Synthesis of Novel Aminomethylphosphine Complexes

by

Nuria Lastra Calvo

A Doctoral Thesis

Submitted in partial fulfilment of the award of Doctor of Philosophy of Loughborough University

Department of Chemistry
Loughborough University
Loughborough
Leicestershire
LE11 3TU

Abstract

A new series of aminomethylphosphine ligands incorporating a PCN backbone and a pendant amine were synthesised using a phosphorus Mannich condensation reaction. Their coordination capabilities were investigated with late transition metal centres. Following a procedure well established within our research group, several phosphines were obtained using $\{P(CH_2OH)_4\}Cl$ (THPC) in two steps. Firstly, THPC was reacted with various *ortho* and *para* anilines to give phosphonium salts $P\{CH_2N(H)R\}_4Cl$ (R = C_6H_5, *o*–MeC_6H_4, *o*–$^{i}PrC_6H_4$, *o*–$^{t}BuC_6H_4$, *o*–FC_6H_4, *o*–$CF_3C_6H_4$, *o*–$\{C(Me)=CH_2\}C_6H_4$, *p*–MeC_6H_4, *p*–$^{i}PrC_6H_4$, *p*–FC_6H_4 and *p*–EtC_6H_4). Secondly, these new salts were reacted with Et_3N to obtain the cyclic $RN(H)CH_2P\{(CH_2)_3(NR)_2\}$ phosphines (R = *para*–substituted anilines) or with $KO^{t}Bu$ to obtain acyclic $P\{CH_2N(H)R\}_3$ phosphines (R = *ortho*-substituted anilines) and cyclic $P\{CH_2N(R)CH_2\}_2P$ diphosphines (R = *ortho*–substituted anilines). Double condensation was observed in the $^{31}P\{^{1}H\}$ NMR of cyclic phosphines $RN(H)CH_2P\{(CH_2)_3(NR)_2\}$ to form $\{(CH_2)_3(NR)_2\}PCH_2N(R)CH_2P\{(CH_2)_3(NR)_2\}$ diphosphines. Some cyclic phosphines were investigated under a wide range of conditions with Ph_2PCH_2OH giving asymmetric $Ph_2PCH_2N(R)CH_2P\{(CH_2)_3(NR)_2\}$ diphosphines along with symmetric diphosphines counterparts and other phosphorus coproducts according to $^{31}P\{^{1}H\}$ NMR and MS. A novel bicyclic $OP\{CH_2N(R)CH_2\}_3PO$ diphosphine (R = *p*–MeC_6H_4) was obtained as crystalline solid from the filtrate of the reaction between $RN(H)CH_2P\{(CH_2)_3(NR)_2\}$ and Ph_2PCH_2OH and it was characterised by X–ray spectroscopy. Attempts to synthesise this diphosphine from $P(CH_2OH)_3$ and *p*–MeC_6H_4 were unsuccessful.

The family of aminomethylphosphine ligands was extended by treating Ph_2PCH_2OH or $CgPCH_2OH$ (Cg = 1,3,5,7–tetramethyl–2,4,8–trioxa–6–phosphaadamantane) with various primary amines to afford $R(H)NCH_2PR'_2$ (R' = Cg or Ph). Symmetric $Ph_2PCH_2N(R)CH_2Ph_2$ diphosphines were observed in the $^{31}P\{^{1}H\}$ NMR spectra indicating that phosphines with Ph_2P– moiety were more susceptible to undertake a second condensation. Novel asymmetric *o*–$\{Ph_2PCH_2C(H)(CH_3)\}C_6H_4N(H)CH_2PPh_2$ diphosphine was synthesised by treatment of *o*-$\{C(Me)=CH_2\}C_6H_4NH_2$ with Ph_2PH to afford *o*–$\{Ph_2PCH_2C(H)(CH_3)\}C_6H_4NH_2$ followed by condensation of the amino group with Ph_2PCH_2OH. Analogous *o*–$\{CgPCH_2C(H)(CH_3)\}C_6H_4NH_2$ phosphine was also obtained.

The coordination capabilities of selected compounds was studied with late transition metal precursor such as Pt(II), Pd(II) and Ru(II). Monophosphine compounds acted as *P*-monodentate ligands to form square planar *cis* and *trans* MCl_2L_2 (M = Pt and Pd) complexes. However, whereas cyclic ligands $RN(H)CH_2P\{(CH_2)_3(NR)_2\}$ afforded *cis*-MCl_2L_2, acyclic ligands $P\{CH_2N(H)R\}_3$ afforded *trans*-MCl_2L_2 along with *cis*-$PtCl_2L_2$ in some cases. Those phosphines which conducted double condensation adopted a *P,P*-chelate mode to form a 6–membered M–P–C–N–C–P to afford *cis*-MCl_2L (M = Pt and Pd). More interesting is the rarely observed *P,P*-bridging mode exhibited by $P\{CH_2N(R)CH_2\}_2P$ ligands to form homobimetallic *cis*–$(PtCl_2L)_2$ complexes and $\{RhCl_2(\eta^5–Cp^*)\}_2L$ complexes. These metal compounds were obtained and characterised by *in situ* NMR however their structures were further supported by simulated $^{31}P\{^1H\}$ NMR and X–ray studies. Asymmetric $Ph_2PCH_2N(R)CH_2P\{(CH_2)_3(NR)_2\}$ diphosphines coordinated to Pt(II) in a *P,P*–chelate fashion affording a mixture of *cis* and *trans* bis(chelate) $(PtL_2)Cl_2$. Complex in *trans* geometry was isolated and the structure was further supported by X–ray crystallography. The coordination capabilities of the ligands were investigated with Ru(II) metal centre revealing "piano–stool" structure of the type $RuCl_2(\eta^6–p–cymene)L$ where the monophosphines adopted a *P*-monodentate mode and $\{RuCl_2(\eta^6–p–cymene)\}_2L$ where the diphosphines adopted a *P,P*-bridging mode. Preliminary studies with selected Ru complexes were carried out to investigate their potential catalytic activity to trap CO_2 by its insertion into the Ru–Cl bond which suggested that the chloride needs to be substituted by a hydride prior the CO_2 insertion. Compounds were characterised by spectroscopic techniques and the structure of some phosphines was further supported by X–ray crystallography.

Acknowledgements

This is probably the only book I will ever publish, so please let me twist a bit the standard format for acknowledgements. This thesis did not start when I did the crystallisation of THPC with ^{i}PrOH for my first reaction, this thesis started nearly six years ago when I came to UK to do an Erasmus exchange. This year I had the opportunity to explore the chemistry of phosphines and late transition metals under the supervision of Dr. Martin B. Smith and one of the chemists that I admire the most, Dr. Chris Raw. In the same lab I also met Allen Ekubo who was doing a PhD in the same research group, but at this time, I did not know that I was going to use this thesis to start mine. It was such a great personal and professional experience that I wanted to continue my studies in the same field. Unfortunately my chemistry background was not sufficient to apply for a PhD grant so I came back to Spain to improve my CV with a Master Thesis in a similar field with my mentor Prof. Jose Vila. Finally, I got the funding and I started my project.

First year was intense. I did not fully understand my chemistry and it was difficult to catch up with names. But I remember from the very beginning the support of the crystallographers Prof. Vickie McKee and Dr. Mark Elsegood, the technicians in the four floor, Andy from stores, Alister for H&S, Mrs Pauline King and Dr. Mark Edgar for long NMR conversations. At that time there were quite a few people in the lab who were finishing but I knew from my Erasmus year like Rob, Leanne, Jenny, Glyn, Andy, Mohammet, Chris and Neil. Others were new like Joe, Andy, Tom and Simon who, to be honest, I shared more beers with than chemist conversations. It was this year when I met people in and out of the Uni who helped me all the way through this thesis like Jason, Cristina, Veronika, Dorota, Vanessa, Bea, Gines, Mario (*acho! Tus comentarios de Facebook me mantuvieron cuerda duerante la tesis*), Juanan, Jayashelaan and Neslihan. *Muchas gracias por compartir tan buenos momentos!*

Second year was confusing. I successfully passed my first year viva, so tons of new ideas wanted my attention. Unfortunately, the chemistry “did not work” and at the end of the year I was panicking with the lack of results. However I learnt that even negative results are meaningful results. For some of them I did not have time to find out the answer, but hopefully future students will reveal the mysteries. New people came to the lab and many left. I met Esther (and her crystallography skills, *tranquila tu secreto esta a salvo con*

Simon y conmigo), Elisa, Oscar and Oscar. I had also the opportunity to go to Netherlands where I met Prof. Karasik and have a chat about diazaphosphorinanes.

Third year finished before started. Or at least this is what I felt. After the second year viva, there were goals to achieve and deadlines to meet. It was the most productive year in terms of chemistry. Everything "worked" but there was no so much time. Luckily, Arturo came to the lab from my home Uni to do an Erasmus exchange as I did years before. I truly thank him for his contribution to this thesis. From a different point of Spain, Alberto also joined to the research group. *A ambos os deseo lo major en vuestra carrera investigadora. Arturo, ti estas seguro de onde te metes?!* I also had the pleasure to share the lab with Eileen, the most determined person and brilliant young chemist I ever met. *Viele danke* for all chemist conversations about cooper and life in general. See you in Manchester!

Finally, fourth year arrived. For one reason or another I was in the lab till Christmas but with so many unfinished bits and reactions to try. It was during my writing period when I realised that my project was only a small contribution to certain chemistry: that I continued the investigation from previous researchers and future investigators will follow mine. The thesis is an open end. It was a year when the support of my family and close friends was the driving force. Hence, special mention merits Dr. Celia Incerti Pradillos (*mi Valencian preferida*), Veronica Varela Mato (*de quimica non entenderas moito pero de cocinar un mundo, gracias polas lambetadas durante a tese!*), Dr. Nolween Derrien (*merci!*) and Dr. Keith MacMillan (thanks for proof reading and music knowledge!). But this thesis would not be possible without the support of my brother Pedro, who visited me every year (*eres incredible brother!*), and my parents, who always let me follow my dreams even if that means to live far away (Pero esta tesis no seria posible sin el apoyo de mi hermano, quien me vino a visitar cada anho, y el de mis padres, quienes siempre me han empujado a perseguir mis suenos aunque eso signifique vivir lejos). And last but not least, I would like to give a big thank to the most important person in my life, the person who passed me his passion for Biology and Ornithology, my best friend and my soul mate, Antonio Lafuente Carballo (*gracias por estar ahi!*).

Table of Abbreviations

Å	Angstrom unit, 10^{-10} m
Acac	acetylacetonate
AIBN	Azobisisobutyronitrile
Ar	substituted arene
Atm	atmosphere
BAr^f_4	Tetra[3,5–bis(trifluoromethyl)phenyl]borane
Bn	Benzyl
^{n}Bu	*n*–butyl
^{i}Bu	iso–butyl
^{t}Bu	tert–butyl
bpy	2,2'–bipyridine
bq	2,2'–biquinoline
bzq	7,8–benzoquinolyl
Cg	1,3,5,7–tetramethyl–2,4,8–trioxa–6–phosphaadamantane
COD	1,5–cylooctadiene
Cp	Cyclopentadienyl
Cy	cyclohexyl
d	doublet
DBU	1,8-Diazabicyclo[5.4.0]undec-7-ene
DCC	*N,N*–Dicyclohexylcarbodiimide
DIPEA	*N,N*-diisopropylethylamine
DMAP	4–dimethylaminopyridine
DMF	*N*,*N*–dimethylformamide
DMSO	Dimethylsulfoxide
dba	dibenzylideneacetone
dmpp	bis(dimethylphosphino)propane
dppmpa	bis(diphenylphosphinomethyl)propionic acid
dppa	bis(diphenylphosphino)amine
dppe	bis(diphenylphosphino)ethane
EA	Elemental Analysis
Et	Ethyl
Fc	Ferrocenyl

g	grams
h	hour(s)
HBTU	O-(benzotriazole-1-yl)-*N,N,N',N'*-tetramethyluronium hexafluorophosphate
Hz	Hertz
IR	Infra red
LDA	Lithium diisopropylamide
Me	Methyl
MS	Mass Spectroscopy
MHz	Megahertz
mins	minutes
mmol	millimoles
NMR	Nuclear Magnetic Resonance
NOe	Nuclear Overhaussen Effect
OAc	acetate
^{n}Oct	*n*–octyl
pip	piperidine
Ph	Phenyl
phen	1,10–phenanthroline
ppm	parts per million
^{i}Pr	iso–propyl
^{n}Pr	*n*–propyl
PTA	1,3,5–triaza–7–phosphaadamantane
r.t.	room temperature
T	Temperature
t	triplet, time
TBAF	Tetra–*n*–butylammonium fluoride
Tf	Triflate
THF	Tetrahydrofuran
THP	tris(hydroxymethyl)phosphine
THPC	tetrakis(hydroxymethyl)phosphonium chloride
tht	tetrahydrothiophene
XRD	X–ray Diffraction
°	Degrees
°C	Degrees centigrade

Key for Mercury Diagrams


C


O


H


P


Cl


N


F


Si


Pt

Key for XP Diagrams


O


F


C


P


Cl


Pd


H


Pt


N


Ru

Table of contents

1. Introduction

1.1 General chemistry of P(III) and P(V) compounds

Phosphines and phosphonium salts are a group of compounds with phosphorus as the central atom. As an element of Group 15, it contains three bonding pairs of electrons and an unshared electron pair. P(III) compounds present a pyramidal structure where the lone non–bonding pair of electrons occupy one of the apical positions (Figure 1.1 **I**). These phosphorus compounds also can form boron–phosphorus adducts with BH_3 as depicted in Figure 1.1 **II**. P(V) compounds can be presented as phosphonium cations (Fig. 1.1 **III**) or as phosphorus chalcogenides (E = O, S, Se) (Fig. 1.1 **IV**). The tetrahedral structure can be distorted by a fourth substituent (R''') or by the lone pair of electrons on the element which compresses the angles R–P–R, respectively.

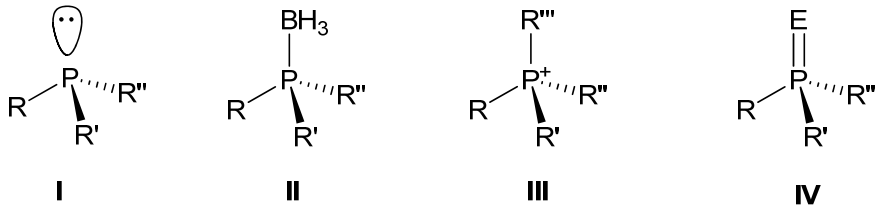

Figure 1.1 Structures of P(III) and P(V) compounds, where R, R', R'' and R''' are H, aryl or alkyl groups and E is O, S or Se.

Organophosphorus compounds incorporate a wide range of substituents, however due to the ligands obtained in this project possessing a PCN backbone, this introduction will review the synthesis, structure and reactivity of heterofunctional phosphorus compounds bearing 'soft' phosphorus and 'hard' nitrogen atoms. In recent years, complexes with PCN ligands have raised great interest due to their versatile coordination chemistry,[1–7] their efficiency as catalysts in electron–transfer process,[8,9] and their biological activity.[1] These important applications reside in the two potential donor atoms (P and N) which can be functionalised by fine tuning of their steric and electronic properties by changing the substituents on both atoms. Therefore, the coordination modes of the aminophosphines may be controlled to bind selected metals too.

One of the most extended methods to obtain tertiary phosphines is the phosphorus based Mannich condensation reaction which will be discussed in more detail in Section 1.2.

1.2 Phosphorus based Mannich condensation reaction

This reaction has been used as an extremely efficient method for the synthesis of PCN phosphorus compounds by reacting hydroxymethylphosphines with primary or secondary amines. Tyler and co–workers showed recently that the lone pair of electrons on the phosphorus atom is essential for reaction to occur, and therefore it is not possible to use this method to functionalise phosphines with the lone pair of electrons occupied.[10] This was demonstrated by treating free (Sch. 1.1 a) and borane–protected (Sch. 1.1 b) hydroxymethyldiphenylphosphines (Ph_2PCH_2OH) with secondary amine (Et_2NH) to get **1.1** in the case of the unprotected phosphine.

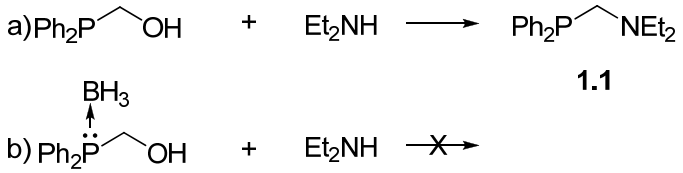

Scheme 1.1 Reactivity of a) free and b) coordinated phosphorus lone pair on Ph_2PCH_2OH.

It has previously been assumed that this reaction proceeds by initial decomposition of the hydroxymethylphosphine, followed by reaction of the amine and formaldehyde to form an iminium salt, and subsequently the nucleophilic attack of the phosphine (Sch. 1.2 where R and R' are H, alkyl or aryl groups).[11] Nevertheless, Tyler *et al*, envisioned an alternative mechanism where the hydroxymethylphosphine eliminates hydroxide to form an electrophilic methylenephosphonium ion salt (analogous to an iminium ion in a classic Mannich reaction), followed by nucleophilic attack of the amine (Sch. 1.2).[10]

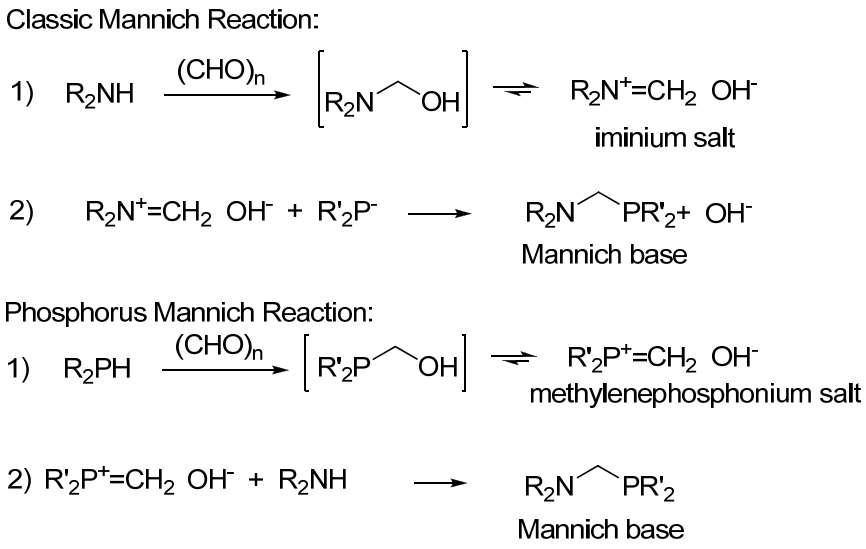

Scheme 1.2 The classic Mannich reaction and suggested mechanism for the phosphorus Mannich reaction.

Scheme 1.2 shows that this is a simple procedure to generate functional tertiary phosphines with no further purification steps hence, phosphorus Mannich condensation reactions are used within this research group[7,12–23] and by others[1–5,8–10,17,18,23–72] working in this field to expand the library of PCN compounds. These tertiary phosphines can contain one, two or more amino groups when the hydroxymethylphosphine precursor reacts with primary amines. This reaction can afford mono– or di–substituted aminophosphines depending upon the nitrogen and phosphorus substituents as well as on the reaction conditions (Sch. 1.3).

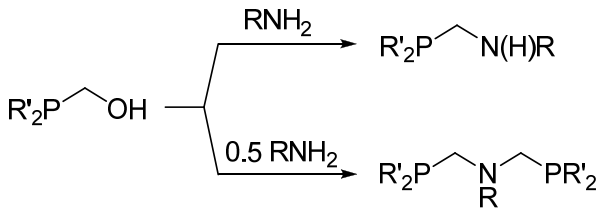

Scheme 1.3 Reactions pathaways for a primary amine in phosphorus based Mannich condensation reactions (R and R' are various alkyl and aryl groups).

1.3 Synthesis, structure, reactivity and applications of PCN compounds

Scheme 1.4 illustrates compounds with a PCN backbone which will be introduced in this chapter as linear (**I** – **V**) and cyclic aminophosphines (**VI** – **X**). The first group of compounds includes phosphonium salts (**I**), monophosphines with one (**II**), two (**III**) or three N atoms (**IV**) and diphosphines with one N (**V**). The second set of compounds contains cyclic aminophosphines with six– (**VI**) or eight–membered rings (**VII**), P–P intrabridgehead phosphines with two five–membered fused rings (**VIII**) or four–membered rings with free rotation along the P–P bond (**IX**) and an eight–membered ring with a CNC bridge between two non–bonded phosphorus centres (**X**).

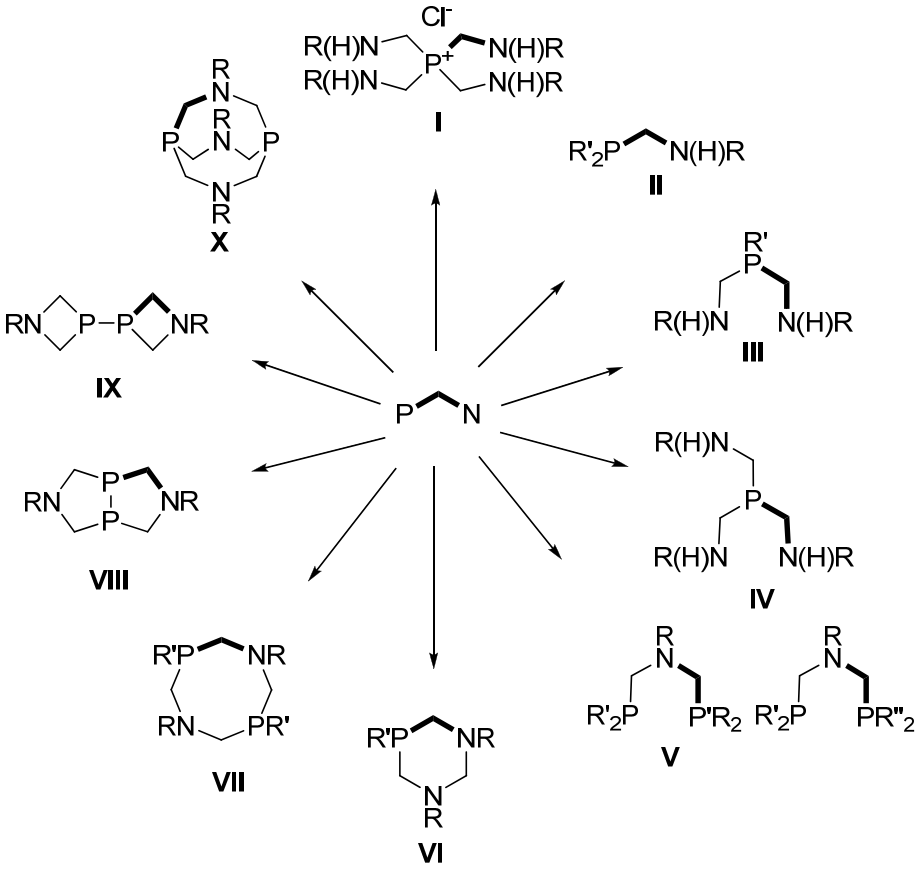

Scheme 1.4 PCN compounds reviewed in this introduction.

1.3.1. Synthesis, structure, reactivity and applications of linear aminomethylphosphines

1.3.1.1 Tetrakis(hydroxymethyl)phosphonium chloride (THPC) as a precursor to phosphonium salts (I) and tris(hydroxymethyl)phosphine (THP)

The preparation of THPC was first documented by Alfred Hoffman, who found a new phosphorus compound when phosphine was absorbed into a warm, aqueous solution of formaldehyde [$(CH_2O)_n$] in HCl (Eqn. 1.1).[24] An 80% aqueous solution of THPC is a commercially available at large scale and relatively cheap reagent due to its industry importance as flame-retardant on cotton textiles and other cellulosic fabrics.[73] THPC which can be used after evaporation of the solution to drynesss, further dried by azeotropic distillation with toluene and finally, the solid is recrystallized with ^{i}PrOH.[27] Reactions of

THPC with primary or secondary amines have gained interest as they provide an insight into the chemistry of the above mentioned flame–retardant cotton finishes prepared from THPC and polyfunctional nitrogen compounds such as ammonia, urea, or melamine.[74]

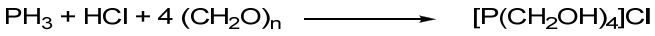

Equation 1.1

Frank and co–workers investigated the chemistry of THPC towards aniline.[25,26] THPC reacts readily with four equivs. of $C_6H_5NH_2$ in ethanol or acetone at r.t., displacing all four hydroxyl groups to obtain $[P\{CH_2N(H)C_6H_5\}_4]Cl$ **1.2** (Sch. 1.5). The reaction of **1.2** with Et_3N gave the cyclic aminomethylphosphine **1.3**. However, when a slurry of **1.2** in acetone was treated with an excess of NH_3 gas, a linear aminomethylphosphine **1.4** was formed. An alternative synthesis for **1.3** and **1.4** was also conducted when THPC was neutralised with NaOEt in EtOH to give tris(hydroxymethyl)phosphine (THP) prior to react with $C_6H_5NH_2$. By this method, the yields of both aminophosphines increased (77% for **1.3** and 81% for **1.4**), however, it implies using THP as an intermediate.

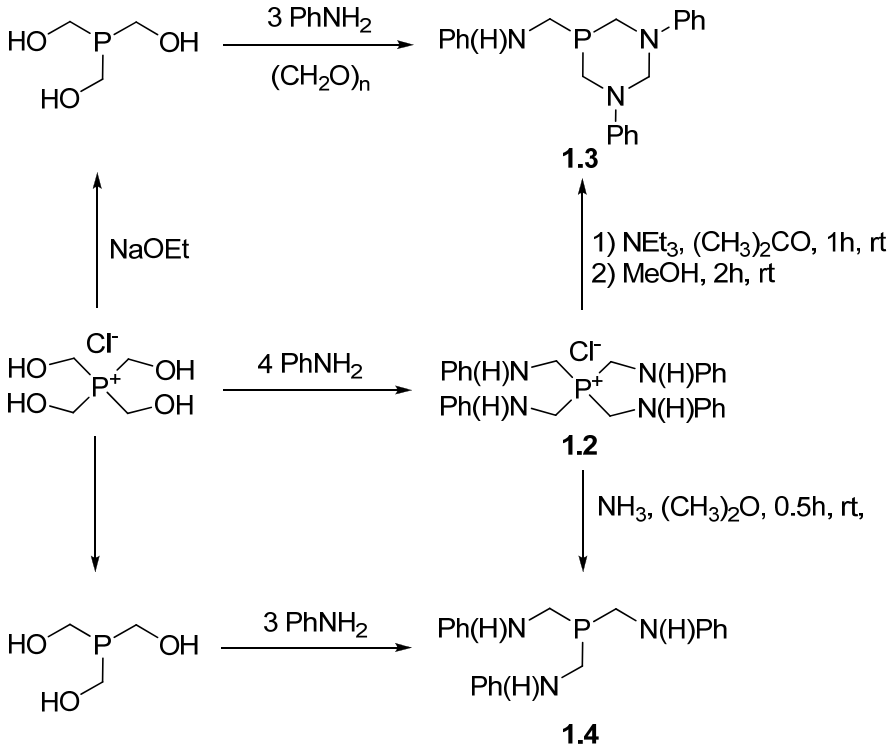

Scheme 1.5 Synthesis of aminomethylphosphines **1.2** – **1.4** from THPC.

Two general methods are extensively used for the synthesis of the water–soluble, moderately air–stable THP. The addition of PH_3 to $(CH_2O)_n$ in water in the presence of $K_2[PtCl_4]$ is an efficient route to THP but requires the handling of highly toxic PH_3 on a

large scale (Sch. 1.6 a).[27] An alternative synthesis of THP, not requiring PH_3, is the reaction of the readily available THPC with a base (Sch. 1.6 b – d).[27,75] Connick and co–workers[28] neutralised THPC with aqueous NaOH to furnish THP (Sch. 1.6 b) in the same manner as the Verkade group[29] who also utilised NaOMe as a base source (Sch. 1.6 b and c). The latter procedure involves adding up to two equivs. of methanolic suspension of NaOMe with THPC to obtain THP in *ca*. 65% conversion as estimated by ^{1}H and $^{31}P\{^{1}H\}$ NMR (δP –24.0 ppm in D_2O). However, along with THP, 30% of unreacted THPC was observed as well as $OP(CH_2OH)_3$ and approximately 5% of formaldehyde too. Ellis *et al.* successfully synthesised THP in *ca*. 99% (by ^{1}H and $^{31}P\{^{1}H\}$ NMR) by treatment of THPC with NEt_3 (Sch. 1.6 d).[27] In addition to the improvement on the purity of the phosphine, this method permitted the generation of THP in a large scale (> 50 g).

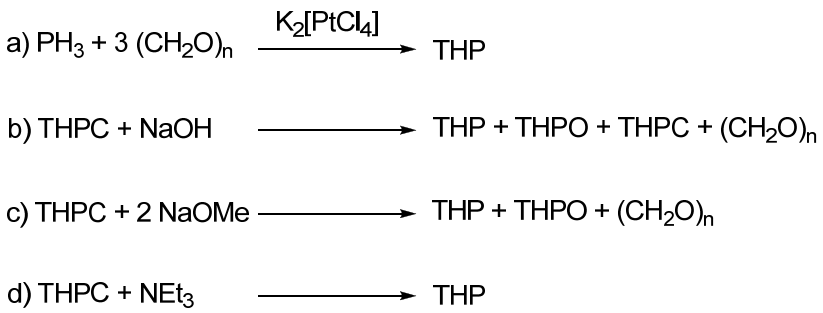

Scheme 1.6 Several methods used to generate THP.

The reliability of this method was manifested by its use to produce THP. Due to this, its coordination chemistry was widely studied with Cu(I),[31] Pt(II), Pd(II) and Ni(II)[27,30] metal centres and as a precursor in the synthesis of aminomethylphosphines.[29,32,33] For instance, the Doud[32] and Griffiths[33] research groups reacted THP with benzyl chloride, to yield benzyltris(hydroxymethyl)phosphonium chloride **1.5** (Sch. 1.7). A second dehydroxymethylation was conducted in neat NEt_3 to form the functional bis(hydroxymethyl)phosphine **1.7**. Furthermore, using methyl iodide, phosphonium salt **1.6** was also synthesised by Doud *et al*. It is remarkable that this new route permits the extension of the family of phosphorus substituents since it is not hampered by the limited availability of primary phosphines and the fact that they are sensitive, noxious, toxic and often pyrophoric.

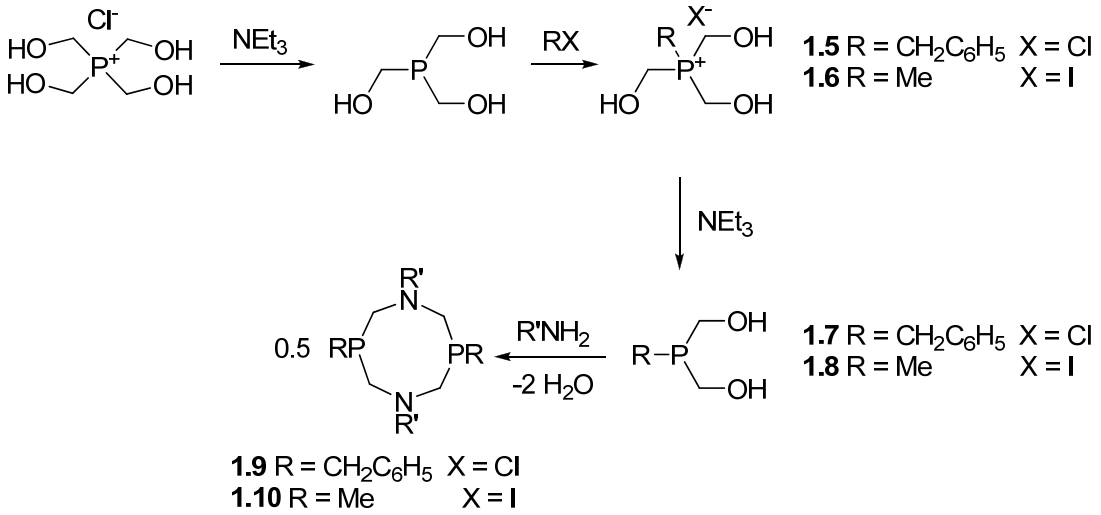

Scheme 1.7 Synthetic route to obtain compounds **1.5** – **1.10**.

However, whereas Griffiths and co–workers isolated **1.5**,[33] Doud *et al*,[32] generated this compound *in situ* from THPC to afford the eight–membered $P_2N_2C_4$ ring aminomethylphosphines **1.9** (13% yield) and **1.10** (63% yield) by addition of the corresponding aniline in methanol. The investigation undertaken by Griffiths revealed that **1.5** was obtained as a mixture of different phosphorus based compounds **1.5**, **1.7**, **1.11** – **1.13** identified by $^{31}P\{^{1}H\}$ NMR studies (Fig. 1.2) which could be the reason of the poor yield for **1.9**.[33]

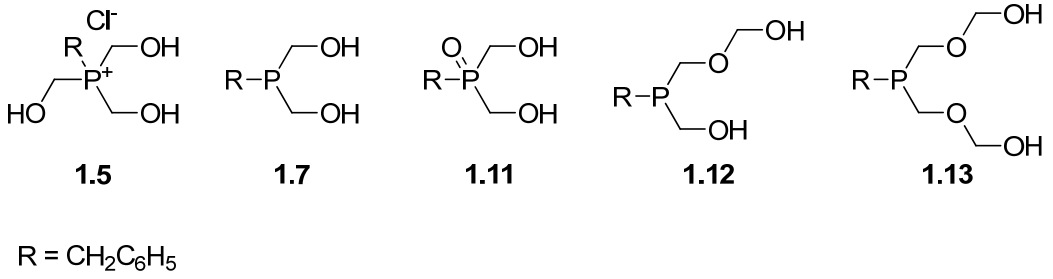

Figure 1.2 Different phosphorus based compounds obtained along with **1.5**.

1.3.1.2 Tertiary aminomethylphosphines R'$_2$PCH$_2$N(H)R (II)

Smith and co–workers have developed new series of $Ph_2PCH_2N(H)R$ phosphines **1.14** – **1.29** (**II** in Sch. 1.4) by treating one equiv. of Ph_2PCH_2OH [generated *in situ* using equimolar amounts of Ph_2PH and $(CH_2O)_n$] with nearly one equiv. of *o,m,p*-aminobenzoic acids (Eqn. 1.2).[15,19] The $^{31}P\{^{1}H\}$ NMR data confirms a single phosphorus species at δP – 20 ppm indicating, in all cases, substituents have negligible effect on the ^{31}P chemical

shifts which are *ca*. 10 ppm upfield with respect to that of Ph_2PCH_2OH [δP –9.9 ppm ($CDCl_3$)].

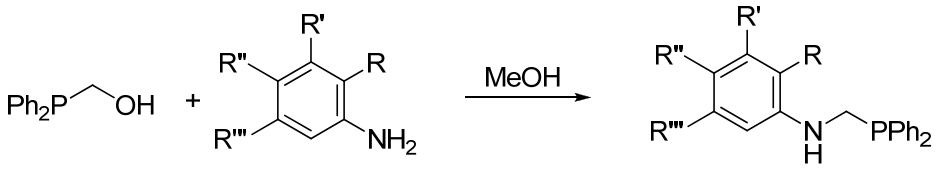

1.14 R = CO_2H R' = H R" = H R''' = H
1.15 R = CO_2H R' = H R" = F R''' = H
1.16 R = CO_2H R' = H R" = Cl R''' = H
1.17 R = CO_2H R' = H R" = H R''' = Cl
1.18 R = CO_2H R' = H R" = Br R''' = H
1.19 R = CO_2H R' = H R" = I R''' = I
1.20 R = CO_2H R' = H R" = OH R''' = H
1.21 R = CO_2H R' = H R" = CO_2H R''' = H
1.22 R = CO_2H R' = H R" = OMe R''' = OMe
1.23 R = CO_2H R' = H R' '= H R''' = CO_2H
1.24 R = OMe R' = H R" = H R''' = CO_2H
1.25 R = H R' = H R" = CO_2H R''' = H
1.26 R = H R' = CO_2H R" = H R'"= H
1.27 R = H R' = H R" = CO_2H R''' = OH
1.28 R = OH R' = H R" = CO_2H R''' = H
1.29 R = H R' = OMe R" = CO_2H R''' = H

Equation 1.2

Small amounts of the di–substituted species were also observed for **1.28** in the $^{31}P\{^1H\}$ NMR so attempts were made to synthesise the non–substituted *bis*(phosphine) derivative of **1.14** from one equiv. of *o*-aminobenzoic acid and two equivs. of Ph_2PCH_2OH which were unsuccessful under these conditions. Similarly reaction of *m*-$(CO_2H)C_6H_4NH_2$ and Ph_2PCH_2OH in a 1:1 molar ratio, in MeOH at ambient temperature, yielded $Ph_2PCH_2N(H)C_6H_4$(*m*–CO_2H) (**1.26**) in addition to small amounts (*ca*. 20%) of the di–substituted phosphine $(Ph_2PCH_2)_2NC_6H_4$(*m*–CO_2H) **1.30** (Eqn. 1.3). Both phosphines could readily be distinguished by their characteristic ^{31}P NMR resonances which differ by *ca*. 10 ppm between both phosphorus species. Despite the substituent on the nitrogen not considerably affecting the basicity of the phosphorus according to the $^{31}P\{^1H\}$ NMR, it does in the product of the Mannich condensation reaction.

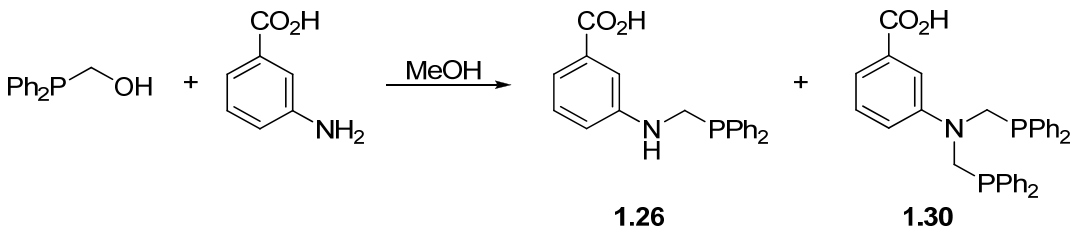

1.26 **1.30**

Equation 1.3

The coordination chemistry of this library of ligands was explored with a Ru(II) metal centre. They were prepared by standard bridge cleavage of $\{RuCl_2(p\text{–cymene})\}_2$ with two equivs. of **1.14**, **1.20, 1.23** – **1.27** in CH_2Cl_2 at r.t. (Fig. 1.3). The $^{31}P\{^1H\}$ NMR data were in good agreement with P–monodentate coordination as inferred by the downfield shift (typically *ca*. 20 ppm) of their ^{31}P resonances [δP 16.1 – 28.3 ppm ($CDCl_3$)]. Furthermore, the ^1H NMR spectra showed well resolved signals for the *p*–cymene and PCH_2N [δH 4.34 – 4.72 ppm] groups.[19]

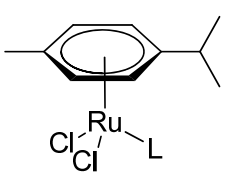

1.31 L = **1.14**
1.32 L = **1.20**
1.33 L = **1.23**
1.34 L = **1.24**
1.35 L = **1.25**
1.36 L = **1.26**
1.37 L = **1.27**

Figure 1.3 Coordination chemistry of various $RN(H)CH_2PPh_2$ ligands with Ru(II).

E. Payet *et al*. synthesised a series of aminophosphines ligands differing in the nature of the phosphorus and nitrogen substituents.[76] They found the reaction was highly dependent upon these groups and due to this, the reaction conditions had to be very carefully monitored in order to avoid the double condensation which forms the corresponding di–substituted PCNCP ligand (Eqn. 1.4). For the synthesis of **1.39** and **1.41**, 1.5 equivs. of $^tBuNH_2$ were used at r.t. in CH_2Cl_2 and the excess of *tert*–butylamine was removed under vacuum. This procedure prevented the formation of the PCNCP phosphine, however, it could not be applied to **1.38** and **1.40** as $C_6H_5NH_2$ proved to be difficult to eliminate. To overcome this issue, aniline was added to a frozen solution of hydroxymethylphosphine (Cy_2PCH_2OH or Ph_2PCH_2OH) and allowed to warm to r.t. under vacuum to eliminate water. The $^{31}P\{^1H\}$ NMR data showed the formation of a unique product exhibiting a singlet at δ(CH_2Cl_2) = –16.7, –5.3, –19.7 and –3.2 ppm for **1.38** – **1.41**, respectively, indicating that the phosphorus substituents has a noticeable effect on the P shift over the nitrogen group.

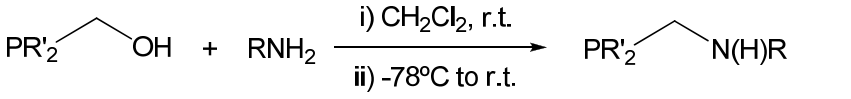

1.38 R' = Cy R = C_6H_5
1.39 R' = Cy R = ^tBu
1.40 R' = C_6H_5 R = C_6H_5
1.41 R' = C_6H_5 R = ^tBu

Equation 1.4

Ligand **1.38** was treated with 0.5 equiv. of $\{Rh(COD)Cl\}_2$ in CH_2Cl_2 for 30 min. The $^{31}P\{^1H\}$ NMR spectrum of the crude mixture indicated the disappearance of the starting material and the formation of a single product **1.42** characterised by a doublet at δP 24.0 ppm [$^1J_{PRh}$ = 144.0 Hz ($CDCl_3$)] (Sch. 1.8). Chloride abstraction from **1.42** was conducted using a silver salt and $NaBAr^f_4$ in CH_2Cl_2 to achieve **1.43** and **1.44**.

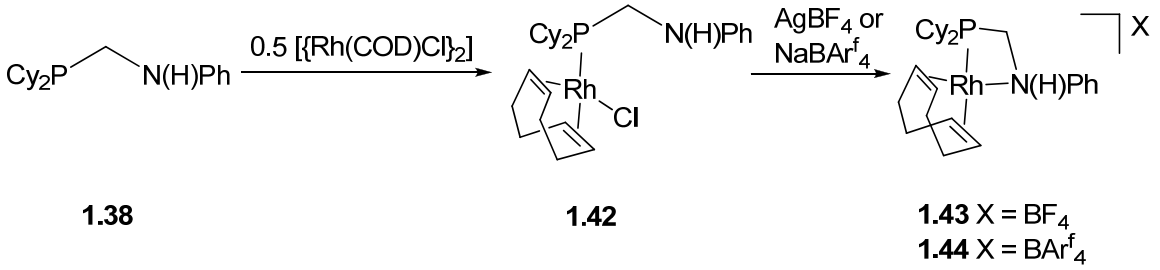

Scheme 1.8 Synthesis of Rh(I) complexes from aminomethylphosphine **1.38**.

As for the previous PCN backboned ligands, Woollins and co–workers obtained **1.45** by condensation of Ph_2PCH_2OH with *o*–$(Ph_2P)C_6H_4NH_2$ but on this occasion in C_7H_8 at 90°C for 20h (Eqn. 1.5).[34] This particular tertiary phosphine possesses an extra 'soft' coordination site with respect to the previous examples discussed. In addition, Ph_2P– is two carbon spacer moieties space from the N atom conferring the ligand a flexible and unsymmetrical $PCNC_2P$ spine suitable for selective coordination modes.

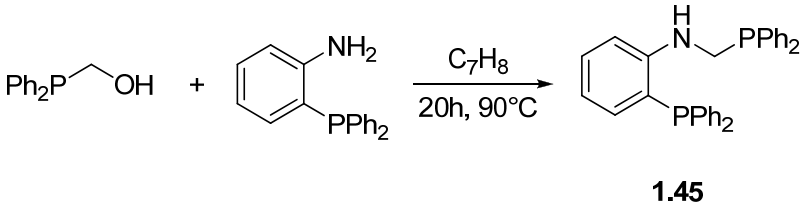

Equation 1.5

Ligand **1.45** demonstrated three distinct binding modes: chelate fashion, bidentate and monodentate as depicted in Figure 1.4. The first mode was observed with $MX_2(COD)$ (M = Pd, Pt; X = Cl, Br, Me) or $Mo(CO)_4(pip)_2$ (complexes **1.46** – **1.50**). The bidentate mode was displayed when **1.45** acts as a bridging ligand after reacting with two equivs. of AuCl(tht) or one equiv. of $\{RhCl(\mu–Cl)(\eta^5–C_5Me_5)\}_2$ to give the bimetallic complexes **1.51** and **1.52**, respectively. Finally, the monodentate binding mode was observed in complex **1.53** due to the reactivity of both phosphorus being different. Hence, ligand **1.45** coordinated selectively through the less bulky phosphorus afford monometallic complex

1.53. The abstraction of the chloride ligands from complex **1.53** with $AgClO_4$ gave the chelate complex **1.54** which again forms a seven–membered M–P–C–N–C–C–P ring as Pt(II) and Pd(II) complexes. The $^{31}P\{^1H\}$ NMR spectrum of **1.45** in $CDCl_3$ showed two distinct singlets at δP –18.8 and δP –22.3 ppm which were assigned to $–NHCH_2PPh_2$ (P_A) group and $–C_6H_4PPh_2$ (P_B), respectively, by comparison with the $^{31}P\{^1H\}$ NMR spectrum of monodentate complex **1.53** [δP –22.8 (P_B), 32.7 ppm (d, $^1J_{RhP}$ = 141 Hz, (P_A))].

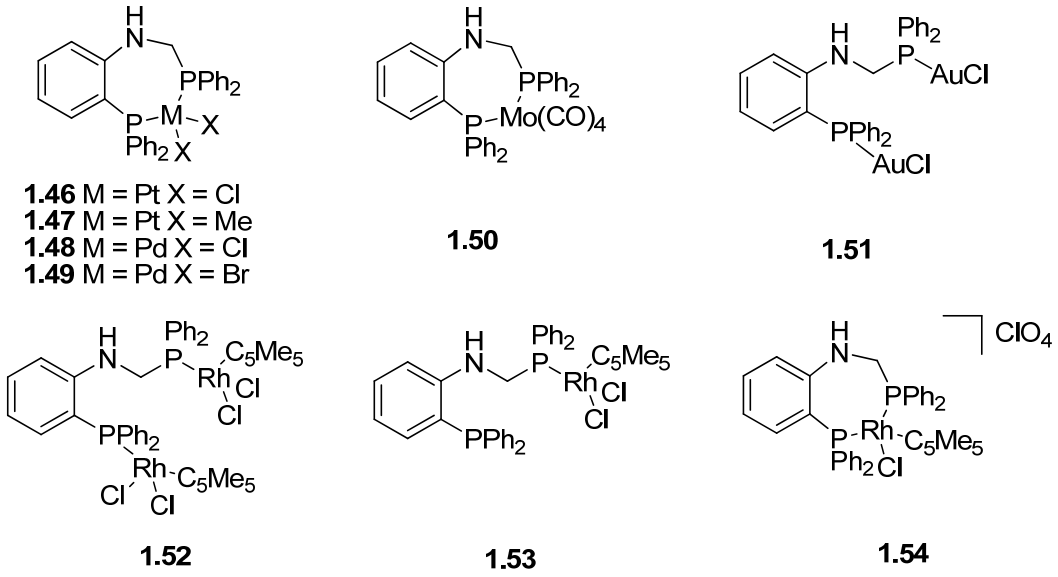

Figure 1.4 Coordination modes of ligand **1.45**.

Several research groups have applied the phosphorus Mannich condensation reaction to incorporate a PCN backbone to pyridyl groups (Py).[14,21,23,34,35] Smith *et al* described the synthesis of a variety of pyridylphosphines using equimolar amounts of Ph_2PCH_2OH and different pyridines with an amino group in *meta* (**1.55**) and *ortho* (**1.56** – **1.62**) positions to the nitrogen (Sch. 1.9).[14,21,23] Furthermore, ligands **1.58** – **1.60** were prepared from **1.57** upon stoichiometric reaction with $ClP(O)Ph_2$, $ClP(O)(OPh)_2$ or $ClPPh_2$, respectively, in C_7H_8 (Sch. 1.9). The $^{31}P\{^1H\}$ NMR spectra of **1.55** – **1.62** showed a single P resonance at approx. δP –19.0 ppm and for **1.58** – **1.60** an additional resonance was observed at δP 34.6, –15.0 and 114.3 ppm, respectively. These values indicate the negligible effect on the phosphorus shift among various pyridylphosphines bearing several functional groups in different positions.

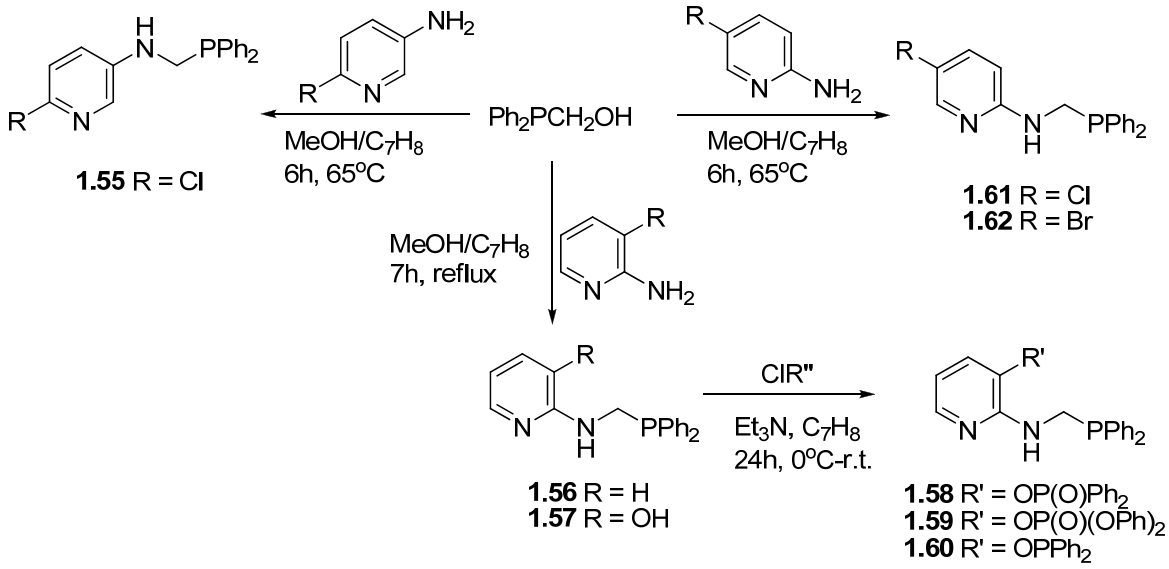

Scheme 1.9 Synthesis of aminomethylphosphines **1.55** – **1.62**.

A detailed study of the ligating ability of aminophosphines **1.55** – **1.62** towards late transition metal centres was undertaken to ascertain the potential for P–co–ordination and $P,N_{pyridyl}$–chelation (Fig. 1.5). The majority of the ligands displayed a monodentate binding mode once reacted with half an equiv. of Pt(II) (**1.63** – **1.67)**, Pd(II) (**1.69** – **1.71**), Ru(II) (**1.76 – 1.82**) and Rh(III) precursors (**1.83 – 1.89**). However, while dichloroplatinum complexes **1.63** – **1.67** possess both phosphorus in a *cis* arrangement, dichloropalladium complexes **1.69** – **1.71** were obtained as a *cis*/*trans* mixture. In addition, the bidentate chelate mode was also observed for ligand **1.60** with Pt(II) (**1.68**) and for **1.61** and **1.62** with Pd(II) (**1.74** – **1.75**) but in a distinct manner. Ligand **1.60** binds platinum through the two phosphorus centres to form a nine–membered ring, though ligands **1.56**, **1.57**, **1.61** and **1.62** coordinate to palladium through the phosphorus and the pyridyl nitrogen to afford a six–membered ring. A bridging coordination mode was also observed after treatment with one equiv. of **1.60** with two equivs. of Ru(II) (**1.90**) and Rh(III) (**1.91**) metal centres.

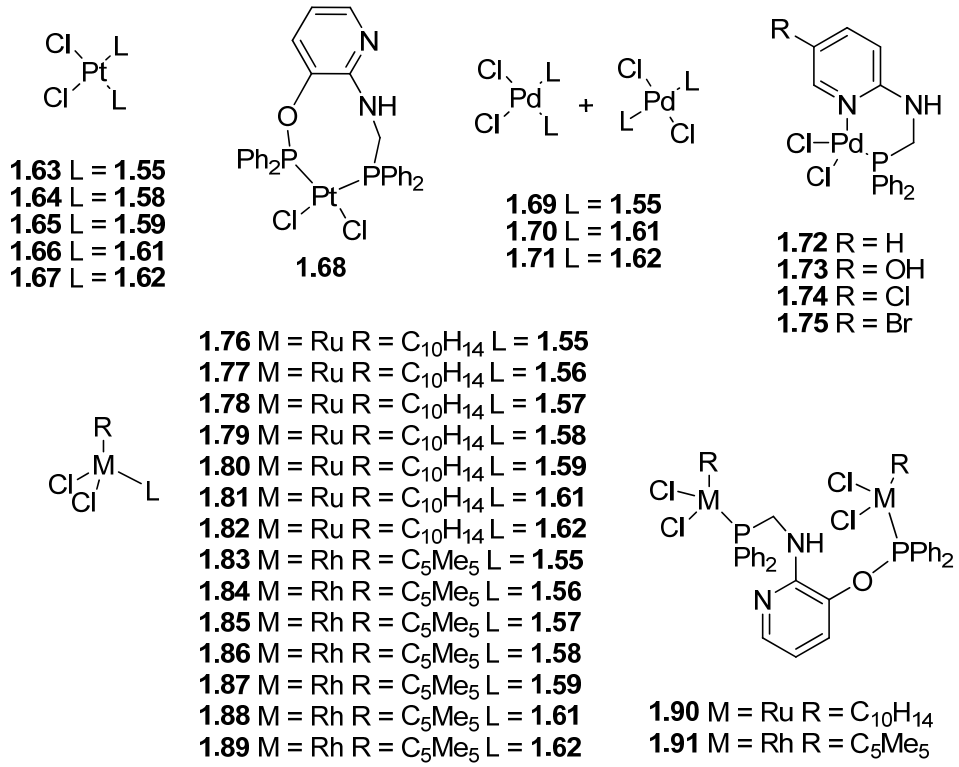

Figure 1.5 Coordinating modes of ligands **1.55** – **1.62** with Pt(II), Pd(II), Ru(II) and Rh(III) metal centres.

Zhang and co–workers prepared a new flexible tridentate naphthyridine–phosphine ligand **1.92** from the condensation of Ph_2PH and $(CH_2O)_n$ with the correspondent naphthyridine derivative upon refluxing in C_7H_8 under a nitrogen atmosphere (Sch. 1.10).[35] The $^{31}P\{^1H\}$ NMR was in agreement with other previously reported secondary aminomethylphosphines at δP –17.2 ppm. This group demonstrated the versatile coordination mode of this type of PCN ligands which incorporate a second potential N donor atom. For example, reaction of **1.92** with $\{Cu(CH_3CN)_4\}BF_4$ and $\{Cu(CH_3CN)_4\}BF_4/PPh_3$ yielded the binuclear copper complexes **1.93** and **1.94**. In the first complex, two copper centres are ligated by two ligands displaying a *P,N,N*–chelating mode and bonded with an intramolecualar Cu···Cu distance of 2.908(3) Å. The second complex (**1.94**), however, did not exhibit this Cu–Cu intrabridgehead due to the ligand **1.92** bridging the two Cu(I) metal centres through the naphthyridine–N atoms and the phosphine group to form a bimetallic 16–membered ring. In contrast, ligand **1.92** coordinates to one Pt(II) metal centre when it was treated with $Pt(SMe_2)_2Cl_2$ in CH_2Cl_2 to form **1.95**. Once more, ligand **1.92** adopted the same coordination as **1.93**, *i.e.* the *P,N*–chelating mode.

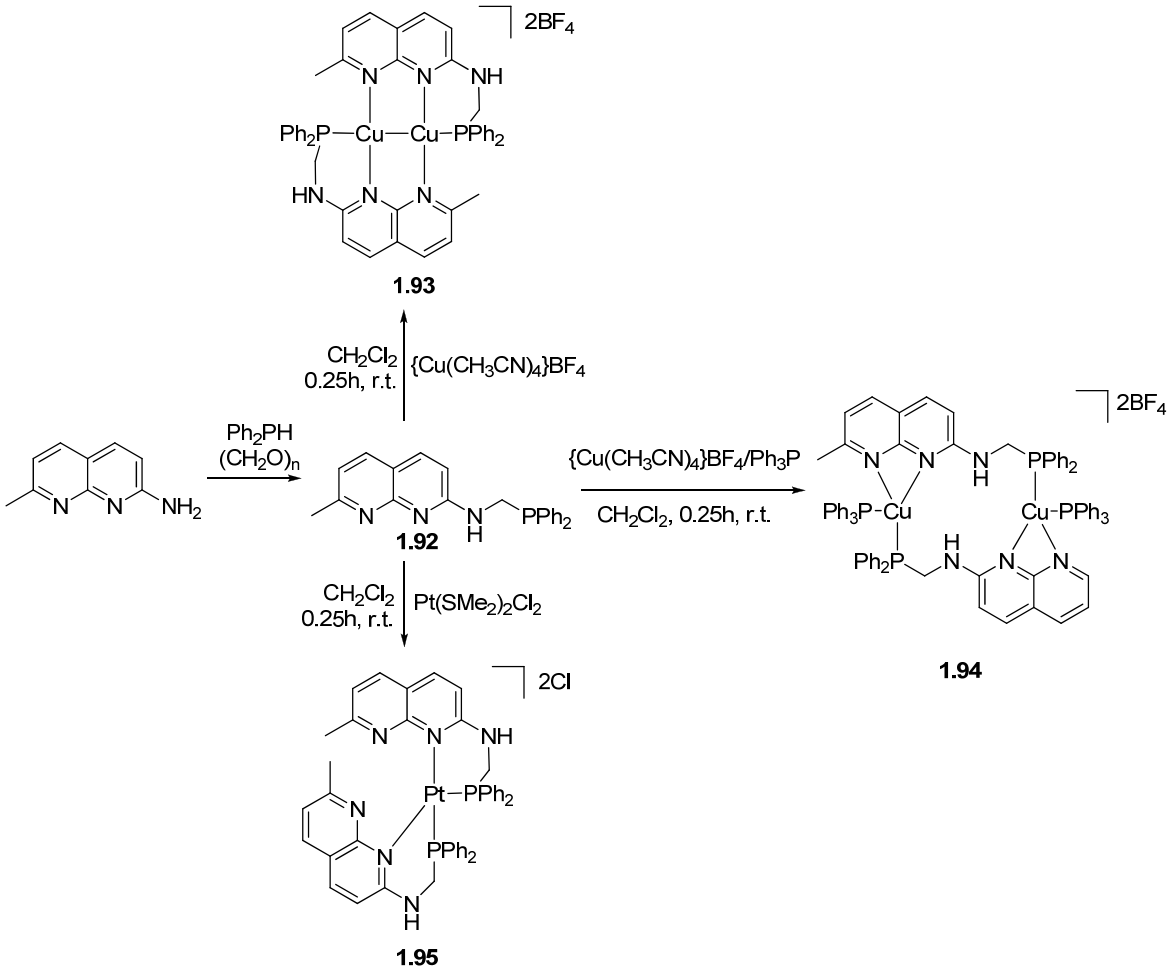

Scheme 1.10 Synthesis and coordination chemistry of ligand **1.92**.

1.3.1.3 Tertiary bisaminomethylphosphines R'P{$CH_2N(H)R$}$_2$ (III)

So far, R'$_2$P$CH_2N(H)R$ aminomethylphosphines have been discussed with identical R' substituents. However, a new type of bisaminomethylphosphine can be generated by incorporation of a second pendant amine as one of the phosphorus substituents, *i.e.* R'P{$CH_2N(H)R$}$_2$ (**III** in Sch. 1.4).

Balch *et al.* synthesised polydentate phosphine ligands with methylene spacers between the donor atoms by condensation of $C_6H_5NH_2$, Ph_2PH and $(CH_2O)_n$ to yield $PhN(CH_2PPh_2)_2$ **1.96** (**V** in Sch. 1.4) or by reaction of $(C_6H_5)_2NH$ and $PhPH_2$ with $(CH_2O)_n$ to obtain $PhP(CH_2NPh_2)_2$ **1.97** (Sch. 1.11).[36] The $^{31}P\{^1H\}$ NMR of each ligand consisted of one sharp peak at δP –27.0 ppm for **1.96** and at –34.7 ppm for **1.97**. Their coordination chemistry was investigated to prove the *P,N*–binding modes by preparing platinum and rhodium complexes (coordination capabilities of **1.96** will be discussed in Section 1.3.1.5 as it belongs to the **V** type of compound in Sch. 1.4). Hence, when one

equiv. of ligand **1.97** was reacted with two equivs. of $Rh_2(CO)_4(\mu\text{–}Cl)_2$ in C_7H_8, the only species observed was *trans*–{$PhP(CH_2NPh_2)_2$}$_2$Rh(CO)Cl **1.98**. Even with an excess of the metal precursor, ligand **1.97** coordinated preferentially to the metal centre through the phosphorus with both phosphorus centres *trans* to each other [δP 26.8 ppm ($^1J_{PRh}$ = 70.2 Hz)].

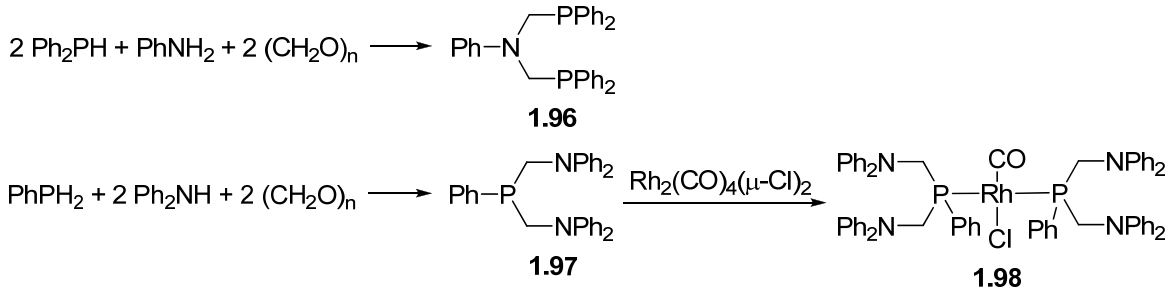

Scheme 1.11 Synthesis of ligands **1.96** and **1.97** and coordination of **1.97** with Rh(I).

A different synthesis was employed by Märkl's research group to produce a family of RN{$CH_2PR'R''$}$_2$ (**1.99** – **1.102**) and R'P{$CH_2N(Me)(CHMePh)$}$_2$ ligands (**1.103** – **1.105**) using various hydroxymethylphosphines (Sch. 1.12).[37] Whereas ligands **1.99 – 1.102** (**V** type in Sch. 1.4) were obtained by condensation of the appropriate hydroxymethylphosphine and the primary amine, ligands **1.103** – **1.105** were achieved by reacting the selected bis(hydroxymethyl)phosphine with a secondary amine that have two unequal substituents. Therefore, ligands **1.99** – **1.102** are optically active at phosphorus and **1.103** – **1.105** are optically active at the carbon bonded to the nitrogen.

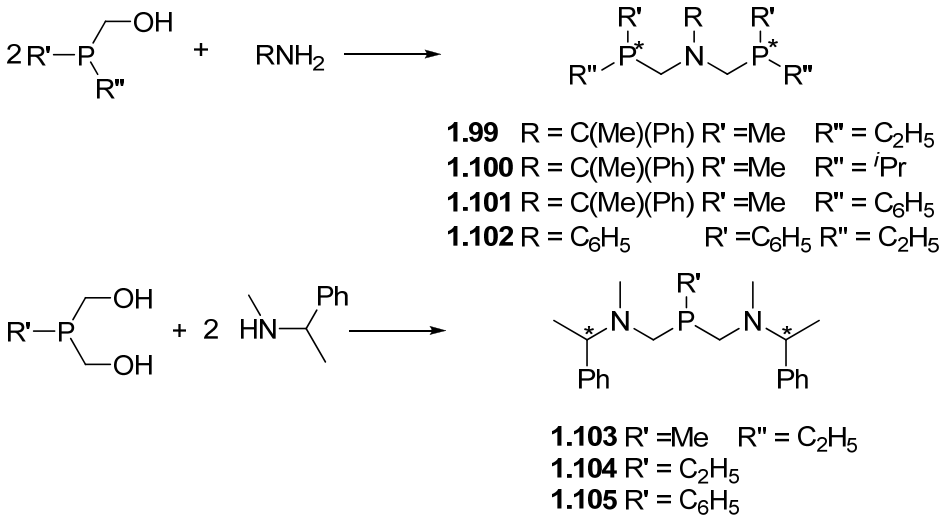

Scheme 1.12 Synthesis of PCNCP **1.99** – **1.102** and NCPCN ligands **1.103** – **1.105**.

Hey–Hawkins, in collaboration with Karasik's research group, developed an extensive library of water soluble tertiary phosphines incorporating an aminoacid group (Sch. 1.13).[38,39] Ligands **1.106** – **1.114** were obtained by condensation of one equiv. of bis(hydroxymethyl)phosphine with two equivs. of *ortho* or *para* aminobenzoic acids. However, even these ligands were obtained as the major products of the reaction (δP –31 to –36 ppm for **1.106** – **1.112** and δP –35.1, –38.2 ppm for **1.113** and **1.114**) the tendency to undergo cyclocondensation is large. This is more noticeable for *p*–aminobenzoic acid derivatives with up to 20% of the eight–membered analogues **1.115** and **1.116**.

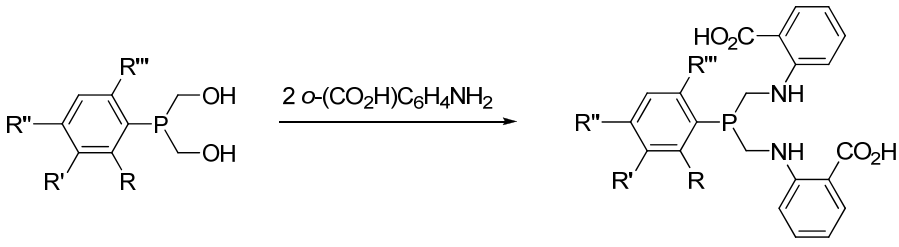

1.106 R = H R' = H R'' = H R''' = H
1.107 R = Me R' = H R'' = Me R''' = Me
1.108 R = ^{i}Pr R' = H R'' = ^{i}Pr R''' = ^{i}Pr
1.109 R = H R' = H R'' = H R''' = OH
1.110 R = H R' = Me R'' = H R''' = OH
1.111 R = H R' = OMe R'' = H R''' = OH
1.112 R = H R' = Me R'' = H R''' = OCH_2Me

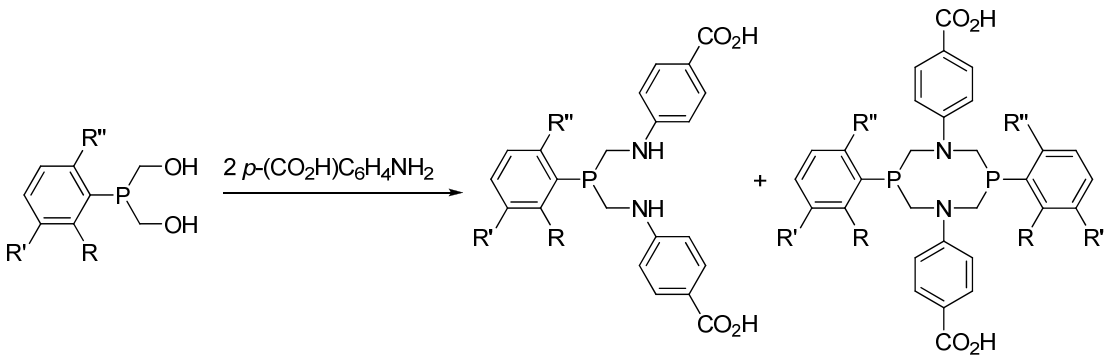

1.113 R = H R' = H R'' = H
1.114 R = H R' = Me R'' = H
1.115 R = H R' = H R'' = H
1.116 R = H R' = Me R'' = H

Scheme 1.13 Synthesis of bisaminomethylphosphines **1.106** – **1.112** and **1.113** – **1.114** along with **1.115** and **1.116**.

These experiments demonstrated that the substituent on the aniline determines the product obtained. Therefore, *ortho* and *para*–aminobenzoic acid derivatives afforded mainly *bis*–aminomethylphosphines but the latter are synthesised with cyclic analogues too. This was further ratified by the synthesis of the *bis*–phosphine **1.117** which contains a *p*–Me aniline and a functionalised benzyl tertiary phosphine for potential polymerisation of the allyl

group (Sch. 1.14).[40] This potential hybrid ligand was not isolated pure (δP –29.4 ppm) due to the presence of the six– and eight–membered cyclic analogues **1.118** (δP –39.9 ppm) and **1.119 [**(δP –49.0 ppm (DMF)], respectively. Compounds **1.115**, **1.116** and **1.119** were easily prepared by adding equimolar amounts of both the phosphine and aniline precursors rather than the 1 to 2 molar ratio required for the analogous linear ligands **1.113, 1.114**, **1.117**; and **1.119** was simply afforded by adding $(CH_2O)_n$.

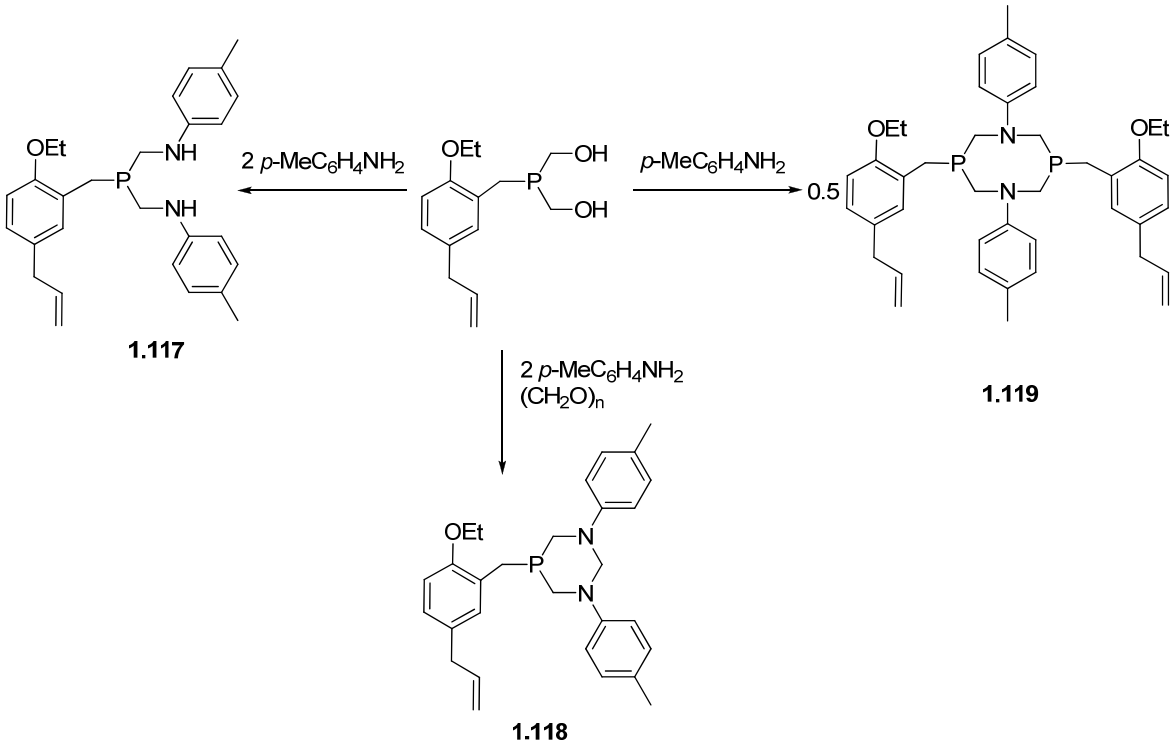

Scheme 1.14 Three synthetic pathways to obtain similar aminomethylphosphines **1.117** – **1.119** by changing the number of equivs. of *p*–$MeC_6H_4NH_2$.

The coordination chemistry of ligands **1.106**, **1.107**, **1.109** – **1.111** was explored towards platinum and nickel metal centres (Fig. 1.6).[38] Platinum complexes were bound by two ligands in a P–monodentate mode (**1.120** – **1.123**) or in a *P,O*–chelate fashion mode (**1.124**). In contrast, Ni(II) complexes were chelated by ligand **1.106** through nitrogen and oxygen to give **1.125**.

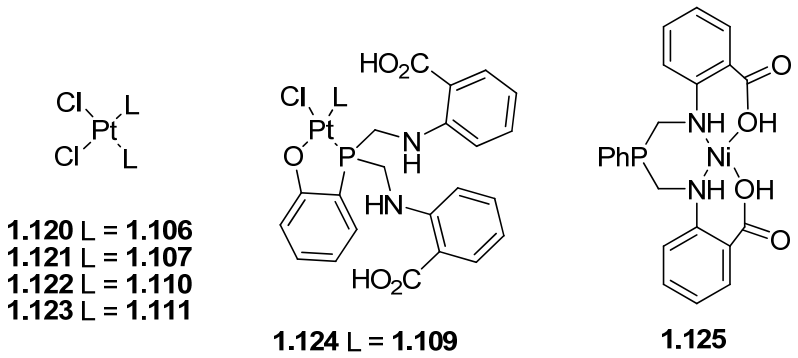

Figure 1.6 Coordination modes of ligands **1.106** – **1.111** with Pt(II) and Ni(II).

Tyler and co–workers have investigated the Mannich condensation reaction between coordinated and uncoordinated hydroxymethylphosphine ligands with NH–functional amines to determine if this reaction is suitable for the synthesis of macrocycles (Sch. 1.15).[10] For these studies 1,2–bis(dihydroxymethylphosphino)ethane (DHMPE) was reacted with $FeCl_2{\cdot}4H_2O$ to give *trans*–$Fe(DHMPE)_2Cl_2$ **1.126** (δP 73.2 ppm) and also with Ru(II) and Ni(II) to form *trans*–$Ru(DHMPE)_2Cl_2$ **1.127** and *trans*–$Ni(DHMPE)_2Cl_2$ **1.128**. Curiously, once **1.127** and **1.128** were treated with a variety of amines ($MeNH_2$, $^{n}BuNH_2$ and $^{t}BuNH_2$) no phosphorus condensation reaction was observed. Furthermore, while no favourable reaction was oberved after 2 weeks under reflux, complex **1.126** underwent removal of two chlorides by one DHMPE ligand to achieve **1.129** (δP 93.3 ppm). This indicates that after coordination of the phosphorus to the metal centre, no condensation was carried out. Hence, experiments illustrated in Scheme 1.15 in conjunction with those previously discussed in Scheme 1.1, supports the necessity of the lone pair of electrons on phosphorus for the Mannich reaction to occur.

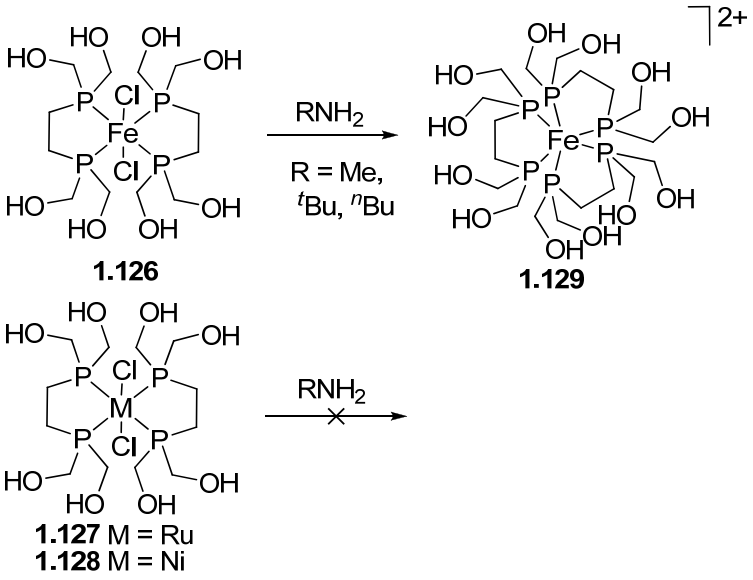

Scheme 1.15 Attemps to condense the HO– groups of **1.126** – **1.128** with primary amines.

The chemistry of DHMPE as well as the rotationally–restricted HMPB (1,2–bis(bis(hydroxymethyl)phosphine)benzene) was investigated against a series of amino acids and secondary amines by Katti and co–workers (Sch. 1.16).[41] Compounds **1.130** – **1.133** were obtained by treatment of DHMPE or HMPB with five equivs. of the corresponding amine in H_2O after stirring for 1 to 3h at r.t. However, only two equivs. of the primary amines react with DHMPE and HMPB to give the cyclic phosphines **1.130** – **1.133**. Whereas, the $^{31}P\{^1H\}$ NMR of HMPB derivatives were in the range of δP –8.3 to –9.9 ppm (D_2O/NaOD), phosphorus in **1.130** resonates at δP –36.3 ppm (D_2O) revealing the noticeable effect in the ^{31}P chemical shift due to the P substituent *versus* the N substituent. Further investigations into the condensation reaction between DHMPE and DHMPB with amines were undertaken using secondary amines $(CH_3)(C_6H_5)NH$ and Et_2NH in stoichiometric amounts in EtOH at r.t. for 1h (Sch. 1.16). In contrast to **1.130** – **1.133**, phosphines **1.134** and **1.135** were obtained as the expected linear tetraamine substituted compound. The $^{31}P\{^1H\}$ NMR showed a single peak at δP –43.6 and –60.3 ppm indicating the noticeable effect of the nitrogen group on the ^{31}P chemical shift.

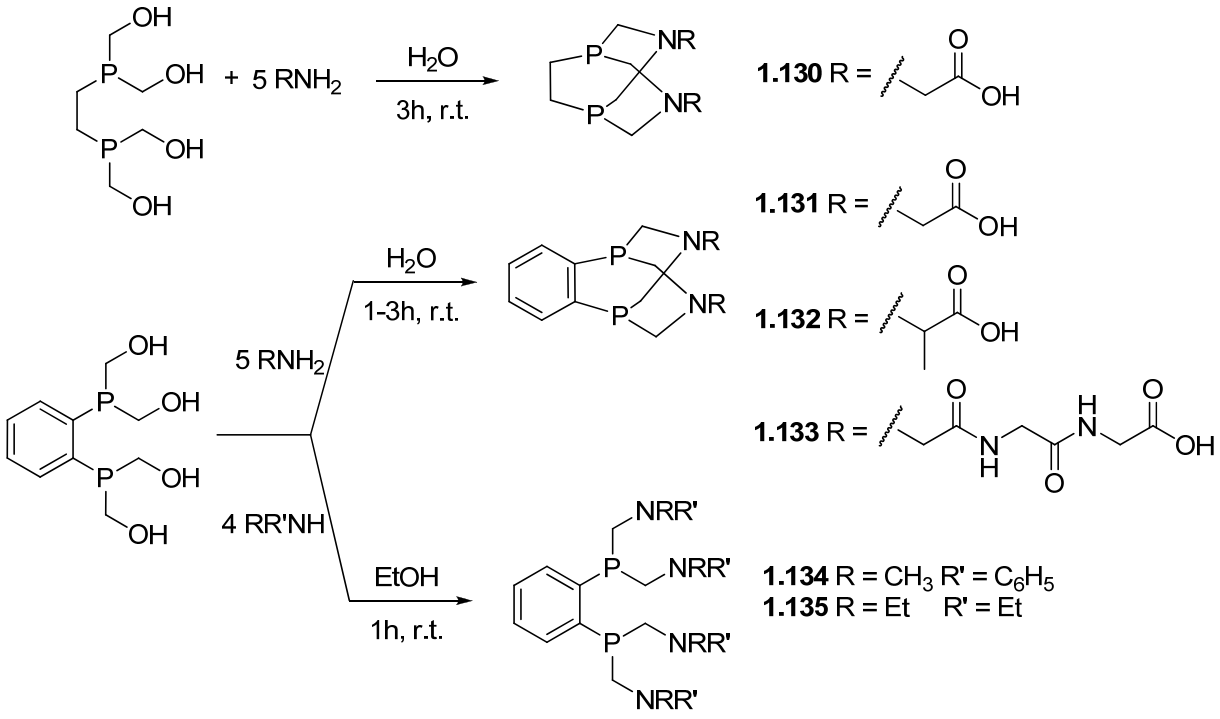

Scheme 1.16 Synthesis of aminomethylphosphines **1.130** – **1.135**. The structure of the phosphine depends on the hydroxymethylphosphine and the amine employed.

1.3.1.4 Tertiary trisaminomethylphosphines $P(CH_2NRR')_3$ (IV)

Katti *et al.* have further developed the conjugation of amino acids with phosphines as a versatile method to expand the spectrum of peptide backbones using glycine and alanine with THP (Eqn. 1.6).[42] New phosphines **1.136** and **1.137** were synthesised by adding five equivs. of glycine or three equivs. of alanine to THP in water at r.t for 3h and 1h, respectively. Compounds **1.136** and **1.137** exhibited high oxidative stability which, in addition to the great water solubility, make them excellent ligands for water–soluble transition metal compounds.[42]

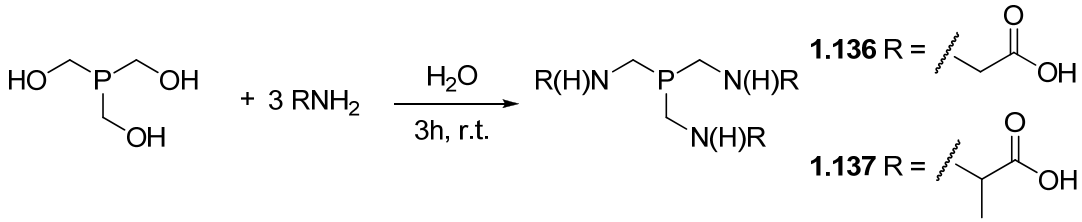

Equation 1.6

Beller *et al.* have also investigated water soluble phosphine ligands due to their practical application in homogenous catalysis once reacted with late transition metals.[77] By employing the same methodology as depicted in Equation 1.6, aminomethylphosphines **1.138** – **1.142** were obtained (Eqn. 1.7). It should be stated that compounds **1.138** – **1.142** could be formed from THPC as starting material but it was not applied for purification reasons. The $^{31}P\{^1H\}$ spectra of **1.138** – **1.142** showed a single peak in the range of δP –57.8 to –69.1 ppm in D_2O which is considerably different to those observed for **1.136** and **1.137** (–38.1 and –39.9 ppm in D_2O), due to the more electron donating substituents in **1.138** – **1.140** compared to the less electron donating carboxylic groups in **1.136** and **1.137**.

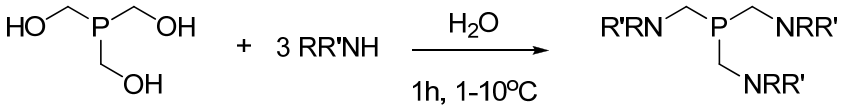

1.138 R = CH_3 R' = CH_2CO_2Na
1.139 R = CH_3 R' = $CH_2CO_2SO_3Na$
1.140 R = CH_3 R' = CH_2CO_2OH
1.141 R = $(CH_2)_2OH$ R' = $(CH_2)_2OH$
1.142 R = ^{n}Bu R' = $(CH_2)_3SO_3Na$

Equation 1.7

Frost and co–workers utilised the simplest trisaminomethylphosphine $P(CH_2NH_2)_3$ **1.143** as precursor to a series of tris(iminomethyl)phosphines or trisubstituted triazaphosphaadamantane ligands depending upon the reaction conditions and the electronics of the aldehyde used (Sch. 1.17).[43] Under basic conditions, **1.144** – **1.146** were obtained by adding the desired aldehyde and NaOH to a solution containing **1.143** (3:1). Likewise, cage ligands **1.147** – **1.150** were synthesised using HCl rather than NaOH. The two isomeric products were easily identified by $^{31}P\{^1H\}$ NMR spectroscopy since **1.144** – **1.146** exhibit a single resonance at approx. δP –21.5 ppm (recorded in DMSO, $CDCl_3$ or CD_3OD depending on the solubility) whereas **1.147** – **1.150** present a singlet too but further upfield [*ca*. δP –110.6 ppm ($CDCl_3$)]. Attempts to convert linear **1.144** – **1.146** to **1.147** – **1.150** were unsuccessful even after heating or addition of acid concluding that the synthesis of the PTA (1,3,5–triaza–7–phosphaadamantane) derivatives involves a condensation followed by nucleophilic attack and ring closure.

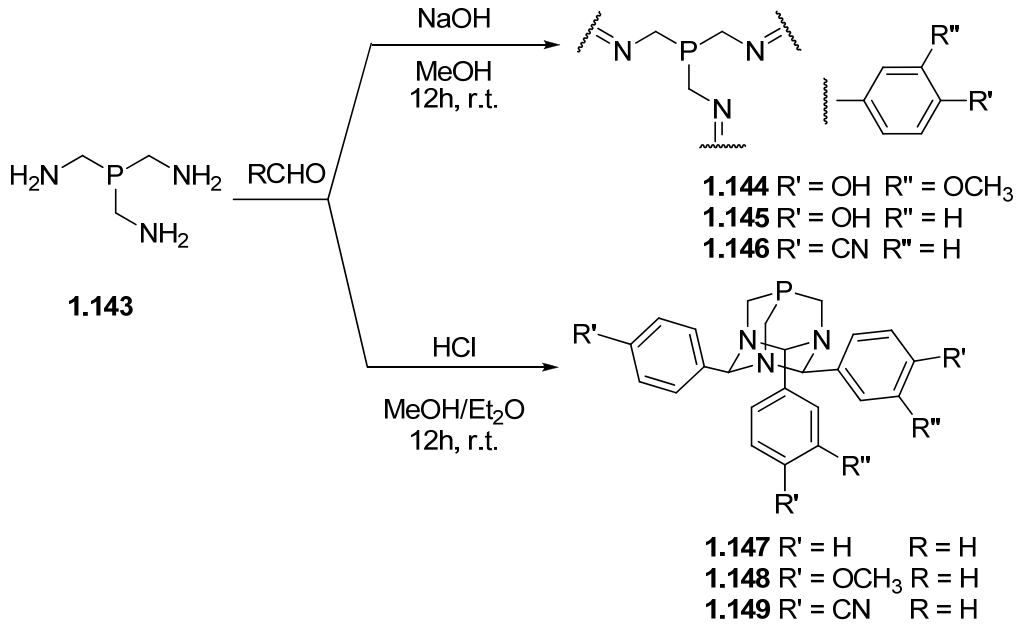

Scheme 1.17 Synthesis of aminomethylphosphines **1.144** – **1.149**.

Recently, Johnson's research group developed trisaminomethylphosphine **1.151** *via* reaction of Boc–protected glycine with oxidised **1.143** (**1.150**) which is reduced using Hunig's base (DIPEA) (Eqn. 1.8).[78] In contrast to the previous PCN synthesis, the phosphine precursor already contains an amino group instead of OH, *i.e.* in hydroxymethylphosphines, so the reaction performed is not a Mannich condensation as previously described. Phosphine **1.143** was synthesised to investigate its capabilities as a tripodal ditopic receptor since it presents H–bond donors (NH) and a phosphine oxide to

potential guests. In fact, **1.151** exhibits great affinity for halides in the presence of Li^+ but not with Na^+. This seems to be related with the "bowl–shaped" cavity with an endohedral P=O displayed by **1.151** in the solid state. This conformation shows that this receptor is able to adopt a geometry with a Lewis basic phosphine oxide to create a ditopic binding pocket capable of binding ion pairs.

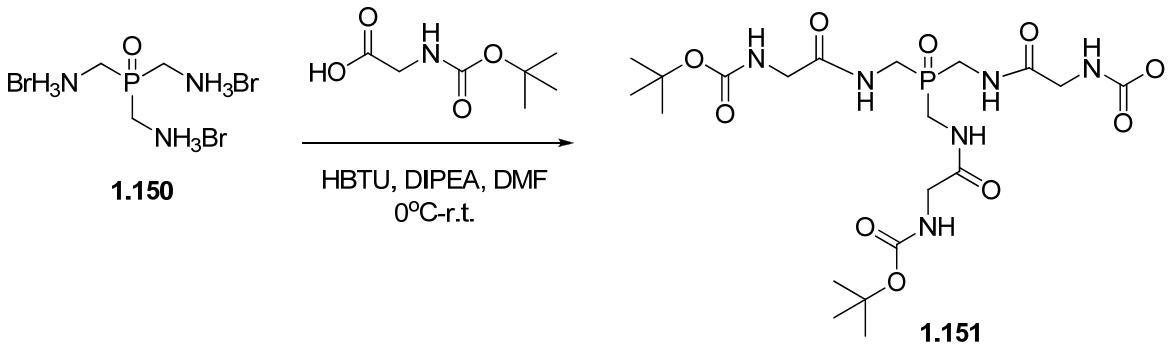

Equation 1.8

Johnson and co–workers prepared ligand precursors **1.152** – **1.154** using THP with the appropriate aniline, as shown in eqn. 1.9.[2,4,5,44] The reaction was solvent free for **1.152** and **1.153** but it was necessary to add C_7H_8 to synthesised **1.154**. Once the reaction was completed, water was removed under vacuum for the solvent–free procedures and using a Dean–Stark apparatus for **1.154**. These three ligands were analytically pure so they were used in subsequent reactions without further purification. The $^{31}P\{^1H\}$ NMR showed a singlet at δP –32.1, –29.6 and –32.6 ppm (C_6D_6) for **1.152** to **1.154**, respectively. The slight difference between **1.153** with respect to **1.152** and **1.154** indicates that two *meta* Me substituents on the aniline affects the phosphorus chemical shift in relation to the unsubstituted or *meta* CF_3 substituted aniline.

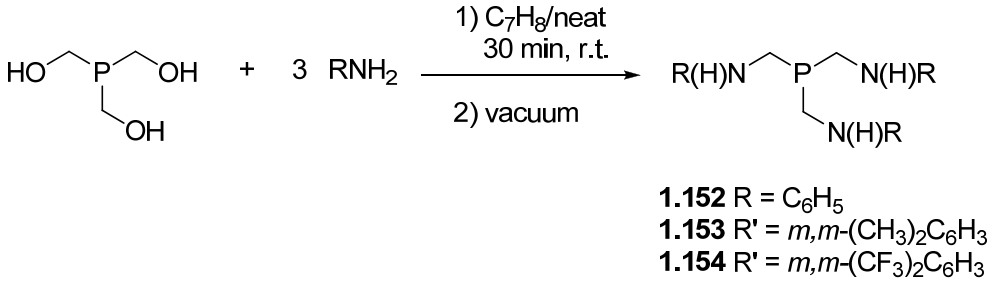

Equation 1.9

Suitable crystals for X–ray single crystal diffraction were grown over several days for ligand **1.154** by slow evaporation in C_7H_8, the same solvent employed for its synthesis.

The structure does not display C_{3v} symmetry because it suffers from disorder of one of the ligand arms and rotational disorder of a majority of the CF_3 substituents. The C–P–C angles are in the range of 99.38(15) – 100.59(16)^o which is much smaller than the tetrahedral angle of 109.5^o.

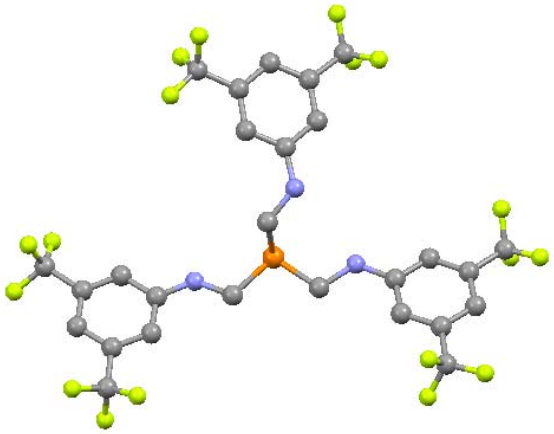

Figure 1.7 X–ray structure of known compound **1.154**.

The binding modes of these three trisaminomethylphosphine ligands were widely explored by coordination to both early and late transition metals to prepare heterobimetallic and polynuclear complexes (Sch. 1.18).[2,4,5,44] The reactions of **1.152** – **1.154** with $Ti\{N(CH_3)_2\}_4$ or $Ta\{N(CH_2CH_3)_2\}_3[N\{C(CH_3)_3\}]$ in C_7H_8 afforded the titanium complexes **1.155** – **1.157** and the tantalum compounds **1.158** – **1.160** where three nitrogens bind to the metal centre as illustrated in Scheme 1.18.[2,44] Likewise, treatment of **1.153** and **1.154** with $Zr\{N(CH_2CH_3)_2\}_4$ in C_7H_8 gave complexes **1.161** and **1.162**. Due to the ring strain, the phosphine lone pair cannot chelate and is available to bind a second metal. Hence, complexes **1.155** – **1.160** were reacted with Rh(I) and Ni(0) precursors to obtain the heterometallic rhodium complexes **1.163** – **1.168** and nickel compounds **1.169** and **1.170**. Compounds **1.163** – **1.168**, were synthesised as *trans*–Rh(I) complexes with the metal centre between two phosphorus donor atoms. In addition to the $^{31}P\{^1H\}$ NMR spectroscopy [average δP 23.0 ppm ($^1J_{PRh}$ = 118 Hz) for **1.163** – **1.165** and δP –32.0 ppm ($^1J_{PRh}$ = 138 Hz) for **1.166** – **1.168**], the adduct of **1.153** was characterised by X–ray crystallography supporting the structure of **1.167** depicted in Scheme 1.18. The nickel complex **1.169** was obtained by reacting ligand **1.153** with an excess of $Ni(CO)_4$ however, it is not stable at r.t. and in solution undergoes ligand redistribution over the course of 48 h to form **1.170** (Sch. 1.18). It is noteworthy the reaction of aryloxyligand (OR' in Sch. 1.18)

with two equivs. of **1.152** in C_7H_8 at r.t. yields the binuclear complex **1.171** where OR' acts a bridging ligand.

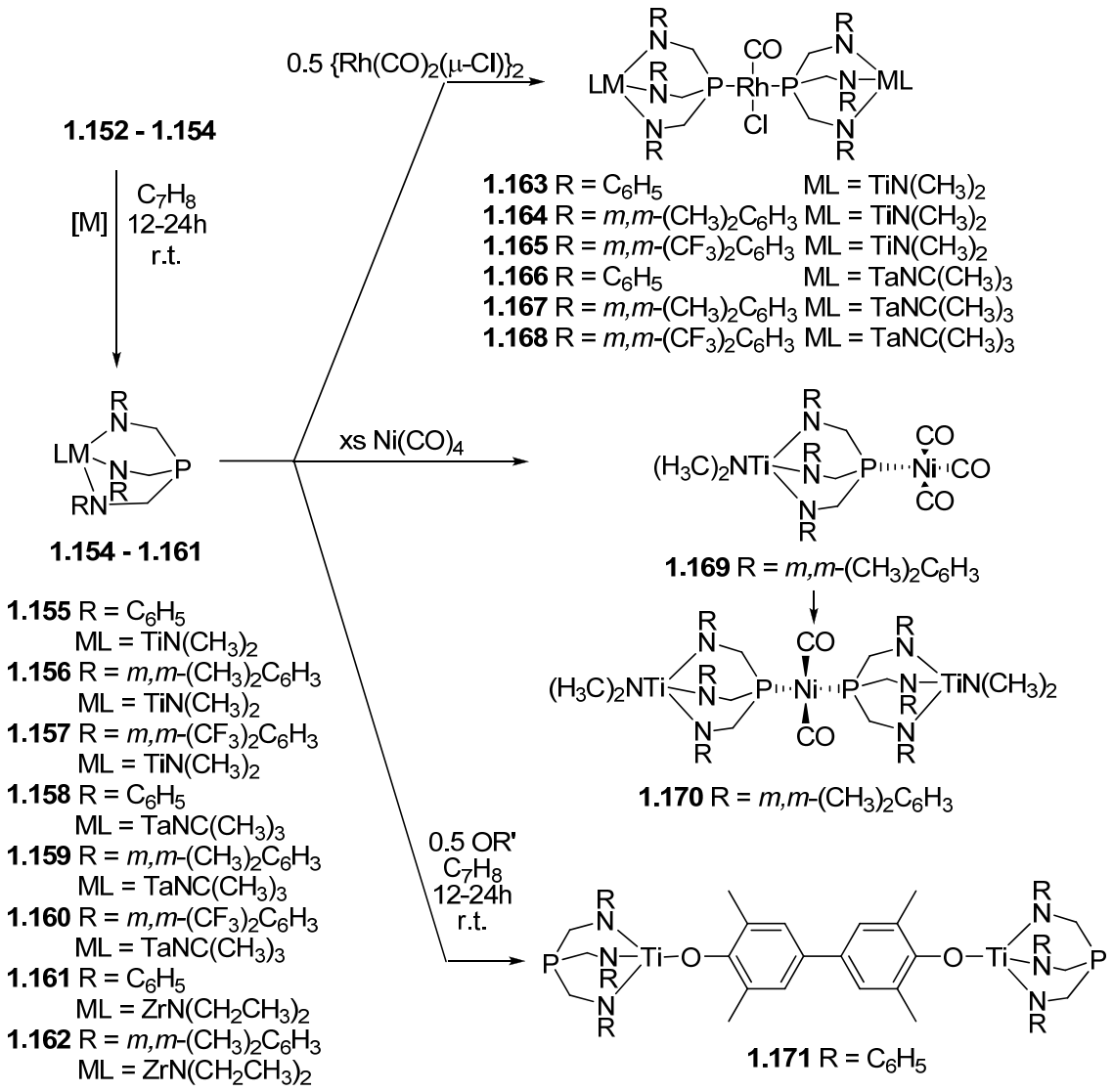

Scheme 1.18 Coordination chemistry of **1.152** – **1.154** with Rh(I), Ni(0) and Ti(IV).

A completely different coordination chemistry was observed for **1.152** – **1.154** once treated with $Al(CH_3)_3$ and selenium (Sch. 1.19).[4] Reaction of ligands **1.152** – **1.154** with two equiv. of $Al(CH_3)_3$ afford the dinuclear aluminium complexes **1.172** – **1.174** prior to yielding the Lewis acid–base adducts **1.175** – **1.176** by adding an excess of $Al(CH_3)_3$. Reactions of **1.152** – **1.154** with selenium produces triaminophosphine selenides **1.177** – **1.179** and subsequent addition of four equivs. of $Al(CH_3)_3$ generates the triangular trinuclear aluminium complexes **1.180** – **1.182**. These adducts incorporate a fourth aluminium centre, bound to phosphorus, by reaction of one equiv. of $Al(CH_3)_3$ to afford **1.183** – **1.184** which can also be obtained by adding an excess of $Al(CH_3)_3$ to **1.152** or

1.153 respectively. X–ray diffraction studies were especially useful to determine the nature of the P–Se and Se–Al bond lengths. Comparisons between **1.181** and **1.183** (and **1.182** and **1.184**) shows that P–Se bond is slightly shorter in **1.182** and **1.184** than in **1.181** and **1.183** respectively by approx. 0.04 Å and consequently Se–Al distance is a bit longer (approx. 0.02 Å). These bond lengths can be interpreted in terms of a contribution from resonance structures where the phosphorus atom is formally an anionic P(V) donor, however the structure is still best described by the resonance structure containing a P–Se single bond in Scheme 1.18.

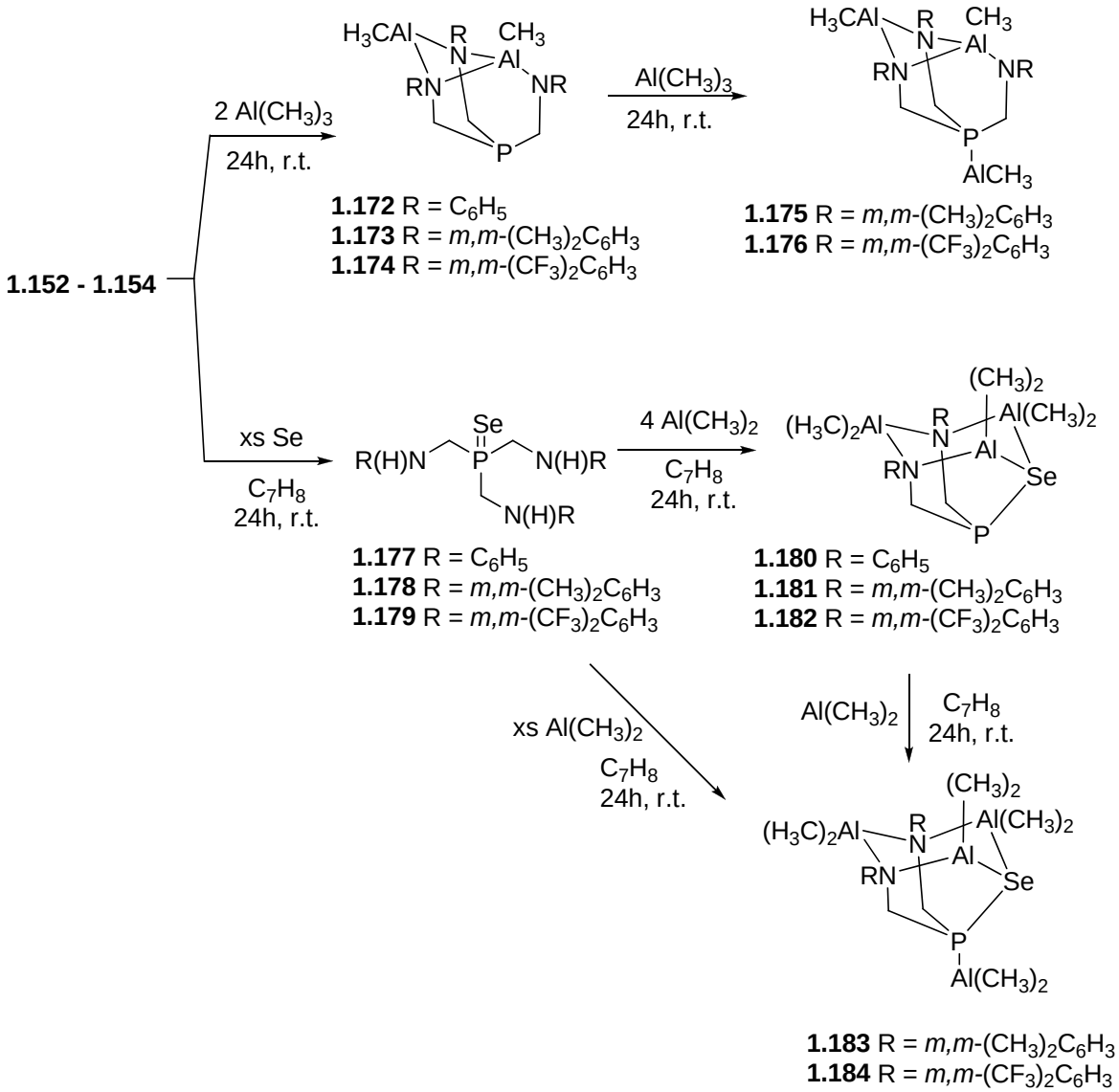

Scheme 1.19 Coordination chemistry of **1.152** – **1.154** with Al(III) and grey Se.

The examples discussed so far demonstrate the wide spectrum of structures adopted by **1.152** – **1.154** with different metal and non–metal nuclei. With the purpose to explore further the binding modes of those ligands, they were treated with Li(I), Mn(II) and Mg(II)

to afford complexes **1.185** – **1.191** as depicted in Scheme 1.20.[5,44] It is noticeable that the different arrangements observed for Li(I) complexes **1.185** and **1.186** in comparison with Mg(II) (**1.187** – **1.189**) and Mn(II) (**1.190** and **1.191**). Whereas **1.185** and **1.186** adopted the same conformation as Al(II) complexes **1.180** – **1.184** (Sch. 1.19), **1.187** – **1.191** readily assemble trinuclear clusters with divalent magnesium and manganese. In both sets of complexes the ^{31}P chemical shift of one of the phosphorus does not differ significantly from the ligand precursors (*ca*. δP –22.0 ppm) however the second phosphorus present in **1.187** – **1.191** is found to be further upfield (*ca.* δP –33.0 ppm). In addition, for **1.187** – **1.191**, ^{31}P–^{31}P coupling was observed with a value of 15 Hz. X–ray diffraction studies in conjunction with density functional theory demonstrate that the coupling observed between phosphorus nuclei occurs *via* a combined through–space, through–bond pathway.

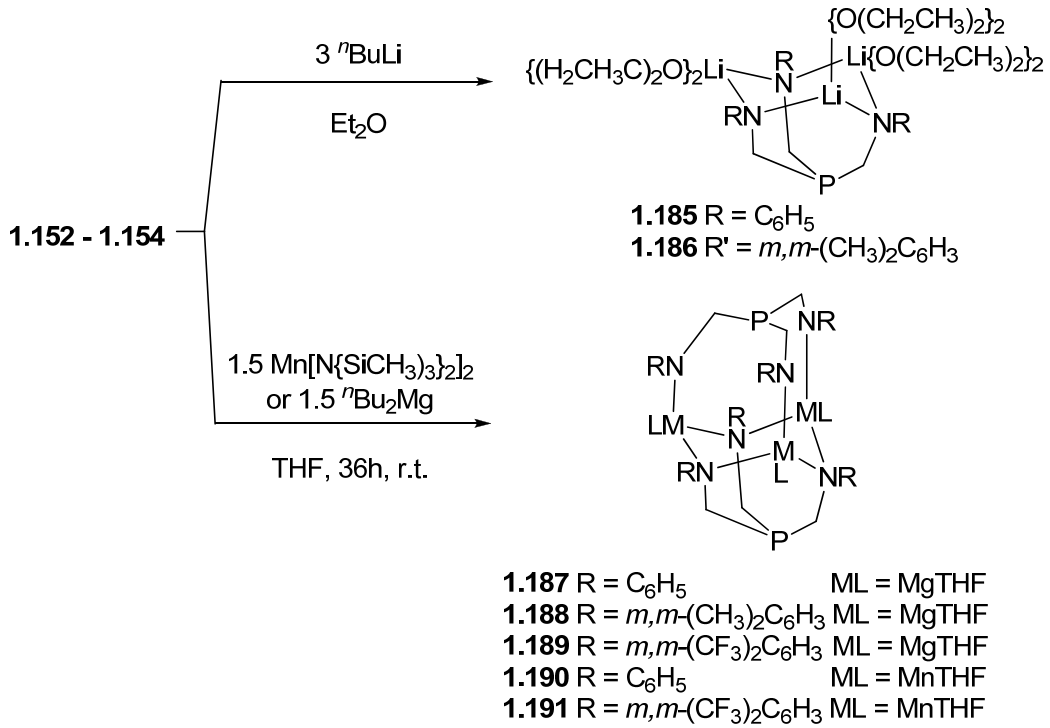

Scheme 1.20 Coordination chemistry of **1.152** – **1.154** with Li(I), Mg(II) and Mn(II).

With the aim to incorporate additional donors to the parent ligand **1.152**, new ligand **1.192** was synthesised by treatment of THP with three equivs. of methyl anthranilate (Sch.1.21).[3] This ligand has a carbonyl substituent in the *ortho* position which in conjunction with the nitrogen donors, bind the lanthanide metal centre in a N,O–chelate fashion to generate **1.193**. The non–bonded phosphorus reacts with the Co(II) precursor as depicted in Scheme 1.21 to form the heterobimetallic complex **1.194**. The ^{31}P{^{1}H} NMR of **1.193** showed a

^{31}P–^{89}Y coupling which is suggested to be mediated by a through–space interaction as was previously observed for **1.187** – **1.191**.

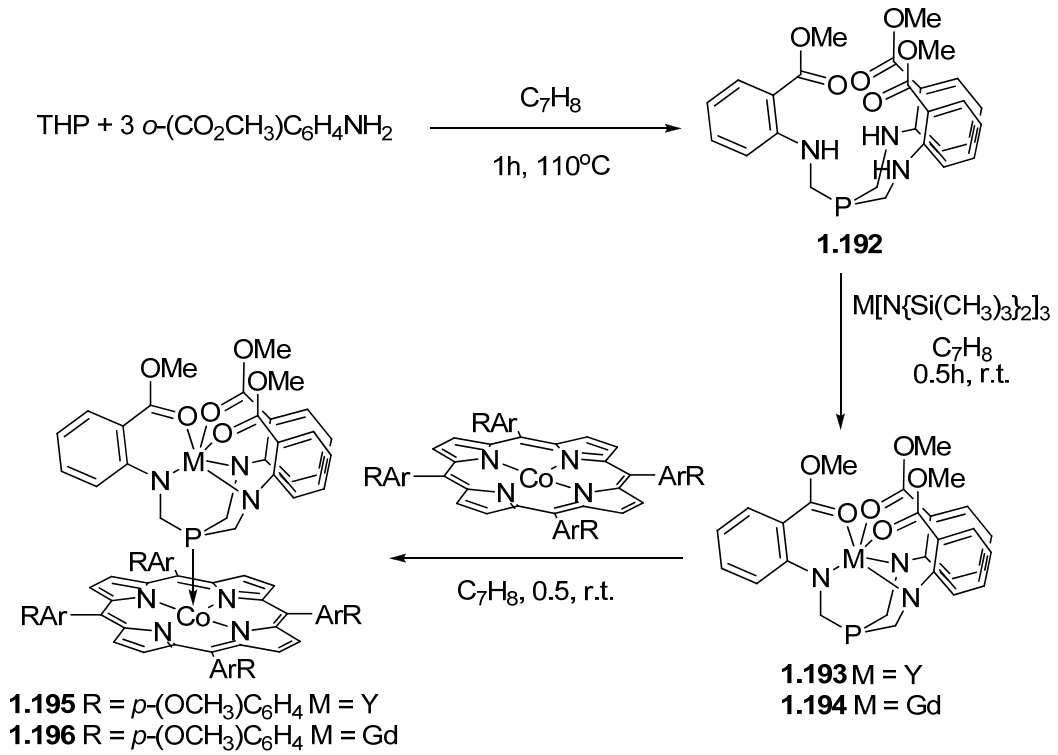

Scheme 1.21 Synthesis and coordination chemistry of ligand **1.192** with Y(III), Gd(III). and Co(II)

In summary, ligands **1.152** – **1.154** and **1.192** are prone to chelate all of nitrogen donor atoms to a single metal with Ti(IV) (**1.155** – **1.157**), Ta(II) (**1.158** – **1.160**), Zr(II) (**1.161** – **1.162**), Y(III) (**1.193**) and Gd(III) (**1.194**). However **1.152** – **1.154** show propensity to form triangular trinuclear structures towards Al(III) (**1.180** – **1.184**), Li(I) (**1.185** and **1.186**), Mg(II) (**1.187** – **1.189**) and Mn(II) (**1.190** and **1.191**).

Three different trisaminomethylphosphines **1.197** – **1.200** were synthesised by Starosta's research group. They were obtained by reaction of $P(CH_2OH)_3$, obtained *in situ* from THPC after addition of a base (Et_3N/KOH), with *N*–methylpiperazine, *N*–ethylpiperazine, morpholine and thiomorpholine in water respectively (Eqn. 1.10).[29,45] Despite this method overcoming the isolation issues of THP, it is noteworthy that the purification step is more complicated. The chemical structures were determined in solution by means of NMR spectroscopy and in the solid state using X–ray crystallography. The $^{31}P\{^1H\}$ NMR displayed a singlet at approx. δP –61.1 ppm which indicates that the chemical shift is independent of the aliphatic ring. Likewise, the ^1H NMR exhibited all of six PC*H*$_2$N

protons having a similar chemical shift at *ca*. 2.6 ppm and a $^{2}J_{HP}$ coupling constant to the phosphorus of approx. 3 Hz. The crystal structure showed a distorted C_{2v} for **1.197** and **1.198** and C_3 for **1.199** with P–C and C–P–C bond lengths and angles in the range of 1.850(2) Å and 97.81(7) – 99.5(1)^{o} respectively. Overall, ligands **1.197** – **1.200** are symmetric in solution and **1.199** in the solid state too.

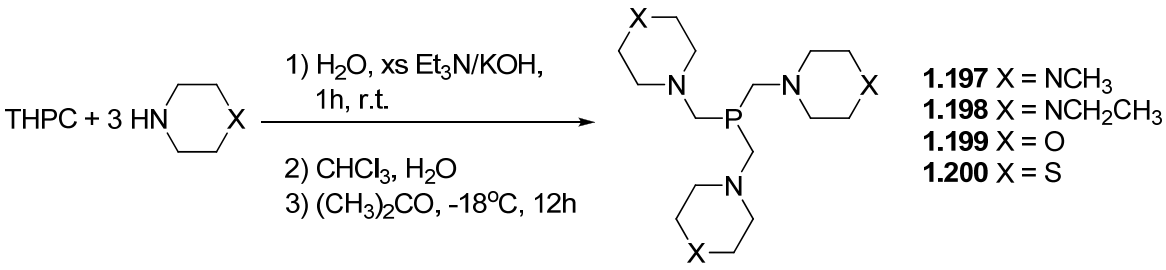

Equation 1.10

Reactions of **1.197** – **1.200** with CuI and bpy, bq, phen and 2,9–dimethyl–1,10–phenanthroline in 1:1:1 molar ratios gave complexes **1.201** – **1.211** (Eqn. 1.11).[29,45–47] The air stable and water soluble copper(I) complexes were synthesised to screen the luminescence properties as well as the antibacterial and antifungal activities indicating that **1.207** showed greater cytotoxic activity than its analogous **1.204**. For the luminescence studies, a set of pyridine derivatives were used because they have delocalisedd electrons. Equation 1.11 illustrates these diimine ligands which can be organised as bpy > bq > phen > dmp in terms of the non–fixed, fixed pyridine rings and fused aromatic rings close to the N donor atoms resulting in considerable steric hindrance. However, this sequence is not linear correlated with the phosphorus chemical shift. The spectra showed similar values (*ca*. δP –34 ppm) for complexes with bpy (**1.201** – **1.203**) and phen (**1.205** – **1.207**) substituents independently of the phosphine. Likewise, complexes with bq (**1.204**) and dmp (**1.208** – **1.211**) displayed one peak at approx. δP –28 ppm slightly downfield with respect to bpy and phen complexes. The single X–ray crystal structure of Cu(I) complexes exhibited a distorted tetrahedral geometry with respect to the metal centre and in particular for **1.208** and **1.209**, π–stacking interactions were observed between two molecules of **1.208** and **1.209**. This supramolecular packing plot is also present in **1.205** and **1.207** however the diimine dmp results in higher luminescence.

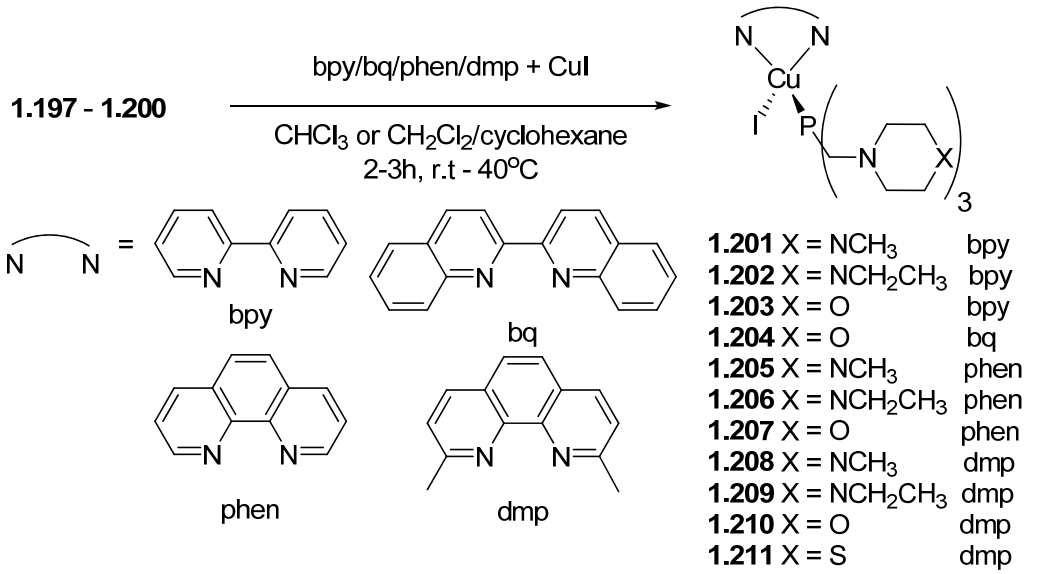

Equation 1.11

The coordination chemistry of **1.197** and **1.199** was also investigated to Pt(II) metal centre due to their potential as chemotherapeutic agents.[1] These two trisaminomethylphosphine ligands were treated with one equiv. of K_2PtCl_4 at r.t. and **1.212** and **1.213** were obtained (Eqn. 1.12). Both reactions afforded complexes with two phosphorus centres *trans* to each other as indicated by the $^{31}P\{^1H\}$ NMR [δP –12.3 ppm ($^1J_{PPt}$ = 2311 Hz) for **1.212** and δP –8.2 ppm ($^1J_{PPt}$ = 2320 Hz) for **1.213**] and further supported by X–ray crystallography (Fig. 1.8 a and b).

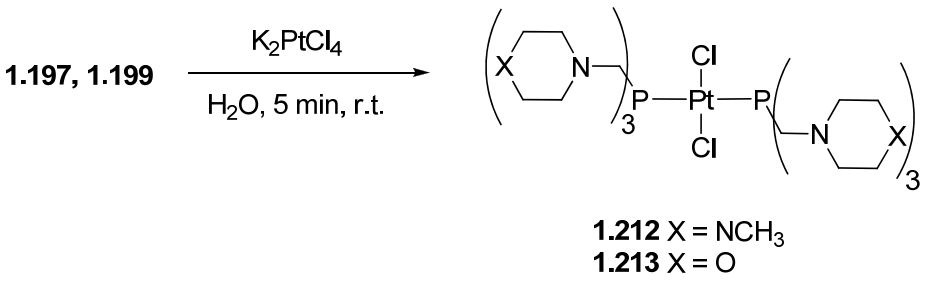

Equation 1.12

The *trans* geometry reflects the large steric demand of the phosphine ligands which prevents the formation of the *cis* isomer. In the solid state both molecules adopt C_i symmetry with the platinum atom lying on a crystallographic centre of symmetry. The P–Pt–Cl bond angles [92.18(18)° and 92.4(2)° for **1.212** and **1.213**] indicate a slightly distorted square–planar geometry with respect to the metal centre.

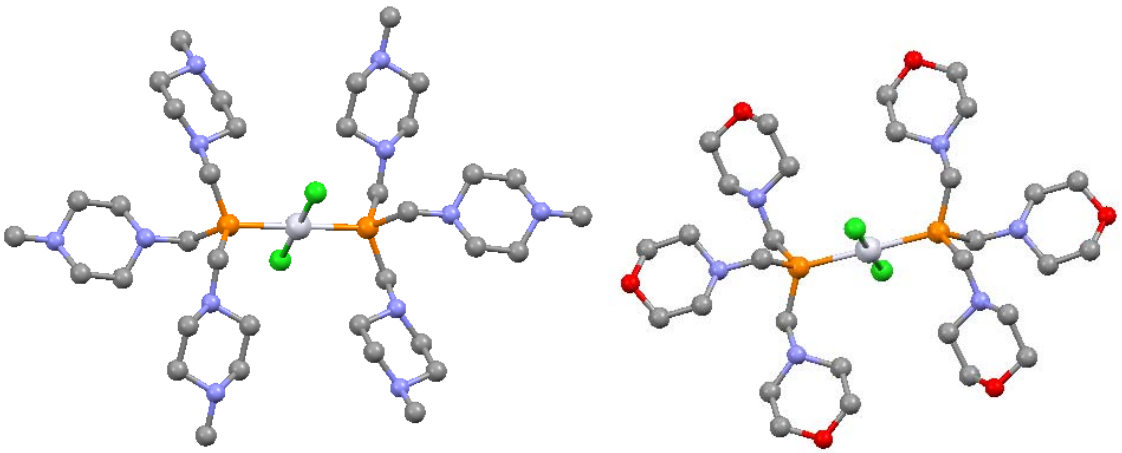

Figure 1.8 Reported X–ray structures of a) **1.212** and b) **1.213**.

Finally, the chalcogenide derivatives of **1.197** – **1.200** were formed by treatment of quantitative amounts of H_2O_2, resublimed sulphur or elemental selenium in H_2O or MeOH to afford **1.214** – **1.222** (Eqn. 1.13).[48] The $^{31}P\{^1H\}$ NMR of these chalcogenides show a singlet at significantly lower field than the parent ligands. For instance, chalcogenide derivatives from **1.197** moved from δP –60.8 [$(CH_3)_2O$] to 105.9 (E = O), 104.1 (E =S) and 88.3 ppm (E = Se). Once again, the phosphorus chemical shift is not determined by the substituent on the aliphatic ring but the chalcogenide. As their initial phosphines, morpholine derivatives **1.216**, **1.217** and **1.222** crystallise in different space groups. Binding the chalcogenide atom to the phosphine causes significant changes in the geometry around the phosphorus atom with respect to the free ligands **1.197** – **1.199**; the P–C distances are shortened and C–P–C bond angles enlarged.

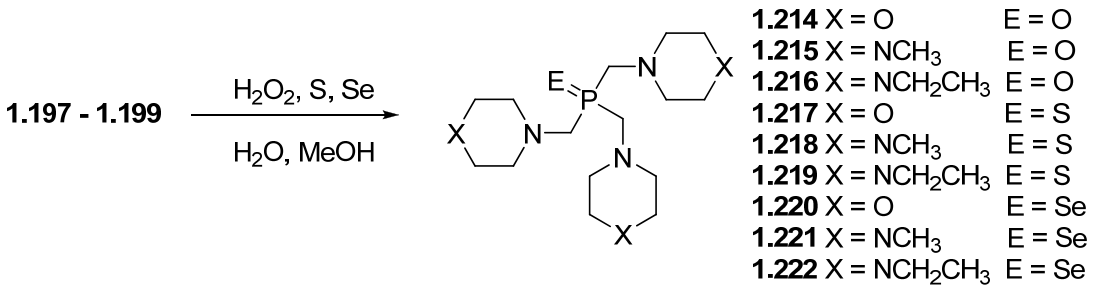

Equation 1.13

1.3.1.5 Tertiary bis(phosphinomethyl)amines $RN(CH_2PR'_2)_2$ (V)

PCN aminomethylphosphines containing a nitrogen atom with two methylenephosphines of the type $RN(CH_2PR'_2)_2$ (**V** in Sch. 1.4) have been widely studied in our research group[7,13,20] and by others.[49–54] Smith and co–workers synthesised a library of tertiary phosphines $RN(CH_2PPh_2)_2$ **1.96** (already discussed in Sch. 1.11), **1.223 – 1.237** by condensation of two equivs. of Ph_2PCH_2OH and the desired primary amine in MeOH (Eqn. 1.14).[13,20] As previously mentioned in Section 1.3.1.2 (Eqns. 1.2 and 1.3) these di–substituted phosphines were observed in small quantities in the $^{31}P\{^1H\}$ NMR. In the course of the synthesis of **1.96**, **1.223** – **1.237**, evidence of the analogous monophosphines were also detected in the phosphorus NMR spectra. This indicates that reactions initially proceed through a singly substituted intermediate prior to yielding **1.96**, **1.223** – **1.237**. In all cases, a single resonance was displayed in the $^{31}P\{^1H\}$ at *ca*. –27 ppm, which is 10 ppm upfield with respect to their monophosphine counterparts (*ca*. δP –18 ppm). The X–ray structure of **1.223** obtained showed an overall geometry of the ditertiary phosphine comprising two O–H···O hydrogen bonds between the two $–CO_2H$ moieties.

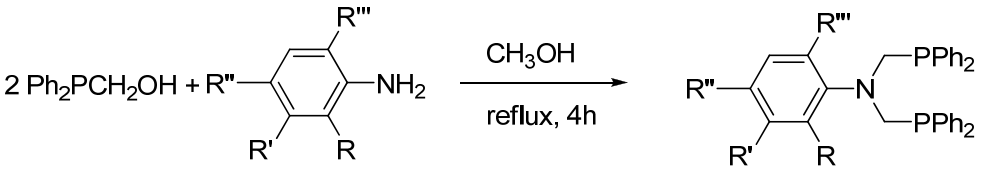

1.96	R = H	R' = H	R'' = H	R''' = H
1.223	R = H	R' = H	R'' = CO_2H	R''' = H
1.224	R = H	R' = H	R'' = CH_2CO_2H	R''' = H
1.225	R = H	R' = H	R'' = $COCH_3$	R''' = H
1.226	R = H	R' = H	R'' = Br	R''' = H
1.227	R = H	R' = H	R'' = I	R''' = H
1.228	R = H	R' = H	R'' = OH	R''' = H
1.229	R = H	R' = H	R'' = $CH=CH_2$	R''' = H
1.230	R = H	R' = H	R'' = OH	R''' = H
1.231	R = H	R' = H	R'' = CH_2OH	R''' = H
1.232	R = H	R' = OH	R'' = CO_2H	R''' = H
1.233	R = OH	R' = CO_2H	R'' = H	R''' = H
1.234	R = OH	R' = H	R'' = H	R''' = CO_2H
1.235	R = H	R' = H	R'' = OH	R''' = CO_2H
1.236	R = H	R' = CO_2H	R'' = H	R''' = OH
1.237	R = H	R' = CO_2H	R'' = OH	R''' = H

Equation 1.14

Coordination of these ligands to give the corresponding Au(I) complexes **1.238 – 1.244** was achieved using 2 equivs. of AuCl(tht) with a single equiv. of the appropriate ligand (Eqn. 1.15). Multiple supramolecular behaviour was displayed by **1.238** – **1.244** through a

combination of Au···Au, C–H···Au, C–H···Cl and O–H···O interactions. For instance, gold interactions were observed in **1.241** – **1.244** in conjunction with O–H···Cl interactions which were not exhibited by **1.238** (due to the lack of oxygen substituents) and only C–H···Cl were present. This study demonstrated that the regioselective incorporation of functional groups in the aniline group has a pronounced effect on the supramolecular structural motifs of complexes **1.238** – **1.245**. Hence, those structures with adjacent groups on the arene core (**1.241** and **1.242**) present dimeric species, however, for complexes **1.243** and **1.244** 1D chain structures were adopted.

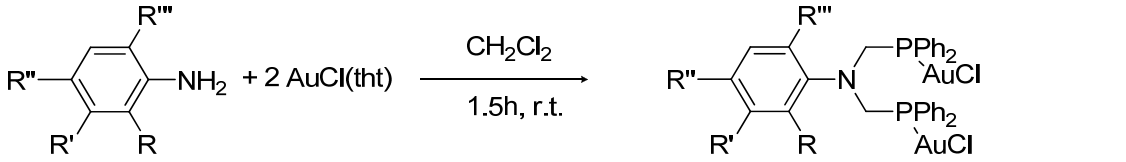

1.238 R = H R' = H R'' = H R''' = H
1.239 R = H R' = H R'' = CO_2H R''' = H
1.240 R = H R' = OH R'' = CO_2H R''' = H
1.241 R = OH R' = CO_2H R'' = H R''' = H
1.242 R = OH R' = H R'' = H R''' = CO_2H
1.243 R = H R' = H R'' = OH R''' = CO_2H
1.244 R = H R' = CO_2H R'' = H R''' = OH
1.245 R = H R' = CO_2H R'' = OH R''' = H

Equation 1.15

The majority of $RN(CH_2PR'_2)_2$ examples mentioned thus far possess phosphorus bearing equivalent groups, mainly Ph, with the exception of **1.99** – **1.102** in Scheme 1.12. However nonsymmetric aminophosphine $RN(CH_2PR'R'')_2$ ligands where R' differrs from the R'' group are less common.[7] To pursue this goal, Smith and co–workers developed novel bis(phosphinomethyl)amines **1.249** and **1.250** using two consecutive Mannich based condensation reactions as illustrated in Scheme 1.22.[7] Accordingly *in situ* generated $CgPCH_2OH$ was treated with an excess of the desired anilines in MeOH to afford **1.247** and **1.248** which was subsequently reacted with one equiv. of Ph_2PCH_2OH to produce non–symmetric phosphines **1.249** and **1.250**. The $^{31}P\{^1H\}$ NMR chemical shifts for the CgP– groups in **1.248** and **1.249** are quite similar to those for $CgPCH_2OH$ (δP –32.2, –32.4 and –31.2 ppm respectively), but differs significantly from CgPH (δP –49.7 ppm). However, they appeared upfield by *ca.* 10 ppm to δP –41.2 (**1.249**) and δP –42.0 ppm (**1.250**) as well as Ph_2P– groups (–27.4 and –27.6 ppm for **1.249** and **1.250**, respectively) comparing to $Ph_2P(CH_2)_3PPh_2$ [δP–17.3 ppm ($CDCl_3$)].

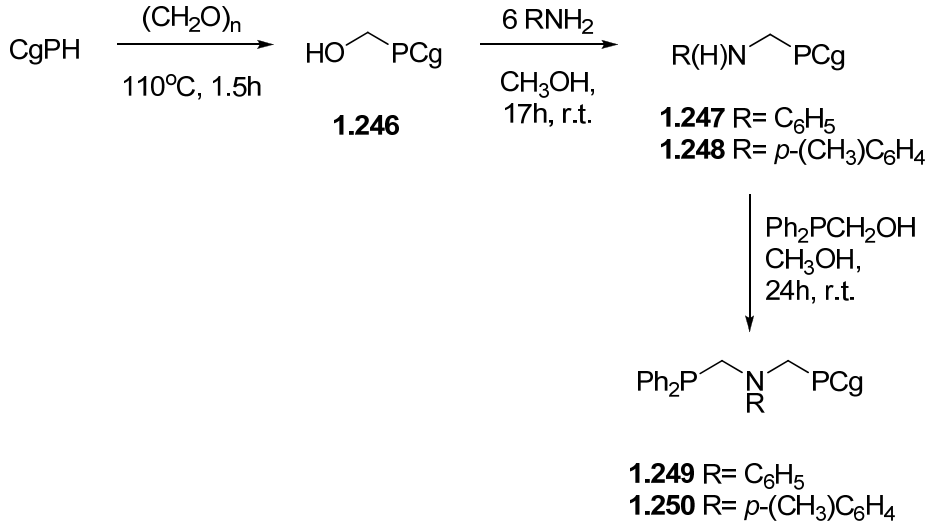

Scheme 1.22 Synthetic route for preparing nonsymmetric tertiary phosphines **1.249** and **1.250**.

Ligands **1.249** and **1.250** demonstrated diverse coordination modes towards a range of late transition metals (Fig. 1.9). For example, *P,P*–chelating mode to a single metal centre was observed for platinum and palladium complexes **1.251** – **1.254**. The $^{31}P\{^{1}H\}$ spectra of these new species showed two doublets due to the two different phosphorus environments with a phosphorus coupling constant $^{4}J_{PP}$, of between 8 and 19 Hz. In addition, platinum complexes **1.251** and **1.252** displayed platinum satellites with an approximate value of $^{1}J_{PPh_2Pt}$ 3231 and $^{1}J_{PCgPt}$ 3489 Hz. These measurements indicated a *cis* arrangement with respect to the platinum centre and by analogy to the palladium too. The structures of **1.251** and **1.253** were further supported by X–ray crystallographic studies revealing a six–membered M–P–C–N–C–P ring with square–planar coordination environment around the platinum. An alternative binding mode was observed for complexes **1.255** and **2.256** where ligands displayed *P*–monodentate coordination towards ruthenium and iridium metal centres. Finally, P,P–bridging coordination between similar metal centres was exhibited by **1.257**, and between disparate metal nuclei by **1.258** and **1.259**. The latter complexes were prepared by adding AuCl(tht) to **1.255** and **1.256**, respectively. These experiments demonstrate the difference in stereoelectronic properties between the two phosphorus centres in ligands **1.249** and **1.250** and how these differences can be used to synthesise mono or heterobimetallic complexes.

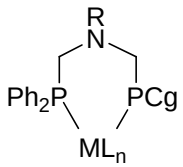

1.251 $ML_n = PtCl_2$, R = C_6H_5
1.252 $ML_n = PtCl_2$, R = *p*-$(CH_3)C_6H_4$
1.253 $ML_n = PdCl_2$, R = C_6H_5
1.254 $ML_n = PdCl_2$, R = *p*-$(CH_3)C_6H_4$

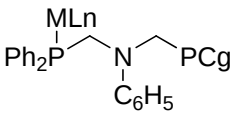

1.255 $ML_n = RuCl_2(\eta^6$-*p*-cymene)
1.256 $ML_n = IrCl_2(\eta^5$-Cp*)

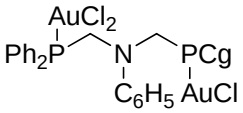

1.257

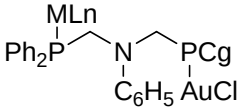

1.258 $ML_n = RuCl_2(\eta^6$-*p*-cymene)
1.259 $ML_n = IrCl_2(\eta^5$-Cp*)

Figure 1.9 Various coordination modes observed for nonsymmetric ligands **1.249** and **1.250**.

Ligands **1.249** and **1.250** are good examples of nonsymmetric PCNCP phosphines with non equivalent phosphorus substituents. However, these diphosphines, as well as **1.223** – **1.238**, only contain functionalised aromatic groups as nitrogen substituents. Serindag *et al*. synthesised a series of $RN(CH_2PR'_2)_2$ ligands with phenyl substituents on the phosphorus but alkyl and aryl groups on the nitrogen.[49,50] Hence, ligands **1.260** – **1.262** were obtained by reaction of the phosphonium salt $[Ph_2P(CH_2OH)_2]Cl$ with the desired primary amine in the presence of Et_3N as a base (Sch. 1.23). The phosphorus chemical shift were in the range of δP –26.4 to –27.5 ppm which does not significantly differ from the Ph_2P– chemical shifts observed in **1.223** – **1.237**, **1.249** and **1.250**. The coordination chemistry of ligands **1.260** – **1.262** was investigated by reaction with $PdCl_2(COD)$ in CH_2Cl_2 and $NiCl_2{\cdot}6H_2O$ in EtOH to yield palladium complexes **1.263** – **1.265** and nickel compounds **1.666** and **1.667** (Sch. 1.27). Complexes **1.260** – **1.262** were applied to the Heck reaction of aryl halides with methyl acrylate and to the hydrogenation of styrene to ethylbenze. It was concluded that **1.263** and **1.264** have shown higher turnover numbers than **1.265** for the Heck reaction and **1.263** showed higher catalytic activities than **1.264** throughout the hydrogenation of styrene to ethylbenzene.

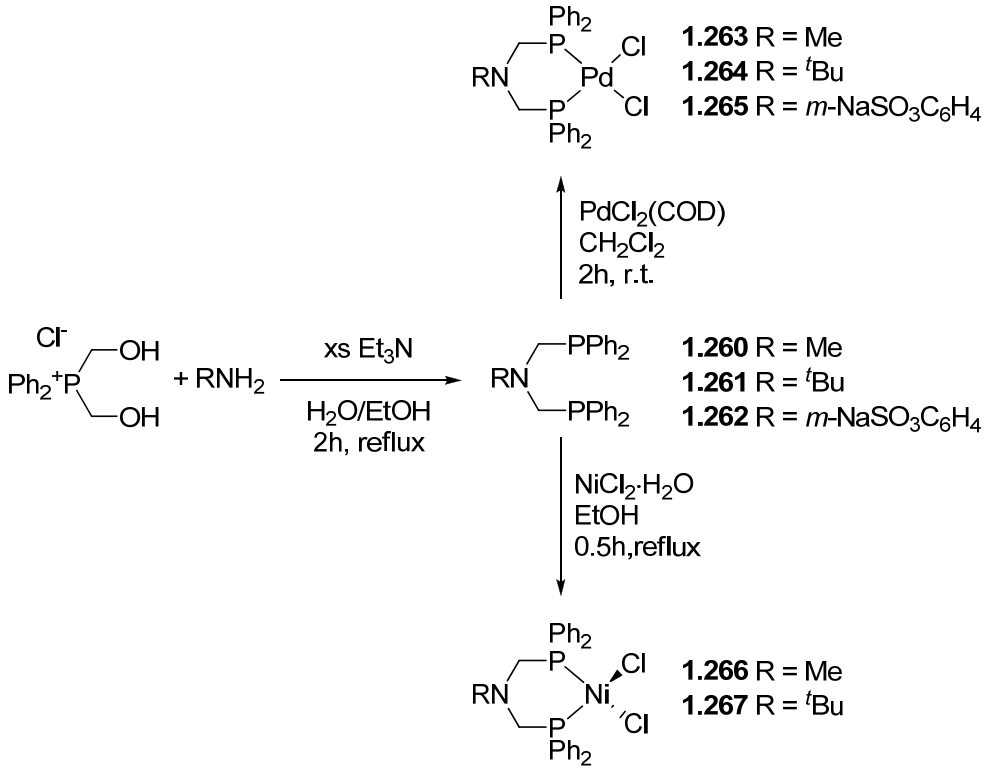

Scheme 1.23 Synthesis and coordination chemistry of bis(phosphinomethyl)amines **1.260** – **1.262**.

Klemps *et al.* prepared symmetric ditertiary aminomethylphosphines **1.268** – **1.274** bearing equal P–substitituents from primary functionalised aryl and alkyl amines (Sch. 1.24).[51] The $^{31}P\{^{1}H\}$ NMR of **1.268** and **1.269** and **1.270**, with Ph_2P– moiety, is in the same range as previous diphenylphophines [*ca*. δP –26 ppm (C_6D_6)] but this value differs considerably for those of **1.271** – **1.273**, with Cy_2P–, at *ca*. δP –15 ppm and for **1.274**, with ^{n}BuP–, at *ca*. δP –48 ppm. These ligands were reacted with one equiv. of $CrCl_3(THF)_3$ to rapidly yield complexes **1.275** – **1.281** which could not be characterised by NMR spectroscopy due to the strong paramagnetic nature of the octahedral d^3 Cr(III) centre. Despite this, the structure of **1.278** was determined by single X–ray crystallography where ligand **1.271** chelates to the metal centre and the overall geometry around chromium was found to be octahedral. Interestingly, the PCNCP ligand behaves as a bidentate ligand and the central nitrogen donor atom does not participate in the coordination as indicated by the very long Cr–N distance of 4.017(1) Å. The chromium complexes were evaluated for the activity in selective oligomerisation of ethylene trimerisation. The catalytic activity was found to be highly dependent upon the steric bulk of the phosphorus bound groups and to a lesser extend the group attached to the nitrogen. Therefore, the most selective and activated

catalysts were **1.277 – 1.279** which contain the bulky cyclohexyl groups attached to the phosphine.

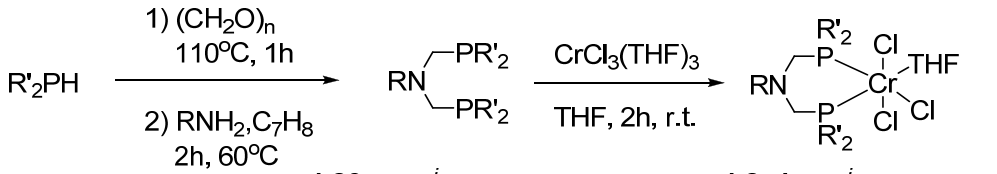

1.267 R = ^{i}Pr R' = Ph
1.268 R = ^{t}Bu R' = Ph
1.269 R = Ph R' = Ph
1.270 R = ^{i}Pr R' = Cy
1.271 R = ^{t}Bu R' = Cy
1.272 R = Ph R' = Cy
1.273 R = ^{i}Pr R' = ^{n}Bu

1.274 R = ^{i}Pr R' = Ph
1.275 R = ^{t}Bu R' = Ph
1.276 R = Ph R' = Ph
1.277 R = ^{i}Pr R' = Cy
1.278 R = ^{t}Bu R' = Cy
1.279 R = Ph R' = Cy
1.280 R = ^{i}Pr R' = ^{n}Bu

Scheme 1.24 Synthesis and coordination chemistry of ligands **1.267** – **1.273** with Cr(III).

Recently, Mock and co–workers synthesised ferrous dinitrogen complexes **1.285** – **1.288** containing a diphosphine ligand with a pendant amine (Sch. 1.25).[52] Complexes **1.285** – **1.288** were obtained via abstraction of the halide from the parent hydrido–halide **1.281** – **1.282** and dihalide **1.283** – **1.284** complexes. These Fe(II/III) complexes possess two phosphines with a phosphorus from each phosphine *trans* to each other and two halide or hydrido–halide ligands in *trans* disposition. The addition of acids to **1.285** – **1.288** results in protonation at the pendent amine of the diphosphine ligand rather than at the dinitrogen ligand (complexes **1.289** and **1.290**). This demonstrates that the basicity of the pendant amine was greater than that on the dinitrogen ligand. The protonated amine did not transfer the proton to the N_2 as desired, concluding that a less basic amine should be employed to achieve the catalytic reduction of N_2 to NH_3. Furthermore, ferrous complexes **1.289** – **1.290** were found to be more stable than **1.285** – **1.286** however, they can be regenerated by addition of a base.

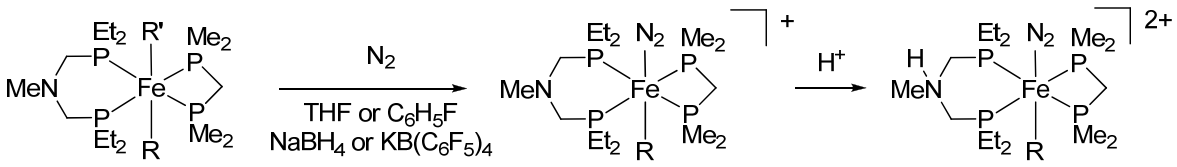

1.281 R = H R' = Cl
1.282 R = H R' = Br
1.283 R = Cl R' = Cl
1.284 R = Br R' = Br

1.285 R = H
1.286 R = H
1.287 R = Cl
1.288 R = Br

1.289 R = H
1.290 R = H

Scheme 1.25 Protonation of ferrous dinitrogen complexes containing a diphosphine ligand with a pendant amine.

Gade and co–workers utilised secondary $^{i}Pr_2PH$ as a phosphorus source to afford secondary amines **1.291** – **1.295** and a tertiary amine **1.301** (Sch. 1.26).[53,54] Bis(diisopropylphosphinomethyl)amines **1.291** – **1.295** were obtained from $[^{i}Pr_2P(CH_2OH)_2]Cl$ and 0.5 equiv. of various primary amines in MeOH in the presence of Et_3N as an auxiliary base. In contrast, tripodal (aminnomethyl)amine **1.301** was produced in a single step from $^{i}Pr_2PH$ with 0.3 equivs. of NH_4Cl. These experiments highlight the synthesis of an easily extendable library of ligands with tuneable steric and electronic backbone properties. In order to gain an insight into the coordination chemistry of ligands **1.291** – **1.295** and **1.301** and the influence of their backbone substituents, the corresponding nickel(II) (**1.296** – **1.300**) and Ru(II) (**1.302**) complexes were synthesised (Sch. 1.26).[54] At r.t., both ^{1}H and $^{31}P\{^{1}H\}$ NMR spectra of complexes **1.296** – **1.300** exhibit significant line broadening so the solution structure was elucidated by elemental analysis and mass spectroscopy in addition to X–ray crystallography for **1.296** – **1.298.** The solid state shows that the Ni(II) is in a slightly distorted square–planar geometry with a bite angle (P–Ni–P) of approx. 96.85(3)°. Ru(II) complex **1.302** was obtained upon stirring a C_7H_8 solution of **1.301** and $\{Ru(COD)(\eta^3–CH_2CMeCH_2)_2\}$ at 90°C for 14 h. The $^{31}P\{^{1}H\}$ NMR spectrum displayed one singlet at δP 26.2 ppm, indicating the formation of a symmetric species this was further corroborated by X–ray diffraction (C_{3v}–symmetry).

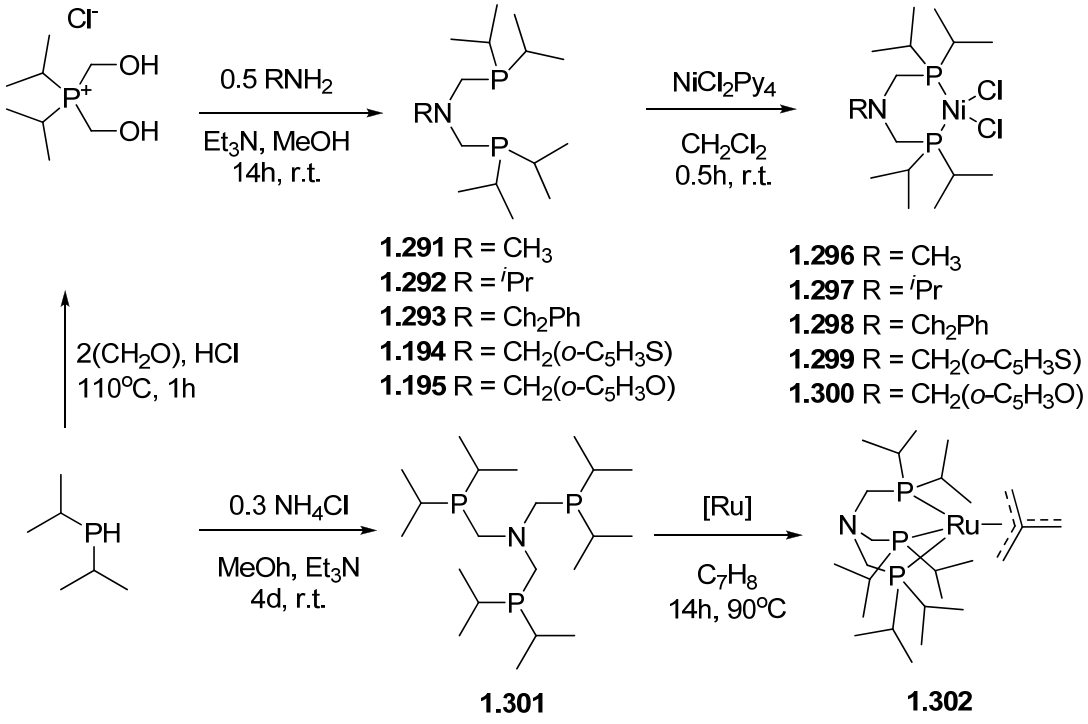

Scheme 1.26 Synthesis and coordination chemistry of ligands **1.291** – **1.295**.

1.3.2 Synthesis, structure, reactivity and applications of cyclic aminomethylphosphines

1.3.2.1 Tertiary 1,3,5–diazaphosphorinanes $R'P\{CH_2N(R)CH_2N(R)CH_2\}$ (VI)

Cyclic monophosphines $R'P\{CH_2N(R)CH_2N(R)CH_2\}$ (R = alkyl or aryl groups) (**VI** in Sch. 1.4), known as 1,3,5–diazaphosphorinanes, contain a six–membered P–C–N–C–N–C ring. These aminomethylphosphines are synthesised mainly by three pathways, as illustrated in Scheme 1.27.[17,18,55–58] In route **A**, one equiv. of a primary phosphine reacts with three equivs. of $(CH_2O)_n$ and two equivs. of a primary amine in a one–pot reaction. Employing the same reagents and stoichiometry, $R'P\{CH_2N(R)CH_2N(R)CH_2\}$ can also be obtained in two steps (route **B**) *via* $R'P(CH_2OH)_2$. The latter procedure has the advantage of that bis(hydroxymethyl)phosphine can be used as precursor of other aminomethylphosphines such as 1,5–diaza–3,7–diphosphacyclooctanes see Scheme 1.7. However, depending on the phosphorus substituents, this synthesis is avoided due to the undesired monosubstituted secondary phosphines $R'P(H)(CH_2OH)$ being obtained as by–products. The third route (**C**) affords $R'P\{CH_2N(R)CH_2N(R)CH_2\}$ by reduction of the appropriate phosphonium salt with Et_3N previously synthesised by reacting THPC with primary amines in a 1:4 molar ratio (see Sch. 1.5 for further explanation). This method permits functionalisation of the R' substituent on the phosphorus as well as it obviates the use of noxious primary phosphines.

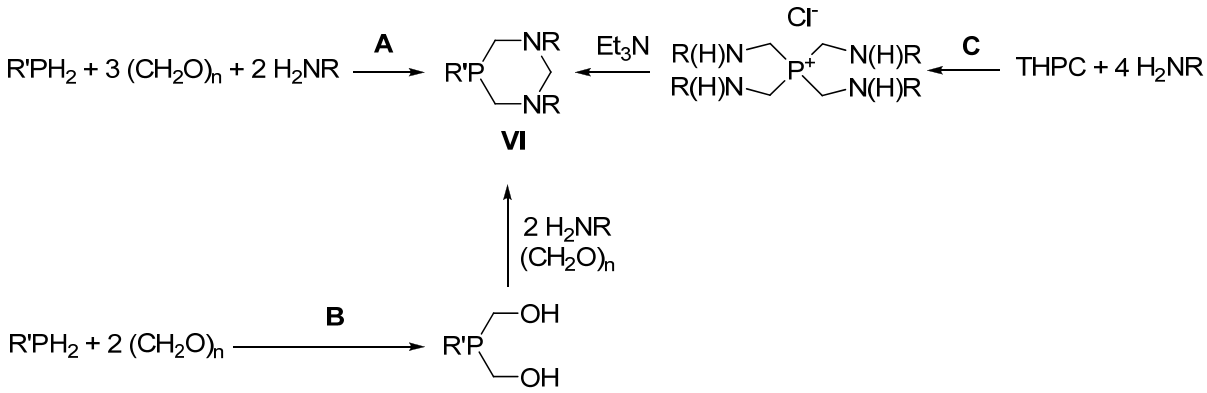

Scheme 1.27 General synthetic routes to achieve 1,3,5–diazaphosphorinanes (**VI**).

In the same manner as phosphines (Fig. 1.10 a and b), 1,3,5–diazaphosphines present a chair shape conformation with at least two possible conformers which is dependant upon if

the substituents are in an axial or equatorial position (Fig. 1.10 c and d respectively). In solution, phosphorinane conformers are in equilibrium showing a single peak in the $^{31}P\{^{1}H\}$ NMR at r.t., but if the temperature is lower than the coalescence temperature, the spectra displays two peaks for R–axial (upfield) and R–equatorial.[79] Likewise, generally, 1,3,5–diazaphosphorinanes exit in solution preferentially in a chair conformation with the triequatorial orientation of the substituents at the heteroatoms.[59]

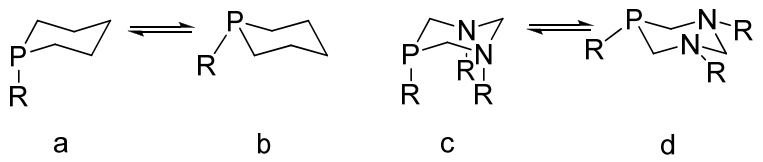

Figure 1.10 a) and b) phosphorinanes and c) and d) diazaphosphorinanes in conformational equilibrium.

However, recently studies from Smith *et al*., reported the crystallographic structure of the 1,3,5–diazaphosphorinane salt **1.304** with a CNC pendant arm on the phosphorus in the axial position and the N–phenyl derivatives equatorial to the plane of the chair (Fig. 1.11).[18] This is favoured because the two hydrogens bound to the nitrogen atom in PNC, are bonded to the nitrogens in an adamantane cage shape.

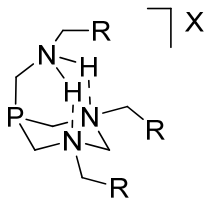

1.303 R = $CH_2C_6H_5$ X = Cl
1.304 R = CH_2-*p*-FC_6H_4 X = Cl
1.305 R = $CH_2C_6H_5$ X = SbF_6
1.306 R = $CH_2C_6H_5$ X = PF_6
1.307 R = CH_2-*p*-FC_6H_4 X = SbF_6
1.308 R = CH_2-*p*-FC_6H_4 X = PF_6

Figure 1.11 Cyclic aminomethylphosphine salts displaying a pseudoadamantane cage due to intramolecular H–bonding.

The phosphorus chemical shifts of **1.303** – **1.308** are *ca*. δP –55 ppm (DMSO), which is in agreement with diazaphosphorinanes documented by Dubois and co–workers[58] [**1.309** and **1.310** *ca*. δP –60 ppm (MeOD)] and by Karasik *et al*[56] (**1.311** – **1.317**) [δP –54.4 to –68.7 ppm (MeOD) and δP –61.0 to –77.1 (D_2O)] (Fig. 1.12). Compounds **1.309** and **1.310** were obtained *via* route **B** (Sch. 1.27) from bis(hydroxymethyl)phosphine in water whereas compounds **1.311** – **1.317** were obtained by route **A** (Sch. 1.27) in MeOH. The ^{1}H NMR showed ABX (X = P) and $(AB)_2X$ spin systems corresponding to the NCH_2N and PCH_2N protons respectively, between 4.21 and 2.65 ppm. The ABX splitting pattern for NCH_2N

protons (equatorial H_e and axial H_a) is characteristic of 1,3,5–diazaphosphorinanes. The chemical shifts of the NCH_2N hydrogen atoms did not change for the low field doublet, but it moved for the high field to further upfield (δP = −0.56 ppm) on changing of the solvent from water to methanol. This high field signal was interpreted as a doublet of doublets with approximate $^2J_{HH}$ = 11.4 Hz and $^4J_{HeP}$ = 1.5 Hz and it was assigned to the equatorial proton in a chair conformation according to the W rule. The axial proton appeared as a doublet due to the coupling to the vicinal equatorial proton and no coupling to the axial PCH_2N protons (PCH_aN). The second spin system [$(AB)_2X$] corresponds to PCH_2N protons (equatorial H_e and axial H_a) with stereospecific geminal ^1H–^{31}P coupling constant. Both H_a and H_e protons were registered as doublets of doublets, but their coupling constants ($^2J_{PH}$) were noticeably different. $^2J_{HeP}$ and $^2J_{HeHa}$ were approximately equal (*ca*. 13 Hz), but the $^2J_{HaP}$ values were smaller than 6.1 Hz, ranging from 4.0 – 6.1 Hz.

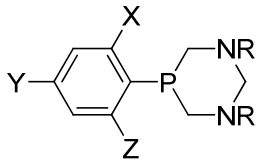

1.309 R = CH_2CO_2H X = Y = Z = H
1.310 R = $CH_2CO_2CH_2CH_3$ X = Y = Z = H
1.311 R = CH_2CO_2Na X = Y = Z = H
1.312 R = CH_2CO_2K X = Y = Z = H
1.313 R = CH_2CO_2Na X = Y = Z = Me
1.314 R = CH_2CO_2K X = Y = Z = Me
1.315 R = CH_2CO_2Na X = Y = Z = ^{i}Pr
1.316 R = CH_2CO_2K X = Y = Z = ^{i}Pr
1.317 R = C(H)(Ph)CO_2K X = Y = Z = H

Figure 1.12 1,3,5–diazaphosphorinanes with *P*–phenyl derivatives.

Karasik's research group expanded the family of 1,3,5–diazaphosphorinanes by reacting bis(hydroxymethyl)(ferrocenylmethyl)phosphine (**1.318**) with two equivs. of glycine in the presence of two equivs. of KOH and one equiv. of $(CH_2O)_n$ to give **1.319** (Eqn. 1.16).[55] The $^{31}P\{^1H\}$ NMR spectrum in NaOD:D_2O (1:10) showed a broad singlet at *ca*. δP –55 ppm along with one sharp peak at δP 35.6 ppm, which was assumed to correspond to the oxidised phosphine of **1.318** and thus indicated that **1.318** was not stable in aqueous solutions.

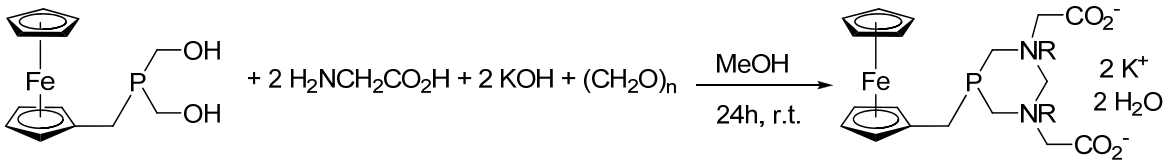

1.318 **1.319**

Equation 1.16

The coordination chemistry of 1,3,5–diazaphosphorinanes towards late transition metals was widely studied with catalytic and structural purposes. For example, Jain and co–workers synthesised complexes **1.320** and **1.321** from compounds **1.309** and **1.310**, respectively, and Pt(II) metal centre with the aim of assessing its potential use in homogeneous catalysis (Eqn. 1.17).[58] The $^{31}P\{^{1}H\}$ spectra consist of resonances in a ratio of 1:4:1, arising from a mixture of Pt isotopes, one of which has a spin of ½. The $^{195}Pt–^{31}P$ coupling varied widely depending on the phosphine ligand ($^{1}J_{PPt}$ = 3930 Hz for **1.320** and 3438 Hz for **1.321**) assumed to be related to the increased distortion form square planar geometry in glycine complexes due to the intra–ligand hydrogen bonding interactions. Both complexes possess phosphine ligands in a *cis* arrangement which was further confirmed by the X–ray structure of **1.321**.

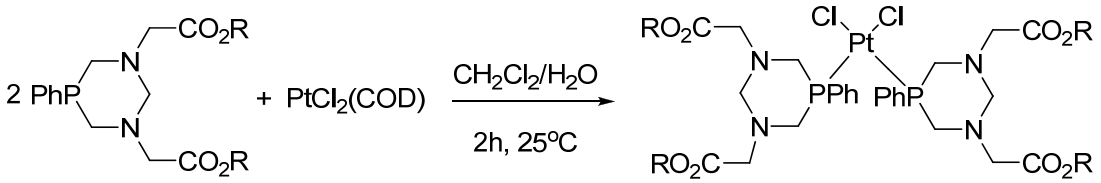

1.309 - 1.310

1.320 R = H
1.321 R = CH_2CH_3

Equation 1.17

In the synthesis of **1.320** the $^{31}P\{^{1}H\}$ NMR spectra showed a minor broad band at δP –50 ppm and the $^{195}Pt\{^{1}H\}$ NMR exhibited a pentuplet at δPt 4914 ppm ($^{1}J_{PPt}$ = 3934 Hz) assigned to the dicationic tetraphosphine Pt(II) complex **1.322** which was observed as a byproduct (Eqn. 1.18). However, compound **1.322** was not isolated by reacting $PtCl_2$(COD) with four equivs. of **1.309**. Likewise, complex **1.323** was observed as a byproduct in the synthesis of **1.321** but not isolated. In addition, no evidence was found for the monocationic $\{ClPt(\mathbf{1.309})_3\}^+$ or $\{PtCl(\mathbf{1.310})_3\}^+$ complexes.

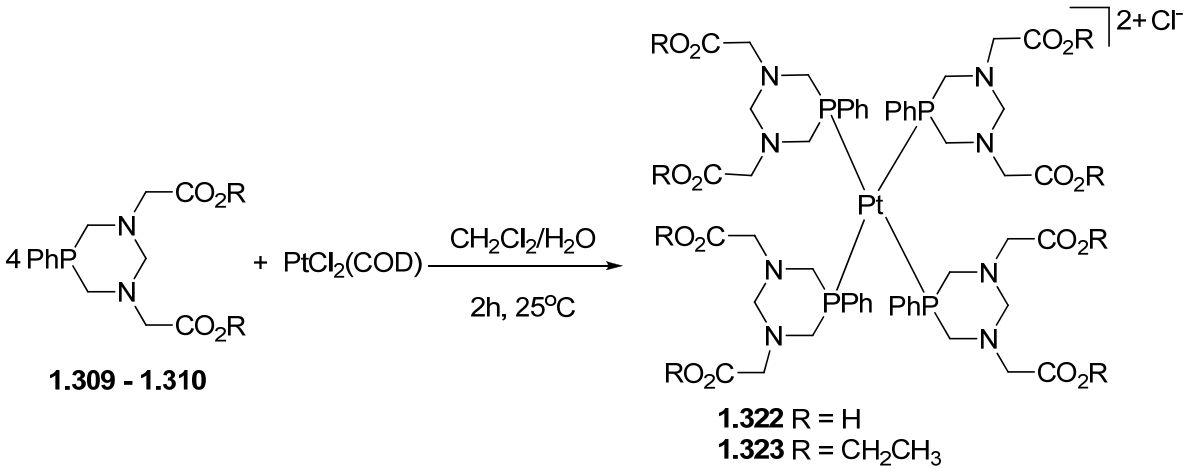

Equation 1.18

Karasik and co–workers did observe a five–coordinate platinum species **1.328a** – **1.331a** in the presence of additional ligands **1.324** – **1.327** to the *cis* platinum complexes **1.332a** – **1.335a** (Sch. 1.28). Complexes **1.328** – **1.331** were intermediates in *cis–trans* isomerisation reactions of square–planar complexes **1.332a** – **1.335a** and **1.332b** – **1.335b**, respectively. The $^{31}P\{^{1}H\}$ NMR of **1.329** showed the signals of three–atom phosphorus coordinated with one metal atom, two phosphorus *cis* to each other ($^{1}J_{PPt}$ = 3366 Hz) and one in *trans* disposition ($^{1}J_{PPt}$ = 2350 Hz), however, this data was not sufficient to elucidate whether **1.329** is a neutral five–coordinated platinum complex (**1.329a**) or ionic square–planar complex (**1.329b**) and by extension this applied to **1.328**, **1.330** and **1.331**.

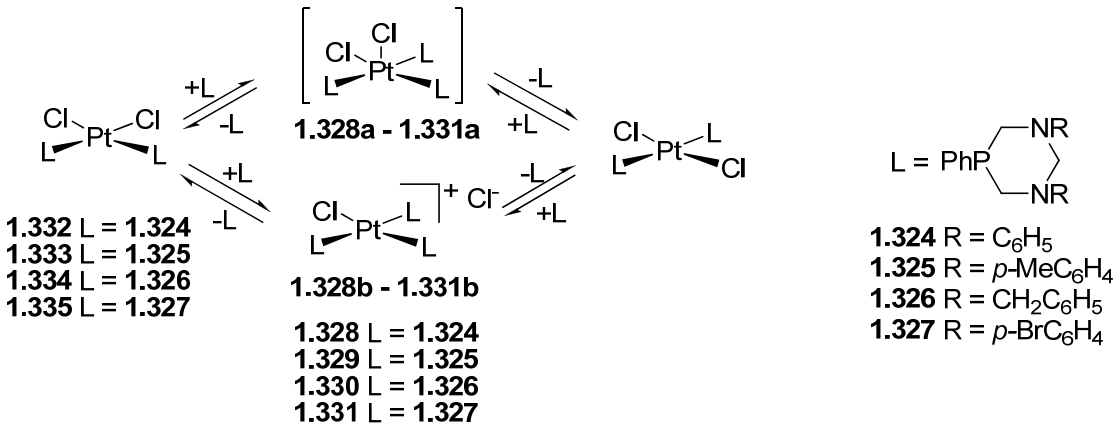

Scheme 1.28 *Cis–trans* isomerisation reaction of dichloroplatinum complexes derivatives of ligands **1.324** – **1.327**.

Dichloroplatinum complex **1.332** was taken as a representative example of 1,3,5–diazaphosphorinanes for isomerism studies using crystallographic and spectroscopic methods.[59] This complex revealed spatial isomerism due to axial or equatorial orientation of the M–P bond relative to the ligand plane (Sch. 1.29) and rotation around the M–P bond (Sch. 1.29).

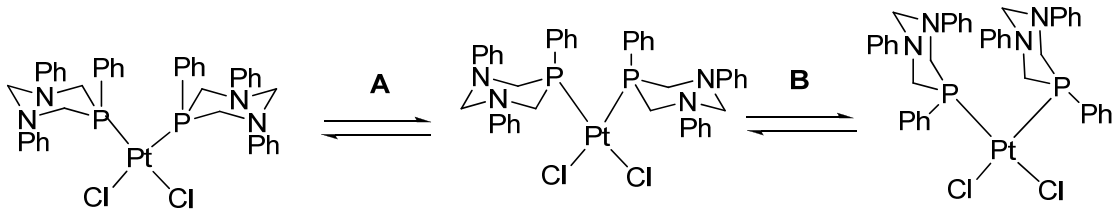

Scheme 1.29 Isomerism of 1,3,5–diazaphosphorinane **1.324**.

Mono and binuclear complexes were obtained by reaction of carbonyl VI transition metal group complexes and ligands **1.324** – **1.327** (Sch. 1.30).[60,61] Mono W(0) complexes **1.336** – **1.339** and Mo(0) **1.340** – **1.343** once reacted with a second metal centre, gave homobitungsten complexes **1.344** – **1.347** and homobimolybdenum complexes **1.348** – **1.351**, respectively. Then, a speculative reorganisation of the phosphorus and nitrogen centres of ligands was proposed to afford **1.352** – **1.355** (M = W) and **1.356** – **1.359** mononuclear tungsten **1.360** – **1.363** and molybdenum **1.364** – **1.367** complexes were formed, by loosing of weakly bonded metal–containing fragment in **1.352** – **1.359**. M–N cleavage in **1.352** – **1.359** was stipulated to occur due to the unfavourable location of the phosphorus atom lone pair.

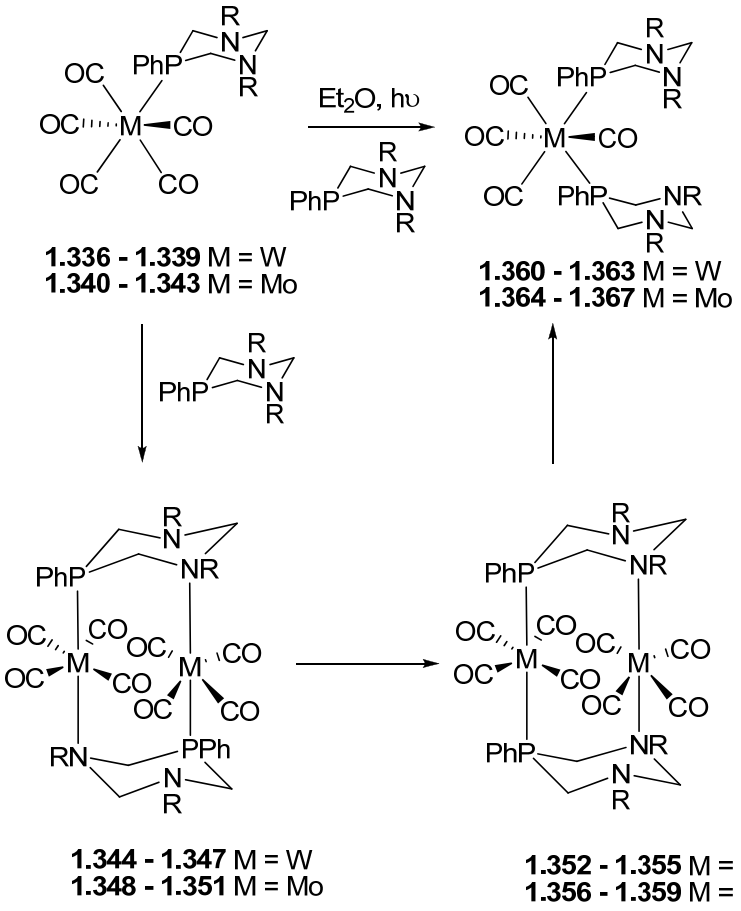

Scheme 1.30 Coordination chemistry of ligands **1.324** – **1.327** with W(0) and Mo(0).

Smith's group studied Ru(II) and Rh(III) complexes of the PTA analogous ligand **1.305** by X–ray diffraction and concluded that **1.305** acted as a *P*–monodentate ligand to maintain the pseudoadamantage cage in piano–stool complexes **1.368** and **1.369** (Fig. 1.13).[18] The coordination chemical shifts for both complexes (**1.368** ΔδP 62 ppm and **1.369** ΔδP 60 ppm) were closely related with $RuCl_2(\eta^6$–*p*–cymene)(PTA) (ΔδP 60 ppm) and $RhCl_2(\eta^5$–Cp*)(PTA) (ΔδP 65 ppm) suggesting comparable stereoelectronic properties. In addition, X–ray structures showed that M–P and M–Cl (M = Ru or Rh) parameters for **1.368** and **1.369** are similar to those of analogous complexes with PTA.

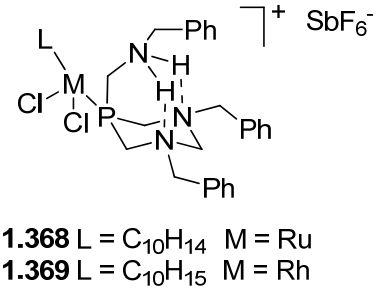

Figure 1.13 Complexes **1.368** and **1.369** showing a pseudoadamantane cage shape.

1.3.2.2 Tertiary 1,5–diaza–3,7–diphosphacyclooctane $R'PCH_2N(R)CH_2P(R')CH_2N(R)CH_2PR'$ (VII)

The synthetic and coordination chemistry of cyclic aminomethylphosphines with two phosphorus centres in the ring have recently been widely studied due to their structural properties and applications in electro catalysis (**VII** in Sch. 1.4).[8,9,32,62–71] The most widely used procedure to achieve 1,5–diaza–3,7–diphosphacyclooctanes is by condensation of primary phosphines with primary amines ($R'PH_2$ and RNH_2, R and R' = aryl and alkyl groups) in the presence of $(CH_2O)_n$ in a one–pot reaction (Eqn. 1.19). An alternative and rarely used route is the alkylation of THP followed by the decomposition of the phosphonium salt with a strong base as previously described in Scheme 1.7. As seen in Equation 1.19, the development of 1,5–diaza–3,7–diphosphacyclooctanes was extremely fruitful, therefore the present section (1.3.2.2) will cover the chemistry in general terms rather than going into specific details each compound synthesised. Most of these ligands are air stable in the solid state and do not undergo decomposition in solution.

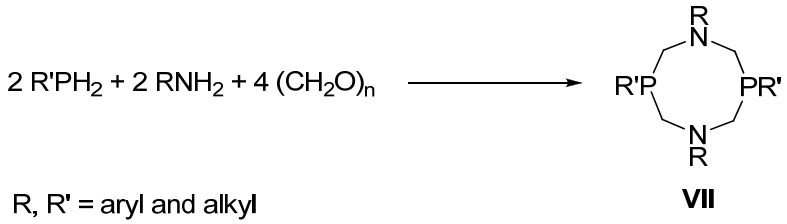

Equation 1.19

In the solid state, 1,5–diaza–3,7–diphosphacyclooctanes **VII** have similar chair–crown (CW) conformations and *syn*–positions of axial phosphorus lone pairs relative to each other as observed by X–ray crystallographic diffraction (Fig. 1.14 b). The pseudoaxial substituents on the nitrogen atoms are also oriented approximately in the same direction relative to the PNPN plane. In solution, 1D and 2D NMR experiments including variable–temperature spectra, the same CW conformations are predominant. However, for phosphines containing R = Bn and R' = Ment, the presence of a minor chair–boat (CB) conformer was observed at –50°C (Fig. 1.14 a and c). Thus, 1,5–diaza–3,7–diphosphacyclooctanes are well predisposed for metal chelation. These phosphines showed a singlet at approx. δP –50 ppm in their $^{31}P\{^1H\}$ NMR spectrum. The ^1H spectra showed the PCH_2N as a doublet of doublets due to the phosphorus coupling with equatorial protons downfield with respect to axial protons ΔδH 0.8 ppm ($^2J_{HH}$ = 15 Hz, $^2J_{HP}$ = 4.8–1.0 Hz).

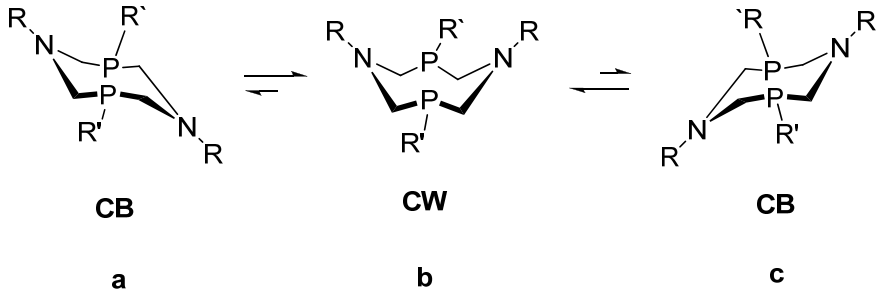

Figure 1.14 General 1,5–diaza–3,7–diphosphacyclooctanes a) in chair–boat b) chair–crown and c) chair–boat conformations.

Employing the same methodology as that in Equation 1.19, but using primary aromatic diamines (R = alkyl or aryl) instead, with spatially divided amine groups, several types of cage *P,N*–containing cyclophanes with two 1,5–diaza–3,7–diphosphacyclooctanes fragments were obtained (Fig. 1.15).[52,70,72] The X–ray structure showed both heterocycles in a CW conformation and for R = R' = Mes and X = S, a molecule of DMF was encapsulated in the hydrophobic cavity. This conformation was supported by $^{31}P\{^{1}H\}$ NMR which exhibited a singlet in the range of *ca*. –41 to –51 ppm in DMF. ^{1}H spectra showed the PCH_2N as doublets of doublets due to the phosphorus coupling with equatorial protons downfield with respect to axial protons [H_e 4.26 ppm ($^{2}J_{HH}$ = 15 Hz, $^{2}J_{HP}$ = 13.4 Hz and H_a 4.69 ppm ($^{2}J_{HH}$ = 15 Hz, $^{2}J_{HP}$ = 4.7 Hz)].

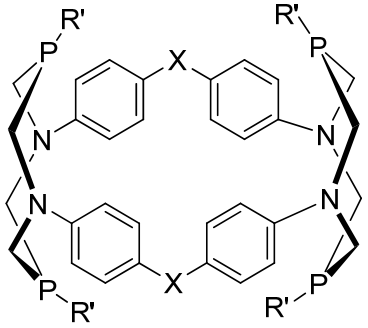

Figure 1.15 Self–assembly of macrocyclic aminomethylphosphine with two 1,5–diaza–3,7–diphosphacyclooctanes fragments.

The coordination chemistry of 1,5–diaza–3,7–diphosphacyclooctanes with soft metal centres has been widely developed.[98] Two different binding modes were observed for these ligands, depending on the metal centre and reaction conditions applied. 1,5–diaza–3,7–diphosphacyclooctanes acted as *P,P*–chelate ligands with platinum or nickel and only with

Pt(II) the *P*,*P*–bidentate mode was observed. For simplicity and relevance to the project here presented, Pt(II), Ni(II) and Fe(II) complexes will be described.

The interaction of ligands **VII** (Eqn. 1.19) (R = Ph, *o,o,p*-$Me_3C_6H_2$, *o,o,p*–$^{i}Pr_3C_6H_2$, CH_2Fc or Ment; R' = Ph, *p*–MeC_6H_4, Bn, CH(Me)Ph, *p*-$NaSO_3C_6H_4$ or *m,m*-$(CO_2H)_2C_6H_3$) with $PtCl_2(COD)$ in a stoichiometric 1:1 ratio in different solvents (from CH_2Cl_2 to DMF and water) gave a wide variety of monoligand neutral *cis*–*P*,*P*–chelate complexes with terminal M–Cl bonds labelled **D** in Scheme 1.31. Ligands with phenyl groups on phosphorus atoms can form two other types of platinum(II) complex. The interaction of **VII** (R' = Ph, *p*–MeC_6H_4 or Bn) with one equiv. of $PtCl_2(PhCN)_2$ in acetone led to binuclear complexes labelled **E** in Scheme 1.31, with two bridging ligands and a *trans*–configuration of platinum metal centres. In the cases of a metal:**VII** ratio of 1:2, unbulky ligands (R = Ph, R' = Ph, *p*–MeC_6H_4, Bn or CH(Me)Ph) readily form dicationic bis–ligand complexes **F** in Scheme 1.31. The formation of complexes **D** and **F** sometimes proceeded simultaneously which has subsequently complicated their separation.

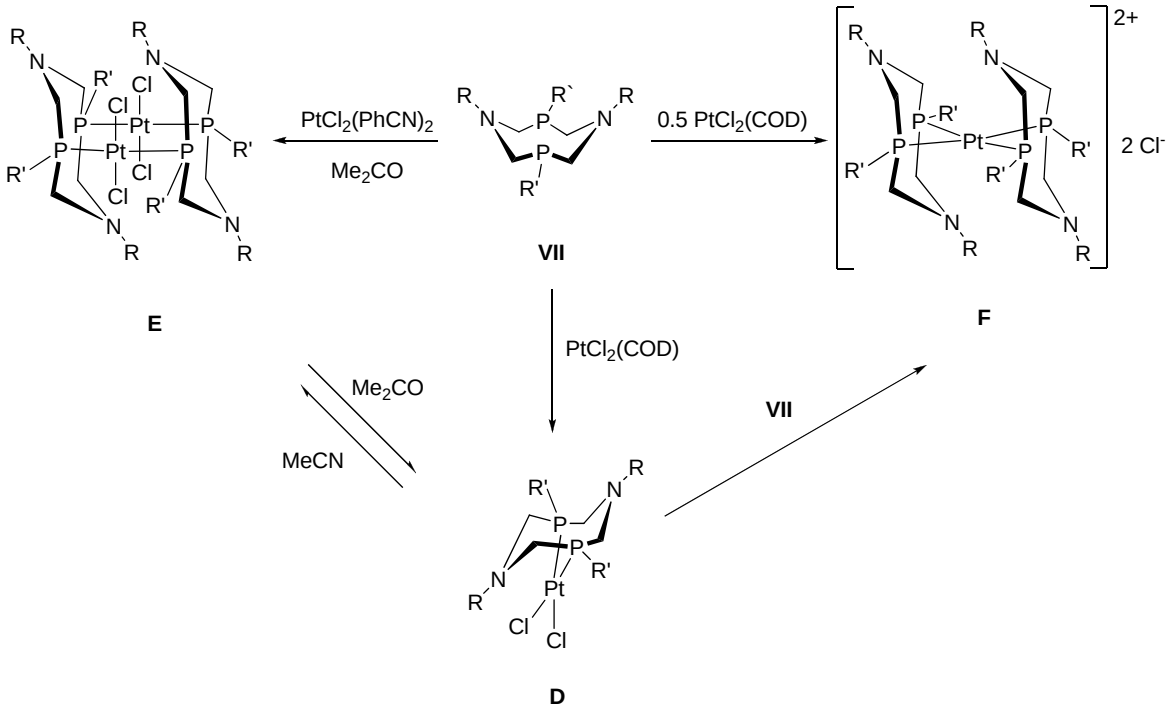

Scheme 1.31 Coordination chemistry of 1,5–diaza–3,7–diphosphacyclooctanes with Pt(II).

The structures of platinum complexes **D** (R = R' = Ph; R = Ph, *o,o,p*-$Me_3C_6H_2$; R' = *m,m*-$(CO_2H)_2C_6H_3$; R = Ment, R' = *p*-MeC_6H_4) were studied by X–ray crystallography, and they were found to be very similar. It has been reported that 1,5–eight–membered rings containing two donor atoms can adopt three conformations with respect to the metal: *endo*-

endo or CW, *endo-exo* or CB or *exo-exo* boat–boat (BB) (Figures 1.16 **G** – **I**, respectively).[80] Likewise, coordinated 1,5–diaza–3,7–diphosphacyclooctanes adopt similar conformations (Figures 1.16 **J** – **L**, respectively). The platinum centres are in slightly distorted *cis* square–planar environments with relatively small bite P–Pt–P angles (84 – 85°) and the ligands in all complexes have chair–boat (CB) conformations, so that one of the nitrogen atoms is located in close proximity of a metal centre (distances N···Pt approx. 3.2 Å). The configurations of the nitrogen atoms vary from trigonal–pyramidal to almost planar. Unlike complexes of the **D** structure, the platinum centre of cationic complexes with the structure **F** (R = Ph, R' = *p*-MeC_6H_4) was in a strongly distorted square–planar environment (the dihedral angle between two P–Pt–P planes was 24.3°). The bite P–Pt–P angles were even smaller (80.6°) than in monoligand complexes of the structure **D**.

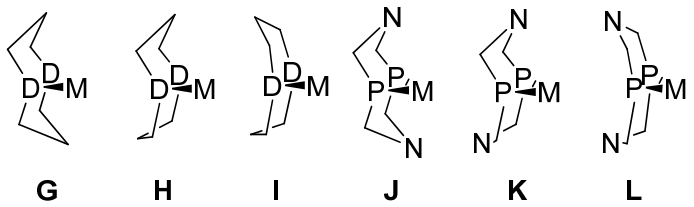

Figure 1.16 Eight–membered ligand ring chelating CW (**G** and **J**), CB (**H** and **K**) and BB (**I** and **L**) conformations. D is a donor atom such as phosphorus.

Complexes of nickel with **VII** (mainly unbulky P–substituents) are of great interest due to their applicability in electro catalysis for the H_2 production and oxidation.[8] Albeit, the most efficient alectrocatalysts use platinum for interconverion of electricity and hydrogen, it is an unabundant and expensive metal. Hence, current efforts are focused on alternative metals such as Ni or Fe. Two 1,5–diaza–3,7–diphosphacyclooctanes chelate one nickel in the same manner as in complexes with the structure **F** in Scheme 1.31. But the main difference between the platinum and the nickel analogoues complexes resides in that the latter can adopt different conformations around the metal centre; *i.e.* distorted square–planar and tetrahedral. Figure 1.17 illustrates the hydride–proton transfer through first, second and third or outer coordination sphere. The first coordination sphere consists of the ligands bound directly to the metal centre, it controls the presence or absence of vacant coordination sites, redox potentials and hydride donor abilities. The second coordination

sphere includes functional groups such as pendent bases that can interact with bound substrates such as H_2 molecules and hydride ligands, but that do not form strong bonds with the metal centre. The outer coordination sphere is defined as that portion of the catalytic system that is beyond the second coordination sphere which assists the delivery of protons and electrons to and from the catalytically active site.

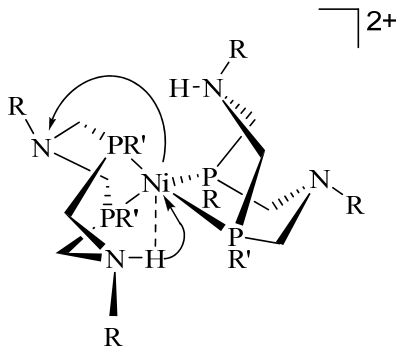

Figure 1.17 Simplified schematic representation of the proton exchange mechanism for one of the complexes conformers. Arrows indicate the metal–mediated proton movement between two nitrogens.

Complexes containing 1,5–diaza–3,7–diphosphacyclooctanes (R = Bn or Ph and R' = ^{t}Bu or Ph) and Fe(II) are illustrated in Scheme 1.32.[71] Treatment of **M** with a strong base led complexes of structure **N** by displacement of Fe–Cl bond to Fe–H. Complexes of structure **M** under H_2 atomosphere gave monocationic iron complexes in form **O** with H_2 as ligand. The deprotonation of **O** with DBU led to **N**, which could be reversibily protonated to give **O**. These mononuclear iron dihydrogen complexes with pendant amines mimic the hydrogenase crucial features of the distal Fe site of the active site of [Fe–Fe]–hydrogenase required for H–H bond formation and cleavage.[81] Although, the electro catalytic oxidation of H_2 of complexes **M** – **O** has not been observed.

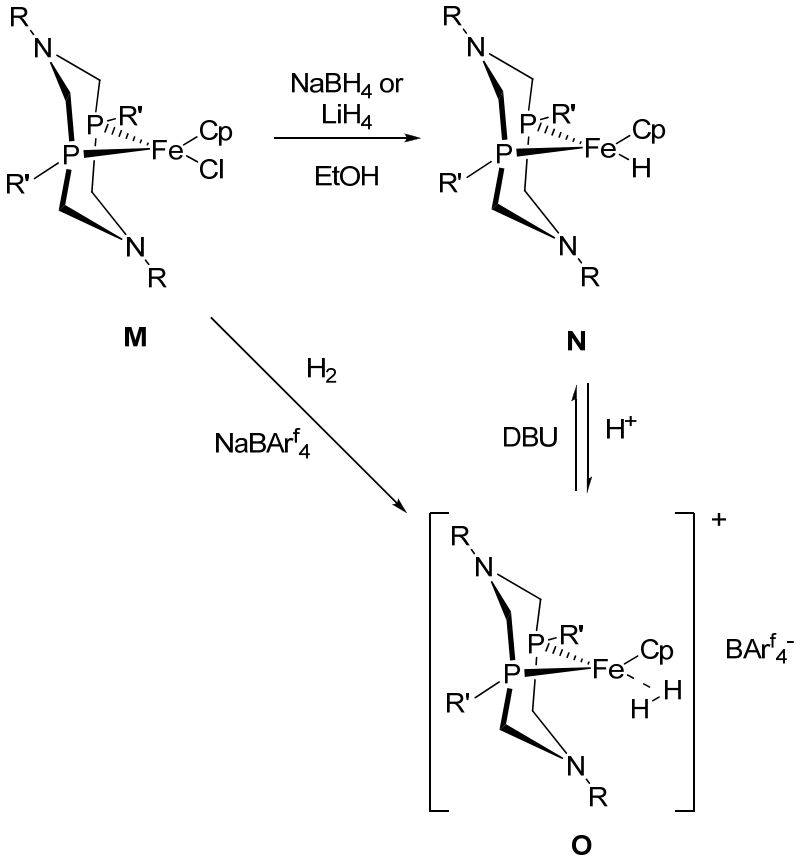

Scheme 1.32 Coordination chemistry of 1,5–diaza–3,7–diphosphacyclooctanes with Fe(II).

1.3.2.3 Tertiary 1,1'–diaza–3,3'–biphosphetidines $\{RN(CH_2)_2P\}_2$ (VIII and IX)

The synthesis and structure of compounds with phosphorus as a bridgehead has previously been studied. Figure 1.18 shows three different groups of diphosphines with a P–P bond: diphosphines with aryl or alkyl groups $R_2P–PR_2$ (**I**),[82,83] with cyclic substituents $[(CH_2)_nP_2]$ ($n \geq 1$) (**II**),[84–88] and with heteroatoms on the ring such as 1,1'–diaza–3,3'–biphosphetidine $\{RN(CH_2)_2P\}$ (R = Ph, *p*-MeC_6H_5) (**III**)[26,89] (**VIII** in Sch. 1.4).

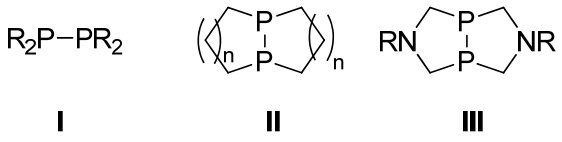

Figure 1.18 Diphosphines with aryl or alkyl substituents (**I**), with fused saturated rings (**II**) and with N on the five–fused rings (**III**).

The saturated bicyclic $(CH_2)_6P_2$ **1.370** was synthesised from 1,3–diphosphinopropane (dppp) in up to 45% yield. The non–isolated cyclic anion was formed by ^{n}BuLi–promoted cyclisation followed by alkylation and an intramolecular cycloalkylation with dihaloalkanes (Sch. 1.33).[88]

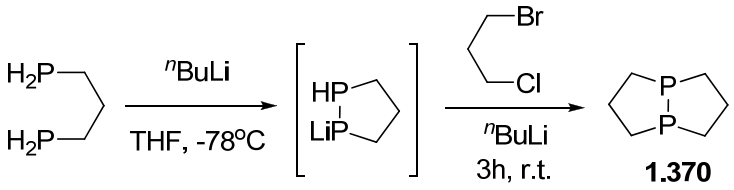

Scheme 1.33 Synthesis of the bicyclic phosphine **1.370**.

Cummins *et al.* synthesised bicyclic phosphines **1.371** and **1.372** from (η^2–MesNPP)Nb{N(Np)Ar}$_3$, (Np = neopentyl, Ar = *m,m*-$Me_2C_6H_3$, Mes = *o,o,p*-$^tBu_3C_6H_2$) as a P–P bond source within the protective coordination sphere of a Nb complex.[87] This complex was reacted in neat cyclodienes (1,3–cyclohexadiene for **1.371** or 1,3–cyclopentadiene for **1.372**) at 65°C for 3h to give quantitative conversion of niobium imido adducts and single phosphorus–containg ring products **1.371** and **1.372** after two [4 + 2] cycloaditions (Sch. 1.34). The $^{31}P\{^1H\}$ NMR showed a singlet at –80 ppm suggesting a symmetric structure in solution. The crystal structure, obtained by single X–ray crystallography, presented a *cis* conformation with C–C double bonds cofacial to each other (Sch. 1.34). The P–P distances are consistent with a single P–P average bond length (2.2 Å).

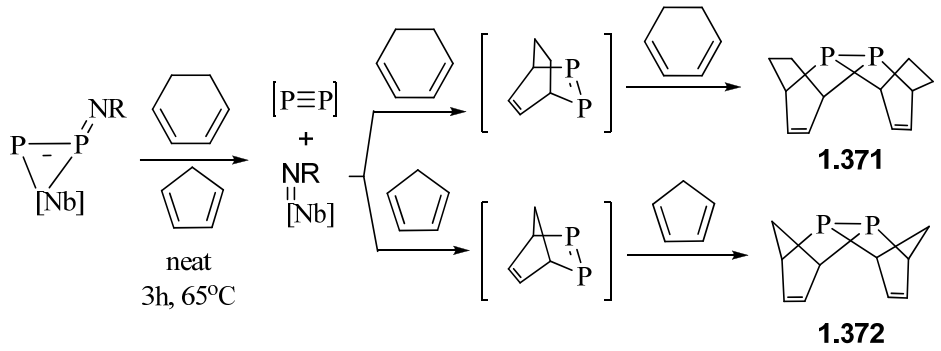

Scheme 1.34 Synthesis of the biphosphacycles **1.371** and **1.372**.

A new route to synthesise similar compounds not limited by the previous synthesis of the Nb complex has recently been discovered. The procedure involves a photochemical reaction of P_4, hexane and 2,3–dimethyl–2–ene to obtain **1.373**. In the novel structure the

C–C double bonds are not cofacial to each other as they were in compounds **1.371** and **1.372** (Sch. 1.35).[87] The reaction of $P_2(C_6H_{10})_2$ (**1.373)** with one equiv. of MeSCN, $SSbPh_3$ and $MesN_3$ led to the diphosphine chalcogenides $EP_2(C_6H_{10})_2$ (**1.374** E = O; **1.375**, E = S and **1.376**, E = NMe) (Sch. 1.35).[85] A second addition of the corresponding O, S or MeN chalcogenide reagents gave $E_2P_2(C_6H_{10})_2$, (**1.377** E = O; **1.378**, E = S and **1.379**, E = NMe) (Sch. 1.35). Compounds **1.377** – **1.379** were also achieved in a one–pot reaction by refluxing two equiv. of MesCN, $SSbPh_3$ and $MesN_3$, respectively, with $P_2(C_6H_{10})_2$. The $^{31}P\{^1H\}$ and ^1H NMR of the mono–chalcogenides showed different shifts for the E*PCH*$_2$ and *PCH*$_2$ moieties (E = O, S). For instance, the $^{31}P\{^1H\}$ NMR of O*P*CH$_2$ is observed at 82.1 ppm ($^1J_{PP}$ = 217 Hz) whereas for *P*CH$_2$ is observed at –84.9 ppm (doublet). Likewise, in the ^1H NMR two sextets are observed (doublet of doublets and doublet) for $OPCH_2C$ and PCH_2C. Suitable crystals of diphosphine **1.373** and diiminophosphorane **1.379** were analysed. The latter presented a notable increase in P–P distance and N–P–P–N dihedral angle compared to the dichalcogenides $E_2P_2(C_6H_{10})_2$ (E = O, S), mainly, due to the steric crowding from the mesityl group.

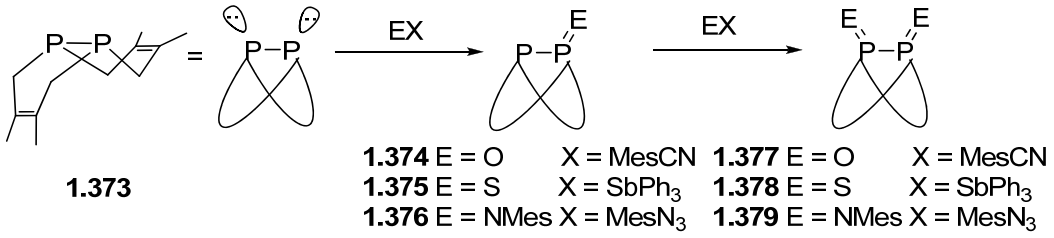

Scheme 1.35 Synthesis of diphosphine **1.373** and chalcogenides derivatives **1.374** – **1.379**.

The coordination capabilities of the ligands $P_2(C_6H_8)_2$ (**1.371)**, $P_2(C_6H_{10})_2$ (**1.373**) and ($MesN_2P_2(C_6H_{10})_2$) **1.379** has been investigated by Piro *et al*.[87] Diphosphines **1.371** and **1.373** have two pair of electrons available to coordinate to a metal centre, however they are not suitable for metal chelation. The bicyclic structure is locked in a *cis* conformation but also restricts the bite angle. The diphosphine framework coordinates to one or two metal centres obtaining mononuclear or polinuclear complexes. Cummins *et al*. isolated $(CO)_5W(P_2(C_6H_8)_2)$ (**1.380**) where only one of the phosphorus atoms coordinates to tungsten [$(CO)_5WP$– δP –84 ppm and P– δP –34 ppm] (Fig. 1.19). Recently, the same

group have developed new complexes with ligand $P_2(C_6H_{10})_2$ which coordinated to two metal centres obtaining $\{M_2P_6\}$ cages [M = Ni, Pt and Pd] (Fig. 1.19).[85] Complexes **1.381** – **1.386** contain three diphosphines acting as bridging ligands and two EPh_3 substituents in a monodentate binding mode (E = P, As or Sb). The Ni(II) complex **1.381** was the only example of a complex with five **1.373** ligands, three of them acting as bidentate and two as monodentates.[86]

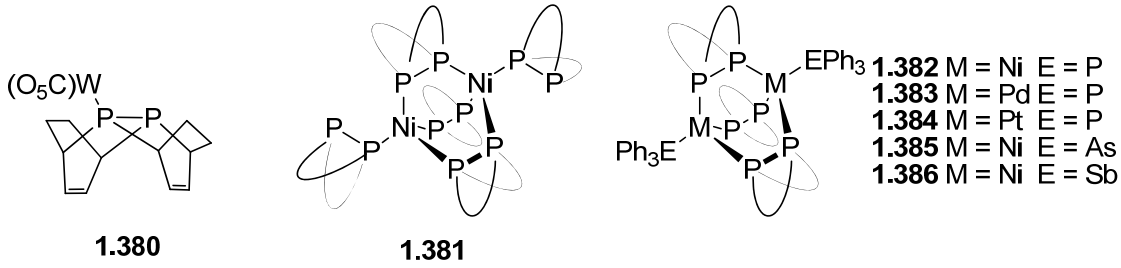

Figure 1.19 Coordination chemistry of **1.371** with W(0) and **1.373** withNi(0), Pd(0) and Pt(0).

The $^{31}P\{^1H\}$ NMR of complex **1.384** revealed that the chemical shift of the axial PPh_3 ligands appeared at δP 26.8 ppm whereas the diphosphines P–P at δP –45.3 ppm. X–ray crystallography studies showed that the cages of complexes **1.381**, **1.383**, **1.384** and **1.386** have a pseudo–D_{3h} symmetry while compounds **1.382** and **1.385** showed a C_3 symmetry. The P–P bond lengths are *ca.* 2.224 Å, slightly larger than the P–P distance in the free ligand [2.2218(5) Å].

In contrast to the non–functionalised ligand **1.373**, the diiminophosphorane c*is*–$(MesN)_2P_2(C_6H_{10})_2$ (**1.379**) possesses a preorganised binding pocket to accommodate early and late transition metals and, therefore, chelated to metal centres.[85] Treatment of molybdenum(II) and nickel(II) with **1.379** allowed for the isolation of the $(MesN)_2P_2(C_6H_{10})_2MoCl(\eta^3–C_3H_5)$ (**1.387**), $(MesN)_2P_2(C_6H_{10})_2NiCl_2$ (**1.388**) and $[(MesN)_2P_2(C_6H_{10})_2Ni(\eta^3–2–C_3H_4Me)][OTf]$ (**1.389**) complexes (Sch. 1.36). The metallacycle exhibited an envelope conformation with a shortened P–P but elongated P–N distances when compared to the free ligand. $^{31}P\{^1H\}$ NMR displayed two broad doublets *ca*. δP 6 ppm for **1.387**, whereas only a singlet was observed for **1.389** at δP 25 ppm.

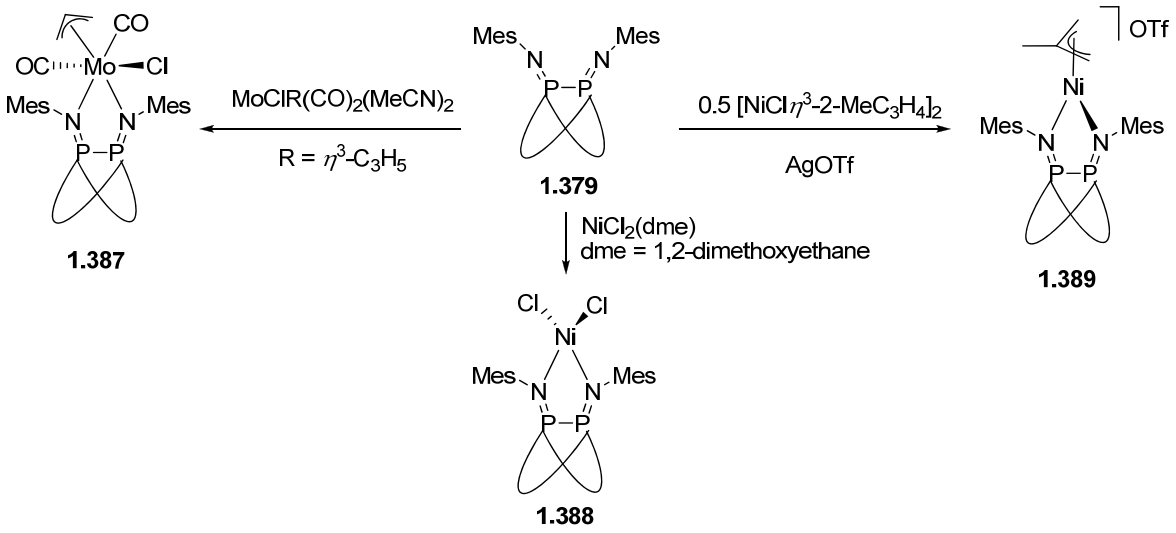

Scheme 1.36 Coordination chemistry of ligand **1.389** with Mo(II) and Ni(II).

Frank *et al.* obtained functionalised diphosphine $\{PhN(CH_2)_2P\}_2$ **1.390** as a result of disproportionation of **1.2** in EtOH (Sch. 1.37).[26] Spectroscopic methods indicated that the synthesis of **1.390** with a molecular formula of $\{PhN(CH_2)_2P\}_2$ was achieved. However two possible structures satisfied this moiety: **I** with two four–membered rings linked through the P atoms and **II** with two five–membered rings fused. While **I** has free rotation through the P–P bond, it is fixed in **II**. The yield of the reaction utilising tripodal phosphine $P\{CH_2N(H)Ph\}_3$ **1.4** gave lower yield (2%) which was improved (17%) when $(CH_2O)_n$ was added to the reaction in an unsuccessful attempt to get cyclic phosphine **1.3**.

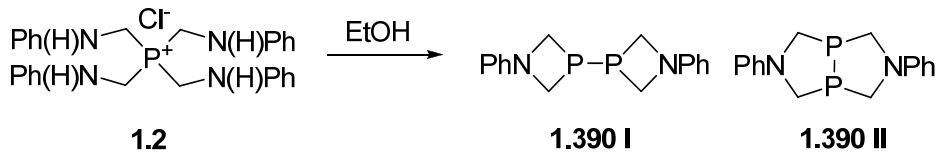

1.2 **1.390 I** **1.390 II**

Scheme 1.37 Synthesis of **1.390**.

Karasik *et al.* isolated the bicyclic diazaphosphacyclootane $\{p\text{-}MeC_6H_5N(CH_2)_2P\}_2$ (**1.392**) as a coproduct of the electrochemical oxidation of **1.391** despite that the aim of the reaction was to obtain the phosphonium salt **1.393** (Eqn. 1.20).[89]

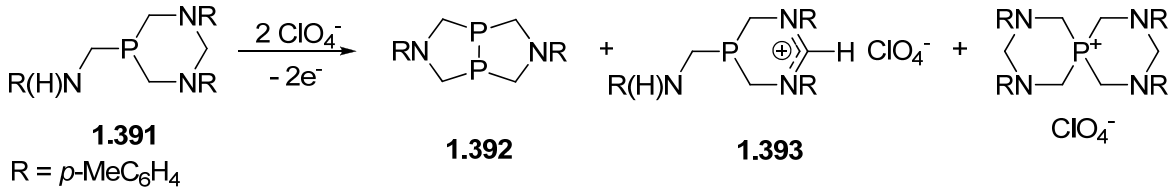

1.391
R = *p*-MeC_6H_4

1.392

1.393

Equation 1.20

The $^{31}P\{^{1}H\}$ NMR of **1.390** and **1.392** revealed a peak at δP –36.0 in DMF which confirms that in solution the two phosphorus centres are equivalent. This value is further shielded compared to **1.370** (no nitrogens on the rings) which showed a singlet at δP –27.8 ppm in $CDCl_3$.[88,89] The ^{1}H NMR of **1.390** and **1.392** showed a multiplet between 3.1 and 3.8 ppm corresponding to the methylene protons PCH_2N with a splitting pattern corresponding to an ABX_2 system. Hence, a doublet of doublets was observed at 3.36 ppm with ^{1}H–^{1}H coupling constant of $^{2}J_{HH}$ = 12.6 Hz and ^{31}P–^{1}H of $^{2}J_{HP}$ = 24.4 Hz and at 3.74 ppm (doublet $^{2}J_{HH}$ = 12.6 Hz).[89]

Analogous compound of **1.390 II** and **1.392** without P–P bond beforehand mentioned in Figure 1.16, can adopt *exo-exo* (**CW** or *cis*), *endo-endo* (**BB**) and *exo-endo* (**CB**) conformations.[84] Compounds **1.390** and **1.392** contain a lone pair of electrons on each nitrogen introducing symmetry, anti or syn depending on the orientation of the lone pairs, in a similar manner as that previously observed for **1.394** in **CW** conformation (Fig. 1.20). Albeit **1.394** has nitrogen and phosphorus exchanged with respect to **1.390** and **1.392**, the C_{2v} symmetry (2–cis,anti,anti and 2–cis,syn,syn) and C_s symmetry (2–cis,syn,syn) observed for **1.394** can be applied to **1.390** and **1.392**.[88]

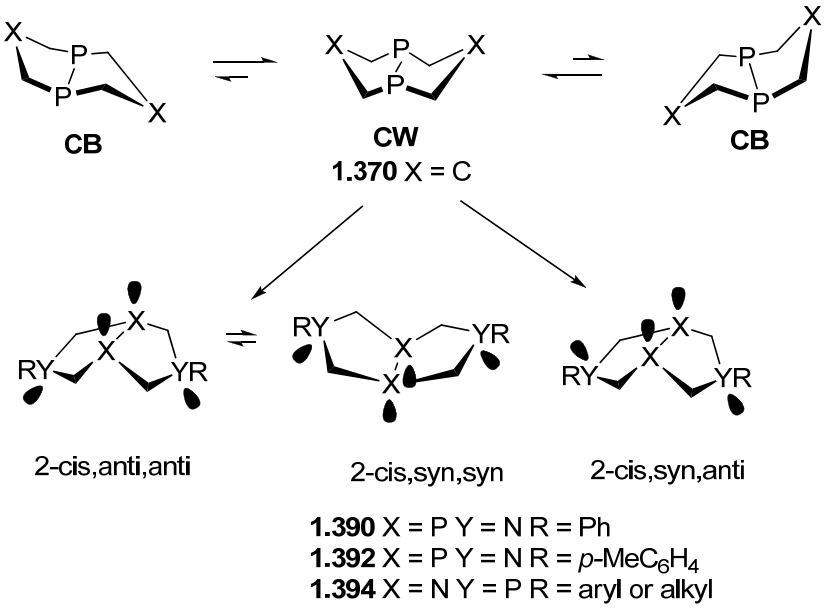

Figure 1.20 Possible conformations for P–P compounds **1.390**, **1.392** and **1.394**.

1.3.2.4 Tertiary (aminomehtyl)phosphines P{$CH_2N(R)CH_2$}$_3$P (X)

The last group of aminomethylphosphines illustrated in Scheme 1.4 (**X**) are those of the type P{$CH_2N(R)CH_2$}$_3$P. A similar family of bicyclic diphosphines that possess three saturated alkylated bridges between phosphorus [P{CH_2}$_n$P] has been developed mainly by Alder and co–workers.[88,90–92] They investigated the structure and basicity of 1,5–diphosphabicyclo[3.3.3]undecane **1.398**, and its analogues diphosphines [*h.k.l*] alkanes (3 < *h, k, l* < 4). Scheme 1.37 shows the synthetic route of **1.398** through P–P intrabridgehead phosphine **1.370**.[88] In the first step, one phosphorus in **1.370** incorporates benzyl to get **1.395** but both phosphorus remained bonded. The P–P bond cleavage occured when both phosphorus are substituted to obtain **1.396** (δP –22.4 ppm). Treatment of **1.396** with bistriflate gave **1.397** which reduction lead to **1.398** (δP –29.4 ppm). Chemical shifts of P–P intrabridgehead **1.370** and non phosphorus bonded **1.396** and **1.398** are between δP –22.4 and –29.4 ppm which indicates that the phosphorus shift is not drastically affected by the phosphorus substituents.[88,90–92]

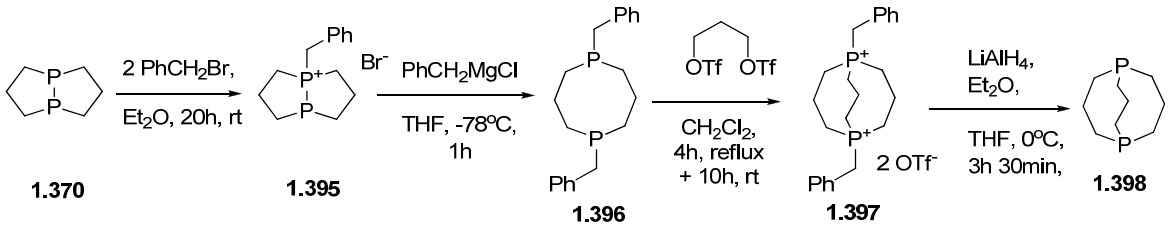

Scheme 1.38 Synthetic route to obtain **1.398**.

Crystals suitable for single crystal X–ray diffraction for **1.397** and **1.398** were obtained by sublimation (Fig. 1.21 a and b).[90,92] Both structures displayed similar P···P distances being approx. 0.383 Å shorter for **1.397** (3.690 Å) than for **1.398** (4.073 Å). Consequently, P–C–P angles are slightly larger for **1.397** (111.7º) than for **1.398** (106.7º). Thus, both phosphorus compounds showed an *out,out* geometry to alleviate restrain. In larger bicyclic [*h.k.l*] analogues, *in,out* and *out,out* isomers were observed when one of the phosphorus is protonated.

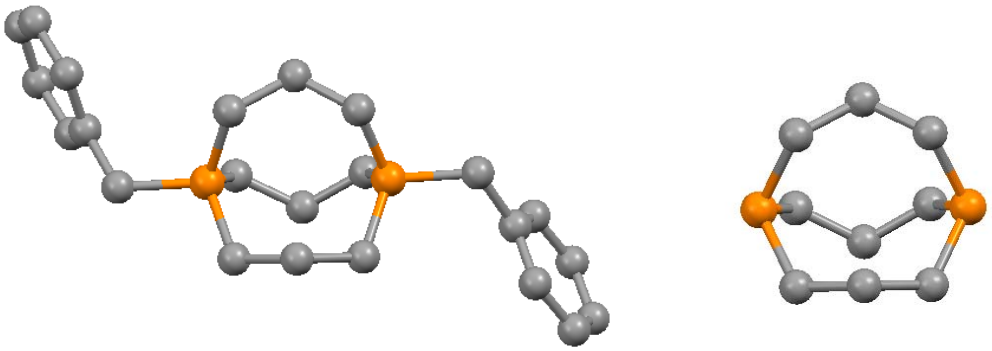

Figure 1.21 X–ray structures of a) **1.397** and b) **1.398**.

Larger bicyclic compounds ([4.3.3], [4.4.3] and [4.4.4]) were oxidised by addition of hydrogen peroxide which changed the inversion of the phosphorus from the *out,out* to the *in,out* with both phosphorus bonded. For instance, the $^{31}P\{^{1}H\}$ NMR of the monoxide [4.4.3] (**1.399**) showed two isomers in equilibrium depending on the concentration of water in THF [δP –48.2 and 48.1 ppm ($^{1}J_{PP}$ = 46 Hz) and at –31.7 and 51.7 ppm) (Fig. 1.22 a and b, respectively). More addition with H_2O_2 yielded the diphosphabicyclic dioxides all in *out,out* inversion. Values for $^{31}P\{^{1}H\}$ NMR varies depending on the ring size, e.g. dioxide [4.3.3] resonates at 57.4 ppm whereas dioxide [4.4.4] shows a peak at 70.7 ppm in D_2O.

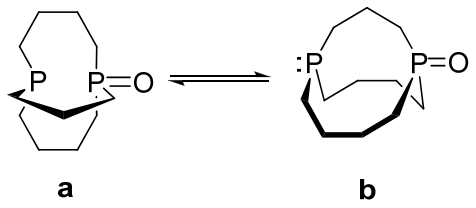

Figure 1.22 a) *in,out* and b) *out,out* isomers of **1.399**.

Verkade and co–workers obtained the nonsymmetric diphosphines $P\{CH_2N(R)\}_3P$ **1.400** (R = Me) and **1.401** (R = C_6H_5) from $[P(CH_2OH)_4]_2SO_4$ (THPS) and THPC respectively (Fig. 1.23).[6,75] Due to the different environments of the two phosphorus atoms in **1.400** and **1.401**, two doublets were observed in the $^{31}P\{^1H\}$ spectra [**1.400**, δP –53.1 (PCH_2–) and δP 82.3 ppm (PNMe–), $^3J_{PP}$ = 27 Hz; **1.401**, δP –45.3 (PCH_2–) and δP 49.7 ppm (PNC_6H_5), $^3J_{PP}$ not reported]. The chalcogenides $O=P\{CH_2NR(R)\}_3P$ **1.402** and $S=P\{CH_2N(R)\}_3P=S$ **1.403** resonated in the region of P(V) compounds [**1.402**, δP 35.6 (PCH_2–) and δP 81.5 ppm (PNMe–), $^3J_{PP}$ = 14 Hz; **1.403**, δP 34.6 (PCH_2–) and δP 62.5 ppm (PNMe–), $^3J_{PP}$ = 108 Hz] (Fig. 1.23).

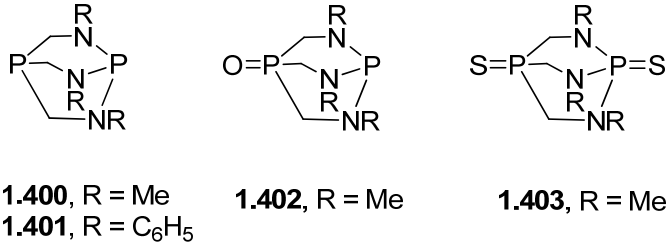

Figure 1.23 Nonsymmetric $P\{CH_2N(R)\}_3P$ compounds.

1.4 Aims

The aims of this project were therefore:

1) To expand the range of PCN ligands using a Mannich–based condensation reaction which contain a pendant amine by varying the N and the P functional groups.
2) To establish a method to afford the ligands obtained utilising THPC and hydroxymethylphosphines as phosphorus precursors.
3) To explore the reactivity of aminic proton in the pendant amine to produce symmetric and nonsymmetric PCNCP ligands.
4) To understand any new ligands synthesised and investigate their coordination capabilities to various transition metal including Pt(II), Pd(II) and Ru(II) and to consequently explore the potential catalytic activity of selected complexes for CO_2 capture.

2. Synthesis, reactivity and characterisation of aminomethylphosphine derivatives of THPC

In recent years, complexes with a PCN backbone have raised great interest due to their versatile coordination chemistry,[1–7] their efficiency as catalysts in electron–transfer process,[8,9] and their biological activity.[1] Complexes with $P_2^RN_2^{R'}$ systems exhibit high electrocatalytic performances in the cleavage of H_2 (See Eqn. 1.19). The success of these complexes lies in the ability of the ligands to take on multiple conformations to assist proton coupled transfer between the metal centre and the amine in the pendant arm (See Fig. 1.17).

Complexes of Pt(II) and Pd(II) with diazaphosphorinanes of the type $RP\{(CH_2)_3(NR)_2\}$ (R = alkyl or aryl substituents) (**VI** in Sch. 1.4) can adopt a *cis* configuration due to the lack of sterically hindrance of the phosphorus substituents (See Eqn. 1.17 and Sch. 1.29).[18,39,40,56–59,93,94] In contrast, Pt(II) and Pd(II) complexes with bulkier PCN ligands such as $P(CH_2NR)_3$ (R = $(CH_2)_4NMe$, **1.197** and R = $(CH_2)_4O$, **1.199**, see Eqn. 1.10) showed a *trans* arrangement of both phosphorus with respect to the metal centre (See Eqn. 1.12).[1] A very different coordination mode was observed for analogous ligands of the kind $P\{CH_2N(H)R\}_3$ (R = C_6H_5, **1.152**; *m,m*–$Me_2C_6H_3$, **1.153**; *m,m*–$(CF_3)_2C_6H_3$, **1.154**, Eqn. 1.9, and *o*–$(CO_2Me)C_6H_4$, **1.192**, Sch. 1.21) which formed a wide range of heteronuclear complexes due to the great flexibility of the multidentate ligand (See Schs. 1.18 – 1.21).[2–5] Moreover, these ligands possess three NH groups for further functionalisation. In fact, the analogue $P\{CH_2N(H)Me\}_3$ was treated with PR_3 (R = Me_3 or Ph_3) to afford bicyclic $P(CH_2NR)_3P$ ligands **1.400** and **1.401** respectively (See Fig. 1.23), which act as monodentate or bidentate towards various metal centres.[6]

Nonsymmetric diphosphines $Ph_2PCH_2N(R)CH_2PCg$ (R = C_6H_5, **1.249** and R = *p*–MeC_6H_4, **1.250**, See Sch. 1.22) were achieved by condensation of a chosen secondary amine $CgPCH_2N(H)R$ with Ph_2PCH_2OH.[7] These PCNCP ligands bind to several metal centres to obtain mononuclear and heteronuclear complexes (See Fig. 1.9). Therefore, the synthesis of ligands incorporating PCN backbone will be explored. They offer an excellent scaffold for the synthesis of PCNCP ligands by functionalisation of the NH group as well as the advantages of the pendant amine required for the cleavage of H_2.[8,9] In this chapter, several methods using THPC and a wide range of *ortho* and *para* anilines to expand the library of PCN ligands were investigated with the aim of studying their coordination capabilities and ultimately their catalytic activity.

2.1 Synthesis of phosphonium salts 2.1 – 2.11

It has been demonstrated that THPC is an excellent phosphorus source for the synthesis of a wide range of aminophosphines.[25,29,32] For instance, Frank and Drake utilised THPC as a starting material for the synthesis of $P\{CH_2N(H)C_6H_5\}_4Cl$ **2.1** (Eqn. 2.1).[25]

Previous work within our group has shown that following this procedure $P\{CH_2N(H)R\}_4Cl$ salts (R = C_6H_5, **2.1**; *o*–FC_6H_4, **2.5**; *p*–MeC_6H_4, **2.8**; *p*–FC_6H_4, **2.10** and *p*–EtC_6H_4, **2.11**) were successfully formed (Eqn. 2.1).[16] In order to expand this library of compounds, new $P\{CH_2N(H)R\}_4Cl$ salts (*o*–MeC_6H_4, **2.2**; *o*–$^{i}PrC_6H_4$, **2.3**; *o*–$^{t}BuC_6H_4$, **2.4**; *o*–$CF_3C_6H_4$, **2.6**; *o*–$\{C(Me)=CH_2\}C_6H_4$, **2.7** and *p*–$^{i}PrC_6H_4$, **2.9**) were synthesised by reacting THPC with four equivs. of the appropriate anilines under aerobic conditions (Eqn. 2.1). Four moles of water were eliminated in this condensation reaction and the desired products isolated in good to excellent yields (62 – 92%).

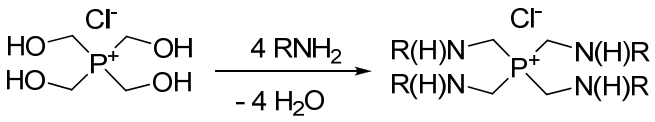

THPC

2.1* R = C_6H_5
2.2 R = *o*-MeC_6H_4
2.3 R = *o*-$^{i}PrC_6H_4$
2.4 R = *o*-$^{t}BuC_6H_4$
2.5* R = *o*-FC_6H_4
2.6 R = *o*-$CF_3C_6H_4$
2.7 R = *o*-$\{C(Me)=CH_2\}C_6H_4$
2.8* R = *p*-MeC_6H_4
2.9 R = *p*-$^{i}PrC_6H_4$
2.10* R = *p*-FC_6H_4
2.11* R = *p*-EtC_6H_4

*Taken from ref[16].

Equation 2.1

The $^{31}P\{^{1}H\}$ NMR of **2.1 – 2.11** showed several peaks indicative of P(V) and P(III) compounds since anilines, as weak bases, can also reduce the phosphonium salts as previously observed Frank *et al.*[25] However they barely investigated these other resonances which were identified and satisfactorily synthesised as the aminomethylphosphines ligands explained in more detail in following sections (Eqns. 2.2, 2.3, 2.6 and 2.10). Figure 2.1 illustrates the $^{31}P\{^{1}H\}$ NMR of **2.1** in $(CD_3)_2SO$, which is representative of the other compounds **2.2** – **2.11**, where resonances in the region of P(V) and P(III) compounds are observed.

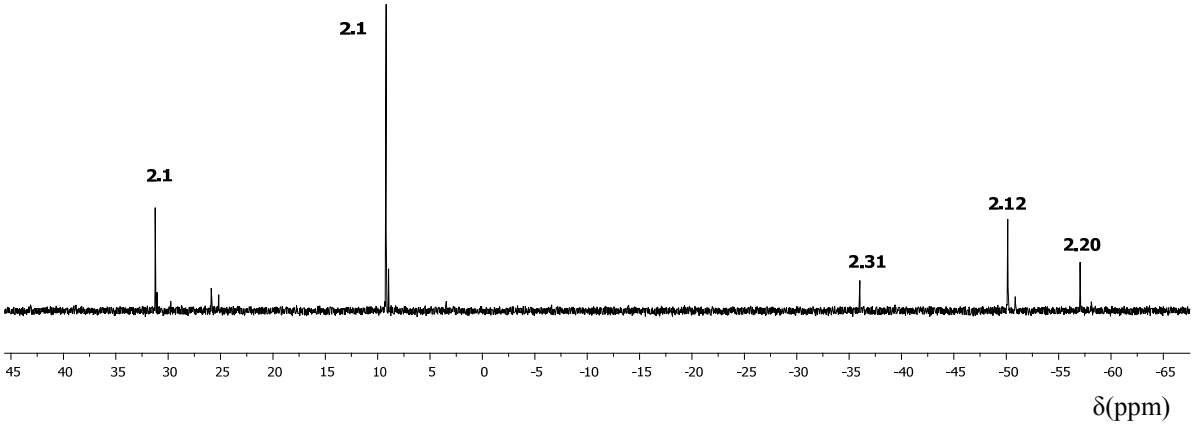

Figure 2.1 $^{31}P\{^{1}H\}$ NMR of the dissociated product obtained between one equiv. of THPC and four equivs. of $C_6H_5NH_2$.

The highest intensity peaks [δ_P 7.53 and 30.11 ppm, $(CD_3)_2SO$] are slightly shifted from THPC [δ_P 26.5 ppm] and close to the resonances observed for $[Et_4P]Cl$ [δ_P 33.7 ppm, $CDCl_3$] and $[Ph_4P]Cl$ [δ_P 23.6 ppm, $CDCl_3$].[95] Albeit the $^{31}P\{^{1}H\}$ NMR were recorded in different solvents, all phosphonium chlorides appears in the positive region of the spectrum with similar values.

The IR spectra of **2.1 – 2.11** were run as KBr disks and showed a band at about 3300 cm^{-1} assigned to νNH stretch. This band was different of that observed for THPC at *ca*. 3467 cm^{-1} due to νOH stretch which confirms that during the condensation reaction, all four hydroxyl groups of THPC were replaced by NH groups. ^{1}H NMR spectra of **2.1 – 2.11** were too complex to analysis due to the overlapping peaks from the mixture but resonances are in the correct region for aryl and alkyl protons.

The ES–MS data result from loss of the chloride ion (*m/z* $[M–Cl]^+$) for the majority of phosphonium salts (Experimental Section). Furthermore, the mass spectrum of **2.1** exhibits the fragmentation pattern of the cyclic **2.12** (*m/z* $[MH]^+$ 362) and acyclic **2.26** (*m/z* $[MH]^+$ 350) aminophosphines. Likewise, the MS of **2.3** shows the fragmentation pattern of cyclic **2.14** (*m/z* $[MH]^+$ 488)] and acyclic **2.27** (*m/z* $[MH]^+$ 476).

2.2 X–ray crystal structure of 2.6

X–ray quality crystals of **2.6** were obtained when a methanol filtrate from the reaction between THPC and *o*-$CF_3C_6H_4NH_2$ was allowed to stand for > 24 h. The X–ray structure depicted in Figure 2.2 shows P(1) atom in a tetrahedral environment with C–P–C bond angles [C(1)–P(1)–C(1A) 106.17(12)º and C(1A)–P(1)–C(1B) 111.14(6)º] comparable to

the previously data obtained for **2.10**[16] and other documented P(V) aminophosphines [between 106.17(12)° and 111.15(6)º] (Table 2.1).[14] Likewise, the P(1)–C(1) [1.8185(19) Å], N(1)–C(1) [1.436(2) Å] distances and P–C–N [110.87 (13)°] bond angles are in agreement with those reported in the literature.[7,12–14,34,96,97]

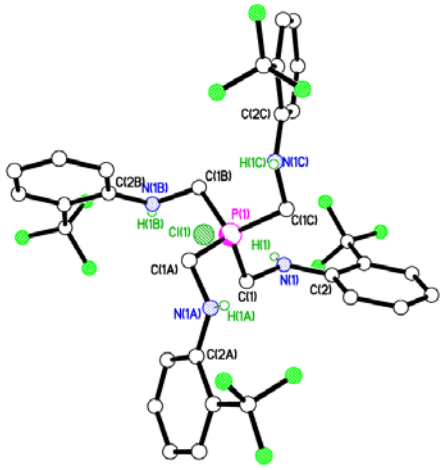

Figure 2.2 X–ray structure of **2.6**. All H atoms except those on N are removed for clarity.

The chloride ion is hydrogen bonded to the secondary amine hydrogens [N(1)···Cl(1) 3.2045(19) Å and 142(2)°] with comparable values observed in **2.10** [3.251(3) – 3.487(3) Å, 154(4) – 172(4)°] and in the literature.[16,98] The fluorine atoms of the CF_3 substituents are bonded to the secondary amine, with an average bond N···F of 2.9325(2) Å. Selected bond lengths, angles as well as hydrogen bond parameters are given in Table 2.1.

Table 2.1 Selected bond lengths (Å), angles (°) and hydrogen bonds lengths (Å) and angles (°) for **2.6**.[a,b]

		2.6		
P(1)–C(1)	1.8185(19)	C(1A)–P(1)–C(1B)		111.14(6)
C(1)–N(1)	1.436(2)	C(1A)–P(1)–C(1C)		111.14(6)
P(1)–C(1)–N(1)	110.87(13)	C(1B)–P(1)–C(1C)		106.17(12)
C(1)–P(1)–C(1A)	106.17(12)	C(1)–P(1)–C(1C)		111.15(6)
C(1)–P(1)–C(1B)	111.14(6)	C(2)–N(1)–C(1)		123.07(18)
D–H···A	**d(D–H)**	**d(H···A)**	**d(D···A)**	**<(DHA)**
N(1)–H(1)···F(2)	0.82(3)	2.45(3)	2.979(2)	123(2)
N(1)–H(1)···F(3)	0.82(3)	2.47(2)	2.886(2)	113(2)
N(1)–H(1)···Cl(1)	0.82(3)	2.52(3)	3.2045(19)	142(2)

[a] Estimated standard deviations in parentheses. [b] Symmetry operations for equivalent atoms: A, –x+1, –y+3/2, z and B: y–1/4, –x+5/4, –z+5/4.

The supramolecular structure of **2.6** (Fig. 2.3 a and b) and **2.10** (Fig. 2.3 c) illustrate the alternation of Cl^- and phosphonium ions along the *b* and *c*–axis (Fig. 2.3 a and c) and *c*–axis (Fig. 2.3 b). It is worth to note that the packing plot of **2.6** along the *c*–axis (Fig. 2.3b) displays Cl^- and P(V) ions eclipsed but this is not observed in **2.10**.

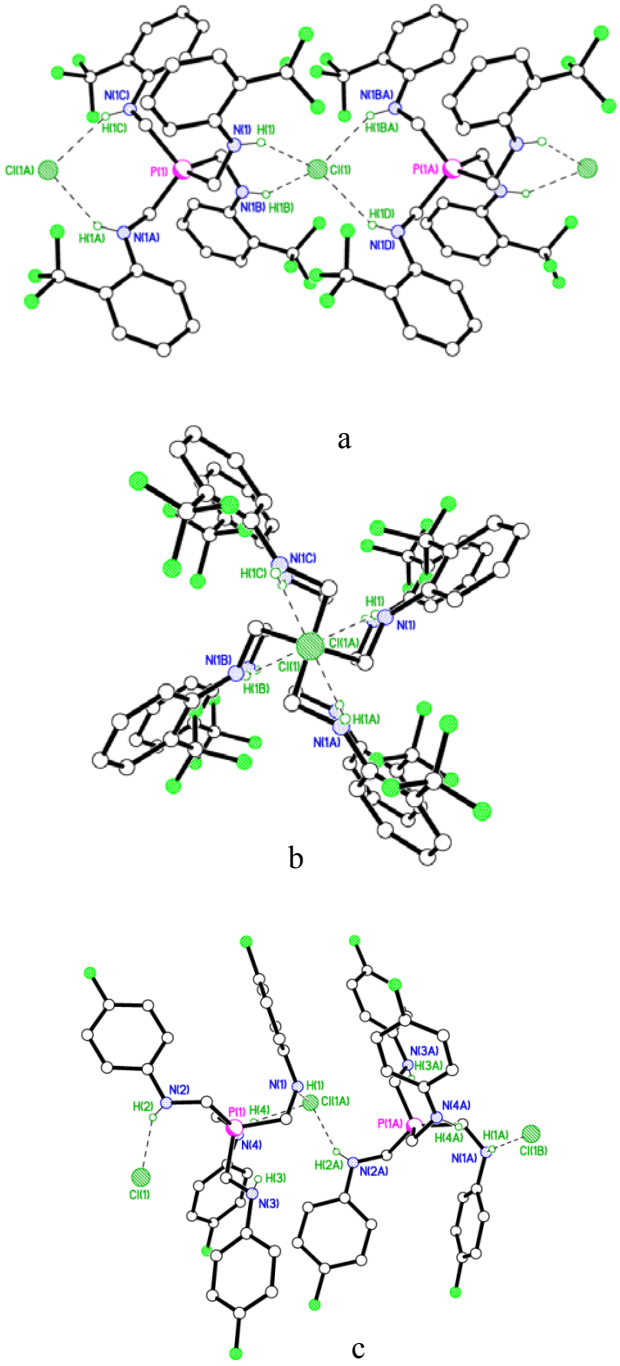

Figure 2.3 Packing plot of a) **2.6** along the *b*–axis, b) **2.6** along the *c*–axis and c) **2.10** along the *c*–axis.

2.3 Synthesis of aminomethylphosphine ligands 2.12 – 2.19

Frank and Drake reported the synthesis of the diazaphosphorinane ligand $R(H)NCH_2P\{(CH_2)_3(NR)_2\}$ (R = C_6H_5, **2.12**) using 1.56 equivs. of Et_3N and one equiv. of **2.1** (Eqn. 2.2).[26] This method was extended, within our group, to include the synthesis of $R(H)NCH_2P\{(CH_2)_3(NR)_2\}$ (R = *o*–FC_6H_5, **2.15**; R = *p*–MeC_6H_4, **2.16**; R = *p*–FC_6H_4, **2.18** and R = *p*–EtC_6H_4, **2.19**) with functionalised anilines. To substantiate this, new $R(H)NCH_2P\{(CH_2)_3(NR)_2\}$ (R = *o*–MeC_6H_4, **2.13**; R = *o*–$^{i}PrC_6H_4$, **2.14;** R = *p*–$^{i}PrC_6H_4$, **2.17**) ligands were obtained in fair to good yields (33 – 84 %) (Eqn. 2.2).

Diazaphosphorinanes with substituted anilines were previously synthesised using $RP(CH_2OH)_2$ as starting material instead of THPC.[18,40,56,59,93,94] These investigations have demonstrated that only *p*-anilines afforded cyclic phosphines of the type $RP\{(CH_2)_3(NR`)_2\}$ whereas *o*-anilines condense with $RP(CH_2OH)_2$ forming $RP(CH_2NHR)_2$ as major products. The method proposed here shows the same tendency for ligands with *p*-anilines (**2.16** – **2.19**) but also cyclic ligands with several *o*–anilines (**2.13** – **2.15**) were achieved. However, more basic Me and ^{i}Pr substituents in **2.13** and **2.14** needed KO^{t}Bu but the electron withdrawing substituent F in **2.15** was obtained with Et_3N. Same conditions were applied to the *ortho* phosphonium salts **2.4** and **2.6** which gave the acyclic ligands **2.28** and **2.29** (Section 2.3, Eqn. 2.3) probably due to the steric hindrance of the *ortho* substituents.

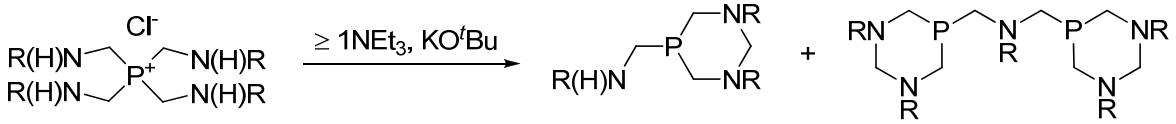

2.1 R = C_6H_5
2.2 R = *o*-MeC_6H_4
2.3 R = *o*-$^{i}PrC_6H_4$
2.5 R = *o*-FC_6H_4
2.8 R = *p*-MeC_6H_4
2.9 R = *p*-$^{i}PrC_6H_4$
2.10 R = *p*-FC_6H_4
2.11 R = *p*-EtC_6H_4

2.12* R = C_6H_5
2.13** R = *o*-MeC_6H_4
2.14** R = *o*-$^{i}PrC_6H_4$
2.15* R = *o*-FC_6H_4
2.16* R = *p*-MeC_6H_4
2.17 R = *p*-$^{i}PrC_6H_4$
2.18* R = *p*-FC_6H_4
2.19* R = *p*-EtC_6H_4

2.20 R = C_6H_5
2.21 R = *p*-MeC_6H_4
2.22 R = *p*-$^{i}PrC_6H_4$
2.23 R = *p*-FC_6H_4
2.24 R = *p*-EtC_6H_4

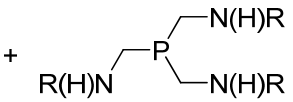

2.25 R = *o*-MeC_6H_4

*Taken from ref[16].

** KO^{t}Bu used for **2.13** and **2.14** only.

Equation 2.2

Compound **2.12** has been previously synthesised and characterised[25] although there is no mention of the minor peak observed at δP –46.7 ppm, in $CDCl_3$, or at δP –54.4 ppm, in $(CD_3)_2SO$. In the $^{31}P\{^1H\}$ NMR of **2.12** it is only reported the major peak at δP –41.0 ($CDCl_3$) or –50.0 ppm $(CD_3)_2SO$. The ratios varied depending on the deuterated solvent used [$CDCl_3$ (**2.12**:**2.20**, approx. 4:1) or $(CD_3)_2SO$ (**2.12**:**2.20**, approx. 6:1)]. This new peak was tentatively assigned to the symmetric diphosphine **2.20** which will be explained in more detail in Section 2.11 (Eqn. 2.10).

For the monophosphines **2.13**, **2.18** and **2.19** the extra minor peak at δP –47.0 ppm in $CDCl_3$ (assigned to diphosphines **2.21**, **2.23** and **2.24** respectively) is even more noticeable (up to approx. 3:1 ratio). For instance, compound **2.18** showed a peak at δP –41.4 ppm and another peak 6 ppm further upfield assigned to **2.23** (Fig. 2.4).

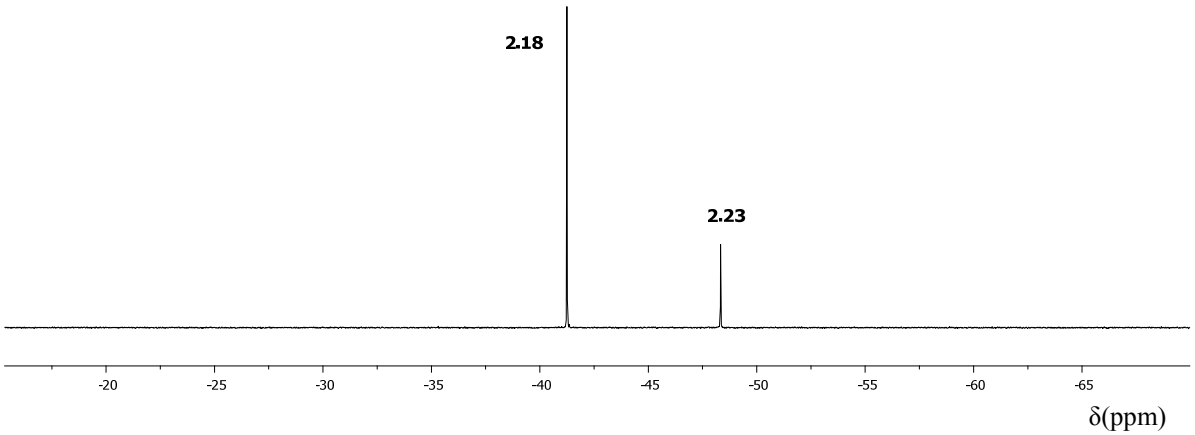

Figure 2.4 $^{31}P\{^1H\}$ NMR of the dissociated product obtained between one equiv. of **2.10** and NEt_3.

The phosphorus shifts of **2.13** (δP –45.1 ppm, broad singlet) and **2.14** (δP –45.1 ppm) slightly stand out from the six–membered ring phosphines which are the only two examples of cyclic ligands with electron donor *ortho* substituents in the aniline. The ^{31}P NMR of **2.14** was run at different temperatures in a range between 40°C and –40°C. It would be anticipated that below the coalescent temperature (–10°C), the broad singlet at –45.1 ppm splits into two signals due to the two possible conformers, *i.e.* fluxionality of the chair. However, the δP did not change significantly with temperature and only the PCH_2N protons became broad. Same broad peak was observed in the $^{31}P\{^1H\}$ spectrum of the crystalline solid, which in addition showed a N···N hydrogen bond (Fig. 2.10a). The IR showed different νNH stretches for the bulk solid (3294 cm^{-1}) and for the crystalline solid (3419 cm^{-1}) which could be related with the N···N hydrogen bond. In the bulk solid this

interaction may not appear and hence the νNH stretch differs noticeable from the crystalline solid where N···N bond is supported by X–ray.

The ^{1}H NMR spectra of **2.12** and **2.14** will be discussed and the explanation can be extended for **2.13**, **2.15** – **2.19** analogues. The ^{1}H NMR of **2.12** shows an ABX pattern (X = P), characteristic of NCH_2N proton in 1,3,5–diazaphosphorinanes.[18,25,39,56] This spin system appears as a sextet, *i.e.* a doublet of doublets owing to the coupling between diastereotopic protons and phosphorus and a doublet (4.31 ppm, dd, $^{2}J_{HH}$ = 12.7 Hz, $^{4}J_{HP}$ = 2.9 Hz and at 5.12 ppm $^{2}J_{HH}$ = 12.7 Hz) (Fig. 2.5). However the latter coupling constant ($^{2}J_{HH}$ = 12.7 Hz) is an average of the coupling of NCH_2N (NCH_aN and NCH_eN) to the axial PCH_2N protons (PCH_aN). Albeit ^{1}H NMR studies by Frank *et al.* concluded that NCH_eN proton resonates at 4.41 ppm[25], NOE NMR experiments of the $PtCl_2$(**2.12**)$_2$ (**3.1**) shows that the peak shifted upfield (3.80 ppm) belongs to the NCH_aN protons (Fig. 3.3). Hence, by analogy of the splitting pattern in the same region of the spectrum for **2.12** and **3.1**, it is presumed that this NCH_aN proton is further upfield than NCH_eN proton (4.31 ppm and 5.12 ppm, respectively). In addition, further recent investigations by Karasik and co–workers documented NCH_aN proton diazaphosphorinanes at lower shifts than NCH_eN proton based in the "W rule".[99] PCH_eN protons are lower field (3.94 ppm) than PCH_aN protons (3.71 ppm) in agreement with PCH_2N protons in the literature.[56,62,63,70]

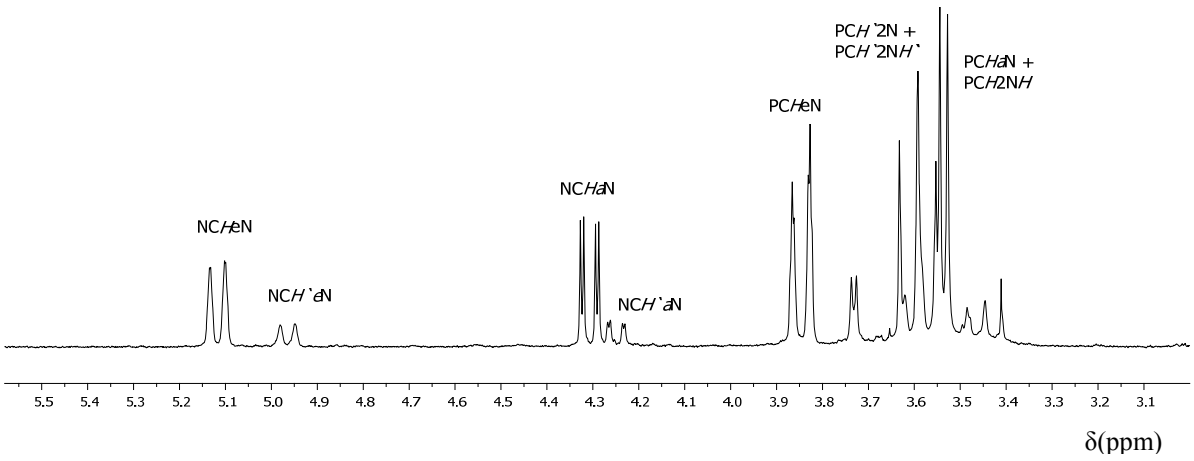

Figure 2.5 Selected region of the ^{1}H NMR spectrum of the dissociated product obtained between one equiv. of **2.1** and NEt_3.

Nevertheless, in the ^{1}H NMR of **2.14**, NCH_2N and PCH_2N protons were recorded as complicated multiplets (Fig. 2.6). They were assigned using the J_{PH}, the COSY, the ^{1}H{^{31}P} and the NOE NMR. PCH_2N protons are equivalents for the pendant arm

(PCH_2NH) but diasterotopics for PCH_2N in the ring. The NCH_2N protons were resolved with a $^1H\{^{31}P\}$ NMR as two doublets at 3.94 (NCH_eN) and 3.90 ppm (NCH_aN) with a $^2J_{HH}$ = 10 Hz in agreement with the two bond ^1H–^1H couplings.[56,99] The COSY revealed that the NCH_aN protons are coupled to the multiplet between 3.34 – 3.27 which resulted in two doublets after the proton was decoupled to phosphorus and hence assigned to PCH_2N.

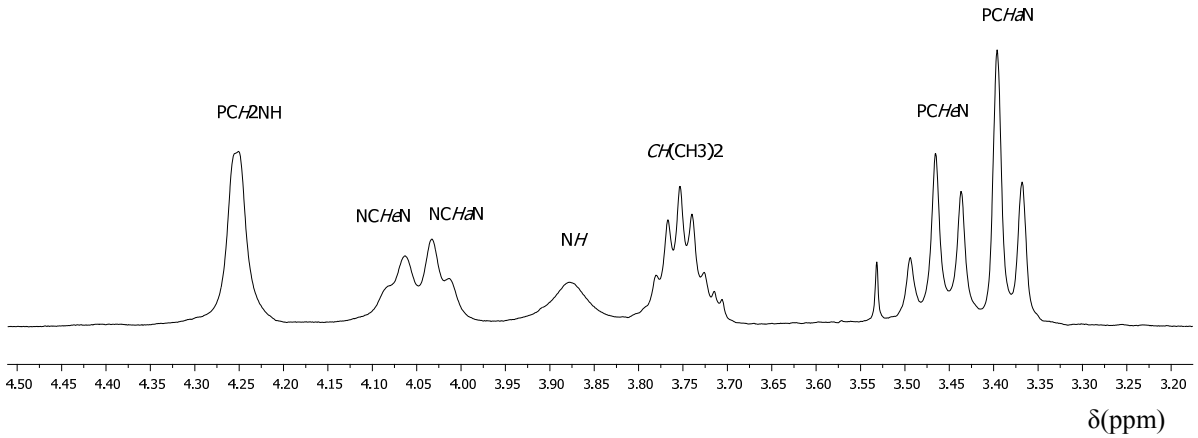

Figure 2.6 Selected region of the ^1H NMR spectrum of **2.14** in $CDCl_3$.

2.4 X–ray structure of 2.12, 2.14, 2.16, 2.17 and 2.19

X–ray quality crystals of ligands **2.12**, **2.14**, **2.16**, **2.17** and **2.19** were obtained from the EtOH filtrate of the reaction between the corresponding phosphonium salt and the base (Fig. 2.7 a, e, d, b and c respectively). Their X–ray structures showed a six–membered P–C–N–C–N–C ring around the phosphorus atom which is at the apical position. The torsion angles in the ring displayed a *chair* conformation between P(1)–C(8)–N(2)–C(9)–N(3)–C(10) with fairly similar values as observed in the first six entries in Table 2.2.

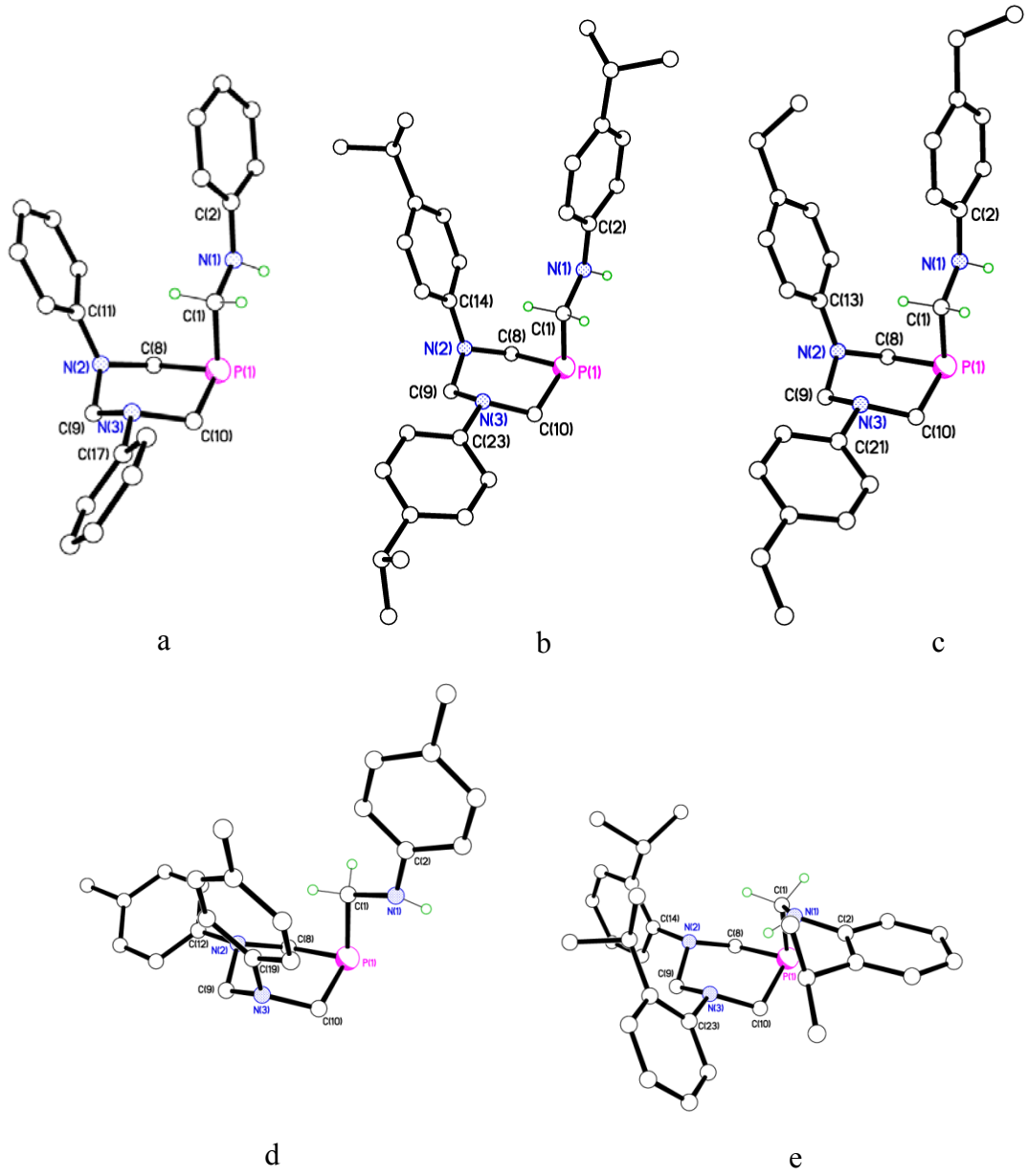

Figure 2.7 X–ray structure of a) **2.12**, b) **2.17**, c) **2.19**, d) **2.16** and e) **2.14**. All H atoms except those on N(1) and C(1) are removed for clarity

In order to compare the orientation of the P pendant arm and the N substituents in the ring of these five structures, selected torsion angles will be discussed. The diagram accompanying Table 2.2 illustrates these torsion angles, named as θ_1 = C(1)–P(1)–C(8)–N(2), θ_2 = C(1)–P(1)–C(10)–N(3), θ_3 = P(1)–C(8)–N(2)–C_{ipso}, θ_4 = P(1)–C(10)–N(3)–C_{ipso} and θ_5 = P(1)–C(1)–N(1)–C(2). When the value of θ_1 to θ_4 is close to 90°, the substituent assessed is in axial position. In contrast if the value is near to 180°, the group is in an equatorial orientation. Figure 2.8 illustrates the orientation of substituents in N(2) by θ_3.

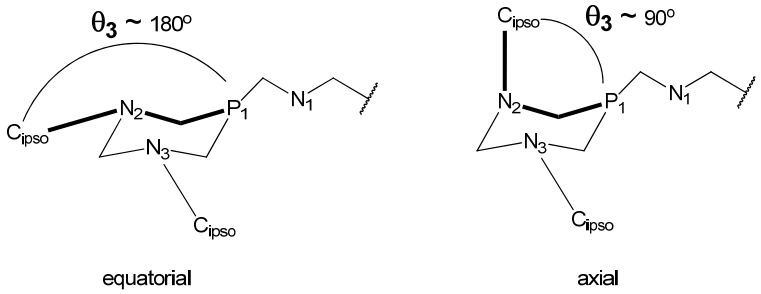

Figure 2.8 Example of the spatial orientation of N(2) substituent by using θ_3 values.

Different approach is pursued for θ_5 which will be used to compare the spatial orientations among structures but it does not give information about the axial–equatorial disposition of the P pendant arm. For example, for all ligands, θ_1 and θ_2 are closer to 90º than to 180º and therefore, the phosphorus pendant arm is in axial position. However, whereas for ligands **2.12**, **2.17** and **2.19**, θ_3 is near to 90º [90.0(4)º – 92.2(3)º], for **2.14** and **2.16** is closer to 180º [173.86(12)º and 173.47(10)º respectively] indicating that for the latter ones, N(3)–aromatic substituents are in equatorial position. Similarly, θ_4 is closer 180º in every ligand except for **2.16** [86.02(18)º] and so N(3)–substituent is in equatorial position. It is remarkable that θ_3 and θ_4 in **2.14** are 173.47(10)º and –156.27(10)º and hence, both N(2) and N(3) aromatic derivatives are in equatorial positions in contrast to the rest of the set.

Table 2.2 Torsion angles (º) for **2.12**, **2.14**, **2.16**, **2.17** and **2.19**.[a]

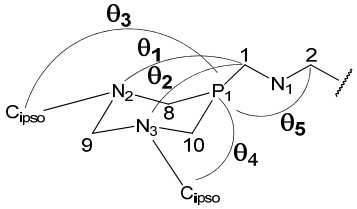

	2.12	**2.14**	**2.16**	**2.17**	**2.19**
P(1)–C(8)–N(2)–C(9)	–56.1(3)	–59.02(18)	–54.09(18)	–57.4(3)	–58.6(4)
C(8)–N(2)–C(9)–N(3)	71.1(3)	68.70(15)	66.9(2)	67.9(3)	68.2(4)
N(2)–C(9)–N(3)–C(10)	–70.7(3)	–73.14(4)	–70.3(2)	–66.6(3)	–67.1(4)
C(9)–N(3)–C(10)–P(1)	55.6(3)	65.57(14)	59.88(18)	57.2(3)	57.6(4)
N(3)–C(10)–P(1)–C(8)	–38.3(2)	–48.26(12)	–42.27(15)	–44.6(2)	–45.5(3)
C(10)–P(1)–C(8)–N(2)	38.1(2)	45.89(12)	40.07(15)	43.3(2)	45.1(3)
θ_1	–64.3(2)	–53.72(12)	–62.98(15)	–57.1(3)	–55.3(3)
θ_2	64.3(2)	51.85(12)	60.27(15)	58.9(2)	58.2(3)
θ_3	91.1(4)	173.47(10)	173.86(12)	92.2(3)	90.9(4)
θ_4	–167.3(4)	–156.27(10)	–86.02(18)	–173.85(18)	–170.9(3)
θ_5	173.2(2)	62.47(17)	–174.73(4)	177.4(2)	177.4(3)

[a] Estandard deviations in parentheses.

All θ_5 angles are in the range of 173.2 – 177.4(3)^o however, for **2.14** the torsion angle decreased to 62.47(17)^o. This structural difference between **2.14** and its analogue **2.12** (chosen as a pattern example) is highlighted in Figure 2.9.

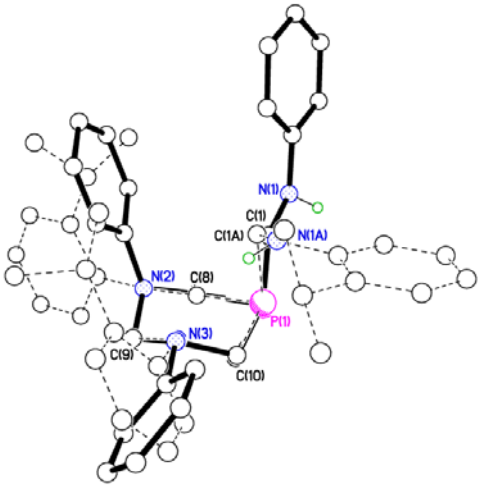

Figure 2.9 X–ray structures of **2.12** (solid bonds) and **2.14** (dashed bonds) superimposed.

Smith *et al*. have determined the X–ray structure of a cationic trialkylphosphine (**1.304**) which is considered as charged versions of PTA (Fig. 2.10 b).[18] Its structure showed intramolecular N–H···N hydrogen bonding between the N(1)···N(2) [N(1)···N(2) 2.915(5) Å, 126°] which fix the structure in a pseudoadamantane cage shape. Similarly, structure of **2.14** revealed a single weak H–bonding interaction [N(1)···N(3) 3.1537 (19) Å, 121.3 (15)^o], which conformationally locks the ligand structure into a pseudoadamantane cage (Fig. 2.10 a). This arrangement could be possible in **2.14** because it is the only structure, among its analogues, which possesses both substituents in equatorial position as it is in **1.304**.

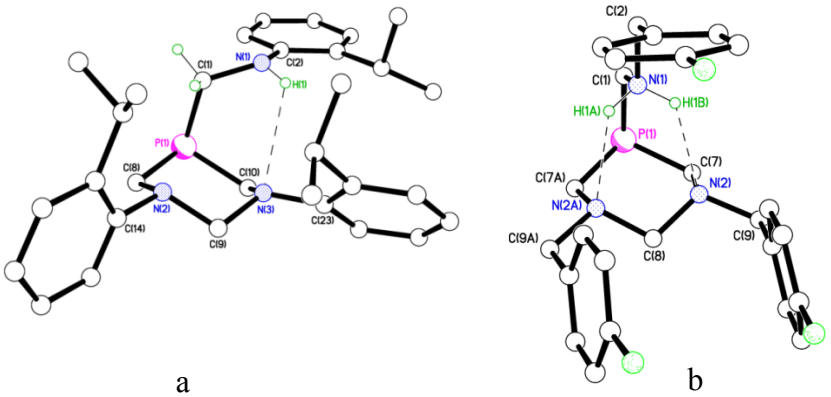

Figure 2.10 X–ray structure of a) **2.14** and b) **1.304**. All H atoms except those on C(1) for **2.14** and N(1) are removed for clarity. Chloride counterion in **1.304** is also removed.

The hindrance of the bulky *ortho*–phenyl substituents in **2.14** prevents formation of the intermolecular eight–membered ring observed for **2.12**, **2.16**, **2.17** and **2.19**. For the latter structures, dimers are formed by two pairs of weak intermolecular P···H–N bonds. Between two molecules an eight–membered ring with a pseudo *chair* conformation between P(1)–C(1)–N(1)–H(1)–P(1A)–C(1A)–N(1A)–H(1C) is formed (Fig. 2.11). The P···N separation [3.647 (3) Å] is similar to values obtained for $Cr(CO)_3\{Ph_2PCH(o\text{-}MeC_6H_4)NHPh\}$[100] and $(o\text{–}MeC_6H_4)_2P(CH_2NHC_{12}H_7)$[101] (Table 2.3).

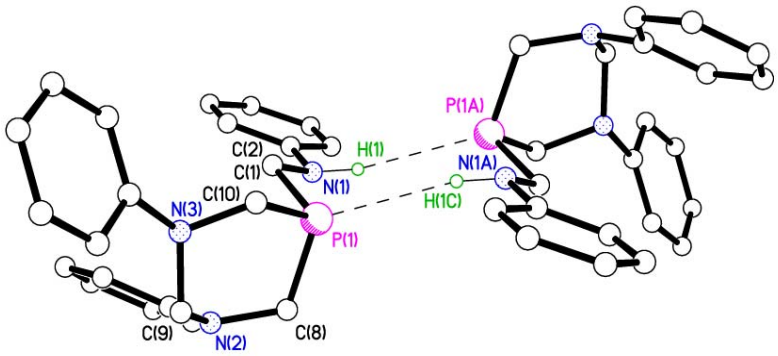

Figure 2.11 Intermolecular H–bonding between two molecules of **2.12.**

Table 2.3 Hydrogen–bond geometry (Å, º).[a]

	D–H···A	d(D–H)	d(H···A)	d(D···A)	<(DHA)
2.12	N(1)–H(1)···P(1A)	0.92(3)	2.72(3)	3.623(2)	168(2)
2.16	N(1)–H(1)···P(1A)	0.87(2)	2.84(3)	3.7007(18)	171(2)
2.17	N(1)–H(1)···P(1A)	0.88(4)	2.81(4)	3.783(3)	170(3)
2.19	N(1)–H(1)···P(1A)	0.89(5)	2.70(5)	3.581(4)	172(4)

[a] Estandard deviations in parentheses. Symmetry operations for equivalent atoms: A: –x, –y+1, –z+1 in **2.12**; –*x*+3, –*y*+1, –*z*+1in **2.16**; –*x*, –*y*+1, –*z* in 2.17; –*x*+1, –*y*+2, –*z*+1 in **2.19**.

The P–C [average [αC–P(1)], αC = C bound to P(1)], C–N [average [αC–αN(X)], αC = C bound to P(1) or N(2) or N(3) and N(X) = N(1), N(2) or N(3)], bonds lengths and the C–P–C angles within the P–C–N–C–N–C ring are similar to those reported for **2.15** and diazaphosphorinanes of the type $R'P\{CH_2N(R)CH_2N(R)CH_2\}$ (Table 2.3).[16–18,59]

Table 2.4 Selected bond lengths (Å) and angles (°) for **2.12**, **2.14**, **2.16**, **2.17** and **2.19**.[a]

	2.12	**2.14**	**2.16**	**2.17**	**2.19**
av.[αC–P(1)][b]	1.840(3)	1.8587(18)	1.8502(19)	1.842(3)	1.842(4)
av.[αC–αN(X)][c]	1.464(4)	1.467(2)	1.464(2)	1.466(4)	1.463(5)
P(1)–C(8)–N(2)	114.9(2)	114.09(12)	115.63(13)	120.8(3)	113.7(3)
C(8)–N(2)–C(9)	111.9(3)	111.56(13)	112.26(15)	112.8(2)	111.9(3)
N(2)–C(9)–N(3)	112.2(2)	110.07(14)	112.83(14)	114.6(2)	114.6(3)
C(9)–N(3)–C(10)	111.2(3)	111.18(13)	112.00(15)	110.0(2)	110.3(3)
N(3)–C(10)–P(1)	115.0(2)	111.35(11)	114.14(13)	115.4(2)	114.5(3)
C(10)–P(1)–C(8)	99.82(16)	97.10(8)	98.38(9)	98.38(14)	98.2(2)
N(1)–C(1)–P(1)	107.27(17)	113.94(12)	108.27(12)	110.7(2)	109.7(3)

[a] Estimated standard deviations in parentheses. [b] Average value of αC–P(1), αC = C bound to P(1). [c] Average value of αC–αN(X), αC = C bound to P(1) or N(2) or N(3) and N(X) = N(1), N(2) or N(3).

2.5 Synthesis of aminomethylphosphines 2.26 – 2.30

The synthesis of ligands of the type $P\{CH_2N(H)R\}_3$ [R = C_6H_5, **1.152**; *m,m*–$Me_2C_6H_3$, **1.153**; *m,m*–$CF_3C_6H_3$, **1.154** and *o*–$(CO_2Me)C_6H_4$, **1.192**] have previously been reported using THP, reduced from THPC, and the relevant primary aniline in a 1:3 stoichiometry.[23] A different approach to synthesise compound **1.152** was also achieved simply by bubbling NH_3 in a solution of the phosphonium salt **2.1** in Me_2CO.[26] This method not only was done under air but also overcomes the issue of synthesising THP first. However, in our hands, even **1.152** was reproduced following this method, the ^1H NMR showed several singlets in the alkyl region probably due to coproducts formed by reaction of the acetone with NH_3. This entailed us to try a different approach to obtain $P\{CH_2N(H)R\}_3$ compounds and hence, the ligands $P\{CH_2N(H)R\}_3$ [R = C_6H_5, **2.26**; R = *o*–^{i}PrC_6H_4, **2.27**; R = *o*–^{t}BuC_6H_4, **2.28**; R = *o*–$CF_3C_6H_4$, **2.29** and R = *o*–$\{C(Me)=CH_2\}C_6H_4$, **2.30**] were accomplished by treatment of the appropriate phosphonium salt with an excess of KO^{t}Bu in MeOH at r.t. in fair to excellent yields (36 – 94%) (Eqn. 2.3).

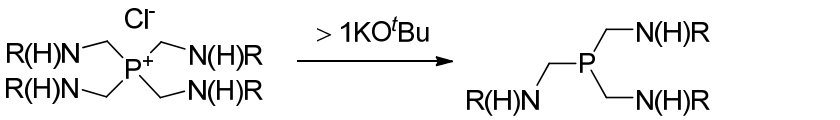

2.1 R = C_6H_5
2.3 R = *o*-^{i}PrC_6H_4
2.4 R = *o*-^{t}BuC_6H_4
2.6 R = *o*-$CF_3C_6H_4$
2.7 R = *o*-{C(Me)=CH_2}C_6H_4

2.26 R = C_6H_4
2.27 R = *o*-^{i}PrC_6H_4
2.28 R = *o*-^{t}BuC_6H_4
2.29 R = *o*-$CF_3C_6H_4$
2.30 R = *o*-{C(Me)=CH_2}C_6H_4

Equation 2.3

Applying the same conditions to P{CH_2N(H)R}$_4$Cl salts with *p*–R$C_6H_4NH_2$ (R = Me, **2.8**; R = ^{i}Pr, **2.9**; R = F, **2.10** and R = Et, **2.11**) did not give P{CH_2N(H)R}$_3$ ligands but cyclic R(H)NCH_2P{$(CH_2)_3(NR)_2$} (R = *p*–MeC_6H_4, **2.16**; R = *p*–^{i}PrC_6H_4, **2.17**; R = *p*–FC_6H_4, **2.18** and R = *p*–EtC_6H_4, **2.19**) ligands (Eqn. 2.2). Aminophosphonium salts with *ortho* (**2.5**) and *para*–FC_6H_4 (**2.10**) on the nitrogen, only lead to the diazaphosphorinanes **2.15** and **2.18** respectively even adding KO^{t}Bu in different ratios (from approx. 1:1 to 1:4).

In the procedure proposed here, KO^{t}Bu was used in excess to achieve **2.26** – **2.30**. However, whereas **2.26** required four equivs. of base to achieve comparable results to those in the literature in terms of yield and purity (based on ^{31}P{^{1}H} NMR); **2.27** – **2.30** only necessitated *ca*. 1.5 equivs of base. Due to the excess of K^{t}BuO used, ligands **2.26**, **2.27** and **2.29** present 2, 1.5 and 1.25 mols of KCl according to EA respectively (see Experimental Section). Attempts to remove KCl by washing compounds **2.26**, **2.27** and **2.29** with methanol were unsuccessful.

The ^{31}P{^{1}H} spectra showed a singlet at *ca*. –32.0 ppm (δP –31.8 ppm, **2.26**; δP –33.2 ppm, **2.27**; δP –31.1 ppm, **2.28**; δP –31.4 ppm, **2.29** and –32.4 ppm, **2.30**) which are comparable with δP shifts for P{CH_2N(H)R}$_3$ [R = C_6H_5, **1.152** (δP –32.6 ppm)[2]; *m,m*–$Me_2C_6H_3$, **1.153** (δP –29.6 ppm)[2]; *m,m*–$CF_3C_6H_3$, **1.154** (δP –32.1 ppm)[2]; *o*–$(CO_2Me)C_6H_4$, **1.192**, (δP –33.6 ppm)[3]]. Similar to ligands **2.12** – **2.19**, the δP shifts of **2.26** – **2.30** are solvent dependant [Δδ*P ca.* 7 ppm downfield in $CDCl_3$ with respect to $(CD_3)_2SO$], *e.g.* the ^{31}P{^{1}H} for **2.26** in $CDCl_3$ appeared at δP –31.8 ppm whereas in $(CD_3)_2SO$ at δP –38.5 ppm. Furthermore, the phosphines were found to be air stable in the solid state although they oxidise slowly overtime in solution. To assign unknown peaks observed in the P(V) region of the spectra, a $CDCl_3$ solution of **2.26**, **2.27** and **2.29** was

treated with an excess of aqueous H_2O_2 in NMR scale (Eqn. 2.4). The $^{31}P\{^1H\}$ spectra showed a singlet at δP 46.0, 45.5 and 45.6 ppm for **2.26a**, **2.27a** and **2.29a** respectively, using H_2O_2 and at δP 44.8, 45.7 and 45.7 ppm for **2.25a**, **2.28a** and **2.30a** over time in $CDCl_3$. No attempts to prepare **2.26a** – **2.30a** on a preparative scale were made.

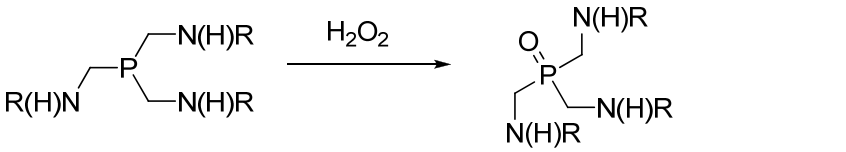

2.26 R = C_6H_5
2.25 R = *o*-MeC_6H_4
2.27 R = *o*-$^iPrC_6H_4$
2.28 R = *o*-$^tBuC_6H_4$
2.29 R = *o*-$CF_3C_6H_4$
2.30 R = *o*-{C(Me)=CH_2}C_6H_4

2.26a R = C_6H_5
2.25a R = *o*-MeC_6H_4
2.27a R = *o*-$^iPrC_6H_4$
2.28a R = *o*-$^tBuC_6H_4$
2.29a R = *o*-$CF_3C_6H_4$
2.30a R = *o*-{C(Me)=CH_2}C_6H_4

Equation 2.4

Since linear phosphines **2.26** and **2.27** and their cyclic analogues **2.12** and **2.14** were successfully obtained, **2.26** and **2.27** were used to acces **2.12** and **2.14** (Eqn. 2.5). Hence, **2.20** was reacted with $(CH_2O)_n$ for up to 4 d in refluxing MeOH, with fairly good conversion (approx. 43% according $^{31}P\{^1H\}$ NMR). Compound **2.27** was reacted with $(CH_2O)_n$ under the same conditions as **2.26** and because no solid precipitated, the solution was kept at r.t. until large block colourless crystals appeared. The $^{31}P\{^1H\}$ NMR showed one peak at δP –45.1 ppm corresponding to **2.14**. It should be mentioned that also large block crystals were deposited overtime when **2.26** was heated in methanol and then kept at r.t. These observations indicate that the role of $(CH_2O)_n$ in the formation of **2.14** by this method is still not clear and crystals of **2.14** could be formed simply by lowering the temperature slowly without $(CH_2O)_n$ overtime.

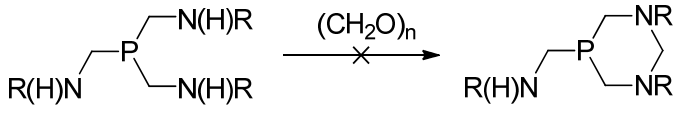

2.26 R = C_6H_5
2.27 R = *o*-$^iPrC_6H_4$

2.12 R = C_6H_5
2.14 R = *o*-$^iPrC_6H_4$

Equation 2.5

^1H NMR spectra of **2.26 – 2.30** run in $CDCl_3$, showed a doublet or a broad singlet between *ca.* 3.42 and 3.99 ppm assigned to the six protons of PCH_2N. The N*H* protons resonated at

lower field around 4.30 ppm in **2.28**, **2.29** and in **2.30**. Despite the aminic protons were not observed in $CDCl_3$ for **2.26** and **2.27**, they appeared as a triplet at 5.5 ppm ($^2J_{HH}$ = 7.0 Hz) in $(CD_3)_2SO$ for **2.27** and the IR shows νNH stretches between 3285 – 3481 cm^{-1} for **2.26** – **2.30**.

2.6 X–ray structures of 2.27 and 2.29a

Crystals of tertiary phosphine **2.27** and tertiary phosphine oxide **2.29a** were obtained from the methanol filtrate of the reactions to get **2.27** or **2.29** respectively, and allowed to stand for > 24 h (Fig. 2.12). Crystal structure of compounds with the formula $P\{CH_2N(H)R\}_3$ are not abundant in the literature and only two examples with R = *m*,*m*–$(CF_3)_2C_6H_3$ (**1.154)** and R = *o*-$CO_2MeC_6H_4$ (**1.192**) have been reported before.[2,3] P–C bond lengths [average αC–P(1), αC = C bound to P(1)] and C–P–C angles for **2.27** and **2.29a** are in agreement with those in the literature (Table 2.5).[2,3]

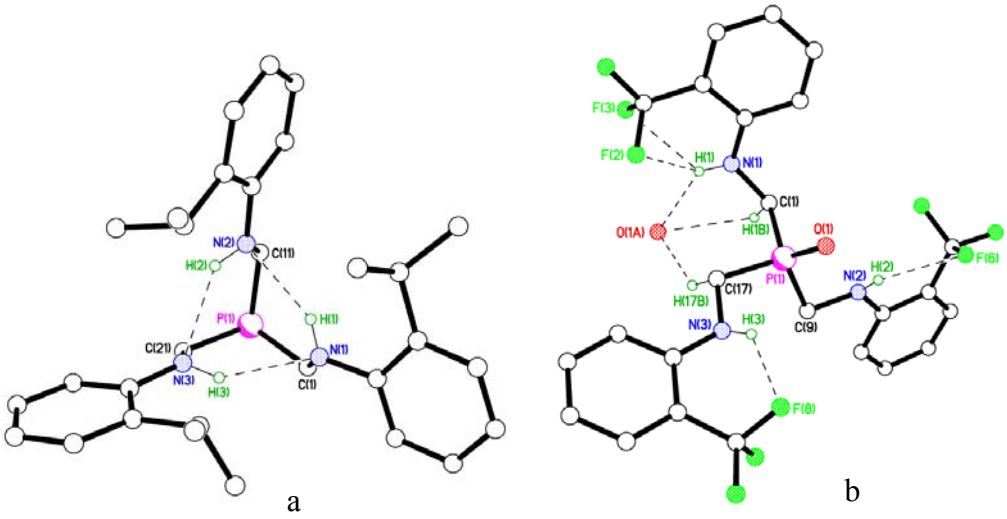

Figure 2.12 X–ray structure of a) tertiary phosphine **2.27** and b) tertiary phosphine oxide **2.29a**. All H atoms except those involved in H–bonds are removed for clarity.

Table 2.5 Selected bond lengths (Å) and angles (°) for **2.27** and **2.29a**.[a]

	2.27	**2.29a**
av.[αC–P(1)][b]	1.845(2)	1.8125(16)
av.[αC–P(1)–αC][c]	102.55(9)	105.90(8)
av.[P(1)–αC–N(X)][d]	116.56(14)	108.77(11)

[a] Estimated standard deviations in parentheses. [b] Average value of αC–P, αC = C bound to P. [c] Average value of αC–P(1)–αC, αC = C bound to P(1). [d] Average value of P(1)–αC–N(X), αC = C bound to P and N(X) = N(1), N(2) or N(3).

Comparison of the structure of tertiary phosphine oxide **2.29a** with **2.27** reveals that the average P–C bond length of **2.29a** is shorter by 0.033 Å, and the sum of C–P–C angles is wider by about 10° [317.69(8)° for **2.29a** and 307.65(9)° for **2.27**]. Closer values of C–P–C bond angles have been reported for selenium chalcogenides S=P{$CH_2N(H)R$}$_3$ (R = *m,m*-$Me_2C_6H_3$, **1.178**) [319.79(12)°].[4] This difference correlates with the larger covalent radii of P(III) compared to P(V) as well as larger repulsion of the lone pair on P(III) versus P=O bond [1.4887(11) Å]. On the other hand, intramolecular N–H···F bonds may affect to alter this value for **2.29a** (Table 2.5). Due to N···F bonds lengths in **2.29a**, NH protons do not show the N···N H–bonds observed in **2.27** between N(1)···N(2) [2.973(2) Å], N(2)···N(3) [2.977(2) Å], N(3)···N(1) [3.007(2) Å] (Fig. 2.12, Table 2.6). Hydrogen–bonds between the aminic proton and the donor atom in the *ortho*–aniline was documented in the previously proposed X–ray structure of P{CH_2NH(*o*-CO_2Me)}$_3$ **1.192**.[3]

Table 2.6 Hydrogen–bond parameter (Å, º) for **2.27** and **2.29a**.[a]

	D–H···A	D—H	H···A	D···A	D—H···A
2.27	N(1)–H(1)···N(2)	0.91(2)	2.18(2)	2.973(2)	145(2)
	N(2)–H(2)···N(3)	0.92(2)	2.22(2)	2.977(2)	138(2)
	N(3)–H(3)···N(1)	0.93(2)	2.22(2)	3.007(2)	142(2)
2.29a	N(1)–H(1)···F(3)	0.847(19)	2.360(19)	2.9205(18)	124.2(16)
	N(1)–H(1)···F(2)	0.847(19)	2.533(18)	2.9374(19)	110.4(15)
	N(2)–H(2)···F(6)	0.84(2)	2.28(2)	2.8854(18)	129.2(17)
	N(3)–H(3)···F(8)	0.814(19)	2.208(19)	2.8030(16)	130.1(17)
	C(1)–H(1B)···O(1A)	0.99	2.50	3.0548(19)	115
	N(1)–H(1)···O(1A)	0.847(19)	2.238(19)	2.9073(18)	136.0(16)
	C(17)–H(17B)···O(1A)	0.99	2.48	3.2652(19)	136

[a] Estimated standard deviations in parentheses. [b] Symmetry operations for equivalent atoms A: $-x+1, y-1/2, -z+1/2$.

2.7 Synthesis of aminomethylphosphines 2.31 – 2.34

The synthesis of bicyclics {$P(CH_2)_2NR$}$_2$ (R = C_6H_5, **1.390** and R = *p*-MeC_6H_4, **1.392**) was previously reported (See section 1.3.2.3, Sch. 1.37, Eqn. 1.20).[26,89] Whereas **1.390** was obtained as a result of disproportionation of THPC with $C_6H_5NH_2$ in isolated yields up to

44%, **1.392** was formed as a co–product of the electrochemical oxidation of **2.16** in up to 14%.

In the procedure proposed here, compounds **2.31** – **2.34** were synthesised from the respective phosphonium salts **2.1**, **2.8**, **2.9** and **2.11** with 0.5 equiv. of KO^{t}Bu in MeOH for 15 min in isolated yield up to 22% (Eqn. 2.6). Phosphonium salts **2.2**, **2.3** and **2.6** were treated with 0.5 equiv. of KO^{t}Bu under the same reaction conditions to give unreacted phosphonium salts according to $^{31}P\{^1H\}$ NMR. This indicates that *ortho* substituents on the aniline do not permit formation of the bicyclic $\{P(CH_2)_2NR\}_2$ presumably because of the steric impact of the Me, ^{i}Pr and CF_3 groups.

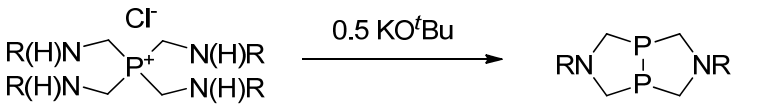

2.1 R = C_6H_5
2.8 R = *p*-MeC_6H_4
2.9 R= *p*-^{i}PrC_6H_4
2.11 R = *p*-EtC_6H_4

2.31 R = C_6H_5
2.32 R = *p*-MeC_6H_4
2.33 R= *p*-^{i}PrC_6H_4
2.34 R = *p*-EtC_6H_4

Equation 2.6

As would be expected, both phosphorus centres in **2.31** – **2.34** are equivalent and hence, a major peak was observed in the $^{31}P\{^1H\}$ NMR (δP –36.0, –35.8, –35.9 and –35.8 ppm respectively). Nevertheless, these values differs by *ca*. 10 ppm from the shift of the analogous $\{P(CH_2)_3\}_2$ (**1.370)** (δP –27.8 ppm) without any heteroatom present in both rings.

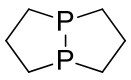

$\{P(CH_2)_3\}_2$

The similar shifts for diphosphines **2.31** – **2.34** indicate that substituents on nitrogen have a negligible effect on the basicity of the phosphine. The $^{31}P\{^1H\}$ NMR of compound **2.31** was run in $(CD_3)_2SO$, $CDCl_3$ and DMF and in all cases the spectra showed a singlet at approximately –36.0 ppm (as previously reported in DMF) proving that the chemical shift of **2.31** is not solvent dependant. The $^{31}P\{^1H\}$ NMR of **2.32** and **2.34** exhibited several resonances. Compound **2.32** was observed along with **2.16** and the diphosphine **2.21** (–47.4 ppm) (Sec. 2.6) in approx. 2:3.5:1 ratios by $^{31}P\{^1H\}$ NMR. Likewise, compound **2.34**

was observed as the major peak (22 % by $^{31}P\{^{1}H\}$ NMR) along with **2.19** (14 % by $^{31}P\{^{1}H\}$ NMR). The formation of both species **2.34** and **2.19** was supported by MS and IR. The MS of **2.34** showed not only the fragmentation pattern for **2.34** (m/z $[MH]^+$ 357) but also the mass to charge ratio for $[p\text{–}EtC_6H_4NH_3]^{2+}$ 122 and $[p\text{–}EtC_6H_4NHCH_2]^{2+}$ 144 resulted from loss of one aniline from the phosphonium salt **2.11**.

Several unsuccessful attempts were tried to purify **2.32** and **2.34**. However, **2.32** was isolated and fully characterised in better yield than reported (42% against 14%). It was obtained from the filtrate of the reaction between THP and $p\text{–}MeC_6H_4NH_2$ (Eqn. 2.7) trying to synthesise **2.35** which will be explained in more detail in Section 2.9.

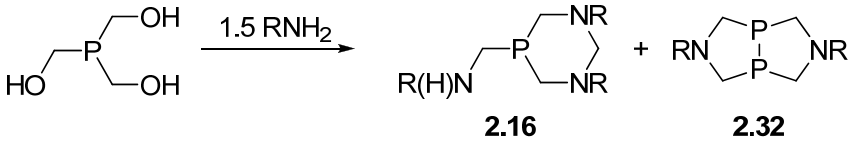

2.16 **2.32**

R = *p*-MeC_6H_4

Equation 2.7

To improve the yield of **2.31 – 2.34**, the reaction was carried out between 15 min and 3 d and from 20°C to 70°C without any change in the $^{31}P\{^{1}H\}$ NMR. The reaction time, low yield and NMR studies suggest that **2.31** – **2.34** are the kinetic product of the reaction. To prove it, same reaction conditions (MeOH, 0.5 equiv. of KO^{t}Bu) were applied to **2.1**, **2.8**, **2.9** and **2.11** but at –20°C for 12 h. A mixture of P(V) and P(III) compounds in different ratios was observed in the $^{31}P\{^{1}H\}$ NMR of **2.31** [**2.1**:THPC:**2.31**:**2.31a**, approx. 3:4:7:8:1], **2.32** [**2.8**:**2.32**:**2.16**:**2.21**, approx. 2:1.5:37:10], **2.33** [**2.9**:THPC:**2.33**:**2.17**, approx. 1:1.25:3:3] and **2.34** [THPC:**2.34**:**2.19**:**2.34a**, approx. 1:2.5:7:5] which demonstrates that the low temperature, but not time, affects the synthesis of **2.31** – **2.34**.

It has been reported in the literature that attempts to prepare chalcogenide derivatives of **2.31** were unsuccessful.[26] However, the $^{31}P\{^{1}H\}$ NMR of **2.31** – **2.34** over time exhibits two doublets at *ca*. 99.0 and –84.0 ppm which were assigned to the monooxide derivatives **2.31a** [δP 98.9, –84.1 ppm ($^1J_{PP}$ = 182 Hz)], **2.32a** [δP 99.4, –84.3 ppm ($^1J_{PP}$ = 181 Hz)], **2.33a** [δP 99.9, –83.6 ppm ($^1J_{PP}$ = 182 Hz)] and **2.34a** [δP 100.1, –83.4 ppm ($^1J_{PP}$ = 181 Hz)] (Eqn. 2.8). These shifts are in agreement with those observed for analogous bicyclic $OP_2(C_6H_{10})_2$, **1.374**, [δP 82.1, –84.9 ppm ($^1J_{PP}$ = 217 Hz)] and for $\{P(CH_2)_6PBz\}Br$, **1.395**, [δP 86.1, –54.2 ppm, ($^1J_{PP}$ = 250 Hz)] (See Schs. 1.35 and 1.38 respectively).[85,88]

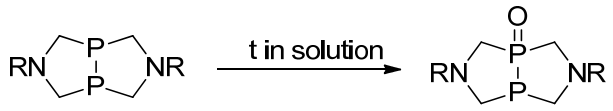

2.31 R = C_6H_5
2.32 R = *p*-MeC_6H_4
2.33 R= *p*-$^{i}PrC_6H_4$
2.34 R = *p*-EtC_6H_4

2.31a R = C_6H_5
2.32a R = *p*-MeC_6H_4
2.33a R= *p*-$^{i}PrC_6H_4$
2.34a R = *p*-EtC_6H_4

Equation 2.8

The PCH_2N protons in **2.31** would be expected to be equivalent however the ^{1}H NMR showed a doublet at 3.64 ppm ($^{2}J_{HH}$ = 12.4 Hz) and a virtual quartet at 3.45 ppm (Fig. 2.13 a) which appeared as a doublet ($^{2}J_{HH}$ = 12.4 Hz) once protons were decoupled to phosphorus (Fig. 2.13 b). This splitting pattern should be analysed in conjunction with X–ray studies, which showed a distorted structure where protons are not eclipsed and therefore they are not equivalent (Fig. 2.14 a and b). In contrast, PCH_2C protons in bicyclic compounds $[(CH_2)_nP]_2$ (**1.371 – 1.373**) were observed as multiplets.

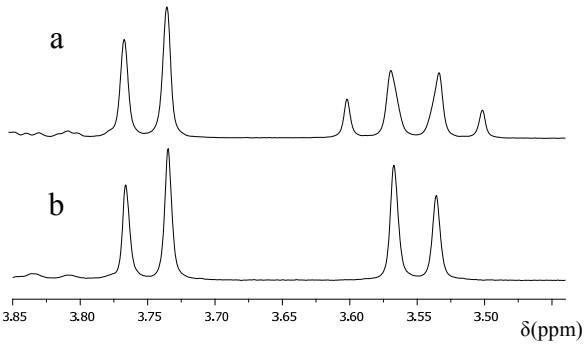

Figure 2.13 Selected region of a) ^{1}H NMR and b) $^{1}H\{^{31}P\}$ for **2.31**.

2.8 X–ray structure of 2.31

Further unambiguous confirmation of the structure of **2.31** was supported by single X–ray crystallography. Suitable crystals were grown by slow evaporation of the MeOH filtrate from the reaction between **2.1** and 0.5 equiv. of KO^{t}Bu. Selected bond lengths and angles are given in Table 2.7 and the molecular structure is shown in Figures 2.14 a and b. Compound **2.31** was found to adopt a distorted five–membered heterobicycled P–P structure in a 2–*cis*–*anti*–*anti* conformation (See Fig. 1.20) where both lone pair of

electrons on phosphorus are in axial position (five–membered ring are in *cis* arrangement) and the substituents on the nitrogen are *anti* to the unshared phosphorus lone pair (Fig. 2.14). No other crystal structure of the type of $\{P(CXC)_3\}_2$ where X = N has previously been reported, therefore **2.31** is the first example of its kind. Nevertheless, there are examples of X–ray structures with X = Si as illustrated in Figure 2.15 a[102] ($\{P(CH_2)C(H)Si(CH_3)_3Si\}_2$) or X = H_2CCH_2, **1.371**[87] in Figure 2.15 b. Whereas the silicon compound (Fig. 2.15 a) shows an overall distorted structure similar as in **2.31**, compound **1.371** is symmetric; but in all cases, the fused rings are *cis* to each other leaving the phosphorus lone pair in the same orientation and potentially suited for future coordination studies. The P(1)–P(2) bond length [2.191(7) Å] is in concordance with a P–P single bond (2.1 – 2.2 Å)[85,87,88,103] and significantly shorter than P–P distance for silicon compound (2.229 Å).[102] The C–P [average αC–αP, αC = C bound to P(1) or P(2) and αP = P(1) or P(2)], C–N [average αC–αN, αC = C bound to N(1) or N(2) and αN = N(1) or N(2)], C–P–C and P–C–N bond angles are also comparable with PCNCP compounds found in the literature.[104]

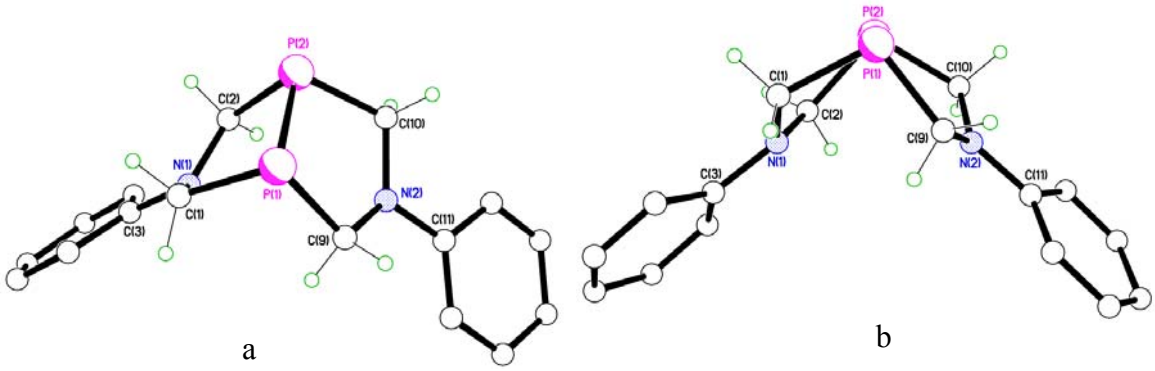

Figure 2.14 X–ray structure of **2.31** a) through the P–P bond and b) along the P–P bond. All H atoms except those on N and αC are removed for clarity.

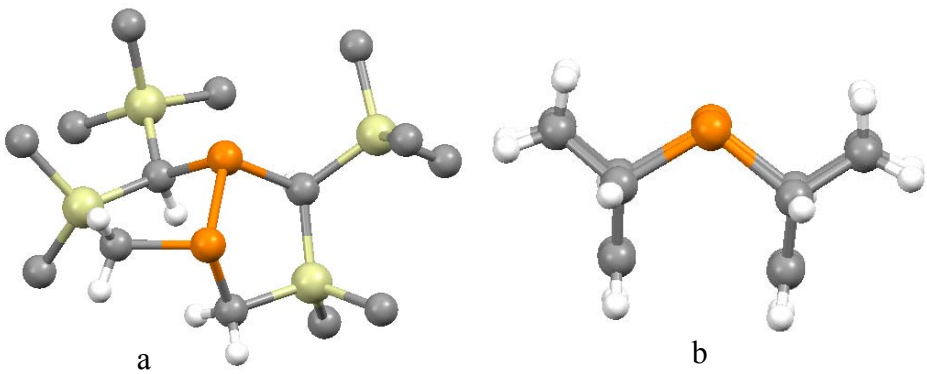

Figure 2.15 X–ray structures of a) $\{P(CH_2)C(H)Si(CH_3)_3Si\}_2$ through the P–P bond and b) **1.371** along the P–P bond. H on CH_3 in $\{P(CH_2)C(H)Si(CH_3)_3Si\}_2$ are omitted for clarity.

Table 2.7 Selected bond lengths (Å) and angles (°) for **2.31**.[a]

2.31			
P(1)–P(2)	2.191(7)	C(9)–N(2)–C(10)	118.9(13)
av.[αC–αP][b]	1.840(16)	N(1)–C(1)–P(1)	108.7(12)
av.[αC–αN][c]	1.437(19)	N(1)–C(2)–P(2)	113.1(12)
C(1)–P(1)–C(9)	100.5(8)	N(2)–C(9)–P(1)	113.5(12)
C(2)–P(2)–C(10)	100.8(7)	N(2)–C(10)–P(2)	112.1(12)
C(1)–N(1)–C(2)	118.1(14)		

[a] Estimated standard deviations in parentheses. [b] Average αC–αP, αC = C bound to P(1) or P(2) and αP = P(1) or P(2). [c] Average αC–αN, αC = C bound to N(1) or N(2) and αN = N(1) or N(2).

2.9 Synthesis and characterisation of 2.35

A novel bicyclic diphosphine O=P{$CH_2N(R)CH_2$}$_3$P=O (R = *p*-MeC_6H_4) **2.35** was obtained as a crystalline solid from the filtrate of the reaction between diazaphosphorinane **2.16** and Ph_2PCH_2OH (Eqn. 2.9). This new aminomethylphosphine possesses three CNC intrabridgehead groups between two phosphorus centres which is the first example of a bicyclic compound with a P{$CH_2N(R)CH_2$}$_3$P backbone.

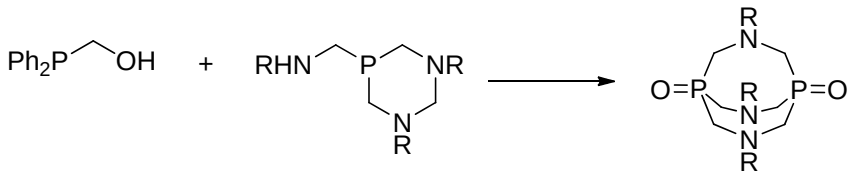

2.16 **2.35**

R = *p*-MeC_6H_4

Equation 2.9

Compound **2.35** was characterised by single X–ray spectroscopy but unfortunately full characterisation was not possible due to the small amount of crystals collected. In order to overcome this issue and obtain **2.35**, a retrosynthetic route using THP and *p*-$MeC_6H_4NH_2$ as starting materials was proposed (Sch. 2.1). The target diphosphine may be achieved from its reduced analogue **2.35a** (pathway **A1**), previously synthesised from THP and *p*-$MeC_6H_4NH_2$ (2:3 molar ratio) (pathway **A2**) or from THP and **2.36** (1:1) (pathway **B1**) which would be obtained from one equiv. of THP and three equivs. of *p*-$MeC_6H_4NH_2$

(pathway **B2**). On the other hand, since **2.35** possess two oxidised phosphorus centres, may be synthesised directly from $O=P(CH_2OH)_3$ (THPO) and *p*-$MeC_6H_4NH_2$ (2:3) (pathway **C1**) previously oxidising THP to THPO (pathway **C2**).

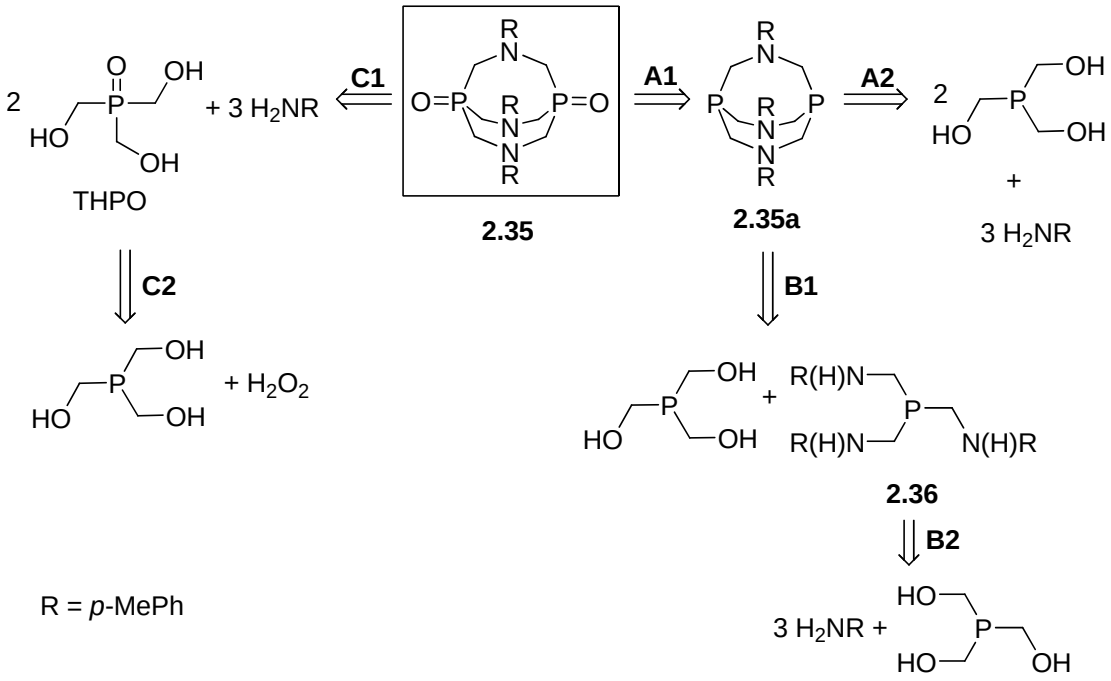

Scheme 2.1 Retrosynthetic approach to **2.35**.

With this retrosynthetic route in mind, three different syntheses were tried to obtain the desired diphosphine **2.35**. In the first method (pathway **A2** in Sch. 2.1), two equivs. of THP were added to three equivs. of *p*-$MeC_6H_4NH_2$ in methanol for 4 h at r.t. (Sch. 2.2). The colourless powder obtained after filtration revealed a peak at δP –41.4 ppm, in the $^{31}P\{^1H\}$ NMR spectrum, corresponding to **2.16** instead of the desired product **2.35a**. This is not unexpected since it has been shown that reaction between THP and *p*-anilines tends to form cyclic diazaphosphorinanes.[38,39,55] The filtrate was stored at low temperature and colourless needles were deposited overtime which were assigned to the P–P diphosphine previously discussed **2.32** (δP –35.8 ppm) according to $^{31}P\{^1H\}$ NMR.

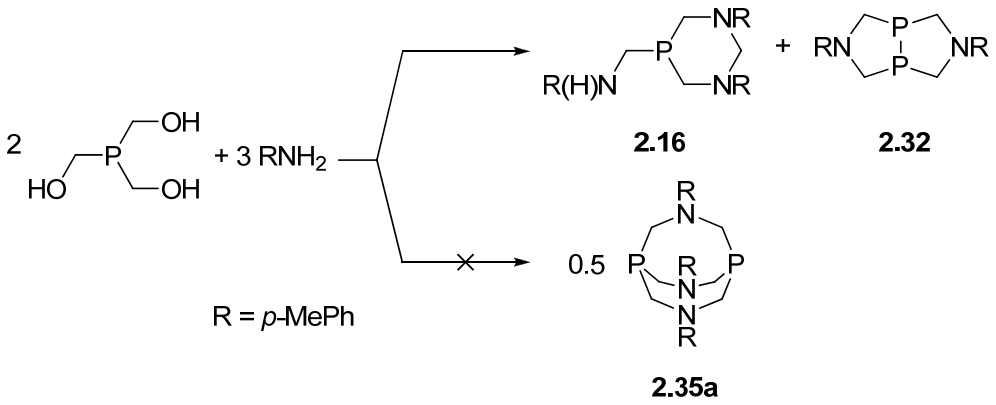

Scheme 2.2 Attempted synthesis of **2.35a**.

An alternative route (pathway **B1** in Sch. 2.1) was proposed which required the previous synthesis of the linear tertiary phosphine $P\{CH_2N(H)(p\text{-}MeC_6H_4)\}_3$ **2.36** (pathway **B2** in Sch. 2.1) (Sch. 2.3). The synthesis of trisaminomethylphosphines from THP was reported before but only satisfactorily with *ortho* and *meta*–anilines.[23] In addition, it was discussed in section 2.5 that the synthesis of linear aminomethylphosphines from phosphonium chloride containing *para*-anilines was not possible. Therefore, when one equuiv. of THP reacted with three equivs. of $p\text{-}MeC_6H_4NH_2$, no traces of the linear **2.36** were observed in the $^{31}P\{^1H\}$ NMR and only **2.16** was synthesised even without $(CH_2O)_n$.

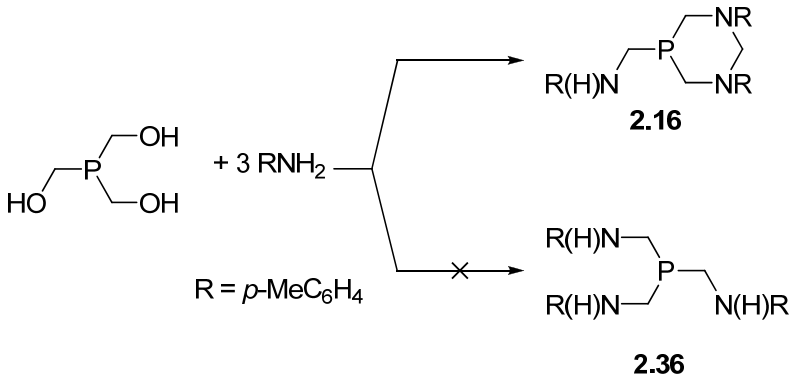

Scheme 2.3 Attempted synthesis of trisaminomethylphosphine **2.36**.

A different approach was tried from $p\text{-}MeC_6H_4NH_2$ and THPO (pathway **C1** in Sch. 2.1), readily formed from THP and an excess of H_2O_2 (pathway **C2** in Sch. 2.1) (Sch. 2.4). Two equivs. of THPO were reacted with three equivs. of $p\text{-}MeC_6H_4NH_2$ in either MeOH or C_7H_8 overnight at rt. under aerobic conditions (Sch. 2.4).

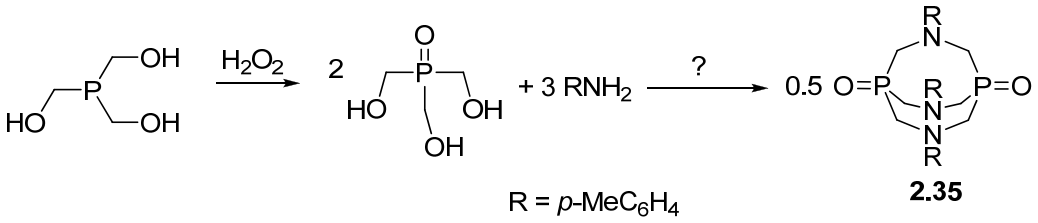

Scheme 2.4 Attempted synthesis of **2.35** using THPO.

The product was collected by filtration and the $^{31}P\{^{1}H\}$ NMR showed two major peaks at δP 49.0 and δP 49.8 ppm in D_2O in approx. 3:1 molar ratio. These values do not differ significantly from THPO (49.0 ppm, D_2O) nevertheless the chemical shift of **2.35** not necessarily has to be different and there are not similar compounds in the literature to compare with. The ^{1}H NMR spectrum showed the same peaks at 4.72 (OH) and 4.05 ppm ($^{2}J_{PH}$ = 1.3 Hz, PCH_2O) than for THPO besides the resonances corresponding to unreacted amine. However there were two doublets close to the doublet for PCH_2O protons at 4.00 ($^{2}J_{PH}$ = 1.0 Hz) and 3.70 ppm ($^{2}J_{PH}$ = 2.1 Hz) that could be related to the unknown minor peak observed in the ^{31}P NMR at 49.8 ppm (approx. 1:3). This indicates that an unknown P(V) compound with PCH_2– moiety was obtained by this method according to $^{31}P\{^{1}H\}$ and ^{1}H NMR. Nevertheless, the similarities between the spectra of the product and the starting material and the work of Tyler *at al.*[10] that demonstrates that the lone pair on phosphorus have to be available for the Mannich reaction to occur, suggests that reaction was not successful and further work is required.

A plausible synthesis of **2.35a** (and therefore **2.35**) could be achieved from diphosphacyclooctane **2.40** in a similar manner as **1.398** was achieved from the 8–membered ring diphosphine **1.396** (Sch. 2.5).[90] The synthesis of **1.398** involved two steps, but **2.40** has the advantage of incorporating an amine on phosphorus which would permit a nucleophilic attack of the nitrogen to the alpha carbon to the amine in a single step without other reagents. This elimination was previously suggested for the synthesis of Pt(II) and Pd(II) chelate complexes.[16] Hence, it would be a potential mechanism for the synthesis of a wide range of compounds of the type of **2.35a** simply by tuning the substituents on nitrogen as illustrated in Scheme 2.5.

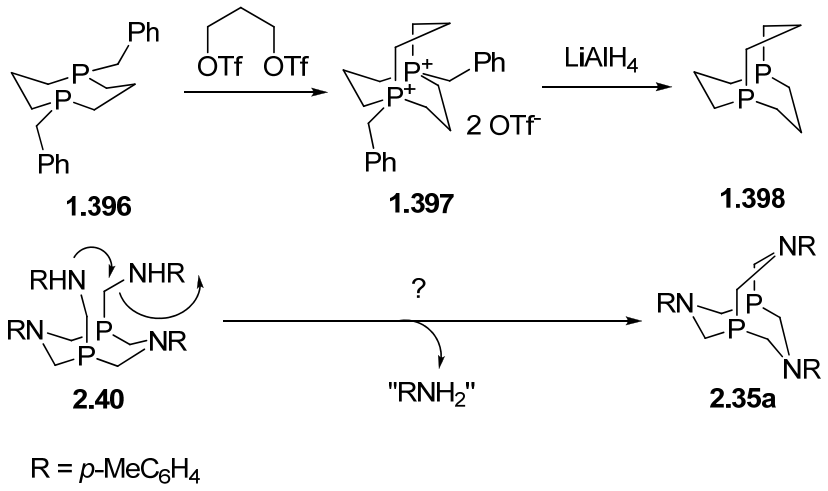

Scheme 2.5 Synthesis of **1.398** and the proposed route for **2.35a**.

2.10 X–ray structure of 2.35

Suitable crystals of **2.35**, for single crystal X–ray diffraction, were grown from a MeOH filtrate of the reaction between **2.16** and Ph_2PCH_2OH (Fig. 2.16).

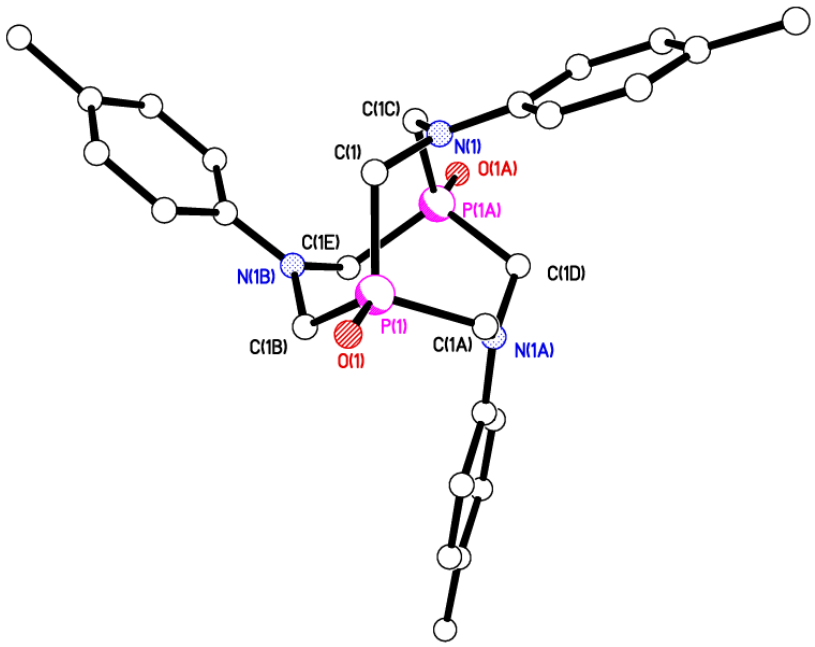

Figure 2.16 X–ray structure of **2.35**. All H atoms and one $CHCl_3$ solvent molecule are removed for clarity. The structure was generated by symmetry operations for equivalent atoms A: $x, y, -z + 3/2$.

The diphosphine oxide **2.35** adopts an *out*,*out*–conformation (Fig. 2.17 a) similar to that of $P(CH_2)_3P$ **1.398** (Figure 2.17 b).[90] Overall both structures show a paddle wheel arrangement around the cage (Fig. 2.18 a and b).

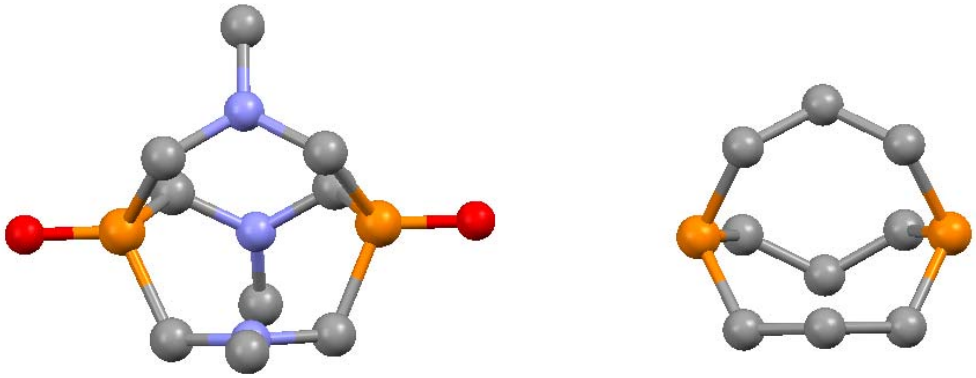

a b

Figure 2.17 X–ray structure of a) **2.35**, where *p*-MeC_6H_4 atoms except C_{ipso} to N were omitted for clarity, and b) **1.398**.

All P–C bond lengths are equal, as are the P–C–N and C–P–C bond angles, owing to the crystallographic symmetry which eclipses the $P(–C–N)_3$ units in **2.35** (Fig. 2.18 a) as PC_3 in $P(CH_2)_3P$ **1.398** (Fig. 2.18 b). Selected bond lengths and angles are summarised in Table 2.8.

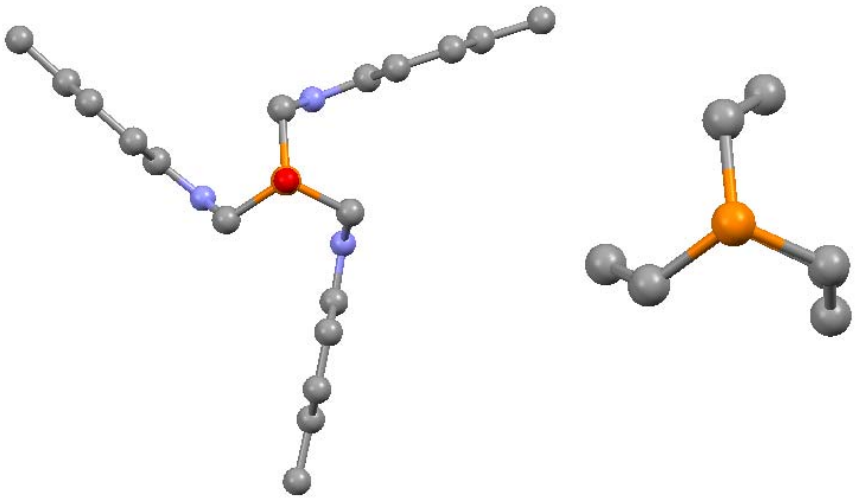

a b

Figure 2.18 X–ray structures of a) **2.35** and b) **1.398** viewed along the non–bonded P···P.

Table 2.8 Selected bond lengths (Å) and angles (°) for **2.35**.[a,b]

2.35			
P(1)–O(1)	1.483(3)	C(1)–P(1)–C(1C)	105.61(7)
P(1)–C(1)	1.8494(19)	N(1)–C(1)–P(1)	116.64(15)
N(1)–C(1)	1.453(2)	O(1)–P(1)–C(1)	113.10(6)
		C(1)–N(1)–C(1A)	117.0(2)

[a] Estimated standard deviations in parentheses. [b] Symmetry operations for equivalent atoms A: *x*, *y*, –*z*+3/2.

The non–bonded P···P distance [3.929 Å] is larger than the normal P–P single bond [2.21 Å] and greater than that seen in **2.31** [2.191(7) Å] but slightly shorter in comparison to $P(CH_2)_3P$ **1.398** [4.073(1) Å].[90] The sum of the angles formed by C–P–C in **2.35** [316.0(7)°] is wider by *ca.* 15° with respect to the P–P diphosphine **2.31** [301.8(7)°] and nearly identical to $P(CH_2)_3P$ **1.398** [317.8(2)°] and the mono tris(aminomethyl)phosphophosphine oxide **2.29a** [317.69(8)°]. This indicates that C–P–C angles are negligible affected by oxygen lone pairs but the strain of the P–P intrabridgehead has an impact on their parameters. In contrast, the P–C–N bond angles in **2.35** [116.64(15)°] are significantly smaller than P–C–C for $P(CH_2)_3P$ **1.398** [123.0(2)° in average]. Likewise, C–N–C bond angles in **2.35** [117.0(2)°] are slightly smaller than C–C–C in $P(CH_2)_3P$ **1.398** [118.1(3)° in average] and C–N–C bond angles in **2.31** [118.5(14)°]. Hence, replacing carbon by nitrogen has a smaller effect on the magnitude of the bond angles than the P(III) versus P(V) oxidation states. On the other hand, the P=O distance [1.483(3) Å] and C–P–C bond angles are comparable with $O=PMe_3$ [1.489(6) Å, 105.8(3)°] and $O=P(CH_2NMe)_3P$ **1.402** [1.485(4) Å and 102.38(12)°]. P–C [1.8494(19) Å] and C–N bond lengths are in agreement with those for ligands **2.12**, **2.14**, **2.16**, **2.17**, **2.19**, **2.27**, **2.29a** and **2.31** and in accordance with those in the literature (Tables 2.4, 2.5, 2.7).[17,18,59,90,105]

Both diphosphines **2.35** and **1.398** adopt an *out*,*out*–disposition and PCN_3– and PC_3– units are eclipsed respectively, although the supramolecular structures are highly different. Figure 2.19 highlights the packing plot of **2.35** versus of **1.398** along the *c*–axis. This organisation may be due to the intermolecular H–bonds between the **2.35** and the solvent [C(1)–H(1B)···Cl(1E) 3.534(2) Å and 118°; C(7)–H(7)···O(1D) 3.166(3) Å and 129°] (Symmetry codes: D: *x*–*y*, *x*, –*z*+1; E: *x*, *y*, –*z*+1/2).

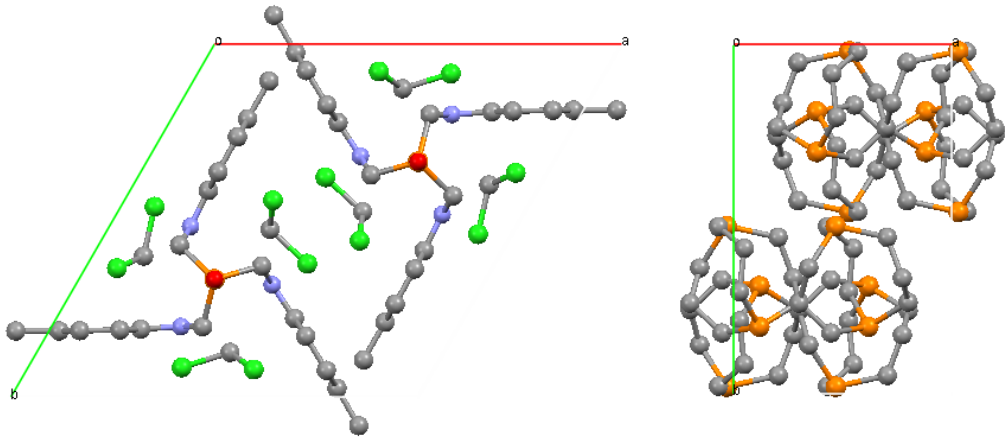

a b

Figure 2.19 X–ray packing plot of a) **2.35** and b) **1.398** along the *c*–axis.

2.11 Reactivity of ligands 2.12, 2.14, 2.15, 2.16 and 2.18 towards Ph_2PCH_2OH

Our research group has been interested in developing new symmetric and nonsymmetric PCNCP aminomethylphosphines using phosphorus based Mannich condensation reactions.[7,12,13] Nonsymmetric tertiary phosphines are less studied so previous research was undertaken to synthesised these phosphines, such as $Ph_2PCH_2N(R)CH_2PCg$ (R = C_6H_5, **1.249** and R = *p*-MeC_6H_4, **1.250**). They were afforded from the secondary amine $HN(R)CH_2PCg$ and Ph_2PCH_2OH in equimolar quantities. Hence, with the aim of expanding the library of nonsymmetric PCNCP aminomethylphosphines, the reactivity of secondary amines **2.12**, **2.14**, **2.15**, **2.16** and **2.18** was explored against Ph_2PCH_2OH to afford the novel PCNCP ligands incorporating $[(CH_2)_3(NR)_2]P$– backbones (R = C_6H_5, **2.36**; R = *o*-$^{i}PrC_6H_4$, **2.37**; R = *o*-FC_6H_4, **2.38**; R = *p*-MeC_6H_4, **2.39** and R = *p*-FC_6H_4, **2.40**) (Eqn. 2.10). The reactions between diazaphosphorinanes **2.12**, **2.14** and **2.15** with Ph_2PCH_2OH led to a mixture of phosphorus compounds according to the $^{31}P\{^{1}H\}$ NMR which some of them were identified as PCN and PCNCP ligands as it is illustrated in Equation 2.10 and summarised in Table 2.9. Similarly, when **2.16** and **2.18** were treated with Ph_2PCH_2OH, the co–products displayed in Eqn. 2.10 were observed as major components and the target compounds **2.39** and **2.40** were achieved in up to 50% according to their $^{31}P\{^{1}H\}$ NMR. Due to that, the reactivity of **2.16** and **2.18** was not only

investigated in more detail than the chemistry of **2.12**, **2.14** and **2.15** but also they are representative examples of electron donor and electron withdrawing diazaphosphorinanes.

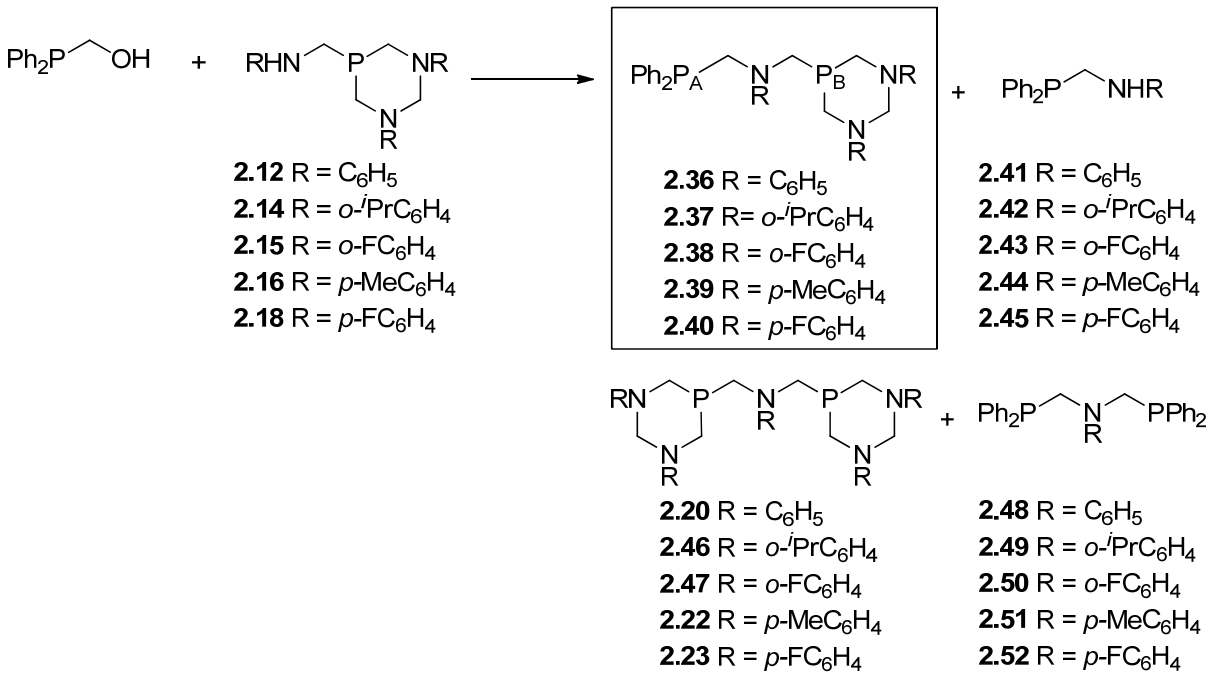

Equation 2.10

Table 2.9 summarises the reaction conditions and approx. percentages of different phosphorus compounds observed in the $^{31}P\{^{1}H\}$ NMR. The previously synthesised $Ph_2PCH_2N(R)CH_2PCg$ ligands (**1.249** and **1.250**) were obtained in MeOH at r.t. under anaerobic conditions therefore, same reaction conditions were applied here. However due to the poor solubility of **2.12**, **2.15**, **2.16** and **2.18** in MeOH at r.t, **2.12** was dissolved in hot MeOH before adding Ph_2PCH_2OH (entry 1), **2.15** and **2.16** were soluble in C_7H_8 (entries 3, 4, 5 and 6) and a mixture of MeOH:C_7H_8 (50:50) was used for **2.18** (entries 12 and 13). Even though **2.40** required 72 h at 110° to achieve a fairly good conversion (36%) (entry 13) and compound **2.37** was not observed even after 24h at r.t in MeOH (entry 2). The higher conversion to **2.39** (approx. 49%) was achieved by using C_7H_8 at 60° and to **2.40** (approx. 45%) when CH_2Cl_2 at r.t. was utilised (entries 5 and 17). In all experiment unreacted diazaphosphorinanes were observed so the number of equivalents of diazaphosphorinane used with respect to Ph_2PCH_2OH was also varied. Adding **2.18** in excess increased the proportion of **2.23** (entry 18) whereas adding less equivalents led to decrease the proportion of **2.23** (entry 19), but in both cases the amount of **2.40** remained moderated (approx. 37%).

To study the effect of solvent, time and temperature, **2.16** and **2.18** were dissolved in $CDCl_3$ and NMR spectrum was run immediately (entries 7, 8, 20 and 21). Conversions to **2.39** and **2.40** increased slightly with the temperature but the use of $CDCl_3$ instead C_7H_8, MeOH or CH_2Cl_2 has a negligible effect. It should be mentioned that albeit high temperatures increased the amount of **2.39** (entries 4, 5, and 6; 7 and 8; 9, 10 and 11), also boosted the decomposition of it and its coproducts to corresponding oxides. In contrast, compound **2.40** was not affected in such way under the same conditions (entries 15, 16, 20, 21, 22, 23 and 24).

Since the procedure was not significantly dependent on the solvent, the method was undertaken without solvents simply using a mortar and a pestle under air (entries 9, 10, 22 and 23). Surprisingly, after 5 minutes grinding **2.16** and Ph_2PCH_2OH, similar $^{31}P\{^1H\}$ NMR spectrum was observed (entry 9) than for that in C_7H_8 at 60°C (entry 5). It must be mentioned that this method generates high temperature due to the friction. However for **2.18** the conversion to **2.40** was really low (approx. 7%) and substantial amount of Ph_2PCH_2OH (approx. 35 %) and **2.18** (approx. 46%) was still present (entry 22). Luckily, the amount of **2.40** increased significantly when the mortar was preheated in the oven (entry 23) with even better conversion than the reaction under anaerobic conditions in CH_2Cl_2 (entry 17). In view of the results, products **2.39** and **2.40** were synthesised simply by melting Ph_2PCH_2OH with **2.16** and **2.18** respectively with fairly good results (entries 11 and 24). However, it is not clear if the proportion of product obtained is boosted under neat conditions due to the grinding since the characterisation ($^{31}P\{^1H\}$ NMR) method was done in solution. This may imply that grinding aids the reaction rate but this still occurs in $CDCl_3$. To overcome this issue, a first attempt of solid state NMR was run. Unfortunately, this method was unsuccessful due to the broadness of the spectrum observed. In summary, it is more than clear that temperature is necessary for the reactions to occur, and that **2.36** – **2.40** were obtained along with phosphorus coproducts under a wide range of conditions.

Table 2.9 Approximate proportion (%) of PCN and PCNCP compounds by $^{31}P\{^{1}H\}$ NMR ($CDCl_3$) under different reaction conditions.

Entry	s. m.	Solvent	T(°C)	t	P_ACNCP_B	P_ACN	$(P_BC)_2N$	$(P_AC)_2N$	P_BCN
1	**2.12**	MeOH	80	4h	30[a]	4[b]	9[c]	17[d]	2[e]
2	**2.14**	MeOH	r.t.	24h	0[f]	15[g]	0[h]	9[i]	51[j]
3	**2.15**	C_7H_8	110	24h	20[k]	15[l]	0[m]	20[n]	9[o]
4	**2.16**	C_7H_8	r.t.	24h	43[p]	2[q]	20[r]	14[s]	2[t]
5	**2.16**	C_7H_8	60	2h	*49*[p]	3[q]	20[r]	18[s]	1[t]
6	**2.16**	C_7H_8	120	24h	18[p]	4[q]	4[r]	14[s]	1[t]
7	**2.16**	neat[z]	r.t.	5min	14[p]	12[q]	32[r]	1[s]	37[t]
8	**2.16**	neat[z]	heat	5min	23[p]	6[q]	10[r]	10[s]	3[t]
9	**2.16**	neat	friction	5min	*48*[p]	7[q]	25[r]	15[s]	1[t]
10	**2.16**	neat	heat	5min	38[p]	4[q]	10[r]	23[s]	1[t]
11	**2.16**	neat	melt	5min	23[p]	7[q]	17[r]	5[s]	7[t]
12	**2.18**	$MeOH/C_7H_8$	r.t.	24h	10[u]	17[v]	1[w]	5[x]	39[y]
13	**2.18**	$MeOH/C_7H_8$	110	72h	36[u]	10[v]	21[w]	11[x]	7[y]
14	**2.18**	C_7H_8	r.t.	144h	28[u]	3[v]	14[w]	10[x]	2[y]
15	**2.18**	C_7H_8	120	4h	42[u]	6[v]	19[w]	15[x]	3[y]
16	**2.18**	C_7H_8	120	24h	43[u]	5[v]	18[w]	19[x]	2[y]
17	**2.18**	CH_2Cl_2	r.t.	5h	*45*[u]	5[v]	23[w]	16[x]	3[y]
18	**2.18**[aa]	C_7H_8	120	24h	37[u]	7[v]	31[w]	8[x]	7[y]
19	**2.18**[bb]	C_7H_8	120	24h	30[u]	5[v]	5[w]	23[x]	1[y]
20	**2.18**	neat[z]	r.t.	5min	34[u]	14[v]	14[w]	7[x]	14[y]
21	**2.18**	neat[z]	heat	5min	44[u]	7[v]	21[w]	16[x]	4[y]
22	**2.18**	neat	friction	5min	7[u]	5[v]	3[w]	0[x]	46[y]
23	**2.18**	neat	heat	5min	*50*[u]	5[v]	13[w]	23[x]	1[y]
24	**2.18**	neat	melt	5min	37[u]	6[v]	23[w]	9[x]	5[y]

[a] **2.36**. [b] **2.41**. [c] **2.20**. [d] **2.48**. [e] **2.12**. [f] **2.37**. [g] **2.42**. [h] **2.46**. [i] **2.49**. [j] **2.14**. [k] **2.38**. [l] **2.43**. [m] **2.47**. [n] **2.50**. [o] **2.15**. [p] **2.39**. [q] **2.44**. [r] **2.21**. [s] **2.51**. [t] **2.16**. [u] **2.40**. [v] **2.45**. [w] **2.23**. [x] **2.52**. [y] **2.18**. [z] Done in $CDCl_3$. [aa] **2.18**: Ph_2PCH_2OH (1.5:1). [bb] **2.18**: Ph_2PCH_2OH (1:1.5).

As summarised in Table 2.9, the reaction between **2.16** or **2.18** with Ph_2PCH_2OH showed several tertiary phosphines present in the $^{31}P\{^{1}H\}$ NMR. The spectrum of **2.39** is shown to illustrate the explanation which can be extended to **2.36 – 2.38** and **2.40** (Fig. 2.20). Two signals would be expected for nonsymmetric compound **2.39** since it possesses two different phosphorus environments (Ph_2P_A– and $\{(CH_2)_3(NR)_2\}P_B$–). Indeed, two doublets were observed at δP –27.4 (P_A) and δP –48.3 (P_B) ppm with a small ^{31}P–^{31}P coupling constant ($^4J_{PP}$ = 8.6 Hz). Resonances for **2.44** (–19.4 ppm) and **2.51** (–27.8 ppm) were assigned according to the literature for secondary and tertiary aminophosphines with aryl substituents respectively. [7,13–15,34,51,76] The singlet at –47.5 ppm was assigned to the symmetric diphosphine **2.21** because its proximity to P_B. Moreover, this peak was already

observed in the phosphorus NMR of the starting material **2.16** in proportion approx. 3:1 which increased at high temperature as well as in **2.18** (Fig. 2.4).

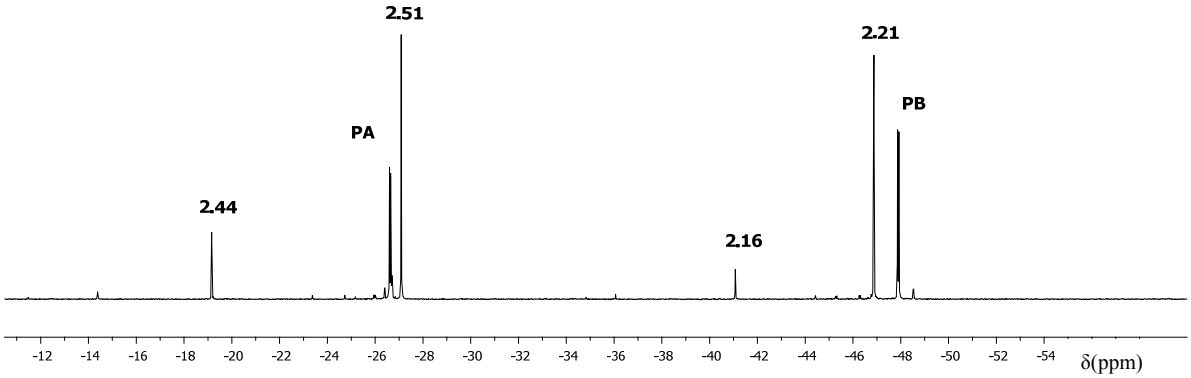

Figure 2.20 $^{31}P\{^{1}H\}$ NMR of the dissociated product obtained between one equiv. of **2.16** and Ph_2PCH_2OH.

Trying to understand the formation of all of these compounds, a mechanism is proposed based on recent studies by Tyler *et al*.[10] They reported that the phosphorus Mannich reaction proceeds through the methylenephosphonium ion which is attacked by diethylamine. In the same manner, Ph_2PCH_2OH eliminates hydroxide to form the methylenephosphonium (Sch. 2.6 second brackets) and the secondary amine (**2.16** or **2.18**) could tautomerise to an electrophilic diazaphosphonium and nucleophilic iminium ions (Sch. 2.6 first brackets). With these four species in solution, the four products observed in the $^{31}P\{^{1}H\}$ NMR could be explained. This mechanism is also supported by MS which revealed a peak at *m/z* 199 due to the $[Ph_2P=]^+$ moiety as well as molecular ions for the oxides of **2.39**, **2.21** and **2.51** (See Exp. Sec).

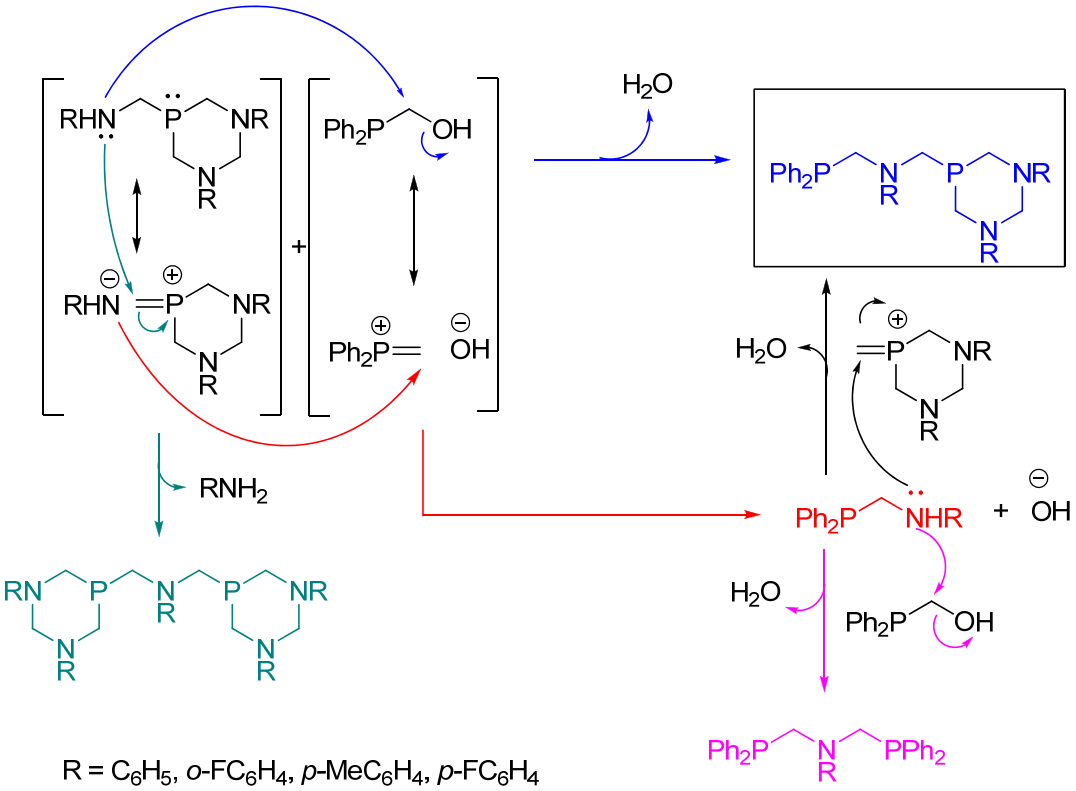

Scheme 2.6 Suggested mechanism for the phosphorus Mannich reaction of compounds **2.12**, **2.15**, **2.16** and **2.18**.

In Scheme 2.7 an alternative method was proposed in order to synthesise **2.36** and **2.40** in better yields. The reported synthesis of $Ph_2PCH_2N(R)CH_2PCg$ (**1.249** and **1.250)**, was achieved in a single step from the secondary $CgPN(H)R$ and Ph_2PCH_2OH. Unfortunately, this method did not lead to pure **2.36** – **2.40**. One possible way to solve it would be to make the alcohol a better electrophile and the amine a better nucleophile. Alcohol would be protected with tosyl chloride (which once converted to tosilate is an excellent leaving group) and lithium diisopropylamide (LDA) would remove the aminic proton which subsequently would attack the alpha carbon to the phosphorus. This route not only may accomplish the pure product but also general asymmetric PCNCP ligands.

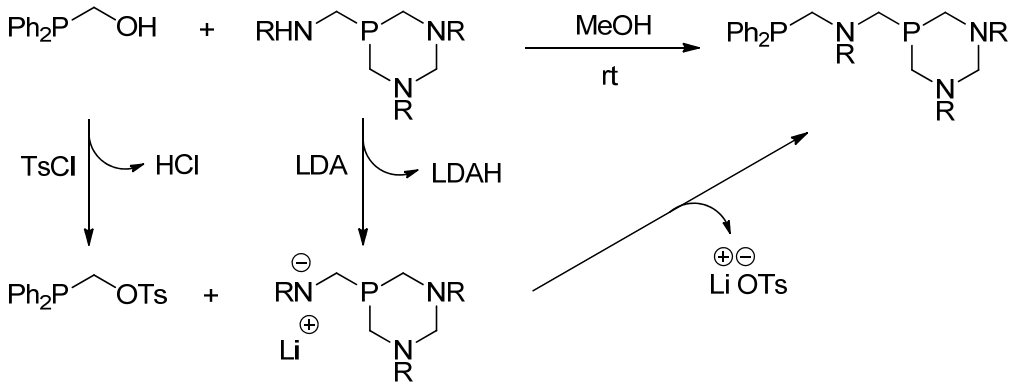

Scheme 2.7 Alternative route for the synthesis of nonsymmetric phosphines.

2.12 Conclusions

In summary, using THPC as starting material, several groups of PCN aminomethylphosphines were obtained with different procedures. A family of aminophosphonium salts incorporating *ortho* and *para* anilines ($C_6H_5NH_2$, *o*–$FC_6H_4NH_2$, *p*–$MeC_6H_4NH_2$, *p*–$FC_6H_4NH_2$ and *p*–$EtC_6H_4NH_2$) were successfully synthesised within our group. Hence, in order to expand this library of compounds further new $P\{CH_2N(H)R\}_4Cl$ salts (*o*–MeC_6H_4, *o*–$^{i}PrC_6H_4$, *o*–$^{t}BuC_6H_4$, *o*–$CF_3C_6H_4$, *o*–$\{C(Me)=CH_2\}C_6H_4$, *p*–$^{i}PrC_6H_4$) were formed.

Cyclic and acyclic PCN ligands were successfully produced by reducing the desired phosphonium salt with the appropriate base. Ligands with 6 and 8–membered ring were only obtained if the nitrogen is not sterically hindered (*i.e.* in *para*-anilines) so the bulkiness and the position of the substituent dictate the synthesis of ligands. In contrast, when the same substituents were close to the amino group (*i.e. ortho*-anilines) free rotational tripod ligands were obtained. The only exceptions were the aminomethylphosphines with *o*–MeC_6H_4 and *o*–$^{i}PrC_6H_4$ which were synthesised as 6–membered cyclic rings too. Note that in solution, several diazaphosphorinanes were observed in more than approx. 80% along with the analogous trisaminomethylphosphine and vice versa, *i.e.* a mixture between trisaminomethylphosphines and diazaphosphorinanes richer in the tripodal phosphine. Furthermore, for some diazaphosphorinanes a third phosphine was present which was assigned to the bisaminomethylphosphine PCNCP. However, in the solid state, only the target phosphine was obtained as was confirmed by EA, IR and in some cases X–ray crystallography.

^{31}P shifts for cyclic and bicyclic P–P ligands are shielded with respect to δP for acyclic analogues in *ca.* 10 and 5 ppm respectively as is illustrated in Figure 2.21. Viewing the δP values, $^{31}P\{^{1}H\}$ NMR demonstrates to be a powerful technique for future prediction of new analogous PCN ligands.

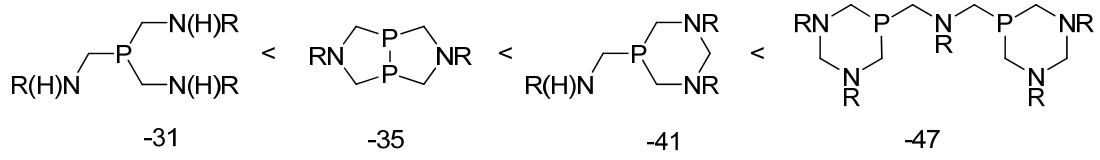

Figure 2.21 Approximate $^{31}P\{^{1}H\}$ values of the aminomethylphosphine ligands in $CDCl_3$.

Suitable crystals were collected in several cases which supports the formula proposed and enables direct comparison between these sets of ligands and analogous previously prepared within the group and within the literature.

These aminomethylphosphines were then utilised in the preparation of a series of novel bis(phosphine)amino compounds. An unprecedented example of symmetric phosphines incorporating three CNC bridges between two phosphorus was obtained as crystals as was shown by the X–ray structure of $OP(CNC)_3PO$. A retrosynthetic route was proposed and attempts to reproduce it seemed promising, however at this stage it is not possible to elucidate if it was obtained based on NMR studies and therefore more research should be conducted. In addition, mimicking a method in the literature, a plausible procedure to accomplish the synthesis of $OP(CNC)_3PO$ was suggested.

As nonsymmetric PCNCP ligands were previously reported with Ph and Cg attached to the P, attempts were made to expand this series by varying the functional group bonded to the phosphorus [$(CH_2)_3(NR)_2$, R = C_6H_5, *o*-^{i}PrC_6H_4, *o*-FC_6H_4, *p*-MeC_6H_4, *p*-FC_6H_4]. This new bis(phosphines) were synthesised by a simple Mannich condensation reaction in up to approx. 50 % by $^{31}P\{^{1}H\}$ NMR. A wide range of reaction conditions were tried to conclude that the temperature is crucial for the reaction to occur as well as the substituent on nitrogen nuclei. The coproducts observed in the $^{31}P\{^{1}H\}$ NMR and MS resulted to be new symmetric bis(aminophosphine) analogues. A mechanism was proposed in based of the $^{31}P\{^{1}H\}$ and MS which might explain the formation of the new ligands. More investigation could be conducted to purify the asymmetric ligands and a plausible route from the same starting materials for future research is given.

3. Coordination chemistry of aminomethylphosphine ligand derivatives of THPC

For more than twenty years, our research group has focused on the development of aminophosphine ligands and their coordination chemistry.[7,12–15,18] Complexes with six–heteroatom–membered rings $RP\{CH_2N(R)CH_2N(R)CH_2\}_2$ (**VI** in Sch. 1.4) have been widely studied with different substituents on the nitrogen but hardly any attention was paid to the phosphorus substituents.[16–18,58,59,93,94,99] Likewise, complexes with $P(CH_2NRR')_3$ (**IV** in Sch. 1.4) with different R and R' substituents have been poorly investigated.[1–5] Fused five–membered rings of the type $\{RN(CH_2)_2P\}_2$ (R = C_6H_5, *p*-MeC_6H_4) (**VIII** and **IX** in Sch. 1.4) are well–known but no examples of their coordination capabilities have been reported.[26,89] Hence, our aim was to investigate the chemistry of the ligands previously synthesised in Chapter 2 towards several metal centres such as Ru(II), Pt(II) and Pd(II).

In recent years, the design of catalysts which emulate hydrogenases that produce and oxidise hydrogen has increased considerably. For example, the DuBois and Bullock[8,71] and Kubiak[32] groups have all reported functional models of the hydrogenase enzyme that demonstrate electrocatalytic reduction of protons to form H_2. The high catalytic activity of these systems resides on the pendant amine whose nitrogen base is poised to deliver or accept a proton during the reversible oxidation of H_2 as it is shown in Figure 3.1.

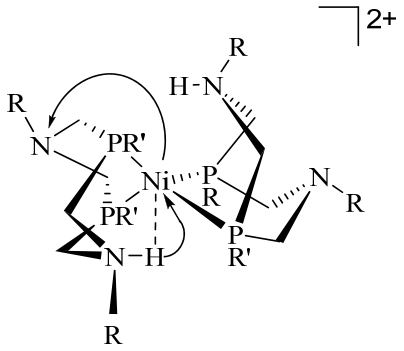

Figure 3.1 Simplified schematic representation of the proton exchange mechanism for one of the complexes conformers. Arrows indicate the metal–mediated proton movement between two nitrogens.

In the past two decades, Karasik and Hawkins expanded the library of aminophosphine ligands and their coordination capabilities with Pt(II) and Pd(II) (Fig. 3.2).[38,55–57,62,64,65,70,72,99] Figure 3.2 illustrates the coordination modes that the ligand can adopt through the phosphorus as bidentate (**I**), monodentate (**II**) and bidentate ligand within a chelating structure (**III**).

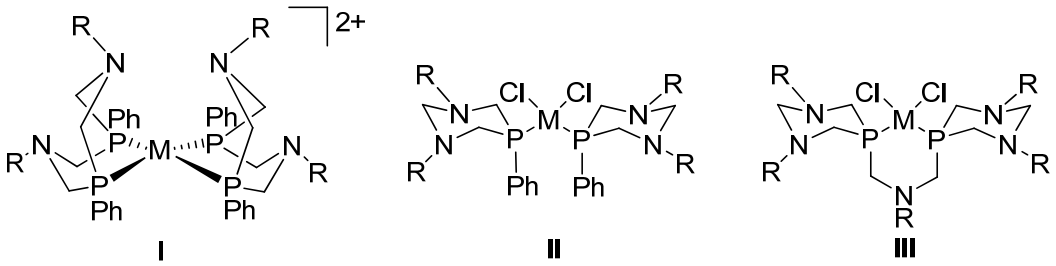

Figure 3.2 Cyclic aminomethylphosphines can adopt a bidentate (**I**), monodentate (**II**) or bidentate within a chelate structure (**III**) with Pt(II) and Pd(II). R and R' are various alkyl and aryl groups.

3.1 Coordination chemistry of cyclic $RN(H)CH_2P\{CH_2N(R)CH_2N(R)CH_2\}$ aminomethylphosphine ligands with Pt(II) and Pd(II)

The Pt(II) and Pd(II) complexes **3.1** – **3.10** were obtained by reacting two equivs. of **2.12**, **2.14** – **2.19** with one equiv. of $MCl_2(COD)$ (M = Pt or Pd) in CH_2Cl_2. After stirring for 1 h, the solution was concentrated to approx. 2 ml under reduced pressure and the complexes precipitated upon addition of Et_2O (Eqn. 3.1). The pale yellow complexes were isolated in up to 95% yield except in the case of chelate Pt(II) complex **3.6a** which was obtained as a crystalline solid in sufficient quantities to allow X–ray diffraction studies but not for full characterisation. The phosphorus chemical shifts and $^{31}P–^{195}Pt$ coupling constants are explained in greater detail later.

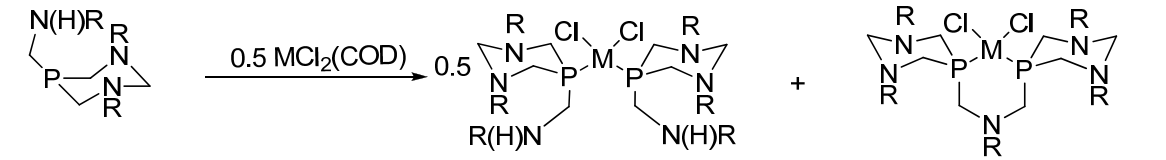

2.12 R = C_6H_5
2.14 R = *o*-$^{i}PrC_6H_4$
2.15 R = *o*-FC_6H_4
2.16 R = *p*-MeC_6H_4
2.17 R = *p*-$^{i}PrC_6H_4$
2.18 R = *p*-FC_6H_4
2.19 R = *p*-EtC_6H_4

3.1 M = Pt R = C_6H_5
3.2 M = Pt R = *o*-$^{i}PrC_6H_4$
3.3* M = Pt R = *o*-FC_6H_4
3.4* M = Pt R = *p*-MeC_6H_4
3.5 M = Pt R = *p*-$^{i}PrC_6H_4$
3.6 M = Pt R = *p*-FC_6H_4
3.7 M = Pt R = *p*-EtC_6H_4
3.8* M = Pd R = C_6H_5
3.9 M = Pd R = *o*-$^{i}PrC_6H_4$
3.10 M = Pd R = *p*-$^{i}PrC_6H_4$

3.6a M = Pt R = *p*-FC_6H_4
3.8a M = Pd R = C_6H_5
3.9a M = Pd R = *o*-$^{i}PrC_6H_4$
3.10a M = Pd R = *p*-$^{i}PrC_6H_4$

*Taken from ref[16]

Equation 3.1

Table 3.1 $^{31}P\{^{1}H\}$ NMR (in ppm, *J* in Hz) data for **3.1** – **3.10a**.[a]

	$^{31}P\{^{1}H\}$	$^{1}J_{PPt}$		$^{31}P\{^{1}H\}$	$^{1}J_{PPt}$
3.1	–6.8	3401	**3.8**	11.2	
3.2	–5.7	3422	**3.9**	13.5	
3.3[b]	–11.3	3369	**3.10**	10.7	
3.4[b]	–5.6	3395	**3.6a**	–23.7	3217
3.5	–7.4	3401	**3.8a**	–6.4	
3.6	–7.4	3403	**3.9a**	–4.8	
3.7	–7.1	3401	**3.10a**	–3.2	

[a] NMR spectra measured in $CDCl_3$. [b] Taken from ref[16].

The $^{31}P\{^{1}H\}$ NMR of Pt(II) complexes **3.1** – **3.7** show a sharp singlet at *ca.* –7.4 ppm, flanked by two platinum satellites with a coupling constant in the range of 3369 - 3422 Hz (Table 3.1). This magnitude is in accordance with values for phosphorus in *trans* arrangement to the chloride.[16,106] The δP of compounds **3.2** and **3.3** differs slightly from the rest but they are the only two examples of aminophosphine Pt(II) complexes with substituents in the *ortho* position with respect to the aniline. However, the δP of **3.3** should be further deshielded with respect to **3.2** as **3.3** possesses an electron withdrawing substituent on the aniline. This substituent should take charge from the amine and therefore from the phosphorus; *i.e.* less electron density relays on the phosphorus. It is clear that the position and the of the substituent in the amine affects its basicity and hence the chemical shift observed in the $^{31}P\{^{1}H\}$ but other factors might be involved.

The ^{1}H NMR spectra of **3.1 – 3.10** exhibit an ABX sextet (H_eH_aP) for NCH_2N protons and $(AB)_2X$ splitting pattern $\{(H_eH_a)_2P\}$ for PCH_2N protons between approximately 5.0 and 3.0 ppm. In a chair conformation, axial protons (PCH_aN and NCH_aN) are closer in the space than the equatorial protons (PCH_eN and NCH_eN) and this feature is observable in the ^{1}H NMR utilising NOE. Figures 3.3 a – d shows the NOE of complex **3.1** and Figure 3.3 e its ^{1}H NMR spectrum. When one of the NCH_2N protons at *ca*. 4.86 ($^{2}J_{HH}$ = 13.1 Hz) is irradiated, the doublet of doublets at *ca*. 3.80 ppm is observed (Fig. 3.3 a) however, when this peak is irradiated, the doublet at *ca*. 3.07 ppm is observed as well as the peak at *ca*. 4.86 ppm (Fig. 3.3 c). This doublet (3.07 ppm) is coupled to the resonance at *ca*. 4.30 ppm but also to the peak at *ca*. 3.80 ppm (Fig. 3.3 d). In conclusion, the equatorial protons are further downfield (δP 4.86 ppm, NCH_eN and δP 4.30 ppm, PCH_eN) than the axial protons (δP 3.80 ppm, NCH_aN and δP 3.07 ppm, PCH_aN) which are four–bond coupled. The $^{1}H\{^{31}P\}$ NMR demonstrates that only the methylene protons in the ring are coupled to phosphorus (PCH_eN $^{2}J_{HP}$ = 5.2 Hz, NCH_aN $^{4}J_{HP}$ = 4.3 Hz, PCH_aN $^{2}J_{HP}$ = 2.5 Hz).

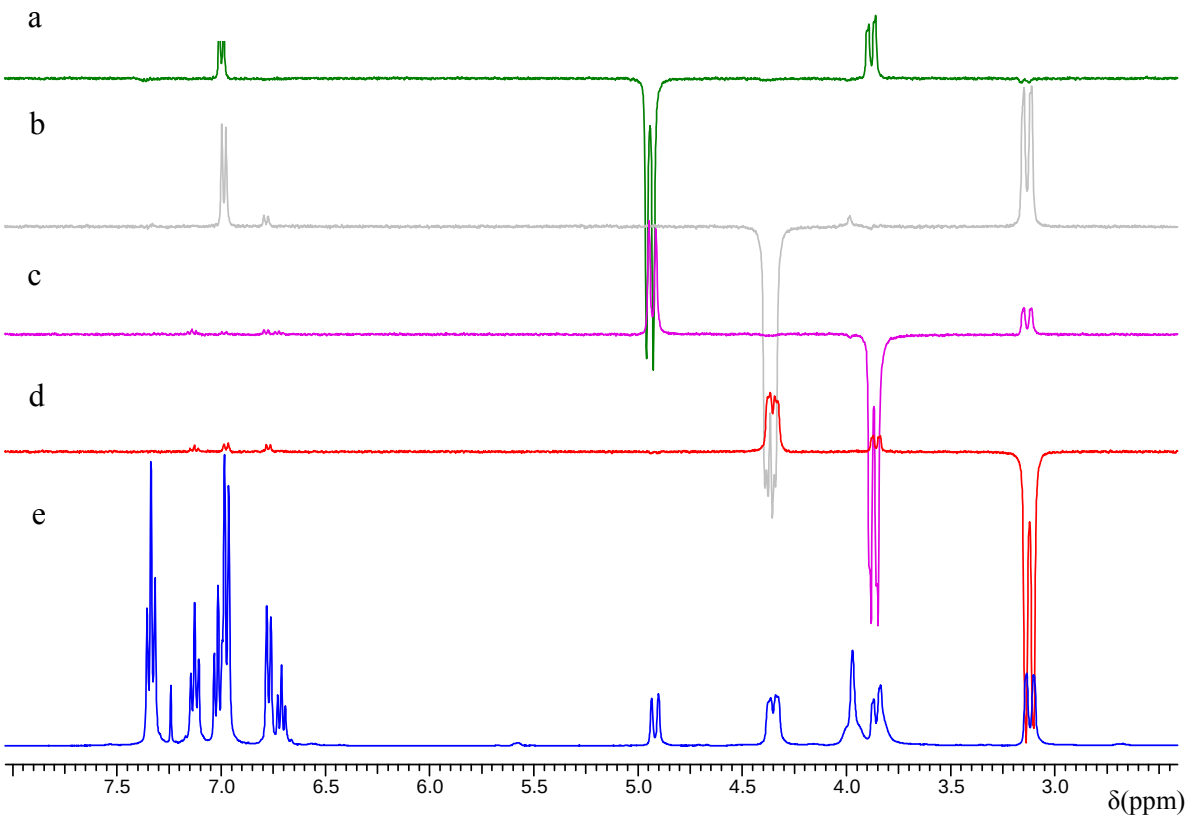

Figure 3.3 NOE spectrum of **3.1**.

In contrast to **3.1** – **3.7**, the $^{31}P\{^{1}H\}$ NMR of Pd(II) complexes with two monophosphines **3.8** – **3.10** show a singlet as the major component at positive values but in addition, a minor peak corresponding to diphosphines Pd(II) complexes **3.8a** – **3.10a** in the ratios of 5:1 for **3.8**:**3.8a**, 3:1 for **3.9**:**3.9a** and 13:1 for **3.10**:**3.10a** was also observed. The assignment of the chemical shifts of **3.8a** – **3.10a** is in agreement with those in the literature.[99] Furthermore, **3.8a** was isolated following a literature procedure[99] which permitted full characterisation of the complex and supported its assignment by comparison. Diphosphine complexes **3.6a**, **3.9a** and **3.10a** were not isolated but they were identified in solution by $^{31}P\{^{1}H\}$ NMR and the structure of **3.6a** was supported by X–ray crystallography analysis. There was a noticeable difference in the ^{1}H NMR spectra of complexes with two monophosphine ligands **3.1** – **3.10** and complexes with one diphosphines ligand **3.6a**, **3.8a** – **3.10a** in the range between approx. 3.00 and 5.00 ppm, where the NCH_2N and PCH_2N protons resonate. Figure 3.4 b illustrates the ^{1}H NMR of **3.8a**, where equatorial protons are shifted downfield with respect to axial protons as it was previously observed for **3.1** in Figure 3.3 e. However, in **3.8a**, protons coupled to phosphorus (NCH_aN, PCH_eN and PCH_aN) were displaced downfield with respect to **3.1**.

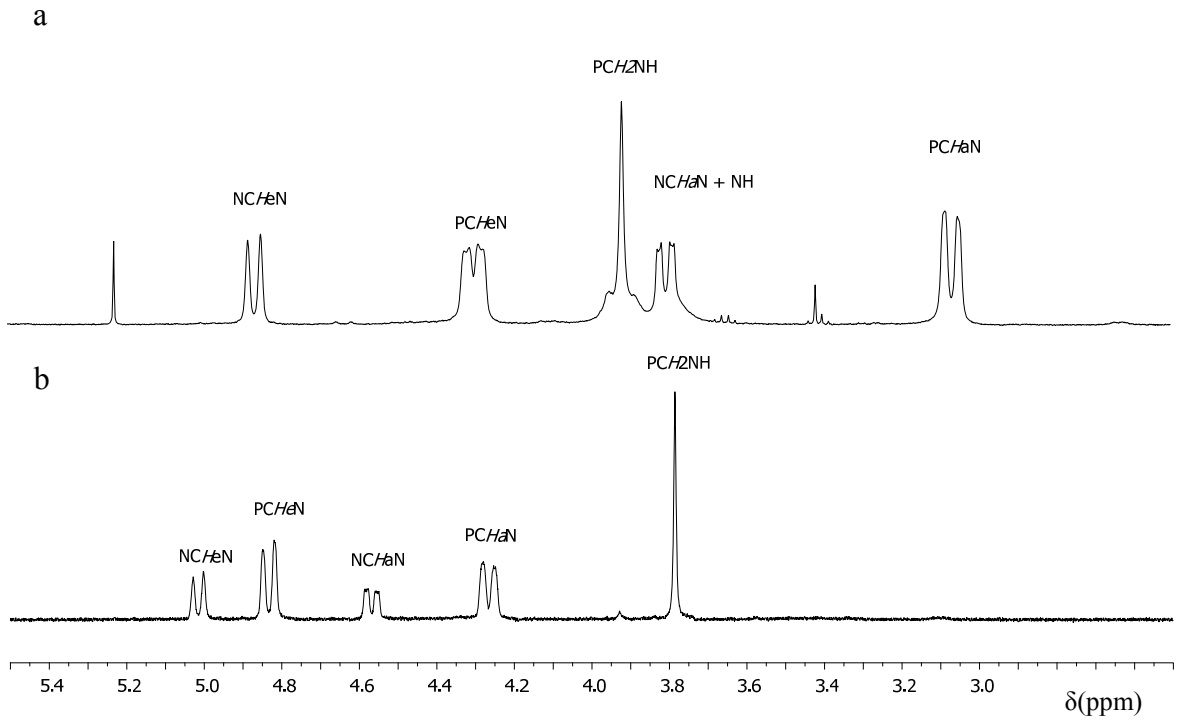

Figure 3.4 ^{1}H NMR spectra of a) **3.1** and b) **3.8a**.

3.2 X–ray crystal structures of 3.1, 3.2, 3.6a and 3.9

Further unambiguous confirmation for the *cis* arrangement of **3.1**, **3.2**, **3.6a** and **3.9** comes from single crystal X–ray diffraction analysis. Crystals were obtained by slow vapour diffusion of Et_2O into solutions of **3.1**, **3.2** and **3.9** in $CDCl_3$ and **3.6a** in CH_2Cl_2 over several days. In all cases, the X–ray structure shows that the complexes adopt a *cis* configuration with the Pt(II) (**3.1**, **3.2**, **3.6a**) or Pd(II) (**3.9**) in a distorted square–planar coordination environment as shown in Figures 3.5a – c and 3.8 and by M–P and M–Cl bond lengths and angles in Tables 3.2 and 3.4. Both phosphorus atoms are coordinated in equatorial disposition leaving the PCN pendant arm substituent in an axial position as was observed in the free ligand (Tables 2.2 and 2.4, Figs. 2.7 a and e). Complexes **3.1**, **3.2** and **3.9** possess two diazaphosphorinane ligands, whereas complex **3.6a** incorporates a diphosphine. This difference is due to the latter complex being obtained from a mixture of bis(phosphine)Pt(II) complexes, which will be explained in more detail in Section 3.10, whereas **3.1**, **3.2** and **3.9** were synthesised from the corresponding monophosphine and metal precursor. The Pt–Cl, Pd–Cl, Pt–P and Pd–P bond lengths are comparable to other previously reported compounds.[7,16,58,59,101]

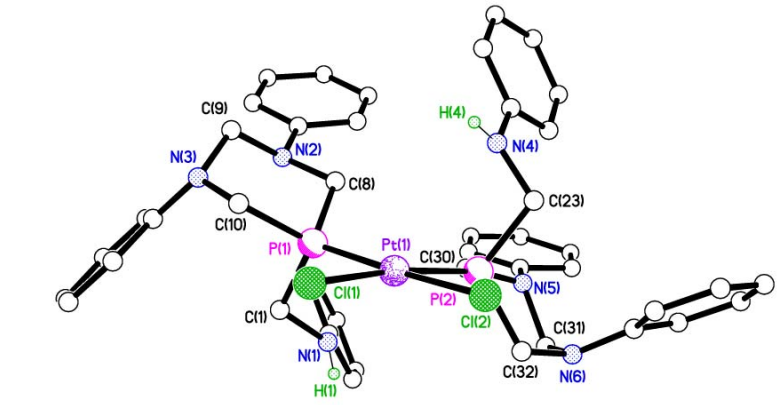

a

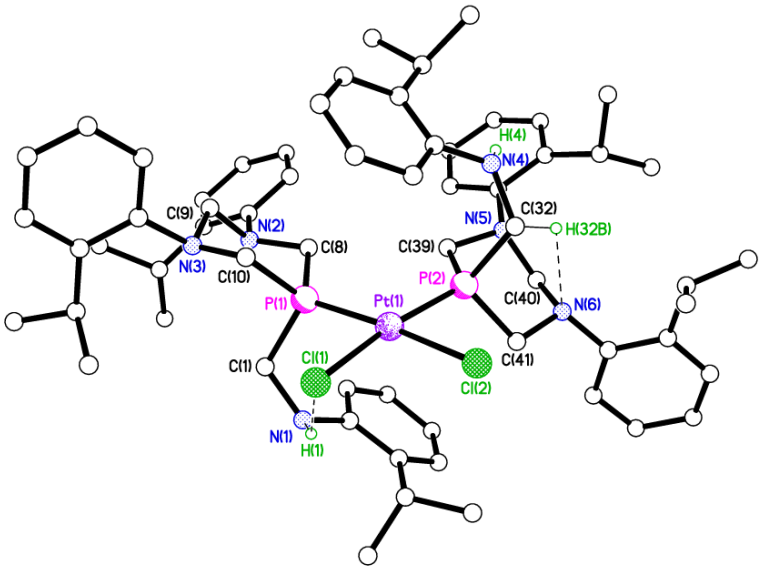

b

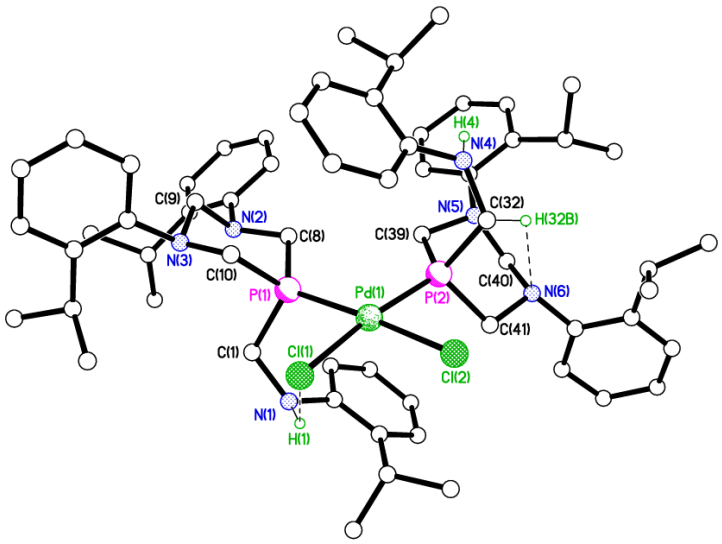

c

Figure 3.5 X–ray structures of a) **3.1** b) **3.2** and c) **3.9**. Only NH protons shown. In **3.1** one molecule of $CHCl_3$ is removed for clarity.

Table 3.2 Selected bond lengths (Å) and angles (°) for **3.1**, **3.2** and **3.9**.

	3.1[a]	**3.2**[a]	**3.9**[b]
M(1)–Cl(1)	2.3737(9)	2.3726(9)	2.374(4)
M(1)–Cl(2)	2.3716(8)	2.3492(9)	2.358(4)
M(1)–P(1)	2.2348(8)	2.2359(9)	2.266(3)
M(1)–P(2)	2.2418(9)	2.2317(9)	2.243(4)
Cl(1)–M(1)–Cl(2)	87.97(2)	89.67(3)	92.02(12)
Cl(1)–M(1)–P(1)	89.29(2)	83.92(3)	83.32(12)
Cl(2)–M(1)–P(2)	82.67(2)	82.64(3)	81.37(12)
P(1)–M(1)–P(2)	100.31(2)	103.67(3)	103.28(12)
P(1)–M(1)–Cl(2)	175.45(2)	173.59(3)	175.34(11)
P(2)–M(1)–Cl(1)	169.76(2)	172.05(3)	172.92(10)

[a] M = Pt, [b] M = Pd.

Complex **3.1** has previously been synthesised, although its crystal structure has not been reported.[16] It is noteworthy that compound **3.1** shows intermolecular N–H···Cl hydrogen bonds between molecules as highlighted in Figure 3.6 (Table 3.3).

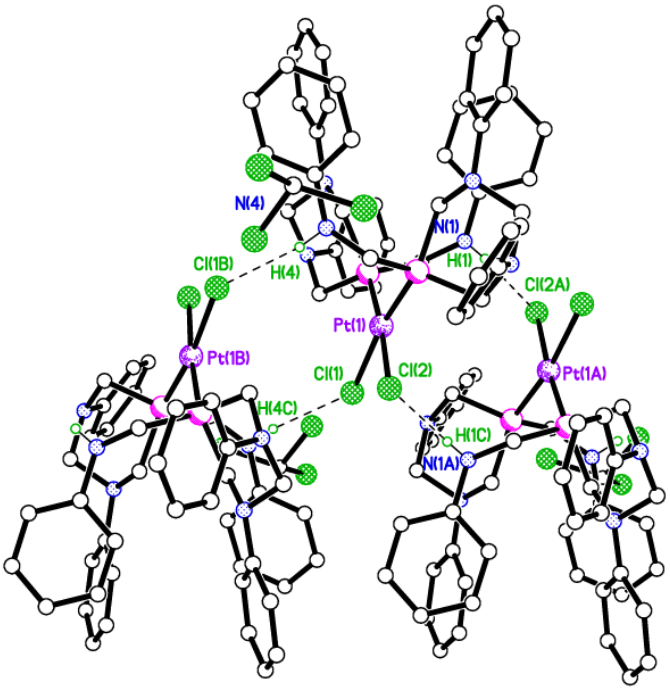

Figure 3.6 Packing diagram of **3.1** exhibiting intermolecular N–H···Cl hydrogen bonds between molecules.

Distances between platinum centres [Pt···Pt *ca*. 5.061 Å and *ca*. 5.071 Å] were found to be much longer in comparison to those previously observed [2.5684(5) – 3.399(1) Å]

suggesting no Pt–Pt bond.[107–113] However, in conjunction with N–H···Cl interactions, the supramolecular structure of **3.1** displayed a zigzag pattern (Figure 3.7).

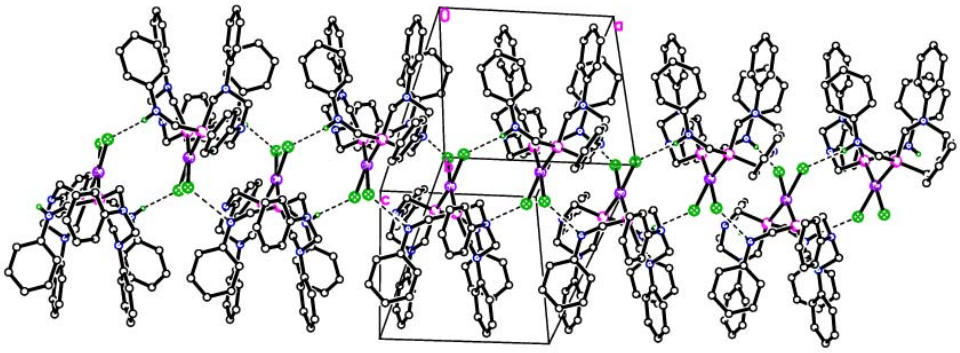

Figure 3.7 Supramolecular motif of **3.1** showing a zigzag pattern through H–bond interactions.

Complexes **3.2** and **3.9** showed intramolecular N–H···Cl hydrogen bonds [N(1)···Cl(1) 3.423(3) Å, 134(3)^{o} for **3.2** and 3.391(11) Å, 119(10)^{o} for **3.9**] with similar values as for **3.1** and for those previously reported but without M···M interactions (Table 3.3).[16,59]

Table 3.3 Selected hydrogen bond lengths (Å) and angles (^{o}) for **3.1**, **3.2** and **3.9**.[a]

	D–H···A	**d(D–H)**	**d(H···A)**	**d(D···A)**	**<(DHA)**
3.1	N(1)–H(1)···Cl(2A)	0.72(4)	2.73(4)	3.290(3)	136(3)
	N(4)–H(4)···Cl(1B)	0.90(4)	2.62(4)	3.507(3)	171(3)
3.2	N(1)–H(1)···Cl(1)	0.82(4)	2.80(4)	3.423(3)	134(3)
	C(32)–H(32B)···N(6)	0.99	2.62	3.144(4)	114
3.9	N(1)–H(1)···Cl(1)	0.84(2)	2.91(11)	3.391(11)	119(10)
	C(32)–H(32B)···N(6)	0.99	2.63	3.157(15)	114

[a] Estimated values in parentheses.

Complex **3.6a** adopts a *cis* configuration with respect to the metal centre in the same manner as **3.1**, **3.2** and **3.9**. However, **3.6a** forms a six–membered chelate ring with a P(1)–Pt(1)–P(2) bite angle of 92.94(4) Å (Fig. 3.8, Table 3.4). This value is in accordance with previous work within our group suggesting that altering the substituents on the N and P atoms has little effect on the bite angle.[7,16,101]

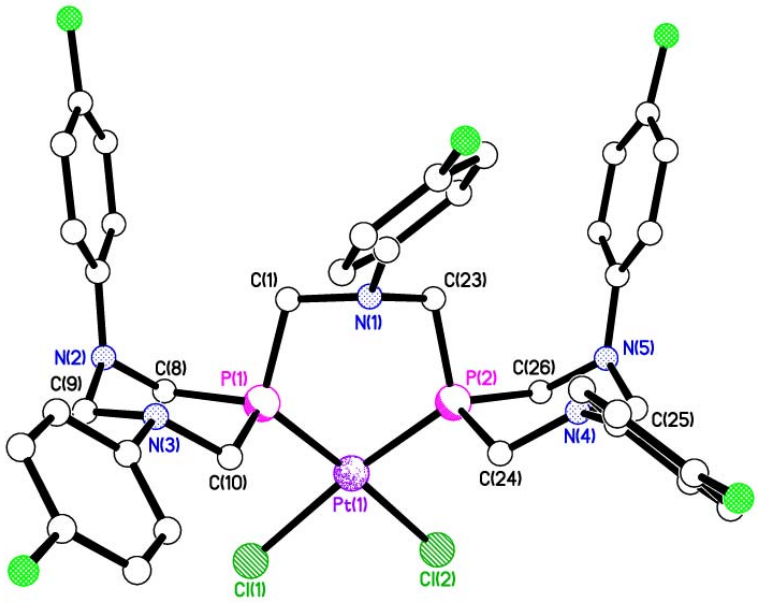

Figure 3.8 X–ray structure of **3.6a**. Two molecules of CH_2Cl_2 and hydrogens are removed for clarity.

Table 3.4 Selected bond lengths (Å) and angles (°) for **3.6a**.

3.6a			
Pt(1)–Cl(1)	2.3768(11)	P(1)–Pt(1)–Cl(2)	176.76(4)
Pt(1)–Cl(2)	2.3736(10)	P(2)–Pt(1)–Cl(1)	171.80(4)
Pt(1)–P(1)	2.2334(10)	Pt(1)–P(1)–C(1)	119.24(14)
Pt(1)–P(2)	2.2193(12)	P(1)–C(1)–N(1)	110.7(3)
Cl(1)–Pt(1)–Cl(2)	88.66(4)	C(1)–N(1)–C(23)	114.1(4)
Cl(1)–Pt(1)–P(1)	88.48(4)	N(1)–C(23)–P(2)	109.8(5)
Cl(2)–Pt(1)–P(2)	89.67(4)	C(23)–P(2)–Pt(1)	117.30(15)
P(1)–Pt(1)–P(2)	92.94(4)		

In contrast to **3.1**, **3.2** and **3.9**, complex **3.6a** does not possess NH protons and hence there is no possibility of intra or intermolecular N–H···Cl bonds. However, as mentioned for **3.1**, weak Pt···Pt interactions [approx. 3.889 Å] between two molecules were observed despite these Pt···Pt distances being longer than those reported previously (Fig. 3.9).[107–113]

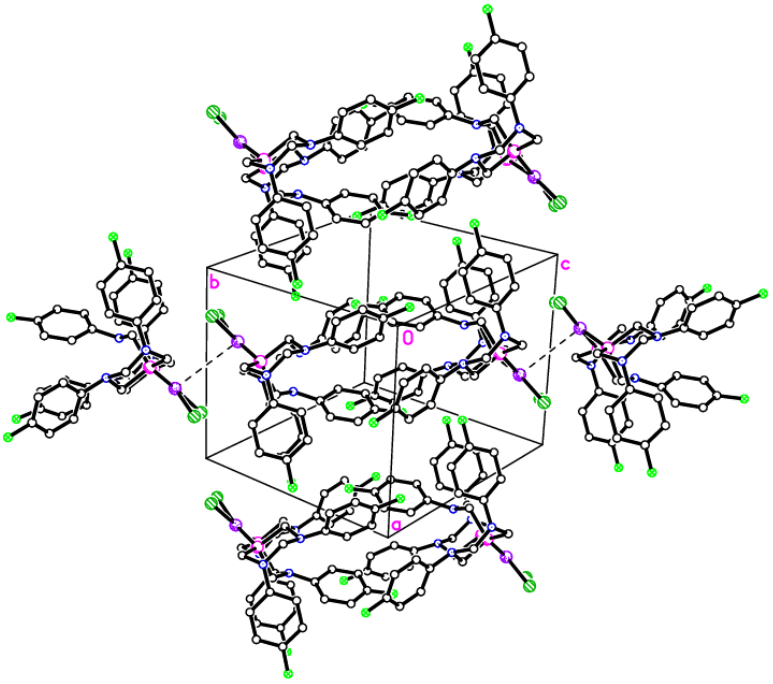

Figure 3.9 Packing diagram of **3.6a** exhibiting Pt···Pt interactions between molecules. Molecules of CH_2Cl_2 and hydrogens are removed for clarity.

In adittion, phenyl interactions are observed between two molecules. The *sextuplet phenyl embrace* (6PE) observed between C(2)–C(3)–C(4)–C(5)–C(6)–C(7) ring and C(17A)–C(18A)–C(19A)–C(20A)–C(21A)–C(22A) and C(27A)–C(28A)–C(29A)–C(30A)–C(31A)–C(32A) rings is illustrated in Figure 3.10. Furthermore, the phenyl rings C(11)–C(12)–C(13)–C(14)–C(15)–C(16) and C(33)–C(34)–C(35)–C(36)–C(37)–C(38) are orientated in a quasi *offset-face-to-face* (off) embrace.

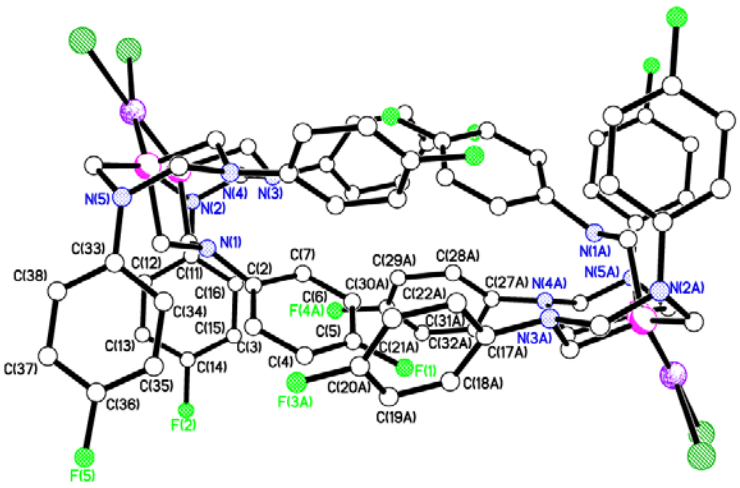

Figure 3.10 X–ray structure of two molecules of **3.6a**. Four molecules of CH_2Cl_2 and hydrogens are removed for clarity. Symmetry operator: x+1, y+1, z+1.

3.3 Coordination chemistry of cyclic RN(H)CH_2P{CH_2N(R)CH_2N(R)CH_2} ligands with Ru(II)

Following the same methodology employed within this research group to synthesise **3.11** and **3.15**,[16] a range of Ru(II) complexes were obtained by reacting **2.14** – **2.16** with $\{RuCl_2(\eta^6\text{–}p\text{-cymene})\}_2$ under aerobic conditions. In all cases, the ligands readily react to form the desired Ru(II) complexes in excellent yields (71 – 90%) as shown in Equation 3.2.

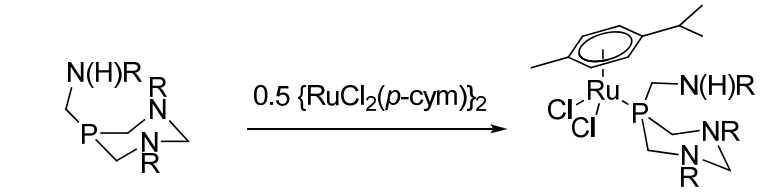

2.12 R = C_6H_5
2.14 R = *o*-^{i}PrC_6H_4
2.15 R = *o*-FC_6H_4
2.16 R = *p*-MeC_6H_4
2.18 R = *p*-FC_6H_4

3.11* R = C_6H_5
3.12 R = *o*-^{i}PrC_6H_4
3.13 R = *o*-FC_6H_4
3.14 R = *p*-MeC_6H_4
3.15* R = *p*-FC_6H_4

Taken from ref [16]

Equation 3.2

The $^{31}P\{^1H\}$ NMR of complexes **3.11** – **3.15** show a sharp peak at *ca*. 13.0 ppm (See Experimental Section). Compound **3.12** was slightly upfield with respect to the rest of the Ru(II) series (δP 8.9 ppm) but it was shifted by 54.0 ppm when deshielded with respect to the ligand which is in agreement with the average value for **3.11** – **3.15** [ΔδP 54.3 ppm, where ΔδP = δP (**3.11** – **3.15**) – δP (**2.12**, **2.14** – **2.18**), respectively]. The chemical shifts of **3.11** – **3.15** are comparable with compounds **3.11** and **3.15** which were synthesised previously.[16] In the same manner as for **3.1** – **3.10**, the ^{1}H NMR spectra show resonances in the range of 4.98 – 3.87 ppm for NCH_2N protons. For **3.13** – **3.15**, an expected ABX splitting pattern for NCH_2N protons was observed at *ca*. 4.88 ppm (NCH_eN, $^2J_{HH}$ = 13.0 Hz) and *ca*. 4.46 (NCH_aN, $^2J_{HH}$ = 13.0 Hz, $^4J_{HH}$ = 4.0 Hz) ppm. These resonances were assigned by analogy with **3.1** – **3.10**. The signal of δNH was observed as a broad singlet at *ca.* 4.30 or was obscured by other peaks; however the presence of the NH is confirmed by the IR spectra of complexes **3.11** – **3.15** which exhibit one absorbing νNH stretch in the range of 3348 – 3400 cm^{-1}.

3.4 Coordination chemistry of acyclic $P(CH_2NRR')_3$ aminomethylphosphine ligands with Pt(II) and Pd(II)

In recent years, Starosta and co–workers have been developing platinum(II) complexes, **1.212** and **1.213**, with tris(anilinomethyl)phosphines to investigate their biological activity (Fig. 3.11).[1] Han and Johnson developed $P\{CH_2N(H)R\}_3$ (R = aryl substituents) ligands with early and late transition metals (Fig. 3.11).[2,3,44]^{2–5} Ligand in **1.195** and **1.196** can adopt a conformation where the phosphine and the amine lone pairs are arranged approximately parallel to each other. The phosphine counterpart cannot bind its lone pair to the chelated metal bound by the amido donors but is well situated to bind a second metal centre. Therefore, $P\{CH_2N(H)R\}_3$ are perfect scaffolds for the synthesis of early–late heterobimetallic complexes.[2,3,44] Trisaminomethylphosphines have been found to be excellent ligands as shown by the previous examples.[2,3,44] Hence, the ligating capabilities of our novel $P\{CH_2N(H)R\}_3$ ligands with Pt(II), Pd(II) and Ru(II) precursors is discussed.

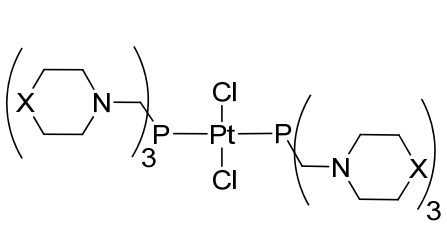

1.212 X = NCH_3
1.213 X = O

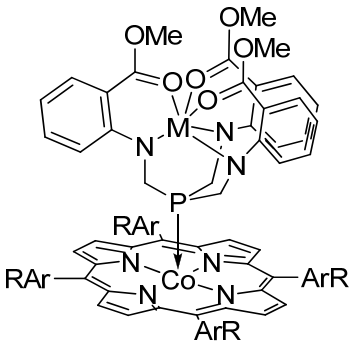

1.195 R = *p*-$(OCH_3)C_6H_4$ M = Y
1.196 R = *p*-$(OCH_3)C_6H_4$ M = Gd

Figure 3.11 Coordination chemistry of $P\{CH_2N(H)R\}_3$.

The coordination nature of **2.27**, **2.29** and **2.30** was investigated with $MCl_2(COD)$ (M = Pt or Pd) to form complexes **3.16** – **3.21** (Eqn. 3.3). Two equivs. of the relevant ligand were added to a solution of one equiv. of $MCl_2(COD)$ (M = Pt or Pd) in CH_2Cl_2. The desired products **3.16** – **3.21** were obtained upon precipitation with either Et_2O or hexanes in moderate to good yields (8 – 84%).

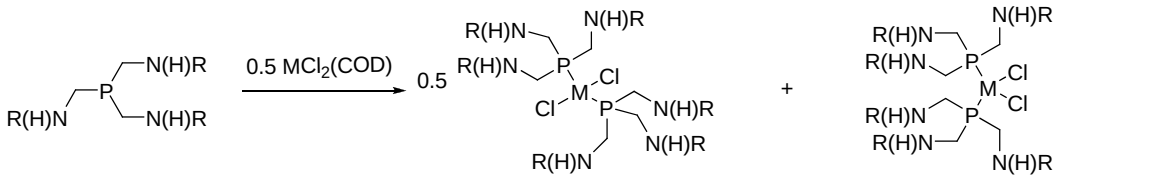

2.27 R = *o*-^{i}PrC$_6$H$_4$
2.29 R = *o*-CF$_3$C$_6$H$_4$
2.30 R = *o*-{C(Me)=CH$_2$}C$_6$H$_4$

3.16 M = Pt R = *o*-^{i}PrC$_6$H$_4$
3.17 M = Pt R = *o*-CF$_3$C$_6$H$_4$
3.18 M = Pt R = *o*-{C(Me)=CH$_2$}C$_6$H$_4$
3.19 M = Pd R = *o*-^{i}PrC$_6$H$_4$
3.20 M = Pd R = *o*-CF$_3$C$_6$H$_4$
3.21 M = Pd R = *o*-{C(Me)=CH$_2$}C$_6$H$_4$

3.16a M = Pt R = *o*-^{i}PrC$_6$H$_4$
3.18a M = Pt R = *o*-{C(Me)=CH$_2$}C$_6$H$_4$

Equation 3.3

Table 3.5 Selected $^{31}P\{^{1}H\}$ NMR (in ppm, *J* in Hz) data for **3.16** – **3.21**.[a]

	$^{31}P\{^{1}H\}$	$^{1}J_{PPt}$		$^{31}P\{^{1}H\}$
3.16	10.9	2392	**3.19**	16.3
3.17	14.1	2417	**3.20**	18.8
3.18	12.2	2403	**3.21**	17.0
3.16a	9.1	3453		
3.18a	11.5	3393		

[a] NMR spectra measured in $CDCl_3$.

The $^{31}P\{^{1}H\}$ NMR spectra of **3.16** – **3.21** displayed higher phosphorus shifts in the δP values compared to the free ligands **2.27**, **2.29** and **2.30** [ΔδP = 44.7 ppm, where ΔδP = δP (**3.16** – **3.21**) – δP (**2.27**, **2.29** – **2.30**) respectively] (Table 3.5). The spectra of the isolated solids **3.16** and **3.18** exhibited one major peak at δP 10.9 ppm ($^{1}J_{PPt}$ = 2392 Hz for **3.16**) and δP 12.2 ppm ($^{1}J_{PPt}$ = 2403 Hz for **3.18**) and a minor peak at δP 9.1 ppm ($^{1}J_{PPt}$ = 3453 Hz for **3.16a**) and δP 11.5 ppm ($^{1}J_{PPt}$ = 3393 Hz for **3.18a**) respectively. The coupling constants indicate that **2.27** and **2.30**, once reacted with $PtCl_2$(COD), resulted in a mixture of Pt(II) complexes with phosphorus *trans* (**3.16** and **3.18**) and *cis* (**3.16a** and **3.18a**) to the chloride. The magnitude of the coupling constants are in agreement with those with phosphorus in *trans* and *cis* positions.[1,27]

Compounds **3.16** and **3.16a** were isolated from the reaction between one equiv. of $PtCl_2$(COD) and two equivs. of **2.27** in CH_2Cl_2 after stirring 24 h or 1 h respectively. Due to the high solubility of **3.16** and **3.16a** in Et_2O, different solvents were used to boost precipitation in the work up. When hexanes or C_7H_8 were used in combination with Et_2O, the yield improved for **3.16a** from 8% to 22% but it did not for **3.16** (from 64% to 25%). Furthermore, the $^{31}P\{^{1}H\}$ NMR showed a mixture of *cis–trans* isomers in different

proportions and ^{1}H NMR of **3.16a** showed one singlet at 7.94 ppm assigned to OH from ^{t}BuOH. Hence reaction time and solvent determine the synthesis of **3.16** and **3.16a** and further investigation would be required to find out the optimal conditions for them to be produced in good yields.

The IR spectra of complexes **3.19** – **3.21** exhibited two absorbing νNH stretches (3341 – 3408 cm^{-1}) and νPdCl stretches (275 – 329 cm^{-1}). The geometry of the complexes was further confirmed by single crystal X–ray diffraction which revealed Pd(II) compounds with phosphorus *cis* to the chloride (Figs. 3.12 b – d). Elemental analysis of **3.19** and **3.20** indicated KCl was present as it was expected due to the residual KCl in **2.27** and **2.29** respectively (See Exp. Sec.).

The ^{1}H NMR spectra of **3.16** – **3.21** showed resonances in the range between 5.01 – 3.94 ppm assigned to N*H* and PCH_2NH protons. They exhibited two signals at *ca.* 4.76 ppm (virtual quartet) for N*H* and at *ca*. 3.99 ppm (virtual triplet) for PCH_2NH protons which are coupled to each other ($^{3}J_{HH}$) as it was observed in ^{1}H–^{1}H NMR. For the analogous P{CH_2N(H)R}$_3$ (R = C_6H_5, **1.152**; *m,m*–$Me_2C_6H_3$, **1.153** and *m,m*–$CF_3C_6H_3$, **1.154**), the $^{2}J_{HP}$ and $^{3}J_{HH}$ for PCH_2NH were also observed but NH displayed a broad singlet.[2] Similar splitting pattern was observed for N*H* and PCH_2NH protons of Ru(II)complex **3.23** (Fig. 3.13) instead of the more defined virtual quartet displayed by **3.16 – 3.21**, which demonstrates that not only was PCH_2NH coupled to the phosphorus but also to the NH protons ($^{3}J_{HP}$). Hence, by extension, N*H* and PCH_2NH protons in Pt and Pd complexes **3.16** – **3.21** are coupled to phosphorus and to each other with an average coupling constant of $J = |\,^{3}J_{HP} + {}^{2}J_{HP} + {}^{3}J_{HH}\,| = 6.8$ Hz.

3.5 X–ray crystal structures of 3.16a, 3.19 – 3.21

Single crystals of **3.16a** and **3.19** – **3.21**, suitable for X–ray crystallography, were grown *via* vapour diffusion of Et_2O into a CH_2Cl_2 solution of **3.16a** and **3.19** – **3.21** (Fig. 3.12 a – d, Tables 3.6 and 3.7). All complexes adopted a near square planar geometry around the metal centre which is confirmed by M–Cl and M–P bond lengths and angles (Table 3.6). The two phosphorus ligands are *trans* to the chloride in **3.16a** and in *cis* disposition in **3.19** – **3.21**. X–ray structures of Pt(II) complexes with P{CH_2N(H)R}$_3$ (R = alkyl derivatives) in a *trans* configuration with respect to the metal centre have been reported before (**1.212** and **1.213**, Eqn. 3.11), however there are not any examples of *cis* isomers in the literature.[1]

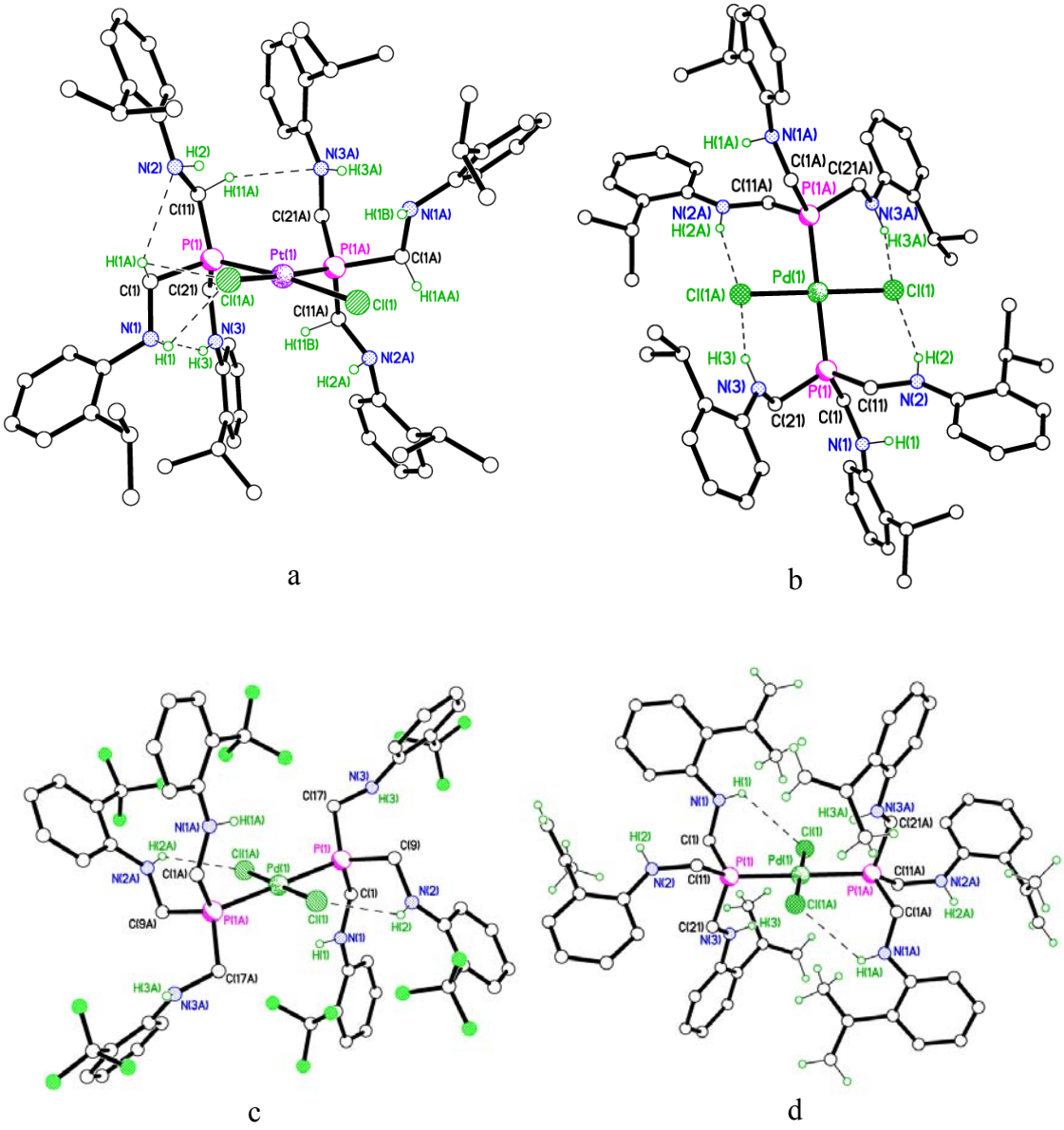

Figure 3.12 X–ray structures of a) **3.16a**, b) **3.19**, c) **3.20** and d) **3.21**. All hydrogen atoms except those on N and/or involved in H–bonds and in *o*–{C(Me)=CH_2}C_6H_4 are removed for clarity.

The substituents on the nitrogen affects the basicity of the phosphorus which is reflected in the M–Cl bond distances. The more basic substituents *o*-^{i}PrC_6H_4 and *o*-{C(Me)=CH_2}C_6H_4 enhances the σ–donor ability of the P(1) and, therefore, weakens the M–Cl bonds causing longer Pd–Cl distances for **3.19** [2.3153(13) Å] and **3.21** [2.3027(7) Å] than for **3.20** [2.3010(17) Å]. The M(1)–Cl(1) bond length in **3.16a** was much longer than the analogues **3.19**, **3.20** and **3.21**, but the Pt(1)–P(1) distance in both *cis* and *trans* compounds **3.16a** and **3.19** were quite similar [2.244(3) and 2.2396(13) Å respectively]

and shorter than **3.20** and **3.21**. This indicates that the *ortho* substituents on the aniline have a noticeable impact on bond lengths but a negligible effect on the geometry of the complex which is determined by the metal centre. The P–C [average αC–P(1), αC = C bound to P(1)], C–P–C and P–C–N bond lengths and angles of **3.16a**, **3.19** and **3.20** are in agreement with the uncoordinated ligands **2.27** and **2.29a** respectively and those in the literature (Table 3.6).[1]

Table 3.6 Selected bond lengths (Å) and angles (°) for **3.16a**, **3.19**, **3.20** and **3.21**.[a]

	3.16a[b]	**3.19**[c]	**3.20**[c]	**3.21**[c]
M(1)–Cl(1)	2.362(3)	2.3153(13)	2.3010(17)	2.3027(7)
M(1)–P(1)	2.244(3)	2.2396(13)	2.319(2)	2.3139(7)
av.[αC–P(1)][d]	1.831(11)	1.846(4)	1.829(7)	1.836(3)
Cl(1)–M–Cl(1A)	87.65(16)	180.00(6)	180.0	180.0
Cl(1)–M–P(1)	174.30(10)	88.40(5)	93.74(6)	91.22(3)
P(1)–M–P(1A)	94.46(15)	180.00	180.0	180.00(3)
P(1)–M–Cl(1A)	89.13(11)	91.60(5)	86.26(6)	88.78(3)
av.[αC–P(1)–αC][e]	101.8(5)	103.01(7)	105.6(3)	104.27(12)
av.[P(1)–αC–N(X)][f]	110.8(8)	110.1(3)	112.8(5)	109.81(18)

[a] Estimated standard deviations in parentheses. [b] M = Pt. [c] M = Pd. [d] Average [αC–P(1)], αC = C bound to P(1). [e] Average value of αC–P–αC, αC = C bound to P. [f] Average value of P(1)–αC–N(X), αC = C bound to P and N(X) is the N bound to αC. Symmetry operator for **3.16a**: *–x*+1, *y*, *–z*+1/2; **3.19**: *–x*, *–y*, *–z*; **3.20**: *x*–1, *y*, *z*; **3.21**: *–x*+1, *–y*+1, *–z*+1.

The intramolecular N–H···N hydrogen bonds observed in **2.27** [N(1)···N(3) 3.007(2) Å, N(3)···N(2) 2.977(2) Å, N(1)···N(3) 2.973(2) Å] were not retained in **3.16a** or **3.19** due to the intramolecular N···Cl bonds (Table 3.7). Only in complex **3.16a**, the bond length between N(1)–H(1)···N(3) was found to be relatively close [N(1)···N(3) 3.047(13) Å] to the distance observed in **2.27** [N(1)···N(3) 3.007(2) Å] (Fig. 3.12 a). All complexes showed intramolecular N···Cl hydrogen bonding and **3.16a** which did not display intermolecular H–bonding. Likewise, only complex **3.20** demonstrated intermolecular H–bond [N(3)···Cl(1B) 3.461(6) Å, 145(6)°] which was longer and therefore weaker than those previously reported.[98]

Table 3.7 Selected H–bond lengths (Å) and angles (°) for **3.16a**, **3.19**, **3.20** and **3.21**.[a]

D–H···A	**D–H**	**H···A**	**D···A**	**D–H···A**

3.16a	C(1)–H(1A)···N(2)	0.99	2.72	3.029(14)	99
	N(3)–H(3)···N(1)	0.84(1)	2.28(5)	3.054(12)	153(9)
	C(1)–H(1A)···Cl(1A)	0.99	2.72	3.153(13)	107
	N(1)–H(1)···Cl(1A)	0.84(1)	2.71(8)	3.305(9)	129(8)
	C(11)–H(11A)···N(3A)	0.99	2.49	3.416(15)	155
3.19	N(2)–H(2)···Cl(1)	0.81(5)	2.48(5)	3.258(4)	160(5)
	N(3)–H(3)···Cl(1A)	0.92(5)	2.44(5)	3.209(4)	141(4)
3.20	N(2)–H(2)···Cl(1)	0.84(2)	2.69(5)	3.332(6)	135(6)
	N(3)–H(3)···Cl(1B)	0.84(2)	2.74(4)	3.461(6)	145(6)
3.21	N(1)–H(1)···Cl(1)	0.80(3)	2.99(3)	3.490(2)	123(3)

[a] Estimated standard deviations in parentheses. Symmetry operator for **3.16a**: $-x+1, y, -z+1/2$; **3.19**: $-x, -y, -z$; **3.20**: $x-1, y, z$.

3.6 Coordination chemistry of acyclic $P(CH_2NRR')_3$ ligands with Ru(II)

Complexes **3.22** – **3.26** were obtained in the same manner as **3.11** – **3.15** (Section 3.3). Two equivs. of **2.26** – **2.30** were treated with one equiv. of $\{RuCl_2(\eta^6\text{–}p\text{-cymene})\}_2$ in CH_2Cl_2. After stirring for 1 h, the solution was concentrated to approximately 2 ml under reduced pressure and the required complexes precipitated upon addition of Et_2O or hexanes in up to 90% yield (Eqn. 3.4).

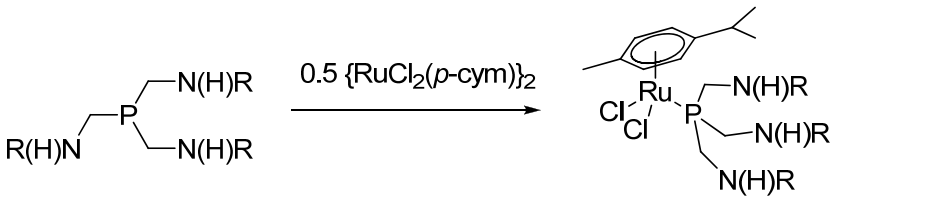

2.26 R = C_6H_5
2.27 R = *o*-^{i}PrC_6H_4
2.28 R = *o*-^{t}BuC_6H_4
2.29 R = *o*-$CF_3C_6H_4$
2.30 R = *o*-{C(Me)=CH_2}C_6H_4

3.22 R = C_6H_5
3.23 R = *o*-^{i}PrC_6H_4
3.24 R = *o*-^{t}BuC_6H_4
3.25 R = *o*-$CF_3C_6H_4$
3.26 R = *o*-{C(Me)=CH_2}C_6H_4

Equation 3.4

The $^{31}P\{^1H\}$ NMR of complexes **3.22** – **3.26** showed a sharp peak in the range of 23.4 – 28.8 ppm (See Experimental Section) with compound **3.25** slightly downfield with respect to the rest of the Ru(II) series (δP 28.8 ppm). This was expected since *o*–CF_3 in **3.25**

withdraws charge from the amine and therefore less electron density relays onto phosphorus and, hence, this resonates slightly further downfield.

The ^{1}H NMR showed resonances in the range of 5.02 – 3.91 ppm for N*H* and PC*H*$_2$NH protons as was previously observed in the spectra of **3.16** – **3.21**. For **3.22** – **3.26**, only two signals were observed at *ca.* 4.88 ppm (broad doublet or virtual quadruplet) for N*H* and at *ca*. 4.03 ppm (virtual triplet) for PC*H*$_2$NH protons. Figure 3.13 highlights the methylene and aminic region of the ^{1}H (a) and the ^{1}H{^{31}P} (b) NMR spectra of the N*H* and PC*H*$_2$NH protons for **3.23**. Both peaks are coupled to phosphorus ($^{3}J_{HP}$ = 4.0 Hz for N*H* and $^{2}J_{HP}$ = 1.6 Hz for PC*H*$_2$NH) and to each other ($^{3}J_{HH}$ = 2.7 Hz) confirmed by 2D ^{1}H–^{1}H NMR.

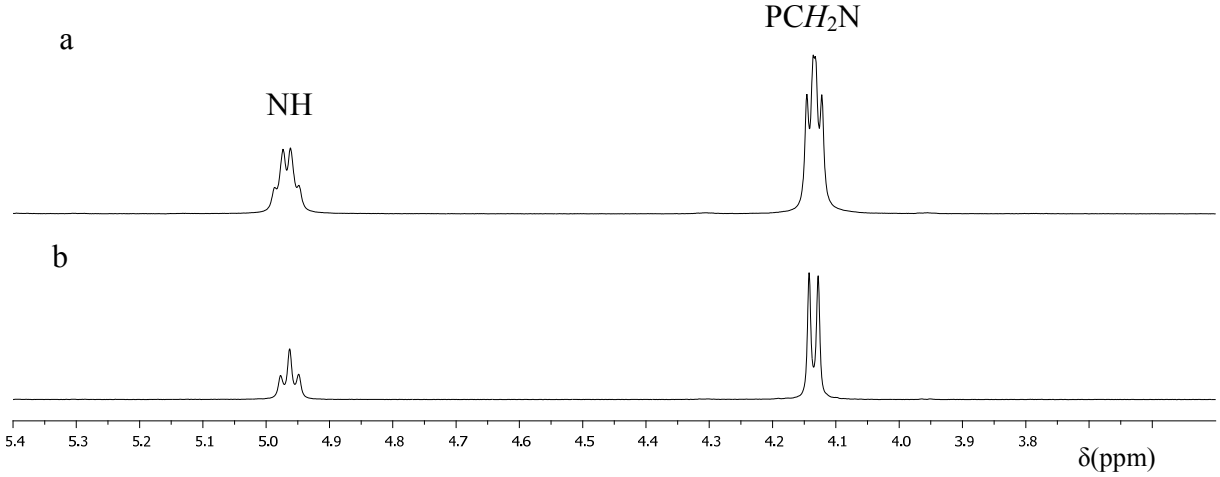

Figure 3.13 Selected **a)** ^{1}H and b) ^{1}H{^{31}P} NMR region of **3.23**.

The presence of the NH in complexes **3.22** – **3.26** was also confirmed by IR spectra which exhibited one absorbing νNH stretch in the range of 3278 – 3367 cm^{-1}. Elemental analysis of **3.22**, **3.23** and **3.25** showed 2, 1.5 and 1.75 molecules of KCl as was expected due to the residual KCl present in **2.26**, **2.27** and **2.29** respectively.

3.7 X–ray crystal structure of 3.25

Crystals of **3.25** suitable for study by single crystal X–ray diffraction were successfully grown by slow evaporation of a CH_2Cl_2 solution. The X–ray structure clearly shows that the desired ruthenium complex has been obtained displaying a classic "piano–stool" geometry formed by the pentamethylcyclopentadienyl ligand, two chloride ligands and a third phosphorus(III) ligand (Fig. 3.14). To the best of our knowledge, **3.25** is the first example of a Ru(II) complex with ligands of the type P{$CH_2N(H)R$}$_3$ (R = aryl or alkyl derivatives). The Ru–Cl, Ru–P and Ru–C_{cent} bond lengths are typical for ruthenium

phosphine complexes with a PCN backbone.[16,18,101] The P–C [average [αC–P(1)], αC = C bound to P(1)], C–P–C [average value of αC–P(1)–αC, αC = C bound to P(1)] and P–C–N [average value of P(1)–αC–αN(X), N(X) = N(2) or N(3)] bond lengths and angles are in agreement with **3.16a**, **3.19** and **3.20** as well as with the uncoordinated ligand **2.29a** and those in the literature (Table 2.5).[1] The structure presents an intramolecular hydrogen bond between one nitrogen and one chloride [N(2)–H(2)···Cl(1) 3.241(4) 123°] but no H–bonds were observed for N(1) and N(3).

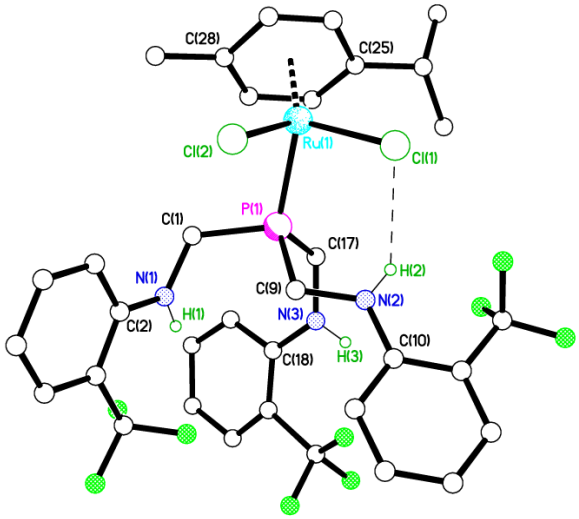

Figure 3.14 X–ray structure of **3.25**. All H atoms except those on N are removed for clarity.

Table 3.8 Selected bond lengths (Å) and angles (°) for **3.25**.[a]

	3.25		
Ru(1)–C_{cent}	1.6959(21)	Cl(1)–Ru(1)–Cl(2)	86.86(4)
Ru(1)–Cl(1)	2.4230(13)	Cl(1)–Ru(1)–P(1)	92.33(4)
Ru(1)–Cl(2)	2.4109(12)	Cl(2)–Ru(1)–P(1)	83.45(4)
Ru(1)–P(1)	2.3219(11)	av.[αC–P(1)–αC][c]	103.6(2)
av.[αC–P(1)][b]	1.8643(5)	av.[P(1)–αC–N(X)][d]	113.9(3)

C_{cent} denotes the centroid of the *p*–cymene ring [C(25)–C(26)–C(27)–C(28)–C(29)–C(30)]. [a] Estimated standard deviations in parentheses. [b] Average αC–P(1), αC = C bound to P(1). [c] Average value of αC–P(1)–αC, αC = C bound to P(1). [d] Average value of P(1)–αC–αN(X), αC = C bound to P(1) and N(X) = N(1), N(2) or N(3).

3.8 Coordination chemistry of bicyclic $\{RN(CH_2)_2P\}_2$ ligands with Pt(II), Rh(III) and Cr(III)

Since Cummins *et al*. developed a one–step procedure to synthesise gram quantities of diphosphines **1.371** and **1.373**, they have been eager to study their coordination capabilities.[114] Scheme 3.1 illustrates several plausible ligating modes for fused six–membered rings along with reported diphosphines. Ligands **1.371** and **1.373** have two electron pairs available to coordinate to a metal centre; however they are not suitable for metal chelation. The bicyclic structure is locked into a *cis* conformation but also restricts the bite angle. In fact, only diphosphines with no–fixed structure by two fused rings such as $R_2P–PR_2$ ligands (R = Ph, Et) showed this *P,P*–chelating mode (structure **I**).[115] Similarly, if the ligand does not contain a P–P bridge, it can bind in a *P,P*–chelate fashion (structure **II**).[9] Therefore, **1.371** and **1.373** showed a pre–configuration ideally suited to form bridges to one metal centre (structure **III**) or to two metal centres (structure **IV**). In fact, ligand **1.371** exhibited a *P*-bridging mode with W(III) (**1.380**) and **1.373** bound to two metal centres in a *P,P*–bridging mode as observed in **1.381**.[86,87] These diphosphines do not possess an heteroatom in the fused rings in contrast to compounds **2.31** and **2.32** (**1.390** in Fig. Sch. 1.37 and **1.392** in Eqn. 1.20) which have been known for more than thirty years, although their potential as ligands has not been investigated.[26,89] Hence, their coordination capabilities were explored towards Pt(II), Rh(III) and Cr(III) metal centres.

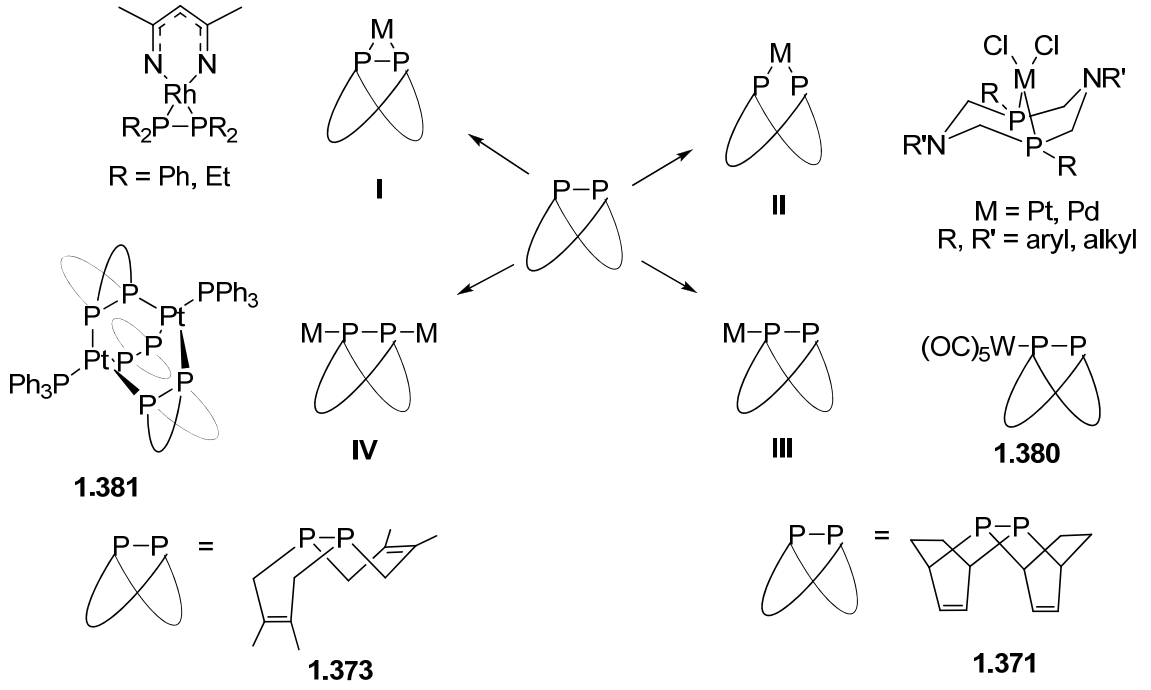

Scheme 3.1 Coordination modes of known P–P and P···P compounds.

When one equiv. of ligands **2.31** – **2.33** was added to a solution of one equiv. of $PtCl_2(COD)$ in $CDCl_3$, new platinum(II) complexes were obtained (Sch. 3.2). Two structures were proposed with one (**3.27a – 3.29a**) or two platinum centres (**3.27b – 3.29b**), as seen in Scheme 3.2. The products precipitated slowly overtime in $CDCl_3$, despite this, they could be analysed by *in situ* $^{31}P\{^1H\}$ and ^1H NMR spectroscopy and single crystal X–ray crystallography for **3.27b**.

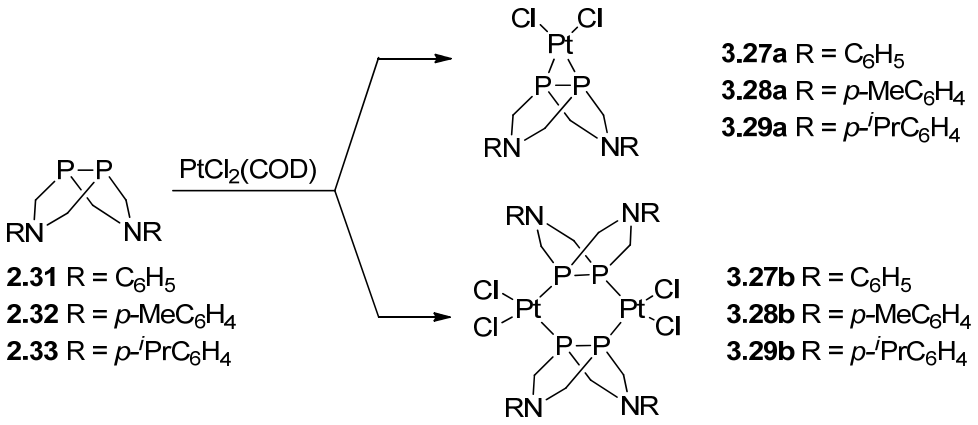

Scheme 3.2 Synthesis of Pt(II) products of **2.31** – **2.33**. Two group of complexes are proposed as possible products: monometallic **3.27a** – **3.29a** and bimetallic **3.27b** – **3.39b**.

The $^{31}P\{^1H\}$ NMR spectra of the new complexes were complicated and poorly resolved (Fig. 3.15 b). Assuming that complexes **3.27a – 3.29a** are symmetric in solution, they would generate a phosphorus NMR with an A_2X (A = P, X = Pt) spin system (singlet flanked by two platinum satellites). Figure 3.15 b shows the $^{31}P\{^1H\}$ NMR for the product of Pt(II) with **2.32** with several peaks flanking a sharp singlet at *ca*. –22.8 ppm. This indicates that mononucleous complexes **3.27a – 3.29a** were not obtained. In addition, due to the fixed bidentate coordination angle of the two adjacent phosphorus atoms, it is unlikely that the structure of the products is that proposed for **3.27a** – **3.29a**. This led us to analyse complexes **3.27b – 3.29b** as possible products. Assuming that these bimetallic compounds are symmetric in solution, they would produce a $^{31}P\{^1H\}$ spectrum with a combination of ABXY (A = P_A, B = P_B, X = Pt_X and Y = Pt_Y), ABX (Pt_X = Pt_Y) and A_2 (P_A = P_B) spin systems. To gain an insight into the NMR, simulated spin–system analysis was used. Figure 3.15 a shows a preliminary simulated $^{31}P\{^1H\}$ NMR spectrum for Pt(II) with **2.32** with estimated δP = –23.3 ppm and $^1J_{PP}$ = –235 Hz, $^1J_{PPt}$ = 3436 Hz and $^2J_{PPt}$ =

20 Hz. A superposition of these spin systems matches with the experimental NMR spectrum, shown in Figures 3.15 a and b, respectively, however an improved signal to noise $^{31}P\{^{1}H\}$ NMR should be obtained in the future for more certain explanation. Moreover, similar spectrum was observed for platinum complex **1.381** (Sch. 3.1) afforded by Cummins *et al*.[86] Further evidence of the synthesis of **3.27b – 3.39b** was supported by crystallographic studies of **3.27b**.

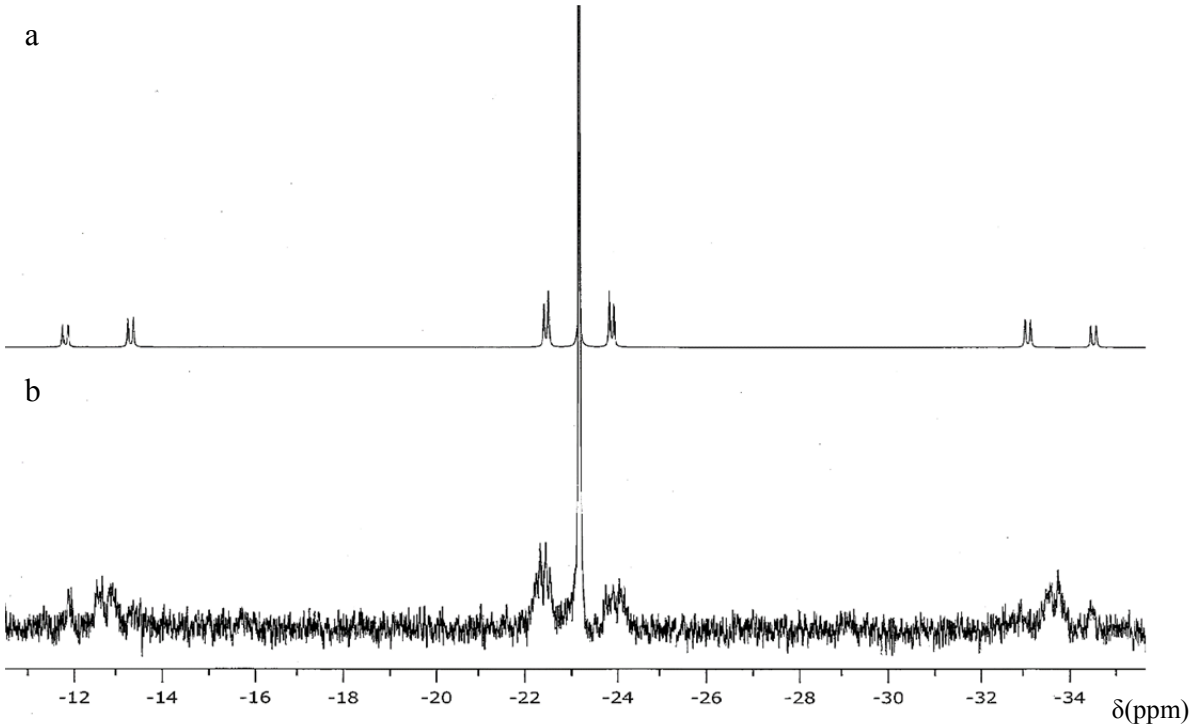

Figure 3.15 a) Preliminary simulated and b) experimental $^{31}P\{^{1}H\}$ NMR spectra of **3.28b**.

To investigate more about the bridging mode of these P–P ligands, *in situ* $^{31}P\{^{1}H\}$ NMR of **2.31** and **2.32** with $Cr(CO)_6$ and $\{RhCl_2(\eta^5\text{–}C_5Me_5)\}_2$ in $CDCl_3$ were made (Eqns. 3.5 and 3.6). Complex **1.380** demonstrated that ligands of the type **1.371** can bind one phosphorus atom to the metal centre leaving the other phosphorus nuclei uncoordinated (structure **III**, Sch. 3.1). In **1.381**, however, both phosphorus atoms are coordinated to Pt(II) metal centre (structure **IV**, Sch. 3.1). When **2.31** was treated with two equivs. of $Cr(CO)_6$, several possible Cr(III) complexes could be formed (**3.30a** – **3.30d**), however, $Cr(CO)_6$ did not react with **2.31** as observed by $^{31}P\{^{1}H\}$ NMR.

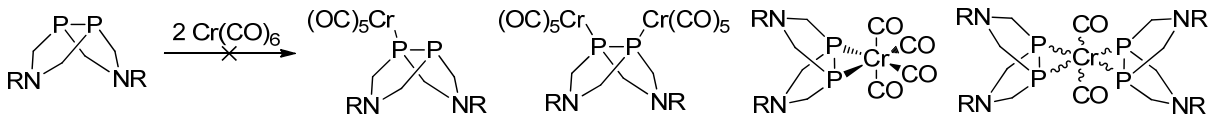

2.31 R = C_6H_5 **3.30a** R = C_6H_5 **3.30b** R = C_6H_5 **3.30c** R = C_6H_5 **3.30d** R = C_6H_5

Equation 3.5

More encouraging results were obtained when one equiv. of either **2.31** or **2.32**, was reacted with one equiv. of $\{RhCl_2(\eta^5\text{–}C_5Me_5)\}_2$ where various structures could be possible as illustrated in Equation 3.6. The MS showed the mass of the molecular ion without one or two chlorides $[M\text{–}Cl]^+$ 881 and $[M\text{–}2Cl]^{2+}$ 423 for the product of **2.31** and Rh precursor and $[M\text{–}Cl]^+$ 909 and $[M\text{–}2Cl]^{2+}$ 437 for the product of **2.32** and Rh precursor. Theses masses to charge belongs to **3.31a** and **3.32a** respectively and therefore, the structure of the products have both phosphorus bound to two Rh(III) metal centres.

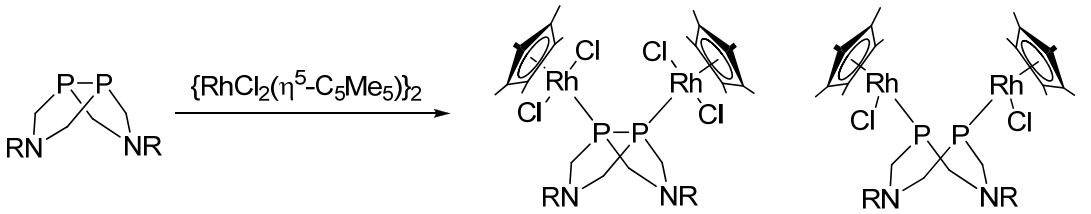

2.31 R = C_6H_5
2.32 R = *p*-MeC_6H_4

3.31a R = C_6H_5
3.32a R = *p*-MeC_6H_4

3.31b R = C_6H_5
3.32b R = *p*-MeC_6H_4

Equation 3.6

The $^{31}P\{^1H\}$ NMR of the Rh(III) complexes revealed resonances further downfield than diphosphines (*ca.* δP 22 ppm, ΔδP = 58 ppm) confirming coordination of **2.31** and **2.32** to Rh(III) metal centre. Figure 3.16 b shows the $^{31}P\{^1H\}$ spectrum of the product obtained from the reaction between **2.31** and Rh(III) precursor. As observed for Pt(II) complexes **3.27b** – **3.29b**, several spin systems are present in the spectrum however it is not first order and therefore the splitting pattern of **3.31** – **3.32** is completely different to those in **3.27b** – **3.29b**. To understand better the NMR, simulated spin–system analysis was employed. Figure 3.16 a shows the simulated $^{31}P\{^1H\}$ NMR for Rh(III) with **2.32** with estimated δP_A = –22.5 ppm, δP_B = –22.6 ppm and $^1J_{PAPB} = {}^1J_{PBPA}$ = –235.5 Hz, $^1J_{PARh} = {}^1J_{PBRh}$ = –150.4 Hz and $^2J_{PARh} = {}^2J_{PBRh}$ = 1 Hz. The latter coupling constant indicates that the products

obtained are likely to be **3.31a** and **3.32a** rather than **3.31b and 3.32b**. A superposition of these spin systems matches with the experimental NMR spectrum, shown in Figures 3.16 a and b, and couplings constants are further supported by the literature.[116–118]

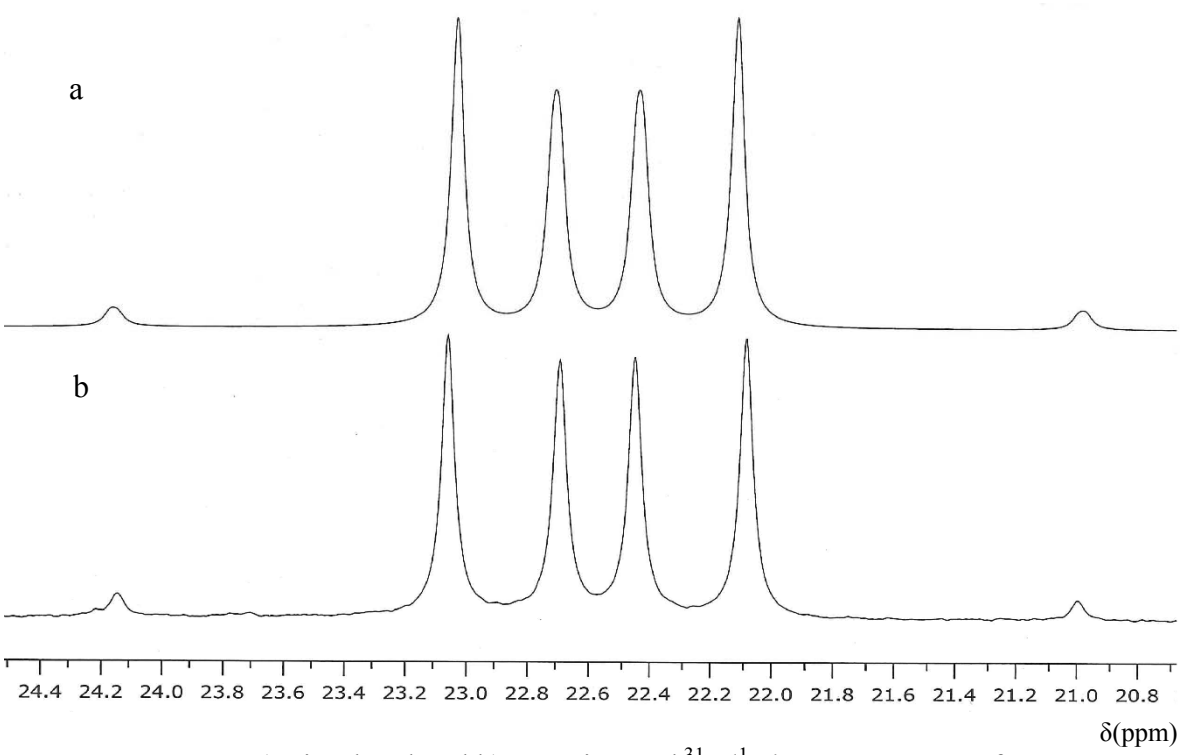

Figure 3.16 a) Simulated and b) experimental $^{31}P\{^{1}H\}$ NMR spectra of **3.31a**.

In summary, the coordination capabilities of the diphosphine ligands **2.31** – **2.34** were investigated towards several metal centres. A wide range of coordination modes are possible, however only the *P,P*-bridging was observed with Pt(II) and Rh(III) complexes **3.27b** – **3.29b** and **3.31a** – **3.32a** respectively and no *P,P*–chelating mode was seen, this was probably due to the restriction of the bite angle. Hence, the first approach to the coordination chemistry of these ligands is promising and further investigation should be conducted to isolate and fully characterise them.

3.9 X–ray crystal structure of 3.27b

Crystals of **3.27b**, suitable for X–ray crystallography, deposited from an *in situ* $CDCl_3$ solution of $PtCl_2$(COD) and **2.31**. The X–ray structure of **3.27b** exhibits a slightly distorted square–planar geometry around the metal centre with a bite angle between P(1)–Pt(1)–P(1A) of 100.11(4)^{o} (Table 3.9). The structure shows that the ligand has successfully coordinated to the Pt(II) metal centre generating a *cis* dinuclear species with a 6–membered ring (Fig. 3.17). This structure confirms the $^{31}P\{^{1}H\}$ spectrum and supports the

complex proposed for **3.27b** in Scheme 3.2. Similar arrangements were recently observed for Ni(II), Pt(II) and Pd(II) complexes (**1.381** – **1.386**, Fig. 1.19) with saturated P–P diphosphines and PPh_3 ligands.[86] These reported diphosphines act as mono or bidentate ligands. In **3.27b**, only the latter coordination mode is observed with two diphosphines between two Pt(II). However, whereas the documented structures form a $\{M(P–P)_3M\}$ cage, **3.27b** contains all metal and phosphorus atoms in a $\{M(P–P)_2M\}$ ring. The diphosphine binding angle (P–P–M) for **1.381** – **1.386** is in the 112 – 114° range, while it is significantly longer for **3.27b** [*ca.* 129.77(5)°]. This difference could be due to two bulky diphosphines having to be accommodated on two platinum(II) centres in **3.27b** while in **1.381** – **1.386** there are three less sterically hindered diphosphines per two metal(0) centres. These bulky diphosphines have the advantage of possessing pendant amines which are well orientated to potentially capture small molecules from the outer sphere and deliver them to the active metal site. Therefore, complex **3.27b** resembles metal systems containing diphosphines with the similar pendant arms but without a P–P bond, which are excellent catalysts for H_2 generation.[8,9,119]

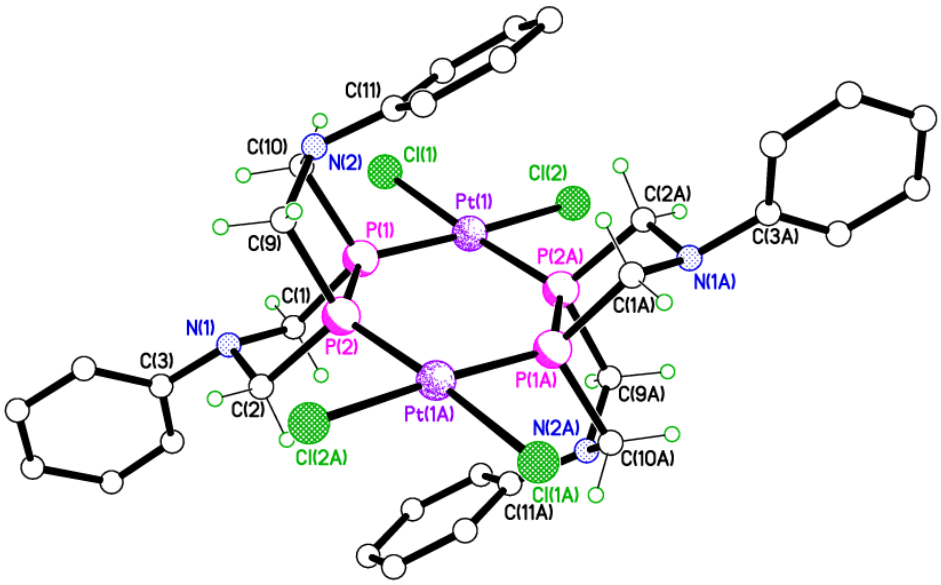

Figure 3.17 X–ray structure of **3.27b**. All H atoms except those on alkyl carbons are removed for clarity.

The P–P distance is slightly longer than the value measured in free phosphine **2.31** [2.191(7) Å] and C–N–C bond angles have comparable values (Table 3.9). The Pt–P and Pt–Cl bond distances are in agreement with those previously synthesised.[7,16,101] Intra or intermolecular H–bonds were not observed.

Table 3.9 Selected bond lengths (Å) and angles (°) for **3.27b**.[a]

3.27b			
Pt(1)–P(1)	2.2056(10)	P(1)–Pt(1)–Cl(2)	174.97(3)
Pt(1)–P(1A)	2.2068(10)	P(1A)–Pt(1)–Cl(1)	176.15(3)
Pt(1)–Cl(1)	2.3595(10)	P(1)–Pt(1)–Cl(1)	83.22(4)
Pt(1)–Cl(2)	2.3446(10)	P(1A)–Pt(1)–Cl(2)	83.87(4)
P(1)–P(2)	2.2147(14)	Cl(1)–Pt(1)–Cl(2)	92.78(3)
P(1)–Pt(1)–P(1A)	100.11(4)	C(1)–N(1)–C(2)	110.1(3)
Pt(1)–P(1)–P(2)	129.82(5)	C(11)–N(2)–C(10)	118.4(3)
Pt(1A)–P(2)–P(1)	129.72(5)		

[a] Estimated standard deviations in parentheses.

3.10 Coordination chemistry of PCNCP ligands with Pt(II)

In recent years, our research group has been investigating the coordination chemistry of ligands with non–equivalents phosphorus substituents of the type $Ph_2PCH_2N(R)CH_2PCg$ (**1.249**, R = C_6H_5, **1.250** and *p*-MeC_6H_4) (Sch. 1.22).[7] Hence, to expand the library of complexes with nonsymmetric diphosphines, the coordination capabilities of several PCNCP aminomethylphosphine ligands have been explored towards Pt(II) and Ru(II) metal centres.

In section 2.11, nonsymmetric PCNCP ligands **2.36** – **2.40** were obtained as major compounds along with their symmetric PCNCP **2.20**, **2.22**, **2.23**, **2.46** and **2.47** counterparts. In order to enhance the proportion of nonsymmetic PCNCP phosphines changes in the solvents, reaction time, reaction temperature and method were explored. However, it was identified that its conversion was not determined by these conditions but the nature of the reagents. In view of this, it is proposed that the isolation of the target compounds is achieved by using a platinum metal centre in a template synthesis as was observed previously by Nikonov *et al*.[99] Scheme 3.3 illustrates the template synthesis in two steps: the coordination of the nonsymmetric $Ph_2P_ACH_2N(R)CH_2P_B\{CH_2N(R)CH_2N(R)CH_2\}$ ligands by adding a platinum(II) precursor which would facilitate formation of the (chelate)platinum(II) complex (pathway **A**) followed by displacement of the diphosphine by a stronger ligand such as cyanide (pathway **B**).

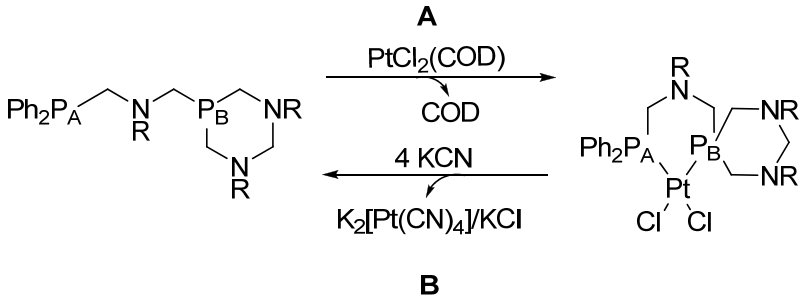

Scheme 3.3 Proposed template synthesis of nonsymmetric PCNCP aminomethylphosphines using $PtCl_2(COD)$ as starting material.

Two equivs. of the nonsymmetric phosphine **2.40** were treated with one equiv. of $PtCl_2(COD)$ in CH_2Cl_2 at r.t for 1 h affording complex **3.33** in up to approx. 50% along with symmetric bis(chelate)phosphines **3.6a** and **3.34** according to the $^{31}P\{^1H\}$ NMR (Eqn. 3.7). This is not surprising since free nonsymmetric ligand **2.40** was achieved in up to approx. 50% (according to the $^{31}P\{^1H\}$ NMR) with symmetric ligands **2.23** and **2.52** (Table 2.9, Eqn. 2.13).

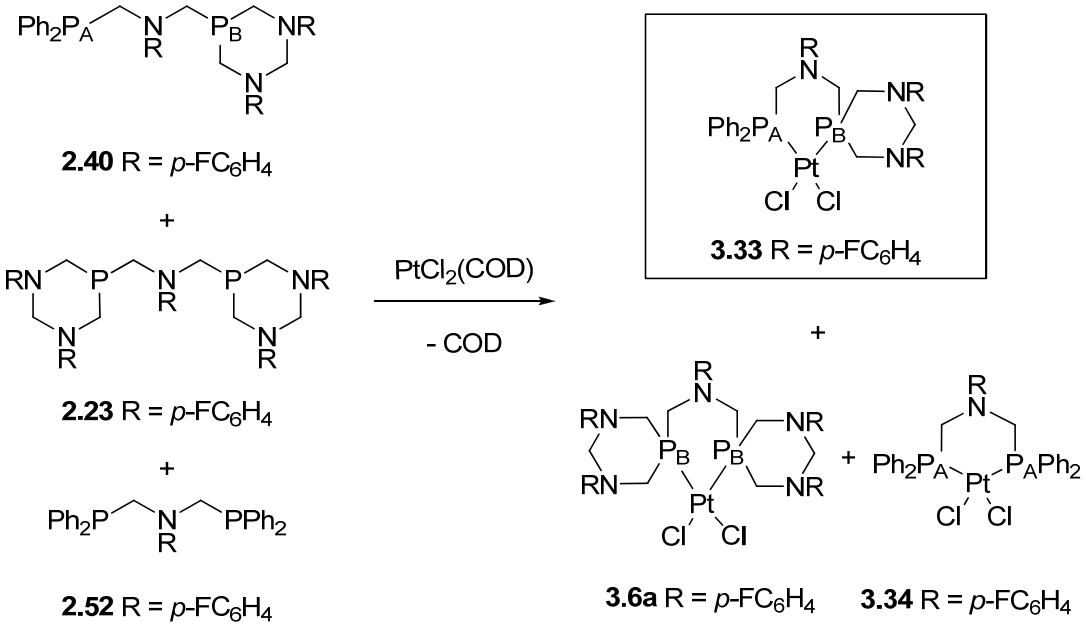

Equation 3.7

The $^{31}P\{^1H\}$ spectrum of **3.33** exhibited two major resonances as two doublets at *ca.* δP_A – 8.5 and δP_B –22.9 ppm ($^2J_{PP}$ = 13.0 Hz) flanked by two platinum satellites ($^1J_{PAPt}$ = 3450 and $^1J_{PBPt}$ = 3201 Hz) (Table 3.10 and Fig. 3.18). The peak at δP –8.5 ppm was assigned to P_A since it is close in chemical shift to P_A in **1.249** and **1.250** (–8.0 ppm, $^2J_{PP}$ = 19 Hz) and so the doublet at δP –22.9 ppm belongs to P_B.[7] However, δP_B in **3.33** is significantly upfield when compared to δP_B in **1.249** and **1.250** (–19.0 and 18.9 ppm respectively) due

to the different substituent on phosphorus ({$CH_2N(R)CH_2N(R)CH_2$}P, R = *p*–FC_6H_4 for **3.33** and Cg for **1.249** and **1.250**). The magnitudes of the $^1J_{PAPt}$, $^1J_{PBPt}$ coupling constants are in accordance with the values for phosphorus in *trans* arrangement to the chloride. The minor resonances at –6.0 ppm ($^1J_{PAPt}$ = 3420 Hz) and –23.7 ppm ($^1J_{PBPt}$ = 3217 Hz) were assigned to the **3.6a** and **3.34** by proximity to P_A and P_B in **3.33** respectively. In addition, assignment of **3.6a** was supported by the minor peak already observed in the $^{31}P\{^1H\}$ spectrum of **3.6** and similar δP values were observed in the literature.[99] Furthermore, assignment of **3.34** was supported by comparison with the phosphorus spectrum of complex **3.34** obtained *in situ* from $PtCl_2(COD)$ and Ph_2PCH_2OH in $CDCl_3$ in 1:2 stoichiometry.

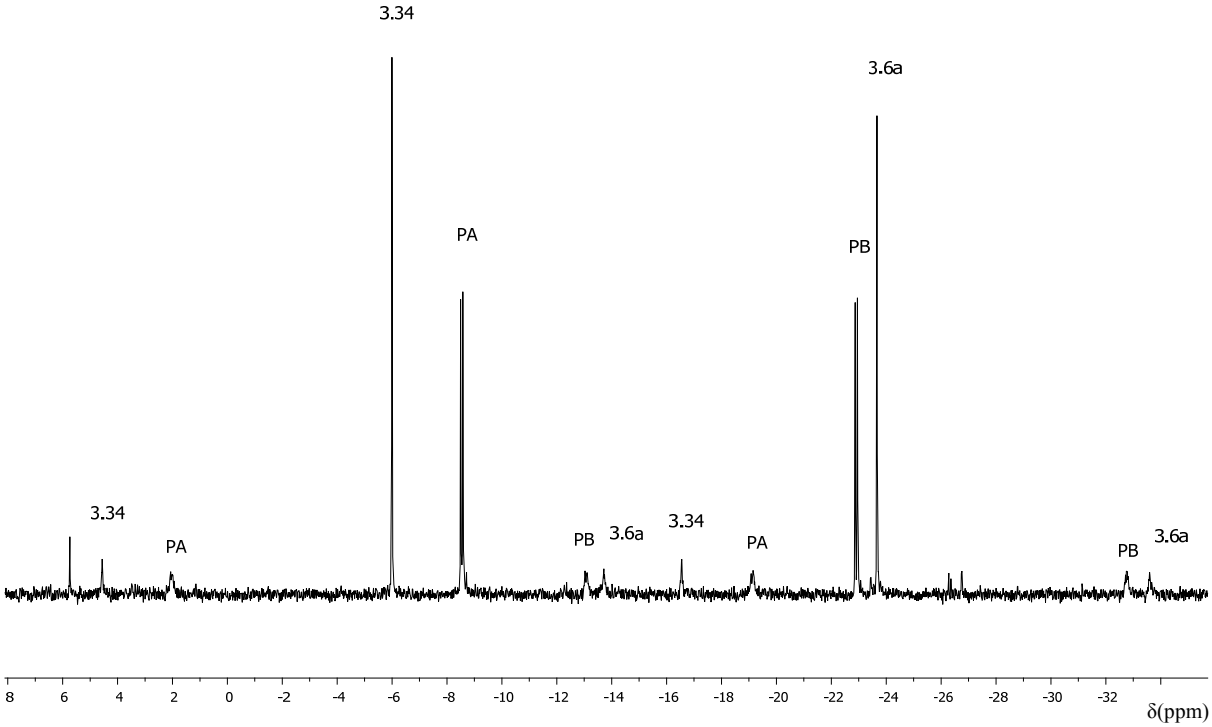

Figure 3.18 $^{31}P\{^1H\}$ of the dissociated product obtained between **2.40, 2.23, 2.52** and Ph_2PCH_2OH.

Ligand **2.40** proved to coordinate with Pt(II) as well as **2.23** and **2.52**, however the bulk solid obtained was a mixture of (chelate)phosphine amine complexes (**3.33**, **3.34** and **3.6a**) and hence, recrystallisation was performed prior to any template reaction (pathway **B** in Sch. 3.3). Purification of **3.33** was attempted by dissolving the complexes in CH_2Cl_2:Et_2O (1:1). Crystals were obtained in solution and the single crystal X–ray diffraction revealed

the *cis*(chelate)Pt(II) complex **3.6a** (Fig. 3.8) rather than the target complex **3.33** which could not be isolated from **3.34**.

A new approach for the template synthesis was proposed (Sch. 3.4). The reasoning is similar to the method depicted in Scheme 3.3 except for the synthesis of **3.33**. Pt(II) is added to ligands Ph_2PCH_2OH and **2.18** (pathway **A**) to get complex **3.33** followed by displacement of diphosphine ligand **2.40** by cyanide (pathway **B**). This alternate synthesis of **3.33** was proposed to avoid the mixture of PCNCP compounds obtained in Equation 3.7.

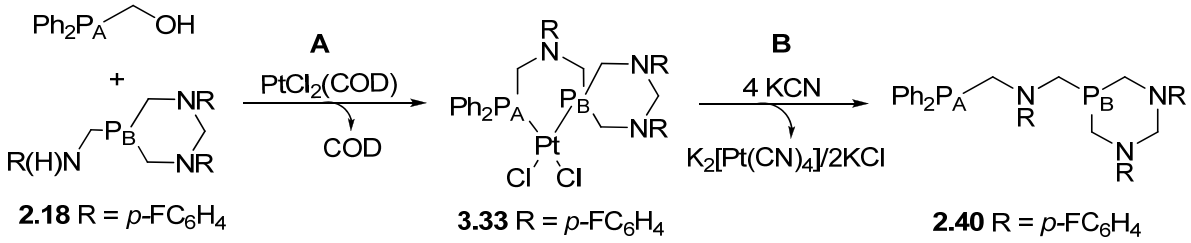

2.18 R = *p*-FC_6H_4 **3.33** R = *p*-FC_6H_4 **2.40** R = *p*-FC_6H_4

Scheme 3.4 Proposed template synthesis of nonsymmetric PCNCP **2.40** using **2.18**, Ph_2PCH_2OH and $PtCl_2(COD)$ as starting materials.

To prevent formation of a mixture of PCNCP aminophosphines **2.40**, **2.23** and **2.52**, $PtCl_2(COD)$, Ph_2PCH_2OH and **2.18** were dissolved in CH_2Cl_2 separately. Solutions containing the ligands were added dropwise to the $PtCl_2(COD)$ solution over a period of 5 min (Sch. 3.5). Surprisingly, cyclic Pt(II) complex **3.33** was not obtained and linear Pt(II) compound **3.35** was synthesised as a major component along with *cis* linear Pt(II) coproducts $PtCl_2(Ph_2PCH_2OH)_2$ and **3.6** (approx. 3:16:1) (Sch. 3.5).

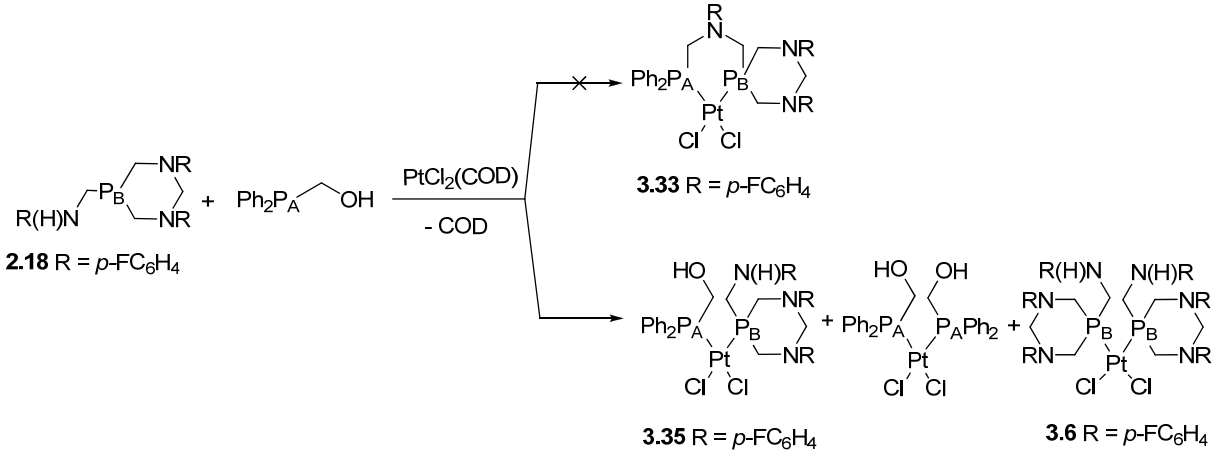

2.18 R = *p*-FC_6H_4 **3.33** R = *p*-FC_6H_4 **3.35** R = *p*-FC_6H_4 **3.6** R = *p*-FC_6H_4

Scheme 3.5 Attempted synthesis of **3.33** and successful production of **3.35** from **2.18** and Ph_2PCH_2OH.

This experiment demonstrated that ligands **2.18** and Ph_2PCH_2OH initially react with the metal centre prior to any condensation between the amino and hydroxyl groups taking place. Recent studies have shown that the Mannich condensation reaction does not occur if the lone pair on phosphorus in Ph_2PCH_2OH is coordinated.[10] Therefore, **3.35** will not proceed to the formation of **3.33** and, accordingly, will not permit the template synthesis.

Different ligands with a variety of substituents on N and P atoms have been utilised in the synthesis of analogues to **3.35**. Complexes **3.36** – **3.40** were prepared under the same reaction conditions as **3.35** and obtained as major components according to the $^{31}P\{^1H\}$ NMR (Eqn. 3.8).

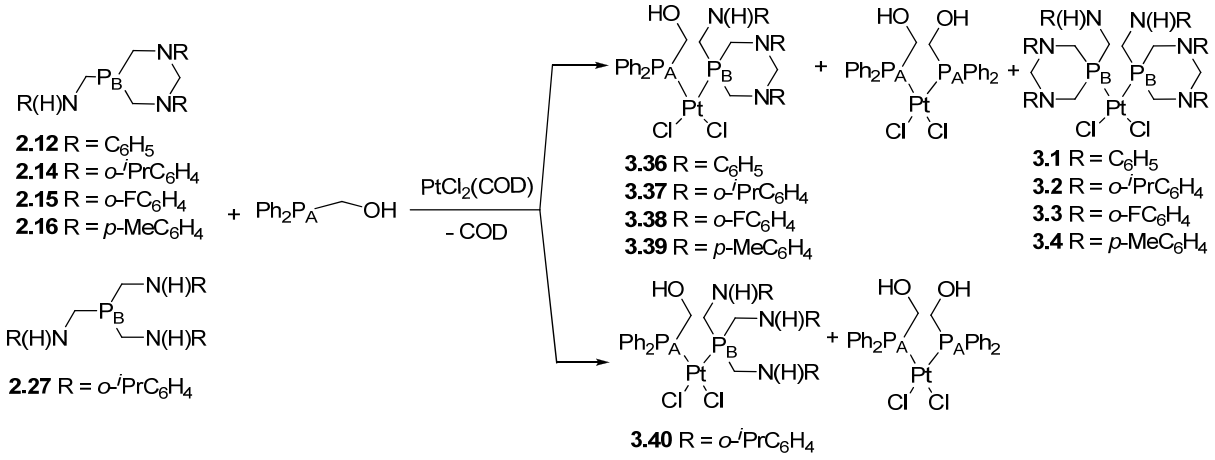

Equation 3.8

Table 3.10 Selected $^{31}P\{^1H\}$ NMR (in ppm, *J* in Hz) for compounds **3.33**, **3.35** – **3.40**.[a]

	$^{31}P_A\{^1H\}$	$^{31}P_B\{^1H\}$	$^1J_{PAPt}$	$^1J_{PBPt}$	$^2J_{PP}$
3.33	–8.5	–22.9	3450	3201	13
$Pt(Ph_2PCH_2OH)_2Cl_2$	7.2 (7.3)[b]		3712 (3687)[b]		
3.35	5.3	–12.3	3693	3356	15
3.36	5.5	–11.1	3742	3285	15
3.37	5.4	–12.7	3696	3146	16
3.38	5.1	–16.3	3735	3311	15
3.39	5.5	–11.9	3965	3285	15
3.40	5.7	5.0	3340	3672	26

[a] NMR spectra measured in $CDCl_3$. [b] Taken from ref[120].

The $^{31}P\{^{1}H\}$ NMR spectra of **3.35** – **3.40** displayed similar splitting patterns as for **3.33** but they exhibited a large downfield shift in the δP_A and δP_B values with respect to **3.33** and Pt**(**$Ph_2PCH_2OH)_2Cl_2$ (Table 3.10). Complexes **3.35** – **3.40** gave two doublets at *ca.* δP_A 5.5 ppm and at *ca.* δP_B –12.9 ppm with coupling constants of approx. $^{2}J_{PP}$ = 15, $^{1}J_{PAPt}$ = 3700 and $^{1}J_{PBPt}$ = 3300 Hz. The coupling between the two phosphorus nuclei do not differ significantly from the value found for **3.33**. Likewise, the coupling constant to platinum is in agreement with **3.33** and $Pt(Ph_2PCH_2OH)_2Cl_2$ which also indicates that the PCNCP ligands adopt a *cis* conformation with respect to the metal centre. Figure 3.19 illustrates the $^{31}P\{^{1}H\}$ NMR spectrum of **3.35** and their coproducts $Pt(Ph_2PCH_2OH)_2Cl_2$ and **3.6**.

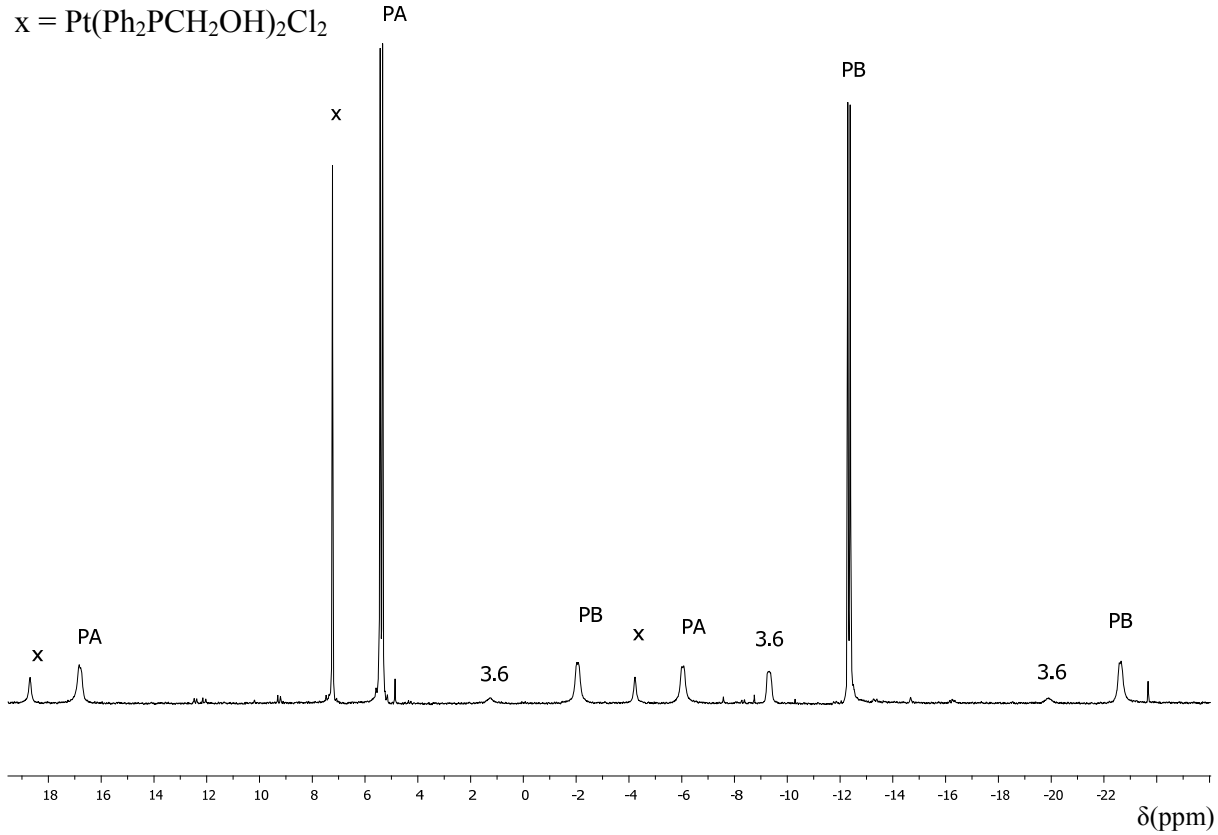

Figure 3.19 $^{31}P\{^{1}H\}$ of the dissociated product obtained between **2.18** and Ph_2PCH_2OH.

Complex **3.40** displayed two doublets as their analogues **3.35** – **3.39** but the value of δP_B is further downfield (δP_B = 5.0 ppm). Likewise, the magnitude of the couplings constants ($^{1}J_{PAPt}$ = 3340 and $^{1}J_{PBPt}$ = 3672 ppm) differs significantly from their analogues. These values indicate that **3.40** possesses both phosphorus atoms in a *cis* arrangement with respect to the platinum. It seems that, independently of the phosphorus substituents (cyclic phosphines **2.12**, **2.14** – **2.16** or linear **2.27**), complexes **3.33**, **3.35** – **3.40** adopt a *cis*

disposition of the phosphorus in relation to the metal centre. Furthermore, whereas the nitrogen substituent in cyclic aminomethylphosphines has a negligible effect on the chemical shift of P_A and P_B of **3.37** – **3.39**, the introduction of a linear phosphorus substituent moves the δP_B shift downfield significantly as has been discussed in **3.40**.

While complexes **3.35** – **3.40** were successfully synthesised, they were not suitable as precursors in the template synthesis depicted in Schemes 3.3 and 3.4. Hence, Scheme 3.6 shows an alternative template synthesis. In this proposed method, Pt(II) complexes containing the coordinated phosphine and free amino group would be treated with the uncoordinated Ph_2PCH_2OH (pathway **A**) to yield the *cis* Pt(II) **I**. Then, the addition of a ligand, which would bind to the metal centre more strongly than the phosphine, would displace two nonsymmetric PCNCP ligands (pathway **B**). The lone pair on Ph_2P_A– in complex **I** could coordinate to the metal centre displacing the chlorides (intermediate **II**) to form a bis(chelate)platinum(II) complex **III** (pathway **C**) which leads to the target PCNCP ligand by displacement with KCN (pathway **D**).

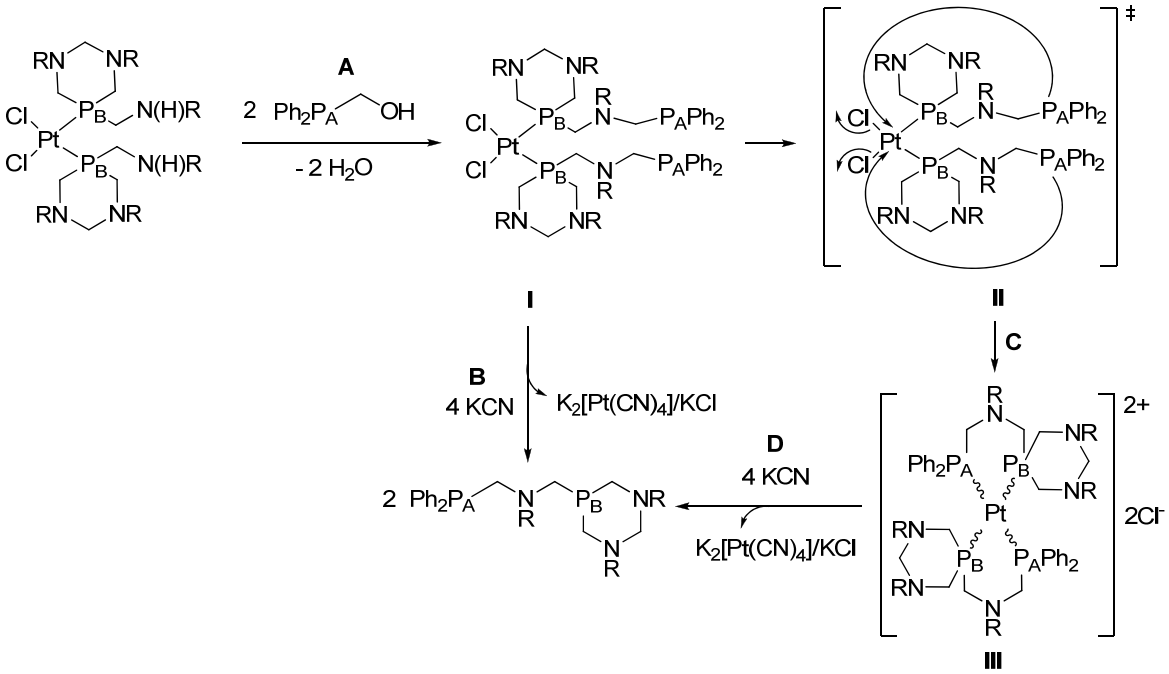

Scheme 3.6 Proposed template synthesis of nonsymmetric PCNCP aminomethylphosphines using $PtCl_2[RN(H)CH_2P_B\{CH_2N(R)CH_2N(R)CH_2\}]_2$ and Ph_2PCH_2OH as starting materials.

Bis(chelate)platinum(II) compounds of the type **III** in Scheme 3.6 were obtained by adding two equivs. of Ph_2PCH_2OH to $PtCl_2[RN(H)CH_2P_B\{CH_2N(R)CH_2N(R)CH_2\}]_2$ in one step. Nevertheless, they could also be achieved in two steps as previously observed by

Gordon and Woollins groups with similar Pt(II) complexes of the type $[Pt(L)]^{2+}$ (L = dppm, dppe, dppa).[121,122] Here we applied both methods and the latter is first discussed since it gives more information about the mechanism of the reaction. Hence, addition of the first equiv. of Ph_2PCH_2OH to **3.3** and **3.6** at r.t. in CH_2Cl_2 gave the monocationic Pt(II) complexes **3.41** and **3.42** respectively as pale yellow powders in 62 and 84% yield (Eqn. 3.9).

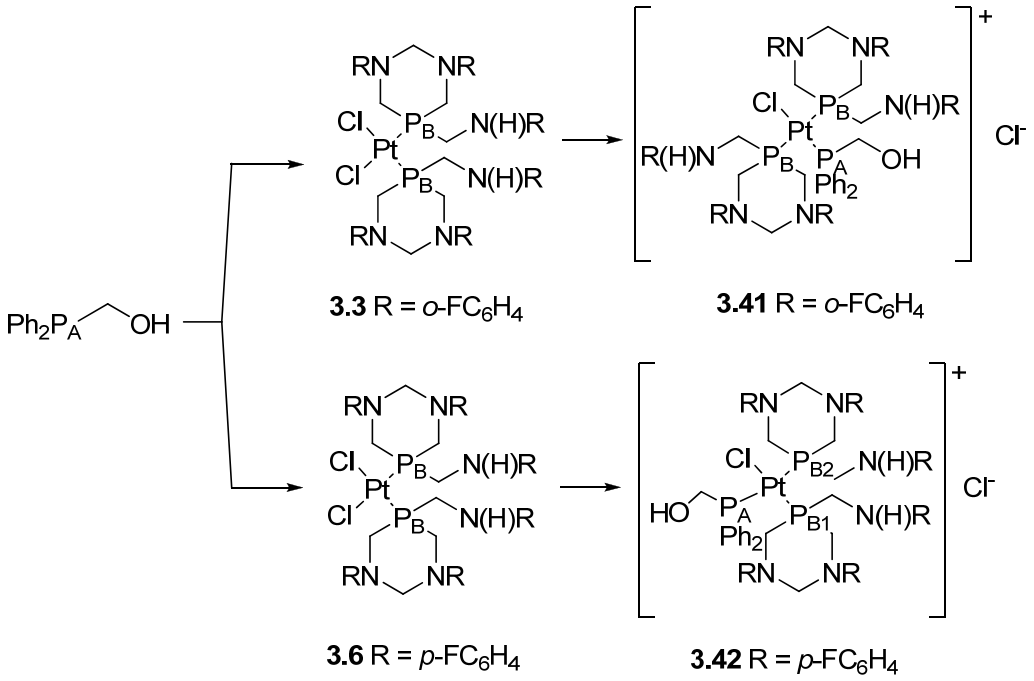

Equation 3.9

Table 3.11 Selected $^{31}P\{^1H\}$ NMR (in ppm) for compounds **3.41** and **3.42**.[a]

Comp	$^{31}P_A$	$^{31}P_B$	$^1J_{PAPt}$	$^1J_{PBPt}$	$^2J_{PAPB}$
3.41	1.0	–10.5	3682	2243	17
3.42	–9.2	–13.4[b]	2307	3714[b]	326[d]
		–26.0[c]		2321[c]	16[e]

[a] NMR spectra measured in $CDCl_3$. [b] P_{B1}. [c] P_{B2}. [d] $^2J_{PAPB2}$. [e] $^2J_{PAPB1} = {}^2J_{PB1PB2}$.

Complexes **3.41** and **3.42** displayed first order $^{31}P\{^1H\}$ NMR spectra, which was in agreement with cationic platinum(II) complexes with three different phosphine groups (Table 3.11).[121,122] Each phosphine group appeared as a doublet of doublets with satellites due to the coupling to ^{195}Pt. However, the *trans* phosphorus nucleus (P_B) in **3.41** have nearly coincident chemical shifts at –10.5 ppm, which showed a simple $^{31}P\{^1H\}$ NMR. The spectrum appeared to consist of a doublet for P_B and a triplet at larger shift (δP_A = 1.0 ppm) for P_A (Fig. 3.20). Likewise, the P_{B2} in **3.42** appeared as a virtual triplet at δP_B –13.4

ppm (Fig. 3.21). The resonances due to the phosphorus *cis* to the chloride were readily identified by the $^{1}J_{PPt}$ coupling constant of $^{1}J_{PBPt}$ = 2243 Hz for **3.41** and $^{1}J_{PB1Pt}$ = 2321 and $^{1}J_{PAPt}$ = 2307 Hz for **3.42**. The $^{1}J_{PAPt}$ coupling constants for δP_A indicated that P_A in **3.41** is *trans* to the chloride ($^{1}J_{PAPt}$ = 3682 Hz) whereas in **3.42** P_A is in a *cis* disposition ($^{1}J_{PAPt}$ = 2307 Hz). Furthermore, the $^{2}J_{PAPB}$ coupling constants between phosphine groups in a *cis* arrangement is smaller than 20 Hz ($^{2}J_{PAPB}$ = 17 Hz for **3.41** and $^{2}J_{PAPB1}$ = $^{2}J_{PBPB2}$ = 16 Hz for **3.42**) while that for phosphorus atoms arranged *trans* to each other is much larger ($^{2}J_{PAPB2}$ = 326 Hz for **3.42**). Hence, **3.41** and **3.42** displayed *cis* and *trans* geometries of P_B with the Pt(II) respectively. The geometry may be related to the position of the fluorine in the aniline. The *trans* geometry in **3.41** could be due to the steric effect of the *ortho* fluorine on the aniline which push apart both diazaphosphorinane substituents. Complex **3.42** possess the fluorine in a *para* position to the nitrogen of the aniline and, therefore, can accommodate two *cis* diazaphosphorinanes.

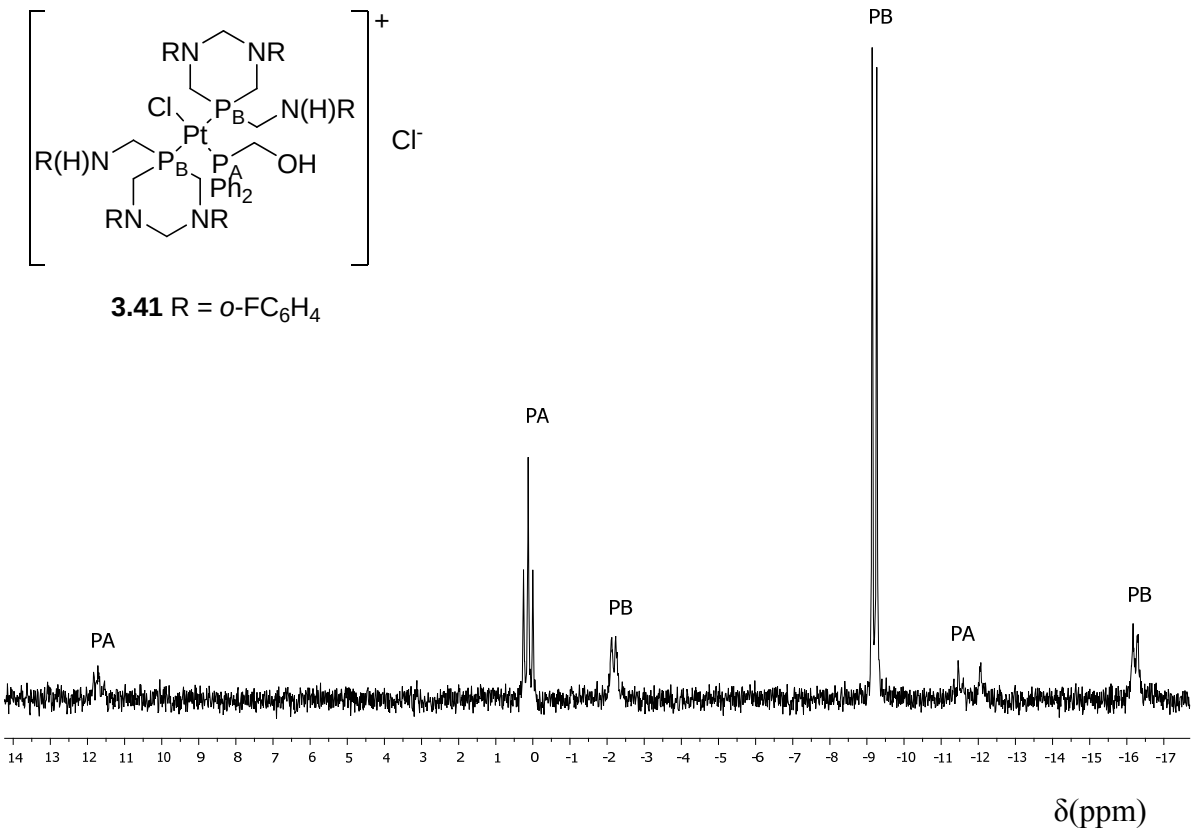

3.41 R = *o*-FC_6H_4

Figure 3.20 $^{31}P\{^{1}H\}$ NMR of **3.41**.

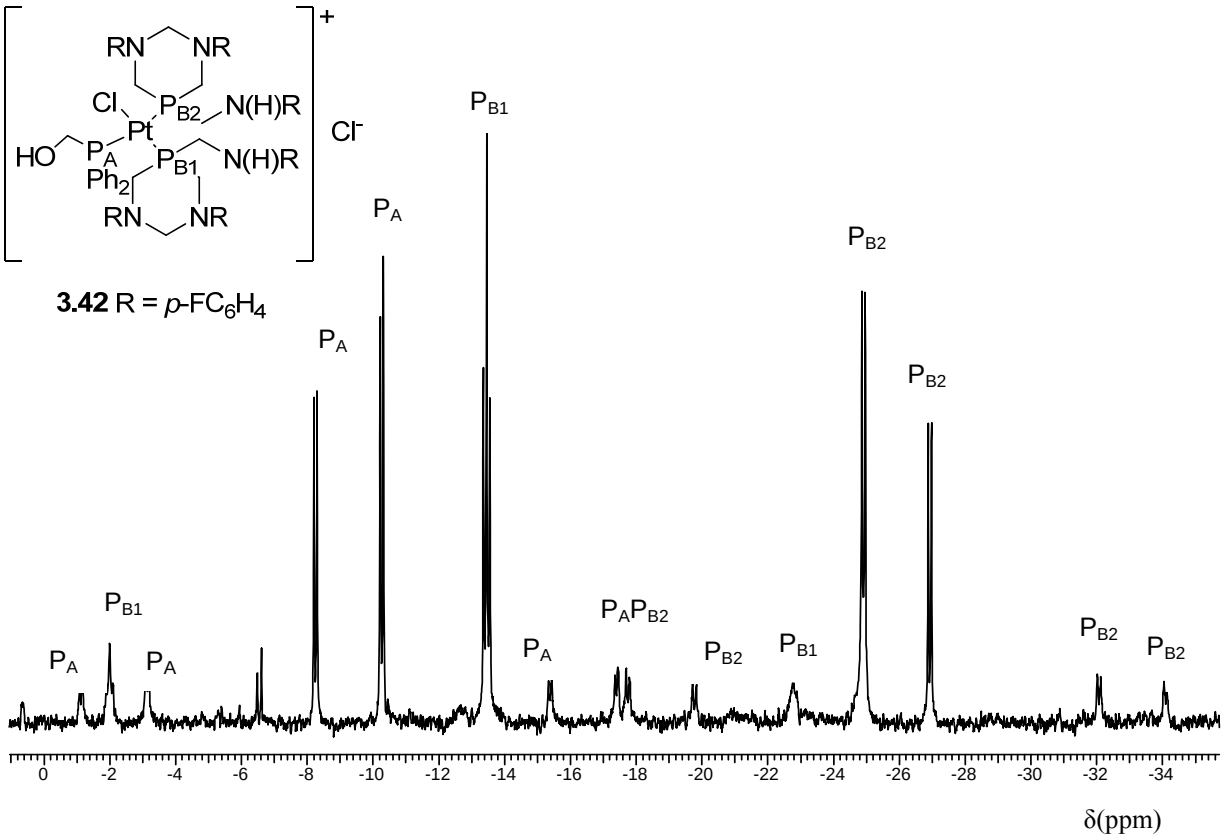

Figure 3.21 $^{31}P\{^{1}H\}$ NMR of **3.42**.

^{1}H NMR of **3.41** showed two peaks at 7.85 and 4.15 ppm which are not observed in the spectrum of **3.42**. Those peaks vanished upon addition of D_2O for **3.41** and a broad singlet at *ca*. 1.70 ppm in **3.42** disappeared too. The latter could be due to 2 NH + OH or due to the H_2O produced in the Mannich condensation since the peak is near to the shift for H_2O in $CDCl_3$.[123] In **3.41**, EA recorded the molecular mass of the compound with H_2O moiety but this was not observed in **3.42**. In both complexes, MS exhibited the mass to charge ratio of the compound without the chloride ion. In addition, in the IR of **3.42** a broad vibration was observed at approx. 3200 cm^{-1}. Overall, IR, MS and EA indicated that a H_2O moiety is present in **3.41** and **3.42** but it is not possible to elucidate if it is produced by the Mannich condensation or due to the NH and OH groups. ^{1}H NMR of **3.41** and **3.42** displayed two and one peaks respectively which disappeared upon adding D_2O but due to the proximity of the δH for H_2O in **3.42**, it is impossible to assign this peak to NH and OH or to H_2O. In summary, the structure proposed in Equation 3.9 for **3.41** satisfied the results obtained but the structure for **3.42** remains unclear.

Why both *cis* and *trans* geometries are formed is still not clear but it may be related to the position of the substituent on the aniline. A possible mechanism *via* a five–coordination complex could explain both conformations. A process of *cis-trans* isomerisation was already observed by Karasik and co–workers with bivalent platinum complexes.[60] Albeit compounds with L_3PtCl_2 composition were isolated as a mixture of *cis*, *trans* and the free ligand, it has been failed to determine if it is a neutral five–coordinated or ionic square–planar platinum complex. Compounds **3.41** and **3.42** have been demonstrated to fit in the last geometry (due to the $^1J_{PPt}$ and MS) with a chloride as a counter ion giving an insight into this chemistry. Although at the present it is impossible to define exactly whether **3.42** underwent condensation or not, the complex is perfectively valid as an intermediate for the next step as it is **3.41**.

Addition of a second equiv. of Ph_2PCH_2OH to **3.41** and **3.42** afforded the bis(chelate) Pt(II) complexes **3.43a**, **3.44a**, **3.43b** and **3.44b** in good to excellent yields (46 – 98%) (Sch. 3.7). Compounds **3.44a** and **3.44b** were also achieved in one–pot reaction from $PtCl_2COD$ and ligands **2.18** and Ph_2PCH_2OH in a stoichiometry of 1:2:2. Likewise compounds **3.45a** and **3.45b** were also obtained.

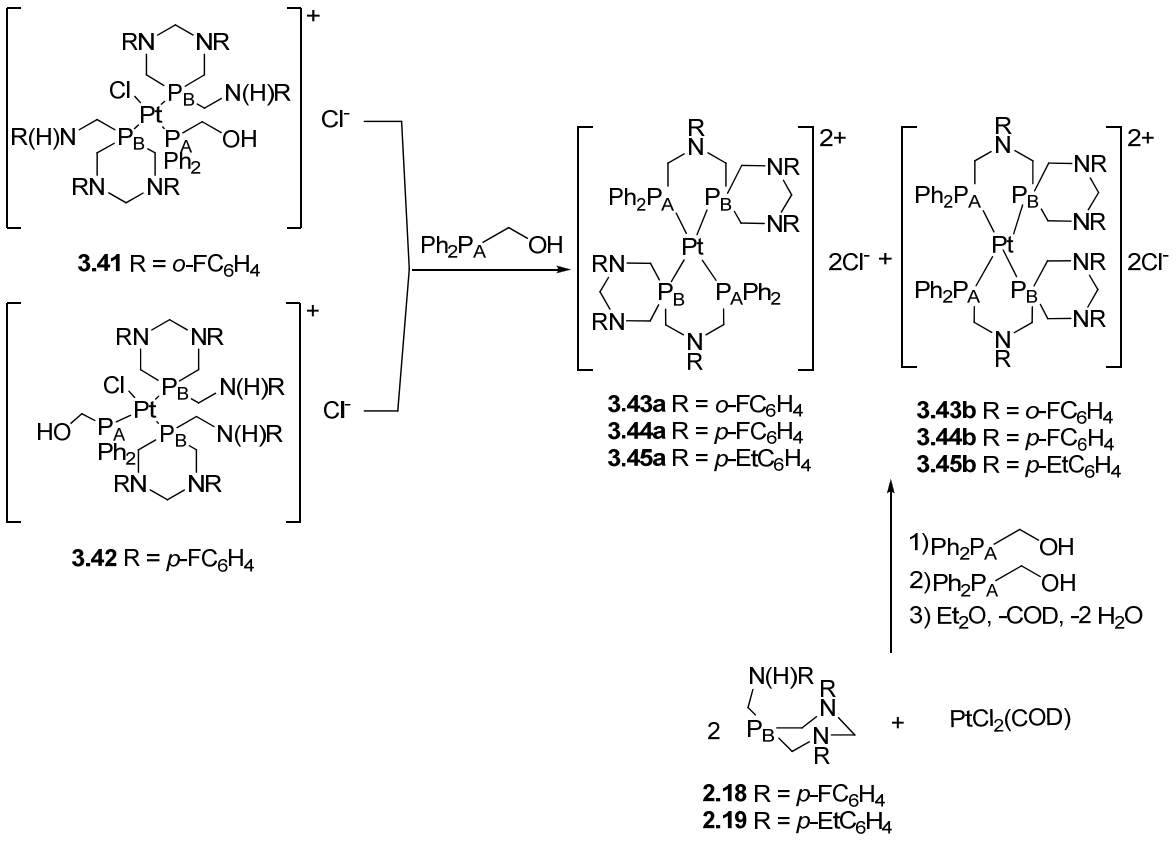

Scheme 3.7 Synthesis of bis(chelate) Pt(II) complexes.

Table 3.12 Selected $^{31}P\{^{1}H\}$ NMR (in ppm, *J* in Hz) for compounds **3.43** – **3.45**.[a]

	$^{31}P_A$	$^{31}P_B$	$^{1}J_{PAPt}$	$^{1}J_{PBPt}$	$^{2}J_{PP}$[b]
3.43a	–20.5	–37.0	2670	2113	31
3.44a	–17.4	–33.5	2628	2139	31
3.45a	–18.4	–34.7	2618	2120	31
3.43b	–25.0	–43.5	n.o.	n.o.	255
3.44b	–22.9	–45.3	n.o.	n.o.	251
3.45b	–24.1	–51.9	n.o.	n.o.	245

[a] NMR spectra in $CDCl_3$. [b] $^{2}J_{PP} = \left| {}^{2}J_{PAPB+} {}^{2}J_{PAPB} \right|$

Signals observed in the $^{31}P\{^{1}H\}$ for **3.43a** – **3.45a** and **3.43b** – **3.45b** were tentatively assigned to P_A and P_B by analogy with platinum precursors where δP_A is further downfield than δP_B. Furthermore, complexes **3.43a** – **3.45a** possess two phosphorus with the same substituents (Ph_2P_A– and $\{CH_2N(R)CH_2N(R)CH_2\}P_B$–) in a *trans* disposition whereas in **3.43b** – **3.45b** they are *cis* to each other. Due to that, it is expected that the $^{31}P\{^{1}H\}$ spectra of **3.43a** – **3.45a** display two triplets and only two doublets for **3.43b** – **3.45b**. The $^{31}P\{^{1}H\}$ of the bulk samples are summarised in Table 3.12. Complexes **3.43a** – **3.45a** showed two major triplets, flanked by platinum satellites ($2618 < {}^{1}J_{PPt} > 2670$ Hz), and two minor doublets for **3.43b** – **3.45b** in different proportions (Exp. Sect.). Using a combination of solvents (CH_2Cl_2/Et_2O 50:50) pure crystals of the *trans*(chelate) isomer **3.44a** were obtained (Fig. 3.23) and the phosphorus NMR (Fig. 3.22) revealed exclusively the two triplets (δP_A –17.4 and δP_B –33.5 ppm) flanked by platinum satellites already observed in the crude product. The X–ray structure of **3.44a** with its NMR supported the assignment of **3.43a** and **3.45a**.

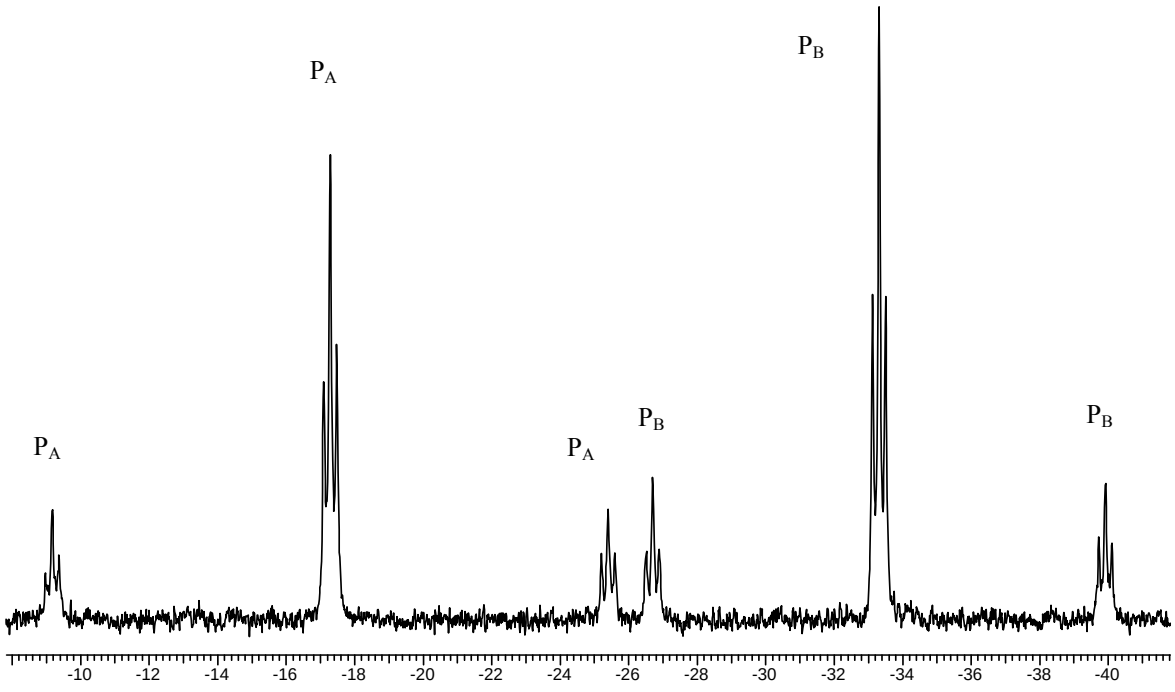

Figure 3.22 $^{31}P\{^{1}H\}$ NMR of **3.44a**.

The synthesis of **3.44a** and **3.45a**, displayed in Scheme 3.7, was further supported by EA and MS. The last technique showed spectra with a fragmentation pattern of the molecular ion without two chloride counter ions but one hydride ($[MH–2Cl]^+$ 1422 for **3.44a** and $[M–Cl]^+$ 1516 for **3.45a**). Five–coordinated platinum(II) complexes have previously been observed with small ligands such as hydride.[27] Furthermore, this fragmentation pattern was also observed for **3.41a** and **3.42a** ($[MH–2Cl]^+$ 1242).

So overall, new *trans* bis(chelate) complex $\{Pt(P_ACNCP_B)_2\}Cl_2$ complexes **3.43a** – **3.45a** and *cis* bischelate complex $\{Pt(P_ACNCP_B)_2\}Cl_2$ complexes **3.43b** – **3.45b** were obtained in a one–pot reaction or in two steps and **3.44a** was purified by crystallisation as *trans* bis(chelate) complex $\{Pt(P_ACNCP_B)_2\}Cl_2$. The procedure conducted in two steps permitted isolation of the intermediates *trans*-**3.41** and *cis*–**3.42** and, therefore, gave better understanding of the mechanism of this reaction. The bis(chelate) complex $\{Pt(P_ACNCP_B)_2\}Cl_2$ are excellent compounds for the template synthesis proposed in Scheme 3.3 so with this aim further investigation should be conducted.

3.11 X–ray crystal structure of 3.44a

Crystals of **3.44a**, suitable for X–ray crystallography, were grown by slow diffusion of Et_2O into a CH_2Cl_2 solution of **3.44a**. The overall geometry is distorted square planar with respect to the platinum(II) centre with angles P–Pt–P close to 90° (Table 3.13, Fig. 3.23).

This structure demonstrates that ligand **2.40** succesfully coordinates with Pt(II), where phosphorus with the same substituents are *trans* to each other [*i.e.* P(1) and P(1A) and P(2) and P(2A)], to form the *trans* bischelate Pt(II) complex **3.44a**. The Pt–P distances in **3.44a** [*ca*. 2.350(4) Å] are comparable with $[Pt(dmpp)_2]^{2+}$ [3.136(11) Å],[124] $[Pt(dppmpa)_2]^{2+}$ [2.355(1) Å][125] and $[Pt(dppe)(dppa)]^{2+}$ [2.317(1) Å].[122] The P(1)–Pt(1)–P(1A) bite angle in the bis chelate **3.44a** [86.72(11)^o] is smaller than the same angle in $[Pt(dmpp)_2]^{2+}$ [88.10(5)^o] and $[Pt(dppmpa)_2]^{2+}$ [87.60(5)^o] and in the analogous mono chelate complex **3.6a** [92.94(4)^o] (Fig. 3.8).

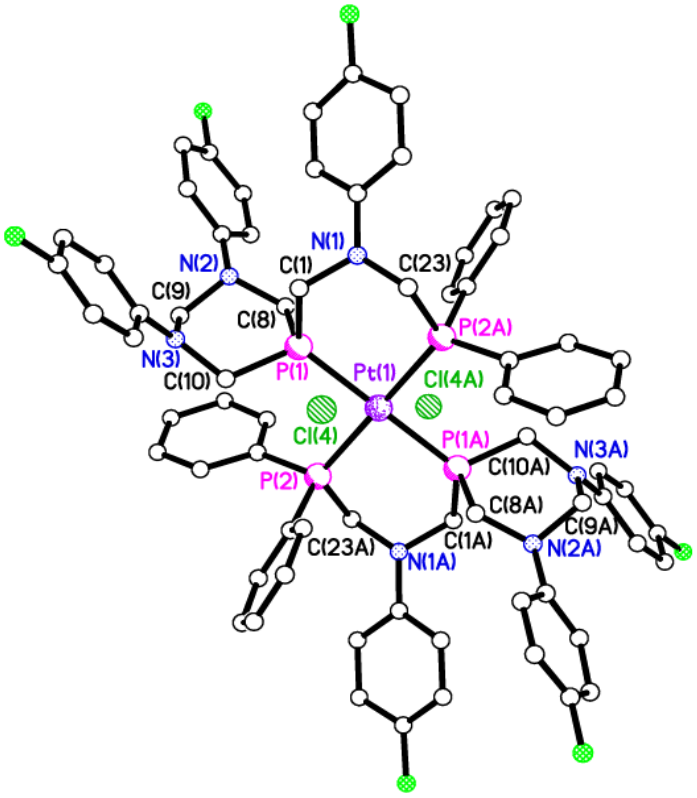

Figure 3.23 X–ray structure of **3.44a**. All H atoms and $CHCl_3$ solvent are removed for clarity.

Table 3.13 Selected bond lengths (Å) and angles (^{o}) for **3.44a**.[a]

3.44a			
Pt(1)–P(1)	2.327(3)	P(2)–Pt(1)–P(1A)	86.72(11)
Pt(1)–P(2)	2.373(4)	P(1A)–Pt(1)–P(2A)	93.28(11)
Pt(1)–P(1A)	2.327(3)	Pt(1)–P(1)–C(1)	123.3 (4)
Pt(1)–P(2A)	2.374(4)	P(1)–C(1)–N(1)	111.6(8)
P(1)–Pt(1)–P(2A)	86.72(11)	C(1)–N(1)–C(23)	111.8(11)
P(1)–Pt(1)–P(2)	93.28(11)	N(1)–C(23)–P(2)	111.3(8)
P(1)–Pt(1)–P(1A)	180.0	C(23)–P(2)–Pt(1)	117.4(5)
P(2)–Pt(1)–P(2A)	180.0		

[a] Estimated standard deviations in parentheses. Symmetry operators: –*x*+1, –*y*+1, –*z*.

The six–membered chelate rings are considerable less twisted in **3.44a** when compared to complex $[Pt(dppmpa)_2]^{2+}$ (Fig. 3.24 a and b respectively). This effect appears to arise because of steric congestion between four phenyl substituents in dppmpa whereas in **3.44a**, Ph_2P– are *trans* to each other. Furthermore, this permits that every atom in the Pt(1)–P(1)–P(2)–P(1A)–P(2A) coordination plane in **3.44** is in the same plane which is in contrast to $[Pt(dppmpa)_2]^{2+}$ (Figs. 3.24 a and b respectively).

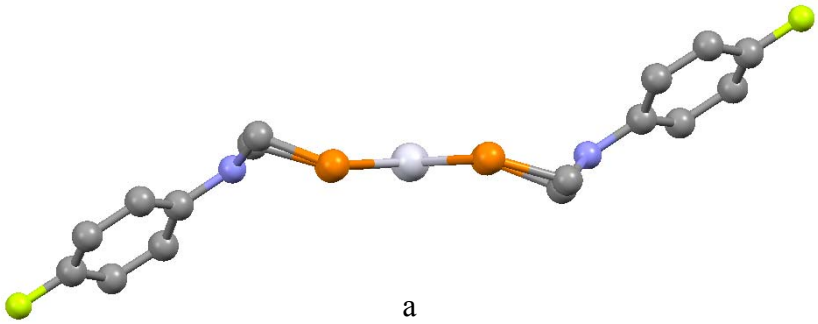

a

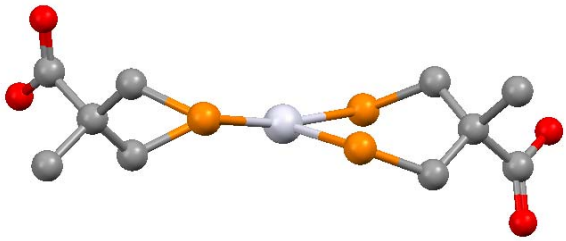

b

Figure 3.24 X–ray structure showing the Pt(1)–P(1)–P(2)–P(1A)–P(2A) coordination plane of a) **3.44a** and b) $[Pt(dppmpa)_2]^{2+}$.[125] Phenyl substituents removed for clarity.

There are weak intermolecular C–H···Cl hydrogen bonds between the Pt(II) dication and the chlorides [C···Cl distances in the range 3.37(2) – 3.596(16) Å] and C–H···Cl interactions were observed too between the counter ions and the chloroform solvent (Table 3.14).

Table 3.14 Selected H–bond lengths (Å) and angles (°) for **3.44**.[a]

D–H···A	D–H	H···A	D···A	D–H···A
C(1)–H(1B)···Cl(4)	0.99	2.64	3.417(15)	136
C(23)–H(23A)···Cl(4)	0.99	2.74	3.596(16)	144
C(35)–H(35)···Cl(4)	0.95	2.68	3.496(15)	144
C(36)–H(36)···Cl(4)	1.00	2.51	3.37(2)	144

[a] Estimated standard deviations in parentheses.

3.12 Coordination chemistry of PCNCP aminomethylphosphine ligands with Ru(II)

To understand more about **2.39** and **2.40**, their coordination chemistry with Ru(II) was investigated. The Ru(II) complexes **3.46** and **3.47** were obtained by reacting **2.39** and **2.40** with $\{RuCl_2(\eta^6\text{–}p\text{-cymene})\}_2$ in equimolar quantities in CH_2Cl_2 (Eqn. 3.10).

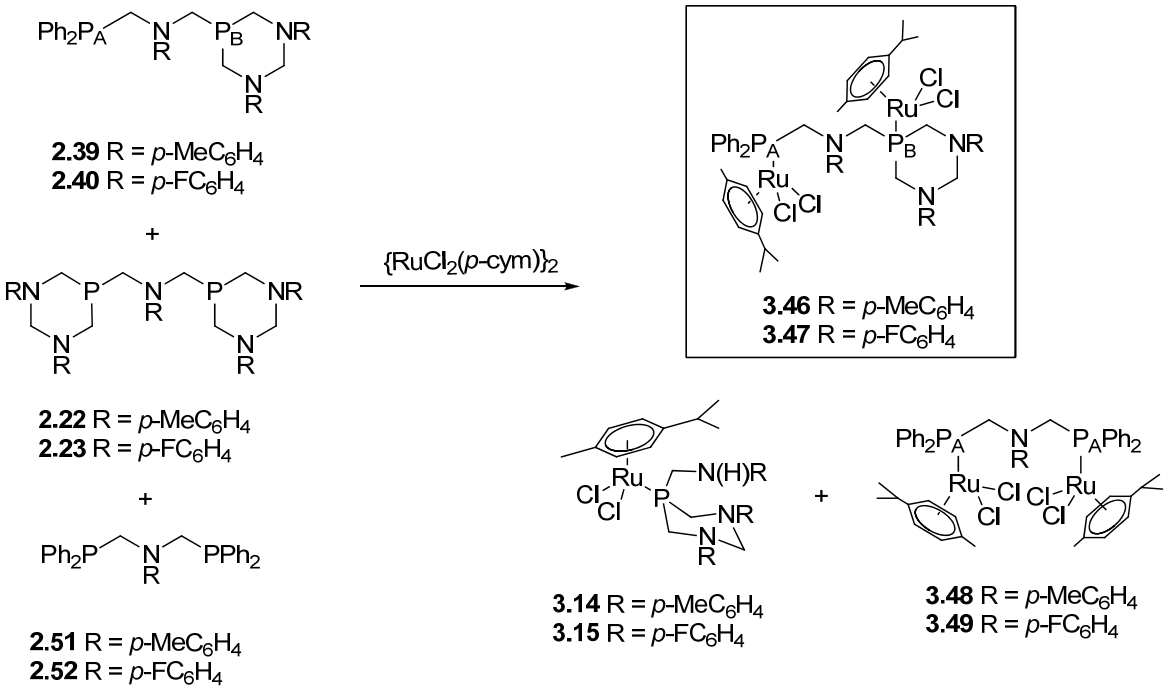

Equation 3.10

The $^{31}P\{^1H\}$ NMR spectra exhibited two doublets as expected for **3.46** (δP 24.6 and 22.3 ppm, $^4J_{PP}$ = 11 Hz, approx. 30% according to $^{31}P\{^1H\}$ NMR) and for **3.47** (δP 23.8 and 22.6 ppm, $^4J_{PP}$ = 10 Hz, approx. 40% according to $^{31}P\{^1H\}$ NMR) along with other two major resonances at *ca*. δP 21.5 and 12.5 ppm. The peak further upfield concurred with those peaks observed for previously synthesised complexes **3.14** and **3.15**, however similar δP shifts were observed in the literature for **3.48** and **3.49** analogues.[101] This was clarified by MS since it revealed a fragmentation pattern not only for [**3.46**–Cl]$^+$, [**3.47**–Cl]$^+$, but also for [**3.14**–Cl]$^+$, [**3.15**–Cl]$^+$ and [**3.48**–Cl]$^+$ and [**3.49**–Cl]$^+$, which demonstrates that all complexes illustrated in Eqn. 3.10 were synthesised. Hence, the peaks at δP 21.4 and 21.7 ppm were assigned to **3.14** and **3.15** respectively and **3.48** and **3.49** resonated at δP 13.2 and 12.0 ppm respectively. The ^1H NMR spectra was not conclusive due to the cluster of

peaks observed. Fortunately, characterisation of **3.47** by single crystal X–ray diffraction supports the proposed structure and by extension the structure of **3.46** was proposed likewise.

3.13 X–ray crystal structure of 3.47

Crystals of **3.47**, suitable for X–ray diffraction, were obtained *via* vapour diffusion of Et_2O into a $CHCl_3$ solution. This structure, along with **3.44a**, confirms the successful synthesis of the PCNCP ligand **2.40** and its coordination capabilities towards Ru(II). As expected, **3.47** displays a "piano–stool" geometry which was previously observed for **3.25** and it is characteristic of Ru(II) complexes with η^6–*p*–cymene, two chlorides and one phosphorus(III) ligand (Fig. 3.25). In complex **3.47** the ligand acts as a bridge between two Ru(II) metal centres. This is the first example of a Ru(II) complex with a nonsymmetric ligand of the type of **2.40**, *i.e.* with diazaphosphorinane as one of the counterparts. Nevertheless, the P–C, P–Ru, Ru–Cl and Ru–C_{cent} bond lengths are similar to those for previous ruthenium complexes with symmetric PCNCP ligands (Ph_2P–) (Table 3.15).[18,101,126]

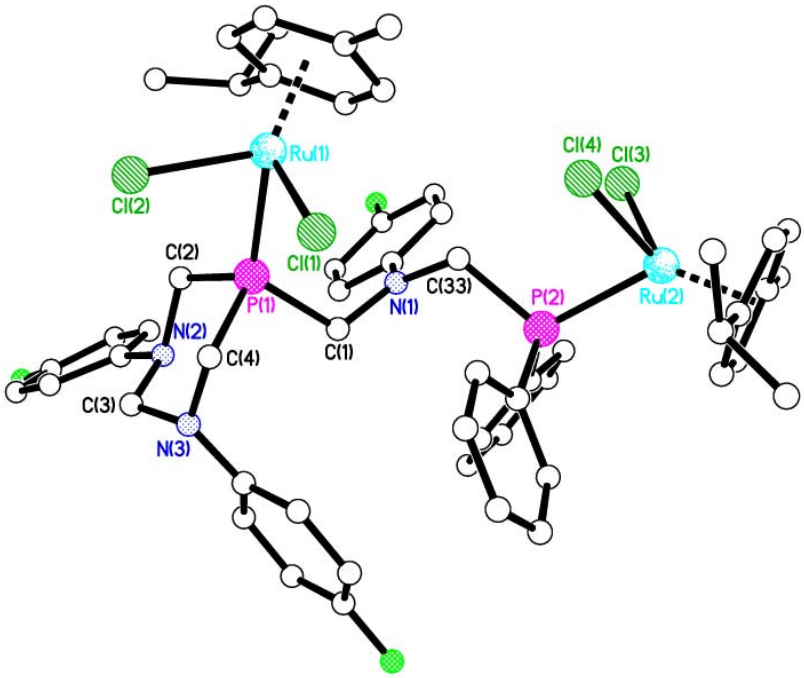

Figure 3.25 X–ray structure of **3.47**. All H atoms are removed for clarity.

Table 3.15 Selected bond lengths (Å) and angles (°) for **3.47**.[a]

3.47			
Ru(1)–Cl(1)	2.4077(13)	Ru(1)–P(1)–C(1)	119.33(17)
Ru(1)–Cl(2)	2.3966(15)	P(1)–C(1)–N(1)	116.6(3)
Ru(1)–P(1)	2.3547(14)	C(1)–N(1)–C(33)	115.0(4)
Ru(1)–C_{cent}	1.7093(19)	N(1)–C(33)–P(2)	116.2(3)
P(1)–C(1)	1.872(5)	C(33)–P(2)–Ru(2)	111.97(17)
Ru(2)–Cl(3)	2.4069(14)	P(1)–Ru(1)–Cl(1)	89.92(5)
Ru(2)–Cl(4)	2.4134(14)	P(1)–Ru(1)–Cl(2)	82.92(5)
Ru(2)–P(2)	2.3455(15)	Cl(1)–Ru(1)–Cl(2)	88.17(5)
Ru(2)–C_{cent}	1.6921(22)	P(2)–Ru(2)–Cl(3)	85.64(5)
P(2)–C(33)	1.884(5)	P(2)–Ru(2)–Cl(4)	84.12(5)
		Cl(3)–Ru(2)–Cl(4)	86.65(5)

[a] Estimated standard deviations in parentheses.

There are no intramolecular contacts but intermolecular H–bonds between the fluorine substituent in C(11)–C(12)–C(13)–C(14)–C(15)–C(16) phenyl ring and aromatic hydrogen in C(11A)–C(12A)–C(13A)–C(14A)–C(15A)–C(16A) [F(2)···C(15A) 3.443(8) Å, 165°, symmetry operators: –*x*+1, –*y*+1, –*z*+1] with similar values to those in the literature [approx. 3.445 Å] (Fig. 3.26).[127]

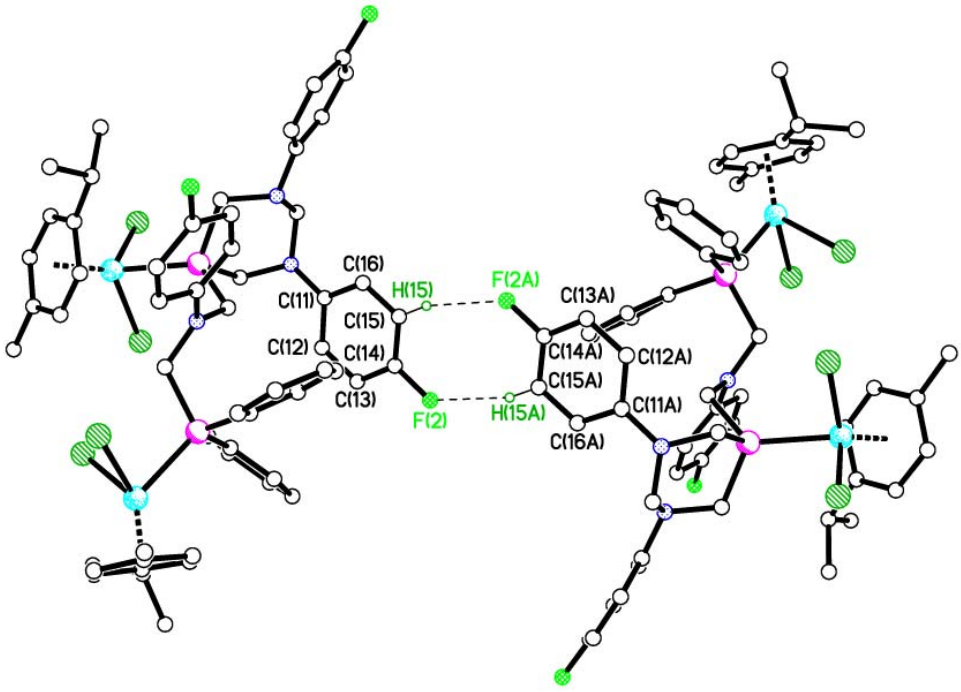

Figure 3.26 Packing diagram of **3.47** exhibiting C–H···F interactions between two molecules. Hydrogens except those involved in H–bonds are removed for clarity.

3.14 Preliminary studies of capture of CO_2 by Ru(II) complexes with PCN ligands

There are plenty of examples in the literature where CO_2 reacts with metal complexes. CO_2 is a weak electrophile and requires a Lewis basic metal centre for coordination. The most common binding modes are the σ bonding of the metal to the carbon atom (Fig. 3.27 a) and the π coordination of one of the C=O bonds to the metal centre (Fig. 3.27 b). However, the cleavage of the transformed CO_2 moiety from the metal centre is still a catalytic challenge. One extended solution is the insertion of CO_2 into metal–element bonds where in the majority of cases, the metal used is a late transition metal such us Pd(II) or Ru(II) and E = H, c or O (Fig. 3.27 c).[128]

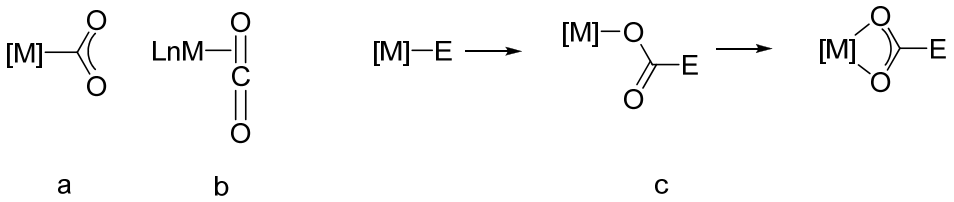

Figure 3.27 CO_2 coordination by a) σ bonding of the metal to the carbon atom and b) the π coordination of one of the C=O bonds to the metal centre and cleavage of the transformed CO_2 moiety by c) insertion of CO_2 into M–E bond.

Recently, DuBois and co–workers reported that the pendant amine in the second coordination sphere of aminomethylphosphines of the type R'$PCH_2N(R)CH_2P(R')CH_2N(R)CH_2PR'$ (**VII** in Sch. 1.4) can bind a proton which makes the reduction of the dioxygen Ru(II) complex with PCN aminomethylphosphines more facile.[129] The same research group demonstrated that nitrogen bases of PCN ligands in a Ni(II) complex can act in concert to stabilise CO adducts.[69]

With these bases in mind, we proposed to use our Ru(II) complexes with PCN ligands for the fixation of CO_2. The pendant amine with an aminic proton would transfer the CO_2 from the outer sphere to the metal *via* H–bond between the NH and the oxygen of CO_2. The Ru(II) complexes synthesised in this project possess up to three NH groups which could enhance the CO_2 trapping. To this end, three complexes with PCN ligands were treated with CO_2 gas at r.t; **3.12**, **3.13** and **3.25**. Potential catalysts **3.12** and **3.13** contain cyclic PCNCNC aminomethylphosphines with and *o*–$^{i}PrC_6H_4$– and *o*–FC_6H_4– substituents on N and **3.25** incorporates acyclic $P(–C–N)_3$ aminomethylphosphines with *o*–$CF_3C_6H_4$–. These three complexes could serve as representative examples of the influence of the

electronic and steric properties in the basicity of the metal centre and so on the ability to coordinate to CO_2.

However, the IR demonstrates that CO_2 was not even weakly bonded to NH since the νNH stretchs remained unchanged in all cases and none of them showed any vibration near 1700 cm^{-1} where the νCO stretches should appear. In addition, the crystal structure obtained for **3.25** did not show any CO_2 either. Therefore, trapping CO_2 gas in a CH_2Cl_2 solution containing the mentioned Ru complexes was unsuccessful. Looking back to the literature, a plausible approach to overcome this issue could be replacing the chloride ligands with a hydride for a subsequent insertion of the CO_2 into the Ru–H bonds.

For the displacement of Cl^- by H^-, the reported procedures utilised K_2CO_3[130] or KBH_4[131] as bases. For an early attempt, two Ru complexes with electron donating substituents on the aniline were used, **3.12** (*o*–^{i}PrC$_6$H$_4$–) and **3.14** (*p*–MeC$_6$H$_4$–), as the ligands employed in documented investigations also donate electron density.[131] In that way, it was expected that the chloride would be easier to be displaced due to the metal centre being more strongly coordinated to the phosphine (more basic) and therefore there being weaker binding to the chloride. Following the procedure in the literature, two equivs. of K_2CO_3 were reacted with one equiv. of **3.12** or **3.14** in MeOH for 30 min at r.t. followed by subsequent refluxing to up 24 h (Eqn. 3.11).[130] According to the reported synthesis, the new complex turned yellow but unfortunately in our hands the suspension did not change in colour.[130] Nevertheless, the orange suspension was filtered and the filtrate was evaporated under vacuum and washed with cold MeOH. In a similar manner, **3.12** was treated with an excess of $NaBH_4$ (molar ratio 1:10) to obtain a dark brown solid Eqn. 3.11. The whole sample was required for ^{1}H NMR characterisation which did not show the expected Ru–H proton at *ca*. –11.0 ppm, this indicates that the hydrogenation was not successful.

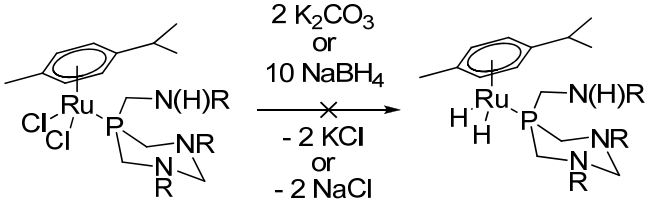

3.12 R = *o*-^{i}PrC$_6$H$_4$
3.14 R = *p*-MeC$_6$H$_4$

Equation 3.11

One of the reasons for these results could be related to the fact the PCN backbones of the phosphines used in this investigation. Previously phosphines did not possess this scaffolding, hence the basicity of the phosphine, *i.e.* its electronic properties, was not affected by the heteroatom. Furthermore, the bulkiness of the substituents plays a role that is still not completely understood which also affects the success of the reaction. Hence, furhter research should be conducted to adapt the documented reaction conditions to the Ru(II) complexes **3.12** and **3.14** as well as to **3.11**, **3.13**, **3.15** and **3.22** – **3.26**.

3.15 Conclusions

In summary, the coordination chemistry of the PCN aminomethylphosphines derivatives of THPC was investigated towards several late transition metals such as Pt(II), Pd(II), Ru(II), Cr(III) and Rh(III).

In order to expand on previous work within our research group, Pt(II), Pd(II) and Ru(II) complexes **3.1** – **3.15** were successfully synthesised with cyclic six–membered ring phosphines. These diazaphosphorinanes reacted to form, not only the expected *cis*–Pt(II) (**3.1** – **3.7**) and *cis*–Pd(II) complexes (**3.8** – **3.10**), but also in some cases chelate complexes with a six–membered M–P–C–N–C–P core ring (**3.6a**, **3.8a** – **3.10a**). Likewise, the desired Ru(II) complexes **3.11** – **3.15** were formed when diazaphosphorinanes were treated with the Ru(II) precursor. The structures proposed were supported by a combination of spectroscopic techniques and further unambiguous confirmation was provided by single crystal X–ray studies for **3.1**, **3.2** and **3.9**.

To the best of our knowledge **3.16** – **3.26** are the first examples of Pt(II), Pd(II) and Ru(II) complexes with $P(CH_2N(H)R)_3$ ligands with aryl derived substituents on the nitrogen. Only two Pt(II) examples (**1.212** and **1.213**, Fig. 1.8) have been reported before with analogues ligands $P(CH_2NR)_3$ (R = $(CH_2)_4X$, X = NMe or O) with alkyl substituents instead.[1] Moreover, **1.212** and **1.213** revealed a geometry where both phosphorus are in *trans* arrangement as was demonstrated for **3.16** – **3.21** whereas $^{31}P\{^1H\}$ NMR of **3.16** and **3.18** show a mixture of *trans* (**3.16** and **3.18**) and *cis* (**3.16a** and **3.18a**) isomers. Furthermore, suitable crystals of **3.16a** were collected confirming the *cis* arrangement of the phosphorus and Pd(II) complexes **3.19** – **3.21** which were achieved exclusively as *trans* isomers as was demonstrated by X–ray analysis. Therefore, in view of the successful

initial results, further investigation should be undertaken with the aim of expanding the library of complexes.

On the other hand, the coordination capabilities of the bicyclic diphosphine ligands **2.31** – **2.33** were investigated towards several metal centres. They were demonstrated to form Pt(II) and Rh(III) complexes but remains unreactive towards Cr(III) according to $^{31}P\{^{1}H\}$ NMR. Several coordination modes are possible, however due to the restriction of the bite angle and, by comparison with previous P–P intrabridgehead diphosphines, it is presumed that **2.31** – **2.33** coordinate in a *P,P*-bridging mode with Pt(II) and Rh(III) to form **3.27b** – **3.29b** and **3.31a** – **3.32a** respectively rather than *P,P*–chelating mode. This binding mode was confirmed by single X–ray crystallography of **3.27b**. Hence, the first approach to the coordination chemistry of these ligands was promising and therefore, further investigation should be conducted.

With the aim of isolating the nonsymmetric PCNCP aminomethylphosphines synthesised in the previous chapter (Section 2.10), a template synthesis approach was proposed using Pt(II). The isolation of the ligand was not completed, although various novel nonsymmetric and symmetric Pt(II) complexes were obtained and a better understanding of the chemistry was achieved. One of these compounds was the interesting *trans* (bischelate) Pt(II) **3.44a**, not only because it is the first example of a platinum complex with two novel nonsymmetric diphosphines but also because it would be utilised in the synthesis template in future work. To investigate further the coordination chemistry of PCNCP ligands, they were treated with a Ru(II) metal centre to afford **3.46** and **3.47**. Crystals of **3.44a** and **3.47** suitable for X–ray studies were obtained to confirm the successful synthesis of the nonsymmetric PCNCP ligand **2.40** and its coordination capabilities towards precious group metals. Due to the successful data collected, future research in this area may be undertaken towards the isolation of PCNCP ligands.

4. Synthesis, reactivity and coordination chemistry of $R(H)NCH_2PR'_2P$ aminomethylphosphines

Previous work within our research group has focused on the synthesis of aminomethylphosphine ligands with a PCN backbone using a Mannich based condensation reaction.[7,13–15] Tuning the substituents on phosphorus and nitrogen gave a wide range of new secondary phosphinoamines R(H)NCH$_2$PR'$_2$ (R = aryl derivatives, R' = Ph, Cg)[7,15] and even symmetric tertiary bis(diphenylphosphinomethyl)amines RN(CH$_2$PR'$_2$)$_2$ (R = *p*–aryl derivatives, R' = Ph).[13] There are plenty of examples in the literature concerning monophosphine PCN ligands of the type R(H)NCH$_2$PR'$_2$ (where R and R' are aryl or alkyl groups) ,[51,54,76] but less for asymmetric diphosphines with a different number of carbons between N and P, *i.e.* PCCNCP [R(H)NCH$_2$PPh$_2$, R = PPh$_2$C$_6$H$_4$].[34] To understand more about these poorly studied species, we proposed a method which involves addition of a secondary phosphine HPR'$_2$ (R' = Ph and Cg) to an amine with a vinyl donor group, followed by a phospha–Mannich reaction to give the asymmetric bis(phosphinomethyl)amines. Once synthesised, the coordination chemistry of the novel PCN, PCNCP and PCCCCNCP phosphorus compounds were studied towards late transition metals.

4.1 Synthesis of tertiary R'$_2$PCH$_2$N(H)R (PCN) aminomethylphosphine ligands

In previous chapters, the chemistry of *o*-{C(Me)=CH$_2$}C$_6$H$_4$NH$_2$ and the phosphonium salt THPC was explored. In this section, the reactivity features of *o*-{C(Me)=CH$_2$}C$_6$H$_4$NH$_2$ were studied versus two tertiary hydroxymethylphosphines (HOCH$_2$PR'$_2$, R' = Ph or Cg). To understand better the influence of the substituents on the nitrogen, *o,o*–(CHPh$_2$)$_2$–*p*–MeC$_6$H$_2$NH$_2$ and 1–adamantylaniline (Ad) were also investigated. Hence, the aminomethylphosphines **4.1 – 4.6** were synthesised in moderate to high yields as colourless powders (48 – 95%). This consisted of one equiv. of R'$_2$PCH$_2$OH (R' = Ph, Cg) (readily prepared from equimolar amounts of (CH$_2$O)$_n$ and Ph$_2$PH or CgPH respectively)[7,132] and one equiv. of the chosen amine at r.t. (Eqn. 4.1).

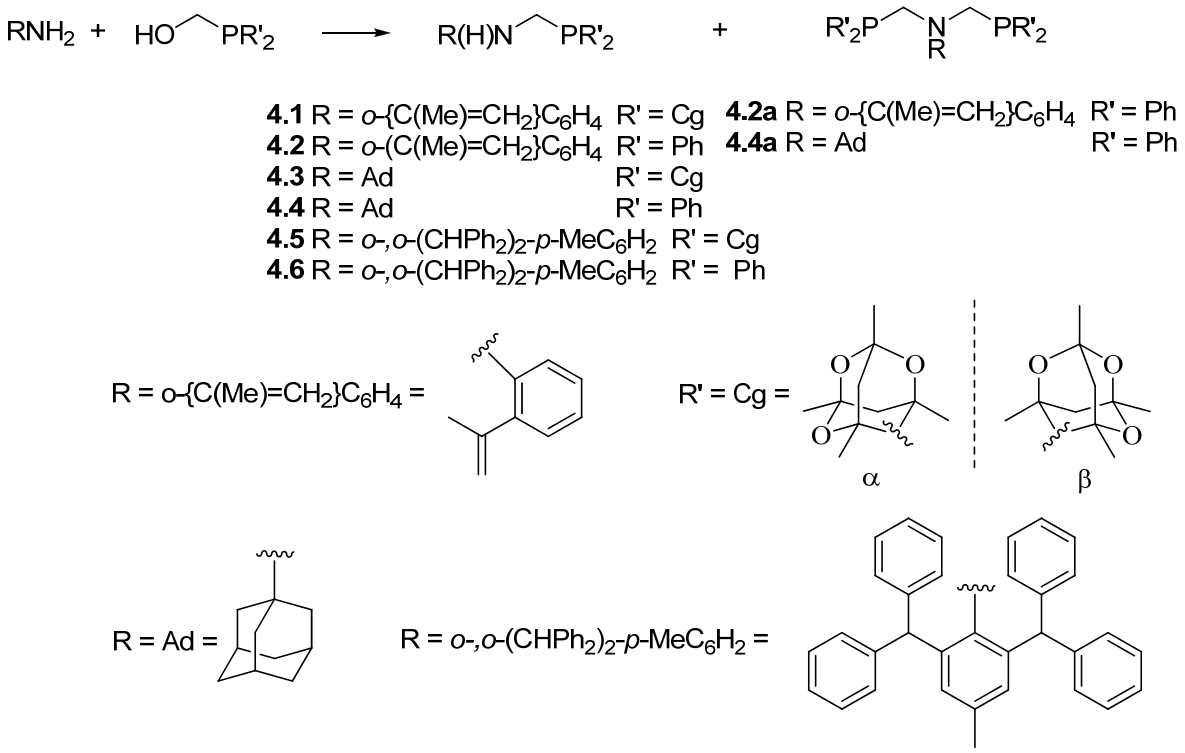

Equation 4.1

All the ligands were prepared in methanol with the exception of **4.6** which was performed in C_7H_8. The synthesis of the compounds was monitored by $^{31}P\{^1H\}$ NMR, with an external C_6D_6 reference, which indicated that reaction was complete within 24 h for **4.1** – **4.5** and after 6 d for **4.6** (Table 4.1). However, the ^1H NMR of the bulk solid **4.6** showed unreacted aniline while the $^{31}P\{^1H\}$ NMR displayed a single peak at δP –19.3 ppm assigned to the desired ligand. Likewise, primary amine *o,o*–$(CHPh_2)_2$–*p*–$MeC_6H_2NH_2$ was also observed in the ^1H NMR of **4.5**. Fortunately, the unreacted aniline was removed from **4.5** and **4.6** upon metal coordination (see Section 4.5).

Table 4.1 $^{31}P\{^1H\}$ NMR (in ppm) data for **4.1 – 4.6**.[a]

	$^{31}P\{^1H\}$		**$^{31}P\{^1H\}$**
4.1	–33.5, –33.3	**4.5**	–27.0
4.2	–18.5	**4.6**	–19.3
4.3	–31.4, –31.1	**4.2a**	–27.3
4.4	–17.7	**4.4a**	–25.0

[a] NMR spectra measured in $CDCl_3$.

The ligands **4.2**, **4.4** and **4.6** showed a major resonance at *ca*. δP –18.5 ppm in the $^{31}P\{^{1}H\}$ NMR, which is characteristic for secondary amines with phenyl substituents.[14,15,34,76] The chemical shifts are *ca.* 10 ppm upfield with respect to that of Ph_2PCH_2OH [δP –9.9 ppm in $CDCl_3$][14] which indicate that Mannich condensation has occurred. The similarity of the ^{31}P chemical shift between **4.2**, **4.4** and **4.6** [–18.5, –17.7 and –19.3 ppm, respectively] suggest that the nature of the amine does not influence significantly the basicity of the phosphorus. It has also a negligible effect for ligands **4.1**, **4.3** and **4.5** [δP –33.5, –33.3; –31.4, –31.1 and –27.0 ppm, respectively] as the shifts do not change drastically from the secondary phosphine precursor $CgPCH_2OH$ [δP –33.7 ppm].[7] Whereas for **4.1** and **4.3**, two closely spaced singlets were observed in the $^{31}P\{^{1}H\}$ NMR due to the racemic mixture of enantiomers α and β, while for **4.5** only one peak was present probably because of accidental equivalence. For **4.2**, **4.4** and **4.6**, small amounts of PCNCP ligand were generated in the course of the reaction as observed by *in situ* NMR at *ca.* δP –26 ppm (C_6D_6). Similar tertiary aminophosphines have previously been seen to display a singlet at *ca*. δP –27.0 ppm.[13,51] However, the $^{31}P\{^{1}H\}$ NMR of the product of the reaction between $AdNH_2$ and Ph_2PCH_2OH showed a mixture of the PCN monophosphine [δP –17.7 ppm, **4.4**] and the PCNCP diphosphine [δP –25.0 ppm, **4.4a**] in a ratio of 4:1. The MS (*m/z* $[MH]^+$ 350) and microanalysis [% C 78.95 (79.05), % H 7.96 (8.08), % N 4.11(4.01)] demonstrate that the product obtained was **4.4** which further reacts in solution to give **4.4** and **4.4a**.

In a similar manner, the *in situ* $^{31}P\{^{1}H\}$ NMR of **4.2** displayed a minor resonance at δP –27.3 ppm. This singlet was assigned to the diphosphine ligand **4.2a** by comparison with the $^{31}P\{^{1}H\}$ NMR for the product obtained by reacting two equivs. of Ph_2PCH_2OH with one equiv. of *o*-$\{C(Me)=CH_2\}C_6H_4NH_2$ (Eqn. 4.2). After 24 h the precipitated solid was collected and the filtrate stored. The colourless powder was confirmed as **4.2** (12% yield) and crystals grown from the filtrate characterised by single crystal X–ray diffraction, $^{31}P\{^{1}H\}$ and ^{1}H NMR. The $^{31}P\{^{1}H\}$ showed two major singlets at –18.5 and –27.3 ppm in a proportion of 1:2.5 whereas the crystal structure obtained was the PCNCP species **4.2a**. These results demonstrate that it was possible to obtain the PCNCP ligand which was proved by its synthesis with the conditions highlighted in Eqn. 4.2.

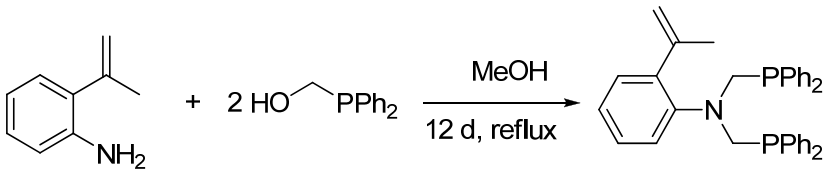

4.2a

Equation 4.2

In the ^{1}H NMR spectra of **4.1** – **4.6** the PC*H*$_2$N methylene protons showed an ABX splitting pattern (A and B for the diastereotopic protons and X for the P) as was observed in previous chapters and in the literature.[7] However, the two doublet of doublets appeared depending on the phosphorus group. For instance, whereas protons in **4.1** resonate as two doublets and **4.3** as doublet of doublets and doublets with a weak coupling to the phosphorus ($^{2}J_{PH}$ = 0.8 Hz), for **4.2** and **4.6** only a doublet was observed with a larger phosphorus coupling constant (4.0 < $^{2}J_{PH}$ < 6.4 Hz).

Whereas the aminophosphines **4.1**, **4.3** and **4.5** are air stable in solid state and in solution; **4.2**, **4.4** and **4.6** are not stable in solution. This feature would be due to the phosphorus in **4.1**, **4.3** and **4.5** being entrenched within the Cg framework and the inherent steric crowding about the P which makes the phosphorus less accessible to the oxygen from the atmosphere, although electronic effects may have an influence too. With the same reasoning, only aminophosphines with Ph_2P– (**4.2**, **4.4** and **4.6**) present evidence of the formation of PCNCP ligands but not those with CgP–.

4.2 X–ray crystal structures of *o,o*–$(CHPh_2)_2$–*p*–$MeC_6H_2NH_2$, 4.3 and 4.2a

Crystals of the aniline precursor of **4.5** and **4.6** [*o,o*–$(CHPh_2)_2$–*p*–MeC_6H_2] were collected from the reaction between *p*–$MeC_6H_4NH_2$ and Ph_2CHOH (Fig. 4.1). Although *o,o*–$(CHPh_2)_2$–*p*–$MeC_6H_2NH_2$ has previously been synthesised,[133] the crystal structure has not been reported. The structure shows the aminic protons in a different plane to the aniline ring [C(6)–C(1)–N(1)···H(1B) 25.84^{o} and C(2)–C(1)–N(1)···H(1A) 28.28^{o}]. They are connected to the *ortho*-phenyl substituents centroids with different distances [N(1)–H(1A)···X(1A) 3.960 Å and N(1)–H(1B)···X(1B) 4.073 Å, X(1A): C(8) to C(13), X(1B): C(22) to C(27)]. These interactions are slightly larger than those previously reported as

well as the *phenyl–phenyl* interactions between C(3)–H(3)···X(1C) [3.814 Å, X(1C): C(14) to C(19)] and C(5)–H(5)···X(1D) [3.700 Å, X(1D): C(28) to C(33)].[134] But overall, the H–phenyl interactions may influence the orientation of the phenyl rings and therefore dictate the structure.

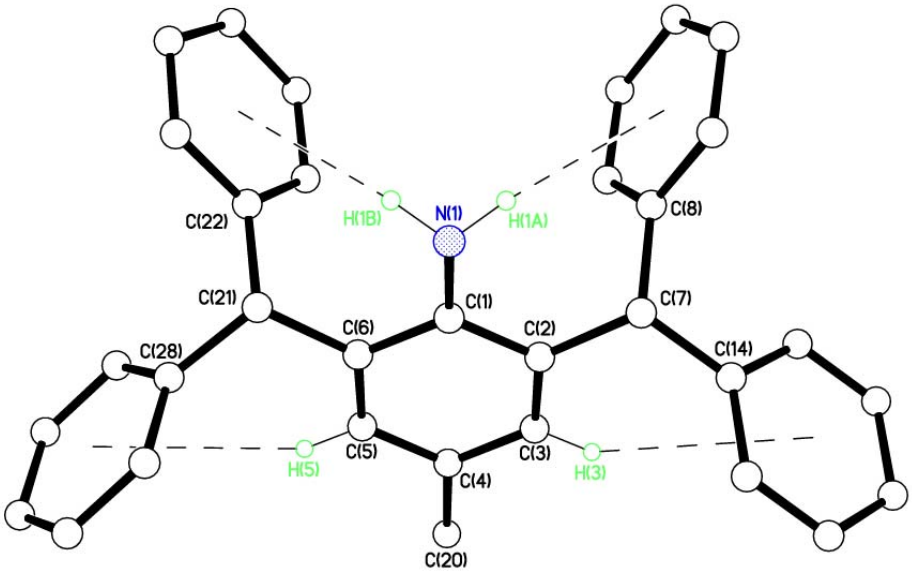

Figure 4.1 X–ray structure of *o,o*–$(CHPh_2)_2$–*p*–$MeC_6H_2NH_2$. All hydrogens except those involved in C–H ···*phenyl* interactions are removed for clarity.

The structure of **4.3** was also elucidated by single crystal X–ray crystallography. Crystals were obtained from a MeOH filtrate standing for more than 24 h (Fig. 4.2). The values for P–C, C–N and C–N–P bonds lengths and angles are in accordance with those for the structure previously reported by Smith *et al*. (**1.249**, Sch. 1.22)[7] [P(1)–C(11) 1.847(4) Å, C(11)–N(1) 1.470(5) and N(1)–C(1)–P(1) 107.9(2)^o for **4.3** vs P(1)–C(11) 1.8591(19) Å, C(11)–N(1) 1.456(2) and N(1)–C(1)–P(1) 108.35(13)^o for **1.249**]. Three molecules crystallised in the asymmetric unit with one of them twisted 180^o with respect to the other two. Due to the different disposition of the molecules in the unit cell, intermolecular H–bonds are not observed for the ligand **4.3**, however they are established in the aminophosphine reported [N(1)–H(1)···O(2A) 3.155 Å].[7]

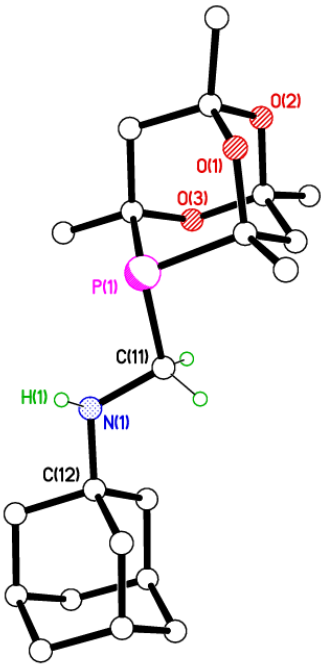

Figure 4.2 X–ray structure for **4.3**. All hydrogens except those on N(1) and C(11) are removed for clarity.

Crystals of **4.2a** were obtained from an *in situ* NMR aliquot of the reaction between one equiv. of *o*-{C(Me)=CH_2}$C_6H_4NH_2$ and two equivs. of Ph_2PCH_2OH (Fig. 4.3). P–C and C–N bond lengths and P–C–N and C–N–C bond angles are in agreement with previously reported PCNCP ligands (Table 4.2).[7]

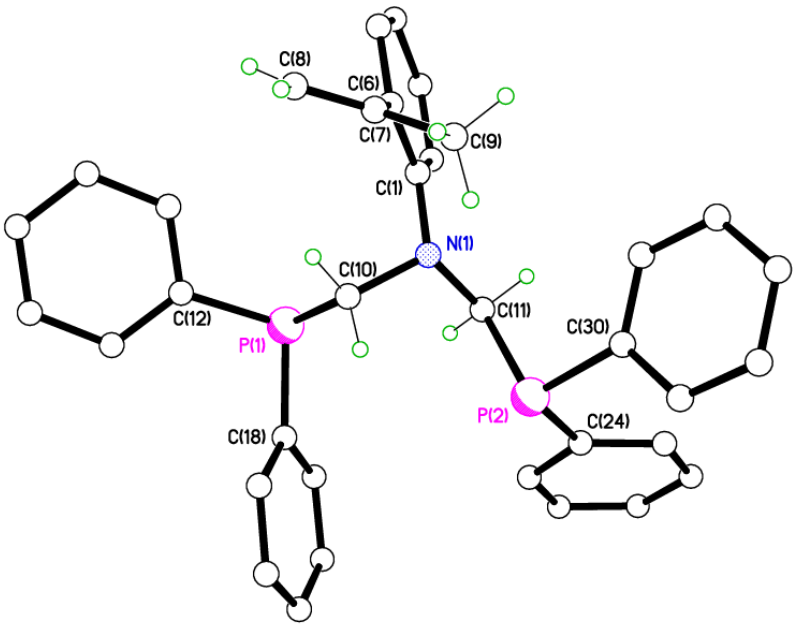

Figure 4.3 X–ray structure of **4.2a**. Selected H atoms on C(8) – C(11) shown.

Table 4.2 Selected bond lengths (Å) and angles (°) for **4.2a**.[a]

4.2a			
N(1)–C(1)	1.429(2)	P(2)–C(24)	1.8358(17)
N(1)–C(10)	1.468(2)	P(2)–C(30)	1.8290(17)
N(1)–C(11)	1.4599(19)	C(7)–C(8)	1.329(3)
P(1)–C(10)	1.8974(16)	C(7)–C(9)	1.506(2)
P(1)–C(12)	1.8349(17)	P(1)–C(10)–N(1)	113.37(11)
P(1)–C(18)	1.8324(16)	C(10)–N(1)–C(11)	112.66(13)
P(2)–C(11)	1.8630(16)	N(1)–C(11)–P(2)	111.91(11)

[a] Estimated standard deviations in parenthesis.

Similar to *o,o*–$(CHPh_2)_2$–*p*–$MeC_6H_2NH_2$, *phenyl–phenyl* interactions were observed in **4.2a**. The supramolecular motif *multiple phenyl embrace* (MPE) is divided in three main classes according to the short distances between *phenyl–phenyl* contacts: sextuple, quadruple and double phenyl embrace (6PE, 4PE, 2PE respectively).[135,136] Within these categories, three orientations are possible: *offset-face-to-face* (*off*), *edge-to-face* (*ef*) and *vertex-to-face* (*vf*). Theoretically, in the *off* conformation two rings are overlapped so the distances between atoms of both rings are equal. When these distances vary, *ef* and *vf* conformations occur. Therefore, these motifs present a range of geometrical arrangements and they are observed in the structure of **4.2a** (Fig. 4.4). For instance, *vf* phenyl embrace is observed between C(33)–H(33)···X(1A) [3.437 Å, X(1A): C(18) to C(23)] and C(28)–H(28)···X(1B) [3.717 Å, X(1B): C(1) to C(6)].

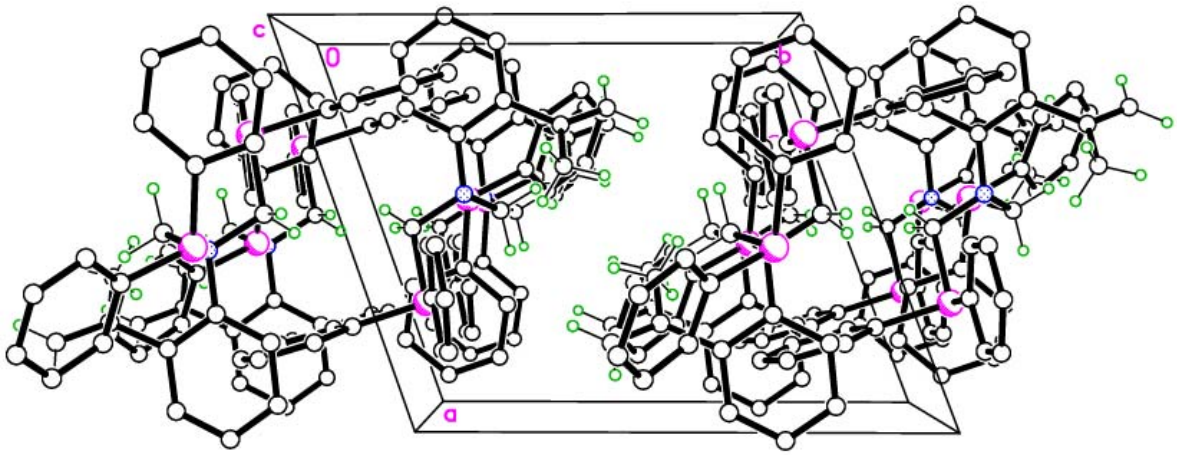

Figure 4.4 Pack plotting of **4.2a** along the *c*-axes.

4.3 Reactivity of PCN aminomethylphosphine ligands with HPR'$_2$ (R = Ph or Cg)

In Section 4.1, the basicity of a family of amines was tested with R_2PCH_2OH (R = Ph or Cg); in this section, the reactivity of the *o*-{C(Me)=CH_2}$C_6H_4NH_2$ against R_2PH (R = Ph or Cg) will be investigated (Sch. 4.1). Symmetric aminophosphine compounds with one CH_2 between N and P, *i.e.* PCNCP scaffolding, are widely studied but those with different numbers of carbons between heteroatoms are not so common. [34,51,54,76] Hence, a simple two step procedure for the synthesis of asymmetric diphosphinoamines containing a P–C–C–C–C–N–C–P skeletal backbone is described here.

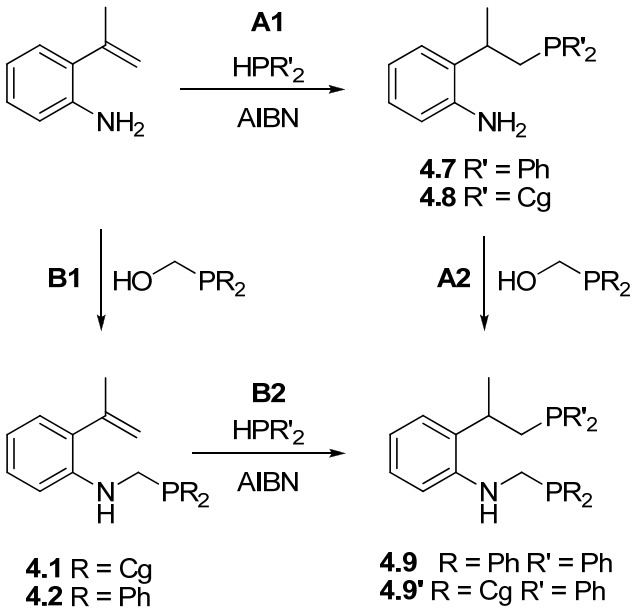

Scheme 4.1 Synthetic pathways to **4.1**, **4.2** and **4.7 – 4.9'**.

Two routes (pathways **A1**, **A2** and **B1**, **B2**) were proposed for the synthesis of the asymmetric bis(diphosphines)amines **4.9** and **4.9'** from *o*-{C(Me)=CH_2}$C_6H_4NH_2$. Diphenylaminomethylphosphine **4.7** was prepared by a hydrophosphination reaction using equimolar amounts of *o*-{C(Me)=CH_2}$C_6H_4NH_2$ and $HPPh_2$ with 14% of 2,2–azo–bisisobutyronitrile (AIBN) as free radical initiator at 110^{o}C for 5 days. The compound was obtained as a yellowish oil which solidified upon adding MeOH and the resulted colourless solid was purified with Et_2O. In the $^{31}P\{^1H\}$ of **4.7** a sharp singlet was observed at –19.6 ppm, only 1 ppm upfield with respect to **4.2**, but the structure proposed was further confirmed by the mass spectroscopy {$[MH]^+$ (320)} and X–ray (Fig. 4.7).

The following step (pathway **A2**) involved treatment of **4.7** with Ph_2PCH_2OH in 1:1 stoichiometry to obtain **4.9**. However, only unreacted starting materials were observed in the *in situ* $^{31}P\{^1H\}$ NMR [–19.5 (**4.2**), –14.0 (Ph_2PCH_2OH) and –40.4 (Ph_2PH) ppm]. Nevertheless, after several hours, a solid precipitated from the *in situ* NMR tube as well as crystals in other *in situ* fractions. $^{31}P\{^1H\}$ and ^1H NMR of the colourless bulk solid product and the crystalline solid revealed two peaks close in the space at –19.7 and –19.8 ppm assigned to the desired product **4.9**. This demonstrates that pathway **A1** – **A2** was followed for the preparation of **4.9** obtained in 66% yield after optimising the conditions [5 d refluxing in MeOH] followed by a simple filtration.

An alternative route to afford **4.9** was also proposed from the already synthesised aminomethylphosphine **4.2** (pathways **B1** and **B2**). $HPPh_2$, **4.2** (1:2) and AIBN (18%) were reacted at 110°C for 5 d and for a further 2 days at r.t in MeOH to give **4.9** in 50% yield according to $^{31}P\{^1H\}$ NMR (pathway **B2**). Hence, compound **4.9** can be synthesised *via* hydrophosphination of *o*-$\{C(Me)=CH_2\}C_6H_4NH_2$ with $HPPh_2$ followed by the condensation of the NH_2– functional group with Ph_2PCH_2OH (pathways **A1** and **A2**) or vice versa (pathways **B1** and **B2**). At this stage, route **B1** – **B2** needs more investigation to purify the product and route **A1** – **A2** gave pure solid, although improvement of the yield (66%) should be conducted. Therefore, this pathway was applied to expand the substituents on phosphorus by the formation of **4.8** and with the aim of future synthesis of **4.9'**.

A similar method to that used for the preparation of **4.7** was employed for the synthesis of compound **4.8**, *i.e.* *o*-$\{C(Me)=CH_2\}C_6H_4NH_2$, CgPH (1:1) and AIBN (14%), but only 24 h were required. In the $^{31}P\{^1H\}$ of **4.8** two closely spaced singlets were observed at –31.7 and –31.9 ppm due to the chirality of the P cage slightly downfield with respect to **4.1** (–33.5, –33.3 ppm).

Scheme 4.1 enables the synthesis of any PC_4NCP ligands offering a potential route to a new class of mono and bidentate phosphine ligands. In addition, this method has only illustrated two possible diphosphines **4.9** and **4.9'**; however more compounds could be achieved by simply varying the substituents on phosphorus. Moreover, the already synthesised **4.9** and the potential synthesis of **4.9'** could be used for further functionalisation due to the aminic proton to get a tridentate phosphine ligand. For all

mentioned above, more investigation should be conducted to expand the series of compounds described in Scheme 4.1.

Products obtained in route **A1** have a general formula of $C_{21}H_{22}NP$ for **4.7** and $C_{19}H_{18}NO_3P$ for **4.8** according to MS and EA. Two possible set of regio isomers (linear ligands **4.7** and **4.8** and branched ligands **4.7'** and **4.8'**) are possible from the reaction between *o*-{C(Me)=CH_2}$C_6H_4NH_2$, R'$_2$PH and AIBN (Sch. 4.2). The linear ligands **4.7** and **4.8** might be expected over **4.7'** and **4.8'** since the phosphorus attacks to the less hindered position in *o*-{C(Me)=CH_2}$C_6H_4NH_2$ (route **A**).

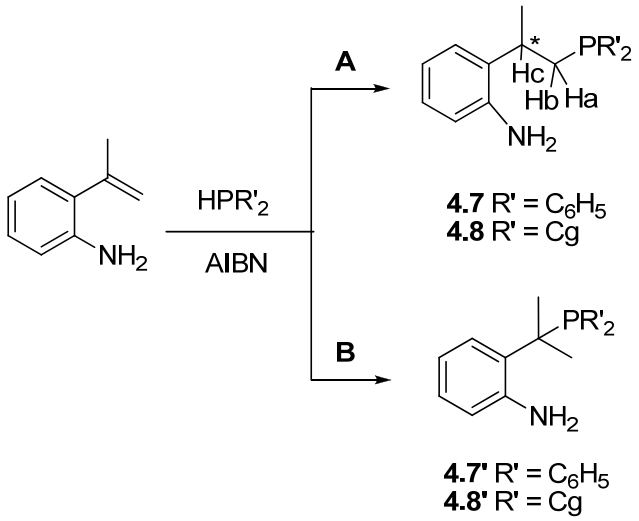

Scheme 4.2 Possible isomers proposed for the anti Markovnikov (route **A**) and for the Markovnikov reaction (route **B**).

The ^{1}H NMR was used to distinguish between both set of structural isomers. The structures synthesised exhibited three peaks in the region between 2.18 and 2.80 ppm for **4.7** (Fig 4.5) and one septuplet at 3.00 ppm and multiplets in the adamantane region for **4.8**. The ^{1}H NMR spectrum of **4.7** will be discussed due to the spectrum of **4.8** shows the alkyl proton peaks obscured by the adamantane resonances being impossible to assign them. Three resonances were observed corresponding to H_c (2.83 – 2.71 ppm), to H_a and to H_b (2.49 ppm, $^2J_{HH}$ = 13.6, $^3J_{HH}$ = 4.0, $^2J_{HP}$ = 3.2 Hz and 2.26 ppm, $^2J_{HH}$ = 13.6, $^3J_{HH}$ = 10.0, $^2J_{HP}$ = 3.2 Hz) (Fig. 4.5). These resonances cannot be possible for structure **4.7'**, in which, only one singlet should be expected for the two methyl groups. The splitting patterns of H_a and H_b were different, which suggests a different coupling to H_c. If one of the protons forms a dihedral torsion angle of 0^o or 180^o with H_c, then the coupling constant is larger according

to the Karplus Equation (Fig. 4.6). Therefore, the assignment of the peak at 2.26 ppm could be elucidated.

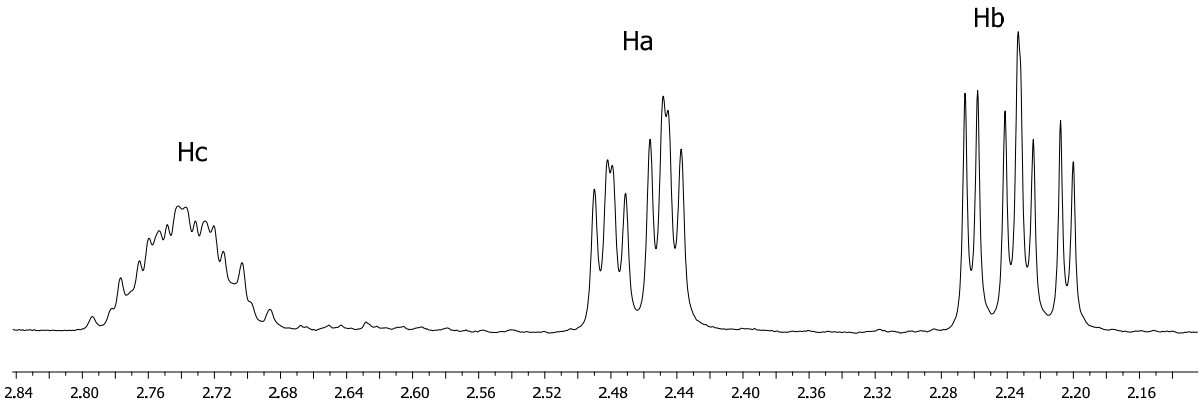

Figure 4.5 Selected ^{1}H NMR region of **4.7**.

Several orientations can be possible with the proton NMR obtained, but the most likely are shown in the Newman projection in Figure 4.6. In the antiperiplanar disposition (**I**), the steric hindrance is the minimum and the dihedral torsion angle between H_a and H_c is 180°, therefore H_a would be the peak at 2.26 ppm with the larger ^{1}H–^{1}H coupling ($^{3}J_{HH}$ = 10.0 Hz). However, in the solid state, the 3D structure (**III**) observed is in agreement with the second possible conformer (**II**) where both bulky groups are as far as possible with H_b and H_c in 180° dihedral angle and so the peak at 2.26 ppm is finally assigned to H_b.

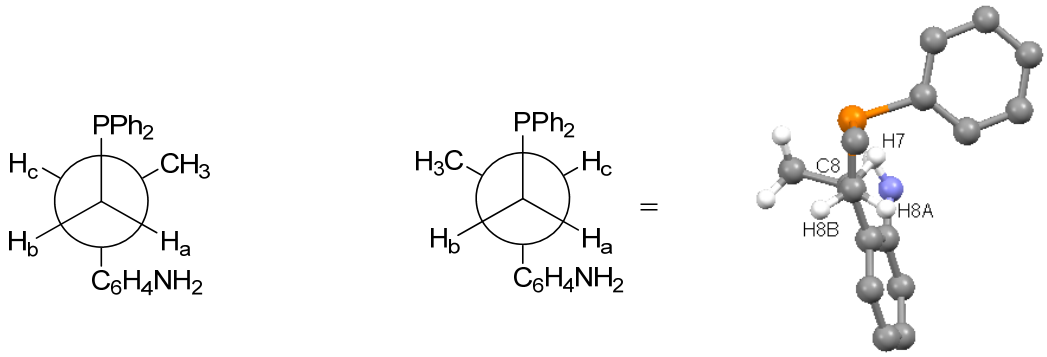

I **II** **III**

Figure 4.6 Newman projection of the two possible conformers (**I** – **II**) and the X–ray structure of **4.7** (**III**).

4.4 X–ray crystal structures of 4.7 and 4.9

Characterisation of compound **4.7** by single X–ray diffraction was possible after collecting suitable crystals from a MeOH filtrate of the reaction between *o*-{C(Me)=CH_2}$C_6H_4NH_2$, Ph_2PH and AIBN (Fig. 4.7). Selected bonds and angles are given in Table 4.3. C–C and C–C–C values for C(8)–C(7), C(7)–C(6) and C(7)–C(9) are in agreement with single C–C bond lengths and C–C–C angles (*ca*. 1.5 Å).

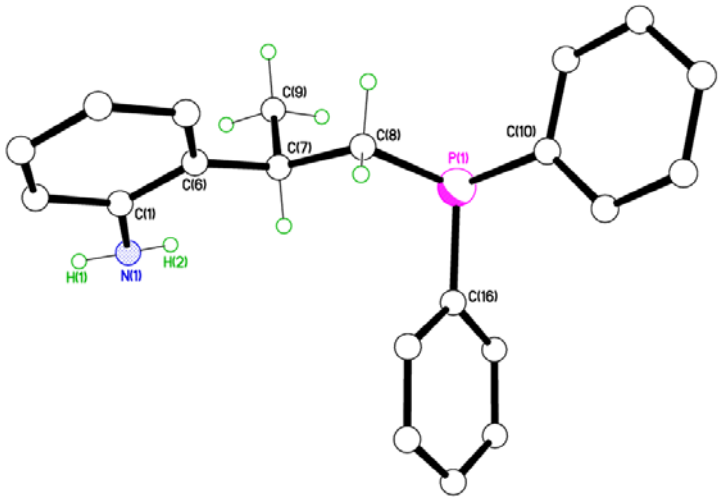

Figure 4.7 X–ray structure of **4.7**. Selected H atoms on C(7) – C(9) and N(1) shown.

Table 4.3 Selected bond lengths (Å) and angles (°) for compound **4.7**.[a]

4.7			
P(1)–C(8)	1.8510(18)	P(1)–C(8)–C(7)	112.49(12)
C(8)–C(7)	1.540(2)	C(16)–P(1)–C(8)	102.19(8)
C(7)–C(6)	1.516(3)	C(8)–C(7)–C(9)	109.56(15)
C(7)–C(9)	1.538(2)	C(8)–C(7)–C(6)	113.28(15)
C(10)–P(1)–C(16)	102.01(8)	C(9)–C(7)–C(6)	111.08(15)
C(10)–P(1)–C(8)	98.36(8)		

[a] Estimated standard deviations in parenthesis.

As previously observed for **4.2a**, the overall geometry of **4.7** showed the *multiple phenyl embrace*. Three phenyl rings are involved in *ef* interaction among three molecules. Hence, one phenyl ring [C(16) to C(21)] is flanked by two other phenyl rings [X(2B): C(10B) to C(15B) and X(3C): C(10C) to C(15C)] with distances of C(18)–H(18)···X(2B) 3.718 Å and C(20)–H(20)···X(3C) 3.573 Å (Fig. 4.8). Each motif is oriented in *ef* conformation slightly distorted with values comparable to those observed before.[134] The aminic

hydrogens are pointing out of the aniline plane ring [C(6)–C(1)–N(1)···H(2) 22.91° and C(2)–C(1)–N(1)···H(1) 26.67°], probably because one of them interacts with X(1A) [X(1A): C(16) to C(21)] with even shorter distance to those in the literature [N(1)–H(1)···X(1A) 3.409 Å].[134]

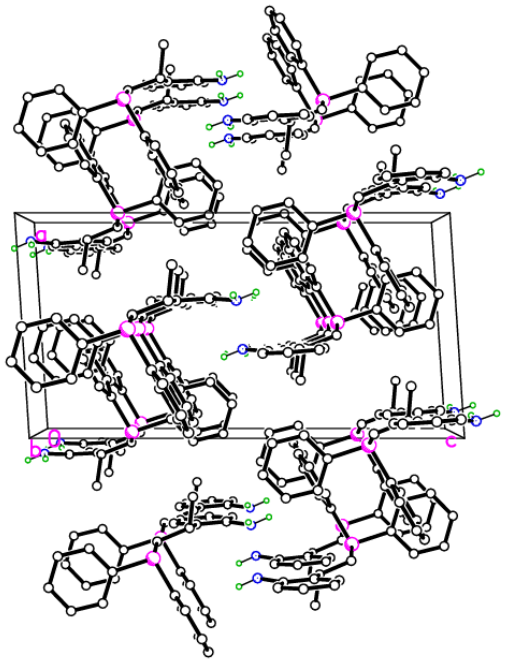

Figure 4.8 Supramolecular motif observed in compound **4.7** along *b*-axis.

Crystals of **4.9** suitable for single X–ray spectroscopy were collected from a MeOH filtrate (Fig. 4.9). P–C and C–C bond lengths are fairly similar for compounds **4.7** and **4.9** as well as P–C–C and C–C–C bonds angles and C–N and P–C–N values are in accordance with the literature (Table 4.3). However, the incorporation of the PCN scaffolding breaks the phenyl embrace observed in **4.7** but another arrangement is adopted. The packing diagram shows a chain of molecules connected by phenyl rings. One phenyl is flanked by two other rings in a *vf* conformation [C(25)–H(25)···X(2A) 2.739 Å and C(28)–H(28)···X(3B) 3.515 Å where X(2A): C(1) to C(6) and X(3B): C(1) to C(6)] and despite the latter interaction is longer than values registered in the literature, it seems to play a role in the supramolecular structure.[134,137,138] There are no H–bonds interactions however the aminic hydrogen may be involved in an intramolecular π interaction [N(1)–H(1)···X(1A) 3.598 Å, X(1A): C(10) to C(15)].

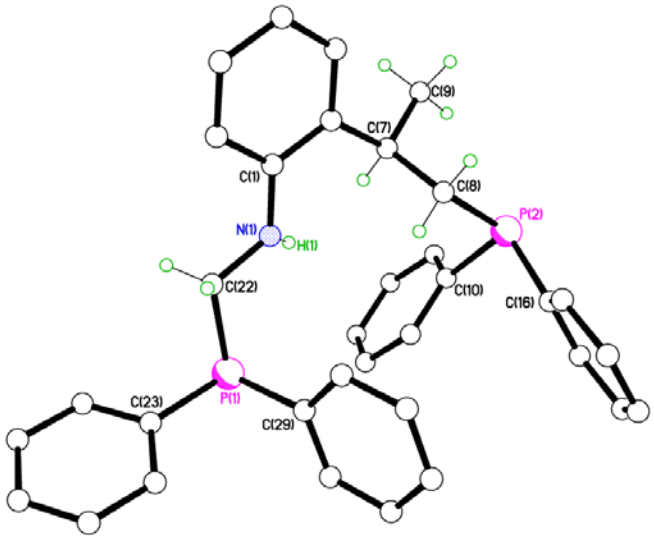

Figure 4.9 X–ray structure of **4.9**. Selected H atoms on C(7) – C(9), C(22) and N(1) shown.

Table 4.4 Selected bond lengths (Å) and angles (°) for compound **4.9**.[a]

4.9			
P(1)–C(22)	1.8565(14)	P(1)–C(22)–N(1)	111.32(9)
C(22)–N(1)	1.4514(17)	C(22)–N(1)–C(1)	120.59(12)
P(2)–C(8)	1.8574(14)	P(2)–C(8)–C(7)	113.12(9)
C(8)–C(7)	1.5471(19)	C(8)–C(7)–C(9)	111.73(12)
C(7) – C(9)	1.531(2)	C(8)–C(7)–C(6)	109.27(11)
C(7) – C(6)	1.5233(19)	C(9)–C(7)–C(6)	113.36(11)

[a] Estimated standard deviations in parenthesis.

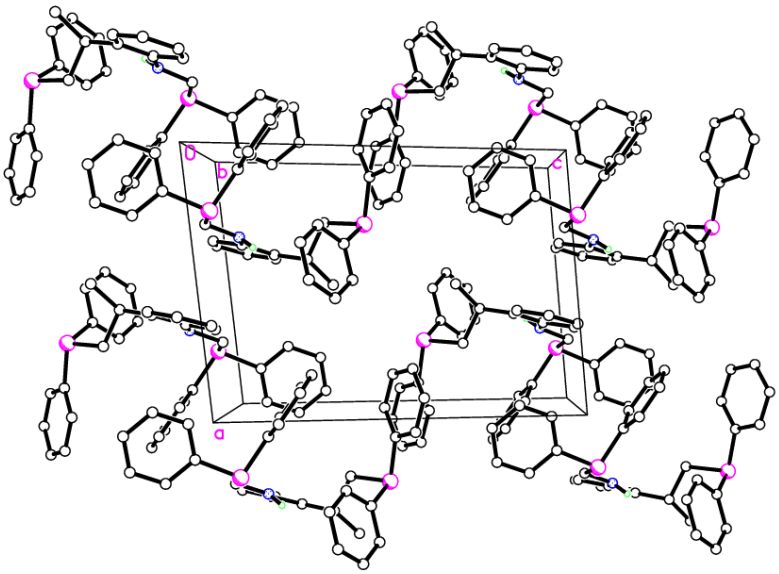

Figure 4.10 Supramolecular motif observed in compound **4.9** along the *b*-axis.

4.5 Coordination chemistry of PCN aminomethylphosphine ligands with Pt(II) and Pd(II) complexes

The coordination chemistry of ligands synthesised in Section 4.1 with $MCl_2(COD)$ (M = Pt and Pd) was investigated. Previous work within our research group has shown that PCN ligands would bind to the metal centre generating linear *cis* and *trans* Pt(II) and Pd(II) complexes, with two PCN ligands acting as P–monodentate, or cyclic compounds with a six–membered M–P–C–N–C–P ring where PCNCP diphosphines chelate the metal centre.[7,14,16,21,101] Following a literature procedure,[14] two equivs of the selected ligand were reacted with one equiv. of $MCl_2(COD)$ in CH_2Cl_2 at r.t. under aerobic conditions as shown in Equation 4.3. A cluster of peaks was observed in the $^{31}P\{^1H\}$ NMR corresponding to **4.10** – **4.15**, **4.10a** – **4.12a**, **4.14a**, **4.15a**, **4.10b** – **4.11b** and **4.15b**. One of the goals of these studies was to identify the mixture of complexes.

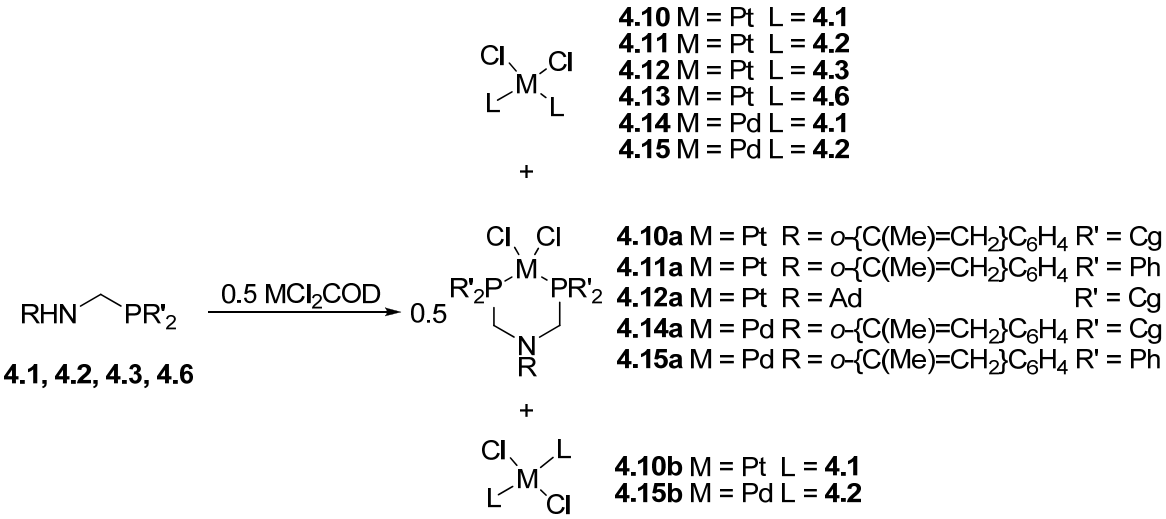

Equation 4.3

Table 4.5 Selected $^{31}P\{^1H\}$ (in ppm, *J* in Hz) for complexes **4.10 – 4.15**, **4.10a – 4.12a**, **4.14a**, **4.15a** and **4.10b** and **4.15b**.[a]

	$^{31}P\{^1H\}$	$^1J_{PPt}$		$^{31}P\{^1H\}$	$^1J_{PPt}$
4.10/4.10a	–19.2	3359	**4.13**	5.4	3649
	–22.5	3327			
4.10b	–3.2	2620	**4.14/4.14a**	3.2, 2.7	
	–3.6	2620			
4.11	6.6	3657	**4.15/4.15b**	26.8, 4.3	
4.11a	–6.1	3418	**4.15a**	9.4	
4.12/4.12a	–20.0	3353			
	–22.9	3324			

[a] NMR spectra measured in $CDCl_3$.

Pt(II) and Pd(II) complexes with a phosphadamantane cage (CgP–) would be expected to present two *meso* (αβ/βα) and two *rac* (αα/ββ) diastereomers due to the chirality on the P centre. In contrast, analogous complexes without a stereogenic centre on P such as Ph_2P– would present only one geometry.[139] Accordingly, the $^{31}P\{^1H\}$ NMR of **4.10** and **4.12** showed at least two major peaks with the phosphorus *trans* to the chloride ($^1J_{PPt}$ ~ 3340 Hz). These *cis* conformers could be the *meso* and the *rac* (αβ and βα and αα or ββ overlapped) or the **4.10** and **4.10a** showed in Equation 4.3. Figure 4.11 shows the $^{31}P\{^1H\}$ NMR of the product of the reaction between $PtCl_2$(COD) and **4.1**. The resonances at δP –19.2, –22.5 ppm, in a proportion of 4:1, showed coupling constants of $^1J_{PPt}$ 3327 and 3359 Hz respectively, indicating that the phosphorus donor atoms are in *cis* arrangement with respect to the metal centre. Two more peaks were observed at δP –3.6 and –3.2 ppm with a ^{31}P–^{195}Pt coupling constant of 2620 Hz, which indicate that both species have two phosphorus in a *trans* geometry (**4.10b**).

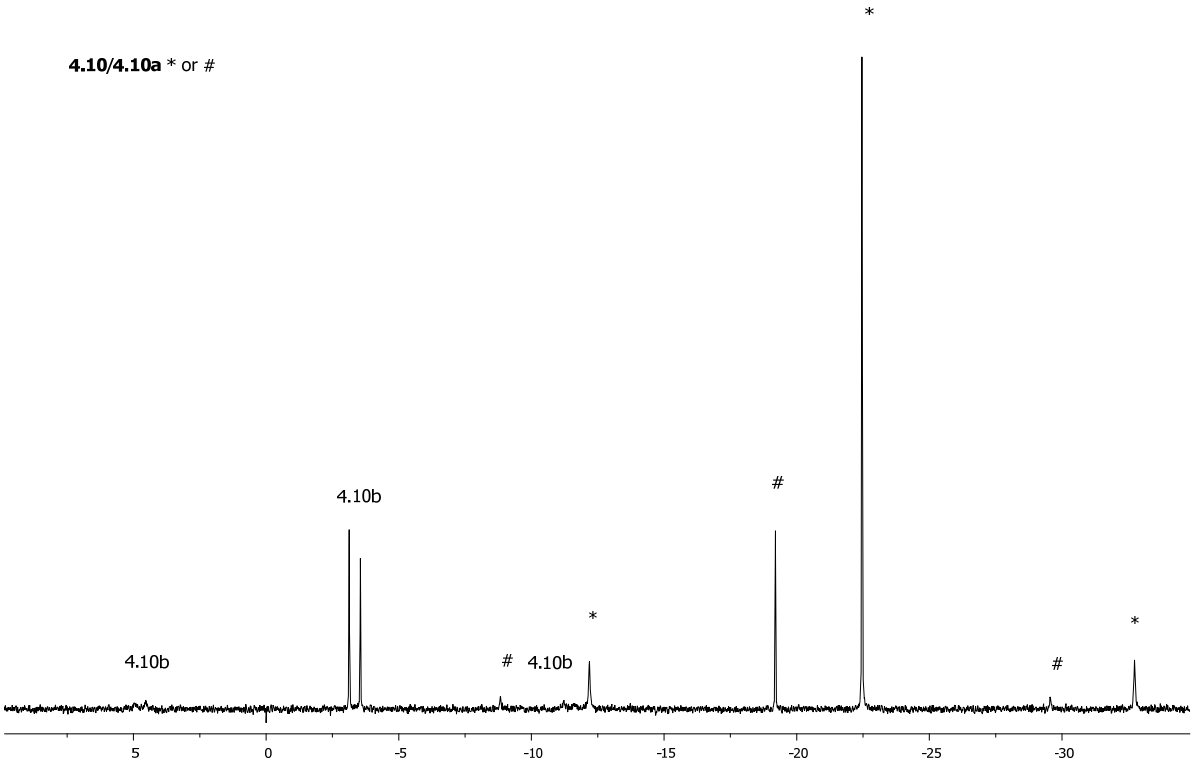

Figure 4.11 $^{31}P\{^1H\}$ NMR from the reaction between **4.1** and $PtCl_2$(COD).

The formula may be elucidated by MS and EA. However, while the mass spectrum displayed a fragmentation pattern of [**4.10aH$_3$O**]$^+$ 873, the EA was not pure enough. Fortunately, crystals that were suitable for single crystal XRD were grown from the P–based mixture, and the resulting structure was found to be **4.10a**. A similar trend was observed for the product obtained by treating $PtCl_2$(COD) with **4.3**. In solution two *cis* Pt(II) species were observed according to $^{31}P\{^1H\}$ NMR; in the solid state, MS shows the mass to charge for linear [**4.12**H]$^+$ 1024 and cyclic [**4.12a**–Cl]$^+$ 837 complexes and [AdNH$_3$]$^+$ 152. Furthermore, the EA was not conclusive due to the coincidence in % of C, H and N for **4.12** and for **4.12a** + AdNH$_2$. Unambiguous confirmation of the structure in the solid state was obtained by single X–ray crystallography revealing the cyclic **4.12a**.

Several species were also observed in the $^{31}P\{^1H\}$ spectrum of the product of the reaction between **4.2** and $PtCl_2$(COD) (Fig. 4.12). Two sharp singlets were displayed at δP 6.6 ($^1J_{PPt}$ = 3658 Hz) and δP –6.0 ppm ($^1J_{PPt}$ = 3418 Hz). The $^1J_{PPt}$ indicates a *cis* arrangement of the phosphorus with respect to the metal centre; hence, it is likely that the two major resonances correspond to **4.11** and **4.11a**. The peak at –6.1 ppm was identified by comparison with the product of the reaction between $PtCl_2$(COD) and **4.2** in equimolar quantities which resulted to be **4.11a** (Eqn. 4.4).

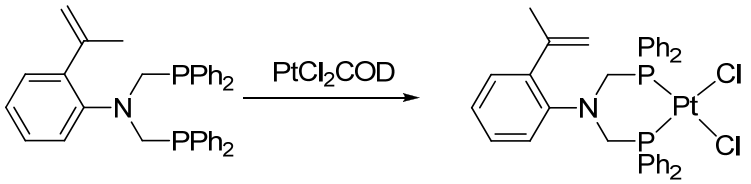

4.2a **4.11a**

Equation 4.4

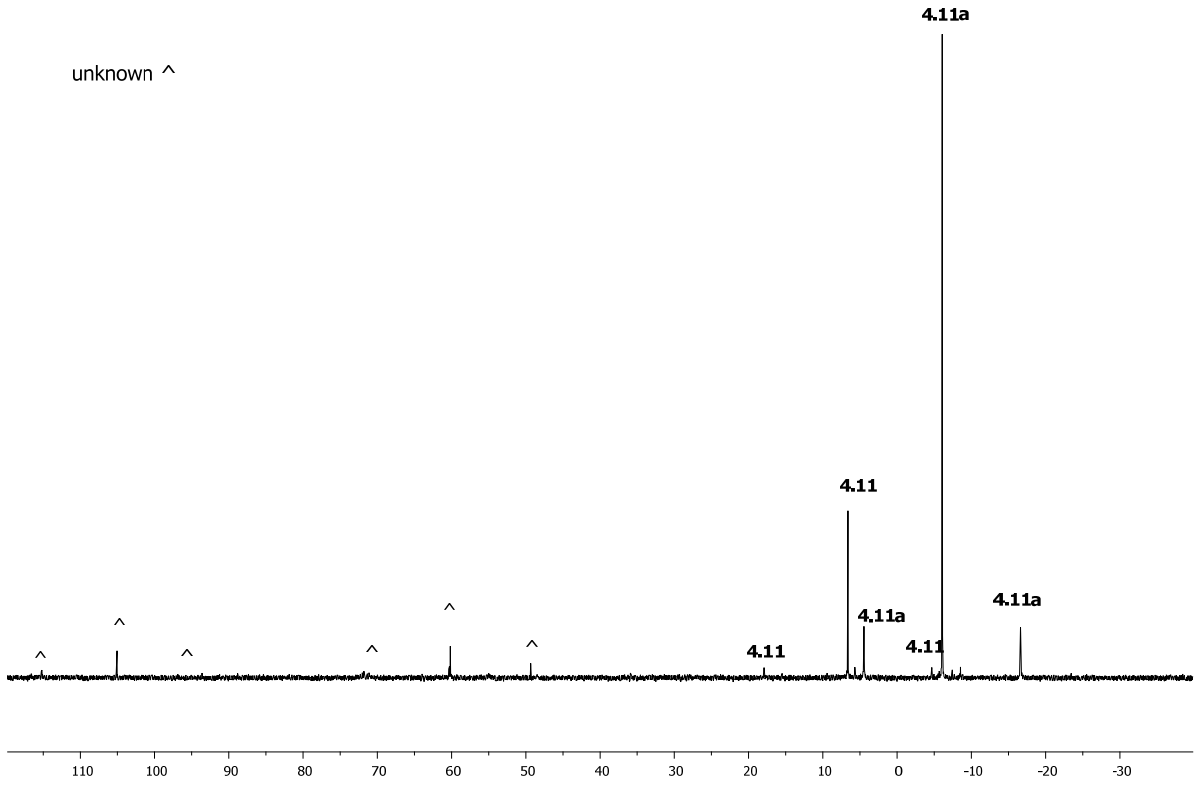

Figure 4.12 $^{31}P\{^{1}H\}$ NMR of the reaction between **4.2** and $PtCl_2(COD)$.

The other peak at 6.6 ppm was assigned by the $^{31}P\{^{1}H\}$ and ^{1}H NMR from experiments illustrated in Scheme 4.3. So far, it was assumed that ligand **4.2** only coordinates to the metal centre through the phosphorus, but in fact, it could act as a monodentate or as a bidentate ligand through the alkene, as previously documented,[140] increasing the number of P–based species in solution. The $^{31}P\{^{1}H\}$ NMR of the reaction between one equiv. of **4.2** and $PtCl_2(COD)$ (pathway **A1** or **B1**) showed a peak at δP 6.6 ppm and after adding another equiv. of the ligand (pathway **A2** and **B2**), the same spectrum was observed. However, the ^{1}H NMR was slightly different for the first and the second addition of **4.2**. The peak of the olefinic protons in the COD displayed two satellites in the first spectrum (pathway **A1** or **B1**) but not in the second (pathways **A2** and **B2**) so COD was initially bonded to the Pt and then removed by a better donor atom. Accordingly, pathway **B1** is rejected because the spectrum observed for the product of **4.2** and $PtCl_2(COD)$ demonstrated that COD remains coordinated to Pt. Therefore, **4.11b** was not formed. These experiments confirm that the peak at 6.6 ppm corresponds to **4.11**.

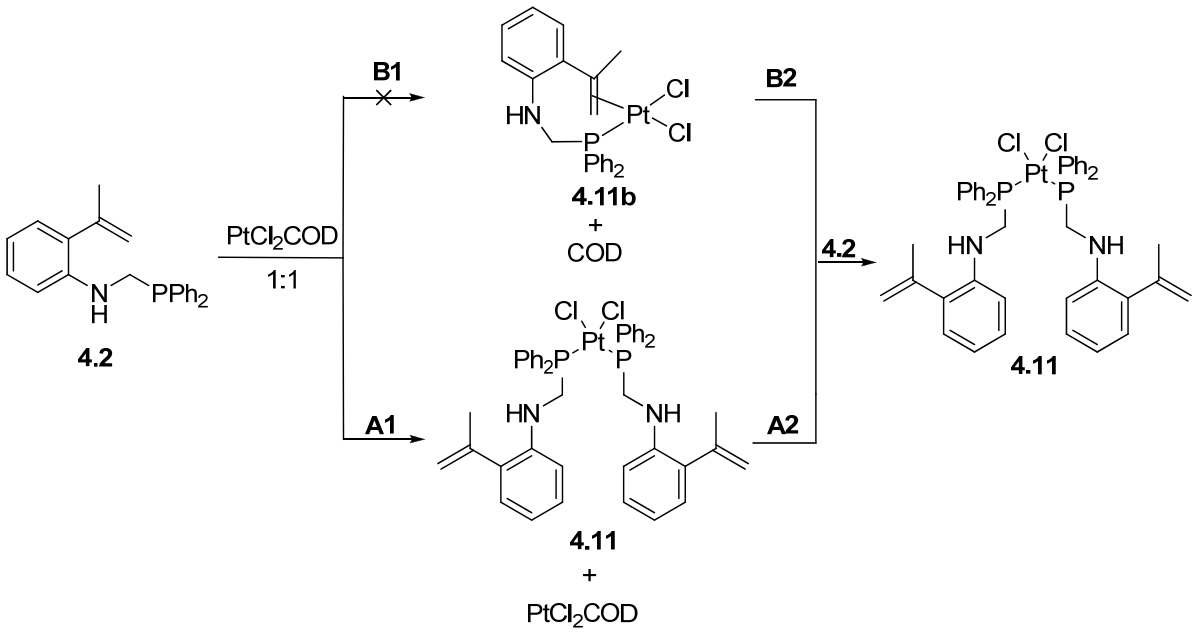

Scheme 4.3 Proposed pathway to compound **4.11**.

Minor resonances observed at δP 105.1 and 60.2 ppm are coupled to each other ($^2J_{PP}$ = 16 Hz) and to platinum ($^1J_{PPt}$ = 3641 Hz) whose magnitude indicates a *trans* arrangement of the phosphorus to the chloride. Therefore, despite the compound not being assigned, it is worthy of further investigation.

Similarly to Pt(II) complexes **4.10** and **4.11**; Pd(II) systems **4.14** and **4.15** displayed more than one peak in the $^{31}P\{^1H\}$ NMR spectrum. Whereas the spectrum of **4.14** showed two peaks close in the space [δP 3.2 and 2.7 ppm], in **4.15** both peaks [δP 26.8 and 14.3 ppm] were separated by more than *ca.* 10 ppm which was observed before for *cis*–/*trans*–$PdCl_2(PR_3)_2$ complexes.[106] To find out whether the *cis* Pd complex corresponds to the linear **4.15** or the cyclic **4.15a** (Sch. 4.3), an *in situ* reaction of **4.2** and $PdCl_2$(COD) in equimolar quantities was performed to produce **4.15a**. The $^{31}P\{^1H\}$ spectrum showed a singlet at δP 9.4 ppm. Therefore, peaks at δP 26.8 and δP 4.13 ppm were assigned to *cis*– and *trans*–Pd(II) complexes **4.15** and **4.15b**, respectively. Furthermore, the ^1H NMR showed a clear mixture of two isomers for the reaction between $PdCl_2$(COD) and **4.1** (Fig. 4.13a) and **4.2** (Fig. 4.13b) with protons slightly displaced. The assignment of the peaks was elucidated by COSY.

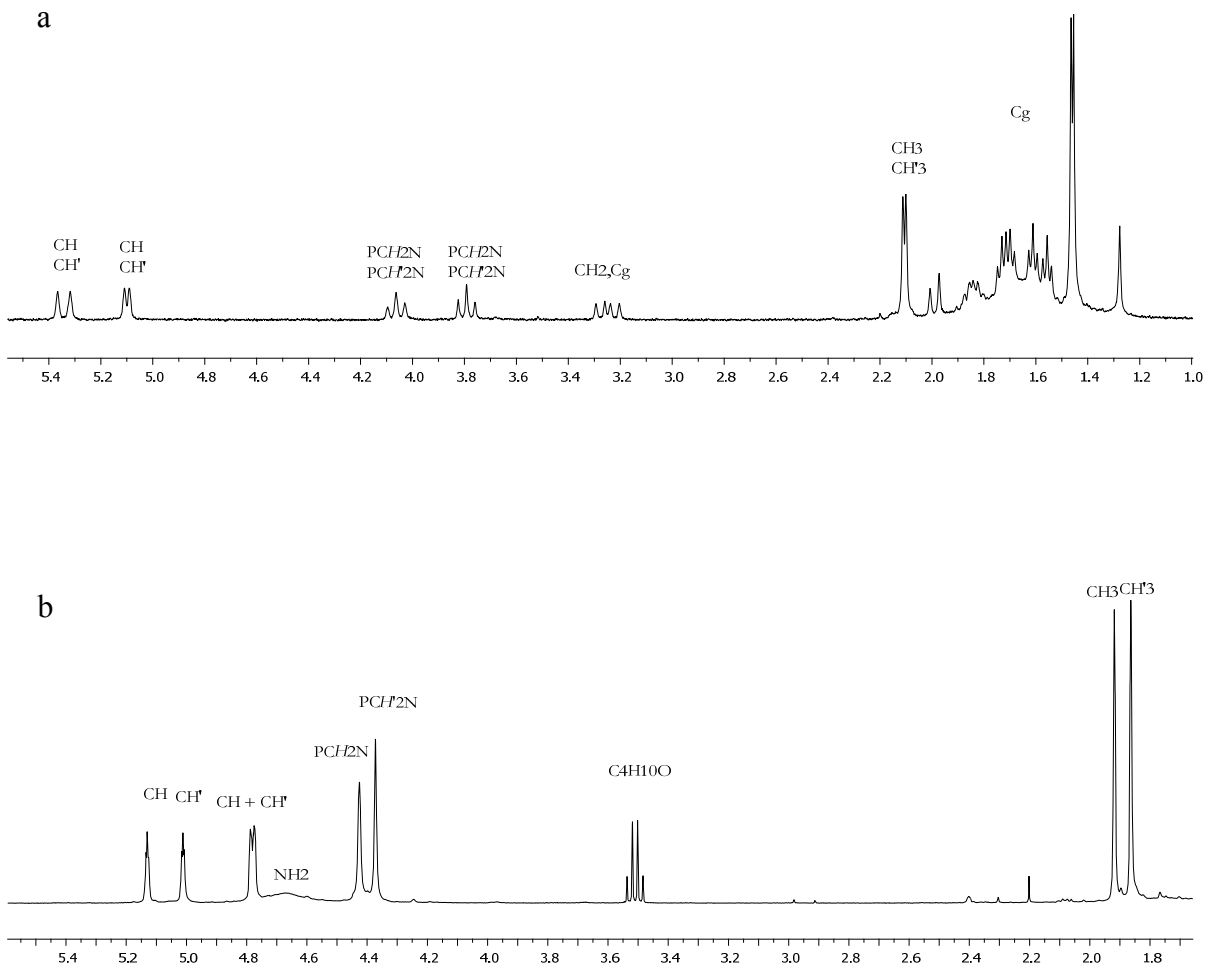

Figure 4.13 Selected region of the ^{1}H spectrum from the reaction of $PdCl_2(COD)$ and a) **4.1** and b) **4.2**.

In contrast to Pt(II) and Pd(II) compounds discussed in this section, the Pt complex obtained after treatment of **4.6** with Pt precursor, only showed a singlet in the $^{31}P\{^{1}H\}$ NMR [δP 5.4 ppm ($^{1}J_{PPt}$ = 3649 Hz)]. This peak was tentatively assigned to the expected *cis* linear Pt complex **4.13** and not to the six–membered Pt–P–C–N–C–P species due to the bulkiness of the amine *o,o*–$(CHPh)_2$–*p*–$MeC_6H_2NH_2$. This is supported by MS which exhibited a fragmentation pattern of 1505 attributed to $[M–Cl]^+$. Further confirmation was obtained by IR spectrum which displayed weakly absorbing νNH stretches (3333, 3332 cm^{-1}) in addition to the weak νPtCl (312, 289 cm^{-1}).

4.6 X–ray structures of 4.10a and 4.12a

X–ray diffraction studies of the Pt(II) complexes with ligands **4.1** and **4.3** confirms a *cis* arrangement of the phosphorus with respect to the metal centre which is in a six–membered Pt–P–C–N–C–P ring. The resulted structures, **4.10a** and **4.12a**, were obtained by slow vapour diffusion of Et_2O into solutions of the bulk products in $CHCl_3$ over several days. The Pt(II) metal centre is in a distorted square–planar coordination environment as shown in Figures 4.14 a and 4.14 b respectively and with typical Pt–P and Pt–Cl bond lengths and angles (Table 4.6). In both complexes the ligand adopts a *P,P*–chelating mode supporting one of the three possible platinum complexes proposed in Equation 4.3 (**4.10a** and **4.12a**). The Pt–Cl, Pt–P are comparable to those in previously synthesised complexes described in Chapter 3 (**3.1**, **3.2**, **3.6a** and **3.9**) and reported compounds.[7,16,58,59,101] The bite angle of **4.10a** and **4.12a** [P(1)–Pt(1)–P(2) 94.20(7)^o and 94.26(5)^o respectively) do not differ significantly from the value for **3.6a** [92.94(4)^o, Table 3.4]. Selected bond lengths and angles are given in Table 4.6.

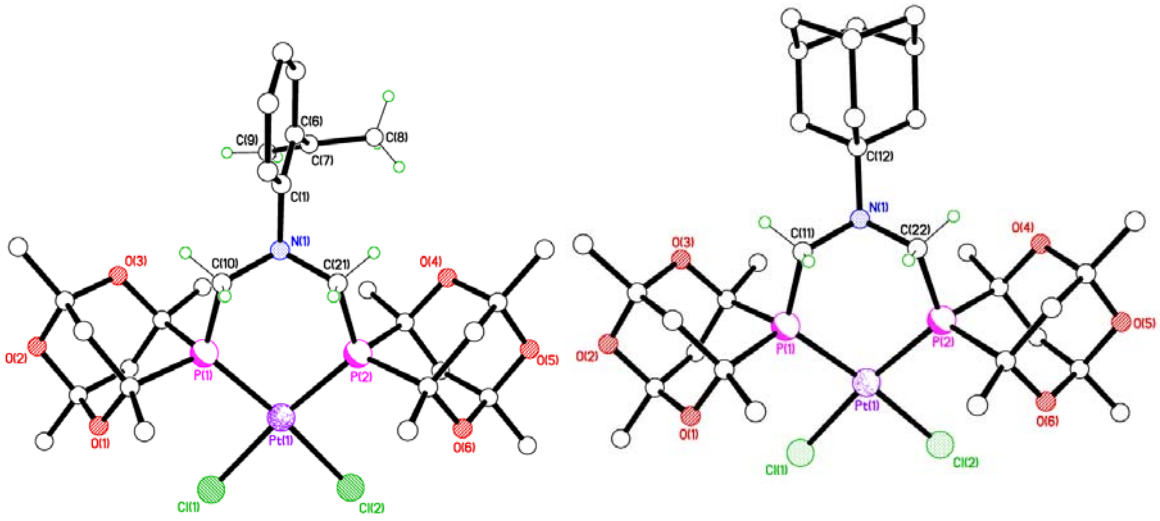

a b

Figure 4.14 X–ray structure of a) **4.10a** and b) **4.12a**. Selected hydrogens are shown and one molecule of $CHCl_3$ is omitted for clarity for **4.10a** and **4.12a**.

Table 4.6 Selected bond lengths (Å) and angles (°) for **4.10a** and **4.12a**.[a]

	4.10a	**4.12a**
Pt(1)–Cl(1)	2.3397(13)	2.3457(19)
Pt(1)–Cl(2)	2.3480(14)	2.337(2)
Pt(1)–P(1)	2.2510(12)	2.2513(18)
Pt(1)–P(2)	2.2496(14)	2.2495(19)
Cl(1)–Pt(1)–Cl(2)	83.11(5)	83.12(7)
Cl(1)–Pt(1)–P(1)	91.01(5)	91.88(7)
Cl(2)–Pt(1)–P(2)	91.68(5)	90.76(7)
P(1)–Pt(1)–P(2)	94.26(5)	94.20(7)
P(1)–Pt(1)–Cl(2)	173.87(5)	174.91(7)
P(2)–Pt(1)–Cl(1)	174.25(5)	173.44(6)
Pt(1)–P(1)–C(11)	118.76(16)	102.4(3)
P(1)–C(10)–N(1)	115.0(3)	113.7(5)[b]
C(10)–N(1)–C(21)	107.7(4)	106.9(5)[c]
N(1)–C(21)–P(2)	116.7(3)	112.7(5)
C(21)–P(2)–Pt(1)	117.54(17)	117.8(2)

[a] Estimated standard deviations in parenthesis. [b] C(10) in **4.10a** is C(11) in **4.12a**. [c] C(21) in **4.10a** is C(22) in **4.12a**.

In contrast to **3.6a**, complexes **4.10a** and **4.12a** do not show weak Pt···Pt interactions, but there are H–bonds between C(11)–H(11)···Cl(2) [3.783(8) Å] and C(22)–H(22)···Cl(1) [3.794(7) Å] for **4.10a**, and likewise between C(2)–H(2)···Cl(1) [3.719(3) Å], C(14)–H(14B)···Cl(1) [3.731(5) Å] and C(29)–H(29B)···Cl(2) [3.934(6) Å] for **4.12a** as illustrated in Figure 4.15 b.

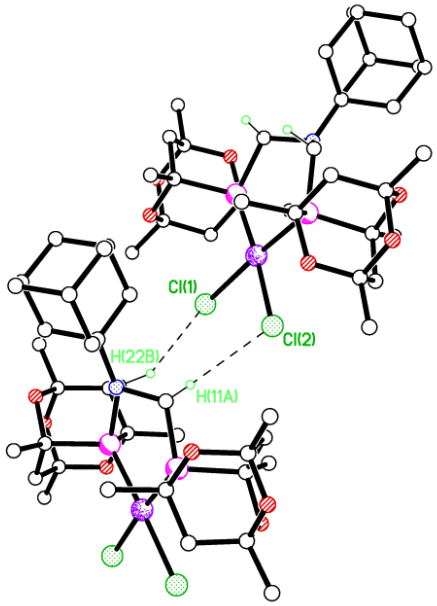

Figure 4.15 Intermolecular C–H···Cl bonding in **4.12a**.

4.7 Coordination chemistry of PCN aminomethylphosphine ligands with Ru(II)

With the aim of studying the coordination capabilities of the novel ligands, different late transition metals were used. In the previous section Pt(II) and Pd(II) complexes were chosen as examples of metal centers with d^8 configuration; in this section we will discuss about the structure of complexes with a d^6 metal center such as Ru(II). Hence, compounds **4.16** – **4.19** were synthesised by reacting one equiv. of $\{RuCl_2(\eta^6\text{–}p\text{–cymene})\}_2$ with two equivs. of the appropriate ligands for 1 h at r.t. in CH_2Cl_2 under aerobic conditions (Eqn. 4.5). Red and orange products were achieved in good yields (43 – 72%).

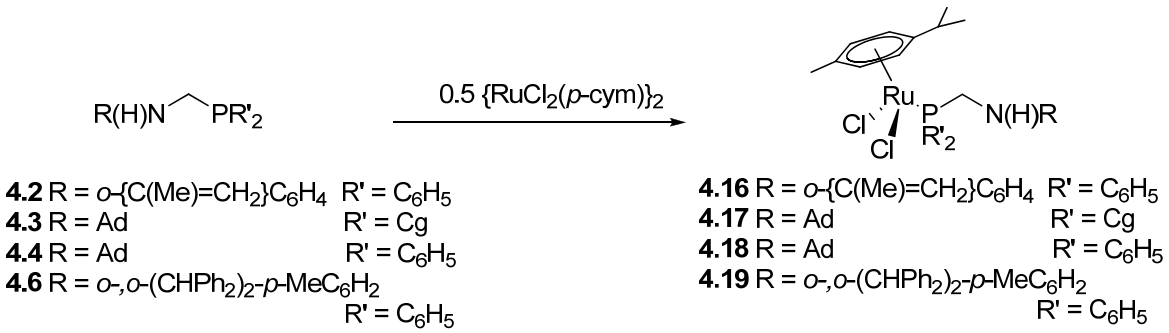

Equation 4.5

The $^{31}P\{^1H\}$ NMR of complexes **4.16** – **4.19** showed a sharp singlet significantly downfield with respect to the corresponding ligands by approx. δP 40 ppm (δP 25.1 ppm for **4.16**, δP 15.1 ppm for **4.17**, δP 26.9 ppm for **4.18** and δP 22.7 ppm for **4.19**). The splitting pattern expected for PC*H*$_2$N protons (ABX, doublet of doublets) was observed for **4.17** at 3.77 ppm ($^3J_{HH}$ = 12.4, $^2J_{HP}$ = 4.9 Hz) and for **4.19** only a doublet at 4.12 ppm ($^2J_{HP}$ = 2.9 Hz) in the ^{1}H NMR. However for **4.16** and **4.18** the protons showed a broad singlet at 4.48 and 3.70 ppm respectively. It should be mentioned that **4.17** was poorly soluble in $CDCl_3$ and hence the ^{1}H NMR was quite weak. Fortunately, even at low concentration, the ^{1}H NMR spectrum was recorded and displayed $\{RuCl_2(\eta^6\text{–}p\text{–cymene})\}_2$ unreacted in 1:1 proportion, even after 24 h stirring at r.t. Furthermore, the ES–MS displayed the mass to charge of **4.3** (*m/z* $[MH]^+$ 380) and in contrast to the EA of **4.12**/**4.12a**, no evidence of 1–adamantylamine was observed. The formulae of the complexes were also supported by

ES–MS data which resulted from loss of the chloride ion for **4.16 – 4.19** (*m/z* $[M–Cl]^+$ 602, 650, 620, 908 respectively).

4.8 X–ray crystal structures of 4.16 and 4.19

Red block crystals of complexes **4.16** and **4.19** suitable for single crystal X–ray analysis were obtained by slow diffusion of diethyl ether into concentrated chloroform solutions at r.t. after a few days. Their analysis confirms the formation of the dichloro(aminophosphine)ruthenium complexes with the expected "piano–stool" geometry for ruthenium. The isopropyl methyl groups in cymene are above the plane of the aromatic ring and they are orientated in opposite direction to the rest of the molecule (Fig 4.16 a and b). It should be mentioned that two molecules of **4.16** crystallised in the unit cell. P–C, Ru–P, Ru–Cl and P–Ru–P bond lengths and angles are in agreement with those previously reported, and C–N and P–C–N bond lengths and angles do not differ significantly between both Ru complexes, **4.16** and **4.19**, and Pt(II) and Pd(II) complexes synthesised in this project [av. P–C–N *ca*. 114.1 Å] (Table 4.7).[126]

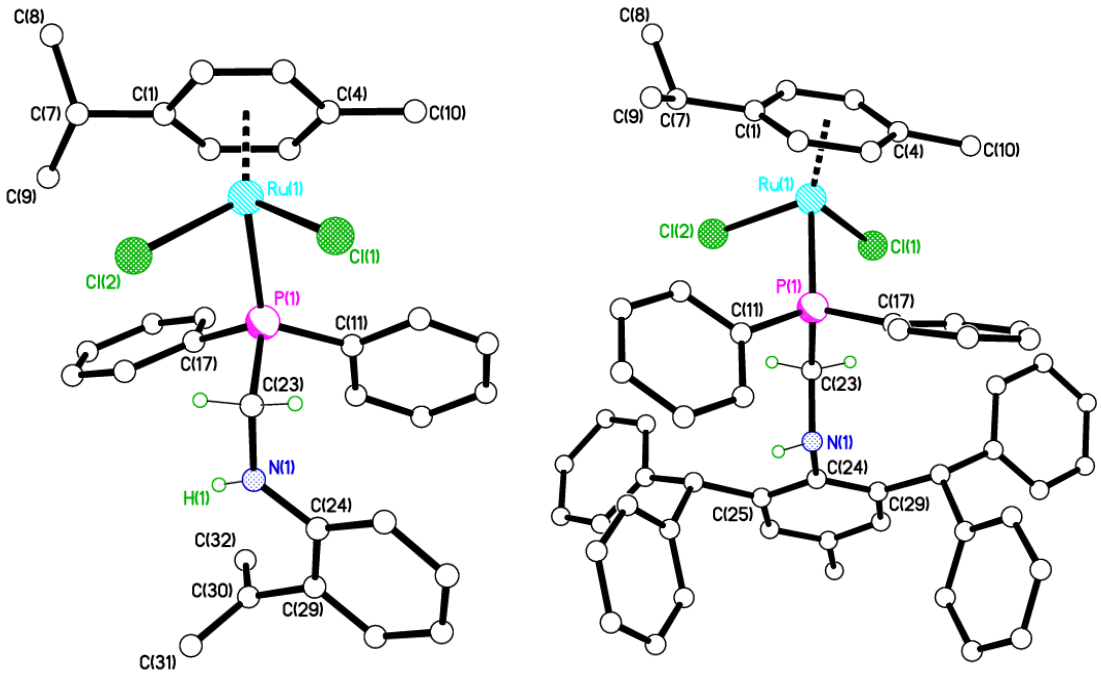

a b

Figure 4.16 X–ray structures of a) **4.16** and b) **4.19**. Selected hydrogens on N(1) and C(23) are shown.

Table 4.7 Selected bond (Å) and angles (°) for **4.16** and **4.19**.[a]

	4.16[b]		**4.19**
Ru(1)–C_{cent}	1.6978(15)	[1.7009(16)]	1.695(2)
Ru(1)–P(1)	2.3360(10)	[2.3249(11)]	2.3416(6)
Ru(1)–Cl(1)	2.4073(10)	[2.4047(11)]	2.4180(6)
Ru(1)–Cl(2)	2.4186(10)	[2.4233(10)]	2.4133(6)
C(30)–C(31)	1.408(7)	[1.491(8)][c]	–
C(30)–C(32)	1.391(7)	[1.346(7)][c]	–
Cl(1)–Ru(1)–Cl(2)	88.68(4)	[88.41(4)]	91.25(7)
P(1)–Ru(1)–Cl(1)	85.80(4)	[85.33(4)]	116.12(7)
P(1)–Ru(1)–Cl(2)	112.20(4)	[84.79(3)]	86.78(2)
N(1)–C(23)–P(1)	114.4(3)	[113.4(3)][d]	116.75(14)

C_{cent} denotes the centroid of the *p*–cymene ring [C(1)–C(2)–C(3)–C(4)–C(5)–C(6)].
[a] Estimated standard deviations in parenthesis. [b] Second molecule denoted in brackets.
[c] C(30) is C(62), C(31) is C(64) and C(32) is C(63). [d] C(23) instead C(55).

In **4.19**, two hydrogens on C(23) are weakly bonded to the two chlorides on Ru(1) with distances between 3.506(2) Å for C(23)···Cl(2) and 3.181(2) Å for C(23)···Cl(1) (Fig. 4.17, Table 4.7). These chlorides are involved in intermolecular hydrogen bonds with aromatic hydrogens of a second molecule in the unit cell [C(2A)···Cl(1) 3.527(2) Å and C(3A)···Cl(2) 3.706(2) Å]. Overall, eight C–H···Cl interactions are involved to lock two molecules as highlighted in Figure 4.17. The same arrangement was observed for the structure of **4.16** and for those in the literature which it was not discussed despite the similarity.[126] Whereas for **4.16**, two molecules are in the unit cell (due to the disorder in one isopropenyl group [C(62)–C(64)]), in **4.19** and those in the literature only one molecule was present.

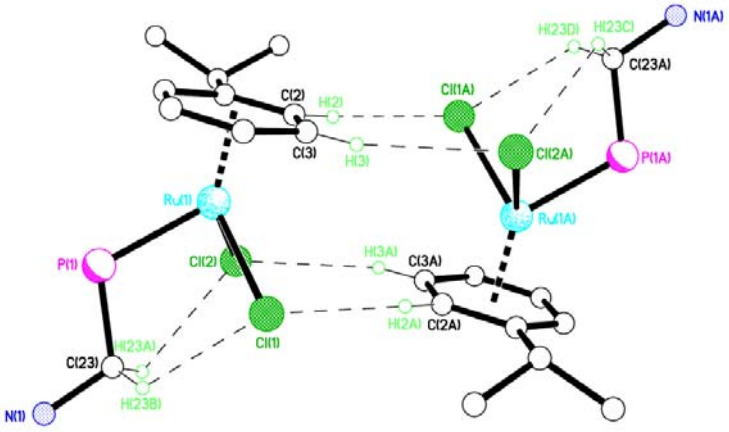

Figure 4.17 Supramolecular structure showing H–bonds between two molecules in the unit cell for **4.19**. Selected atoms on N, P and *p*–cymene are omitted for clarity.

Table 4.8 Hydrogen–bond contacts (Å, º) for **4.16** and **4.19**.[a]

	D–H···A	*D*–H	H···A	*D*···A	*D*–H···A
4.16	C(23)–H(23A)···Cl(1)	0.99	2.93	3.445(4)	113
	C(23)–H(23B)···Cl(2)	0.99	2.66	3.291(4)	122
	C(55)–H(55A)···Cl(3)	0.99	2.67	3.334(4)	125
4.19	C(23)–H(23A)···Cl(2)	0.99	2.90	3.506(2)	121
	C(23)–H(23B)···Cl(1)	0.99	2.59	3.181(2)	119
	C(2)–H(2)···Cl(1A)	0.95	2.62	3.527(2)	159
	C(3)–H(3)···Cl(2B)	0.95	2.79	3.706(2)	162

[a] Estimated standard deviations in parenthesis.

4.9 Coordination chemistry of PC_4CN and PC_4NCP aminomethylphosphine ligands with Pt(II)

To understand more about the primary amines PC_4N, **4.7** and **4.8**, their coordination chemistry was briefly investigated. The reaction of two equivs. of **4.7** or **4.8** with one equiv. of $PtCl_2(COD)$ in CH_2Cl_2 showed a complicated $^{31}P\{^1H\}$ NMR and therefore plausible new Pt(II) complexes **4.20** – **4.20d** and **4.21** – **4.21d** depicted in Equation 4.6 could be obtained.

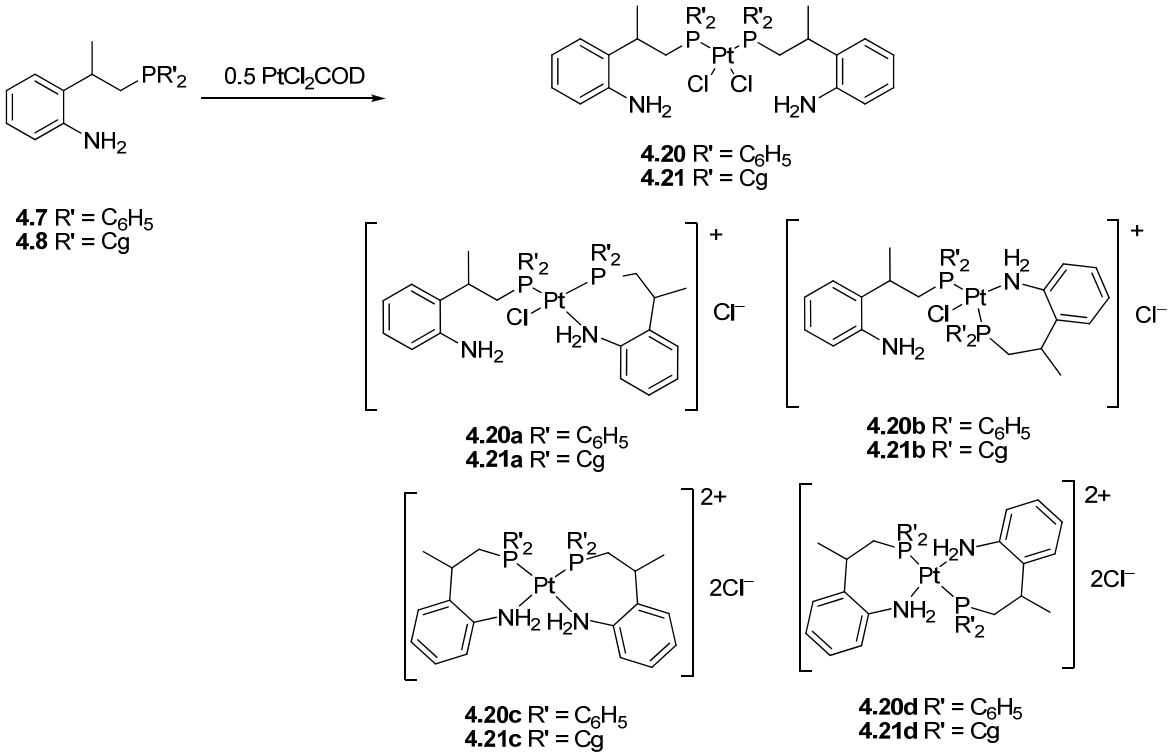

Equation 4.6

The $^{31}P\{^{1}H\}$ NMR of the product between **4.7** with $PtCl_2(COD)$ showed a sharp singlet at *ca*. δP 53.4 ppm and various overlapping broad signals around 10 ppm. In a similar manner, the $^{31}P\{^{1}H\}$ NMR of the product between **4.8** with $PtCl_2(COD)$ showed several peaks in the range of δP 6.00 and 0.00 but no platinum satellites were observed which impedes any characterisation. Because of the broadness of the resonances, only a tentative estimation could be done according to the shape and integration of the signals. The resonance observed for the product between **4.7** and $PtCl_2(COD)$ at 53.4 ppm was flanked by two platinum satellites with a coupling constant of $^{1}J_{PPt}$ = 4020 Hz suggesting that the phosphorus were positioning *trans* to a coordinated amine and therefore this signal might be due to the formation of *cis*-dication **4.20c**.[141,142] The resonances at approx. δP 12.1 ppm (*ca*. $^{1}J_{PPt}$ = 3552 Hz) and 9.55 ppm (*ca*. $^{1}J_{PPt}$ = 3508 Hz) could correspond to the dichloro platinum (II) complex **4.20**. Moreover, the MS of the product between **4.7** and $PtCl_2(COD)$ exhibited a mass to charge of [**4.20**–Cl]$^{+}$ 868. Future investigation using variable temperature NMR studies would aid the resolution of the spectra and therefore give more insight into the structure of these complexes.

Trying to elucidate this mixture, an excess of KO^{t}Bu was added to **4.20** – **4.40d** and **4.21** – **4.21d** to enhance the formation of the presumed new species *cis* **4.20e** and **4.21e** or *trans* **4.20f** and **4.21f** (Eqn. 4.7). Once the salt was added, the colourless solutions turned to bright yellow as previously observed for similar chelated amidophosphines.[142] Unfortunately, a more broad spectrum was observed for the $^{31}P\{^{1}H\}$ and ^{1}H NMR of the product of **4.20 – 4.20d** and KO^{t}Bu, and even more resonances were observed for **4.21 – 4.21d** with KO^{t}Bu. It is clear that there are several species in solution which are difficult to assign. It is worth noting that the ligands used in these experiments were very clean and of high purity and are therefore not a factor in the formation of these species.

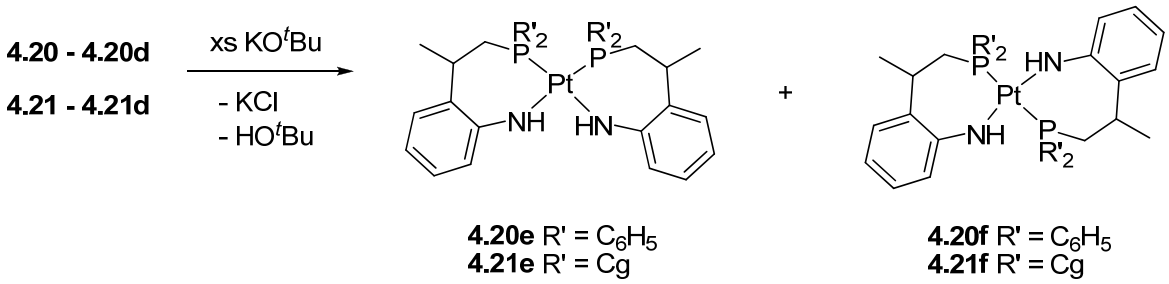

Equation 4.7

The coordination capabilities of the novel asymmetric PC_4NCP aminomethylphosphine **4.9** was also investigated towards Pt(II) precursor. The synthesis of the *cis*–Pt(II) complex **4.22** was achieved by reacting $PtCl_2(COD)$ and **4.9** in equimolar quantities in the same manner as **4.20** and **4.21** (Eqn. 4.8).

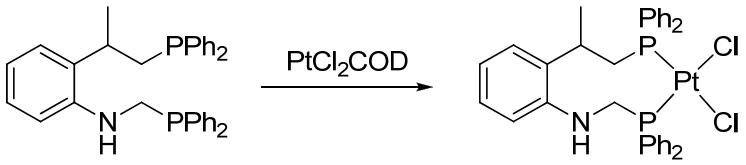

4.9 **4.22**

Equation 4.8

The target platinum complex was formed in 80% yield and exhibited two resonances at δP 23.9 ($^1J_{PPt}$ = 3768, $^2J_{PP}$ = 9 Hz) and 11.3 ppm ($^1J_{PPt}$ = 3479, $^2J_{PP}$ = 9 Hz) in the $^{31}P\{^1H\}$ NMR spectrum, which are significantly downfield from the free ligand **4.9** (δP –19.6, –19.8 ppm). The large downfield shift and the magnitudes of $^{31}P–^{195}Pt$ coupling constants indicate that the ligand coordinates in a *P,P*–chelate fashion give a nine–membered Pt–P–C–N–C–C–C–C–P ring. Similar compounds with a seven–membered Pt–P–C–N–C–C–P ring showed two phosphorus peaks flanked by platinum satellites with values in accordance with **4.22**.[34] In addition, both phosphorus are coupled with a value in agreement to those in the literature for Pt(II) complexes with two phosphorus in a *cis* arrangement.[34] This geometry is supported by the absorbing νPtCl (316 and 291 cm^{-1}) and νNH (3357) stretches observed in the IR characteristic of the *cis* disposition. Further unambiguous confirmation of the empirical formula was made by MS ($[M–Cl]^+$ 747) and EA.

4.10 Preliminary studies of capture of CO_2 by Ru(II) complexes with PCN ligands

Following the investigation conducted in Chapter 3 with Ru(II) complexes **3.11** – **3.15**, **3.25** and **3.26**, compounds **4.16** – **4.18** were dissolved in CH_2Cl_2 and treated with CO_2 at r.t. for 1 h. Then, the brown suspensions were kept for several days to see any changes in colour. After evaporation of the solvent, the products were collected and characterised by IR. The spectra revealed the same νNH and νRuCl stretches as for previously treated **4.16**

– **4.18**, with no evidence of the characteristic ν*C*O stretch around 1765 – 1645 cm^{-1}. Therefore, under these conditions no reaction occured.

The X–ray structure of **4.16** was obtained and a packing model shows that ruthenium is not widely accessible to CO_2 (Fig. 4.18). However, as the NH is not involved in H–bond, it could bind the oxygen on CO_2 facilitating the approach to the metal centre. In view of the results, it is clear that this hypothesis merits considerable further investigation.

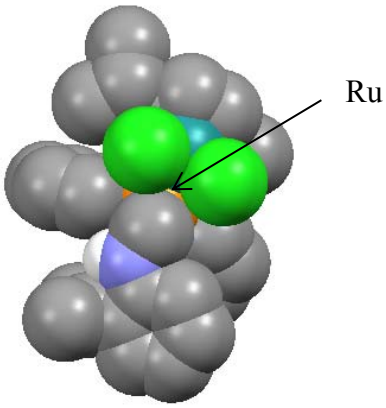

Figure 4.18 Space filling model of **4.16**.

As mentioned in Section 3.5 the fixation of CO_2 by organometallics is favoured by displacement of the chloride ligands by hydrides and a subsequent sequestration of the small molecule in the M–H bond. So, future efforts should be addressed to pursue the conversion of the M–Cl into the M–H bond in the fully characterised novel Ru(II) complexes **4.16 – 4.18**.

4.11 Conclusions

In summary, new PCN aminomethylphosphine ligands incorporating a variety of substituents on the N and P atoms were prepared *via* simple Mannich based condensation reactions. The reaction was dependant on the bulkiness of the *ortho*–aniline; thus less hindered phosphines were more susceptible to a double condensation reaction. With the aim of investigating the reactivity of the *ortho*–anilines towards secondary and tertiary

amines, *o*–{C(Me)=CH_2}$C_6H_4NH_2$ was used to obtain novel PC_4N and asymmetric PC_4NCP ligands by a hydrophosphination reaction followed by a condensation reaction.

The coordination capabilities of these ligands was explored towards Pt(II), Pd(II) and Ru(II) metal centres. While the PCN ligands showed several *cis* and *trans* Pt(II) and Pd(II) species, the same ligands afforded exclusively the expected Ru(II) compounds. In some cases, crystals were obtained showing *cis* chelate Pt(II) complexes with a square–planar conformation and Ru(II) compounds exhibit piano–stool geometry. For the latter, C–H···Cl interactions between two molecules were comparable to those for previously reported structures. The coordination chemistry of PC_4N with Pt(II) precursors revealed a complicated $^{31}P\{^1H\}$ NMR presumably due to the wide range of binding modes through the N and P donor atoms. The asymmetric PC_4NCP ligand was also treated with $PtCl_2COD$ which conducted to a nine–membered Pt–P–C–N–C–C–C–C–P ring.

Overall, the library of PCN and PC_4N ligands were expanded and novel PC_4NCP were synthesised which were reacted with various transition metal centres. Hence, future investigation should be pursued not only to gain an insight into the formation of the chelating ligands in coordination studies but also in the purification and/or the isolation and crystallisation of these complexes.

5. Conclusions and future work

A new series of PCN backbone ligands was synthesised *via* a phosphorus Mannich condensation reaction and their coordination chemistry investigated. These novel phosphines incorporate a pendant amine to mimic similar PCN compounds found in the literature which demonstrated high efficiency as catalysts in electron–transfer processes and versatile binding modes to various metal centres.

A novel family of aminomethylphosphines was obtained by using THPC as phosphorus precursor. This salt offers the advantage of being cheap, readily available and easy to handle under air conditions. Hence following a literature procedure, THPC was reacted with various anilines to give phosphonium salts $P\{CH_2N(H)R\}_4Cl$ (R = C_6H_5, **2.1**; *o*–MeC_6H_4, **2.2**; *o*–$^{i}PrC_6H_4$, **2.3**; *o*–$^{t}BuC_6H_4$, **2.4**; *o*–FC_6H_4, **2.5**; *o*–$CF_3C_6H_4$, **2.6**; *o*–$\{C(Me)=CH_2\}C_6H_4$, **2.7**; *p*–MeC_6H_4, **2.8**; *p*–$^{i}PrC_6H_4$, **2.9**; *p*–FC_6H_4, **2.10** and *p*–EtC_6H_4, **2.11**).[25] Applying a well–stablished method employed by our research group,[16] these phosphonium salts were reduced with Et_3N to afford the cyclic $N(H)CH_2P\{(CH_2)_3(NR)_2\}$ phosphines (R = C_6H_5, **2.12**; *o*–FC_6H_4, **2.15**; *p*–MeC_6H_4, **2.16**; *p*–$^{i}PrC_6H_4$, **2.17**; *p*–FC_6H_4, **2.18** and *p*–EtC_6H_4, **2.19**). Acyclic $P\{CH_2N(H)R\}_3$ phosphines [R = C_6H_5, **2.26**; *o*–$^{i}PrC_6H_4$, **2.27**; *o*–$^{t}BuC_6H_4$, **2.28**; *o*–$CF_3C_6H_4$, **2.29** and *o*–$\{C(Me)=CH_2\}C_6H_4$, **2.30**] were obtained by changing Et_3N by $KO^{t}Bu$ and using phosphonium salts with *ortho*–groups relative to the nitrogen. Other methods for the synthesis of acyclic $P\{CH_2N(H)R\}_3$ phosphines (R = aryl and alkyl groups) were employed by the Starosta and Han research groups which involves the synthesis of $P\{CH_2OH\}_3$ (THP) and therefore, inert atmosphere.[2,29,45] However using our method, **2.26 – 2.30** were obtained under aerobic conditions. Double condensation was observed in the $^{31}P\{^{1}H\}$ NMR of cyclic phosphines **2.12**, **2.16 – 2.19**, which possess *para* substituents relative to the amine, to form diphosphines $\{(CH_2)_3(NR)_2\}PCH_2N(R)CH_2P\{(CH_2)_3(NR)_2\}$ (R = C_6H_5, **2.20**; *p*–MeC_6H_4, **2.21**; *p*–$^{i}PrC_6H_4$, **2.22**; *p*–FC_6H_4, **2.23** and *p*–EtC_6H_4, **2.24**). Therefore, reduction of phosphonium salts containing *ortho*–aniline substituents relative to the amine afforded linear phosphines **2.26 – 2.30**, whereas *para* substituted anilines produced cyclic phosphines **2.12 – 2.19**, with the exception of **2.13** and **2.14 (***o*–MeC_6H_4 and *o*–$^{i}PrC_6H_4$, respectively). In the solid state, only one phosphine species was obtained as confirmed by EA, MS and the structure of **2.6**, **2.12**, **2.14**, **2.16**, **2.17**, **2.19**, **2.27**, **2.29a** (**2.29** with a P=O bond) was further supported by single crystal X–ray diffraction.

Poorly investigated $P\{CH_2N(R)CH_2\}_2P$ (R = C_6H_5, **2.31**; *p*–MeC_6H_4, **2.32**; *p*–$^{i}PrC_6H_4$, **2.33** and *p*–EtC_6H_4, **2.34**) diphosphines with a P–P intrabridghead were obtained from

phosphonium chlorides **2.1**, **2.8**, **2.9** and **2.11** and KO^{t}Bu. Diphosphines **2.31** and **2.32** were previously documented as co–products in lower yields.[26,89] Despite the yields achieved here were not higher than those in the literature (*ca*. 21% vs 44%), a procedure was stablished for their synthesis and crystals were obtained for **2.31** confirming the structure. Phosphonium salt **2.11** afforded the target P–P diphosphines **2.34** along with cyclic **2.19** counterpart so purification of **2.34** merits further investigation. Reaction of phosphonium salts containing *ortho*–RC_6H_4N– amines was unsuccessful which suggests that the formation of diphosphines of the type of $P\{CH_2N(R)CH_2\}_2P$ is related to the accessibility of the nitrogen. Accordingly, further research should be undertaken to expand the library of these ligands, *e.g.* incorporating no hindered amines.

This research group has been interested in developing new symmetric and asymmetric PCNCP aminomethylphosphines of the type $Ph_2PCH_2N(R)CH_2PR'$.[7,12,13] Asymmetric diphosphines $Ph_2PCH_2N(R)CH_2PCg$ (R = C_6H_5 and *p*–MeC_6H_4 and Cg =1,3,5,7–tetramethyl–2,4,8–trioxa–6–phosphaadamantane) were achieved when secondary aminomethylphosphines $HN(R)CH_2PCg$ were reacted with Ph_2PCH_2OH. Therefore, to expand the library of asymmetric phosphines, cyclic **2.12**, **2.14 – 2.16** and **2.18** phosphines were utilised as secondary amines. These compounds proved to react with Ph_2PCH_2OH according to $^{31}P\{^1H\}$ NMR and MS to afford $Ph_2PCH_2N(R)CH_2P\{(CH_2)_3(NR)_2\}$ (R = C_6H_5, **2.36**; *o*–^{i}PrC_6H_4, **2.37**; *o*–FC_6H_4, **2.38**; *p*–MeC_6H_4, **2.39** and *p*–FC_6H_4, **2.40**). However they were observed in up to 50% yields according to $^{31}P\{^1H\}$ NMR, along with symmetric $\{(CH_2)_3(NR)_2\}PCH_2N(R)CH_2P\{(CH_2)_3(NR)_2\}$ diphosphines (R = C_6H_5, **2.20**; *p*–MeC_6H_4, **2.21**; *p*–FC_6H_4, **2.23**; *o*–^{i}PrC_6H_4, **2.46** and *o*–FC_6H_4, **2.47**) and $\{Ph_2PCH_2N(R)CH_2PPh_2\}$ diphosphines (R = C_6H_5, **2.48**; *o*–^{i}PrC_6H_4, **2.49** and *o*–FC_6H_4, **2.50**; *p*–MeC_6H_4, **2.51** and *p*–FC_6H_4, **2.52**). A wide range of conditions were applied to conclude that the product could also be formed in the absence of solvents and required high temperature. This suggested that the nature of the reagents (Ph_2PCH_2OH and **2.12**, **2.14 – 2.16** and **2.18** phosphines) may dictate the formation of these products and, therefore, trying to optimise the reaction conditions is not the best direction for further research. Consequently, a mechanism was suggested which was independent of the P and N substituents, where the phosphines and Ph_2PCH_2OH were in equilibrium with their tautomers as previously observed in the literature.[10] To prevent this equilibrium, an alternative method was proposed for future investigation. This procedure involves the protection of the alcohol group of Ph_2PCH_2OH and the elimination of the aminic proton

from the aminomethylphosphine to produce an amido group which would attack to the protected alcohol. This route may not only yield the pure product but also general asymmetric PCNCP ligands.

A novel bicyclic OP{$CH_2N(R)CH_2$}$_3$PO diphosphine (R = *p*–MeC_6H_4, **2.35**) was obtained as a crystalline solid in the filtrate of the reaction between **2.16** and Ph_2PCH_2OH. To the best of our knowledge, this is the first example of symmetric diphosphine with three –$CH_2N(R)CH_2$– bridges between two phosphorus atoms. The oxygen free version of this diphosphine, *i.e.* P{$CH_2N(R)CH_2$}$_3$P, could be used in the synthesis of complexes with several metal centres as previously observed for analogous asymmetric P{$CH_2N(R)$}$_3$P (R = Me and C_6H_5) diphosphines which demonstrated selective coordination towards various metal centres.[6,75] The synthesis of **2.35** was attempted from THP and *p*–$MeC_6H_4NH_2$ using different routes without success. Nevertheless, during its investigation, the reaction between THP and *p*–$MeC_6H_4NH_2$ afforded exclusively cyclic N(H)CH_2P{$(CH_2)_3(NR)_2$} and not acyclic P{$CH_2N(H)R$}$_3$ phosphines, corroborating previous examples in the literature.[38–40] Promising results were achieved using an alternative method from OP{CH_2OH}$_3$ (THPO) (readily formed from THP and an excess of H_2O_2) and *p*–$MeC_6H_4NH_2$. Tyler *et al.* demonstrated that the lone pair on phosphorus has to be available for the phosphorus Mannich reaction to occur.[10] Accordingly, in THPO the lone pair is unavailable and, therefore, the phosphorus should not react. However, the $^{31}P\{^1H\}$ NMR of the product and the starting material are slightly different and hence the product of this reaction could be the target **2.35** but is still not clear. Future research could include other substituents or undertake a proposed synthesis for P{$CH_2N(R)CH_2$}$_3$P ligands mimicking a literature procedure from a cyclic R'$PCH_2N(R)CH_2PR'CH_2N(R)CH_2$ diphosphine with two pendant amines.

The family of aminomethylphosphines was extended by treating Ph_2PCH_2OH or $CgPCH_2OH$ (Cg = 1,3,5,7–tetramethyl–2,4,8–trioxa–6–phosphaadamantane) with various primary amines to afford R(H)$NCH_2PR'_2$ [R = *o*-{$C(Me)=CH_2$}C_6H_4, R' = Cg, **4.1**; R = *o*-{$C(Me)=CH_2$}C_6H_4, R' = C_6H_5, **4.2**; R = Adamantane, R' = Cg, **4.3**; R = Adamantane, R' = C_6H_5, **4.4**; R = *o,o*-$(CHPh_2)_2$–*p*-MeC_6H_2, R' = Cg, **4.5**; R = *o,o*-$(CHPh_2)_2$–*p*-MeC_6H_2, R' = C_6H_5, **4.6**] *via* a phosphorus Mannich condensation reaction. Unlikely to the aminomethylphosphines derivatives of THPC (**2.12 – 2.34**), ligands **4.1 – 4.6** were synthesised under inert atmosphere. Symmetric $R'_2PCH_2N(R)CH_2PR'_2$ diphosphines (R = *o*-{$C(Me)=CH_2$}C_6H_4, R' = C_6H_5, **4.2a** and R = Adamantane, R' = C_6H_5, **4.4a**) were

observed in the $^{31}P\{^{1}H\}$ NMR spectra (and **4.2a** was also isolated) of **4.2** and **4.4a** indicating that phosphines with Ph_2P– moiety were more susceptible to undertake a second condensation. This seems to be related with the structural and electronic properties of phosphorus and nitrogen substituents. In addition, also unreacted anilines with bulky *ortho* substituents on the nitrogen (*o,o*-$(CHPh_2)_2$-*p*-MeC_6H_2– and *o,o*-$(CHPh_2)_2$-*p*-MeC_6H_2–) were present in solution along with the monophosphine, but these anilines were removed upon coordination. Two routes were proposed to achieve novel asymmetric *o*-$\{Ph_2PCH_2C(H)(CH_3)\}C_6H_4N(H)CH_2PPh_2$ diphosphine **4.9** which involved either a hydrogenation of the vinyl group in *o*-$\{C(Me)=CH_2\}C_6H_4NH_2$ with Ph_2PH to get *o*-$\{Ph_2PCH_2C(H)(CH_3)\}C_6H_4NH_2$ **4.7** followed by condensation of the amino group with Ph_2PCH_2OH or vice versa. Both pathways gave **4.9** but further improvement of the yield should be undertaken. The procedure was applied using CgPH to successfully achieve *o*-$\{CgPCH_2C(H)(CH_3)\}C_6H_4NH_2$ **4.8** with the future aim of condensing the amino group in **4.8** to afford the *o*-$\{CgPCH_2C(H)(CH_3)\}C_6H_4N(H)CH_2PPh_2$ diphosphine. Moreover, the novel diphosphine **4.9** possesses an aminic proton available for potential functionalisation to give triphosphine ligands of the type of *o*-$\{Ph_2PCH_2C(H)(CH_3)\}C_6H_4N(CH_2PPh_2)_2$. Future work should be focus in the expansion of the family of diphosphines using more amines with vinyl groups. Compounds **4.1** – **4.9** were fully characterised by spectroscopic techniques and the structure of **4.2a**, **4.3**, **4.7** and **4.9** was further elucidated by X–ray diffraction studies.

The coordination chemistry of selected compounds was investigated with late transition metal centres including Pt(II), Pd(II) and Ru(II) following a well–stablished procedure within this research group.[16,101] Monophosphine compounds **2.12**, **2.14 – 2.19**, **2.27**, **2.29**, **2.30**, **4.1 – 4.3** and **4.6** acted as *P*-monodentate ligands to form square planar *cis* and *trans* MCl_2L_2 (M = Pt and Pd) complexes. However, whereas cyclic ligands **2.12**, **2.14 – 2.19** afforded *cis*-MCl_2L_2 (M = Pt, L = **2.12**, **3.1**; M = Pt, L = **2.14**, **3.2**; M = Pt, L = **2.15**, **3.3**; M = Pt, L = **2.16**, **3.4**; M = Pt, L = **2.17**, **3.5**; M = Pt, L = **2.18**, **3.6**; M = Pt, L = **2.19**, **3.7**; M = Pd, L = **2.12**, **3.8**; M = Pd, L = **2.14**, **3.9**; M = Pd, L = **2.17**, **3.10**), acyclic ligands **2.27**, **2.29** and **2.30** afforded *trans*-MCl_2L_2 (M = Pt, L = **2.27**, **3.16**; M = Pt, L = **2.29**, **3.17**; M = Pt, L = **2.30**, **3.18**; M = Pd, L = **2.27**, **3.19**; M = Pd, L = **2.29**, **3.20**; M = Pd, L = **2.30**, **3.21**) along with *cis*-$PtCl_2L_2$ (L = **2.27**, **3.16a**; L = **2.30**, **3.18a**). Furthermore, $^{31}P\{^{1}H\}$ NMR and X–ray diffraction studies of **3.16a**, **3.19**, **3.20** and **3.21** support both *cis* and *trans* structural isomers. The isolation of *cis* and *trans* Pt(II) complexes containing *o*-

$^{i}PrC_6H_5N$– groups (**3.16** and **3.16a**) was investigated using different reaction conditions. The $^{31}P\{^{1}H\}$ NMR suggests that the proportion of one of the isomers was enhanced with respect to the other by varying the reaction time and solvents during work up so further investigation should be conducted for complete purification. Complexes **3.6**, **3.8 – 3.10** were achieved along with 6–membered M–P–C–N–C–P to afford *cis*-MCl_2L (M = Pt, L = **2.23**, **3.6a**; M = Pd, L = **2.20**, **3.8a**; M = Pd, L = **2.46**, **3.9a** and M = Pd, L = **2.22**, **3.10a**) in minor proportion showing that cyclic monophosphine **2.12**, **2.17, 2.18** and **2.14** ligands may undergo a condensation to afford the diphosphines **2.20**, **2.22**, **2.23** and **2.46**, respectively, which coordinate in a *P,P*-chelate mode. Ligands **4.1 – 4.3** and **4.6** gave *cis*-MCl_2L_2 (M = Pt, L = **4.1**, **4.10**; M = Pt, L = **4.2**, **4.11**; M = Pt, L = **4.3**, **4.12**; M = Pt, L = **4.6**, **4.13**; M = Pd, L = **4.1**, **4.14**; M = Pd, L = **4.2**, **4.15**) along with *trans*-MCl_2L_2 (M = Pt, L = **4.1**, **4.10b** and M = Pd, L = **4.2**, **4.15b**). Those phosphines which underwent double condensation adopted a *P,P*-chelate mode to form *cis*–$MCl_2(R'_2PCH_2N(R)CH_2PR'_2)$ [M = Pt, R = *o*-{C(Me)=CH_2}C_6H_4, R' = Cg, **4.10a**; M = Pt, R = *o*-{C(Me)=CH_2}C_6H_4, R' = C_6H_5, **4.11a**; M = Pt, R = Adamantane, R' = Cg, **4.12a**; M = Pd, R = *o*-{C(Me)=CH_2}C_6H_4, R' = Cg, **4.14a**; M = Pd, R = *o*-{C(Me)=CH_2}C_6H_4, R' = C_6H_5, **4.15a**].

The coordination capabilities of asymmetric $Ph_2PCH_2N(R)CH_2P\{(CH_2)_3(NR)_2\}$ (R = C_6H_5, **2.36**; *o*–$^{i}PrC_6H_4$, **2.37**; *o*–FC_6H_4, **2.38**; *p*–MeC_6H_4, **2.39** and *p*–FC_6H_4, **2.40**) ligands were investigated with Pt(II) and Ru(II) metal centres. These ligands were not isolated as pure compounds and therefore a template synthesis was proposed with Pt(II). This procedure involved the coordination of the ligand to the metal centre in a *P,P*–chelate fashion to get Pt complexes ($PtCl_2L$) with a Pt–P–C–N–C–P ring, purification of the target complex and displacement of the desired $Ph_2PCH_2N(R)CH_2P\{(CH_2)_3(NR)_2\}$ diphosphine by a stronger π acceptor ligand. Several methods were attempted to achieve the desired chelate $PtCl_2L$ complex with asymmetric $Ph_2PCH_2N(R)CH_2P\{(CH_2)_3(NR)_2\}$ ligand **2.40**. In one method, the mixture of diphosphine ligands including **2.40**, was reacted with $PtCl_2(COD)$ to afford the target $PtCl_2L$ complex **3.33** (L = **2.40**) along with platinum coproducts **3.6a** and $Ph_2PCH_2N(R)CH_2PPh_2$ **3.34**. The isolation of **3.33** was not possible by recrystallisation instead **3.6a** was obtained and characterised by X–ray. An alternative method involved the reaction between one equiv. of the monophosphine **2.18**, one equiv. of Ph_2PCH_2OH and one equiv. of $PtCl_2(COD)$ to prove whether the Mannich condensation take place. However, this procedure led to *cis* linear Pt complexes

$PtCl_2$(**2.18**)(Ph_2PCH_2OH) **3.35**, $PtCl_2$(**2.18**)$_2$ **3.6** and $PtCl_2(Ph_2PCH_2OH)_2$. Therefore **3.33** was not achieve so the condensation between **2.18** and Ph_2PCH_2OH did not occur. These two methods suggest that not only is the coordination more rapid than the condensation but also that once ligands are coordinated they are incapable of condensing. A third approach involved the reaction between linear *cis* **3.3** and **3.6** complexes and Ph_2PCH_2OH which was added in one or two steps. The first addition of Ph_2PCH_2OH gave novel triphosphine monocationic Pt(II) complexes {PtCl(**2.15**)$_2$(Ph_2PCH_2OH)}Cl **3.41** and {PtCl(**2.18**)$_2$(Ph_2PCH_2OH)}Cl **3.42**; the second addition yielded unprecedented dicationic bis chelate Pt(II) complexes *trans*–{Pt(**2.38**)$_2$}Cl_2 **3.43a** and *cis*–{Pt(**2.38**)$_2$}Cl_2 **3.43b** and *trans*-{Pt(**2.40**)$_2$}Cl_2 **3.44a** and *cis*-{Pt(**2.40**)$_2$}Cl_2 **3.44b**. The structure of **3.44a** was further supported by single X–ray crystallography. This chemistry gave an insight into the poorly studied mono and dicationic Pt(II) complexes with nonsymmetric diphodphines with a PCNCP backbone so it would worthy to further investigate the reactivity with more ligands such as tripodal P{$CH_2N(H)R$}$_3$ and different hydroxymethylphosphines such as $CgPCH_2OH$. Complexes **3.43a**, **3.43b**, **3.44a** and **3.44b** are excellent precursors to achieve the target asymmetric $Ph_2PCH_2N(R)CH_2P\{(CH_2)_3(NR)_2\}$ ligands by a synthesis template. However, this final step was not studied and treatment of **3.43a**, **3.43b**, **3.44a** and **3.44b** with a strong π acceptor ligand such as CN^- should be carried out to complete the template synthesis. To understand more about the coordination chemistry of these $Ph_2PCH_2N(R)CH_2P\{(CH_2)_3(NR)_2\}$ ligands, **2.39** and **2.40** were reacted with ruthenium centre giving bimetallic complexes {$RuCl_2$(η^6–*p*–cymene)}$_2$L (L = **2.39**, **3.46** and L = **2.40**, **3.47**) where **2.39** and **2.40** adopted a *P,P*–bridging mode between two Ru metals whose structure was further supported by single crystal X–ray diffraction studies of **3.47**.

The coordination chemistry of ligands with a P–P bond of the type P{$CH_2N(R)CH_2$}$_2$P has not been documented despite ligands **2.31** and **2.32** being well known.[26,89] While they remained unreacted towards Cr(III), ligands **2.31 – 2.33** coordinated to Pt(II) and Rh(III) in a *P,P*-bridging mode to afford *cis*–($PtCl_2L$)$_2$ complexes (L = **2.31**, **3.27b**; L = **2.32**, **3.28b** and L = **2.33**, **3.29b**) and {$RhCl_2(C_{10}H_{15})$}$_2$L complexes (L = **2.31**, **3.31a**; L = **2.32**, **3.32a**). Characterisation by $^{31}P\{^1H\}$ NMR showed complicated spectra which were elucidated by simulated spin–system NMR and further supported by X–ray crystallography of **3.27b**. Pt complexes **3.27b – 3.29b** resembles metal systems containing diphosphines with the similar pendant arms but without a P–P bond, which are excellent catalysts for H_2 reduction.[8,9,119] A potential *P,P*-chelating mode was not observed

presumably due to the restriction of the bite angle as previously observed in analogous ligands.[86,87,114] These *in situ* studies demonstrated that P{$CH_2N(R)CH_2$}$_2$P ligands with a P–P bond coordinate selectively to some metal precursors so other transition metals should be screened to gain an insight into this novel chemistry.

The coordination capabilities of the monophosphines **4.7** and **4.8** and asymmetric diphosphine **4.9** ligands were briefly explored towards Pt(II). The $^{31}P\{^1H\}$ NMR observed for **4.7** and **4.8** was broad hence only a tentative assignment of the peaks was discussed to conclude that several complexes with *P,N*–donor ligands are involved. The displacement of the chlorides ligands in $PtCl_2$(COD) by phosphorus or nitrogen donor atoms could be overcome by using a different platinum precursor such as $PtMe_2$(COD). Accordingly, the Pt–Me bonds would remain intact decreasing the number of complexes formed. The diphosphine **4.9** adopted a *P,P*–chelating mode with Pt(II) to give a nine–membered Pt–P–C_4–P ring complex $PtCl_2$(**4.9**) **4.22**. Future investigation of the reactivity of both, mono and diphosphines, **4.7**, **4.8** and **4.9** with other metal centres should be conducted.

The coordination chemistry of selected ligands was more investigated with Ru(II) metal centre revealing "piano–stool" structure of the type $RuCl_2(\eta^6$–*p*–cymene)L where the monophosphines adopted a *P*-monodentate mode (L = **2.12**, **3.11**; L = **2.14**, **3.12**; L = **2.15**, **3.13**; L = **2.16**, **3.14**; L = **2.18**, **3.15**; L = **2.26**, **3.22**; L = **2.27**, **3.23**; L = **2.28**, **3.24**; L = **2.29**, **3.25**; L = **2.30**, **3.26**; L = **4.2**, **4.16**; L = **4.3**, **4.17**; L = **4.4**, **4.18** and L = **4.6**, **4.19**) and {$RuCl_2(\eta^6$–*p*–cymene)}$_2$L (L = **2.39**, **3.46** and L = **2.40**, **3.47**) where the diphosphines adopted a *P,P*-bridging mode. Despite similar linear ligands to **3.22** – **3.26** were investigated towards a wide range of d–block elements, they were poorly studied with late transition metals.[1,2] To the best of our knowledge, these complexes are the first example of P{$CH_2N(H)R$}$_3$ ligands with a ruthenium metal centre. The structure of **3.22** – **3.26** was supported by X–ray diffraction studies of **3.25**. To evaluate the catalytic activity of complexes **4.16 – 4.18** for CO_2 capture, they were dissolved in CH_2Cl_2 and treated with CO_2 gas at r.t. for 1 h. After slow evaporation of the solvent, the product was characterised by IR but the characteristic νCO stretch was not observed. The packing model of **4.16** showed that the metal centre is not widely accessible to CO_2. However, due to aminic proton is not involved in H–bond, NH could bind the oxygen on CO_2 facilitating the approach to the metal centre. Furthermore the fixation of CO_2 by organometallics is favoured by displacement of the chloride ligands by hydrides and a subsequent sequestration of the small molecule in the M–H bond. So, complexes **3.12** and **3.14** were

treated with K_2CO_3 or KBH_4 bases to displace the chloride ligands by hydrides using a literature procedure.[130,131] Unfortunately, in our hands, the reaction did not occur so the insertion of CO_2 into the M–H bond was not undertaken. Nevertheless, these reactions are in an early stage so further development is required to optimise conditions and, once successful, they may also be applied to Pt(II) and Pd(II) complexes.

In summary, a new series of aminomethylphosphines incorporating a PCN backbone has been synthesised using a phosphorus Mannich condensation reaction. These phosphines were obtained by treatment of THPC or R'_2PCH_2OH as phosphorus sources with a wide series of primary amines. The structure of the phosphines was found to be dictated by the substituents on nitrogen and phosphorus. The reactivity of various monophosphines was further explored to get symmetric and asymmetric diphosphines with a PCNCP backbone. The coordination capabilities of selected ligands has been explored with a variety of transition metal centres including Pt(II), Pd(II) and Ru(II) confirming the versatility of these compounds when acting as bi– and mono–dentate ligands. Preliminary investigations with Ru(II) complexes suggested that the displacement of the M–Cl bond by M–H bond has to be undertaken for the incorporation of CO_2 into the M–H bond, so more future research should be focus in the formation of this bond.

6. Experimental

6.1 General

Unless otherwise stated, all reactions were performed in air. Standard Schlenk techniques were used for experiments carried out under an oxygen–free nitrogen atmosphere. All solvents were purchased from Aldrich, Fisher, Alfa Aesar and Acros. Any freeze thawed solution was degassed three times through a freeze–pump thaw cycle. The transition metal precursors $MCl_2(COD)$ (M = Pt or Pd and COD = cycloocta–1,5–diene),[143,144] $\{RhCl_2(\eta^5–C_5Me_5)\}_2$,[145] $RuCl_2(\eta^5–p\text{-cymene})\}_2$,[146] were prepared according to literature methods. Ph_2PCH_2OH was readily preformed from equimolar amounts of Ph_2PH and $(CH_2O)_n$[132] and the $CgPCH_2OH$ was readily preformed from equimolar amounts of CgPH and $(CH_2O)_n$.[7] THP was synthesised according with reported procedure from THPC.[27]

NMR spectra were recorded in $CDCl_3$, $(CD_3)_2SO$ or DMF. ^1H NMR spectra (400 MHz or 500 MHz) was recorded on a Bruker Advance or in JEOL ECS spectrometer with chemical shifts in ppm relative to $SiMe_4$. $^{31}P\{^1H\}$ NMR spectra on a Bruker Advance or in JEOL ECS spectrometer operating at 161.9755 MHz for P with chemical shifts in ppm relative to 85% H_3PO_4. Values given in decoupled $^{31}P\{^1H\}$ NMR for phosphorus ratios were approximate. The following abbreviations are used b, broad; v, virtual; s, singlet; d, doublet; t, triplet; q, quartet; sept, septuplet m, multiplet. Infrared spectra were recorded as KBr discs in the range 4000–200 cm^{-1} on a Perkin–Elmer System 2009 Fourier transform spectrometer. Elemental analyses (Perkin–Elmer 2400 CHN elemental analyser) were carried out by the Loughborough University Analytical Service within the Department of Chemistry. Mass spectra were recorded on a Thermo Fisher Exactive + Triversa Nanomate mass spectrometer (ESI) within the Department of Chemistry at Loughborough University.

6.2 Chapter 2 Experimental

Compounds **2.1** – **2.11** were prepared following a known procedure which is explained for **2.1** as an example but it can be extended to **2.2** – **2.11**.[16,25]

Preparation of $C_{28}H_{32}ClN_4P$ (2.1):

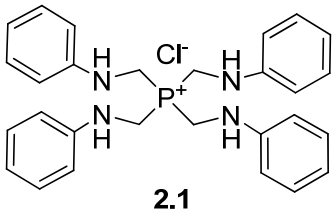

2.1

A solution of THPC (3.830 g, 20.099 mmol) in EtOH (100%, 75 ml) was prepared. $C_6H_5NH_2$ (7.488 g, 80.395 mmol) was added dropwise to the THPC solution and the mixture stirred for 2 h at room temperature. A colourless solid precipitated which was filtered on a glass sinter, dried under vacuum and kept in the dark. Yield: 8.735 g, 89%. Selected data: IR (KBr, cm^{-1}): (νNH) 3234. ^1H NMR (400 MHz, DMSO) 7.39 – 6.36 (m, CH), 5.04 – 3.66 (m, PC*H*$_2$N, NH) ppm. $^{31}P\{^1H\}$ NMR (DMSO) 9.1, 31.5 ppm. EI–MS (*m/z*, $[M–Cl]^+$) 455. $C_{28}H_{32}ClN_4P$ (490). EA found (calculated): 68.38 (68.50), 6.37 (6.52), 11.31 (11.41). This compound was previously synthesised and the data presented here is in agreement with that observed for the reported compound.[16,25]

Preparation of $C_{32}H_{40}N_4PCl$ (2.2):

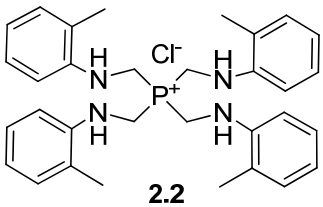

2.2

THPC (3.830 g, 20.099 mmol), *o*–$MeC_6H_4NH_2$ (8.614 g, 80.395 mmol). Yield: 10.270 g, 93%. Selected data: IR (KBr, cm^{-1}): (νNH) 3307. ^1H NMR (400 MHz, DMSO) 7.40 – 6.47 (m, CH), 5.86 – 2.06 (m, PC*H*$_2$N, NH, CH_3) ppm. $^{31}P\{^1H\}$ NMR (DMSO) 10.3, 30.4 ppm. EI–MS (*m/z*, $[M–Cl]^+$) 511. $C_{32}H_{40}N_4PCl$ (547). EA found (calculated)(%): C 69.95 (70.23), H 7.36 (7.37), N 10.25 (10.24).

Preparation of $C_{40}H_{56}N_4PCl$ (2.3):

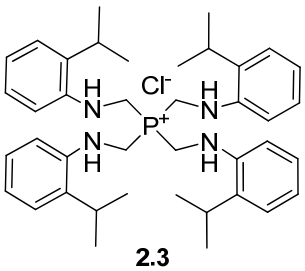

2.3

THPC (1.500 g, 7.871 mmol), EtOH (100%, 35 ml), *o*–$^{i}PrC_6H_4NH_2$ (4.257 g, 31.486 mmol). Yield: 3.352 g, 65%. Selected data: IR (KBr, cm^{-1}) (νNH) 3292. ^1H NMR: poor solubility in DMSO or $CDCl_3$ therefore no meaningful spectrum could be obtained. $^{31}P\{^1H\}$ NMR (DMSO) 28.3 ppm. EI–MS (*m/z*) $[C_{31}H_{43}N_3P]^+$ 488 (**2.14**), $[C_{30}H_{43}N_3P]^+$ 476 (**2.21**). $C_{40}H_{56}N_4PCl$ (659). EA found (calculated)(%): C 72.29 (72.87), H 8.31 (8.56), N 8.47 (8.50).

Preparation of $C_{44}H_{64}N_4PCl$ (2.4):

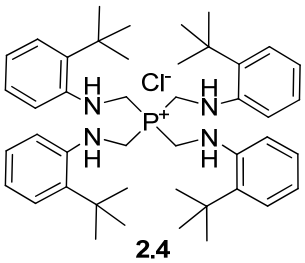

2.4

THPC (2.500 g, 13.123 mmol), *o*–$^{t}BuC_6H_4NH_2$ (7.872 g, 52.493 mmol). Yield: 7.693 g, 82 %. Selected data: IR (KBr, cm^{-1}) (νNH) 3370. ^1H NMR: poor solubility in DMSO or $CDCl_3$ to assign peaks. $^{31}P\{^1H\}$ NMR poor solubility in DMSO or $CDCl_3$ therefore no meaningful spectrum could be obtained. EI–MS (*m/z,* $[M–Cl]^+$): 680, $[C_{33}H_{48}N_3P]^+$ 518. $C_{44}H_{64}N_4PCl{\cdot}2H_2O$ (750). EA found (calculated)(%): C 70.28 (70.33), H 8.86 (9.12), N 7.24 (7.46).

Preparation of $C_{28}H_{28}N_4F_4PCl$ (2.5):

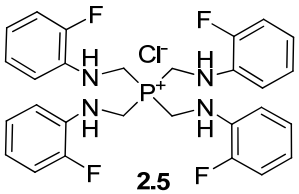

2.5

THPC (3.830 g, 20.105 mmol), *o*–$FC_6H_4NH_2$ (8.936 g, 80.420 mmol). Yield: 10.222 g, 90%. Selected data: ^1H NMR (400 MHz, DMSO) 7.41 – 6.15 (m, CH), 4.55 – 3.55 (m,

PC*H*$_2$N*H*) ppm. $^{31}P\{^1H\}$ NMR (DMSO) 8.5, 31.5 ppm. $C_{28}H_{28}N_4F_4PCl{\cdot}H_2O$ (581). EA found (calculated)(%): C 57.65 (57.89), H 4.65 (5.20), N 9.11 (9.64). This compound was previously synthesised and the data presented here is in agreement with that observed for the reported compound.[16]

Preparation of $C_{32}H_{28}N_4F_{12}PCl$ (2.6):

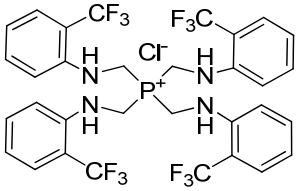

2.6

THPC (1.173 g, 6.150 mmol), *o*–$CF_3C_6H_4NH_2$ (3.967 g, 24.622 mmol). Yield: 3.401 g, 72%. Selected data: IR (KBr, cm^{-1}) (νNH) 3286. ^1H (400 MHz, DMSO) 7.54 – 6.76 (m, CH), 6.06 – 4.64 (m, PC*H*$_2$N*H*) ppm. $^{31}P\{^1H\}$ NMR (DMSO) 29.7 ppm. EI–MS (*m/z,* $[M–Cl]^+$): 727. $C_{32}H_{28}N_4F_{12}PCl{\cdot}H_2O$ (781). EA found (calculated)(%): C 49.20 (49.21), H 3.79 (3.87), N 6.97 (7.17).

Preparation of $C_{40}H_{48}N_4P_4Cl$ (2.7):

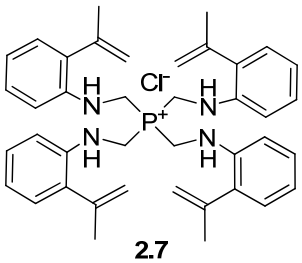

2.7

THPC (0.343 g, 1.801 mmol), *o*-{(C(Me)=CH_2}$C_6H_4NH_2$ (0.958 g, 7.203 mmol). Yield: 0.974 g, 83%. Selected data: IR (KBr, cm^{-1}) (νNH) 3284. ^1H NMR: poor solubility in DMSO or $CDCl_3$ therefore no meaningful spectrum could be obtained. $^{31}P\{^1H\}$ NMR (DMSO): 7.0, 29.0 ppm. EI–MS (*m/z,* $[M–Cl]^+$): 615. $C_{40}H_{48}N_4PCl{\cdot}H_2O$ (668). EA found (calculated)(%): C 71.88 (71.78), H 7.30 (7.53), N 8.40 (8.37).

Preparation of $C_{32}H_{40}N_4PCl$ (2.8):

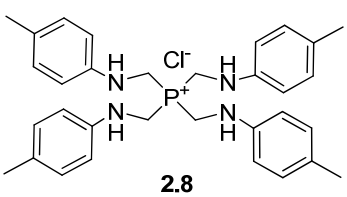

2.8

THPC (3.850 g, 20.210 mmol), *p*–$MeC_6H_4NH_2$ (8.658 g, 80.840 mmol). Yield: 10.165 g, 92%. Selected data: IR (KBr, cm^{-1}) (νNH) 3220. ^1H (400 MHz, DMSO) 6.86 (m, CH), 4.79 – 4.26 (m, PC*H*$_2$N*H*), 2.36 – 1.96 (m, CH_3) ppm. $^{31}P\{^1H\}$ NMR (DMSO) 8.0, 31.1 ppm. $C_{32}H_{40}N_4PCl$ (547). EA found (calculated)(%): C 70.39 (70.27), H 7.28 (7.32), N 10.23 (10.25). This compound was previously synthesised and the data presented here is in agreement with that observed for the reported compound.[16]

Preparation of $C_{40}H_{56}N_4PCl$ (2.9):

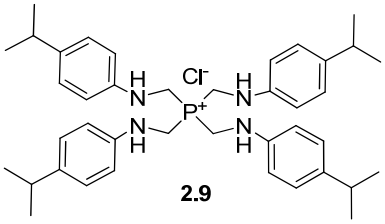

2.9

THPC (2.469 g, 12.961 mmol), *p*–$^iPrC_6H_4NH_2$ (6.999 g, 51.842 mmol). Yield: 7.605 g, 87%. Selected data: IR (KBr, cm^{-1}) (νNH) 3261. ^1H (400 MHz, DMSO) 7.27 – 6.26 (m, CH), 4.97 – 2.38 (m, PC*H*$_2$N*H*, CH), 1.28 – 0.99 (1 H, m, CH_3) ppm. $^{31}P\{^1H\}$ NMR (DMSO) 8.2, 30.7 ppm. EI–MS (*m/z,* $[M–Cl]^+$): n.o. $C_{40}H_{56}N_4PCl$ (658). EA found (calculated)(%): C 72.81 (72.87), H 8.63 (8.56), N 8.58 (8.50).

Preparation of $C_{28}H_{28}N_4F_4PCl$ (2.10):

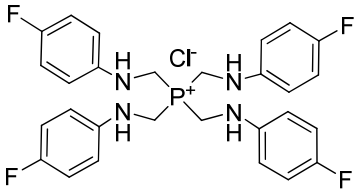

2.10

THPC (3.830 g, 20.105 mmol), *p*–$FC_6H_4NH_2$ (8.927 g, 80.420 mmol). Yield: 9.244 g, 82%. Selected data: ^1H (400 MHz, DMSO) 7.28 – 6.40 (m, CH), 4.94 – 3.64 (m, PC*H*$_2$N*H*) ppm. $^{31}P\{^1H\}$ NMR (DMSO) 8.7, 30.6 ppm. $C_{28}H_{28}N_4F_4PCl$ (562). EA found (calculated)(%): C 59.55 (59.74), H 5.03 (5.01), N 9.93 (9.95). This compound was previously synthesised and the data presented here is in agreement with that observed for the reported compound.[16]

Preparation of $C_{36}H_{48}N_4PCl$ (2.11):

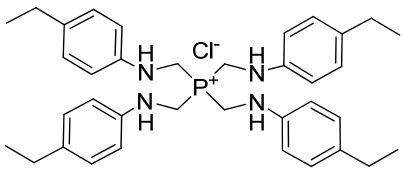

2.11

THPC (3.830 g, 20.105 mmol), *p*–$EtC_6H_4NH_2$ (9.745 g, 80.420 mmol). Yield: 11.205 g, 92%. Selected data: IR (KBr, cm^{-1}) (νNH) 3220. ^1H (400 MHz, DMSO) 7.25 – 6.13 (m, CH), 4.93 – 3.62 (m, PC*H*$_2$N*H*), 2.69 – 2.18 (m, CH_2), 1.27 – 0.95 (m, CH_3) ppm. $^{31}P\{^1H\}$ NMR (DMSO) 8.2, 30.9 ppm. EI–MS (*m/z,* $[C_{28}H_{37}N_3P]^+$): 446. $C_{36}H_{48}N_4PCl$ (603). EA found (calculated)(%): C 71.51 (71.68), H 7.78 (8.02), N 9.21 (9.29). This compound was previously synthesised and the presented here data is in agreement with that observed for the reported compound.[16]

Compounds **2.12**, **2.15** – **2.19** were prepare following a known procedure which is explained for **2.12** as an example but it can be extended to **2.15** – **2.19**.[16]

Preparation of $C_{22}H_{24}N_3P$ (2.12):

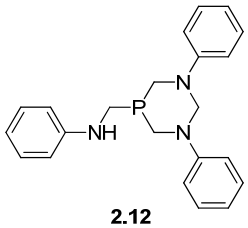

2.12

A suspension of **2.1** (5.000 g, 10.193 mmol) in HPLC grade Me_2CO (75 ml) was prepared. Et_3N (1.627 g, 16.106 mmol) was added dropwise to the suspension. The mixture was stirred for 1 h at r.t. and the colourless precipitate filtered using a glass sinter and dried under vacuum. The filtrate was concentrated under high pressure to 1–2 ml affording an oil. Absolute EtOH (10 ml) was added and the mixture was stirred for 2 h at r.t. to give a colourless solid which was filtered and dried under vacuum. Yield: 2.751 g, 75%. Selected data: IR (KBr, cm^{-1}) (νNH) 3303. ^1H NMR (400 MHz, $CDCl_3$, *J* in Hz, H for **2.12** and H` for **2.20**) 7.27 – 6.39 (m, CH, m, CH`), 5.12 (1 H, d, $^2J_{HH}$ = 12.7, NC*H*$_e$N), 4.97 (d, $^2J_{HH}$ = 12.7, NC*H*`$_e$N), 4.31 (1 H, dd, $^2J_{HH}$ = 12.7, $^4J_{HP}$ = 2.9, NC*H*$_a$N), 4.25 (dd, $^2J_{HH}$ = 12.9, $^4J_{HP}$ = 2.4, NC*H*`$_a$N), 3.85 (2 H, d, $^2J_{HH}$ = 15.6, PC*H*$_e$N), 3.61 (2 H, d, $^2J_{HH}$ = 15.6, PC*H*$_a$N), 3.55 (1 H, s, NH), 3.54 (2 H, d, $^2J_{HP}$ = 6.6, PC*H*$_2$NH), 3.87 – 3.80 (m, PC*H*`$_2$N*H* obscured by PC*H*$_2$N*H*) ppm. $^1H$ NMR (400 MHz, DMSO, *J* in Hz, H for **2.12** and H` for **2.20**) 7.22

(4 H, t, $^{3}J_{HH}$ = 8.0, *m*–CH), 7.07 (4 H, d, $^{3}J_{HH}$ = 8.0, *o*–CH), 7.02 (2 H, dd, $^{4}J_{HH}$ = 2.1, $^{3}J_{HH}$ = 8.0, *m*–CH), 6.77 (2 H, t, $^{3}J_{HH}$ = 8.0, *p*–CH), 6.53 (2 H, d, $^{3}J_{HH}$ = 8.0, *o*–CH), 6.49 (1 H, d, $^{3}J_{HH}$ = 8.0, *p*–CH), 7.22 – 6.48 (m, CH` obscured by CH), 5.76 (1 H, s, NH), 5.02 (1 H, d, $^{2}J_{HH}$ = 13.3, NC*H*$_{e}$N), 4.79 (vq, $^{2}J_{HH}$ = 13.3, NC*H*`$_{2}$N), 4.70 (1 H, dd, $^{2}J_{HH}$ = 13.3, $^{4}J_{HP}$ = 0.48 Hz, NC*H*$_{a}$N), 3.97 – 3.74 (6 H, m, PC*H*$_{2}$N, PC*H*$_{2}$NH), 3.63 – 3.71 (m, PC*H*`$_{2}$N*H*) ppm. $^{31}P\{^{1}H\}$ NMR ($CDCl_3$) –41.0, –46.7 (approx. 4:1) ppm; (DMSO) –50.0, –54.4 (approx. 6:1) ppm. EI–MS (*m/z*) $[MH]^+$ 362, $[MNa]^+$ 384, $[MK]^+$ 400, $[C_{21}H_{24}N_3PK]^+$ 388 (**2.20**). $C_{22}H_{24}N_3P{\cdot}0.25C_3H_6O$ (376). EA found (calculated)(%): C 72.66 (73.11), H 6.60 (6.69), N 11.45 (11.63). This compound was previously synthesised and the data presented is in agreement with that observed for the reported compound.[16,25] However, $^{31}P\{^{1}H\}$ and here ^{1}H NMR in this thesis showed a mixture between **2.12** and **2.20** not previously observed.

From **2.26**: $(CH_2O)_n$ (0.094 g, 0.313 mmol) was added to **2.26** (0.100 g, 0.282 mmol) previously dissolved in MeOH (10 ml). The mixture was stirred for 1 – 4 days at r.t or refluxed and the solvent evaporated under reduced pressure to give a mixture richer in **2.12** (up to 43%) and **2.26** (up to 25%).

Preparation of $C_{25}H_{30}N_3P$ (2.13):

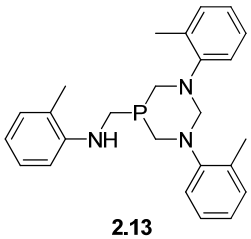

2.13

A suspension of **2.2** (1.000 g, 1.830 mmol) in HPLC grade MeOH (5 ml) was prepared. KO^{t}Bu (0.205 g, 1.830 mmol) was dissolved in the minimum amount of HPLC MeOH (5 ml) and added dropwise to the suspension of the phosphonium salt. The mixture was stirred for 19 h at r.t. and the resulting colourless precipitate was filtered in a glass sinter and dried under vacuum. Yield: 0.245 g, 33%. Selected data: ^{1}H NMR ($CDCl_3$, *J* in Hz, H for **2.13** and H` for **2.25**): 7.23 – 6.62 (m, CH, CH`), 4.24 – 3.44 (m, PC*H*$_{2}$N*H*, PC*H*`$_{2}$N*H*`), 2.12 (s, CH`$_{3}$), 2.04 (9 H, s, CH_3) ppm. $^{31}P\{^{1}H\}$ NMR ($CDCl_3$): –45.1, –33.6 (approx. 4:1) ppm. EI–MS (*m/z*) $[MH]^+$ 404, $[MK]^+$ 442. A pure sample of **2.13** could not be obtained for elemental analysis. No exhaustive attempts to improve the quality of the elemental analysis were made due to the mixture encountered in the NMR.

Preparation of $C_{31}H_{42}N_3P$ (2.14):

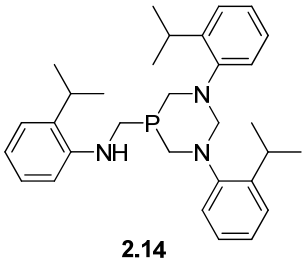

2.14

A suspension of **2.3** (1.000 g, 1.517 mmol) in HPLC grade MeOH (35 ml) was prepared. KO^{t}Bu (0.179 g, 1.592 mmol) was dissolved in the minimum amount of HPLC MeOH (5 ml) and added dropwise to the suspension with the aniline. The mixture was stirred for 18 h at r.t. and the resulting colourless precipitate was filtered. Yield: 0.330 g, 45%. In some cases, the filtrate was concentrated to give a crystalline material which was filtered off. Alternatively, the solvent was stripped to dryness obtaining an oil which was recrystallised from EtOH after standing for more than 12 h at r.t. Yield: 0.415 g, 56%. Selected data: IR (KBr, cm^{-1}) (νNH) 3294, 3419. ^{1}H NMR ($CDCl_3$, *J* in Hz): ^{1}H NMR (400 MHz, $CDCl_3$, *J* in Hz) 7.21–7.16 (2 H, m, *o-,p*-CH), 7.05 (8 H, m, *o-,m*-CH), 6.78 (1 H, d, $^3J_{HH}$ = 7.6, *o*-CH), 6.67 (1 H, t, $^3J_{HH}$ = 7.6, *p*-CH), 4.12 (2 H, d, $^2J_{HP}$ = 4.0, PCH_2NH), 3.94 – 3.90 (2 H, m, NCH_2N), 3.60 (1 H, bs, NH), 3.62 (2 H, sept, $^3J_{HH}$ = 7.0, CH), 3.34 – 3.27 (4 H, m, PCH_2N), 2.71 (1 H, sept, $^3J_{HH}$ = 6.6, CH), 1.12 (6 H, d, $^3J_{HH}$ = 6.6, CH_3), 1.08 (6 H, d, $^3J_{HH}$ = 7.0, CH_3), 1.06 (6 H, d, $^3J_{HH}$ = 7.0, CH_3) ppm. ^{31}P{^{1}H} NMR ($CDCl_3$): –45.1 ppm. EI–MS (*m/z,* [MH]$^+$) 488. $C_{31}H_{42}N_3P{\cdot}0.25H_2O$ (501). EA found (calculated)(%): 74.26 (74.29), 8.60 (8.75), 8.70 (8.30).

From **2.27:** $(CH_2O)_n$ (0.032 g, 1.052 mmol) was added to **2.27** (0.500 g, 1.052 mmol) previously dissolved in MeOH (10 ml). The mixture was refluxed for 3 d, the solvent was evaporated under reduced pressure to give a mixture richer in **2.14** (up to 60%) and **2.27** (up to 37%).

Preparation of $C_{22}H_{21}N_3F_3P$ (2.15):

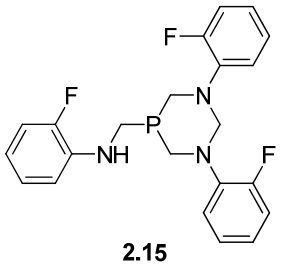

2.15

From **2.5** (5.000 g, 8.894 mmol), Et_3N (1.419 g, 14.053 mmol). Yield: 2.853 g, 77%. Selected data: IR (KBr, cm^{-1}) (νNH) 3302. ^1H NMR (400 MHz, $CDCl_3$, *J* in Hz) 7.23 (2 H, dt, $^3J_{HH}$ = 8.0, $^4J_{HH}$ = 1.4, *m*–CH), 7.14 – 7.05 (4 H, m, *m*–CH), 7.05 – 6.98 (2 H, m, *o*–CH), 6.94 (2 H, dt, $^3J_{HH}$ = 8.0, $^4J_{HH}$ = 1.4, *p*–CH), 6.74 – 6.65 (1 H, dt, $^3J_{HH}$ = 8.0, $^4J_{HH}$ = 1.4, *o*–CH), 6.60 (1 H, dt, $^3J_{HH}$ = 8.0, $^4J_{HH}$ = 1.4, *p*–CH), 4.83 (1 H, dd, $^2J_{HH}$ = 12.2, $^4J_{HP}$ = 1.2, NC*H*$_e$N), 4.43 (1 H, dd, $^2J_{HH}$ = 12.2, $^4J_{HP}$ = 2.8, NC*H*$_a$N), 4.06 (1 H, bs, NH), 3.94 – 3.81 (4 H, m, PC*H*$_e$N, PC*H*$_2$NH), 3.76 – 3.66 (2 H, m, PC*H*$_a$N) ppm. $^{31}P\{^1H\}$ NMR ($CDCl_3$): –41.8 ppm, (DMSO) –53.1 ppm. EI–MS (*m/z,* $[MH]^+$) 416. $C_{22}H_{21}N_3F_3P$ (415). EA found (calculated)(%): 63.22 (63.61), 5.03 (5.10), 9.91 (10.12). This compound was previously synthesised and the data presented here is in agreement with that observed for the reported compound.[16]

Preparation of $C_{25}H_{30}N_3P$ (2.16):

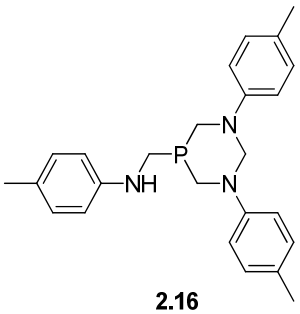

2.16

From **2.8** (5.000 g, 9.217 mmol) and Et_3N (1.471 g, 14.562 mmol). Yield: 3.136 g, 84%. Selected data: IR (KBr, cm^{-1}) (νNH) 3303. ^1H NMR (400 MHz, $CDCl_3$, *J* in Hz, H for **2.16** and H` for **2.21**) 7.13 (4 H, d, $^3J_{HH}$ = 8.6, *m*–CH), 7.00 (4 H, d, $^3J_{HH}$ = 8.6, *o*–CH), 6.94 (2 H, t, $^3J_{HH}$ = 8.6, *m*–CH), 6.47 (2 H, d, $^3J_{HH}$ = 8.6, *o*–CH), 7.10 – 6.60 (m, CH`), 5.09 (1 H, d, $^2J_{HH}$ = 12.9, NC*H*$_e$N), 4.33 (1 H, dd, $^2J_{HH}$ = 12.9, $^4J_{HP}$ = 2.9, NC*H*$_a$N), 3.93 – 3.44 (m, PC*H*$_2$N, PC*H*$_2$N*H*, PC*H*`$_2$N, PC*H*`$_2$N*H*`), 2.43 – 2.12 (m, $CH_3$, CH`$_3$) ppm. ^1H NMR (400 MHz, DMSO, *J* in Hz, H for **2.16** and H` for **2.21**) 7.03 (4 H, t, $^3J_{HH}$ = 8.0, *m*–CH), 6.96 (4 H, d, $^3J_{HH}$ = 8.0, *o*–CH), 6.83 (2 H, dd, $^4J_{HH}$ = 2.1, $^3J_{HH}$ = 8.0, *m*–CH), 6.44 (2 H, d, $^3J_{HH}$ = 8.0, *o*–CH), 7.04 – 6.43 (m, CH` obscured by CH), 5.51 (1 H, s, NH), 4.86 (1 H, d, $^2J_{HH}$ = 13.3, NC*H*$_e$N), 4.79 (vq, $^2J_{HH}$ = 13.3, NC*H*`$_2$N), 4.59 (1 H, d, $^2J_{HH}$ = 13.3,

NCH_aN), 3.83 (2 H, d, $^2J_{HH}$ = 14.3, PCH_eN), 3.75 – 3.54 (m, PCH_2N, PCH_2NH, PCH`$_2$N, PC$H$`$_2$NH`), 2.20 – 2.12 (m, $CH_3$, CH`$_3$) ppm. $^{31}P\{^1H\}$ NMR ($CDCl_3$): –41.4, –47.4 (approx. 3.5:1) ppm, (DMSO) –50.4, –54.4 (approx. 4:1) ppm. EI–MS (*m/z,* $[MH]^+$) 404. $C_{25}H_{30}N_3P$ (403). EA found (calculated)(%): 74.50 (74.42), 7.40 (7.49), 10.37 (10.41). This compound was previously synthesised and the data here presented is in agreement with that observed for the reported compound.[16]

Preparation of $C_{31}H_{42}N_3P$ (2.17):

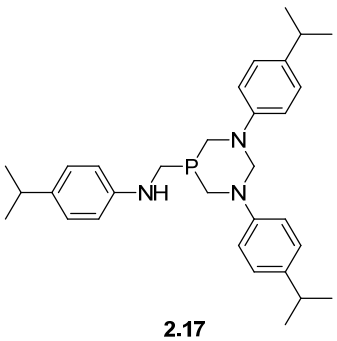

2.17

From **2.9** (1.000 g, 1.519 mmol) and Et_3N (0.242 g, 2.400 mmol). Yield: 0.530 g, 72%. Selected data: IR (KBr, cm^{-1}) (νNH) 3357. ^1H NMR (400 MHz, $CDCl_3$, *J* in Hz, H for **2.17** and H` for **2.22**) 7.19 (4 H, d, $^3J_{HH}$ = 8.6, *m*–CH), 7.05 (4 H, d, $^3J_{HH}$ = 8.6, *o*–CH), 7.01 – 6.94 (2 H, m, $^3J_{HH}$ = 8.6, *m*–CH), 6.47 (2 H, d, $^3J_{HH}$ = 8.6, *o*–CH), 7.19 – 6.51 (m, CH`), 5.14 (1 H, d, $^2J_{HH}$ = 12.8, NCH_eN), 4.99 (1 H, d, $^2J_{HH}$ = 12.7, NCH`$_e$N), 4.34 (1 H, dd, $^2J_{HH}$ = 12.8, $^4J_{HP}$ = 2.9, NC$H_a$N), 4.24 (1 H, dd, $^2J_{HH}$ = 12.9, $^4J_{HP}$ = 2.4, NC$H$`$_a$N), 3.91 – 3.60 (m, PCH_2NH, PCH`$_2$NH), 2.95 – 2.74 (3 H, m, CH), 1.30 – 1.17 (m, $CH_3$, CH`$_3$) ppm. ^1H NMR (400 MHz, DMSO, *J* in Hz, H for **2.17** and H` for **2.22**) 7.09 (5 H, t, $^3J_{HH}$ = 8.7, *m*–CH), 6.99 (4 H, d, $^3J_{HH}$ = 8.7, *o*–CH), 6.86 (2 H, d, $^3J_{HH}$ = 8.5, *m*–CH), 6.43 (2 H, d, $^3J_{HH}$ = 8.5, *o*–CH), 7.11 – 6.42 (m , CH`), 5.49 (1 H, s, NH), 4.93 (1 H, d, $^3J_{HH}$ = 13.0, NCH_eN), 4.74 (d, $^3J_{HH}$ = 13.0, NCH`$_e$N), 4.55 (1 H, d, $^3J_{HH}$ = 13.0, NC$H_a$N), 4.59 – 4.53 (m, NC$H$`$_a$N obscured by NCH_aN), 3.92 – 3.60 (m, PCH_2N, PCH_2NH, PCH`$_2$N, PC$H$`$_2$NH), 2.75 (m, CH, CH`), 1.17 – 1.07 (m, $CH_3$, CH`$_3$) ppm. $^{31}P\{^1H\}$ NMR ($CDCl_3$) –41.2, –47.8 (approx. 4:1) ppm, (DMSO) –49.2, –53.7 (approx. 5:1) ppm. EI–MS (*m/z,* $[MH]^+$) 488. $C_{31}H_{42}N_3P$ (487). EA found (calculated)(%): 76.37 (76.37), 8.58 (8.62), 8.68 (8.62).

Preparation of $C_{22}H_{21}N_3F_3P$ (2.18):

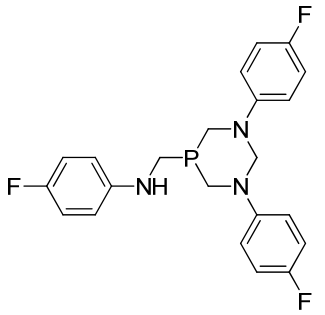

2.18

From **2.10** (5.000 g, 8.889 mmol) and Et_3N (1.419 g, 14.053 mmol). Yield: 2.548 g, 69%. Selected data: IR (KBr, cm^{-1}) (νNH) 3351. ^1H (400 MHz, $CDCl_3$, *J* in Hz, H for **2.18** and H` for **2.23**) 7.02 – 6.42 (m, CH, CH`), 4.95 (1 H, dd, $^2J_{HH}$ = 12.9, $^4J_{HP}$ = 1.2, NC*H*$_e$N), 4.84 (1 H, dd, $^2J_{HH}$ = 13.0, NC*H*`$_e$N), 4.35 (1 H, dd, $^2J_{HH}$ = 12.9, $^4J_{HP}$ = 2.9, NC*H*$_a$N), 4.24 (1 H, dd, $^2J_{HH}$ = 13.0, $^4J_{HP}$ = 2.4, NC*H*`$_a$N), 3.84 – 3.47 (m, PC*H*$_2$N, PC*H*$_2$NH, PC*H*`$_2$N, PC*H*`$_2$NH) ppm. ^1H (400 MHz, DMSO, *J* in Hz, H for **2.18** and H` for **2.23**) 7.40 – 6.97 (8 H, m, *o*–, *p*–CH), 6.86 (2 H, t, $^3J_{HH}$ = 8.9, *m*–CH), 6.61 – 6.33 (2 H, m, *o*–CH), 5.73 (1 H, s, N*H*), 4.87 (1 H, d, $^2J_{HH}$ = 13.3, NC*H*$_e$N), 4.62 (1 H, d, $^2J_{HH}$ = 13.3, NC*H*$_a$N), 4.06 – 3.58 (4 H, m, PC*H*$_2$N), 3.39 – 3.32 (2 H, m, PC*H*$_2$NH) ppm. $^{31}P\{^1H\}$ (162 MHz, $CDCl_3$): –41.2, – 48.3 (approx. 3:1) ppm, (DMSO) –51.4 ppm. EI–MS (*m/z,* $[MH]^+$) 416, $[MK]^+$ 454. $C_{22}H_{21}N_3F_3P$ (415). EA found (calculated)(%): 63.56 (63.61), 5.04 (5.10), 9.93 (10.12). This compound was previously synthesised and the data presented here is in agreement with that observed for the reported compound.[16] However, $^{31}P\{^1H\}$ and ^1H NMR in $CDCl_3$ in this thesis showed a mixture between **2.18** and **2.23** not previously observed.

Preparation of $C_{28}H_{36}N_3P$ (2.19):

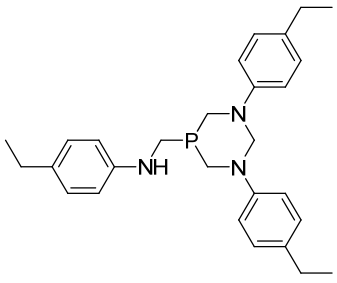

2.19

From **2.11** (5.000 g, 8.301 mmol) and Et_3N (1.325 g, 13.116 mmol). Yield: 2.772 g, 75%. Selected data: IR (KBr, cm^{-1}) (νNH) 3307. ^1H NMR (400 MHz, $CDCl_3$, *J* in Hz, H for **2.19** and H` for **2.24**) 7.16 (4 H, d, $^3J_{HH}$ = 8.6, *m*–CH), 7.13 (4 H, d, $^3J_{HH}$ = 8.6, *o*–CH), 6.98 – 6.91 (2 H, m, *m*–CH), 6.47 (2 H, d, $^3J_{HH}$ = 8.6, *o*–CH), 7.17 – 6.39 (m, CH`), 5.12

(1 H, d, $^{2}J_{HH}$ = 13.0, NCH_{e}N), 4.96 (d, $^{2}J_{HH}$ = 13.1, NC$H`_{e}$N), 4.34 (1 H, dd, $^{2}J_{HH}$ = 13.0, $^{4}J_{HP}$ = 2.9, NC$H_{a}$N), 4.27 (d, $^{2}J_{HH}$ = 13.1, NC$H`_{a}$N), 3.96 – 3.38 (m, PCH_2N, PCH_2NH, PC$H`_2$N, PC$H`_2$N$H`$), 2.68 – 2.40 (m, $CH_2$, $CH`_2$), 1.35 – 1.05 (m, CH_3, $CH`_3$) ppm. $^{1}$H NMR (400 MHz, DMSO, *J* in Hz, H for **2.19** and H` for **2.24**) 7.06 (4 H, d, $^{3}J_{HH}$ = 8.6, *m*–CH), 6.99 (4 H, d, $^{3}J_{HH}$ = 8.6, *o*–CH), 6.85 (2 H, d, $^{3}J_{HH}$ = 8.6, *m*–CH), 6.44 (2 H, d, $^{3}J_{HH}$ = 8.6, *o*–CH), 7.08 – 6.43 (m, CH`), 5.52 (1 H, s, NH), 4.91 (1 H, d, $^{2}J_{HH}$ = 13.6, NC$H_{e}$N), 4.57 (1 H, d, $^{2}J_{HH}$ = 13.6, NC$H_{a}$N), 4.74 – 4.59 (m, NC$H`_2$N), 3.89 – 3.66 (m, PC$H_2N, PCH_2NH, PCH`_2$N, PC$H`_2$NH), 1.17 – 1.06 (m, CH_2, CH_3, $CH`_2$, $CH`_3$ peaks obscured by solvent) ppm. ^{31}P{^{1}H} (162 MHz, $CDCl_3$) –41.4, –47.7 (approx. 4:1) ppm, (DMSO) –49.8, –54.2 (approx. 4:1) ppm. EI–MS (*m/z,* $[MH]^+$) 446. $C_{28}H_{36}N_3P{\cdot}0.25H_2O$ (450). EA found (calculated)(%): 74.78 (74.72), 7.79 (8.17), 9.33 (9.34). This compound was previously synthesised and the data presented here is in agreement with that observed for the reported compound.[16] However, ^{31}P{^{1}H} and ^{1}H NMR in $CDCl_3$ in this thesis showed a mixture between **2.18** and **2.23** not previously observed.

Preparation of $C_{21}H_{24}N_3P$ (2.26):

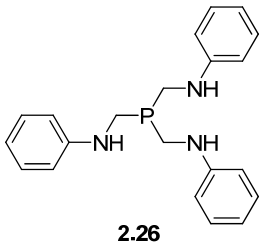

2.26

A suspension of **2.1** (1.000 g, 2.37 mmol) in HPLC grade MeOH (10 ml) was prepared. KO^{t}Bu (0.914 g, 8.146 mmol) was dissolved in the minimum amount of HPLC MeOH (5 ml) and added dropwise to the suspension of **2.1**. The mixture was stirred for 2 h at room temperature and the resulting colourless precipitate was filtered using a glass sinter and dried under vacuum. Yield: 0.613 g, 86%. Selected data: ^{1}H NMR (500 MHz, $CDCl_3$, *J* in Hz) 7.22 (6 H, t, $^{3}J_{HH}$ = 7.8, *m*–CH), 6.79 (3 H, t, $^{3}J_{HH}$ = 7.8, *p*–CH), 6.70 (6 H, d, $^{3}J_{HH}$ = 7.8, *o*–CH), 3.99 (6 H, s, PCH_2NH) ppm. ^{1}H NMR (400 MHz, DMSO, *J* in Hz) 7.05 (6 H, dd, $^{3}J_{HH}$ = 7.8, *m*–CH), 6.65 (6 H, d, $^{3}J_{HH}$ = 7.8, *o*-CH), 6.51 (3 H, t, $^{3}J_{HH}$ = 7.8, *p*-CH), 3.44 (6 H, d, $^{2}J_{HP}$ = 3.8). ^{31}P{^{1}H} NMR ($CDCl_3$) –31.5, –36.1, –41.0 (approx. 8:1:1) ppm; (DMSO) –38.5, –50.1 (approx. 7:1) ppm. EI–MS (*m/z,* $[MH]^+$) 350, $[MNa]^+$ 372, $[MK]^+$ 388. $C_{21}H_{24}N_3P{\cdot}2KCl$ 536. EA found (calculated)(%): C 47.12 (47.08), H 4.67 (4.51), N 7.59 (7.84). This compound was previously synthesised with a different method and the data presented here is in agreement with that observed for the reported compound.[16,25] The

inclusion of KCl in the formula came from the excess of KO^{t}Bu using in the reaction with the chloride counter ion from the phosphonium salt **2.1**. Attempts to remove it with methanol were unsuccessful.

Preparation of $C_{30}H_{42}N_3P$ (2.27):

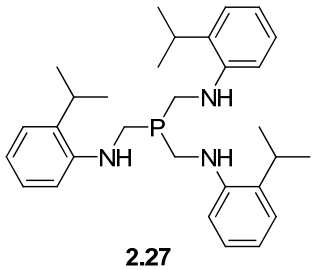

2.27

Method **A**) A suspension of **2.3** (1.000 g, 1.519 mmol) in HPLC grade MeOH (5 ml) was prepared. KO^{t}Bu (0.682 g, 6.074 mmol) was dissolved in the minimum amount of HPLC MeOH (5 ml) and added dropwise to the suspension **2.3**. The mixture was stirred for 5 min at r.t. and the resulting colourless precipitate was filtered in a glass sinter and dried under vacuum. Yield: 0.581 g, 81%. Method **B**) A suspension of **2.3** (2.000 g, 3.033 mmol) in HPLC grade MeOH (75 ml) was prepared. KO^{t}Bu (0.357 g, 3.185 mmol) was dissolved in the minimum amount of HPLC MeOH (5 ml) and added dropwise to the suspension with **2.3**. The mixture was stirred for 20 h at r.t. and the volume was reduced to 10 ml. Colourless crystals precipitated and they were filtered in a glass sinter and dried under vacuum. Yield: 0.721 g, 50%. Selected data: IR (KBr, cm^{-1}) (vNH) 3425. ^{1}H NMR (400 MHz, $CDCl_3$, *J* in Hz) 7.09 – 7.02 (6H, m, *m*–CH), 6.75 – 6.67 (6H, m, p–,o–CH), 4,29 (3H, bs, NH), 3.58 (6H, d, $^2J_{HP}$ = 4.6, PC*H*$_2$NH), 2.73 (3H, sept, $^3J_{HH}$ = 6.7, CH), 1.06 (18 H, t, $^3J_{HH}$ = 6.7, CH_3) ppm. ^{1}H NMR (400 MHz, DMSO) 7.02 (3H, dd, $^3J_{HH}$ = 7.6, $^4J_{HH}$ = 1.3, *m*–CH), 6.93 – 6.87 (3H, t, $^3J_{HH}$ = 1.3, *m*–CH), 6.63 (3H, d, $^3J_{HH}$ = 7.6, *o*–CH), 6.54 (3H, t, $^3J_{HH}$ = 7.6, *p*–CH), 5.32 (3H, t, $^3J_{HP}$ = 7.0, NH), 3.61 – 3.52 (6H, $^3J_{HH}$ = 7.0, PC*H*$_2$NH), 2.96 (3H, sept, $^3J_{HH}$ = 7.4, CH), 1.14 (18H, d, $^3J_{HH}$ = 7.4, CH_3) ppm. ^{31}P{^{1}H} NMR ($CDCl_3$): –33.2 ppm, (DMSO): –42.9 ppm. EI–MS (*m/z,* $[MH]^+$) 476. Method **A**) $C_{30}H_{42}N_3P$·1.5KCl (589). EA found (calculated)(%): C 60.82 (61.33), H 6.84 (7.21), N 7.08 (7.15). The inclusion of KCl in the formula came from the excess of KO^{t}Bu using in the reaction with the chloride counter ion from the phosphonium salt **2.3**. KCl was not observed in the single X–ray structure of **2.27**. Method **B**) $C_{30}H_{42}N_3P$ (475). EA found (calculated)(%): C 75.44 (75.75), H 8.55 (8.90), N 8.98 (8.83).

Preparation of $C_{33}H_{48}N_3P$ (2.28):

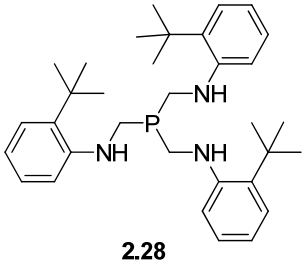

2.28

A suspension of **2.4** (1.000 g, 1.392 mmol) in HPLC grade MeOH (35 ml) was prepared. KO^{t}Bu (0.164 g, 1.461 mmol) was dissolved in the minimum amount of HPLC MeOH (5 ml) and added dropwise to the suspension with **2.4**. The mixture was stirred for 20 h at r.t. and the resulting colourless precipitate filtered using a glass sinter and dried under vacuum. Yield: 0.480 g, 67%. Selected data: IR (KBr, cm^{-1}) (νNH) 3363, 3481. ^{1}H NMR (400 MHz, $CDCl_3$, *J* in Hz) 7.18 (3 H, multiplicity obscured by solvents, *m*–CH), 7.06 (3 H, t, $^3J_{HH}$ = 7.9, *m*–CH), 6.74 (3 H, d, $^3J_{HH}$ = 7.9, *o*–CH), 6.68 (3 H, t, $^3J_{HH}$ = 7.9, *p*–CH), 4.07 (3 H, s, NH), 3.57 (6 H, d, $^2J_{HP}$ = 3.7, PCH_2N), 1.33 (27 H, s, CH_3) ppm. ^{31}P{^{1}H} NMR ($CDCl_3$): –31.1, –44.5 (approx. 10:1) ppm. EI–MS (*m/z,* $[MH]^+$) 518. $C_{33}H_{48}N_3P{\cdot}H_2O$ (536). EA found (calculated, %): C 73.61 (73.98), H 9.07 (9.41), N 7.74 (7.84).

Preparation of $C_{24}H_{21}F_9N_3P$ (2.29):

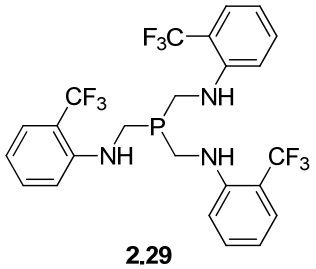

2.29

A suspension of **2.6** (0.500 g, 0.655 mmol) in HPLC grade MeOH (15 ml) was prepared. KO^{t}Bu (0.116 g, 1.035 mmol) was dissolved in the minimum amount of HPLC MeOH (5 ml) and added dropwise to the suspension with **2.6**. The mixture was stirred for 20 h at r.t. and the solvent reduced in volume to *ca*. 1 ml. The resulting colourless precipitate was filtered using a glass sinter and dried under vacuum. Yield: 0.130 g, 36%. Selected data: IR (KBr, cm^{-1}) (νNH) 3285, (νCF_3) 1104. ^{1}H NMR (400 MHz, $CDCl_3$, *J* in Hz) 7.38 (3 H, d, $^3J_{HH}$ = 8.0, *m*–CH), 7.28 (3 H, t, $^3J_{HH}$ = 8.0, *m*–CH), 6.76 (3 H, d, $^3J_{HH}$ = 8.0, *o*–CH), 6.70 (3 H, t, $^3J_{HH}$ = 7.6, *p*–CH), 4.46 (3H, s, NH), 3.53 (6 H, t, $^2J_{HP}$ = 5.6, PCH_2NH) ppm. δ ^{31}P{^{1}H} NMR ($CDCl_3$): –31.4, 45.2 (approx. 9:1) ppm. EI–MS (*m/z,* $[MK]^+$) 592, $[MOK]^+$ 608. $C_{24}H_{21}F_9N_3P{\cdot}1.25KCl$ (645). EA found (calculated)(%): 45.17 (44.58), 3.24 (3.27),

6.43 (6.50). The inclusion of KCl in the formula came from the excess of KO^{t}Bu using in the reaction with the chloride counter ion from the phosphonium salt **2.6**. KCl was not observed in the single X–ray structure of **2.27a** (**2.27** with a P=O bond).

Preparation of $C_{30}H_{36}N_3P$ (2.30):

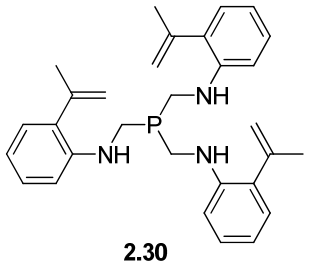

2.30

A suspension of **2.7** (0.433 g, 0.666 mmol) in HPLC grade MeOH (5 ml) was prepared. KO^{t}Bu (0.118 g, 1.052 mmol) was dissolved in the minimum amount of HPLC MeOH (5 ml) and added dropwise to the suspension with **2.7**. The mixture was stirred for 10 min at r.t. The resulting colourless precipitate was filtered using a glass sinter and dried under vacuum. Yield: 0.304 g, 97%. Selected data: IR (KBr, cm^{-1}) (vNH) 3419. ^{1}H NMR (400 MHz, $CDCl_3$, *J* in Hz) 7.18 (1 H, td, $^3J_{HH}$ = 8.0, $^4J_{HH}$ = 1.6, *m*–CH), 7.06 (1 H, dd, $^3J_{HH}$ = 7.7, $^4J_{HH}$ = 1.6, *o*–CH), 6.67 (2 H, m, *m*–, *p*–CH), 5.31 – 5.24 (1 H, m, CH), 5.05 – 4.96 (1 H, m, CH), 4.42 (3 H, s, NH), 3.53 (6 H, vt, $^2J_{HP}$ = 4.7, PCH_2NH), 2.09 – 2.01 (6 H, m, CH_3) ppm. ^{1}H NMR (400 MHz, DMSO, *J* in Hz) 7.03 – 6.97 (3 H, m, *m*–CH), 6.90 (3 H, dd, $^3J_{HH}$ = 7.5, $^4J_{HH}$ = 1.6, *o*–CH), 6.64 (3 H, d, $^3J_{HH}$ = 7.5, *m*–CH), 6.55 (3 H, td, $^3J_{HH}$ = 7.5, $^4J_{HH}$ = 0.9, *p*–CH), 5.25 – 5.22 (3 H, m, CH), 5.01 (3 H, t, $^3J_{HP}$ = 6.2, NH), 4.94 – 4.91 (3 H, m, CH), 3.50 – 3.40 (2 H, PCH_2NH obscured by solvent), 1.98 (3 H, s, CH_3) ppm. ^{31}P{^{1}H} NMR ($CDCl_3$) –32.4, –46.1 (approx. 23:1) ppm; (DMSO) –38.0 ppm. EI–MS (*m/z*) $[MH]^+$ 470. $C_{30}H_{36}N_3P$ 469. EA found (calculated)(%): 76.48 (76.76), 7.70 (7.68), 8.90 (8.96).

Preparation of $C_{16}H_{18}N_2P_2$ (2.31):

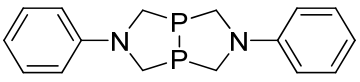

2.31

A suspension of **2.1** (1.000 g, 2.038 mmol) in HPLC grade MeOH (45 ml) was prepared. KO^{t}Bu (0.114 g, 1.019 mmol) was dissolved in the minimum amount of HPLC MeOH (5 ml) and added dropwise to the suspension of the phosphonium salt. The mixture was stirred for 15 min at r.t. and filtered off. The filtrate was stripped to 2 ml and filtered in a

glass sinter and dried under vacuum. Yield: 0.067 g, 22%. Selected data: ^{1}H NMR (400 MHz, $CDCl_3$, *J* in Hz) 7.13 (4 H, dd, $^{3}J_{HH}$ = 8.4, $^{3}J_{HH}$ = 7.4, *m*–CH), 6.80 (4 H, d, $^{3}J_{HH}$ = 8.4, *o*-CH), 6.72 (2 H, t, $^{3}J_{HH}$ = 7.4, *p*-CH), 3.65 (4 H, d, $^{3}J_{HH}$ = 12.6, PCH_2N), 3.45 (4 H, vq, *J* = 12.8, PCH_2N) ppm. ^{31}P{^{1}H} NMR (162 MHz, $CDCl_3$) –36.1 ppm. EI–MS (*m/z,* $[MH]^+$) 301, $[MK]^+$ 339. $C_{16}H_{18}N_2P_2$ 300. EA found (calculated)(%): C 63.88 (64.00), H 5.78 (6.00), N 9.30 (9.33). This compound was previously synthesised and the data presented here is in agreement with that observed for the reported compound.[26] In addition, single crystal X–ray diffraction for **2.31** was obtained which supported the structure.

Preparation of $C_{18}H_{22}N_2P_2$ (2.32):

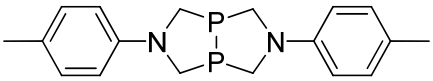

2.32

Compound **2.32** was collected as fine colourless needles from the filtrate of the reaction between THP and *p*-$MeC_6H_4NH_2$ (2:3) after leaving the solution to stand for more than 24 h at –18^{o}C. Yield: 0.140 g, 21%. Selected data: IR (cm^{-1}) (vNH) 3482, 3363. ^{1}H NMR (400 MHz, $CDCl_3$, *J* in Hz) 6.74 (4 H, d, $^{3}J_{HH}$ = 2.0, *m*–CH), 6.72 (4 H, d, $^{3}J_{HH}$ = 2.0, *o*-CH), 6.72 (2 H, t, $^{3}J_{HH}$ = 7.4, *p*-CH), 3.56 – 3.40 (8 H, m, PCH_2N) ppm. ^{31}P{^{1}H} NMR (162 MHz, $CDCl_3$) –35.8 ppm. EI–MS (*m/z,* $[MH]^+$) 329, $[MK]^+$ 367. $C_{18}H_{22}N_2P_2$ 328. EA found (calculated)(%): C 65.30 (65.85), H 6.38 (6.71), N 8.50 (8.54).

From **2.8**: A suspension of **2.8** (0.500 g, 0.915 mmol) in HPLC grade MeOH (20 ml) was prepared. KO^{t}Bu (0.051 g, 0.457 mmol) was dissolved in the minimum amount of HPLC MeOH (5 ml) and added dropwise to the suspension of the phosphonium salt. The mixture was stirred for 15 min at r.t. and filtered off. ^{31}P{^{1}H} NMR (162 MHz, $CDCl_3$) –35.8, –41.4, –47.4 (approx. 2:3.5:1) ppm.

Preparation of $C_{22}H_{30}N_2P_2$ (2.33):

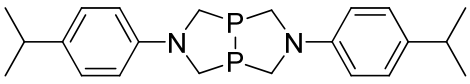

2.33

A suspension of **2.9** (0.500 g, 0.758 mmol) in MeOH (45 ml) was prepared. KO^{t}Bu (0.043 g, 0.379 mmol) was dissolved in the minimum amount of MeOH (5 ml) and added dropwise to the suspension of the phosphonium salt. The mixture was stirred at r.t. for 15

min and the solid filtered off. Yield: 0.020 g, 14%. Selected data: ^{1}H NMR (400 MHz, $CDCl_3$, *J* in Hz) 6.99 (4 H, d, $^{3}J_{HH}$ = 6.8, *m*–CH), 6.75 (4 H, d, $^{3}J_{HH}$ = 6.8, *o*-CH), 3.58 (4 H, d, $^{3}J_{HH}$ = 12.4, PC*H*$_2$N), 3.43 (4 H, vq, *J* = 12.6, PC*H*$_2$N), 2.73 (2 H, sept, $^{3}J_{HH}$ = 6.8, CH), 1.12 (12 H, d, $^{3}J_{HH}$ = 6.8, CH_3) ppm. $^{31}P\{^{1}H\}$ NMR (162 MHz, $CDCl_3$) –35.8 ppm. EI–MS (*m/z,* $[MH]^+$) 385. $C_{22}H_{30}N_2P_2 \cdot 1.20\ H_2O$ 407. EA found (calculated)(%): C 63.89 (65.07), H 6.78 (8.04), N 6.69 (6.90).

Preparation of $C_{20}H_{26}N_2P_2$ (2.34):

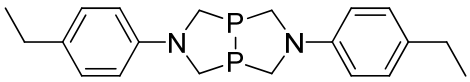

2.34

A suspension of **2.11** (0.500 g, 0.830 mmol) in MeOH (45 ml) was prepared. KO^{t}Bu (0.047 g, 0.415 mmol) was dissolved in the minimum amount of MeOH (5 ml) and added dropwise to the suspension of the phosphonium salt. The mixture was stirred at r.t for 15 min and the solid filtered off. Selected data: IR (cm^{-1}) (vNH) 3481, 3363. ^{1}H NMR (400 MHz, $CDCl_3$, *J* in Hz) 7.11 – 6.66 (m, CH), 5.01 – 3.40 (m, PCH_2N), 2.54 – 2.38 (m, C*H*$_2$), 1.19 – 1.04 (m, CH_3) ppm. $^{31}P\{^{1}H\}$ NMR (162 MHz, $CDCl_3$) –35.8 (32%) ppm. EI–MS (*m/z,* $[MH]^+$) 357. A pure sample of **2.34** could not be obtained for elemental analysis despite drying the sample in the desiccator overnight.

Preparation of $C_{27}H_{33}N_3P_2O_2$ (2.35):

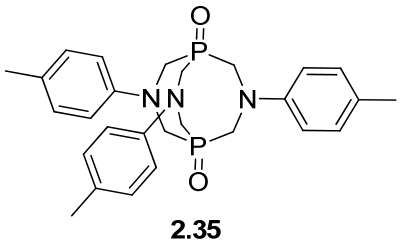

2.35

Route **A**: THP (0.250 g, 2.016 mmol) and *p*-$MeC_6H_4NH_2$ (0.323 g, 3.024 mmol) were dissolved in MeOH (5 ml) at r.t. for 4 h under nitrogen atmosphere. The colourless solid precipitated was filtered off and shown to be **2.16**. Yield: 0.072 g, 18%. The filtrate was kept at low temperature and after approx. 12 h, colourless needles were collected and analysed to get **2.32**. Yield: 0.140 g, 21%. Route **B**: THP (0.500 g, 4.032 mmol) and *p*-$MeC_6H_4NH_2$ (1.294 g, 12.097 mmol) were dissolved in MeOH (25 ml) at r.t. for 4 h under

nitrogen atmosphere. A colourless solid precipitated and was filtered off, and shown to be **2.16**. Yield: 0.166 g, 11%. The filtrate was kept at low temperature and the colourless solid collected shown to be **2.16**. Total yield: 0.494 g, 30%. Route **C**: THP (0.402 g, 3.242 mmol) and H_2O_2 (30 %) (0.367 g, 3.242 mmol) in acetone (6 ml) were stirred for 1 h at r.t. then, the solvent was removed under high vacuum to get the crude THPO which was used for next step. $^{31}P\{^1H\}$ NMR (162 MHz, D_2O) 49.0 ppm. THPO (0.260 g, 1.857 mmol) was dissolved in MeOH:C_7H_8 (1:1) and *p*-$MeC_6H_4NH_2$ (0.299 g, 2.786 mmol) was added in several portions. The solution was stirred for 6 d at r.t. and monitored by external C_6D_6 NMR. After this time, the solvent was reduced under high vacuum. A mixture containing unreacted THPO and *p*-$MeC_6H_4NH_2$ was observed in NMR: ^1H NMR (400 MHz, D_2O, *J* in Hz) 7.00 (2 H, d, $^3J_{HH}$ = 8, *m*-CH), 6.68 (2 H, d, $^3J_{HH}$ = 8, *o*-CH), 4.72 (18 H, s, H_2O + OH), 4.05 (3 H, d, $^2J_{PH}$ = 1.3, PCH_2O), 4.00 (< 1 H, $^2J_{PH}$ = 1.0, PCH_2O), 3.70 (< 1 H, $^2J_{PH}$ = 2.1, PCH_2O), 3.23 (2H, s, NH_2), 2.12 (3 H, s, CH_3) ppm. $^{31}P\{^1H\}$ NMR (162 MHz, D_3O) 49.8, 49.0 (approx. 1:3) ppm.

Several methods were used to obtain the ligands **2.36** – **2.40** as indicated in Table 2.9 in Chapter 2. Here is compiled those procedures which gave the highest conversions under specific conditions. Tertiary ligands were identified by $^{31}P\{^1H\}$ NMR spectroscopy. IR and elemental analysis were not recorded since NMR studies indicated mixtures of aminomethylphosphines.

Preparation of $C_{35}H_{35}N_3P_2$ (2.36):

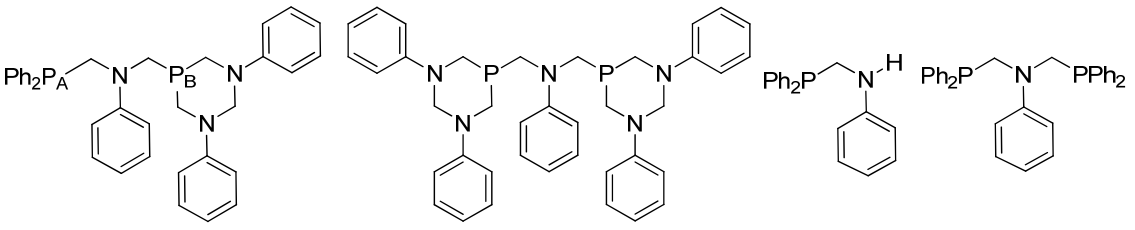

2.36 **2.20** **2.41** **2.48**

Compound **2.12** (0.281 g, 0.778 mmol) and Ph_2PCH_2OH (0.168 g, 0.778 mmol) were suspended in MeOH (10 ml) for 4 h at 80°C under nitrogen. Once the solution was cooled to r.t., the solvent was evacuated until some solid precipitated. This solid was filtered off and washed with MeOH and Et_2O. Selected data: ^1H NMR (400 MHz, $CDCl_3$) 7.78 – 7.56 (m, CH), 5.02 – 3.05 (m, CH_2) ppm. $^{31}P\{^1H\}$ NMR (162 MHz, $CDCl_3$, *J* in Hz) –17.9 (**2.41**), –27.4 (d, $^4J_{PP}$ = 8.1, P_A), –27.7 (**2.48**), –36.2 (**2.31**), –41.0 (**2.12**), –46.7 (**2.20**), –47.8 (d, $^4J_{PP}$ = 8.1, P_B) (approx. 4:30:17:5:1:9) ppm.

Preparation of $C_{44}H_{53}N_3P_2$ (2.37):

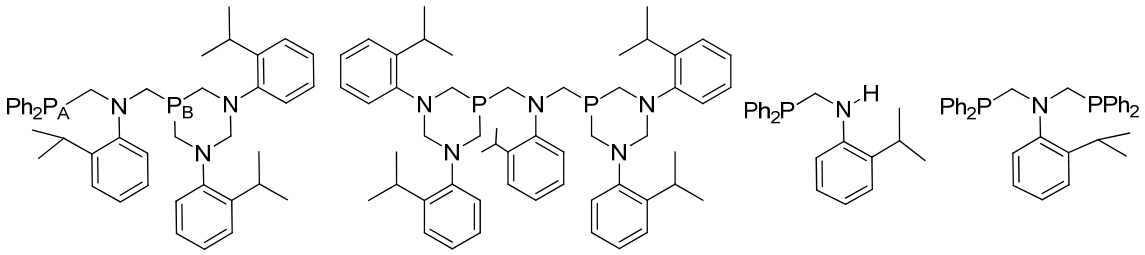

2.37 **2.46** **2.42** **2.49**

Compound **2.14** (0.349 g, 0.718 mmol) and Ph_2PCH_2OH (0.155 g, 0.718 mmol) were suspended in MeOH (15 ml) for 24 h at r.t. under nitrogen. The solid was filter off under vacuum. Selected data: ^{1}H NMR (400 MHz, $CDCl_3$) 7.49 – 7.66 (m, CH), 4.13 – 2.66 (m, CH, CH_2), 1.19 – 0.80 (CH_3) ppm. $^{31}P\{^1H\}$ NMR (162 MHz, $CDCl_3$, J in Hz) –17.8 (**2.42**), –27.6 (**2.49**), –45.0 (**2.14**) (approx. 1:2:3) ppm.

Preparation of $C_{35}H_{32}F_3N_3P_2$ (2.38):

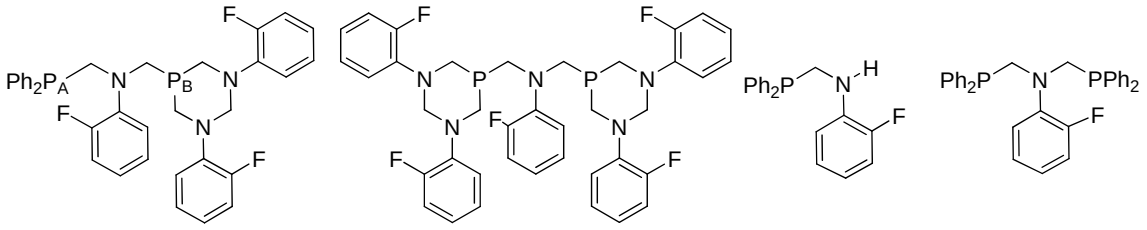

2.38 **2.47** **2.43** **2.50**

Compound **2.15** (0.250 g, 0.602 mmol) and Ph_2PCH_2OH (0.130 g, 0.602 mmol) were suspended in C_7H_8 (10 ml) for 24 h at 110^{o}C under nitrogen. Once the solution was cooled to r.t., the solvent was reduced to a third, the solid filtered off and washed with hexanes. Selected data: ^{1}H NMR (400 MHz, $CDCl_3$) 7.78 – 7.55 (m, CH), 4.72 – 3.43 (m, CH_2) ppm. $^{31}P\{^1H\}$ NMR (162 MHz, $CDCl_3$, J in Hz) –19.6 (**2.43**), –26.8 (t, $^4J_{PP}$ = 4.5, P_A), –26.2 (d, J = 4.5, **2.50**), –40.8 (**2.15**), –51.0 (**2.38**) (approx. 1.5:2.5:1.5:1) ppm.

Preparation of $C_{38}H_{41}N_3P_2$ (2.39):

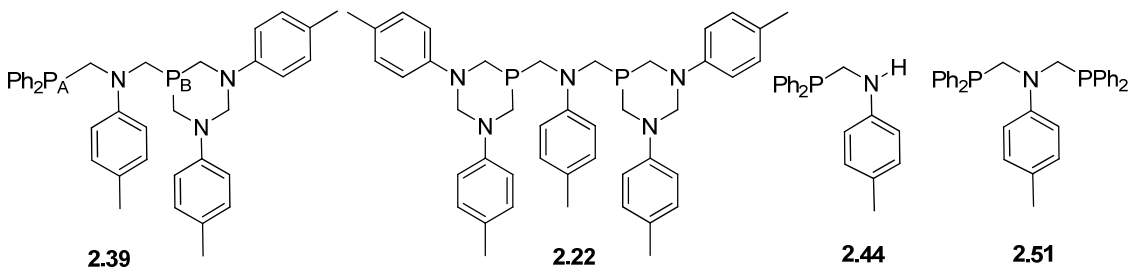

2.39 **2.22** **2.44** **2.51**

Method **A** (entry 5 Table 2.9): **2.16** (0.250 g, 0.620 mmol) and Ph_2PCH_2OH (0.134 g, 0.620 mmol) were dissolved in C_7H_8 (10 ml) and stirred at 60°C for 2 h. Then, the solvent was evaporated to dryness under reduced pressure to give a colourless precipitate. The solid became waxy after minutes. The purity was shown, by $^{31}P\{^1H\}$ NMR, to be 49%. Method **B** (entry 9 in Table 2.9): **2.16** (0.100 g, 0.248 mmol) and Ph_2PCH_2OH (0.054 g, 0.248 mmol) were placed in a mortar and triturated until a waxy product was formed (*ca.* 1 min). The purity was shown, by $^{31}P\{^1H\}$ NMR, to be 48%. Method **C** (entry 8 Table 2.9): **2.16** (0.010 g, 0.025 mmol) and Ph_2PCH_2OH (0.005 g, 0.025 mmol) were dissolved in $CDCl_3$ and heated for 5 min. The purity was shown, by $^{31}P\{^1H\}$ NMR, to be 23%. Method **D** (entry 11 Table 2.9): **2.16** (0.010 g, 0.025 mmol) and Ph_2PCH_2OH (0.005 g, 0.025 mmol) were melted for approx. 5 min and then dissolved in $CDCl_3$. The purity was shown, by $^{31}P\{^1H\}$ NMR, to be 23%. Selected data: $^{31}P\{^1H\}$ NMR (162 MHz, $CDCl_3$, *J* in Hz) – 19.4 (**2.44**), –27.4 (d, $^4J_{PP}$ = 8.6 Hz, P_A), –27.8 (**2.51**), –47.5 (**2.21**), –48.3 (d, $^4J_{PP}$ = 8.6 Hz, P_B) ppm. EI–MS (*m/z,* $[MO_2H]^+$) 634, $[C_{43}H_{51}N_5P_2O_2H]^+$ 732, $[C_{33}H_{31}NP_2O_2H]^+$ 536.

Preparation of $C_{35}H_{32}N_3F_3P_2$ (2.40):

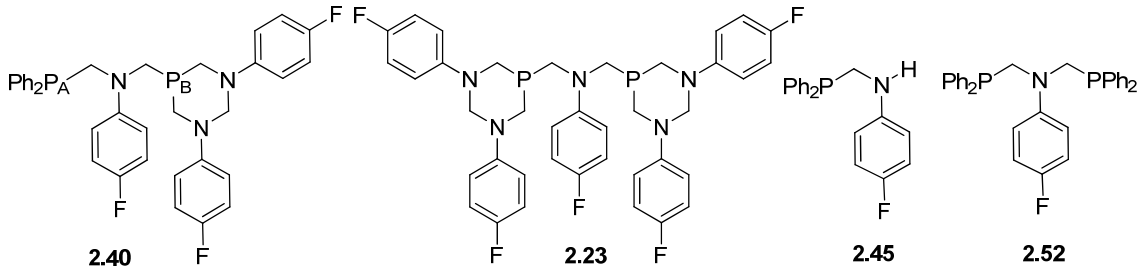

Method **A** (entry 17 Table 2.9): **2.18** (0.250 g, 0.602 mmol) and Ph_2PCH_2OH (0.130 g, 0.602 mmol) were dissolved in CH_2Cl_2 (50 ml) and stirred at r.t. for 5 h. The solvent was evaporated to dryness under reduced pressure to give a colourless precipitate which was washed with Et_2O. The solid became waxy after minutes. The purity was shown, by $^{31}P\{^1H\}$ NMR, to be 45%. Method **B** (entry 23 in Table 2.9): **2.18** (0.100 g, 0.240 mmol) and Ph_2PCH_2OH (0.052 g, 0.240 mmol) were placed in a preheated mortar (in the oven) and triturated until a waxy product was formed (*ca.* 5 min). The purity was shown, by $^{31}P\{^1H\}$ NMR, to be 50%. Method **C** (entry 21 Table 2.9): **2.18** (0.010 g, 0.024 mmol) and Ph_2PCH_2OH (0.005 g, 0.024 mmol) were dissolved in $CDCl_3$ and heated for 5 min. The purity was shown, by $^{31}P\{^1H\}$ NMR, to be 44 %. Method **D** (entry 24 Table 2.9): **2.16** (0.010 g, 0.024 mmol) and Ph_2PCH_2OH (0.005 g, 0.024 mmol) were melted for approx. 5 min and then dissolved in $CDCl_3$. The purity was shown, by $^{31}P\{^1H\}$ NMR, to be 37%.

Method **E** (entry 18 Table 2.9): **2.18** (0.250 g, 0.602 mmol) and Ph_2PCH_2OH (0.195 g, 0.903 mmol) were dissolved in C_7H_8 (10 ml) and stirred at 120°C for 24 h. The solvent was evaporated to dryness under reduced pressure to give a colourless precipitate. The purity was shown, by $^{31}P\{^1H\}$ NMR, to be 37%. Method **F** (entry 19 Table 2.9): **2.18** (0.250 g, 0.602 mmol) and Ph_2PCH_2OH (0.087 g, 0.401 mmol) were dissolved in C_7H_8 (10 ml) and stirred at rt. for 24 h and for further 24 h at 120°C. Then, the solvent was evaporated to dryness under reduced pressure to give a colourless precipitate. The purity was shown, by $^{31}P\{^1H\}$ NMR, to be 30%. Selected data: $^{31}P\{^1H\}$ NMR (162 MHz, $CDCl_3$, *J* in Hz) –19.4 (**2.45**), –27.85 (**2.52**), –27.4 (d, $^4J_{PP}$ = 7.9, P_A), –48.4 (**2.23**), –49.0 (d, $^4J_{PP}$ = 7.9, P_B) ppm.

6.3 Chapter 3 Experimental

Unless otherwise stated, new Pt(II), Pd(II) and Ru(II) complexes were synthesised by reacting appropriate metal precursors with phosphine ligands in CH_2Cl_2 and stirring at r.t. for 1 or 24 h. The solids were dried under vacuum after precipitation with Et_2O upon concentration of the solution.

Preparation of $C_{44}H_{48}N_6P_2PtCl_2$ (3.1):

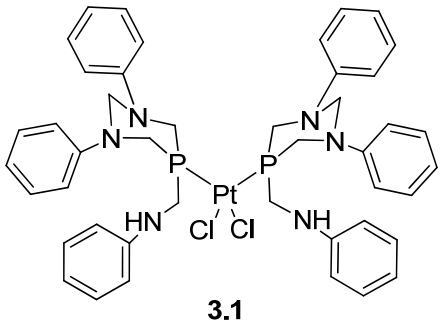

3.1

From **2.12** (0.100 g, 0.277 mmol) and $PtCl_2COD$ (0.052 g, 0.139 mmol). Yield: 0.130 g, 95%. Selected data: IR (KBr, cm^1): (νNH) 3350, (νPtCl) 306, 280. ^1H NMR (400 MHz, $CDCl_3$, *J* in Hz) 7.28 (8 H, t, $^3J_{HH}$ = 7.9, *m*–CH), 7.07 (4 H, t, $^3J_{HH}$ = 7.9, *m*–CH), 6.99 – 6.89 (12 H, m, *o*–CH), 6.72 (4 H, d, $^3J_{HH}$ = 7.9, *o*–CH), 6.66 (2 H, t, $^3J_{HH}$ = 7.9, *p*–CH), 4.86 (2 H, d, $^2J_{HH}$ = 13.2, NC*H*$_e$N), 4.30 (4 H, d, $^3J_{HH}$ = 13.2, $^2J_{HP}$ = 5.2, PC*H*$_e$N), 3.92 (4 H, vs, PC*H*$_2$NH), 3.80 (4 H, d, $^3J_{HH}$ = 13.2, $^4J_{HP}$ = 4.3, NC*H*$_a$N, PCH$_2$N*H*), 3.07 (4 H, d, $^3J_{HH}$ = 13.2, $^2J_{HP}$ = 2.5, PC*H*$_a$N) ppm. $^{31}P\{^1H\}$ NMR (162 MHz, $CDCl_3$, *J* in Hz) –6.8 ppm ($^1J_{PPt}$ = 3401 Hz). $C_{44}H_{48}N_6P_2PtCl_2{\cdot}CH_2Cl_2$ 1073. EA found (calculated) (%): C 50.14 (50.14), H 4.33 (4.69), N 7.83 (7.83).

Preparation of $C_{62}H_{84}N_6P_2PtCl_2$ (3.2):

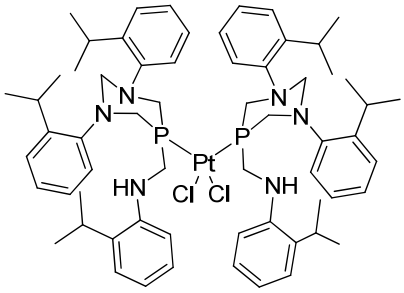

3.2

From **2.14** (0.100 g, 0.206 mmol) and $PtCl_2COD$ (0.038 g, 0.103 mmol). Yield: 0.068 g, 54%. Selected data: IR (KBr, cm^{-1}): (vNH) 3424, 3379. ^1H NMR (400 MHz, $CDCl_3$, *J* in Hz): 7.19 (8 H, m, *m*-CH), 7.12 (2 H, t, $^3J_{HH}$ = 7.2, *m*-CH), 7.03 (8 H, t, $^3J_{HH}$ = 6.4, *p-, o*-CH), 6.91 (2 H, d, $^3J_{HH}$ = 7.2, *o*–CH), 6.82 (2 H, t, $^3J_{HH}$ = 7.2, *m*–CH), 6.77 (2 H, s, *p*–CH), 4.55 – 3.44 (18 H, m, PC*H*$_2$N*H*, NC*H*$_2$N), 2.80 (4 H, s, CH), 2.65 (2 H, s, CH), 1.19 (12 H, d, $^3J_{HH}$ = 6.8, CH_3), 1.08 (24 H, d, $^3J_{HH}$ = 6.4, CH_3) ppm. $^{31}P\{^1H\}$ NMR (162 MHz, $CDCl_3$, *J* in Hz) –5.7 ($^1J_{PPt}$ = 3422 Hz) ppm. EI–MS (*m/z* $[M–Cl]^+$) 1204. A pure sample of **3.2** (several batches) could not be obtained for elemental analysis despite drying the sample in the desiccator overnight.

Preparation of $C_{44}H_{42}N_6P_2F_6PtCl_2$ (3.3):

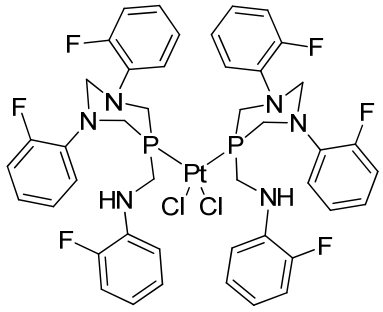

3.3

From **2.15** (0.100 g, 0.241 mmol) and $PtCl_2COD$ (0.045 g, 0.120 mmol). Yield: 0.105 g, 80%. Selected data: ^1H NMR (400 MHz, $CDCl_3$, *J* in Hz): 7.33 (2 H, m, *p*-CH), 7.20 – 7.07 (18 H, m, *m-,o*-CH), 7.04 (2 H, m, *p*-CH), 6.76 (2 H, m, *p*-CH), 4.60 (2 H, d, $^2J_{HH}$ = 12.6, NC*H*eN), 4.36 – 4.28 (8 H, m, PC*H*$_2$NH, PC*H*eN), 3.94 – 3.78 (4 H, m, NC*H*aN, PCH$_2$N*H*), 3.10 (4 H, dd, $^2J_{HH}$ = 14.8, $^2J_{PH}$ = 4.4, PC*H*aN) ppm. $^{31}P\{^1H\}$ NMR (162 MHz, $CDCl_3$, *J* in Hz) –11.3 ($^1J_{PPt}$ = 3369) ppm. This compound was previously synthesised and the data here presented is in agreement with that observed for the reported compound.[16]

Preparation of $C_{50}H_{60}N_6P_2PtCl_2$ (3.4):

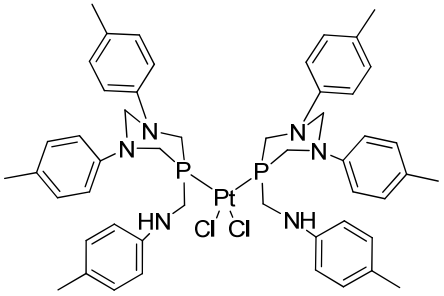

3.4

From **2.16** (0.100 g, 0.248 mmol) and $PtCl_2COD$ (0.046 g, 0.124 mmol). Yield: 0.112 g, 84%. Selected data: ^{1}H NMR (400 MHz, $CDCl_3$, *J* in Hz): 7.17 (8 H, d, $^3J_{HH}$ = 8.3, *m*-CH), 6.98 (4 H, d, $^3J_{HH}$ = 8.1, *m*-CH), 6.93 (8 H, d, $^3J_{HH}$ = 8.3, *o*-CH), 6.73 (2 H, d, $^3J_{HH}$ = 8.1, *o*-CH), 4.83 (2 H, d, $^2J_{HH}$ = 11.7, NCH_eN), 4.29 (4 H, bd, $^2J_{HH}$ =10.7, PCH_eN), 4.20 – 4.05 (2 H, m), 3.98 (4 H, vs, PCH_2NH), 3.79 (4 H, bd, $^2J_{HH}$ =11.7, NCH_aN), 3.05 (4 H, bd, $^2J_{HH}$ = 14.0, PCH_aN), 2.36 (12 H, s, CH_3), 2.14 (6 H, s, CH_3) ppm. ^{31}P{^{1}H} NMR (162 MHz, $CDCl_3$, *J* in Hz) –5.6 ($^1J_{PPt}$ = 3395) ppm. $C_{50}H_{60}N_6P_2PtCl_2 \cdot 0.75CH_2Cl_2$ 1136. EA found (calculated) (%): 53.76 (53.62), 5.17 (5.45), 7.43 (7.39). This compound was previously synthesised and the data here presented is in agreement with that observed for the reported compound.[16]

Preparation of $C_{62}H_{84}N_6P_2PtCl_2$ (3.5):

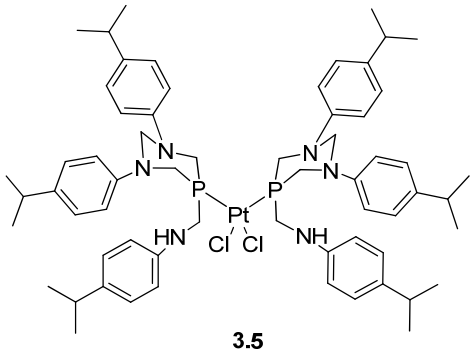

3.5

From **2.17** (0.100 g, 0.203 mmol) and $PtCl_2COD$ (0.038 g, 0.101 mmol). Yield: 0.096 g, 75%. Selected data: IR (KBr, cm^{-1}): (νNH) 3356, (νPtCl) 314, 285. ^{1}H NMR (400 MHz, $CDCl_3$, *J* in Hz) 7.12 (8 H, d, $^3J_{HH}$ = 8.5, *m*–CH), 6.93 (4 H, d, $^3J_{HH}$ = 8.5, *m*–CH), 6.86 (8 H, d, $^3J_{HH}$ = 8.5, *o*–CH), 6.66 (4 H, d, $^3J_{HH}$ = 8.5, *o*–CH), 4.81 (2 H, d, $^2J_{HH}$ = 13.1, NCH_eN), 4.26 (4 H, bd, $^2J_{HH}$ = 9.5, PCH_eN), 3.89 (4 H, vd, $^2J_{HP}$ = 5.5, PCH_2NH), 3.79 – 3.60 (4 H, m, NCH_aN, NH), 3.06 (4 H, d, $^2J_{HH}$ = 13.1, PCH_aN), 2.83 (4 H, sept, $^3J_{HH}$ = 6.9, CH), 2.62 (2H, sept, $^3J_{HH}$ = 6.9, CH), 1.19 (24 H, d, $^3J_{HH}$ = 6.9, CH_3), 0.99 (12 H, d, $^3J_{HH}$ =

6.9, CH_3) ppm. $^{31}P\{^1H\}$ NMR (162 MHz, $CDCl_3$, *J* in Hz) –7.4 ($^1J_{PPt}$ = 3401) ppm. EI–MS (*m/z* $[M–Cl]^+$) 1204. $C_{62}H_{84}Cl_2N_6P_2Pt$ 1240. EA found (calculated) (%): C 59.50 (59.71), N 6.38 (6.74), H 6.85 (6.74).

Preparation of $C_{44}H_{42}N_6P_2F_6PtCl_2$ (3.6):

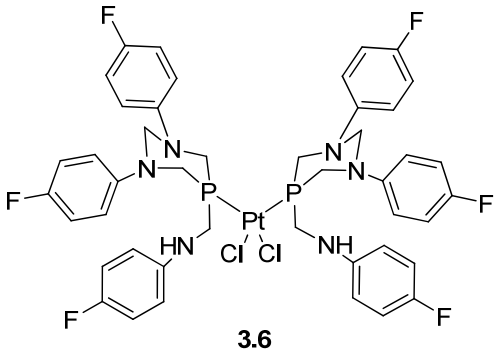

3.6

From **2.18** (0.200 g, 0.482 mmol) and $PtCl_2COD$ (0.090 g, 0.241 mmol). Yield: 0.237 g, 90%. Selected data: IR (KBr, cm^{-1}) (νNH) 3409, 3442, (νPtCl) 314, 286. ^1H NMR (400 MHz, $CDCl_3$, *J* in Hz): 7.10 – 6.54 (m, CH), 4.73 (2 H, d, $^2J_{HH}$ = 12.7, NCH_eN), 4.11 (4 H, bd, $^2J_{HH}$ = 12.5, PCH_eN), 3.90 – 3.87 (8 H, m, NCH_aN, PCH_2NH, N*H*), 3.26 (4 H, bd, $^2J_{HH}$ = 13.6, PCH_aN) ppm. $^{31}P\{^1H\}$ NMR (162 MHz, $CDCl_3$, *J* in Hz) –7.4 ($^1J_{PPt}$ = 3401) ppm. EI–MS (*m/z* $[M+Na]^+$) 1119. $C_{44}H_{42}N_6P_2F_6PtCl_2$ 1096. EA found (calculated) (%): C 47.97 (48.18), H 3.70 (3.86), N 7.59 (7.66).

Preparation of $C_{56}H_{72}N_6P_2PtCl_2$ (3.7):

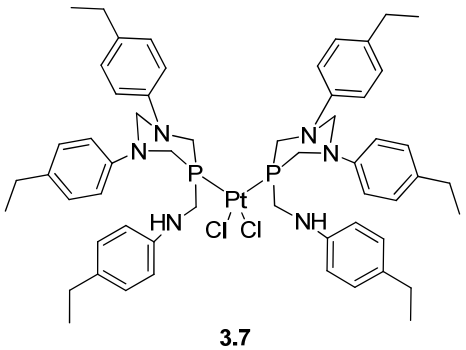

3.7

From **2.19** (0.100 g, 0.224 mmol) and $PtCl_2COD$ (0.032 g, 0.112 mmol). Yield: 0.080 g, 62%. Selected data: IR (KBr, cm^{-1}): (νNH) 3352, (νPtCl) 311, 284. ^1H NMR (400 MHz, $CDCl_3$, *J* in Hz) 7.10 (8 H, d, $^3J_{HH}$ = 8.4, *m*–CH), 6.90 (4 H, d, $^3J_{HH}$ = 8.4, *o*–CH), 6.85 (8 H, d, $^3J_{HH}$ = 8.4, *o*–CH), 6.66 (4 H, d, $^3J_{HH}$ = 8.4, *m*–CH), 4.77 (2 H, d, $^2J_{HH}$ = 11.1, NCH_eN), 4.23 (4 H, bd, $^2J_{HH}$ = 9.3, PC*H*eN), 3.89 (4 H, vs, PCH_2NH), 3.71 (4 H, bd, $^2J_{HH}$ = 11.1, NCH_aN, NH), 3.00 (4 H, bd, $^2J_{HH}$ = 13.1, PCH_aN), 2.56 (8 H, q, $^3J_{HH}$ = 7.6, CH_2),

2.35 (4 H, q, $^3J_{HH}$ = 7.6, CH_2), 1.16 (17 H, vt, $^3J_{HH}$ = 7.6, CH_3) ppm. $^{31}P\{^1H\}$ NMR (162 MHz, $CDCl_3$, *J* in Hz) –7.1 ($^1J_{PPt}$ = 3401) ppm. EI–MS (*m/z* $[M–Cl]^+$) 1120. $C_{56}H_{72}N_6P_2PtCl_2 \cdot 0.5CH_2Cl_2$ (1198). EA found (calculated) (%): C 56.72 (56.57), N 6.02 (6.13), H 6.96 (7.01).

Preparation of $C_{44}H_{48}N_6P_2PdCl_2$ (3.8):

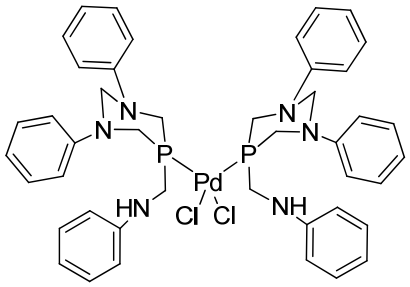

3.8

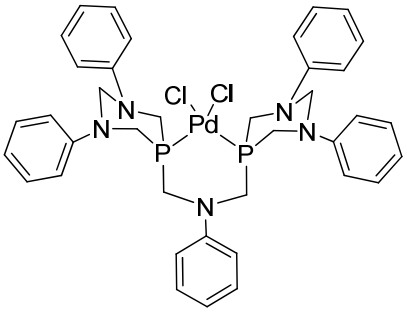

3.8a

From **2.12** (0.100 g, 0.278 mmol) and $PdCl_2COD$ (0.040 g, 0.139 mmol). Selected data: ^1H NMR (400 MHz, $CDCl_3$, *J* in Hz, *H* for the **3.8** and *H`* for **3.8a**) 7.38 (8 H, t, $^3J_{HH}$ = 12.0, *m*–CH), 7.25 (4 H, t, $^3J_{HH}$ = 7.9, *m*–CH), 7.14 – 6.97 (12 H, m, *p*–, *o*–CH), 6.91 (4 H, d, $^3J_{HH}$ = 7.9, *o*-CH), 6.80 (2 H, t, $^3J_{HH}$ = 7.9, *p*-CH), 6.68 (t, $^3J_{HH}$ = 12.0, *p*-CH`), 6.40 (d, $^3J_{HH}$ = 12.0, *o*-CH`), 5.19 (d, $^2J_{HH}$ = 16.0, NC*H*`$_e$N), 4.94 (2 H, d, $^2J_{HH}$ = 13.3, NCH_eN), 4.43 (4 H, d, $^2J_{HH}$ = 13.3, $^2J_{HP}$ = 6.4, PCH_eN+ PC*H*`$_e$N), 4.10 (d, $^2J_{HH}$ = 16.0, NC*H*`$_a$N), 4.02 (4 H, d, $^2J_{HP}$ = 7.0, PCH_2NH), 3.93 – 3.83 (4 H, m, NCH_aN, NH` + NC*H*`$_a$N, NH`), 3.16 (4 H, dd, $^2J_{HH}$ = 13.3, $^2J_{HP}$ = 6.3, PCH_aN) ppm. $^{31}P\{^1H\}$ NMR (162 MHz, $CDCl_3$): 11.2, –6.4 (approx. 5:1) ppm. EI–MS (*m/z*) $[M–Cl]^+$ 864. This compound was previously synthesised and the data here presented is in agreement with that observed for the reported compound.[16] However the $^{31}P\{^1H\}$ and ^1H NMR spectra of **3.8** showed **3.8a** which was not observed in the literature.

Preparation of $C_{38}H_{41}Cl_2N_5P_2Pd$ (3.8a): From **2.12** (0.900 g, 2.493 mmol) and $PdCl_2$ (0.22 g, 1.242 mmol) were dissolved in 20 ml of $CHCl_3$, stirred for 24 h at r.t. The suspension was filtered and the filtrate was reduced to 1 ml. The solid was dried under vacuum after precipitation with Et_2O. Yield: 0.735 g, 73%. Selected data: IR (KBr, cm^{-1}): (νNH) 3468 (νPdCl) 306, 280. ^1H NMR (400 MHz, $CDCl_3$, *J* in Hz,) 7.25 (8 H, t, $^3J_{HH}$ = 8.0, *m*-CH), 7.04 (8 H, d, $^3J_{HH}$ = 8.0, *o*-CH), 6.92 (4 H, t, $^3J_{HH}$ = 7.8, *p*-CH), 6.61 (2 H, t, $^3J_{HH}$ = 8.0, *m*-CH), 6.51 (1 H, d, $^3J_{HH}$ = 8.0, *p*-CH), 6.37 (2 H, d, $^3J_{HH}$ = 8.0, *o*-CH), 5.02 (2 H, d, $^2J_{HH}$ = 13.2, NCH_eN), 4.83 (4 H, d, $^2J_{HH}$ = 14.8, PCH_eN), 4.57 (2 H, d, $^2J_{HH}$ = 10.4,

$^4J_{HP}$ = 4.6, NCH_aN), 4.27 (4 H, d, $^2J_{HH}$ = 13.3, PCH_aN), 3.79 (4 H, vs, PCH_2NH) ppm. $^{31}P\{^1H\}$ NMR (162 MHz, $CDCl_3$) –6.4 ppm. EI–MS (*m/z*) $[M–Cl]^+$ n.o. $C_{38}H_{41}Cl_2N_5P_2Pd$ 807. EA found (calculated) (%): C 56.31 (56.55), H 5.09 (5.12), N 8.76 (8.68).

Preparation of $C_{62}H_{84}N_6P_2PdCl_2$ (3.9):

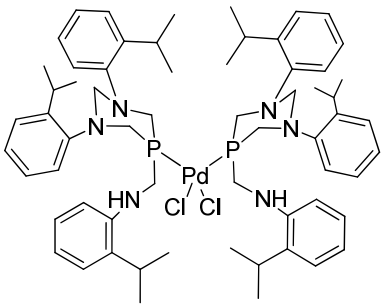

3.9

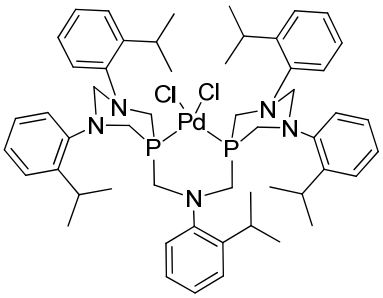

3.9a

From **2.14** (0.100 g, 0.206 mmol) and $PdCl_2COD$ (0.029 g, 0.103 mmol). Selected data: ^1H NMR (400 MHz, $CDCl_3$, *J* in Hz, *H* for **3.9** and *H`* for **3.9a**) 7.34 – 6.74 (m, CH + CH`), 4.75 – 2.71 (m, CH_2 + C$H`_2$), 1.31 – 1.10 (m, C$H_3$ + C$H`_3$) ppm. $^{31}P\{^1H\}$ NMR (162 MHz, $CDCl_3$) 13.5, –4.8 (approx. 3:1) ppm. EI–MS (*m/z*) $[M–Cl]^+$ n.o.

Preparation of $C_{62}H_{84}N_6P_2PdCl_2$ (3.10):

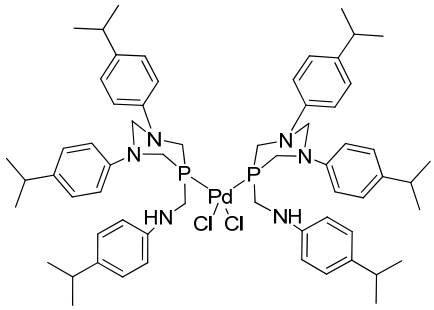

3.10

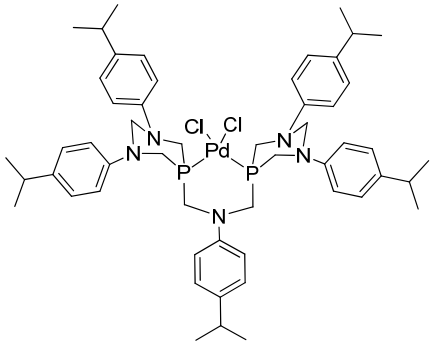

3.10a

From **2.17** (0.100 g, 0.205 mmol) and $PdCl_2COD$ (0.029 g, 0.103 mmol). Yield: 0.060 g, 51%. Selected data: IR (KBr, cm^{-1}): (νNH) 3347, (νPdCl) n.o. ^1H NMR (400 MHz, $CDCl_3$, *J* in Hz) 7.12 (8 H, d, $^3J_{HH}$ = 8.5, *m*–CH), 6.93 (4 H, d, $^3J_{HH}$ = 8.5, *m*–CH), 6.86 (8 H, d, $^3J_{HH}$ = 8.5, *o*–CH), 6.66 (4 H, d, $^3J_{HH}$ = 8.5, *o*–CH), 4.81 (2 H, d, $^2J_{HH}$ = 13.1, NCH_eN), 4.26 (4 H, bd, $^2J_{HH}$ = 9.5, PCH_eN), 3.89 (4 H, bd, $^2J_{HP}$ = 5.5, PCH_2NH), 3.79 – 3.50 (4 H, m, NCH_aN, NH), 3.06 (4 H, bd, $^3J_{HH}$ = 13.1, PCH_aN), 2.83 (4 H, sept, $^3J_{HH}$ = 6.9, CH), 2.62 (2 H, sept, $^3J_{HH}$ = 6.9, CH), 1.19 (24 H, d, $^3J_{HH}$ = 6.9, CH_3), 0.99 (12 H, d, $^3J_{HH}$ = 6.9, CH_3) ppm. $^{31}P\{^1H\}$ NMR (162 MHz, $CDCl_3$) 10.7, –3.2 (approx. 13:1) ppm.

EI–MS (*m/z*) $[M–Cl]^+$ 1115. $C_{62}H_{84}N_6P_2PdCl_2$ (1151). EA found (calculated) (%): C 64.29 (64.28), H 7.09 (7.26), N 7.35 (7.26).

Preparation of $C_{32}H_{38}N_3PRuCl_2$ (3.11):

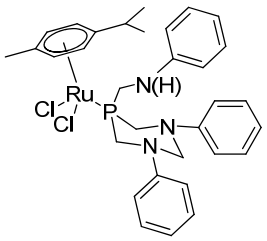

3.11

From **2.12** (0.100 g, 0.277 mmol) and $\{RuCl_2(\eta^6–p–cymene)\}_2$ (0.085g, 0.138 mmol). Yield: 0.168g, 90%. Selected data: IR (KBr, cm^{-1}): (νNH) 3352, (νRuCl) 295. ^1H NMR (400 MHz, $CDCl_3$, *J* in Hz) 7.22 – 6.83 (15 H, m, CH), 5.60 (4 H, bs, CH_{cym}), 5.03 (1 H, d, $^2J_{HH}$ = 13.0, NC*H*$_e$N), 4.35 – 4.12 (6 H, m, PC*H*$_2$N*H*, NC*H*$_a$N), 3.77 (2 H, d, $^2J_{HH}$ = 6.0, PC*H*$_2$NH), 2.77 (1 H, sept, , $^3J_{HH}$ = 6.8, CH), 2.03 (3 H, s, CH_3), 1.17 (6 H, d, $^3J_{HH}$ = 6.8, CH_3) ppm. $^{31}P\{^1H\}$ NMR (162 MHz, $CDCl_3$) 13.2 ppm. EI–MS (*m/z* $[MK]^+$) 706. $C_{32}H_{38}Cl_2N_3PRu{\cdot}CH_2Cl_2$ (752). EA found (calculated) (%): 53.10 (52.67), 5.27 (5.36), 5.49 (5.58). This compound was previously synthesised and the data here presented is in agreement with that observed for the reported compound.[16]

Preparation of $C_{41}H_{56}N_3PRuCl_2$ (3.12):

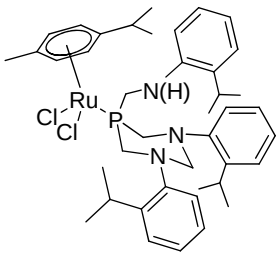

3.12

From **2.14** (0.100 g, 0.205 mmol) and $\{RuCl_2(\eta^6–p–cymene)\}_2$ (0.063g, 0.102 mmol). Yield: 0.137g, 83%. Selected data: IR (KBr, cm^{-1}): (νNH) 3364, (νRuCl) 297. ^1H NMR (400 MHz, $CDCl_3$, *J* in Hz) 7.19–6.68 (12 H, m, CH), 5.46 (2 H, d, $^3J_{HH}$ = 6.0, CH_{cym}), 5.40 (2 H, d, $^3J_{HH}$ = 6.0, CH_{cym}), 4.43 (2 H, d, $^2J_{HH}$ = 3.2, PC*H*$_e$NH), 4.13 (1 H, d, $^2J_{HH}$ = 10.4, NC*H*$_e$N), 3.91 – 3.82 (3 H, m, PC*H*$_e$N, NC*H*$_a$N), 3.76 – 3.71 (2 H, m, PC*H*$_a$N), 3.35 (1 H, sept, $^3J_{HH}$ = 6.8, CH_{cym}), 2.29 (1 H, sept, $^3J_{HH}$ = 6.8, CH), 2.29 (2 H, sept, $^3J_{HH}$ = 6.8, CH), 2.05 (3 H, s, CH_{3cym}), 1.19 (6 H, d, $^3J_{HH}$ = 6.8, CH_{3cym}), 1.09 (6H, d, $^3J_{HH}$ = 6.8 Hz, CH_3), 1.04 (6 H, d, $^3J_{HH}$ = 6.8, CH_3), 0.94 (6 H, d, $^3J_{HH}$ = 6.8, CH_3) ppm. $^{31}P\{^1H\}$ NMR (162

MHz, $CDCl_3$) 8.8 ppm. EI–MS (*m/z* $[MH]^+$) 794. A pure sample of **3.12** could not be obtained for elemental analysis despite drying the sample in the desiccator overnight.

Preparation of $C_{32}H_{35}N_3F_3PRuCl_2$ (3.13):

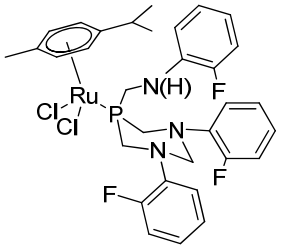

3.13

From **2.15** (0.100 g, 0.241 mmol) and $\{RuCl_2(\eta^6\text{–}p\text{–cymene})\}_2$ (0.074 g, 0.102 mmol). Yield: 0.125 g, 72%. Selected data: IR (KBr, cm^{-1}): (νNH) 3377 (bb), 3350, 3400, (νRuCl) 295. ^{1}H NMR (400 MHz, $CDCl_3$, *J* in Hz) 7.21 – 6.89 (10 H, m, CH), 6.66 (1 H, dd, $^3J_{HH}$ = 12.0, $^3J_{HH}$ = 7.0, *m*-CH), 6.54 (1 H, t, $^3J_{HH}$ = 8.3, *p*–CH), 5.58 (4 H, s, CH_{cym}), 4.67 (1 H, d, $^2J_{HH}$ = 12.4, NC*H*eN), 4.60 (1 H, s, NH), 4.56 (1 H, dd, $^2J_{HH}$ = 12.4, $^4J_{HP}$ = 3.8, NC*H*aN), 4.23 (4 H, s, PCH_2N), 4.11 (2 H, bs, PCH_2NH), 2.83 (1 H, sept, $^3J_{HH}$ = 6.9, CH_{cym}), 2.09 (3 H, s, CH_{3cym}), 1.23 (5 H, d, $^3J_{HH}$ = 6.9, CH_{3cym}) ppm. ^{31}P{^{1}H} NMR (162 MHz, $CDCl_3$) 12.9 ppm. EI–MS (*m/z* $[M\text{–}Cl]^+$) 686. $C_{32}H_{35}Cl_2N_3F_3PRu$ (720). EA found (calculated) (%): 52.04 (51.93), 4.61 (4.82), 5.77 (5.63).

Preparation of $C_{35}H_{44}N_3PRuCl_2$ (3.14):

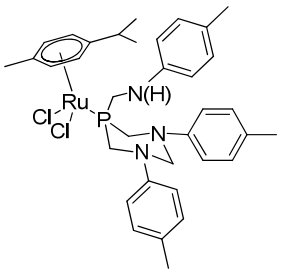

3.14

From **2.16** (0.800 g, 1.985 mmol) and $\{RuCl_2(\eta^6\text{–}p\text{–cymene})\}_2$ (0.479 g, 0.993 mmol). Yield: 0.997 g, 71%. Selected data: IR (KBr, cm^{-1}): (νNH) 3352, (νRuCl) 292. ^{1}H NMR (400 MHz, $CDCl_3$, *J* in Hz): 7.07 (4 H, d, $^3J_{HH}$ = 8.4, *m*-CH), 6.96 (4 H, d, $^3J_{HH}$ = 8.4, *o*-CH), 6.91 (2 H, d, $^3J_{HH}$ = 8.2, *m*-CH), 6.34 (2 H, d, $^3J_{HH}$ = 8.2, *o*-CH), 5.53 (4 H, s, CH_{cym}), 4.98 (1 H, d, $^2J_{HH}$ = 13.1, NCH_eN), 4.44 (1 H, dd, $^2J_{HH}$ = 13.1, $^4J_{HP}$ = 4.2, NCH_aN), 4.30 (3 H, dd, $^2J_{HH}$ = 14.8, $^2J_{HP}$ = 5.0, PCH_eN, N*H*), 4.18 (2 H, dd, $^2J_{HH}$ = 14.8, $^2J_{HP}$ = 5.0, PCH_aN), 3.85 (2 H, bs, PCH_2NH), 2.85 (1 H, sept, $^3J_{HH}$ = 6.9, CH_{cym}), 2.28 (6

H, s, CH_3), 2.23 (3 H, s, CH_3), 2.09 (3 H, s, CH_{3cym}), 1.25 (6 H, d, $^3J_{HH}$ = 6.9, CH_{3cym}) ppm. $^{31}P\{^1H\}$ NMR (162 MHz, $CDCl_3$) 13.2 ppm. EI–MS (*m/z* $[M–Cl]^+$) 674. $C_{35}H_{44}N_3PRuCl_2{\cdot}H_2O$ (728). EA found (calculated) (%): 57.79 (57.77), 5.94 (6.37), 5.81 (5.77).

Preparation of $C_{32}H_{35}N_3F_3PRuCl_2$ (3.15):

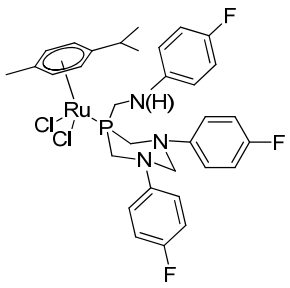

3.15

From **2.18** (0.100 g, 0.241 mmol) and $\{RuCl_2(\eta^6–p–cymene)\}_2$ (0.074 g, 0.121 mmol). Yield: 0.143 g, 83%. Selected data: ^1H NMR (400 MHz, $CDCl_3$, *J* in Hz) 6.97 (8 H, d, $^3J_{HH}$ = 6.1, *o*-,*m*-CH), 6.82 (2 H, vt, $^3J_{HH}$ = 8.3, *m*-CH), 6.34 (2 H, dd, $^3J_{HH}$ = 8.3, $^3J_{HH}$ = 3.9, *o*-CH), 5.56 (2 H, dd, $^3J_{HH}$ = 5.8, CH_{cym}), 5.52 (2 H, dd, $^3J_{HH}$ = 5.8, CH_{cym}), 4.88 (1 H, d, $^2J_{HH}$ = 13.4, NCH_eN), 4.63 (1 H, s, NH), 4.46 (1 H, dd, $^2J_{HH}$ = 13.1, $^4J_{HP}$ = 4.0, NCH_aN), 4.29 – 4.17 (4 H, m, PCH_2N), 3.84 (2 H, d, $^2J_{HP}$ = 5.9, PCH_2NH), 2.86 (1 H, sept, $^3J_{HH}$ = 6.9, CH_{cym}), 1.27 (8 H, d, $^3J_{HH}$ = 6.9, CH_{3cym}) ppm. $^{31}P\{^1H\}$ NMR (162 MHz, $CDCl_3$) 12.6 ppm. This compound was previously synthesised and the data here presented is in agreement with that observed for the reported compound.[16]

Preparation of $C_{60}H_{84}Cl_2N_6P_2Pt$ (3.16):

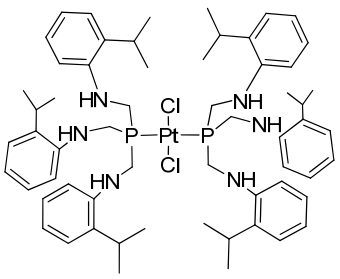

3.16

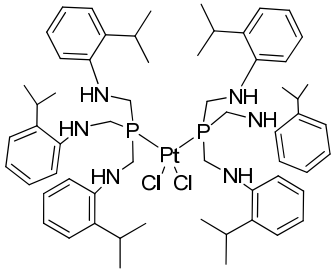

3.16a

From **2.27** (0.100 g, 0.210 mmol) and $PtCl_2COD$ (0.039 g, 0.105 mmol). Yield: 0.011 g, 8%. The filtrate was dried and the solid characterised by $^{31}P\{^1H\}$ and ^1H NMR which showed peaks corresponding to **3.16** and **3.16a**. Selected data: IR (KBr, cm^{-1}): (vNH) 3414, 3348, (vPtCl) 333. ^1H NMR (400 MHz, $CDCl_3$, *J* in Hz) 7.08 (6 H, d, $^3J_{HH}$ = 7.5, *o*-CH), 7.01 (6 H, t, $^3J_{HH}$ = 7.5, *m*-CH), 6.74 (6 H, t, $^3J_{HH}$ = 7.5, *p*-CH), 6.66 (6 H, d, $^3J_{HH}$ =

7.5, *o*-CH), 4.47 (6 H, t, $^3J_{HH}$ = 6.5, NH), 4.03 (12 H, d, $^3J_{HH}$ = 6.5, PC*H*$_2$NH), 2.74 (6 H, sept, $^3J_{HH}$ = 6.8, CH), 1.08 (36 H, d, $^3J_{HH}$ = 6.8, CH_3) ppm. $^{31}P\{^1H\}$ NMR (162 MHz, $CDCl_3$, *J* in Hz) 10.9 ($^1J_{PPt}$ = 2392) ppm. EI–MS (*m/z*, $[M–Cl]^+$) n.o. A pure sample of **3.16** could not be obtained for elemental analysis despite drying the sample in the desiccator overnight.

Preparation of $C_{60}H_{84}Cl_2N_6P_2Pt$ (3.16a):

From **2.27** (0.100 g, 0.210 mmol) and $PtCl_2COD$ (0.039 g, 0.105 mmol). Yield: 0.067 g, 64%. The filtrate was dried and the solid characterised by $^{31}P\{^1H\}$ and ^1H NMR which showed peaks corresponding to **3.16** and **3.16a**. Selected data: IR (KBr, cm^{-1}): (νNH) 3414, 3348, (νPtCl) 318, 298. ^1H NMR (400 MHz, $CDCl_3$, *J* in Hz) 8.04 (2 H, s, OH), 7.18 (7 H, dd, $^3J_{HH}$ = 7.5, $^4J_{HH}$ = 1.3, *m*-CH), 7.01 (6 H, dt, $^4J_{HH}$ = 1.3, $^3J_{HH}$ = 7.5, *m*-CH), 6.86 (7 H, t, $^3J_{HH}$ = 7.5, *p*-CH), 6.53 (6 H, d, $^3J_{HH}$ = 7.5, *o*-CH), 4.92 (6 H, s, NH), 4.05 (12 H, s, PC*H*$_2$NH), 2.98 (6 H, s, CH_3), 2.91 (6 H, s, CH_3), 2.86 (7 H, sept, $^3J_{HH}$ = 6.7, CH), 2.20 (6 H, s, CH_3), 1.12 (36 H, d, $^3J_{HH}$ = 6.7, CH_3) ppm. $^{31}P\{^1H\}$ NMR (162 MHz, $CDCl_3$, *J* in Hz) 9.1 ($^1J_{PPt}$ = 3446) ppm. In addition, single crystal X–ray diffraction for **2.16a** was obtained which supported the proposed structure. A pure sample of **3.16a** could not be obtained for elemental analysis despite drying the sample in the desiccator overnight. MS not recorded due to the poor solubility of **3.16a** in MeOH, acetonitrile or MeOH:H_2O.

Preparation of $C_{48}H_{42}N_6F_{18}P_2PtCl_2$ (3.17):

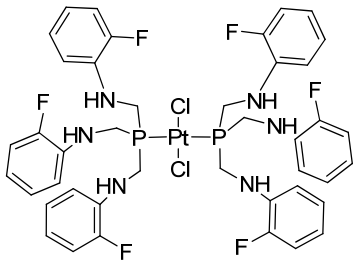

3.17

From **2.29** (0.100 g, 0.181 mmol) and $PtCl_2COD$ (0.034 g, 0.090 mmol). Yield: 0.066 g, 53%. Selected data: IR (KBr, cm^{-1}): (νNH) 3443, 3391, (νPtCl) 341. ^1H NMR (400 MHz, $CDCl_3$, *J* in Hz): 7.39 (3 H, dd, $^3J_{HH}$ = 7.3, $^4J_{HH}$ = 1.2, *m*-CH), 7.24 (3 H, dt, $^3J_{HH}$ = 7.3, $^4J_{HH}$ = 1.2, *m*-CH), 6.78 (3 H, d, $^3J_{HH}$ = 7.3, *o*-CH), 6.71 (6 H, t, $^3J_{HH}$ = 7.3, *p*-CH), 4.94 – 4.92 (4 H, m, NH), 4.10 (6 H, d, $^3J_{HH}$ = 6.3, PC*H*$_2$NH) ppm. $^{31}P\{^1H\}$ NMR (162 MHz, $CDCl_3$, *J* in Hz) 14.1 ($^1J_{PPt}$ = 2417) ppm. EI–MS (*m/z*) [**2.29a**K]$^+$ 608. A pure enough sample of **3.17** could not be obtained for elemental analysis.

Preparation of $C_{60}H_{72}N_6P_2PtCl_2$ (3.18):

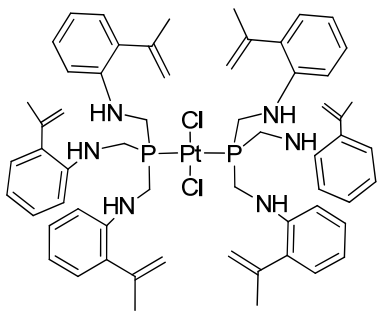

3.18

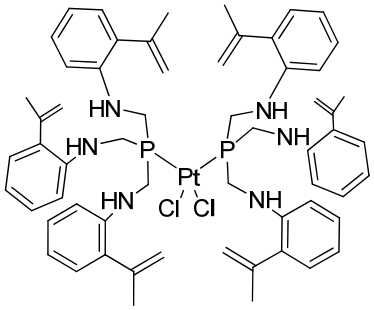

3.18a

From **2.30** (0.100 g, 0.253 mmol) and $\{RuCl_2(\eta^6\text{–}p\text{–cymene})\}_2$ (0.047 g, 0.127 mmol). Yield: 0.098 g, 74%. Selected data: IR (KBr, cm^{-1}): (νNH) 3367, 3324, (νPtCl) 317, 283. ^{1}H NMR (400 MHz, $CDCl_3$, *J* in Hz H **3.18a**, H' **3.18**) 7.16 – 6.73 (m, CH, CH'), 6.53 (3 H, d, $^3J_{HH}$ = 7.9, *o*-CH), 5.18 – 5.16 (m, CH, CH'), 5.01 – 5.00 (m, CH', NH), 4.92 (3 H, s, CH), 4.77 (s, NH'), 4.00 (bs, PCH_2NH, PCH'_2NH), 2.02 (s, CH'$_3$), 1.95 (9 H, s, CH_3) ppm. ^{31}P{^{1}H} NMR (162 MHz, $CDCl_3$, *J* in Hz) 11.5 ($^1J_{PPt}$ = 3393), 12.3 ($^1J_{PPt}$ = 2403) ppm (approx. 4:1 **3.18a:3.18**). EI–MS (*m/z,* $[M–Cl]^+$) 1168. A pure enough sample of **3.18** could not be obtained for elemental analysis.

Preparation of $C_{60}H_{84}N_6P_2PdCl_2$ (3.19):

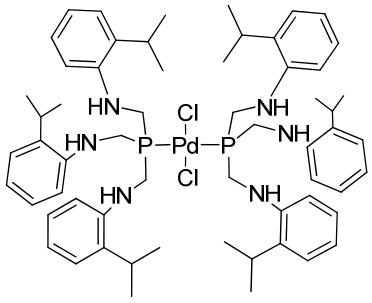

3.19

From **2.27** (0.100 g, 0.210 mmol) and $PdCl_2COD$ (0.030 g, 0.105 mmol). Yield: 0.088 g, 84%. Selected data: IR (KBr, cm^1): (νNH) 3408, 3341, (νPdCl) 329, 305. ^{1}H NMR (400 MHz, $CDCl_3$, *J* in Hz) 7.09 (6 H, dd, $^3J_{HH}$ = 7.5, $^4J_{HH}$ = 1.3, *m*-CH), 7.04 – 6.98 (6 H, $^3J_{HH}$ = 6.6, $^4J_{HH}$ = 1.3, *m*-CH), 6.73 (6 H, t, $^3J_{HH}$ = 7.5, $^4J_{HH}$ = 1.3, *p*-CH), 6.66 (6 H, d, $^3J_{HH}$ = 7.5, *o*-CH), 4.51 (6 H, t, $^3J_{HH}$ = 6.5, NH), 3.98 (10 H, d, $^3J_{HH}$ = 6.5, PCH_2NH), 2.73 (6 H, $^3J_{HH}$ = 6.80, CH), 1.09 (36 H, d, $^3J_{HH}$ = 6.8, CH_3). ^{31}P{^{1}H} NMR (162 MHz, $CDCl_3$): 16.3 ppm. EI–MS (*m/z*) $[M–Cl]^+$ n.o., $[\mathbf{2.27}K]^+$ 514. $C_{60}H_{84}Cl_2N_6P_2Pd{\cdot}3KCl$ (1326). EA found (calculated, %): C 53.20 (53.29), H 5.75 (6.26), N 5.93 (6.21). The inclusion of KCl in the formula came from the excess of KO^{t}Bu using in the reaction to obtain **2.27**, with the

chloride counter ion from the phosphonium salt **2.3**. KCl was not observed in the single X–ray structure of **3.19**.

Preparation of $C_{48}H_{42}N_6F_{18}P_2PdCl_2$ (3.20):

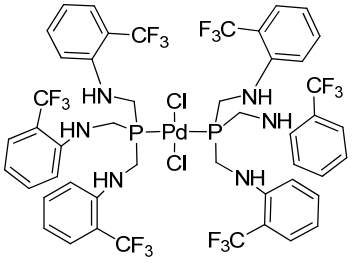

3.20

From **2.29** (0.100 g, 0.180 mmol) and $PdCl_2COD$ (0.026 g, 0.090 mmol). Yield: 0.064 g, 55%. Selected data: IR (KBr, cm^1): (νNH) 3445, 3425, ν(PdCl) 317. ^1H NMR (400 MHz, $CDCl_3$, *J* in Hz) 7.39 (3 H, dd, $^3J_{HH}$ = 7.6, $^4J_{HH}$ = 1.1, *m*–CH), 7.25 (3 H, dt, $^3J_{HH}$ = 7.6, $^4J_{HH}$ = 1.1, *m*–CH), 6.80 (3 H, d, $^3J_{HH}$ = 7.6, *o*–CH), 6.72 (3 H, t, $^3J_{HH}$ = 7.6, *p*–CH), 4.84 (3 H, vt, $^3J_{HH}$ = 6.3, NH), 3.96 (6 H, d, $^3J_{HH}$ = 6.3, PC*H*$_2$NH) ppm. $^{31}P\{^1H\}$ NMR (162 MHz, $CDCl_3$) 18.8 ppm. EI–MS (*m/z*) $[MH]^+$ 1285. $C_{48}H_{42}N_6F_{18}P_2PdCl_2 \cdot 3KCl$ (1580). EA found (calculated, %): C 36.49 (36.44), H 2.42 (2.68), N 5.04 (5.31). The inclusion of KCl in the formula came from the excess of KO^{t}Bu using in the reaction to obtain **2.29**, with the chloride counter ion from the phosphonium salt **2.6**. KCl was not observed in the single X–ray structure of **3.20**.

Preparation of $C_{60}H_{72}N_6P_2PdCl_2$ (3.21):

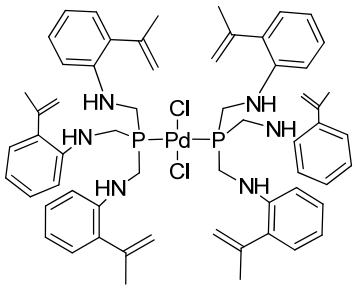

3.21

From **2.30** (0.100 g, 0.212 mmol) and $PdCl_2COD$ (0.030 g, 0.106 mmol). Yield: 0.025 g, 22%. Selected data: IR (KBr, cm^1): (νNH) 3380, 3401, 3358, ν(PdCl) 275. ^1H NMR (400 MHz, $CDCl_3$, *J* in Hz) 7.15 (6 H, td, $^3J_{HH}$ = 7.9, 1.4, *m*-CH), 7.05 (6 H, dd, $^3J_{HH}$ = 7.5, 1.4, *m*-CH), 6.77 (12 H, vt, $^3J_{HH}$ = 7.6, *o*-, *p*-CH), 5.20 (6 H, d, $^3J_{HH}$ = 1.0, CH), 5.01 (6 H, d, $^3J_{HH}$ = 1.0, CH), 4.78 (6 H, t, $^3J_{HH}$ = 6.8, NH), 3.94 (12 H, d, $^3J_{HH}$ = 6.8, PC*H*$_2$NH), 2.03 (18 H, s, CH_3) ppm. $^{31}P\{^1H\}$ NMR (162 MHz, $CDCl_3$, *J* in Hz): 17.0 ppm. EI–MS (*m/z*)

$[MH]^+$ n.o. $C_{60}H_{72}N_6P_2PdCl_2{\cdot}2H_2O$ (1134). EA found (calculated) (%): C 62.52 (62.53), H 6.39 (6.65), N 7.17 (7.29). In addition, X–ray structure was obtained for **3.21**.

Preparation of $C_{31}H_{38}Cl_2N_3PRu$ (3.22):

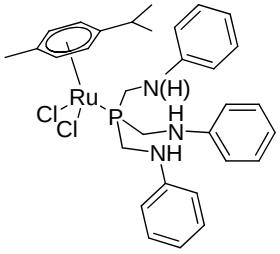

3.22

From **2.26** (0.100 g, 0.277 mmol) and $\{RuCl_2(\eta^6\text{–}p\text{–cymene})\}_2$ (0.087g, 0.143 mmol. Yield: 0.170 g, 90%. Selected data: IR (KBr, cm^{-1}): (νNH) 3327, (νRuCl) 282. ^{1}H NMR (400 MHz, $CDCl_3$, *J* in Hz) 7.05 (6 H, t, $^3J_{HH}$ = 7.7, *m*-CH), 6.65 (3 H, t, $^3J_{HH}$ = 7.7, *p*-CH), 6.53 (6 H, d, $^3J_{HH}$ = 7.7, *o*-CH), 5.50 (2 H, d, $^3J_{HH}$ = 5.8, CH_{cym}), 5.41 (2 H, d, $^3J_{HH}$ = 5.8, CH_{cym}), 4.71 (3 H, bs, NH), 3.91 (6 H, bs, PC*H*$_2$NH), 2.73 (1 H, sept, $^3J_{HH}$ = 8.0, CH_{cym}), 2.01 (3 H, s, CH_{3cym}), 1.14 (6 H, m, CH_{3cym}) ppm. $^{31}P\{^1H\}$ NMR (162 MHz, $CDCl_3$): 25.1 ppm. EI–MS (*m/z*) $[M–Cl]^+$ 620. $C_{31}H_{38}Cl_2N_3PRu{\cdot}2KCl$ (803). EA found (calculated) (%): C 45.02 (46.27), H 4.39 (4.76), N 4.59 (5.22). The inclusion of KCl in the formula came from the excess of KO^{t}Bu using in the reaction to obtain **2.26**, with the chloride counter ion from the phosphonium salt **2.1**.

Preparation of $C_{40}H_{59}N_3PRuCl_2$ (3.23):

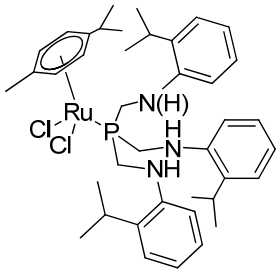

3.23

From **2.27** (0.100 g, 0.211 mmol) and $\{RuCl_2(\eta^6\text{–}p\text{–cymene})\}_2$ (0.064g, 0.105 mmol). Yield: 0.136 g, 82%. Selected data: IR (KBr, cm^{-1}): (νNH) 3343, (νRuCl) 290. ^{1}H NMR (400 MHz, $CDCl_3$, *J* in Hz) 7.06 (3 H, dd, $^3J_{HH}$ = 7.6, $^4J_{HH}$=1.3, *o*-CH), 6.93 (3 H, t, $^3J_{HH}$ = 7.6, $^4J_{HH}$=1.3, *m*-CH), 6.69 (3 H, t, $^3J_{HH}$ = 7.6, *p*-CH), 6.56 (3 H, d, $^3J_{HH}$ = 7.6, *o*-CH), 5.50 (2 H, d, $^3J_{HH}$ = 5.9, CH_{cym}), 5.40 (2 H, d, $^3J_{HH}$ = 5.9, CH_{cym}), 4.86 (3 H, t, $^3J_{HH}$ = 2.7, NH), 4.03 (6 H, d, $^3J_{HH}$ = 2.7, PC*H*$_2$NH), 2.74 (4 H, 2 sept, $^3J_{HH}$ = 6.8, CH, CH_{cym}), 2.03

(3 H, s, CH_{3cym}), 1.03 (18 H, d, $^3J_{HH}$ = 6.8, CH_3) ppm. $^{31}P\{^1H\}$ NMR (162 MHz, $CDCl_3$): 23.4 ppm. EI–MS (*m/z*) $[MH]^+$ 782, $[MK]^+$ 820. $C_{40}H_{59}N_3PRuCl_2 \cdot 1.5KCl$ (896). EA found (calculated) (%): C 53.32 (53.58), H 5.82 (6.63), N 4.50 (4.69). The inclusion of KCl in the formula came from the excess of KO^{t}Bu using in the reaction to obtain **2.27**, with the chloride counter ion from the phosphonium salt **2.3**.

Preparation of $C_{44}H_{65}N_3PRuCl_2$ (3.24):

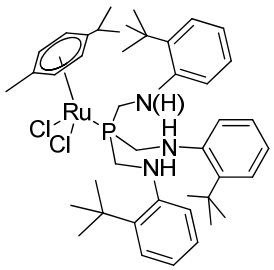

3.24

From **2.28** (0.100 g, 0.193 mmol) and $\{RuCl_2(\eta^6\text{–}p\text{–cymene})\}_2$ (0.059 g, 0.097 mmol). Yield: 0.120 g, 76%. Selected data: IR (KBr, cm^{-1}): (νNH) 3367, (νRuCl) 296. ^1H NMR (400 MHz, $CDCl_3$, *J* in Hz) 7.28 – 6.66 (12 H, m, CH), 5.60 (2 H, d, $^3J_{HH}$ = 5.6, CH_{cym}), 5.55 (2 H, d, $^3J_{HH}$ = 5.6, CH_{cym}) 4.81 (3 H, bs, NH), 4.20 (6 H, d, $^3J_{HH}$ = 2.8, PC*H*$_2$NH), 2.17 (3 H, s, CH_{3cym}), 1.40 – 1.27 (27 H, m, CH_3) ppm. $^{31}P\{^1H\}$ NMR (162 MHz, $CDCl_3$): 24.9, 7.9 (11:1) ppm. EI–MS (*m/z*) $[MH]^+$ 824, $[M–Cl]^–$ 788. $C_{44}H_{65}N_3PRuCl_2 \cdot 0.25CH_2Cl_2 \cdot 0.5H_2O$ (890). EA found (calculated) (%): C 61.07 (61.15), H 7.44 (7.71), N 4.88 (4.83).

Preparation of $C_{34}H_{35}N_3F_9PRuCl_2$ (3.25):

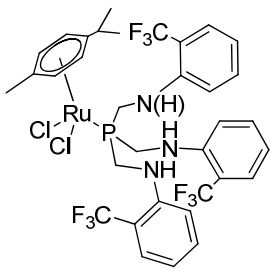

3.25

From **2.29** (0.153 g, 0.278 mmol) and $\{RuCl_2(\eta^6\text{–}p\text{–cymene})\}_2$ (0.055g, 0.139 mmol). Yield: 0.108 g, 45%. Selected data: IR (KBr, cm^{-1}): (νNH) 3468, 3442, (νRuCl) 335. ^1H NMR (400 MHz, $CDCl_3$, *J* in Hz): 7.66 – 6.67 (12 H, m, CH), 5.52 (2 H, d, $^3J_{HH}$ = 5.6, CH_{cym}), 5.40 (2 H, d, $^3J_{HH}$ = 5.6, CH_{cym}) 5.02 (3 H, s, NH), 4.00 (6 H, s, PC*H*$_2$NH), 2.81 (1

H, sept, $^{3}J_{HH}$ = 6.8, $CH_{cym,}$), 2.02 (3 H, s, CH_{3cym}), 1.17 (6 H, d, $^{3}J_{HH}$ = 6.8, CH_{3cym}) ppm. $^{31}P\{^{1}H\}$ NMR (162 MHz, $CDCl_3$): 28.8 ppm. EI–MS (*m/z*) $[MH]^+$ 860, $[MK]^+$ 898. $C_{34}H_{35}N_3F_9PRuCl_2 \cdot 1.75KCl$ (989). EA found (calculated) (%): C 41.25 (41.83), H 3.56 (3.00), N 4.24 (4.49). The inclusion of KCl in the formula came from the excess of KO^{t}Bu using in the reaction to obtain **2.29**, with the chloride counter ion from the phosphonium salt **2.6**. KCl was not observed in the single X–ray structure of **3.25**.

Preparation of $C_{40}H_{50}N_3PRuCl_2$ (3.26):

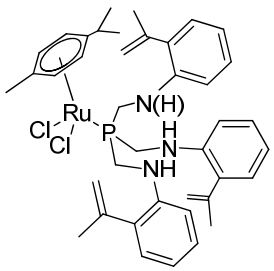

3.26

From **2.30** (0.100 g, 0.213 mmol) and $\{RuCl_2(\eta^6\text{–}p\text{–cymene})\}_2$ (0.065 g, 0.107 mmol). Yield: 0.147 g, 89%. Selected data: IR (KBr, cm^{-1}): (νNH) 3317, (νRuCl) 294. ^{1}H NMR (400 MHz, $CDCl_3$, *J* in Hz) 7.00 (3 H, td, $^{3}J_{HH}$ = 7.8, $^{4}J_{HH}$ =1.5, *m*–CH), 6.93 (3 H, dd, $^{3}J_{HH}$ = 7.8, $^{4}J_{HH}$ =1.5, *m*–CH), 6.65 (3 H, td, $^{3}J_{HH}$ = 7.8, $^{4}J_{HH}$ = 0.8, *p*–CH), 6.56 (3 H, d, $^{3}J_{HH}$ = 7.8, *o*–CH), 5.45 (2 H, d, $^{3}J_{HH}$ = 5.9, CH_{cym}), 5.37 (2 H, d, $^{3}J_{HH}$ = 5.9, CH_{cym}), 5.05 (3 H, s, CH), 4.99 (3 H, bs, NH), 4.81 (3 H, s, CH), 4.01 (6 H, d, $^{3}J_{HH}$ = 1.1, PCH_2NH), 2.75 (1 H, sept, $^{3}J_{HH}$ = 6.9, CH_{cym}), 1.99 (3 H, s, CH_{3cym}), 1.88 (9 H, s, CH_3), 1.13 (6 H, d, $^{3}J_{HH}$ = 6.9, CH_{3cym}) ppm. $^{31}P\{^{1}H\}$ NMR (162 MHz, $CDCl_3$) 26.0 ppm. EI–MS (*m/z*) $[M–Cl]^+$ 740. $C_{40}H_{50}N_3PRuCl_2 \cdot 0.5CH_2Cl_2$ (817). EA found (calculated) (%): 59.97 (59.45), 5.96 (6.28), 5.35 (5.14).

Preparation of $C_{32}H_{36}N_4P_4Pt_2Cl_4$ (3.27b):

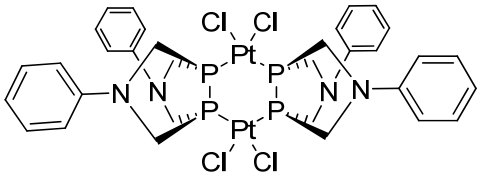

3.27b

From **2.31** (0.016 g, 0. 053 mmol) and $PtCl_2COD$ (0.020 g, 0.053 mmol) were dissolved in $CDCl_3$ (0.7 ml) and stirred for 5 min. at r.t. A green solid formed overtime in the yellow

solution. ^{1}H NMR (400 MHz, $CDCl_3$, *J* in Hz) poor solubility in $CDCl_3$ therefore no meaningful spectrum could be obtained. $^{31}P\{^{1}H\}$ NMR ($CDCl_3$): discussed in Chapter 3, Section 3.8.

Preparation of $C_{36}H_{44}N_4P_4Pt_2Cl_4$ (3.28b):

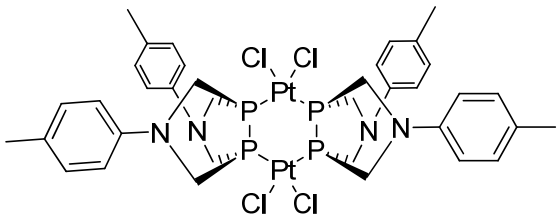

3.28b

From **2.32** (0.018 g, 0. 053 mmol) and $PtCl_2COD$ (0.020 g, 0.053 mmol) were dissolved in $CDCl_3$ (0.7 ml) and stirred for 5 min. at r.t. A colourless solid formed overtime in the yellow solution. ^{1}H NMR (400 MHz, $CDCl_3$, *J* in Hz) poor solubility in $CDCl_3$ therefore no meaningful spectrum could be obtained. $^{31}P\{^{1}H\}$ NMR (162 MHz, $CDCl_3$, *J* in Hz): discussed in Chapter 3, Section 3.8.

Preparation of $C_{44}H_{60}N_4P_4Pt_2Cl_4$ (3.29b):

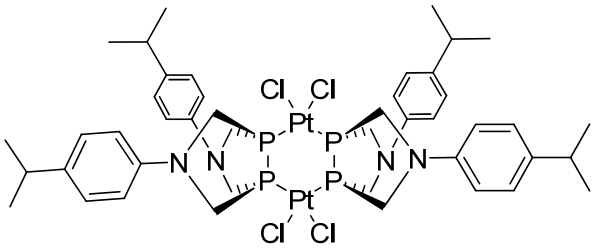

3.29b

From **2.33** (0.010 g, 0. 026 mmol) and $PtCl_2COD$ (0.010 g, 0.026 mmol) were dissolved in $CDCl_3$ (0.7 ml) and stirred for 5 min. at r.t. An orange solution was obtained. ^{1}H NMR (400 MHz, $CDCl_3$, *J* in Hz) 7.11 (4 H, d, $^{3}J_{HH}$ = 8.4, *m*-CH), 6.98 (4 H, d, $^{3}J_{HH}$ = 8.4, *o*-CH), 5.52 (4 H, CH_{COD}), 4.06 (8 H, bs, PCH_2N), 2.70 (2 H, sept, $^{3}J_{HH}$ = 7.2, CH), 2.30 (8 H, s, CH_{2COD}), 1.03 (12 H, d, $^{3}J_{HH}$ = 7.2, CH_3) ppm. $^{31}P\{^{1}H\}$ NMR (162 MHz, $CDCl_3$, *J* in Hz): discussed in Chapter 3, Section 3.8.

Preparation of $[C_{16}H_{18}N_2P_2]_nCr(CO)_m$ (n =1, m = 4, 5; n = 2, m = 2) (3.30a – 3.30e):

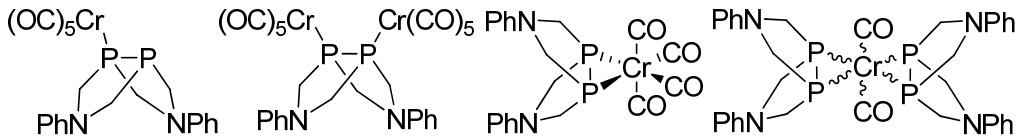

3.30a **3.30b** **3.30c** **3.30d**

From **2.31** (0.007 g, 0. 023 mmol) and $Cr(CO)_6$ (0.005 g, 0.053 mmol) dissolved in $CDCl_3$ (0.7 ml), stirred for 12 h at r.t. and for further 12 h at 50°C. A red solution was obtained due to the unreacted $Cr(CO)_6$ (red) and **2.31** (colourless).

Preparation of $C_{26}H_{48}N_2P_2Rh_2Cl_4$ (3.31):

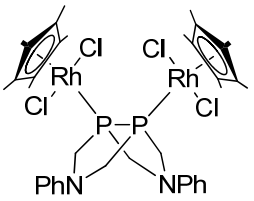

3.31a

From **2.31** (0.010 g, 0.033 mmol) and $\{RhCl_2(\eta^5\text{–}C_5Me_5)\}_2$ (0.021 g, 0.033 mmol) dissolved in $CDCl_3$ (0.7 ml) and stirred for 5 min. A red solution was formed. ^{1}H NMR (400 MHz, $CDCl_3$, *J* in Hz) 7.23 (4 H, t, $^3J_{HH}$ = 8.0, *m*-CH), 6.91 (4 H, d, $^3J_{HH}$ = 8.0, *o*-CH), 6.86 (2 H, t, $^3J_{HH}$ = 8.0, *p*-CH), 4.37 (8 H, bs, PC*H*$_2$N), 1.80 (30 H, s, CH_3) ppm. $^{31}P\{^1H\}$ NMR (162 MHz, $CDCl_3$, *J* in Hz): discussed in Chapter 3, Section 3.8. EI–MS (m/z $[M–Cl]^+$) 881, (m/z $[M–2Cl]^{+2}$) 423.

Preparation of $C_{28}H_{52}N_2P_2Rh_2Cl_4$ (3.32):

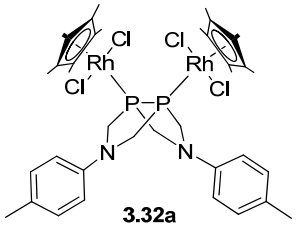

3.32a

From **2.32** (0.010 g, 0. 030 mmol) and $\{RhCl_2(\eta^5\text{–}C_5Me_5)\}_2$ (0.019 g, 0.030 mmol) dissolved in $CDCl_3$ (0.7 ml) and stirred for 5 min. A red solution was formed. ^{1}H NMR (400 MHz, $CDCl_3$, *J* in Hz) 7.01 (4 H, d, $^3J_{HH}$ = 3.4, *m*-CH), 6.81 (4 H, d, $^3J_{HH}$ = 3.4, *o*-CH), 4.27 (8 H, bs, PC*H*$_2$N), 2.23 (6 H, s, CH_3), 1.80 (30 H, s, CH_3) ppm. $^{31}P\{^1H\}$ NMR (162 MHz, $CDCl_3$, *J* in Hz): discussed in Chapter 3, Section 3.8. EI–MS (m/z $[M–Cl]^+$) 909, (m/z $[M–2Cl]^{+2}$) 437.

Preparation or $C_{35}H_{32}N_3F_3P_2PtCl_2$ (3.33):

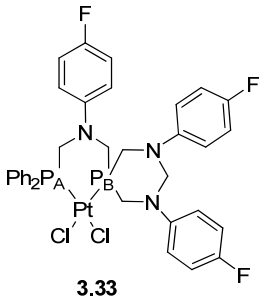

3.33

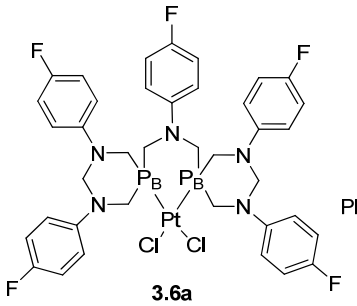

3.6a

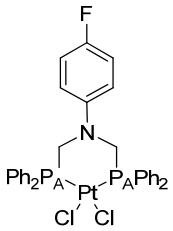

3.34

From **2.40** (0.263 g, 0.429 mmol) and $PtCl_2$(COD) (0.160 g, 0.429 mmol). Selected data: $^{31}P\{^1H\}$ NMR (162 MHz, $CDCl_3$, *J* in Hz): –6.0 ($^1J_{PPt}$ = 3420, **3.34**), –8.5 ($^1J_{PPt}$ = 3450, $^2J_{PP}$ = 13, P_A, **3.33**), –22.9 ($^1J_{PPt}$ = 3201, $^2J_{PP}$ = 15, P_B, **3.33**), –23.7 ($^1J_{PPt}$ = 3217, **3.6a**) (approx. 1:3:1) ppm.

Preparation of $C_{35}H_{34}N_3OF_3P_2PtCl_2$ (3.35):

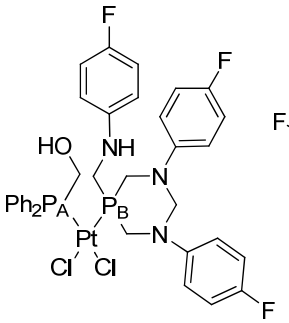

3.35

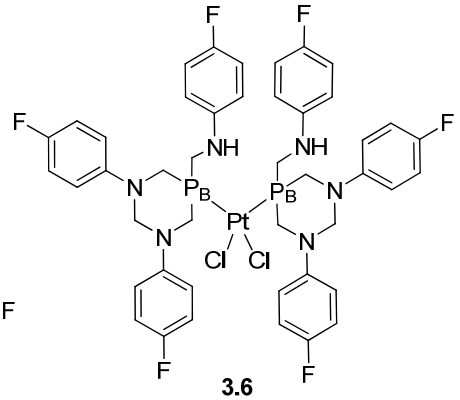

3.6

From **2.18** (0.250 g, 0.602 mmol), Ph_2PCH_2OH (0.130 g, 0.602 mmol), $PtCl_2COD$ (0.225 g, 0.602 mmol). Selected data: ^1H NMR (400 MHz, $CDCl_3$, *J* in Hz): 7.87 – 6.39 (m, CH), 4.71 – 3.34 (m, CH_2) ppm. $^{31}P\{^1H\}$ NMR (162 MHz, $CDCl_3$, *J* in Hz): 7.2 [$^1J_{PPt}$ = 3712, ***cis*–$PtCl_2(Ph_2PCH_2OH)_2$**], 5.3 ($^1J_{PPt}$ = 3693, $^2J_{PP}$ = 15, P_A, **3.35**), –9.3 ($^1J_{PPt}$ = 3427, **3.6**), –12.3 ($^1J_{PPt}$ = 3356, $^2J_{PP}$ = 15, P_B, **3.35**), (approx. 3:16:1) ppm. EI–MS (*m/z*) $[M–Cl]^+$ 861.

Preparation of $C_{35}H_{37}N_3OP_2PtCl_2$ (3.36):

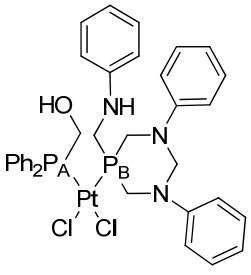

3.36

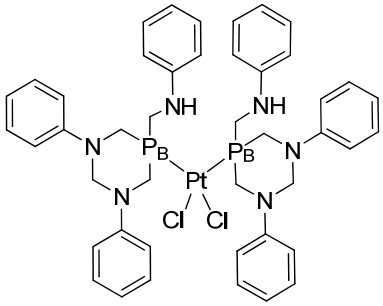

3.1

From **2.12** (0.125 g, 0.346 mmol) and Ph_2PCH_2OH (0.075 g, 0.346 mmol) were dissolved in CH_2Cl_2 (10 ml) separately and then added dropwise simultaneously to a solution of $PtCl_2COD$ (0.129 g, 0.346 mmol) in CH_2Cl_2 (15 ml) for a period of 5 min. The yellow solution was stirred at r.t. for 1 h. The solid was dried under vacuum after precipitation with hexanes upon concentration of the solution. Selected data: ^1H NMR (400 MHz, $CDCl_3$, *J* in Hz): 7.77 – 6.34 (m, CH), 4.72 – 3.20 (m, CH_2), 2.30 – 2.03 (m, *hexane*) ppm. $^{31}P\{^1H\}$ NMR (162 MHz, $CDCl_3$, *J* in Hz): 7.2 [$^1J_{PPt}$ = 3712, ***cis*–PtCl$_2$(Ph$_2$PCH$_2$OH)$_2$**], 5.5 ($^1J_{PPt}$ = 3742, $^2J_{PP}$ = 15, P_A, **3.36**), –6.6 ($^1J_{PPt}$ = 3395, **3.1**), –11.1 ($^1J_{PPt}$ = 3285, $^2J_{PP}$ = 15, P_B, **3.36**), –24.0 ($^1J_{PPt}$ = 3181) (approx. 2:8:1:1) ppm. EI–MS (*m/z*) $[MH]^+$ n.o., $[PtCl_2(Ph_2PCH_2OH)_2HK–Cl]^+$ 703.

Preparation of $C_{44}H_{55}N_3OP_2PtCl_2$ (3.37):

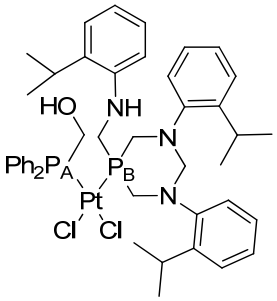

3.37

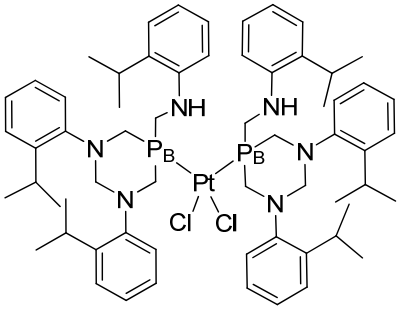

3.2

Same procedure as **3.36**. From **2.14** (0.097 g, 0.199 mmol), Ph_2PCH_2OH (0.043 g, 0.199 mmol), $PtCl_2COD$ (0.074 g, 0.199 mmol). Selected data: ^1H NMR ($CDCl_3$, *J* in Hz): 7.74 – 6.65 (m, CH), 4.66 – 2.90 (m, CH_2), 1.17 – 0.98 (m, *hexane*) ppm. $^{31}P\{^1H\}$ NMR ($CDCl_3$, *J* in Hz): 7.2 [$^1J_{PPt}$ = 3712, ***cis*–PtCl$_2$(Ph$_2$PCH$_2$OH)$_2$**], 5.4 ($^1J_{PPt}$ = 3696, $^2J_{PP}$ = 16, P_A, **3.37**), –6.0 ($^1J_{PPt}$ = 3431, **3.2**), –12.7 ($^1J_{PPt}$ = 3146, $^2J_{PP}$ = 16, P_B, **3.37**) (approx. 1:4:1) ppm. EI–MS (*m/z*) $[M]^+$ n.o.

Preparation of $C_{35}H_{34}N_3OF_3P_2PtCl_2$ (3.38):

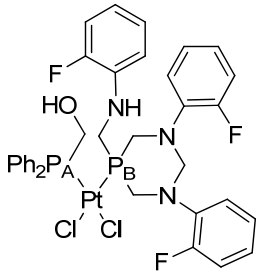

3.38

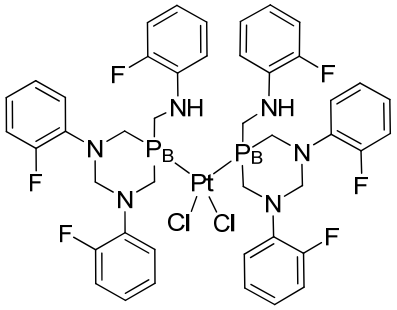

3.3

Same procedure as **3.36**. From **2.15** (0.125 g, 0.301 mmol), Ph_2PCH_2OH (0.065 g, 0.301 mmol), $PtCl_2COD$ (0.113 g, 0.301 mmol). Selected data: ^1H NMR (400 MHz, 162 MHz, $CDCl_3$, *J* in Hz): 7.79 – 6.71 (m, CH), 4.60 – 3.10 (m, CH_2) ppm. $^{31}P\{^1H\}$ NMR ($CDCl_3$, *J* in Hz): 7.2 [$^1J_{PPt}$ = 3712, ***cis*-PtCl$_2$(Ph$_2$PCH$_2$OH)$_2$**], 5.1 ($^1J_{PPt}$ = 3735, $^2J_{PP}$ = 15, P_A, **3.38**), –11.9 ($^1J_{PPt}$ = 3363, **3.3**), –16.3 ($^1J_{PPt}$ = 3311, $^2J_{PP}$ = 15, P_B, **3.38**), (approx. 2:3:2) ppm. EI–MS (*m/z*) $[M]^+$ n.o.

Preparation of $C_{38}H_{43}N_3OP_2PtCl_2$ (3.39):

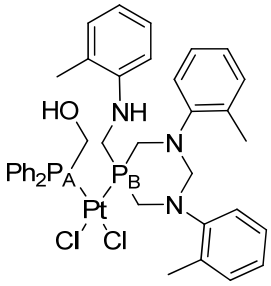

3.39

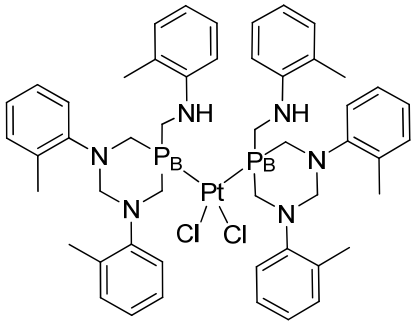

3.4

Same procedure as **3.36**. From **2.16** (0.125 g, 0.310 mmol), Ph_2PCH_2OH (0.067 g, 0.310 mmol), $PtCl_2COD$ (0.116 g, 0.310 mmol). Selected data: ^1H NMR (400 MHz, $CDCl_3$, *J* in Hz): 7.78 – 6.34 (m, CH), 4.72 – 2.92 (m, CH_2), 2.31 – 2.17 (m, *hexane*) ppm. $^{31}P\{^1H\}$ NMR (162 MHz, $CDCl_3$, *J* in Hz): 7.2 [$^1J_{PPt}$ = 3712, ***cis*-PtCl$_2$(Ph$_2$PCH$_2$OH)$_2$**], 5.5 ($^1J_{PPt}$ = 3965, $^2J_{PP}$ = 15, P_A, **3.39**), –6.62 ($^1J_{PPt}$ = 3394, **3.4**), –11.9 ($^1J_{PPt}$ = 3285, $^2J_{PP}$ = 15, P_B, **3.39**) (approx. 2:7:1) ppm. EI–MS (*m/z*) $[M–Cl]^+$ 849.

Preparation of $C_{43}H_{55}N_3OP_2PtCl_2$ (3.40):

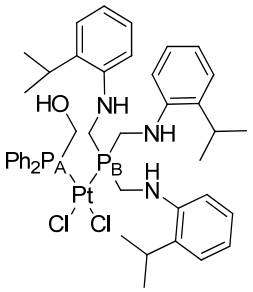

3.40

Same procedure as **3.36**. From **2.27** (0.095 g, 0.199 mmol), Ph_2PCH_2OH (0.043 g, 0.199 mmol), $PtCl_2COD$ (0.074 g, 0.199 mmol). Selected data: ^1H NMR (400 MHz, $CDCl_3$, *J* in Hz) 7.98 – 6.12 (m, CH), 4.53 – 4.44 (m, PCH_2OH), 3.61 (6 H, d, $^2J_{HP}$ = 1.62, PCH_2NH), 2.71, (1 H, d, $^3J_{HH}$ = 3.24, CH), 1.29 – 0.86 (m, CH_3 + *hexane*) ppm. $^{31}P\{^1H\}$ NMR (162

MHz, $CDCl_3$, *J* in Hz): 7.2 ($^1J_{PPt}$ = 3712, ***cis*-$PtCl_2(Ph_2PCH_2OH)_2$**], 5.7 ($^1J_{PPt}$ = 3340, $^2J_{PP}$ = 16, P_A, **3.40**), 5.0 ($^1J_{PPt}$ = 3657, $^2J_{PP}$ = 16, P_B, **3.40**), (approx. 1:9) ppm.

Preparation of $C_{57}H_{55}N_6OF_6P_3PtCl_2$ (3.41):

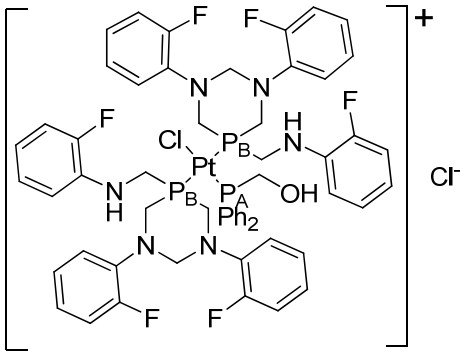

3.41

From **3.3** (0.090 g, 0.082 mmol) and Ph_2PCH_2OH (0.018 g, 0.082 mmol) were dissolved in 5 ml of CH_2Cl_2 and stirred for 1 h at r.t. The solid was dried under vacuum after precipitation with Et_2O (10 ml) upon concentration of the solution. Yield: 0.067 g, 62%. Selected data: IR (KBr, cm^{-1}): (νNH) 3424, (νPtCl) 301. ^{1}H NMR (400 MHz, $CDCl_3$, *J* in Hz) 7.85 (1 H, s, OH/NH), 7.42 – 6.62 (34 H, m, CH), 5.33 (2 H, vs, PC*H*$_2$OH), 4.61 (4 H, vs, PC*H*$_2$NH), 4.46 (4 H, d, *J* 15.3, CH_2), 4.26 (4 H, d, *J* 6.5, CH_2), 4.15 (2 H, s, OH/NH), 3.55 (4 H, d, *J* 13.2, CH_2) ppm. ^{31}P{^{1}H} NMR (162 MHz, $CDCl_3$, *J* in Hz) 1.0 (1 P, t, $^1J_{PPt}$ = 3682, $^2J_{PP}$ = 17, P_A), –10.5 (2 P, d, $^1J_{PPt}$ = 2243, $^2J_{PP}$ = 17, P_B) ppm. EI–MS (*m/z*) $[M–Cl]^+$ 1276, $[MH–2Cl]^+$ 1242. $C_{57}H_{55}N_6OF_6P_3PtCl_2 \cdot H_2O$ 1329. EA found (calculate) (%): C 51.53 (51.44), H 4.19 (4.32), N 6.40 (6.31).

Preparation of $C_{57}H_{55}N_6OF_6P_3PtCl_2$ (3.42):

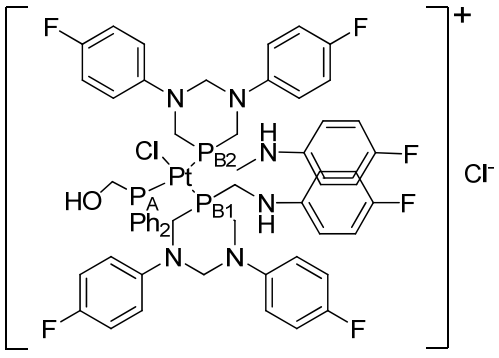

3.42

Compound **3.6** (0.100 g, 0.091 mmol) and Ph_2PCH_2OH (0.020 g, 0.091 mmol) were dissolved in 5 ml of CH_2Cl_2 and stirred for 1 h at r.t. The solid was dried under vacuum after precipitation with Et_2O (10 ml) upon concentration of the solution. Yield: 0.100 g, 84%. Selected data: IR (KBr, cm^{-1}): (νNH) 3234, (νPtCl) 301. ^{1}H NMR (400 MHz, $CDCl_3$,

J in Hz): 8.06 – 6.34 (34 H, m, CH), 4.86 (1 H, d, $^{2}J_{HH}$ = 14.3, NC*H*eN), 4.78 (1H, d, $^{2}J_{HH}$ = 12.8, NC*H*eN), 4.64 (2 H, d, *J* 14.9, 3, CH_2), 4.50 – 4.37 (6 H, m, CH_2), 4.29 (2 H, vs, CH_2), 4.02 (1 H, dd, $^{2}J_{HH}$ = 12.8, $^{4}J_{HP}$ = 4.6, NC*H*aN), 3.74 (2 H, vd, *J* 5.0, CH_2), 3.59 (2 H, bs, CH_2), 3.27 (1 H, dd, $^{2}J_{HH}$ = 14.3, $^{4}J_{HP}$ = 6.4, NC*H*aN), 1.69 (2 H, s, OH+NH/OH) ppm. $^{31}P\{^{1}H\}$ NMR (162 MHz, $CDCl_3$, *J* in Hz): –9.2 (1 P, dd, $^{1}J_{PAPt}$ = 2307, $^{2}J_{PAPB1}$ = 16, $^{2}J_{PAPB2}$ = 326, P_A), –13.4 (1 P, vt, $^{1}J_{PB1Pt}$ = 3714, $^{2}J_{PB1PB2}$ = 16, P_{B1}), –26.0 (1 P, dd, $^{1}J_{PB2Pt}$ = 2321, $^{2}J_{PB1PB2}$ = 16, $^{2}J_{PAPB2}$ = 326, P_{B2}) ppm. EI–MS (*m/z*) $[M–Cl]^+$ 1276, $[MH–2Cl]^+$ 1242. $C_{57}H_{55}N_6OF_6P_3PtCl_2$ 1311. EA found (calculate) %: C 52.09 (52.14), H 4.17 (4.22), N 6.19 (6.40).

Preparation of $C_{70}H_{64}N_6F_6P_4PtCl_2$ (3.43):

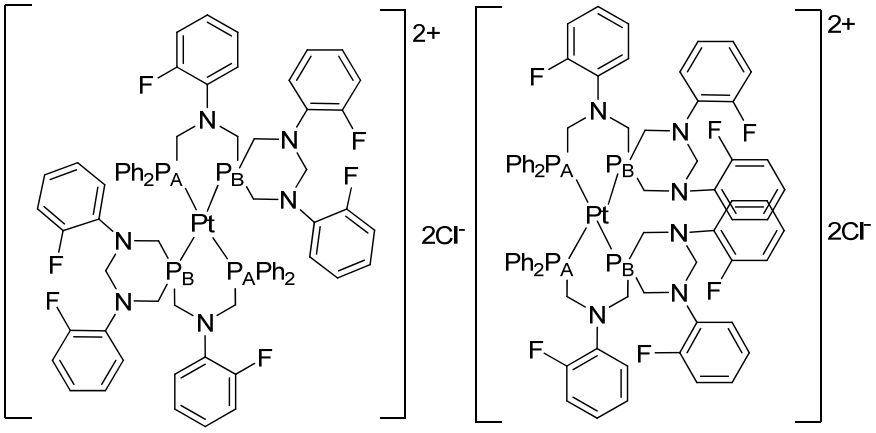

3.43a **3.43b**

Compound **3.41** (0.015 g, 0.011 mmol) and Ph_2PCH_2OH (0.003 g, 0.012 mmol) were dissolved in 1 ml of CH_2Cl_2 and stirred for 1 h at r.t. The resulted colourless solid was filtered off. Yield: 0.016 g, 98%. Selected data: ^{1}H NMR (400 MHz, $CDCl_3$, *J* in Hz) 8.40 – 6.01 (m, CH), 5.01 – 1.11 (m, CH_2) ppm. $^{31}P\{^{1}H\}$ NMR (162 MHz, $CDCl_3$, *J* in Hz) – 20.5 (2 P, vt, $^{1}J_{PPt}$ = 2670, $^{2}J_{PP}$ = 31, P_A, **3.43a**), 25.0 (2 P, d, $^{2}J_{PP}$ = 255, P_A, **3.43b**), –37.0 (2 P, vt, $^{1}J_{PPt}$ = 2113, $^{2}J_{PP}$ = 31, P_B, **3.43a**), –43.5 (2 P, d, $^{2}J_{PP}$ = 255, P_B, **3.43b**) ppm.

Preparation of $C_{70}H_{64}N_6F_6P_4PtCl_2$ (3.44):

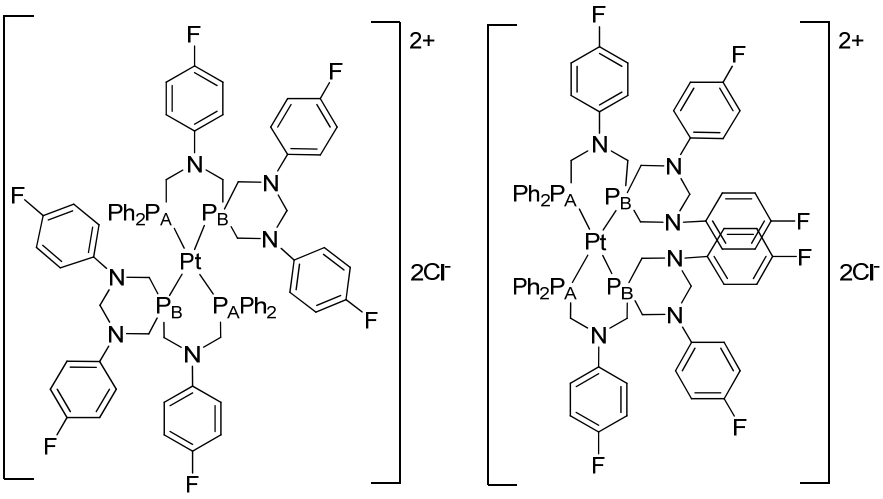

3.44a **3.44b**

Method **A**: **3.42** (0.100 g, 0.076 mmol) and Ph_2PCH_2OH (0.016 g, 0.076 mmol) were dissolved in 5 ml of CH_2Cl_2 and stirred for 1 h at r.t. The solid was dried under vacuum after removal of the solvent. Yield: 0.045 g, 40%. Method **B**: **2.18** (0.200 g, 0.482 mmol) and $PtCl_2COD$ (0.090 g, 0.241 mmol) were dissolved in CH_2Cl_2 (5 ml) and stirred for 1 h at r.t. After that, Ph_2PCH_2OH (0.052 g, 0.241 mmol) was added to the solution and stirred for further 1 h. and then, another eq. of Ph_2PCH_2OH (0.052 g, 0.241 mmol) was added and stirred for an additional hour. The solid was dried under vacuum after precipitation with Et_2O (10 ml) upon concentration of the solution. Yield: 0.326 g, 91%. Product was purified by recrystallisation form CH_2Cl_2\$Et_2O$ (50:50). Yield: 0.129 g, 35%. Selected data: IR (KBr, cm^{-1}): (νNH) 3392, 3226, 3052, (νPtCl) 302. ^{1}H NMR (400 MHz, $CDCl_3$, *J* in Hz) 8.24 (6 H, bs, CH + OH), 7.68 – 6.31 (42 H, m, CH + NH), 5.10 (4 H, vs, PCH_2OH), 4.31 (2 H, d, $^2J_{HH}$ = 13.4, NCH_eN), 4.27 – 4.20 (8 H, vs, PCH_eN, PCH_2NH), 3.22 (4 H, d, $^2J_{HH}$ = 15.2, PCH_aN), 2.94 (2 H, d, $^2J_{HH}$ = 13.4, NCH_aN) ppm. ^{31}P{^{1}H} NMR (162 MHz, $CDCl_3$, *J* in Hz) –17.4 (2 P, t, $^1J_{PPt}$ = 2628, $^2J_{PP}$ = 31, P_A, **3.44a**), –33.5 (2 P, t, $^1J_{PPt}$ = 2139, $^2J_{PP}$ = 31, P_B, **3.44a**) ppm. EI–MS (*m/z*) $[MH–2Cl]^+$ 1422. $C_{70}H_{64}N_6F_6P_4PtCl_2$ 1491. EA found (calculate) (%): C 54.83 (54.94), H 4.32 (4.45), N 5.10 (5.63).

Preparation of $C_{82}H_{94}N_6P_4PtCl_2$ (3.45):

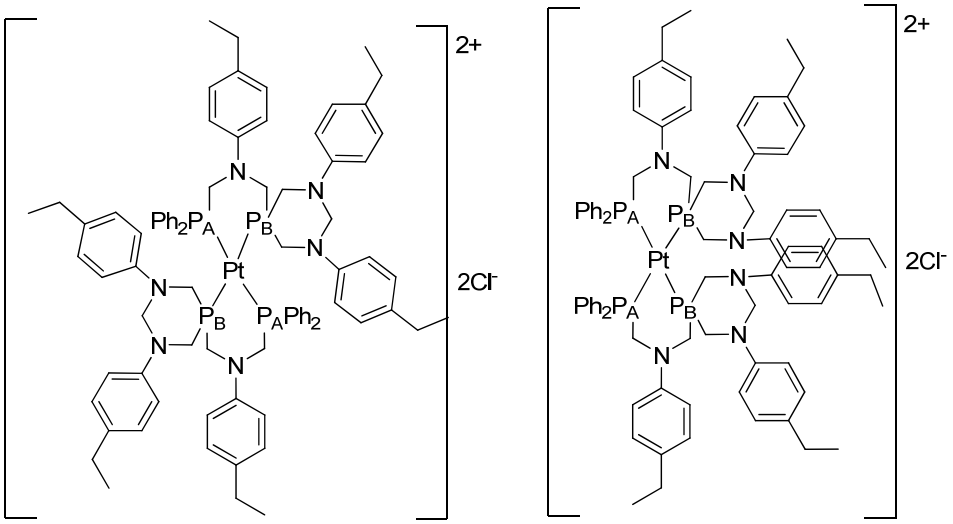

3.45a **3.45b**

Method **B**: **2.19** (0.100 g, 0.206 mmol) and $PtCl_2COD$ (0.039 g, 0.103 mmol) were dissolved in CH_2Cl_2 (2.5 ml) and stirred for 1 h at r.t. After that, Ph_2PCH_2OH (0.022 g, 0.103 mmol) was added to the solution and stirred for further 1 h. and then, another equiv. of Ph_2PCH_2OH (0.027 g, 0.103 mmol) was added and stirred for an additional hour. The solid was dried under vacuum after precipitation with Et_2O (10 ml) upon concentration of the solution. Yield: 0.080 g, 46%. Product was purified by recrystallisation from CH_2Cl_2\$Et_2O$ (50:50). Selected data: IR (KBr, cm^{-1}): (νNH) 3392, (νPtCl) n.o. ^1H NMR (400 MHz, $CDCl_3$, *J* in Hz) 8.25 (8 H, bs, CH + OH), 7.67 – 6.27 (m, CH + NH), 5.08 (4 H, vs, PC*H*$_2$OH), 4.47 (2 H, d, $^2J_{HH}$ = 13.4, NC*H*eN), 4.21– 4.18 (8 H, vs, PC*H*eN, PC*H*$_2$NH), 3.28 (4 H, d, J_{HH} = 15.1, PC*H*aN), 2.96 (2 H, d, $^2J_{HH}$ = 13.4, NC*H*aN), 2.56 – 2.38 (m, CH_2), 1.25 – 1.07 (m, CH_3) ppm. $^{31}P\{^1H\}$ NMR (162 MHz, $CDCl_3$, *J* in Hz) – 18.4 (2 P, t, $^1J_{PPt}$ = 2618, $^2J_{PP}$ = 31, P_A, **3.45a**), –24.1 (2 P, d, $^2J_{PP}$ = 245, P_A, **3.45b**), –34.7 (2 P, t, $^1J_{PPt}$ = 2120, $^2J_{PP}$ = 31, P_B, **3.45a**), –51.9 (2 P, d, $^2J_{PP}$ = 245, P_B, **3.45b**) (approx. 8:2) ppm. EI–MS (*m/z*) $[M–Cl]^+$ 1516. $C_{82}H_{96}N_6P_4PtCl_2 \cdot 2.5H_2O$ (1596). EA found (calculate) (%): C 61.27 (61.61), H 5.86 (6.24), N 5.18 (5.26).

Preparation of $C_{58}H_{69}N_3P_2Ru_2Cl_4$ (3.46):

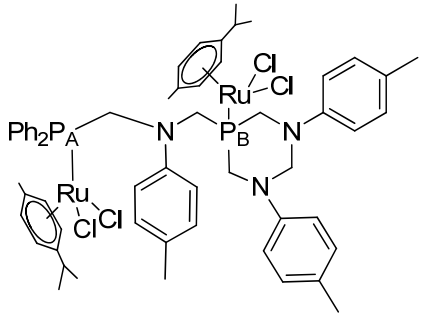

3.46

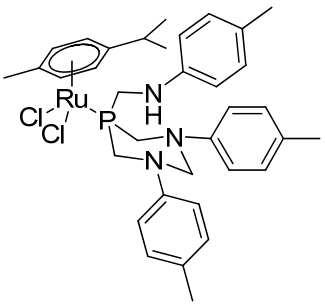

3.14

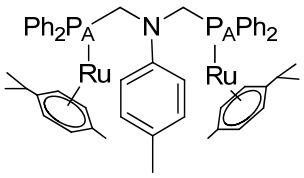

3.48

From **2.39** (0.097 g, 0.161 mmol) and $\{RuCl_2(\eta^6\text{–}p\text{–cymene})\}_2$ (0.099 g, 0.161 mmol). Selected data: $^{31}P\{^1H\}$ NMR (162 MHz, $CDCl_3$, *J* in Hz) 24.6 (1 P, d, $^4J_{PP}$ = 11, P_A, **3.46**), 22.3 (1 P, d, $^4J_{PP}$ = 11, P_B, **3.46**), 21.7 (**3.48**), 13.2 (**3.14**) (approx. 1.5:1:1.5) ppm. EI–MS (*m/z*) $[M–Cl]^+$ 1178, $[\mathbf{3.48}–Cl]^+$ 1080, $[\mathbf{3.14}–Cl]^+$ 674.

Preparation of $C_{55}H_{60}N_3P_2F_3Ru_2Cl_4$ (3.47):

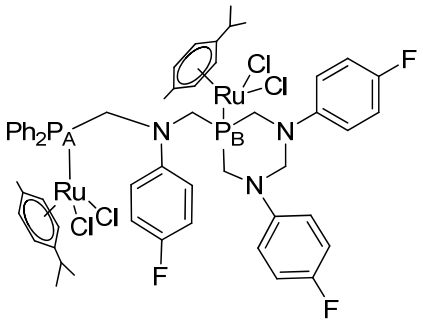

3.47

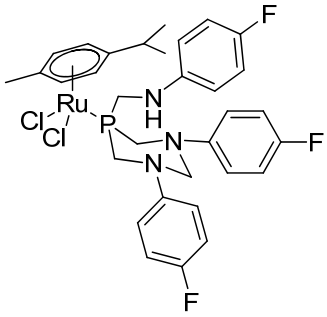

3.15

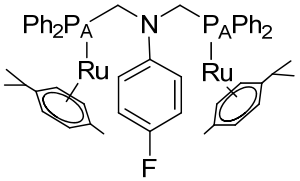

3.49

From **2.40** (0.100 g, 0.163 mmol) and $\{RuCl_2(\eta^6\text{–}p\text{–cymene})\}_2$ (0.100 g, 0.163 mmol). Selected data: $^{31}P\{^1H\}$ NMR (400 MHZ, $CDCl_3$, *J* in Hz) 23.8 (1 P, d, $^4J_{PP}$ = 10, P_A, **3.47**), 22.6 (1 P, d, $^4J_{PP}$ = 10, P_B, **3.47**), 21.4 (**3.49**), 12.0 (**3.15**) (approx. 1.5:1:1.5) ppm. EI–MS (*m/z*) $[M–Cl]^+$ 1192, $[\mathbf{3.49}–Cl]^+$ 1086, $[\mathbf{3.15}–Cl]^+$ 686.

6.4 Chapter 4 Experimental

Preparation of $C_{20}H_{28}NO_3P$ (4.1):

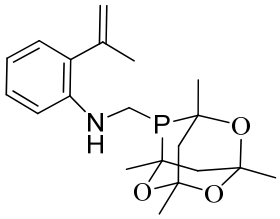

4.1

A solution $CgPCH_2OH$ (0.635 g, 2.568 mmol) in methanol (10 ml) was added to *o*-{C(Me)=CH_2}$C_6H_4NH_2$ (0.342 g, 2.568 mmol) and the solution stirred for 24h at r.t. The suspension was kept in the freezer for 12 h and the solid collected by suction filtration and dried in vacuo. Yield: 0.600 g, 64%. Selected data: IR (KBr, cm^{-1}): (νNH) 3428. ^{1}H NMR (400 MHz, $CDCl_3$) 7.21 (1 H, vt, $^3J_{HH}$ = 7.2, *m*-CH), 7.05 (1 H, d, $^3J_{HH}$ = 6.8, *m*-CH), 6.75 (2 H, *m*, *o*-, *p*-CH), 5.33 (1 H, s, CH), 5.05 (1 H, s, CH), 4.74 (1 H, bs, NH), 3.52 (1 H, d, $^2J_{HH}$ = 12.7, PC*H*$_2$N), 3.02 (1 H, d, $^2J_{HH}$ = 12.7, PC*H*$_2$N), 2.17 – 1.21 (19 H, m, CHadamantane + CH_3) ppm. ^{31}P{^{1}H} NMR (400 MHZ, $CDCl_3$, *J* in Hz) –33.5 ppm. EI–MS (*m/z*) $[MH]^+$ 362. $C_{20}H_{28}NO_3P{\cdot}0.5H_2O$ (370). EA found (calculated) (%): C 64.63 (64.85), H 7.32 (7.89), N 3.86 (3.78).

Preparation of $C_{22}H_{22}NP$ (4.2):

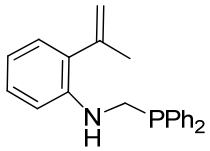

4.2

A solution of *o*-{C(Me)=CH_2}$C_6H_4NH_2$ (0.300 g, 2.252 mmol) in methanol (7.5 ml) was added to a methanol solution (7.5 ml) of Ph_2PCH_2OH (0.487 g, 2.252 mmol) by cannula. The resulting mixture was stirred for 24 h and the solvent concentrated under reduced pressure to *ca.* 5ml. The suspension was kept in the freezer for 12 h and the solid collected by suction filtration and dried in vacuo. Yield: 0.449 g, 60%. Selected data: IR (KBr, cm^{-1}): (νNH) 3401 cm^{-1}. ^{1}H NMR (400 MHz, $CDCl_3$, *J* in Hz) 7.54 – 7.32 (10 H, m, CH), 7.23 – 7.16 (1 H, dt, $^3J_{HH}$ = 7.3, $^4J_{HH}$ = 1.5, *m*-CH,), 6.99 (1 H, dd, $^3J_{HH}$ = 7.4, $^4J_{HH}$ = 1.5, *m*-CH), 6.81 (1 H, d, $^3J_{HH}$ = 8.1, *o*-CH), 6.72 (1 H, vt, $^3J_{HH}$ = 7.4, *p*-CH), 5.06 (1 H, s, $^2J_{HH}$ = 1.3, CH), 4.74 (1 H, s, $^2J_{HH}$ = 1.3, CH), 4.23 (1 H, bs, NH), 3.83 (2 H, d, $^2J_{HP}$ = 4.5, PC*H*$_2$N), 1.86 (3 H, s, CH_3) ppm. ^{31}P{^{1}H} NMR ($CDCl_3$): –18.5 ppm. EI–MS (*m/z*) $[MH]^+$

332. $C_{22}H_{22}NP{\cdot}0.75CH_4O$ (347). EA found (calculated) (%): C 78.65 (79.74), H 6.41 (6.69), N 4.16 (4.23).

Preparation of $C_{35}H_{34}NP_2$ (4.2a):

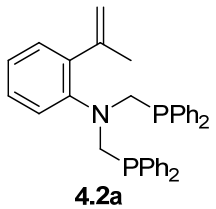

4.2a

A solution of *o*-{C(Me)=CH_2}$C_6H_4NH_2$ (0.300 g, 2.252 mmol) and Ph_2PCH_2OH (0.974 g, 4.505 mmol) in methanol (10 ml) was refluxed for 12 d and concentrated under reduced pressure to dryness resulting a colourless solid. Yield: 0.695 g, 58%. Selected data: IR (cm^{-1}): (νNH) 3272 (vw) cm^{-1}. ^{1}H NMR (400 MHz, $CDCl_3$, *J* in Hz) 7.67 – 6.95 (24 H, m, CH), 5.00 (1 H, s, CH), 4.84 (1 H, d, $^2J_{HH}$ = 1.4, CH), 4.41 (3 H, s, PCH_2N), 1.81 (3 H, s, CH_3) ppm. $^{31}P\{^1H\}$ NMR (162 MHz, $CDCl_3$) –27.3 ppm. EI–MS (*m/z*) $[MH]^+$ 530. $C_{35}H_{34}NP_2$ 529. EA found (calculated) (%): C 79.26 (79.38), H 6.30 (6.28), N 2.72 (2.64).

Preparation of $C_{21}H_{34}NO_3P$ (4.3):

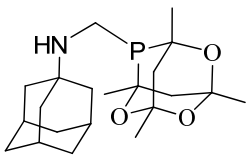

4.3

A solution of CgPCH_2OH (1.150 g, 3.736 mmol) in methanol (20 ml) was added to 1–adamantylamine (0.565 g, 3.736 mmol). The mixture was stirred for 24 h at r.t., stored in the freezer for 12 h and colourless solid filtered and dried under vacuum. Yield: 0.994 g, 70%. Selected data: IR (KBr, cm^{-1}): (νNH) 3436 cm^{-1}. ^{1}H NMR (400 MHz, $CDCl_3$, *J* in Hz) 2.91 (1 H, dd, $^2J_{HH}$ = 11.8, $^2J_{HP}$ = 0.8, PC*H*$_2$N), 2.45 (1 H, d, $^2J_{HH}$ = 11.8 , PCH_2N), 1.99 – 1.28 (32 H, m, CH, NH, CH_2, CH_3) ppm. $^{31}P\{^1H\}$ NMR (162 MHz, $CDCl_3$): –31.40, –31.10 ppm. EI–MS (*m/z,* $[MH]^+$): 380. $C_{21}H_{34}NO_3P$ (379). EA found (calculated) (%): C 66.01(66.47), H 8.59(9.03), N 3.83 (3.68).

Preparation of $C_{23}H_{28}NP$ (4.4):

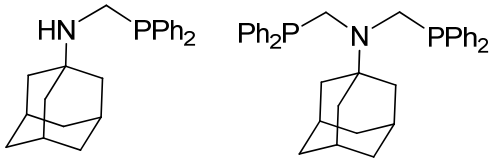

4.4 **4.4a**

1–adamantylamine (0.500 g, 3.306 mmol) and Ph_2PCH_2OH (0.715 g, 3.306 mmol) were dissolved in methanol (30 ml) and the solution was stirred for 24 h at r.t., stored in the freezer for 12 h and the colourless deposited was filtered, washed with Et_2O (10 ml) and dried under vacuum. Yield: 0.428 g, 64%. Selected data: IR (KBr, cm^{-1}): (νNH) 3272. ^1H NMR (400 MHz, $CDCl_3$) 7.84 – 7.27 (m, CH), 3.90 – 3.37 (m, PCH_2N), 2.07 – 1.49 (m, Ad cage) ppm. $^{31}P\{^1H\}$ NMR (162 MHz, $CDCl_3$): –17.7 (**4.4**), –25.3 (**4.4a**) (approx. 4:1) ppm. EI–MS (*m/z*) $[MH]^+$ 350. $C_{23}H_{28}NP{\cdot}0.25CH_4O$ (358). EA found (calculated) (%): C 78.95 (79.05), H 7.96 (8.08), N 4.11 (4.01).

Preparation of $C_{44}H_{46}NO_3P$ (4.5):

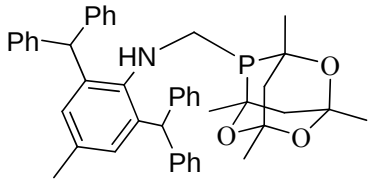

4.5

A solution of $CgPCH_2OH$ (0.555 g, 2.245 mmol) in C_7H_8 (10 ml) was added to *o,o*-$(CHPh_2)_2$–*p*–$MeC_6H_2NH_2$ (0.987 g, 2.245 mmol) and then more toluene was added (20 ml). After stirring for 24 h at r.t., the solvent was evaporated to dryness under reduced pressure to give a colourless solid. Yield: 1.430 g, 95%. Selected data: IR (KBr, cm^{-1}): (νNH) 3272. ^1H NMR (400 MHz, $CDCl_3$, J in Hz) 7.40 – 7.01 (m, CH), 6.61 (2 H, s, CH), 6.40 (s, CH), 5.96 (2 H, s, CH), 5.47 (s, CH), 3.09 (1 H, dd, $^3J_{HH}$ = 13.2, $^2J_{HP}$ = 2.2, PCH_2N), 2.94 (1 H, m, NH), 2.37 (1 H, d, $^3J_{HH}$ = 13.2, PCH_2N), 2.15 – 0.79 (m, CH_2 + CH_3) ppm. $^{31}P\{^1H\}$ NMR (162 MHz, $CDCl_3$) –27.0 ppm. EI–MS (*m/z*) $[MH]^+$ 668. $C_{44}H_{46}NO_3P{\cdot}0.25C_{33}H_{29}N$ (777). EA found (calculated) (%): C 80.38 (80.69), H 6.79 (6.90), N 2.26 (2.25).

Preparation of $C_{46}H_{40}NP$ (4.6):

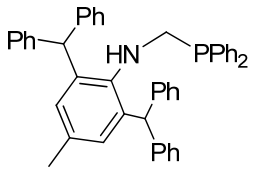

4.6

Compound *o,o*-$(CHPh_2)_2$–*p*–$MeC_6H_2NH_2$ (0.752 g, 1.71 mmol) and Ph_2PCH_2OH (0.370 g, 1.71 mmol) were dissolved in C_7H_8 (30 ml) and stirrer for 6 d at r.t. The colourless solid was filtered under N_2 and dried under vacuum. Yield: 0.546 g, 48%. Selected data: IR (KBr, cm^{-1}): (νNH) 3444, 3366. ^1H NMR (400 MHz, $CDCl_3$, *J* in Hz) 7.38 – 6.92 (m, CH), 6.58 (2 H, s, CH), 6.40 (s, CH), 5.78 (2 H, s, CH), 5.48 (s, CH), 3.46 (2 H, s, PCH_2N), 2.91 (1 H, bs, NH), 2.10 (s, CH_3), 2.04 (1 H, s, CH_3) ppm. $^{31}P\{^1H\}$ NMR (162 MHz, $CDCl_3$): –19.3 ppm. EI–MS (*m/z*) $[M–Na]^+$ 660. $C_{46}H_{40}NP{\cdot}0.5H_2O$ (647). EA found (calculated) (%): C 85.63 (85.42), H 6.07 (6.39), N 2.32 (2.17).

Preparation of $C_{21}H_{22}NP$ (4.7):

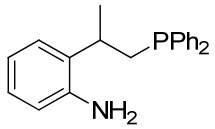

4.7

Compound *o*-{C(Me)=CH_2}$C_6H_4NH_2$ (0.500 g, 3.754 mmol), $HPPh_2$ (0.698 g, 3.754 mmol) and AIBN (0.085 g, 0.526 mmol) were placed in a Schlenk tube. The mixture was freeze–thawed three times and then stirred at 110°C for 3 d. After that time more AIBN was added (0.024 g, 0.146 mmol) and left for a further 2 d. The colourless oily product solidified upon addition of MeOH (10 ml) and purified by adding Et_2O (5 ml). The solid was collected by suction filtration and dried in vacuum. Yield: 0.789 g, 66%. Selected data: IR (KBr, cm^{-1}): (νNH) 3462, 3377. ^1H NMR (400 MHz, $CDCl_3$, *J* in Hz) 7.57 – 7.33 (10 H, m, CH), 7.25 (1 H, dd, $^3J_{HH}$ = 7.7, $^4J_{HH}$ = 1.4, *m*–CH), 7.06 (1 H, td, $^3J_{HH}$ = 7.6, $^4J_{HH}$ = 1.5, *m*–CH), 6.84 (1 H, td, $^3J_{HH}$ = 7.5, $^4J_{HH}$ = 1.2, *p*–CH), 6.65 (1 H, dd, $^3J_{HH}$ = 7.9, $^4J_{HH}$ = 1.2, *o*–CH), 3.30 (2 H, bs, NH), 2.83 – 2.71 (1 H, m, CH), 2.49 (1 H, dvt, $^2J_{HH}$ = 13.6, $^3J_{HH}$ = 4.0, $^2J_{HP}$ = 3.2, CH_2), 2.26 (1 H, ddd, $^2J_{HH}$ = 13.6, $^3J_{HH}$ = 10.0, $^2J_{HP}$ = 3.2, CH_2), 1.52 (3 H, d, $^3J_{HH}$ = 6.8, CH_3) ppm. $^{31}P\{^1H\}$ NMR (162 MHz, $CDCl_3$) –19.5 ppm. EI–MS (*m/z*) $[MH]^+$ 320. $C_{21}H_{22}NP{\cdot}0.25CH_4O$ 319. EA found (calculated) (%): C 77.65 (77.96), H 6.64 (7.08), N 3.99 (4.28).

Preparation of $C_{19}H_{28}NO_3P$ (4.8):

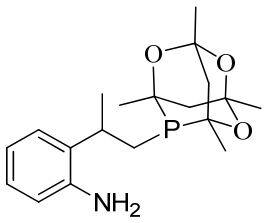

4.8

Compound *o*-{C(Me)=CH_2}$C_6H_4NH_2$ (0.500 g, 3.754 mmol), CgPH (0.812 g, 3.754 mmol) and AIBN (0.085 g, 0.526 mmol) were placed in a Schlenk tube. The mixture was freeze–thawed and stirred at 110°C for 24 h. The yellow oily product was solidified upon cooling in the freezer. Yield: 1.112 g, 85%. Selected data: IR (KBr, cm^{-1}): (νNH) 3460, 3369. ^{1}H NMR (400 MHz, $CDCl_3$, *J* in Hz) 7.17 (1 H, dd, $^3J_{HH}$ = 3.2, $^4J_{HH}$ = 0.6, *m*–CH), 7.05 (1 H, dd, $^3J_{HH}$ = 3.2, $^4J_{HH}$ = 0.6, *m*-CH), 6.83 (1 H, vt, $^3J_{HH}$ = 3.2, *p*-CH), 6.71 (1 H, d, $^3J_{HH}$ = 3.2, *o*-CH), 3.61 (2 H, bs, NH), 3.02 (1 H, m, CH), 2.27 – 1.12 (23 H, m, CH_2, CH_3) ppm. ^{31}P{^{1}H} NMR (162 MHz, $CDCl_3$) –31.7, –31.9 ppm. EI–MS (*m/z*) $[MH]^+$ 350. $C_{19}H_{28}NO_3P$ 349. EA found (calculated) (%): C 65.96 (65.31), 8.30 (8.08), 4.04 (4.01).

Preparation of $C_{34}H_{33}NP_2$ (4.9):

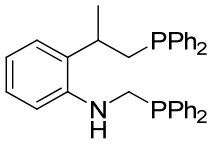

4.9

Pathway **A2**) **4.7** (0.100 g, 0.313 mmol) and Ph_2PCH_2OH (0.081 g, 0.376 mmol) were placed in a Schlenk tube and degassed MeOH (10 ml) added. The mixture was refluxed for 3 d and then concentrated under reduced pressure to *ca*. 1 ml. The resulting solid was filtered off under vacuum. Yield: 0.074 g, 46%. Pathway **B2**) **4.2** (0.200 g, 0.603 mmol) and $HPPh_2$ (0.224 g, 1.206 mmol) and AIBN (0.018 g, 0.108 mmol) were placed in a Schlenk tube and degassed MeOH (10 ml) added. The mixture was refluxed for 5 d, stirred for a further 2 d at r.t. and concentrated under reduced pressure to dryness. The resulted oil was solidified with Et_2O (10 ml) and filtered off under vacuum. Yield: 0.052 g, 17%. Selected data: IR (KBr, cm^{-1}): (νNH) 3400. ^{1}H NMR (400 MHz, $CDCl_3$, *J* in Hz) 7.60 – 7.27 (10 H, m, CH), 7.25 (1 H, dd, $^3J_{HH}$ = 7.7, $^4J_{HH}$ = 1.4, *m*-CH), 7.06 (1 H, td, $^3J_{HH}$ = 7.7, $^4J_{HH}$ = 1.4, *m*-CH), 6.84 (1 H, td, $^3J_{HH}$ = 7.7, $^4J_{HH}$ = 1.4, *p*-CH), 6.65 (1 H, dd, $^3J_{HH}$ = 7.7, $^4J_{HH}$ = 1.4, *o*-CH), 3.30 (2 H, bs, NH_2), 2.84 – 2.70 (1 H, m, CH), 2.56 – 2.44 (1 H, dvt,

$^2J_{HH}$ = 12.3, $^2J_{HP}$ = 4.0, $^3J_{HH}$ = 4.0, CH_2), 2.26 (1 H, ddd, $^2J_{HH}$ = 12.3, $^2J_{HP}$ = 4.0, $^3J_{HH}$ = 8.0, CH_2), 1.52 (3 H, d, $^3J_{HH}$ = 6.8, CH_3) ppm. $^{31}P\{^1H\}$ NMR (162 MHz, $CDCl_3$) –19.6, –19.8 ppm. EI–MS (*m/z*) $[MOH]^+$ 534, $[MO_2H]^+$ 550. $C_{34}H_{33}NP_2$ 517. EA found (calculated) (%): C 78.80 (78.90), 6.45 (6.43), 2.80 (2.71).

Unless otherwise stated, new Pt(II), Pd(II) and Ru(II) complexes were synthesised by reacting the metal precursors with phosphine ligands in CH_2Cl_2 and stirring at r.t. for 1 h. The solids were dried under vacuum after precipitation with Et_2O upon concentration of the solution.

Preparation of $C_{40}H_{56}Cl_2N_2P_2Pt$ (4.10):

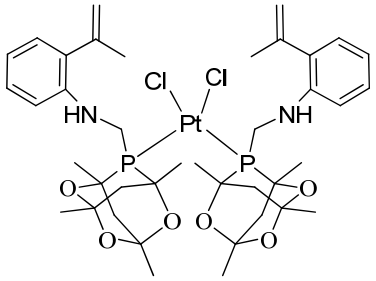

4.10

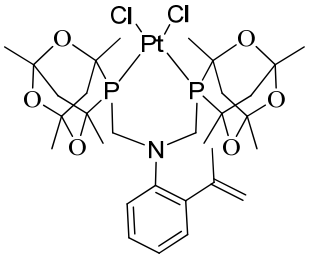

4.10a

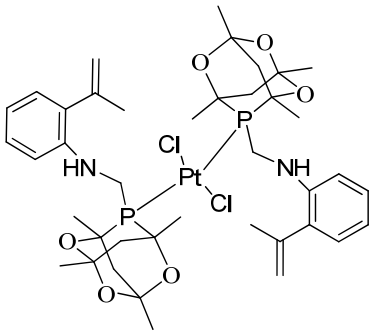

4.10b

From **4.1** (0.100 g, 0.276 mmol) and $PtCl_2COD$ (0.051 g, 0.138 mmol). Yield: 0.046 g, 33%. Selected data: IR (KBr, cm^{-1}): (νNH) 3394, (νPtCl) 320, 291. ^1H NMR (400 MHz, $CDCl_3$, *J* in Hz) 6.45 – 6.70 (m, CH), 5.42 – 4.95 (m, CH_2), 4.20 – 3.08 (m, CH_2), 2.44 – 1.15 (m, CH_2, CH_3) ppm. $^{31}P\{^1H\}$ NMR ($CDCl_3$) –3.2, –3.6 ($^1J_{PPt}$ = 2620 Hz) (**4.10b**), –19.2 ($^1J_{PPt}$ = 3359 Hz), –22.5 ($^1J_{PPt}$ = 3327 Hz) ppm. EI–MS (*m/z*) [**4.10aH$_3$O**]$^+$ 873. A pure enough sample of **4.10** could not be obtained for elemental analysis due to the mixture of **4.10**, **4.10a** and **4.10b**.

Preparation of $C_{44}H_{44}Cl_2N_2P_2Pt$ (4.11):

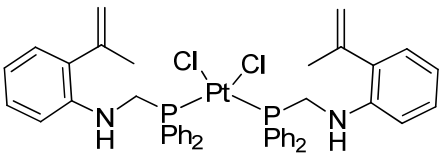

4.11

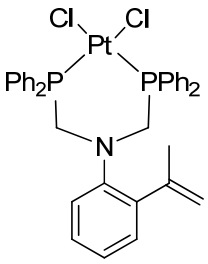

4.11a

From **4.2** (0.100 g, 0.302 mmol) and $PtCl_2COD$ (0.056 g, 0.151 mmol). Yield: 0.053 g, 38%. Selected data: IR (KBr, cm^{-1}): (νNH) 3412 (νPtCl) 315, 290. ^1H NMR (400 MHz, $CDCl_3$, *J* in Hz) due to the mixture of **4.11** and **4.11a** the spectrum could not be assigned. $^{31}P\{^1H\}$ NMR ($CDCl_3$) –5.6 ($^1J_{PPt}$ = 3420 Hz, **4.11a**), 6.6 ($^1J_{PPt}$ = 3657 Hz, **4.11**), 60.7 (*ca.* $^2J_{PP}$ = 45 Hz, *ca.* $^1J_{PPt}$ = 3641 Hz), 105.7 (*ca.* $^2J_{PP}$ = 45 Hz, *ca.* $^1J_{PPt}$ = 3641 Hz) (approx. 3:3:1) ppm. EI–MS (*m/z*) $[M–Cl]^+$ 892, [**4.11a**–Cl]$^+$ 759. A pure enough sample of **4.11** could not be obtained for elemental analysis due to the mixture of **4.11**, **4.11a**, and unknown.

Preparation of $C_{35}H_{33}Cl_2NP_2Pt$ (4.11a):

From **4.2a** (0.100 g, 0.189 mmol) and $PtCl_2COD$ (0.071 g, 0.189 mmol). Yield: 0.141 g, 94%. Selected data: IR (KBr, cm^{-1}): (νNH) n.o. ^1H NMR (400 MHz, $CDCl_3$, *J* in Hz) 7.96 – 7.36 (20 H, m, CH), 7.14 – 6.97 (3 H, m, *m-, m-, p*-CH), 6.64 (1 H, d, $^3J_{HH}$ = 7.1, *o*-CH), 4.74 (1 H, s, CH), 4.67 (1 H, s, CH), 4.16 – 3.86 (4 H, m, PCH_2N,), 1.46 (3 H, s, CH_3) ppm. $^{31}P\{^1H\}$ NMR (400 MHz, $CDCl_3$, *J* in Hz) –6.1 ($^1J_{PPt}$ = 3418) ppm. EI–MS (*m/z*) $[M–Cl]^+$ 759. $C_{35}H_{33}Cl_2NP_2Pt{\cdot}0.5C_4H_{10}O$ 832. EA found (calculated) (%): C 53.85 (53.37), H 4.64 (4.60), N 1.60 (1.68).

Preparation of $C_{42}H_{68}Cl_2N_2O_6P_2Pt$ (4.12):

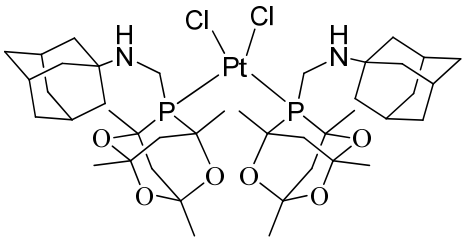

4.12

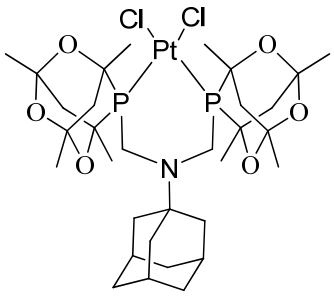

4.12a

From **4.3** (0.100 g, 0.263 mmol) and $PtCl_2COD$ (0.049 g, 0.132 mmol). Yield: 0.039 g, 29%. Selected data: IR (KBr, cm^{-1}): (νNH) 3435, (νPtCl) 317, 289. ^1H) NMR ($CDCl_3$, *J* in Hz) 8.30 (6 H, bs, NH), 4.30 (1 H, vt, $^2J_{HH}$ = 14.4, PCH_2N), 3.82 (1 H, dd, $^2J_{HH}$ = 14.0, $^2J_{HP}$ = 3.0, PCH_2N), 3.56 (1 H, dd, $^2J_{HH}$ = 14.0, $^2J_{HP}$ = 3.0, PCH_2N), 2.95 (1 H, bd, $^2J_{HH}$ = 12.0, PCH_2N), 2.23 – 1.29 (87 H, m, Ad + Cg cages) ppm. $^{31}P\{^1H\}$ NMR (400 MHz, $CDCl_3$) –20.0 ($^1J_{PPt}$ = 3350 Hz) –22.9 ($^1J_{PPt}$ = 3322 Hz) ppm. EI–MS (*m/z*) $[MH]^+$ 1024, [**4.12a**–Cl]$^+$ 837. $C_{42}H_{68}Cl_2N_2O_6P_2Pt$ 1023. EA found (calculated) (%): C 49.63 (49.22), H 6.35 (6.64), N 3.21 (2.73).

Preparation of $C_{92}H_{80}Cl_2N_2P_2Pt$ (4.13):

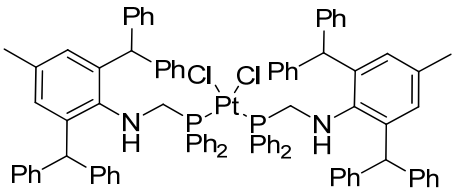

4.13

From **4.6** (0.100 g, 0.157 mmol) and $PtCl_2COD$ (0.029 g, 0.078 mmol). Yield: 0.072 g, 61%. Selected data: IR (KBr, cm^{-1}): (νNH) 3333, 3332, (νPtCl) 312, 289. ^1H NMR (400 MHz, $CDCl_3$, *J* in Hz) 7.10 (60 H, m, CH), 6.56 (4 H, s, CH), 5.87 (4 H, s, CH), 4.29 (2 H, bs, NH), 3.63 (4 H, bs, PC*H*$_2$N), 2.06 (6 H, s, CH_3) ppm. $^{31}P\{^1H\}$ NMR (400 MHz, $CDCl_3$) 5.4 ($^1J_{PPt}$ = 3649 Hz) ppm. EI–MS (*m/z*) $[M–Cl]^+$ 1505, [**4.6**K]$^+$ 676. $C_{92}H_{80}Cl_2N_2P_2Pt{\cdot}H_2O$. EA found (calculated) (%): C 70.00 (70.85), H 4.71 (5.30), N 2.14 (1.80).

Preparation of $C_{40}H_{56}Cl_2N_2O_6P_2Pd$ (4.14):

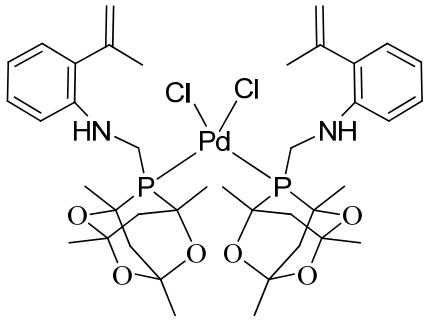

4.14

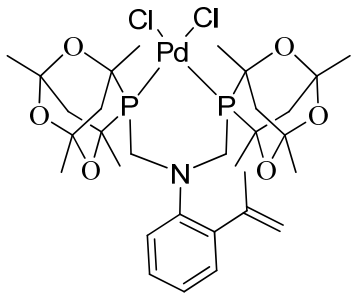

4.14a

From **4.1** (0.100 g, 0.277 mmol) and $PtCl_2COD$ (0.040 g, 0.138 mmol). Yield: 0.094 g, 76%. Selected data: IR (KBr, cm^{-1}): (νNH) 3388, (νPtCl) 374, 310. ^1H NMR (400 MHz, $CDCl_3$, *J* in Hz) 7.22 (3 H, s, *p*-CH), 7.07 (2 H, d, $^3J_{HH}$ = 6.5, *o*-CH), 6.80 (5 H, q, $^3J_{HH}$ = 7.8, *m*-CH), 5.37 (1 H, s, CH), 5.32 (1 H, s, CH), 5.11 (1 H, s, CH), 5.09 (1 H, s, CH), 4.06 (2 H, vt, $^2J_{HH}$ = 12.8, PCH_2N), 3.79 (2 H, vt, $^2J_{HH}$ = 12.8, PCH_2N), 3.29 – 3.20 (2 H, m, CH_2), 2.15 – 1.23 (m, CH_2, CH_3) ppm. EI–MS (*m/z*) $[HPCgNa]^+$ 239. $^{31}P\{^1H\}$ NMR (400 MHz, $CDCl_3$) 3.2, 2.7 ppm. $C_{40}H_{56}Cl_2N_2O_6P_2Pd$ 900. EA found (calculated) (%): C 53.07 (53.27), H 6.03 (6.27), N 3.20 (3.11).

Preparation of $C_{44}H_{44}Cl_2N_2P_2Pd$ (4.15):

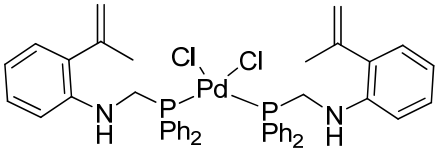

4.15

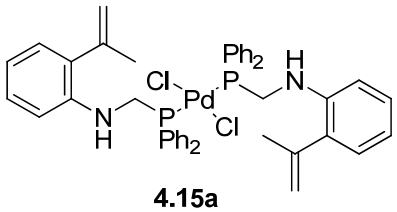

4.15a

From **4.2** (0.100 g, 0.302 mmol) and $PtCl_2COD$ (0.043 g, 0.151 mmol). Yield: 0.087 g, 69%. Selected data: IR (KBr, cm^{-1}): (νNH) 3402, (νPtCl) 307, 283. ^1H NMR (400 MHz, $CDCl_3$, *J* in Hz) 7.91 – 6.36 (m, CH), 5.18 – 5.08 (2 H, m, CH), 5.08 – 4.96 (2 H, m, CH), 4.83 – 4.73 (4 H, m, CH), 4.67 (4 H, s, NH), 4.43 (4 H, s, PCH_2N), 4.37 (4 H, s, PCH_2N), 1.92 (6 H, s, CH_3), 1.86 (6 H, s, CH_3) ppm. $^{31}P\{^1H\}$ NMR (400 MHz, $CDCl_3$): 26.8, 14.3 ppm. EI–MS (*m/z*) $[M–Cl]^+$ 803. A pure sample of **4.15** (several batches) could not be obtained for elemental analysis despite drying the sample in the desiccator overnight.

Preparation of $C_{32}H_{36}Cl_2NPRu$ (4.16):

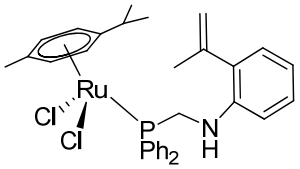

4.16

From **4.2** (0.084 g, 0.255 mmol) and $\{RuCl_2(\eta^6–p–cymene)\}_2$ (0.092 g, 0.127 mmol). Yield: 0.132 g, 69%. Selected data: IR (KBr, cm^{-1}): (νNH) 3390, (νRuCl) 294. ^1H NMR (400 MHz, $CDCl_3$, *J* in Hz) 7.93 – 7.37 (10 H, m, CH), 7.00 – 6.81 (1 H, m, *m*-CH), 6.78 (1 H, dd, $^3J_{HH}$ = 7.8, $^4J_{HH}$ = 1.5, *m*-CH), 6.49 (1 H, t, $^3J_{HH}$ = 7.8, *p*-CH), 6.34 (1 H, d, $^3J_{HH}$ = 7.8, *o*-CH), 5.33 (2 H, d, $^3J_{HH}$ = 6.2, CH), 5.20 (2 H, d, $^3J_{HH}$ = 6.2, CH), 4.98 (1 H, s, CH), 4.56 (1 H, s, CH), 4.48 (2 H, s, PCH_2N), 4.18 (1 H, bs, NH), 2.57 (1 H, q, $^3J_{HH}$ = 7.0, CH), 1.94 (3 H, s, CH_3), 1.70 (3 H, s, CH_3), 0.87 (6 H, d, $^3J_{HH}$ = 7.0, CH_3) ppm. $^{31}P\{^1H\}$ NMR (162 MHz, $CDCl_3$) 25.2 ppm. EI–MS (*m/z*) $[M–Cl]^+$ 602. $C_{32}H_{36}NPRuCl_2·2H_2O$ 673. EA found (calculated) (%): C 56.46 (57.06), H 5.21(5.99), N 2.06 (2.08).

Preparation of $C_{31}H_{48}Cl_2NO_3PRu$ (4.17):

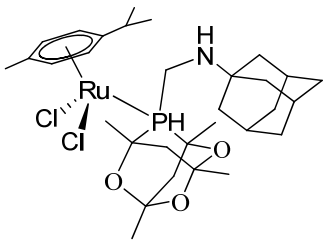

4.17

From **4.3** (0.100 g, 0.263 mmol) and $\{RuCl_2(\eta^6–p–cymene)\}_2$ (0.081 g, 0.132 mmol). Yield: 0.078g, 43%. Selected data: IR (KBr, cm^{-1}): (νNH) 3278, 3415, (νRuCl) 285, 296. ^1H NMR (400 MHz, $CDCl_3$, *J* in Hz) 5.83 (1 H, d, $^3J_{HH}$ = 5.8, CH), 5.78 (1 H, d, $^3J_{HH}$ = 6.3, CH), 5.65 (1 H, d, $^3J_{HH}$ = 6.3, CH), 5.30 (1 H, d, $^3J_{HH}$ = 5.8, CH), 3.77 (1 H, dd, $^3J_{HH}$ = 12.4, $^2J_{HP}$ = 4.9, PCH_2N), 3.14 – 2.98 (1 H, m, CH), 2.96 – 2.90 (2 H, m, CH, NH), 2.37 (1 H, dd, $^2J_{HP}$ = 12.4, $^2J_{HP}$ = 3.0, PCH_2N), 2.23 – 1.19 (56 H, m, CH, CH_2, CH_3) ppm. $^{31}P\{^1H\}$ NMR (162 MHz, $CDCl_3$) 15.1 ppm. EI–MS (*m/z*) $[M–Cl]^+$ 650. A pure sample of **4.15** (several batches) could not be obtained for elemental analysis despite drying the sample in the desiccator overnight.

Preparation of $C_{34}H_{45}Cl_2NPRu$ (4.18):

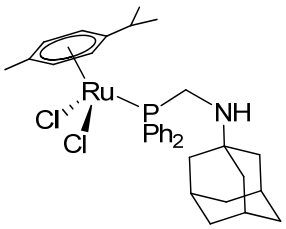

4.18

From **4.4** (0.100 g, 0.286 mmol) and $\{RuCl_2(\eta^6–p–cymene)\}_2$ (0.087 g, 0.143 mmol). Yield: 0.135 g, 72%. Selected data: IR (KBr, cm^{-1}): (νNH) 3309, (νRuCl) 287. ^1H NMR (400 MHz, $CDCl_3$, *J* in Hz) 7.90 – 7.28 (10 H, m, CH), 5.20 (2 H, d, $^3J_{HH}$ = 5.6, CH), 5.05 (2 H, d, $^3J_{HH}$ = 5.6, CH), 3.70 (2 H, s, PCH_2N), 2.46 (1 H, q, $^3J_{HH}$ = 6.8, CH), 1.82 (6 H, s, CH_3), 1.55 – 1.02 (15 H, m, CHadamantane+ CH_3), 0.79 (6 H, d, $^3J_{HH}$ = 6.8, CH_3) ppm. $^{31}P\{^1H\}$ NMR (162 MHz, $CDCl_3$) 26.9 ppm. EI–MS (*m/z*) $[M–Cl]^+$ 620. A pure sample of **4.15** (several batches) could not be obtained for elemental analysis despite drying the sample in the desiccator overnight.

Preparation of $C_{56}H_{54}Cl_2NPRu$ (4.19):

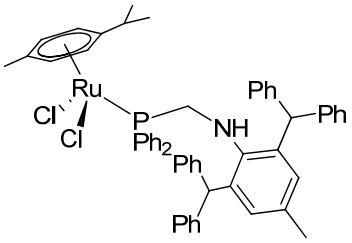

4.19

From **4.6** (0.100 g, 0.302 mmol) and $\{RuCl_2(\eta^6–p–cymene)\}_2$ (0.094 g, 0.151 mmol). Yield: 0.099 g, 67%. Selected data: IR (KBr, cm^{-1}): (νNH) 3320, (νRuCl) 294. ^1H NMR (400 MHz, $CDCl_3$, *J* in Hz) 7.85 – 6.65 (30 H, m, CH), 6.49 (2 H, s, CH), 5.61 (2 H, s,

CH), 5.20 (2 H, d, $^3J_{HH}$ = 5.6, CH), 5.14 (2 H, d, $^3J_{HH}$ = 5.6, CH), 4.12 (2 H, d, $^2J_{HP}$ = 2.9, PCH_2N), 2.43 (1 H, q, $^3J_{HH}$ = 6.9, CH), 2.02 (2 H, s, CH_3), 1.78 (3 H, s, CH_3), 0.94 (6 H, d, $^3J_{HH}$ = 6.9, CH_3) ppm.$^{31}P\{^1H\}$ NMR (162 MHz, $CDCl_3$) 22.7 ppm. EI–MS (*m/z*) $[M–Cl]^+$ 908. $C_{56}H_{54}NPRuCl_2{\cdot}2H_2O$ 981. EA found (calculated) (%): C 68.33 (68.63), H 5.52 (5.97), N 1.55 (1.43).

Preparation of $C_{42}H_{44}Cl_2N_2P_2Pt$ (4.20 – 4.20d):

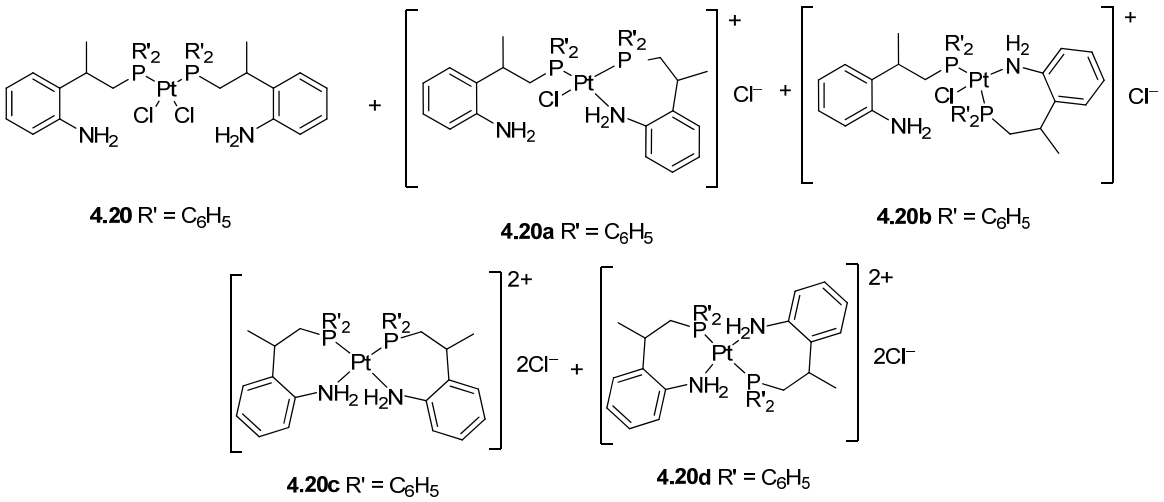

From **4.8** (0.100 g, 0.313 mmol) and $PtCl_2$(COD) (0.059 g, 0.157 mmol). Yield: 0.126 g, 89%. Selected data: ^1H NMR (400 MHz, $CDCl_3$, *J* in Hz) 7.95 – 6.45 (52 H, m, CH), 4.46 (3 H, bs, NH_2), 2.89 (2 H, bs, PCH_2N), 2.73 (2 H, bs, PCH_2N), 2.38 (2 H, s, CH), 1.51 – 1.27 (6 H, m, CH_3) ppm. $^{31}P\{^1H\}$ NMR (400 MHz, $CDCl_3$, *J* in Hz) 53.4 ($^1J_{PPt}$ = 4023), 23.0 – 0.6 (bm) ppm. EI–MS (*m/z*) $[M–Cl]^+$ 868.

Preparation of $C_{38}H_{56}O_6Cl_2N_2P_2Pt$ (4.21 – 4.21d):

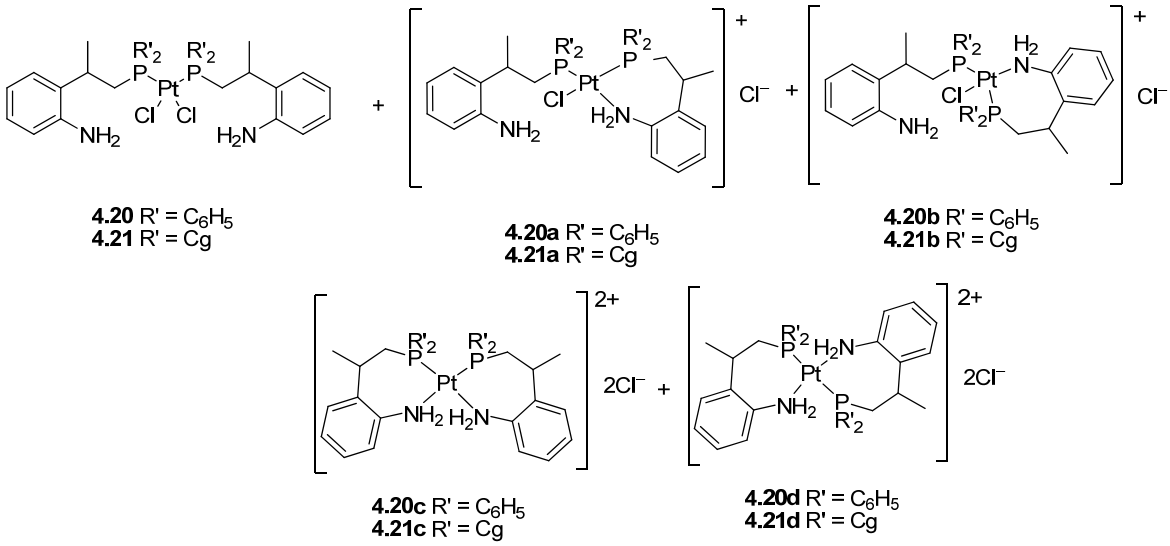

From **4.8** (0.100 g, 0.286 mmol) and $PtCl_2$(COD) (0.053 g, 0.143 mmol). Yield: 0.079 g, 57%. Selected data: ^{1}H NMR (400 MHz, $CDCl_3$, *J* in Hz) due to the mixture of compounds the spectrum could not be assigned. $^{31}P\{^1H\}$ NMR (400 MHz, $CDCl_3$, *J* in Hz) 5.6, 3.6, 2.4, 1.5, 0.6, 0.0, –1.2 ppm.

Preparation of $C_{34}H_{33}NP_2PtCl_2$ (4.22):

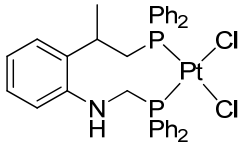

4.22

From **4.9** (0.050 g, 0.096 mmol) and $PtCl_2$(COD) (0.036 g, 0.096 mmol). Yield: 0.060 g, 80%. Selected data: IR (KBr, cm^{-1}): (νNH) 3357, (νPtCl) 316, 291. ^{1}H NMR (400 MHz, $CDCl_3$, *J* in Hz) 7.92 – 6.95 (20 H, m, CH), 6.47 (2 H, t, $^3J_{HH}$ = 6.0, *p*-,*m*-CH), 6.34 (1 H, dd, $^3J_{HH}$ = 8.0, $^4J_{HH}$ = 1.2, *o*-CH), 6.18 (1 H, d, $^3J_{HH}$ = 9.2, *m*-CH), 5.32 – 5.27 (1 H, m, PCH_2N), 4.30 (1 H, m, NH), 3.57 – 3.47 (1 H, m, CH), 3.42 (1 H, bt, $^3J_{HH}$ = 12.8, PCH_2N), 2.67 (1 H, q, $^3J_{HH}$ = 13.6, CH), 1.97 (1 H, q, $^3J_{HH}$ = 8.4, CH), 1.78 (3 H, dd, $^3J_{HH}$ = 16.0, *J* 2.0, CH_3) ppm. $^{31}P\{^1H\}$ NMR (162 MHz, $CDCl_3$, *J* in Hz) 23.9 ($^1J_{PPt}$ = 3768, $^2J_{PP}$ = 9), 11.3 ($^1J_{PPt}$ = 3479, $^2J_{PP}$ = 9) ppm. EI–MS (*m/z*) $[M–Cl]^+$ 747. $C_{34}H_{33}NP_2PtC_{l2}$ 783. EA found (calculated) (%): C 51.74 (52.12), 4.13 (4.24), 1.76 (1.79).

6.5 X–ray Crystallographic Experimental

Measurements were made either by using a diffractometer and radiation source in the home laboratory or at the ESPRC National Service at Southampton (see Appendix for details). The structural study of **2.19** was performed at the Diamond Light Source (station I19) using synchrotron radiation, due to its small size and weakly diffracting nature. All data collections were performed at low temperature (typically in the range of 120–150 K) using a suitable crystal (typically with dimensions in the range 0.1 to 0.8 mm) mounted onto a glass fibre on the goniometer head using a drop of inert oil. Each data collection was run in two stages: firstly with the determination of the orientation matrix, unit cell and crystal system, followed by a longer data collection to measure the full sphere of the total diffraction pattern. Programs used were APEX 2[147] or Rigaku CrystalClear[148] for diffractometer control and Bruker SAINT[149] or Rigaku CrystalClear.[148] A semi–empirical absorption correction was applied using the SADABS program based on equivalent and repeated reflections and the data reduction carried out.[150] The program XPREP within the

SHELXTL suite of programs was used to check for any higher or missed symmetry, and the space group was determined.[151] The structure was solved using the program XS using direct methods.[151] The structure was refined using the program SHELXL–97 or SHELX–2013/4 by full–matrix least squares methods on F^2.[151] Non–hydrogen atoms were initially refined isotropically and then anisotropically. All C*H* atoms were placed in geometrically calculated positions and were refined using a riding model (aryl C–H 0.95 Å, methyl C–H 0.98 Å, methylene C–H 0.99 Å). The NH atoms in **2.6**, **2.14, 2.16, 2.17, 2.19, 2.29, 3.1, 3.2, 3.21, 3.25, 4.3, 4.7, 4.9, 4.16** and **4.19** were freely refined. $U_{iso}(H)$ values were set be 1.2 times U_{eq} of the carrier atom for aryl C*H* and methylene CH_2, and 1.5 times U_{eq} of the carrier atom for O*H*, N*H* and CH_3. The program XP was used to produce graphics.[152] Programs that were used during data collection, refinement and production of graphics were Bruker APEX 2,[147] SAINT,[149] SHELXTL[152] and local programs. Hydrogen bonds are shown as thin dashed lines and thick dashed lines are used to signify the η^6–bonding of the *p*–cymene to the Ru(II) metal centres in the structures in this thesis.

Data for compounds **2.6**, **2.12**, **2.14**, **2.29**, **2.35**, **3.6a**, **3.20**, **3.21**, **o,o–(CHPh$_2$)$_2$–*p*–MeC$_6$H$_2$NH$_2$**, **4.7**, **4.9**, **4.10a**, **4.12a**, **4.16** and **4.19** were collected using a Bruker APEX 2 CCD diffractometer using graphite–monochromated Mo–K_α radiation (λ = 0.71073 Å). Data for **2.16**, **2.17**, **2.27**, **2.31**, **3.1**, **3.2**, **3.9**, **3.16, 3.19**, **3.25**, **3.27b** and **3.44** were collected at the Rigaku AFC6 with Saturn724+ (2x2 bin mode) diffractometer using graphite–monochromated Mo–K_α radiation (λ = 0.71073 Å). Data for **3.47** and **4.3** were collected at the Bruker–Nonius Roper CCD camera on κ–goniostat diffractometer using graphite–monochromated Mo–K_α radiation (λ = 0.71073 Å). Data for **4.2a** was collected on an Agilent SuperNova, Dual, Cu at zero, Atlas diffractometer using graphite–monochromated Cu–K_α radiation (λ = 1.54184 Å). Data for **4.12a** was collected on and Agilent SuperNova, Dual, Cu at zero, Atlas diffractometer using graphite–monochromated Mo–K_α radiation (λ = 0.71073 Å). Data for compound **2.19** was collected at the Diamond Light Source (station I19) using synchrotron radiation (0.6889 Å).

Compound **2.12** was found to contain a disordered phenyl ring with C(17) > C(22) modelled over two sets of positions [major: minor components = 0.514(14):0.486(14)%].

Compound **2.16** contains a peak (Q1 = 1.40 electrons) which belongs to the lone pair of electrons on phosphorus with a d(P–Q1) < 1.20 Å.

Compound **2.17** was found to contain a disordered isopropyl group with C(20) > C(22) modelled over two sets of positions [major: minor components = 0.654(12):0.346(12)%].

Compound **2.19** was found to contain a disordered ethyl group with C(27) > C(28) modelled over two sets of positions [major: minor components = 0.532(19):0.468(19)%].

Compound **3.6a** was found to contain a disordered *o*–F phenyl groups with C(2) > F(1) modelled over two sets of positions [major: minor components = 0.501(5):0.499(5)%] with C(2) being coincident and C(27) > F(4) modelled over two sets of positions [major: minor components = 0.503(5):0.497(5)%].

Compound **3.25** was found to contain a disordered phenyl groups with C(17) > F(9) modelled over two sets of positions [major: minor components = 0.605(5):0.395(5)%] with C(17) and C(23) being coincident.

Compound **3.47** was found to contain a disordered isopropyl groups with C(53) > C(55) modelled over two sets of positions [major: minor components = 0.861(10):0.139(10)%].

Compound **4.10a** was found to contain a total of two solvent accessible voids of 371 $Å^3$, each containing 116 electrons, which is equivalent to two $CHCl_3$ moieties which contain 58 electrons per void within its crystal structure which were modelled as areas of diffuse electron density using SQUEEZE.[153]

Compound **4.12a** was found to contain a total of two solvent accessible voids of 416 $Å^3$, each containing 128 electrons, which is equivalent to two $CHCl_3$ moieties which contain 58 electrons per void within its crystal structure which were modelled as areas of diffuse electron density using SQUEEZE.[153] The 1,3,5,7–tetramethyl–2,4,8–trioxa–6–phosphaadamantane was found to have O(4) and C(25) in the same position.

Compounds **3.1** and **3.44** were found to contain a total of one and two $CHCl_3$ molecules respectively whereas **3.6a** contains a total of two CH_2Cl_2 molecules.

Accompanying CD at the back of this thesis containing tables and data for the crystal structures given in this thesis.

7. References

1. R. Starosta, A. Bykowska, M. Barys, A. K. Wieliczko, Z. Staroniewicz, and M. Jeżowska-Bojczuk, *Polyhedron*, 2011, **30**, 2914.

2. H. Han, M. Elsmaili, and S. A. Johnson, *Inorg. Chem.*, 2006, **45**, 7435.

3. R. Raturi, J. Lefebvre, D. B. Leznoff, B. R. McGarvey, and S. A. Johnson, *Chem. Eur. J.*, 2008, **14**, 721.

4. H. Han and S. A. Johnson, *Organometallics*, 2006, **25**, 5594.

5. J. A. Hatnean, R. Raturi, J. Lefebvre, D. B. Leznoff, G. Lawes, and S. A. Johnson, *J. Am. Chem. Soc.*, 2006, **128**, 14992.

6. N. Thirupathi, P. M. Stricklen, X. Liu, R. Oshel, I. Guzei, A. Ellern, and J. G. Verkade, *Inorg. Chem.*, 2007, **46**, 9351.

7. G. M. Brown, M. R. J. Elsegood, A. J. Lake, N. M. Sanchez-Ballester, M. B. Smith, T. S. Varley, and K. Blann, *E. J. Inorg. Chem.*, 2007, 1405.

8. W. J. Shaw, M. L. Helm, and D. L. DuBois, *Biochim. Biophys. Acta*, 2013, **1827**, 1123.

9. A. A. Karasik, A. S. Balueva, E. I. Musina, and O. G. Sinyashin, *Mendeleev Commun.*, 2013, **23**, 237.

10. C. D. Swor, K. R. Hanson, L. N. Zakharov, and D. R. Tyler, *Dalt. Trans.*, 2011, **40**, 8604.

11. K. Kellner, B. Seidel, and A. Tzschach, *J. Organomet. Chem.*, 1978, **149**, 167.

12. S. E. Durran, M. R. J. Elsegood, and M. B. Smith, *New J. Chem.*, 2002, **26**, 1402.

13. S. E. Durran, M. R. J. Elsegood, N. Hawkins, M. B. Smith, and S. Talib, *Tetrahedron Lett.*, 2003, **44**, 5255.

14. S. E. Durran, M. B. Smith, A. M. Z. Slawin, and J. W. Steed, *J. Chem. Soc. Dalt. Trans.*, 2000, **16**, 2771.

15. M. B. Smith and M. R. J. Elsegood, *Tetrahedron Lett.*, 2002, **43**, 1299.

16. A. T. Ekubo, Loughborough University, Leicestershire, UK, PhD Thesis, 2009.

17. A. T. Ekubo, M. R. J. Elsegood, A. J. Lake, and M. B. Smith, *Inorg. Chem.*, 2010, **49**, 3703.

18. A. T. Ekubo, M. R. J. Elsegood, A. J. Lake, and M. B. Smith, *Inorg. Chem.*, 2009, **48**, 2633.

19. S. E. Dann, S. E. Durran, M. R. J. Elsegood, M. B. Smith, P. M. Staniland, S. Talib, and S. H. Dale, *J. Organomet. Chem.*, 2006, **691**, 4829.

20. M. B. Smith, S. H. Dale, S. J. Coles, T. Gelbrich, M. B. Hursthouse, and M. E. Light, *Cryst. Eng. Comm.*, 2006, **8**, 140.

21. S. E. Durran, M. B. Smith, S. H. Dale, S. J. Coles, M. B. Hursthouse, and M. E. Light, *Inorg. Chim. Acta*, 2006, **359**, 2980.

22. M. R. J. Elsegood, A. J. Lake, R. J. Mortimer, M. B. Smith, and G. W. Weaver, *J. Organomet. Chem.*, 2008, **693**, 2317.

23. S. J. Coles, S. E. Durran, M. B. Hursthouse, M. Z. Slawin, and M. B. Smith, *New J. Chem.*, 2001, **25**, 416.

24. A. Hoffman, *J. Am. Chem. Soc.*, 1921, **2**, 1684.

25. A. W. Frank, A. S. D. George, and L. Drake, *J. Org. Chem.*, 1979, **37**, 2752.

26. A. W. Frank and G. L. Drake, *J. Org. Chem.*, 1977, **42**, 4125.

27. J. W. Ellis, K. N. Harrison, P. A. T. Hoye, A. G. Orpen, P. G. Pringle, and M. B. Smith, *Inorg. Chem.*, 1992, **31**, 3026.

28. W. J. Connick and J. Boudreaux, *J. Org. Chem.*, 1972, **37**, 3453.

29. R. Starosta, M. Florek, J. Król, M. Puchalska, and A. Kochel, *New J. Chem.*, 2010, **34**, 1441.

30. P. A. T. Hoye, P. G. Pringle, M. B. Smith, and K. Worboys, *J. Chem. Soc. Dalt. Trans*, 1993, 269.

31. D. S. Bharathi, M. A. Sridhar, J. S. Prasad, and A. G. Samuelson, *Inorg. Chem. Comm.*, 2001, **4**, 490.

32. M. D. Doud, K. A. Grice, A. M. Lilio, C. S. Seu, and C. P. Kubiak, *Organometallics*, 2012, **31**, 779.

33. D. V. Griffiths, H. J. Groombridge, and M. C. Salt, *Phosphorus, Sulfur and Silicon*, 2008, **183**, 473.

34. Q. Zhang, S. M. Aucott, A. M. Z. Slawin, and J. D. Woollins, *Eur. J. Inorg. Chem.*, 2002, **7**, 1635.

35. J. F. Zhang, W. F. Fu, X. Gan, and J. H. Chen, *Dalt. Trans.*, 2008, 3093.

36. A. L. Balch, M. M. Olmstead, and S. P. Rowley, *Inorg. Chim. Acta*, 1990, **168**, 255.

37. V. G. Markl, G. Y. Jin, and C. Schoerner, *Tetrahedron Lett.*, 1980, **21**, 1845.

38. A. A. Karasik, O. G. Sinyashin, J. Heinicke, and E. Hey-Hawkins, *Phosphorus, Sulfur and Silicon*, 2002, **177**, 1469.

39. A. A. Karasik, I. O. Georgiev, E. I. Musina, O. G. Sinyashin, and J. Heinicke, *Polyhedron*, 2001, **20**, 3321.

40. F. Z. Baimukhametov, V. F. Zheltukhin, G. N. Nikonov, and A. S. Balueva, *Russ. J. Gen. Chem.*, 2002, **72**, 1754.

41. D. E. Berning, K. V. Katti, C. L. Barnes, and W. A. Volkert, *J. Am. Chem. Soc.*, 1999, **121**, 1658.

42. K. Raghuraman, K. K. Katti, L. J. Barbour, N. Pillarsetty, C. L. Barnes, and K. V Katti, *J. Am. Chem. Soc.*, 2003, **125**, 6955.

43. R. Huang and B. J. Frost, *Inorg. Chem.*, 2007, **46**, 1221.

44. H. Han and S. A. Johnson, *Eur. J. Inorg. Chem.*, 2008, **3**, 471.

45. R. Starosta, U. K. Komarnicka, M. Puchalska, and M. Barys, *New J. Chem.*, 2012, **36**, 1673.

46. R. Starosta, M. Puchalska, J. Cybińska, M. Barys, and A. V Mudring, *Dalt. Trans.*, 2011, **40**, 2459.

47. R. Starosta, A. Brzuszkiewicz, A. Bykowska, U. K. Komarnicka, B. Bażanów, M. Florek, Ł. Gadzała, N. Jackulak, J. Król, and K. Marycz, *Polyhedron*, 2013, **50**, 481.

48. R. Starosta, B. Bazanów, and W. Barszczewski, *Dalt. Trans.*, 2010, **39**, 7547.

49. M. Keles, Z. Aydin, and O. Serindag, *J. Organomet. Chem.*, 2007, **692**, 1951.

50. M. Keles, O. Altan, and O. Seridag, *Heteroat. Chem*, 2008, **19**, 113.

51. C. Klemps, E. Payet, L. Magna, L. Saussine, X. F. Le Goff, and P. Le Floch, *Chem. Eur. J.*, 2009, **15**, 8259.

52. Z. M. Heiden, S. Chen, M. T. Mock, W. G. Dougherty, W. S. Kassel, R. Rousseau, and R. M. Bullock, *Inorg. Chem.*, 2013, **52**, 4026.

53. P. Scherl, A. Kruckenberg, H. Wadepohl, and L. H. Gade, *Organometallics*, 2012, **31**, 7024.

54. A. Kruckenberg, H. Wadepohl, and L. H. Gade, *Organometallics*, 2013, **32**, 5153.

55. A. A. Karasik, R. N. Naumov, R. Sommer, O. G. Sinyashin, and E. Hey-Hawkins, *Polyhedron*, 2002, **21**, 2251.

56. A. A. Karasik, I. O. Georgiev, O. G. Sinyashin, and E. Hey-Hawkins, *Polyhedron*, 2000, **19**, 1455.

57. A. A. Karasik, I. O. Georgiev, R. I. Vasiliev, and O. G. Sinyashin, *Mendeleev Commun.*, 1998, **8**, 140.

58. A. Jain, M. L. Helm, J. C. Linehan, D. L. DuBois, and W. J. Shaw, *Inorg. Chem. Comm.*, 2012, **22**, 65.

59. I. A. Litivinov, A. A. Karasik, S. V Bobrov, V. A. Naumov, and A. G. Akhmadullin, *Russ. Chem. Bull.*, 1994, **42**, 1587.

60. S. V. Bobrov, A. A. Karasik, and O. G. Sinyashin, *Phosphorus, Sulfur and Silicon*, 1999, **144**, 289.

61. S. V. Bobrov, A. A. Karasik, and O. G. Sinyashin, *Chem. Comput. Simulation. Butlerov Commun.*, 1999, **1**, 35.

62. S. K. Latypov, A. G. Strelnik, S. N. Ignatieva, E. Hey-Hawkins, A. S. Balueva, A. A. Karasik, and O. G. Sinyashin, *J. Phys. Chem. A*, 2012, **116**, 3182.

63. S. N. Ignatieva, A. S. Balueva, A. A. Karasik, S. K. Latypov, A. G. Nikonova, O. E. Naumova, P. Lönnecke, E. Hey-Hawkins, and O. G. Sinyashin, *Inorg. Chem.*, 2010, **49**, 5407.

64. A. A. Karasik, R. N. Naumov, O. G. Sinyashin, G. P. Belov, H. V Novikova, and E. Hey-hawkins, *Dalt. Trans.*, 2003, 2209.

65. A. A. Karasik, R. N. Naumov, A. S. Balueva, Y. S. Spiridonova, O. N. Golodkov, H. V. Novikova, G. P. Belov, S. A. Katsyuba, E. E. Vandyukova, L. Peter, E. Hey-Hawkins, and O. G. Sinyashin, *Heteroat. Chem*, 2006, **17**, 499.

66. M. T. Mock, S. Chen, R. Rousseau, M. J. O'Hagan, W. G. Dougherty, W. S. Kassel, D. L. DuBois, and R. M. Bullock, *Chem. Commun.*, 2011, **47**, 12212.

67. G. M. Jacobsen, J. Y. Yang, B. Twamley, A. D. Wilson, R. M. Bullock, M. Rakowski DuBois, and D. L. DuBois, *Energy Environ. Sci.*, 2008, **1**, 167.

68. U. J. Kilgore, J. a S. Roberts, D. H. Pool, A. M. Appel, M. P. Stewart, M. R. DuBois, W. G. Dougherty, W. S. Kassel, R. M. Bullock, and D. L. DuBois, *J. Am. Chem. Soc.*, 2011, **133**, 5861–72.

69. A. D. Wilson, K. Fraze, B. Twamley, S. M. Miller, D. L. DuBois, and M. R. DuBois, *J. Am. Chem. Soc.*, 2008, **130**, 1061.

70. A. S. Balueva, R. M. Kuznetsov, S. N. Ignat'eva, A. A. Karasik, A. T. Gubaidullin, I. A. Litvinov, O. G. Sinyashin, P. Lönnecke, and E. Hey-Hawkins, *Dalt. Trans.*, 2004, 442.

71. T. Liu, D. L. Dubois, and R. M. Bullock, *Nat. Chem.*, 2013, **5**, 228.

72. A. A. Karasik, D. V Kulikov, a S. Balueva, S. N. Ignat'eva, O. N. Kataeva, P. Lönnecke, a V Kozlov, S. K. Latypov, E. Hey-Hawkins, and O. G. Sinyashin, *Dalt. Trans.*, 2009, 490.

73. E. D. Weil and S. V. Levchik, *J. Fire Sci.*, 2008, **26**, 243.

74. W. A. Reeves, O. J. McMillan, and J. D. Guthrie, *Text. Res. J.*, 1953, **23**, 527.

75. P. Kisanga and J. Verkade, *Heteroat. Chem*, 2001, **12**, 114.

76. E. Payet, A. Auffrant, X. F. Le Goff, and P. Le Floch, *J. Organomet. Chem.*, 2010, **695**, 1499.

77. J. G. E. Krauter and M. Beller, *Tetrahedron*, 2000, **56**, 771.

78. J. V Gavette, J. Lara, O. B. Berryman, L. N. Zakharov, M. M. Haley, and D. W. Johnson, *Chem. Commun.*, 2011, **47**, 7653.

79. S. I. Featherman and L. D. Quin, *J. Am. Chem. Soc.*, 1974, **97**, 4349.

80. J. C. Kane, E. H. Wong, G. P. A. Yap, and A. L. Rheingold, *Polyhedron*, 1999, **18**, 1183.

81. J. W. Peters, W. N. Lanzilotta, B. J. Lemon, and L. C. Seefeldt, *Science*, 1998, **282**, 1853.

82. D. Förster, H. Dilger, F. Ehret, M. Nieger, and D. Gudat, *Eur. J. Inorg. Chem.*, 2012, **25**, 3989.

83. R. Tian, Y. Mei, Z. Duan, and F. Mathey, *Organometallics*, 2013, **32**, 5615.

84. O. Disulfid, J. Kaiser, R. Richter, and H. Hartung, *Tetrahedron*, 1978, **34**, 1.

85. D. Tofan, M. Temprado, S. Majumdar, C. D. Hoff, and C. C. Cummins, *Inorg. Chem.*, 2013, **52**, 8851.

86. D. Tofan and C. C. Cummins, *Chem. Sci.*, 2012, **3**, 2474.

87. N. A. Piro, J. S. Figueroa, J. T. McKellar, and C. C. Cummins, *Science*, 2006, **313**, 1276.

88. R. W. Alder, C. Ganter, M. Gil, R. Gleiter, C. J. Harris, S. E. Harris, H. Lange, a. G. Orpen, and P. N. Taylor, *J. Chem. Soc. Perkin Trans. 1*, 1998, **10**, 1643.

89. E. V. N. and G. N. N. V. A. Zagummennov, A. A. Karasik, *Russ. J. Gen. Chem.*, 1999, **69**, 886.

90. R. W. Alder, D. D. Ellis, R. Gleiter, C. J. Harris, H. Lange, a. G. Orpen, D. Read, and P. N. Taylor, *J. Chem. Soc. Perkin Trans. 1*, 1998, **10**, 1657.

91. R. W. Alder, C. P. Butts, A. G. Orpen, D. Read, and J. M. Oliva, *J. Chem. Soc. Perkin Trans. 2*, 2001, **3**, 282.

92. R. W. Alder, D. D. Ellis, A. G. Orpen, and P. N. Taylor, *Chem. Comm.*, 1996, 539.

93. A. A. Karasik, O. A. Erastov, and B. A. Arbuzov, *Bull. Acad. Sci. USSR*, 1989, **6**, 1375.

94. V. A. Zagumennov, A. A. Karasik, E. V Nikitin, and G. N. Nikonov, *Russ. Chem. Bull.*, 1997, **46**, 1154.

95. D. Weber, S. H. Hausner, A. Eisengräber-Pabst, S. Yun, J. a. Krause-Bauer, and H. Zimmer, *Inorganica Chim. Acta*, 2004, **357**, 125.

96. P. A. Dub, A. Béthegnies, J. Daran, and R. Poli, *Organometallics*, 2012, **31**, 3081.

97. S. Osman, R. D. W. Kemmitt, J. Fawcett, and D. R. Russell, *Transit. Met. Chem.*, 1999, **491**, 486.

98. H. Yin, L. Dong, M. Hong, and J. Cui, *J. Organomet. Chem.*, 2011, **696**, 1824.

99. G. N. Nikonov, A. A. Karasik, E. V. Malova, and K. M. Enikeev, *Heteroat. Chem*, 1992, **3**, 439.

100. J. Andrieu, C. Baldoli, S. Maiorana, R. Poli, and P. Richard, *Eur. J. Inorg. Chem.*, 1999, **1**, 3095.

101. C. R. Raw, Loughborough University, Leicestershire, UK, PhD Thesis, 2011.

102. P. G. Jones and F. Ruthe, *Priv. Commun.*, 2004.

103. A. Kreienbrink, M. B. Sárosi, E. G. Rys, P. Lönnecke, and E. Hey-Hawkins, *Angew. Chemie*, 2011, **50**, 4701.

104. A. Kreienbrink, P. Lönnecke, M. Findeisen, and E. Hey-Hawkins, *Chem. Comm.*, 2012, **48**, 9385.

105. T. Brenstrum, J. Clattenburg, J. Britten, S. Zavorine, J. Dyck, A. J. Robertson, J. Mcnulty, and A. Capretta, *Org. Lett.*, 2006, **8**, 103.

106. R. A. Baber, M. F. Haddow, A. J. Middleton, A. G. Orpen, P. G. Pringle, A. Haynes, and G. L. Williams, *Organometallics*, 2007, **26**, 713.

107. T. R. Cook, Y. Surendranath, and D. G. Nocera, *J. Am. Chem. Soc.*, 2009, **131**, 28.

108. R. Chi, F. P. Fanizzi, F. P. Intini, and G. Natile, *J. Am. Chem. Soc.*, 1991, **113**, 7805.

109. R. Cini, F. P. Fanizzi, F. P. Inti, L. Maresca, and G. Natile, *J. Am. Chem. Soc.*, 1993, **115**, 5123.

110. C. Albrecht, S. Schwieger, T. Ru, C. Bruhn, T. Lis, D. Steinborn, and D. Halle, *Organometallics*, 2007, **2**, 6000.

111. A. Díez, J. Forniés, C. Larraz, E. Lalinde, J. a López, A. Martín, M. T. Moreno, and V. Sicilia, *Inorg. Chem.*, 2010, **49**, 3239.

112. L. S. Hollis, M. M. Roberts, and S. J. Lippard, *Inorg. Chem.*, 1983, **22**, 3637.

113. A. Santoro, M. Wegrzyn, A. C. Whitwood, B. Donnio, and D. W. Bruce, *J. Am. Chem. Soc.*, 2010, **132**, 10689.

114. D. Tofan and C. C. Cummins, *Angew. Chemie Int. Ed.*, 2010, **49**, 7516.

115. S. J. Geier and D. W. Stephan, *Chem. Comm.*, 2008, **054**, 99.

116. A. L. Crumbliss, R. J. Topping, J. Szewczyk, A. T. Mcphail, and L. D. Quin, *J. Chem. Soc. Chem. Comm*, 1986, 1895.

117. H. Werner and B. Klingert, *J. Organomet. Chem.*, 1981, **218**, 395.

118. S. Y. Zhang, S. Yemul, H. B. Kagan, R. Stern, D. Commereuc, and Y. Chauvin, *Tetrahedron Lett.*, 1981, **22**, 3955.

119. E. S. Wiedner and M. L. Helm, *Organometallics*, 2013, **2**, 3.

120. L. D. Davies, J. Neild, L. J. S. Prouse, and D. R. Russell, *Polyhedron*, 1993, **12**, 2121.

121. G. K. Anderson and G. J. Lumetta, *Inorg. Chem.*, 1987, **26**, 1518.

122. P. Bhattacharyya, R. N. Sheppard, A. M. Slawin, D. J. Williams, and J. D. Woollins, *J. Chem. Soc. Dalt. Trans*, 1993, 2393.

123. G. R. Fulmer, A. J. M. Miller, N. H. Sherden, H. E. Gottlieb, A. Nudelman, B. M. Stoltz, J. E. Bercaw, and K. I. Goldberg, *Organometallics*, 2010, **29**, 2176.

124. D. E. Berning, B. C. Noll, and D. L. Dubois, *J. Am. Chem. Soc.*, 1999, **121**, 11432.

125. C.-Q. Zhao, M. C. Jennings, and R. J. Puddephatt, *Inorg. Chim. Acta*, 2008, **361**, 3301.

126. R. García-Álvarez, J. Díez, P. Crochet, and V. Cadierno, *Organometallics*, 2010, **29**, 3955.

127. R. J. H. K. Fun, M. Hemamalini, P. Shanmugavelan, A. Ponnuswamy, *Acta Crystallogr., Sect.E Struct. Rep. Online*, 2010, **67**, o2776.

128. M. Cokoja, C. Bruckmeier, B. Rieger, W. A. Herrmann, and F. E. Kühn, *Angew. Chemie Int. Ed.*, 2011, **50**, 8510.

129. T. A. Tronic, M. Rakowski DuBois, W. Kaminsky, M. K. Coggins, T. Liu, and J. M. Mayer, *Angew. Chemie Int. Ed.*, 2011, **50**, 10936.

130. B. Demerseman, M. D. Mbaye, D. Sémeril, L. Toupet, C. Bruneau, and P. H. Dixneuf, *Eur. J. Inorg. Chem.*, 2006, **6**, 1174.

131. G. Espino, B. R. Manzano, M. Moreno, N. Agustin Caballero, B. R. Manzano, L. Santos, M. Perez Manrique, and F. A. Jalon, *Organometallics*, 2012, **31**, 3087.

132. H. Hellmann, J. Bader, H. Birkner, and O. Schumacher, *Ann. Der Chemie Justus Liebig*, 1962, **659**, 49.

133. G. Berthon-Gelloz, M. A. Siegler, A. L. Spek, B. Tinant, J. N. H. Reek, and I. E. Markó, *Dalt. trans.*, 2010, **39**, 1444.

134. J. M. Antelo, L. Adrio, B. Bermúdez, J. Martínez, M. Teresa Pereira, J. M. Ortigueira, M. López-Torres, and J. M. Vila, *J. Organomet. Chem.*, 2013, **740**, 83.

135. I. Dance and M. Scudder, *J. Chem. Soc. Chem. Comm*, 1995, 1039.

136. E. D'Oria, D. Braga, and J. J. Novoa, *Cryst. Eng. Comm.*, 2012, **14**, 792.

137. M. Revés, C. Ferrer, T. León, S. Doran, P. Etayo, A. Vidal-Ferran, A. Riera, and X. Verdaguer, *Angew. Chem. Int. Ed. Engl.*, 2010, **49**, 9452.

138. T. Ogawa, Y. Kajita, Y. Wasada-Tsutsui, H. Wasada, and H. Masuda, *Inorg. Chem.*, 2013, **52**, 182.

139. P. G. Pringle and M. B. Smith, in *Phosphorus(III) Ligands in Homogeneus Catalysis: Design and Synthesis*, eds. P. C. J. Kamer and P. W. N. M. Van Leeuwen, John Wiley & Sons, Ltd., First., 2012, p. 391.

140. A. Baber, C. Fan, D. W. Norman, a. G. Orpen, P. G. Pringle, and R. L. Wingad, *Organometallics*, 2008, **27**, 5906.

141. M. K. Cooper and J. M. Downes, *J. Chem. Soc. Chem. Comm*, 1981, 381.

142. M. K. Cooper and J. M. Downes, *Inorg. Chem.*, 1978, **17**, 880.

143. D. Drew and J. R. Doyle, *Inorg. Synth.*, 1972, **13**, 47.

144. J. X. Mcdermott, J. F. White, and G. M. Whitesides, *J. Am. Chem. Soc.*, 1976, **98**, 6521.

145. C. White, A. Yates, and P. M. Maitlis, *Inorg. Synsthesis*, 1992, 228.

146. M. A. Bennett and A. K. Smith, *Dalt. Trans.*, 1974, 233.

147. Bruker APEX2 Softw. CCD Diffractom. Bruler AXS INc., Madison, USA, 2008.

148. Rigaku (2011), CrystalClear-SM Expert. Version 3.1 b10, Rigaku Am. Woodlands, Texas, USA., 2011.

149. SAINT Softw. CCD Diffractom. 2008, Bruker AXS Inc., Madison, USA., 2008.

150. G. M. Sheldrick, SADABS, 2012, Version 2012/1, Univ. Göttingen, Ger., 2012.

151. G. M. Sheldrick, *Acta Crystallogr.*, 2008, **A64**, 112., 2008.

152. G. M. Sheldrick, *SHELXTL user Man.*, 2001, version 6.12, Bruker AXS Inc., Madison, WI., 2001.

153. P. V. D. Sluis A. L. Spek, *Acta Cryst. Sect. A,* 1990, **46**, 194, 1990.

8. Appendices

2.6

Crystal data

$C_{16}H_{14}Cl_{0.50}F_6N_2P_{0.50}$	V = 3215.1 (4) Å^3
M_r = 381.50	Z = 8
Tetragonal, $P4_1$	F(000) = 1552
a = 19.5774 (14) Å	D_x = 1.576 Mg m^{-3}
b = 19.5774 (14) Å	Mo $K\alpha$ radiation, λ = 0.71073 Å
c = 8.3885 (6) Å	μ = 0.27 mm^{-1}
α = 90°	T = 150 K
β = 90°	0.54 × 0.30 × 0.14 mm
γ = 90°	

Data collection

Radiation source: fine–focus sealed tube	R_{int} = 0.046
Graphite monochromator	θ_{max} = 29.3°, θ_{min} = 2.1°
17177 measured reflections	h = –26→26
2201 independent reflections	k = –26→26
1598 reflections with $I > 2\sigma(I)$	l = –11→11

Refinement

Refinement on F^2	Primary atom site location: structure–invariant direct methods
Least–squares matrix: full	Secondary atom site location: difference Fourier map
$R[F^2 > 2\sigma(F^2)]$ = 0.052	Hydrogen site location: inferred from neighbouring sites
$wR(F^2)$ = 0.160	H atoms treated by a mixture of independent and constrained refinement
S = 1.11	$w = 1/[\sigma^2(F_o^2) + (0.0753P)^2 + 2.7933P]$ where $P = (F_o^2 + 2F_c^2)/3$
2201 reflections	$(\Delta/\sigma)_{max}$ = 0.001
116 parameters	$\Delta\rangle_{max}$ = 0.37 e Å^{-3}
0 restraints	$\Delta\rangle_{min}$ = –0.85 e Å^{-3}

2.12

Crystal data

$C_{22}H_{24}N_3P$	$Z = 2$
$M_r = 361.41$	$F(000) = 384$
Triclinic, $P\bar{1}$	$D_x = 1.274$ Mg m^{-3}
Hall symbol: –P 1	Mo $K\alpha$ radiation, $\lambda = 0.71073$ Å
$a = 6.1323$ (3) Å	Cell parameters from 11948 reflections
$b = 11.8760$ (7) Å	$\theta = 2.9$–$27.5°$
$c = 13.8702$ (9) Å	$\mu = 0.16$ mm^{-1}
$\alpha = 100.148$ (3)°	$T = 120$ K
$\beta = 100.568$ (3)°	Rod, colourless
$\gamma = 103.092$ (4)°	0.30 × 0.07 × 0.06 mm
$V = 941.84$ (9) Å^3	

Data collection

Bruker–Nonius Roper CCD camera on κ–goniostat diffractometer	3322 independent reflections
Radiation source: Bruker–Nonius FR591 rotating anode	2306 reflections with $I > 2\sigma(I)$
Graphite monochromator	$R_{int} = 0.081$
Detector resolution: 9.091 pixels mm^{-1}	$\theta_{max} = 25.0°$, $\theta_{min} = 3.2°$
ϕ & ω scans	$h = -7 \rightarrow 7$
Absorption correction: multi–scan *SADABS* v2007/2, Sheldrick, G.M., (2007)	$k = -14 \rightarrow 14$
$T_{min} = 0.955$, $T_{max} = 0.991$	$l = -16 \rightarrow 16$
16860 measured reflections	

Refinement

Refinement on F^2	Secondary atom site location: difference Fourier map
Least–squares matrix: full	Hydrogen site location: geom except NH coords freely refined
$R[F^2 > 2\sigma(F^2)] = 0.060$	H atoms treated by a mixture of independent and constrained refinement
$wR(F^2) = 0.155$	$w = 1/[\sigma^2(F_o^2) + (0.0561P)^2 + 0.7115P]$ where $P = (F_o^2 + 2F_c^2)/3$
$S = 1.06$	$(\Delta/\sigma)_{max} < 0.001$
3322 reflections	$\Delta\rangle_{max} = 0.29$ e Å^{-3}
294 parameters	$\Delta\rangle_{min} = -0.24$ e Å^{-3}
224 restraints	Extinction correction: *SHELXL*, $Fc^* = kFc[1+0.001xFc^2\lambda^3/\sin(2\theta)]^{-1/4}$
Primary atom site location: structure–invariant direct methods	Extinction coefficient: 0.020 (4)

2.14

Crystal data

$C_{31}H_{42}N_3P$	$Z = 2$
$M_r = 487.64$	$F(000) = 528$
Triclinic, $P\bar{1}$	$D_x = 1.154$ Mg m^{-3}
$a = 10.4521$ (6) Å	Mo $K\alpha$ radiation, $\lambda = 0.71073$ Å
$b = 11.7150$ (6) Å	Cell parameters from 4297 reflections
$c = 12.9759$ (7) Å	$\theta = 2.2$–$28.1°$
$\alpha = 74.4351$ (8)°	$\mu = 0.12$ mm^{-1}
$\beta = 66.8811$ (8)°	$T = 150$ K
$\gamma = 79.8508$ (9)°	Block, colourless
$V = 1403.16$ (13) Å^3	0.32 × 0.21 × 0.09 mm

Data collection

Bruker APEX 2 CCD diffractometer	6921 independent reflections
Radiation source: sealed tube	5055 reflections with $I > 2\sigma(I)$
Graphite monochromator	$R_{int} = 0.028$
ω rotation with narrow frames scans	$\theta_{max} = 28.3°$, $\theta_{min} = 1.8°$
Absorption correction: multi–scan *SADABS* v2008/1, Sheldrick, G.M., (2008)	$h = -13 \rightarrow 13$
$T_{min} = 0.962$, $T_{max} = 0.989$	$k = -15 \rightarrow 15$
14514 measured reflections	$l = -17 \rightarrow 17$

Refinement

Refinement on F^2	0 restraints
Least–squares matrix: full	Hydrogen site location: mixed
$R[F^2 > 2\sigma(F^2)] = 0.044$	H atoms treated by a mixture of independent and constrained refinement
$wR(F^2) = 0.110$	$w = 1/[\sigma^2(F_o^2) + (0.0442P)^2 + 0.3132P]$ where $P = (F_o^2 + 2F_c^2)/3$
$S = 1.03$	$(\Delta/\sigma)_{max} < 0.001$
6921 reflections	$\Delta\rangle_{max} = 0.40$ e Å^{-3}
325 parameters	$\Delta\rangle_{min} = -0.22$ e Å^{-3}

2.16

Crystal data

$C_{25}H_{30}N_3P$	$Z = 2$
$M_r = 403.49$	$F(000) = 432$
Triclinic, $P\bar{1}$	$D_x = 1.240$ Mg m^{-3}
$a = 5.9410$ (3) Å	Mo $K\alpha$ radiation, $\lambda = 0.71073$ Å
$b = 13.7654$ (10) Å	Cell parameters from 3907 reflections
$c = 13.7686$ (10) Å	$\theta = 3.0$–$27.5°$
$\alpha = 81.151$ (6)°	$\mu = 0.14$ mm^{-1}
$\beta = 78.428$ (6)°	$T = 120$ K
$\gamma = 80.814$ (6)°	Plate, colourless
$V = 1080.29$ (13) Å^3	0.17 × 0.07 × 0.02 mm^3

Data collection

Rigaku AFC6 with Saturn724+ (2x2 bin mode) diffractometer	4950 independent reflections
Radiation source: Rotating Anode	3964 reflections with $I > 2\sigma(I)$
Detector resolution: 28.5714 pixels mm^{-1}	$R_{int} = 0.041$
profile data from ω–scans	$\theta_{max} = 27.5°$, $\theta_{min} = 3.0°$
Absorption correction: multi–scan *CrystalClear*–SM Expert 3.1 b18 (Rigaku, 20112)	$h = -7 \rightarrow 7$
$T_{min} = 0.976$, $T_{max} = 0.997$	$k = -17 \rightarrow 17$
14694 measured reflections	$l = -17 \rightarrow 17$

Refinement

Refinement on F^2	Primary atom site location: structure–invariant direct methods
Least–squares matrix: full	Secondary atom site location: all non–H atoms found by direct methods
$R[F^2 > 2\sigma(F^2)] = 0.052$	Hydrogen site location: mixed
$wR(F^2) = 0.135$	H atoms treated by a mixture of independent and constrained refinement
$S = 1.04$	$w = 1/[\sigma^2(F_o^2) + (0.0547P)^2 + 0.8468P]$ where $P = (F_o^2 + 2F_c^2)/3$
4950 reflections	$(\Delta/\sigma)_{max} = 0.001$
266 parameters	$\Delta\rangle_{max} = 1.40$ e Å^{-3}
0 restraints	$\Delta\rangle_{min} = -0.38$ e Å^{-3}

2.17

Crystal data

$C_{31}H_{42}N_3P$	V = 1386.06 (17) Å^3
M_r = 487.64	Z = 2
Triclinic, $P\bar{1}$	$F(000)$ = 528
a = 5.9928 (4) Å	D_x = 1.168 Mg m^{-3}
b = 14.9505 (11) Å	Mo $K\alpha$ radiation, λ = 0.71073 Å
c = 15.5973 (11) Å	μ = 0.12 mm^{-1}
α = 96.038 (9)°	T = 100 K
β = 93.851 (9)°	Needle, colourless
γ = 91.114 (9)°	0.31 × 0.03 × 0.03 mm^3

Data collection

Rigaku Saturn724+ (2x2 bin mode) diffractometer	4303 independent reflections
Radiation source: Sealed Tube	2926 reflections with $I > 2\sigma(I)$
Detector resolution: 28.5714 pixels mm^{-1}	R_{int} = 0.056
profile data from ω–scans	θ_{max} = 24.0°, θ_{min} = 2.7°
Absorption correction: multi–scan *CrystalClear*–SM Expert 3.1 b27 (Rigaku, 20112)	h = –6→6
T_{min} = 0.768, T_{max} = 1.000	k = –17→17
13862 measured reflections	l = –17→17

Refinement

Refinement on F^2	Secondary atom site location: difference Fourier map
Least–squares matrix: full	Hydrogen site location: mixed
$R[F^2 > 2\sigma(F^2)]$ = 0.057	H atoms treated by a mixture of independent and constrained refinement
$wR(F^2)$ = 0.149	$w = 1/[\sigma^2(F_o^2) + (0.0572P)^2 + 1.0516P]$ where $P = (F_o^2 + 2F_c^2)/3$
S = 1.03	$(\Delta/\sigma)_{max}$ = 0.003
4303 reflections	$\Delta\rangle_{max}$ = 0.33 e Å^{-3}
356 parameters	$\Delta\rangle_{min}$ = –0.31 e Å^{-3}
75 restraints	Extinction correction: *SHELXL*, $Fc^*=kFc[1+0.001xFc^2\lambda^3/\sin(2\theta)]^{-1/4}$
Primary atom site location: structure–invariant direct methods	Extinction coefficient: 0.015 (2)

2.19

Crystal data

$C_{28}H_{36}N_3P$	$F(000) = 960$
$M_r = 445.57$	$D_x = 1.193$ Mg m^{-3}
Monoclinic, $P2/c$	Synchrotron radiation, $\lambda = 0.6889$ Å
$a = 14.084$ (15) Å	Cell parameters from 5295 reflections
$b = 6.012$ (6) Å	$\theta = 2.0$–$26.8°$
$c = 29.37$ (3) Å	$\mu = 0.12$ mm^{-1}
$\beta = 94.015$ (10)°	$T = 100$ K
$V = 2481$ (4) Å^3	Needle, colourless
$Z = 4$	$0.22 \times 0.03 \times 0.02$ mm^3

Data collection

CrystalLogic diffractometer	5634 independent reflections
Radiation source: DLS beamline I19	4397 reflections with $I > 2\sigma(I)$
Double crystal silicon monochromator	$R_{int} = 0.087$
Detector resolution: 28.5714 pixels mm^{-1}	$\theta_{max} = 26.7°$, $\theta_{min} = 1.9°$
profile data from ω–scans	$h = -18 \rightarrow 18$
Absorption correction: multi–scan *CrystalClear*–SM Expert 3.1 b18 (Rigaku, 20112)	$k = -6 \rightarrow 7$
$T_{min} = 0.973$, $T_{max} = 0.998$	$l = -38 \rightarrow 37$
21688 measured reflections	

Refinement

Refinement on F^2	Secondary atom site location: all non–H atoms found by direct methods
Least–squares matrix: full	Hydrogen site location: mixed
$R[F^2 > 2\sigma(F^2)] = 0.098$	H atoms treated by a mixture of independent and constrained refinement
$wR(F^2) = 0.295$	$w = 1/[\sigma^2(F_o^2) + (0.1148P)^2 + 4.8065P]$ where $P = (F_o^2 + 2F_c^2)/3$
$S = 1.11$	$(\Delta/\sigma)_{max} < 0.001$
5634 reflections	$\Delta\rangle_{max} = 0.34$ e Å^{-3}
306 parameters	$\Delta\rangle_{min} = -0.36$ e Å^{-3}
20 restraints	Extinction correction: *SHELXL*, $Fc^* = kFc[1+0.001xFc^2\lambda^3/\sin(2\theta)]^{-1/4}$
Primary atom site location: structure–invariant direct methods	Extinction coefficient: 0.013 (6)

2.27

Crystal data

$C_{30}H_{42}N_3P$	$F(000) = 2064$
$M_r = 475.63$	$D_x = 1.132$ Mg m^{-3}
Monoclinic, $C2/c$	Mo $K\alpha$ radiation, $\lambda = 0.71073$ Å
$a = 19.5578$ (13) Å	Cell parameters from 11660 reflections
$b = 15.7697$ (10) Å	$\theta = 3.1–27.5°$
$c = 19.4430$ (14) Å	$\mu = 0.12$ mm^{-1}
$\beta = 111.380$ (8)°	$T = 100$ K
$V = 5584.0$ (7) Å^3	Chip, colourless
$Z = 8$	0.15 × 0.10 × 0.06 mm

Data collection

Rigaku Saturn724+ (2x2 bin mode) diffractometer	6377 independent reflections
Radiation source: 'fine–focus sealed tube'	4054 reflections with $I > 2\sigma(I)$
Detector resolution: 28.5714 pixels mm^{-1}	$R_{int} = 0.063$
profile data from ω–scans	$\theta_{max} = 27.5°$, $\theta_{min} = 3.1°$
Absorption correction: multi–scan '*CrystalClear*–SM Expert 3.1 b5 (Rigaku, 2011)'	$h = –25\rightarrow25$
$T_{min} = 0.982$, $T_{max} = 0.993$	$k = –20\rightarrow20$
19433 measured reflections	$l = –14\rightarrow25$

Refinement

Refinement on F^2	Primary atom site location: structure–invariant direct methods
Least–squares matrix: full	Secondary atom site location: difference Fourier map
$R[F^2 > 2\sigma(F^2)] = 0.059$	Hydrogen site location: inferred from neighbouring sites
$wR(F^2) = 0.146$	H atoms treated by a mixture of independent and constrained refinement
$S = 1.07$	$w = 1/[\sigma^2(F_o^2) + (0.0643P)^2]$ where $P = (F_o^2 + 2F_c^2)/3$
6377 reflections	$(\Delta/\sigma)_{max} < 0.001$
322 parameters	$\Delta\rangle_{max} = 0.61$ e Å^{-3}
3 restraints	$\Delta\rangle_{min} = –0.29$ e Å^{-3}

2.29

Crystal data

$C_{24}H_{21}F_9N_3OP$	$F(000) = 1160$
$M_r = 569.41$	$D_x = 1.542$ Mg m^{-3}
Monoclinic, $P2_1/c$	Mo $K\alpha$ radiation, $\lambda = 0.71073$ Å
Hall symbol: –P 2ybc	Cell parameters from 5595 reflections
$a = 12.0249$ (10) Å	$\theta = 2.4$–$27.0°$
$b = 9.7826$ (8) Å	$\mu = 0.21$ mm^{-1}
$c = 21.1367$ (18) Å	$T = 150$ K
$\beta = 99.5356$ (14)°	Block, colourless
$V = 2452.1$ (4) Å^3	0.47 × 0.16 × 0.14 mm
$Z = 4$	

Data collection

Bruker APEX 2 CCD diffractometer	6096 independent reflections
Radiation source: fine–focus sealed tube	4445 reflections with $I > 2\sigma(I)$
Graphite monchromator	$R_{int} = 0.032$
ω rotation with narrow frames scans	$\theta_{max} = 28.4°$, $\theta_{min} = 1.7°$
Absorption correction: multi–scan *SADABS* v2008/1, Sheldrick, G.M., (2008)	$h = -16 \rightarrow 15$
$T_{min} = 0.910$, $T_{max} = 0.972$	$k = -13 \rightarrow 12$
24275 measured reflections	$l = -28 \rightarrow 28$

Refinement

Refinement on F^2	Primary atom site location: structure–invariant direct methods
Least–squares matrix: full	Secondary atom site location: all non–H atoms found by direct methods
$R[F^2 > 2\sigma(F^2)] = 0.038$	Hydrogen site location: geom except NH coords freely refined
$wR(F^2) = 0.099$	H atoms treated by a mixture of independent and constrained refinement
$S = 1.03$	$w = 1/[\sigma^2(F_o^2) + (0.0423P)^2 + 0.6943P]$ where $P = (F_o^2 + 2F_c^2)/3$
6096 reflections	$(\Delta/\sigma)_{max} = 0.001$
352 parameters	$\Delta\rangle_{max} = 0.31$ e Å^{-3}
0 restraints	$\Delta\rangle_{min} = -0.31$ e Å^{-3}

2.31

Crystal data

$C_{24}H_{27}N_3P_3$	$F(000) = 948$
$M_r = 450.39$	$D_x = 1.413$ Mg m^{-3}
Monoclinic, *I*2	Mo *K*α radiation, λ = 0.71073 Å
$a = 13.549$ (6) Å	Cell parameters from 1380 reflections
$b = 5.1596$ (19) Å	θ = 3.5–24.9°
$c = 30.618$ (14) Å	μ = 0.30 mm^{-1}
β = 98.489 (9)°	$T = 100$ K
$V = 2117.0$ (16) Å^3	Lath, colourless
$Z = 4$	0.06 × 0.02 × 0.01 mm

Data collection

Rigaku Saturn724+ (2x2 bin mode) diffractometer	1226 reflections with $I > 2\sigma(I)$
profile data from ω–scans	$R_{int} = 0.154$
Absorption correction: multi–scan *SADABS* v2009/1, Sheldrick, G.M., (2009)	$\theta_{max} = 25.0°$, $\theta_{min} = 3.0°$
$T_{min} = 0.982$, $T_{max} = 0.997$	$h = -16 \rightarrow 11$
4032 measured reflections	$k = -6 \rightarrow 4$
2683 independent reflections	$l = -36 \rightarrow 36$

Refinement

Refinement on F^2	Secondary atom site location: all non–H atoms found by direct methods
Least–squares matrix: full	Hydrogen site location: inferred from neighbouring sites
$R[F^2 > 2\sigma(F^2)] = 0.101$	H–atom parameters constrained
$wR(F^2) = 0.279$	$w = 1/[\sigma^2(F_o^2) + (0.1227P)^2]$ where $P = (F_o^2 + 2F_c^2)/3$
$S = 0.96$	$(\Delta/\sigma)_{max} < 0.001$
2683 reflections	$\Delta\rangle_{max} = 0.69$ e Å^{-3}
271 parameters	$\Delta\rangle_{min} = -0.66$ e Å^{-3}
288 restraints	Absolute structure: Flack x determined using 214 quotients [(I+)–I(–)]/[(I+)+(I–)] (Parsons and Flack (2004), Acta Cryst. A60, s61).
Primary atom site location: structure–invariant direct methods	Flack parameter: 0.6 (5)

2.35

Crystal data

$C_{27}H_{33}N_3O_2P_2$	D_x = 1.545 Mg m^{-3}
M_r = 851.61	Mo $K\alpha$ radiation, λ = 0.71073 Å
Hexagonal, $P6_3/m$	Cell parameters from 2164 reflections
a = 14.1799 (19) Å	θ = 2.6–25.4°
c = 10.5101 (14) Å	μ = 0.81 mm^{-1}
V = 1830.1 (5) Å^3	T = 150 K
Z = 2	Block, colourless
F(000) = 872	0.19 × 0.15 × 0.13 mm

Data collection

Bruker APEX 2 CCD diffractometer	1193 reflections with $I > 2\sigma(I)$
Radiation source: fine–focus sealed tube	R_{int} = 0.085
ω rotation with narrow frames scans	θ_{max} = 28.4°, θ_{min} = 1.7°
Absorption correction: multi–scan *SADABS* v2012/1, Sheldrick, G.M., (2012)	h = –18→18
T_{min} = 0.861, T_{max} = 0.902	k = –18→18
19111 measured reflections	l = –14→14
1608 independent reflections	

Refinement

Refinement on F^2	Primary atom site location: structure–invariant direct methods
Least–squares matrix: full	Secondary atom site location: all non–H atoms found by direct methods
$R[F^2 > 2\sigma(F^2)]$ = 0.037	Hydrogen site location: inferred from neighbouring sites
$wR(F^2)$ = 0.090	H–atom parameters constrained
S = 1.06	$w = 1/[\sigma^2(F_o^2) + (0.0339P)^2 + 0.9347P]$ where $P = (F_o^2 + 2F_c^2)/3$
1608 reflections	$(\Delta/\sigma)_{max} < 0.001$
80 parameters	$\Delta\rangle_{max}$ = 0.31 e Å^{-3}
0 restraints	$\Delta\rangle_{min}$ = –0.33 e Å^{-3}

3.1

Crystal data

$C_{44}H_{48}Cl_2N_6P_2Pt\cdot(CHCl_3)$	$Z = 2$
$M_r = 1108.18$	$F(000) = 1108$
Triclinic, $P\bar{1}$	$D_x = 1.608$ Mg m^{-3}
$a = 9.628$ (3) Å	Mo $K\alpha$ radiation, $\lambda = 0.71073$ Å
$b = 13.794$ (3) Å	Cell parameters from 7084 reflections
$c = 18.423$ (5) Å	$\theta = 2.8$–$31.2°$
$\alpha = 109.724$ (7)°	$\mu = 3.47$ mm^{-1}
$\beta = 93.982$ (16)°	$T = 120$ K
$\gamma = 93.384$ (11)°	Lath, colourless
$V = 2288.7$ (10) Å^3	0.25 × 0.06 × 0.04 mm

Data collection

Rigaku Saturn724+ (2x2 bin mode) diffractometer	13173 independent reflections
Radiation source: rotating anode	12710 reflections with $I > 2\sigma(I)$
Confocal mirrors monochromator	$R_{int} = 0.029$
Detector resolution: 28.5714 pixels mm^{-1}	$\theta_{max} = 31.2°$, $\theta_{min} = 2.7°$
profile data from ω–scans	$h = -13\rightarrow8$
Absorption correction: multi–scan	$k = -19\rightarrow20$
$T_{min} = 0.478$, $T_{max} = 0.874$	$l = -25\rightarrow26$
30790 measured reflections	

Refinement

Refinement on F^2	Secondary atom site location: difference Fourier map
Least–squares matrix: full	Hydrogen site location: inferred from neighbouring sites
$R[F^2 > 2\sigma(F^2)] = 0.031$	H atoms treated by a mixture of independent and constrained refinement
$wR(F^2) = 0.073$	$w = 1/[\sigma^2(F_o^2) + (0.0334P)^2 + 3.8421P]$ where $P = (F_o^2 + 2F_c^2)/3$
$S = 1.06$	$(\Delta/\sigma)_{max} = 0.003$
13173 reflections	$\Delta\rangle_{max} = 1.78$ e Å^{-3}
539 parameters	$\Delta\rangle_{min} = -1.75$ e Å^{-3}
0 restraints	Extinction correction: *SHELXL*, $Fc^* = kFc[1+0.001xFc^2\lambda^3/\sin(2\theta)]^{-1/4}$
Primary atom site location: structure–invariant direct methods	Extinction coefficient: 0.00035 (15)

3.2

Crystal data

$C_{62}H_{84}Cl_2N_6P_2Pt$	$F(000) = 2560$
$M_r = 1241.28$	$D_x = 1.359$ Mg m^{-3}
Monoclinic, $P2_1/c$	Mo $K\alpha$ radiation, $\lambda = 0.71073$ Å
$a = 10.772$ (3) Å	Cell parameters from 14107 reflections
$b = 50.015$ (14) Å	$\theta = 2.4$–$28.9°$
$c = 12.142$ (4) Å	$\mu = 2.50$ mm^{-1}
$\beta = 112.011$ (3)°	$T = 100$ K
$V = 6065$ (3) Å^3	Cut blade, colourless
$Z = 4$	0.16 × 0.11 × 0.04 mm

Data collection

Rigaku Saturn724+ (2x2 bin mode) diffractometer with confocal mirrors	14906 independent reflections
Radiation source: Rotating Anode	13250 reflections with $I > 2\sigma(I)$
Detector resolution: 28.5714 pixels mm^{-1}	$R_{int} = 0.039$
profile data from ω–scans	$\theta_{max} = 29.1°$, $\theta_{min} = 2.4°$
Absorption correction: multi–scan	$h = -13 \rightarrow 14$
$T_{min} = 0.862$, $T_{max} = 1.000$	$k = -66 \rightarrow 56$
56239 measured reflections	$l = -16 \rightarrow 15$

Refinement

Refinement on F^2	Primary atom site location: structure–invariant direct methods
Least–squares matrix: full	Secondary atom site location: all non–H atoms found by direct methods
$R[F^2 > 2\sigma(F^2)] = 0.036$	Hydrogen site location: mixed
$wR(F^2) = 0.071$	H atoms treated by a mixture of independent and constrained refinement
$S = 1.09$	$w = 1/[\sigma^2(F_o^2) + (0.0162P)^2 + 13.3738P]$ where $P = (F_o^2 + 2F_c^2)/3$
14906 reflections	$(\Delta/\sigma)_{max} = 0.001$
676 parameters	$\Delta\rangle_{max} = 3.40$ e Å^{-3}
0 restraints	$\Delta\rangle_{min} = -1.31$ e Å^{-3}

3.9

Crystal data

$C_{62}H_{84}Cl_2N_6P_2Pd$	$F(000) = 2432$
$M_r = 1152.59$	$D_x = 1.252$ Mg m^{-3}
Monoclinic, $P2_1/c$	Mo $K\alpha$ radiation, $\lambda = 0.71073$ Å
$a = 10.756$ (13) Å	Cell parameters from 9347 reflections
$b = 50.18$ (6) Å	$\theta = 2.3$–$27.4°$
$c = 12.220$ (16) Å	$\mu = 0.49$ mm^{-1}
$\beta = 111.977$ (13)°	$T = 100$ K
$V = 6117$ (13) Å^3	Platelet, yellow
$Z = 4$	$0.06 \times 0.04 \times 0.02$ mm^3

Data collection

Rigaku Saturn724+ (2x2 bin mode) diffractometer	13589 independent reflections
Radiation source: Rotating Anode	9331 reflections with $I > 2\sigma(I)$
Detector resolution: 28.5714 pixels mm^{-1}	$R_{int} = 0.168$
profile data from ω–scans	$\theta_{max} = 27.4°$, $\theta_{min} = 2.4°$
Absorption correction: multi–scan	$h = -13 \rightarrow 13$
$T_{min} = 0.469$, $T_{max} = 1.000$	$k = -50 \rightarrow 64$
36654 measured reflections	$l = -15 \rightarrow 15$

Refinement

Refinement on F^2	Primary atom site location: structure–invariant direct methods
Least–squares matrix: full	Secondary atom site location: all non H–atoms found by direct methods
$R[F^2 > 2\sigma(F^2)] = 0.150$	Hydrogen site location: mixed
$wR(F^2) = 0.362$	H atoms treated by a mixture of independent and constrained refinement
$S = 1.20$	$w = 1/[\sigma^2(F_o^2) + (0.0901P)^2 + 67.0164P]$ where $P = (F_o^2 + 2F_c^2)/3$
13589 reflections	$(\Delta/\sigma)_{max} = 0.001$
676 parameters	$\Delta\rangle_{max} = 1.32$ e Å^{-3}
2 restraints	$\Delta\rangle_{min} = -2.22$ e Å^{-3}

3.6a

Crystal data

$C_{38}H_{36}Cl_2F_5N_5P_2Pt \cdot 2CH_2Cl_2$	$Z = 2$
$M_r = 1155.50$	$F(000) = 1140$
Triclinic, $P\bar{1}$	$D_x = 1.726$ Mg m^{-3}
$a = 10.4753$ (11) Å	Mo $K\alpha$ radiation, $\lambda = 0.71073$ Å
$b = 15.2335$ (16) Å	Cell parameters from 8056 reflections
$c = 15.2621$ (16) Å	$\theta = 2.3$–$23.3°$
$\alpha = 68.1582$ (16)°	$\mu = 3.65$ mm^{-1}
$\beta = 83.5847$ (18)°	$T = 150$ K
$\gamma = 79.9839$ (18)°	Block, colorless
$V = 2223.2$ (4) Å^3	0.25 × 0.13 × 0.04 mm

Data collection

Bruker APEX 2 CCD diffractometer	8957 reflections with $I > 2\sigma(I)$
Radiation source: fine–focus sealed tube	$R_{int} = 0.063$
ω rotation with narrow frames scans	$\theta_{max} = 28.3°$, $\theta_{min} = 1.5°$
Absorption correction: multi–scan TWINABS v2012/1, Sheldrick, G.M., (2012)	$h = -13 \rightarrow 13$
$T_{min} = 0.463$, $T_{max} = 0.868$	$k = -18 \rightarrow 20$
58164 measured reflections	$l = 0 \rightarrow 20$
11005 independent reflections	

Refinement

Refinement on F^2	Primary atom site location: structure–invariant direct methods
Least–squares matrix: full	Secondary atom site location: all non–H atoms found by direct methods
$R[F^2 > 2\sigma(F^2)] = 0.039$	Hydrogen site location: inferred from neighbouring sites
$wR(F^2) = 0.087$	H–atom parameters constrained
$S = 1.01$	$w = 1/[\sigma^2(F_o^2) + (0.040P)^2]$ where $P = (F_o^2 + 2F_c^2)/3$
11005 reflections	$(\Delta/\sigma)_{max} = 0.001$
652 parameters	$\Delta\rangle_{max} = 1.05$ e Å^{-3}
471 restraints	$\Delta\rangle_{min} = -0.91$ e Å^{-3}

3.16a

Crystal data

$C_{60}H_{84}Cl_2N_6P_2Pt$	$F(000) = 2512$
$M_r = 1217.26$	$D_x = 1.394$ Mg m^{-3}
Monoclinic, $C2/c$	Mo $K\alpha$ radiation, $\lambda = 0.71073$ Å
$a = 23.882$ (18) Å	Cell parameters from 5247 reflections
$b = 8.231$ (5) Å	$\theta = 3.4$–$30.2°$
$c = 29.68$ (3) Å	$\mu = 2.61$ mm^{-1}
$\beta = 96.070$ (6)°	$T = 100$ K
$V = 5802$ (8) Å^3	Lath, colourless
$Z = 4$	0.05 × 0.02 × 0.01 mm

Data collection

Rigaku Saturn724+ (2x2 bin mode) diffractometer	6664 independent reflections
Radiation source: Rotating Anode	5037 reflections with $I > 2\sigma(I)$
Confocal monochromator	$R_{int} = 0.149$
Detector resolution: 28.5714 pixels mm^{-1}	$\theta_{max} = 27.7°$, $\theta_{min} = 2.6°$
profile data from ω–scans	$h = -31 \rightarrow 20$
Absorption correction: multi–scan *CrystalClear*–SM Expert 3.1 b13a (Rigaku, 20112)	$k = -10 \rightarrow 10$
$T_{min} = 0.747$, $T_{max} = 1.000$	$l = -38 \rightarrow 38$
26108 measured reflections	

Refinement

Refinement on F^2	Hydrogen site location: mixed
Least–squares matrix: full	H atoms treated by a mixture of independent and constrained refinement
$R[F^2 > 2\sigma(F^2)] = 0.106$	$w = 1/[\sigma^2(F_o^2) + (0.0454P)^2 + 104.0805P]$ where $P = (F_o^2 + 2F_c^2)/3$
$wR(F^2) = 0.217$	$(\Delta/\sigma)_{max} = 0.001$
$S = 1.15$	$\Delta\rangle_{max} = 1.91$ e Å^{-3}
6664 reflections	$\Delta\rangle_{min} = -2.98$ e Å^{-3}
337 parameters	Extinction correction: *SHELXL*, $Fc^* = kFc[1+0.001xFc^2\lambda^3/\sin(2\theta)]^{-1/4}$
18 restraints	Extinction coefficient: 0.00043 (8)
Primary atom site location: structure–invariant direct methods	

3.19

Crystal data

$C_{60}H_{84}Cl_2N_6P_2Pd$	$Z = 1$
$M_r = 1128.57$	$F(000) = 596$
Triclinic, $P\bar{1}$	$D_x = 1.311$ Mg m^{-3}
$a = 10.047$ (5) Å	Mo $K\alpha$ radiation, $\lambda = 0.71073$ Å
$b = 11.388$ (6) Å	Cell parameters from 8326 reflections
$c = 13.210$ (7) Å	$\theta = 2.2$–$31.4°$
$\alpha = 75.79$ (2)°	$\mu = 0.52$ mm^{-1}
$\beta = 78.92$ (2)°	$T = 100$ K
$\gamma = 81.52$ (2)°	Needle, yellow
$V = 1429.9$ (13) Å^3	0.21 × 0.02 × 0.01 mm

Data collection

Rigaku Saturn724+ (2x2 bin mode) diffractometer	8326 independent reflections
Radiation source: Rotating Anode	7387 reflections with $I > 2\sigma(I)$
Confocal	$R_{int} = 0.052$
profile data from ω–scans	$\theta_{max} = 31.4°$, $\theta_{min} = 2.1°$
Absorption correction: multi–scan *SADABS* v2009/1, Sheldrick, G.M., (2009)	$h = -14 \rightarrow 8$
$T_{min} = 0.899$, $T_{max} = 0.995$	$k = -16 \rightarrow 15$
18827 measured reflections	$l = -19 \rightarrow 18$

Refinement

Refinement on F^2	Secondary atom site location: difference Fourier map
Least–squares matrix: full	Hydrogen site location: inferred from neighbouring sites
$R[F^2 > 2\sigma(F^2)] = 0.076$	H atoms treated by a mixture of independent and constrained refinement
$wR(F^2) = 0.173$	$w = 1/[\sigma^2(F_o^2) + (0.0605P)^2 + 3.7142P]$ where $P = (F_o^2 + 2F_c^2)/3$
$S = 1.11$	$(\Delta/\sigma)_{max} < 0.001$
8326 reflections	$\Delta\rangle_{max} = 1.30$ e Å^{-3}
338 parameters	$\Delta\rangle_{min} = -2.11$ e Å^{-3}
1 restraint	Extinction correction: *SHELXL*, $c^*=kFc[1+0.001xFc^2\lambda^3/\sin(2\theta)]^{-1/4}$
Primary atom site location: structure–invariant direct methods	Extinction coefficient: 0.0210 (18)

3.20

Crystal data

$C_{48}H_{42}Cl_2F_{18}N_6P_2Pd$	$Z = 1$
$M_r = 1284.11$	$F(000) = 644$
Triclinic, $P\bar{1}$	$D_x = 1.676$ Mg m^{-3}
$a = 7.9244$ (19) Å	Mo Ka radiation, l = 0.71073 Å
$b = 13.158$ (3) Å	Cell parameters from 838 reflections
$c = 13.821$ (3) Å	q = 2.6–17.0°
a = 114.893 (3)°	m = 0.64 mm^{-1}
b = 100.494 (4)°	$T = 150$ K
g = 92.876 (4)°	Block, orange
$V = 1272.3$ (5) Å^3	0.14 × 0.13 × 0.06 mm

Data collection

Bruker SMART APEX 2 CCD diffractometer	4498 independent reflections
Radiation source: fine–focus sealed tube	2125 reflections with $I > 2s(I)$
graphite	$R_{int} = 0.151$
w rotation with narrow frames scans	$q_{max} = 25.0°$, $q_{min} = 1.7°$
Absorption correction: multi–scan *SADABS* v2009/1, Sheldrick, G.M., (2009)	$h = -9 \rightarrow 9$
$T_{min} = 0.916$, $T_{max} = 0.963$	$k = -15 \rightarrow 15$
13153 measured reflections	$l = -16 \rightarrow 16$

Refinement

Refinement on F^2	Secondary atom site location: all non–H atoms found by direct methods
Least–squares matrix: full	Hydrogen site location: mixed
$R[F^2 > 2s(F^2)] = 0.062$	H atoms treated by a mixture of independent and constrained refinement
$wR(F^2) = 0.132$	$w = 1/[s^2(F_o^2) + (0.0407P)^2]$ where $P = (F_o^2 + 2F_c^2)/3$
$S = 0.92$	$(D/s)_{max} = 0.001$
4498 reflections	$D\rho_{max} = 0.63$ e Å^{-3}
359 parameters	$D\rho_{min} = -0.74$ e Å^{-3}
3 restraints	Extinction correction: *SHELXL*, $Fc^* = kFc[1+0.001xFc^2l^3/\sin(2q)]^{-1/4}$
Primary atom site location: structure–invariant direct methods	Extinction coefficient: 0.0066 (8)

3.21

Crystal data

$C_{60}H_{72}Cl_2N_6P_2Pd$	$Z = 1$
$M_r = 1116.47$	$F(000) = 584$
Triclinic, $P\bar{1}$	$D_x = 1.352$ Mg m^{-3}
$a = 11.2149$ (16) Å	Mo $K\alpha$ radiation, $\lambda = 0.71073$ Å
$b = 11.7544$ (17) Å	Cell parameters from 4970 reflections
$c = 12.0517$ (17) Å	$\theta = 2.3$–$22.5°$
$\alpha = 70.435$ (2)°	$\mu = 0.54$ mm^{-1}
$\beta = 74.029$ (2)°	$T = 150$ K
$\gamma = 68.498$ (2)°	Block, yellow
$V = 1371.6$ (3) Å^3	0.31 × 0.14 × 0.10 mm

Data collection

Bruker APEX 2 CCD diffractometer	4494 reflections with $I > 2\sigma(I)$
Radiation source: fine–focus sealed tube	$R_{int} = 0.051$
ω rotation with narrow frames scans	$\theta_{max} = 26.4°$, $\theta_{min} = 1.8°$
Absorption correction: multi–scan *SADABS* v2012/1, Sheldrick, G.M., (2012)	$h = -14 \rightarrow 14$
$T_{min} = 0.851$, $T_{max} = 0.948$	$k = -14 \rightarrow 14$
16458 measured reflections	$l = -15 \rightarrow 15$
5624 independent reflections	

Refinement

Refinement on F^2	Primary atom site location: structure–invariant direct methods
Least–squares matrix: full	Secondary atom site location: all non–H atoms found by direct methods
$R[F^2 > 2\sigma(F^2)] = 0.039$	Hydrogen site location: mixed
$wR(F^2) = 0.090$	H atoms treated by a mixture of independent and constrained refinement
$S = 1.08$	$w = 1/[\sigma^2(F_o^2) + (0.0375P)^2 + 0.074P]$ where $P = (F_o^2 + 2F_c^2)/3$
5624 reflections	$(\Delta/\sigma)_{max} < 0.001$
334 parameters	$\Delta\rangle_{max} = 0.67$ e Å^{-3}
0 restraints	$\Delta\rangle_{min} = -0.44$ e Å^{-3}

3.25

Crystal data

$C_{34}H_{35}Cl_2F_9N_3PRu$	$F(000) = 868$
$M_r = 859.59$	$D_x = 1.637$ Mg m^{-3}
Monoclinic, $P2_1$	Mo $K\alpha$ radiation, $\lambda = 0.71073$ Å
$a = 11.1316$ (8) Å	Cell parameters from 3312 reflections
$b = 13.1145$ (9) Å	$\theta = 2.2–27.5°$
$c = 12.3389$ (9) Å	$\mu = 0.73$ mm^{-1}
$\beta = 104.5020$ (12)°	$T = 100$ K
$V = 1743.9$ (2) Å^3	Needle, brown
$Z = 2$	0.30 × 0.03 × 0.01 mm

Data collection

Rigaku Saturn724+ (2x2 bin mode) diffractometer	7848 independent reflections
Radiation source: Sealed Tube	7023 reflections with $I > 2\sigma(I)$
Detector resolution: 28.5714 pixels mm^{-1}	$R_{int} = 0.044$
profile data from ω–scans	$\theta_{max} = 27.5°$, $\theta_{min} = 2.3°$
Absorption correction: multi–scan *CrystalClear*–SM Expert 3.1 b27 (Rigaku, 20112)	$h = -14 \rightarrow 14$
$T_{min} = 0.811$, $T_{max} = 0.993$	$k = -16 \rightarrow 17$
22354 measured reflections	$l = -16 \rightarrow 15$

Refinement

Refinement on F^2	Secondary atom site location: all non–H atoms found by direct methods
Least–squares matrix: full	Hydrogen site location: inferred from neighbouring sites
$R[F^2 > 2\sigma(F^2)] = 0.035$	H–atom parameters constrained
$wR(F^2) = 0.077$	$w = 1/[\sigma^2(F_o^2) + (0.032P)^2 + 0.6117P]$ where $P = (F_o^2 + 2F_c^2)/3$
$S = 1.03$	$(\Delta/\sigma)_{max} = 0.001$
7848 reflections	$\Delta\rangle_{max} = 0.80$ e Å^{-3}
545 parameters	$\Delta\rangle_{min} = -0.45$ e Å^{-3}
875 restraints	Absolute structure: Flack x determined using 3011 quotients [(I+)–(I–)]/[(I+)+(I–)] (Parsons, Flack and Wagner, Acta Cryst. B69 (2013) 249–259).
Primary atom site location: structure–invariant direct methods	Absolute structure parameter: –0.006 (15)

3.27b

Crystal data

$C_{32}H_{36}Cl_4N_4P_4Pt_2$	$Z = 1$
$M_r = 1132.51$	$F(000) = 540$
Triclinic, $P\bar{1}$	$D_x = 2.175$ Mg m^{-3}
$a = 9.0417$ (6) Å	Mo $K\alpha$ radiation, $\lambda = 0.71073$ Å
$b = 9.5759$ (7) Å	Cell parameters from 3135 reflections
$c = 10.6803$ (7) Å	$\theta = 2.2$–$27.5°$
$\alpha = 94.137$ (6)°	$\mu = 8.61$ mm^{-1}
$\beta = 100.938$ (6)°	$T = 100$ K
$\gamma = 106.115$ (6)°	Plate, colourless
$V = 864.58$ (11) Å^3	0.12 × 0.06 × 0.01 mm

Data collection

Rigaku Saturn724+ (2x2 bin mode) diffractometer	3931 independent reflections
Radiation source: Sealed Tube	3753 reflections with $I > 2\sigma(I)$
Detector resolution: 28.5714 pixels mm^{-1}	$R_{int} = 0.029$
profile data from ω–scans	$\theta_{max} = 27.5°$, $\theta_{min} = 2.4°$
Absorption correction: multi–scan *CrystalClear*–SM Expert 3.1 b27 (Rigaku, 20112)	$h = -11 \rightarrow 9$
$T_{min} = 0.742$, $T_{max} = 1.000$	$k = -9 \rightarrow 12$
11569 measured reflections	$l = -13 \rightarrow 13$

Refinement

Refinement on F^2	Primary atom site location: structure–invariant direct methods
Least–squares matrix: full	Hydrogen site location: inferred from neighbouring sites
$R[F^2 > 2\sigma(F^2)] = 0.023$	H–atom parameters constrained
$wR(F^2) = 0.061$	$w = 1/[\sigma^2(F_o^2) + (0.0309P)^2 + 2.8489P]$ where $P = (F_o^2 + 2F_c^2)/3$
$S = 1.03$	$(\Delta/\sigma)_{max} = 0.002$
3931 reflections	$\Delta\rangle_{max} = 1.49$ e Å^{-3}
208 parameters	$\Delta\rangle_{min} = -0.81$ e Å^{-3}
0 restraints	

3.44

Crystal data

$C_{70}H_{64}Cl_2F_6N_6P_4Pt{\cdot}2(CHCl_3)$	$F(000) = 1736$
$M_r = 1731.87$	$D_x = 1.604$ Mg m^{-3}
Monoclinic, $P2_1/n$	Mo $K\alpha$ radiation, $\lambda = 0.71073$ Å
$a = 14.4491$ (16) Å	Cell parameters from 6479 reflections
$b = 9.6868$ (10) Å	$\theta = 3.0$–$27.5°$
$c = 26.016$ (3) Å	$\mu = 2.41$ mm^{-1}
$\beta = 99.955$ (7)°	$T = 100$ K
$V = 3586.5$ (6) Å^3	Plate, colorless
$Z = 2$	0.04 × 0.02 × 0.01 mm

Data collection

Rigaku Saturn724+ (2x2 bin mode) diffractometer	5615 independent reflections
Radiation source: Rotating Anode	3031 reflections with $I > 2\sigma(I)$
Detector resolution: 28.5714 pixels mm^{-1}	$R_{int} = 0.159$
profile data from ω–scans	$\theta_{max} = 24.0°$, $\theta_{min} = 3.0°$
Absorption correction: multi–scan *CrystalClear*–SM Expert 3.1 b18 (Rigaku, 20112)	$h = -16 \rightarrow 16$
$T_{min} = 0.910$, $T_{max} = 0.976$	$k = -11 \rightarrow 11$
18794 measured reflections	$l = -29 \rightarrow 29$

Refinement

Refinement on F^2	Primary atom site location: structure–invariant direct methods
Least–squares matrix: full	Secondary atom site location: all non–H atoms found by direct methods
$R[F^2 > 2\sigma(F^2)] = 0.084$	Hydrogen site location: inferred from neighbouring sites
$wR(F^2) = 0.208$	H–atom parameters constrained
$S = 1.00$	$w = 1/[\sigma^2(F_o^2) + (0.0801P)^2]$ where $P = (F_o^2 + 2F_c^2)/3$
5615 reflections	$(\Delta/\sigma)_{max} < 0.001$
439 parameters	$\Delta\rangle_{max} = 2.62$ e Å^{-3}
0 restraints	$\Delta\rangle_{min} = -0.90$ e Å^{-3}

3.47

Crystal data

$C_{55}H_{60}Cl_4F_3N_3P_2Ru_2$	$F(000) = 2496$
$M_r = 1225.94$	$D_x = 1.513$ Mg m^{-3}
Monoclinic, $P2_1/n$	Mo $K\alpha$ radiation, $\lambda = 0.71073$ Å
$a = 15.0979$ (5) Å	Cell parameters from 9737 reflections
$b = 16.8930$ (7) Å	$\theta = 2.9$–$27.5°$
$c = 21.3212$ (7) Å	$\mu = 0.87$ mm^{-1}
$\beta = 98.195$ (2)°	$T = 120$ K
$V = 5382.4$ (3) Å^3	Block, orange
$Z = 4$	0.16 × 0.14 × 0.09 mm

Data collection

Bruker–Nonius Roper CCD camera on κ–goniostat diffractometer	9446 independent reflections
Radiation source: Bruker–Nonius FR591 rotating anode	6429 reflections with $I > 2\sigma(I)$
Graphite monochromator	$R_{int} = 0.117$
Detector resolution: 9.091 pixels mm^{-1}	$\theta_{max} = 25.0°$, $\theta_{min} = 3.0°$
ϕ & ω scans	$h = -17 \rightarrow 17$
Absorption correction: multi–scan *SADABS* 2007/2 (Sheldrick, G.M., 2007)	$k = -20 \rightarrow 19$
$T_{min} = 0.873$, $T_{max} = 0.926$	$l = -25 \rightarrow 25$
51505 measured reflections	

Refinement

Refinement on F^2	Hydrogen site location: inferred from neighbouring sites
Least–squares matrix: full	H–atom parameters constrained
$R[F^2 > 2\sigma(F^2)] = 0.054$	$w = 1/[\sigma^2(F_o^2) + (0.0093P)^2 + 14.8565P]$ where $P = (F_o^2 + 2F_c^2)/3$
$wR(F^2) = 0.105$	$(\Delta/\sigma)_{max} = 0.001$
$S = 1.01$	$\Delta\rangle_{max} = 0.49$ e Å^{-3}
9446 reflections	$\Delta\rangle_{min} = -0.61$ e Å^{-3}
650 parameters	Extinction correction: *SHELXL*, $Fc^* = kFc[1+0.001xFc^2\lambda^3/\sin(2\theta)]^{-1/4}$
31 restraints	Extinction coefficient: 0.00060 (8)
Primary atom site location: structure–invariant direct methods	

o,o–$(CHPh_2)_2$–*p*–$MeC_6H_2NH_2$

Crystal data

$C_{33}H_{29}N$	$F(000) = 936$
$M_r = 439.57$	$D_x = 1.201$ Mg m^{-3}
Monoclinic, $P2_1/n$	Mo $K\alpha$ radiation, $\lambda = 0.71073$ Å
Hall symbol: –P 2yn	Cell parameters from 12919 reflections
$a = 9.6117$ (13) Å	$\theta = 2.4$–$30.5°$
$b = 11.3752$ (15) Å	$\mu = 0.07$ mm^{-1}
$c = 22.269$ (3) Å	$T = 150$ K
$\beta = 93.278$ (2)°	Block, colourless
$V = 2430.8$ (6) Å^3	0.89 × 0.58 × 0.45 mm
$Z = 4$	

Data collection

Bruker APEX 2 CCD diffractometer	7370 independent reflections
Radiation source: sealed tube	6161 reflections with $I > 2\sigma(I)$
Graphite monochromator	$R_{int} = 0.021$
ω rotation with narrow frames scans	$\theta_{max} = 30.6°$, $\theta_{min} = 1.8°$
Absorption correction: multi–scan *SADABS* v2008/1, Sheldrick, G.M., (2008)	$h = -13 \rightarrow 13$
$T_{min} = 0.941$, $T_{max} = 0.970$	$k = -16 \rightarrow 16$
27588 measured reflections	$l = -31 \rightarrow 31$

Refinement

Refinement on F^2	Primary atom site location: structure–invariant direct methods
Least–squares matrix: full	Secondary atom site location: all non–H atoms found by direct methods
$R[F^2 > 2\sigma(F^2)] = 0.047$	Hydrogen site location: geom except NH coords freely refined
$wR(F^2) = 0.136$	H atoms treated by a mixture of independent and constrained refinement
$S = 1.03$	$w = 1/[\sigma^2(F_o^2) + (0.0783P)^2 + 0.5687P]$ where $P = (F_o^2 + 2F_c^2)/3$
7370 reflections	$(\Delta/\sigma)_{max} = 0.001$
314 parameters	$\Delta\rangle_{max} = 0.44$ e Å^{-3}
0 restraints	$\Delta\rangle_{min} = -0.24$ e Å^{-3}

4.2a

Crystal data

$C_{35}H_{33}NP_2$	$Z = 2$
$M_r = 529.56$	$F(000) = 560$
Triclinic, $P\bar{1}$	$D_x = 1.217$ Mg m^{-3}
$a = 10.2553$ (5) Å	Cu $K\alpha$ radiation, $\lambda = 1.54184$ Å
$b = 12.2752$ (5) Å	Cell parameters from 5245 reflections
$c = 12.3781$ (6) Å	$\theta = 3.6$–$74.0°$
$\alpha = 87.619$ (4)°	$\mu = 1.54$ mm^{-1}
$\beta = 81.388$ (4)°	$T = 100$ K
$\gamma = 69.780$ (4)°	Block, colourless
$V = 1445.62$ (12) Å^3	0.13 × 0.07 × 0.07 mm

Data collection

SuperNova, Dual, Cu at zero, Atlas diffractometer	4616 reflections with $I > 2\sigma(I)$
Radiation source: SuperNova (Cu) X–ray Source	$R_{int} = 0.032$
ω scans	$\theta_{max} = 74.4°$, $\theta_{min} = 3.6°$
Absorption correction: multi–scan *CrysAlis PRO*, Agilent Technologies, Version 1.171.36.31a (release 02–08–2013 CrysAlis171 .NET) (compiled Aug 2 2013,12:40:55) Empirical absorption correction using spherical harmonics, implemented in SCALE3 ABSPACK scaling algorithm.	$h = -12 \rightarrow 12$
$T_{min} = 0.825$, $T_{max} = 0.900$	$k = -12 \rightarrow 15$
8504 measured reflections	$l = -11 \rightarrow 15$
5563 independent reflections	

Refinement

Refinement on F^2	Primary atom site location: structure–invariant direct methods
Least–squares matrix: full	Secondary atom site location: difference Fourier map
$R[F^2 > 2\sigma(F^2)] = 0.037$	Hydrogen site location: inferred from neighbouring sites
$wR(F^2) = 0.093$	H–atom parameters constrained
$S = 1.03$	$w = 1/[\sigma^2(F_o^2) + (0.0378P)^2 + 0.1206P]$ where $P = (F_o^2 + 2F_c^2)/3$
5563 reflections	$(\Delta/\sigma)_{max} = 0.001$
344 parameters	$\Delta\rangle_{max} = 0.28$ e Å^{-3}
0 restraints	$\Delta\rangle_{min} = -0.29$ e Å^{-3}

4.3

Crystal data

$C_{21}H_{34}NO_3P$	$F(000) = 2472$
$M_r = 379.46$	$D_x = 1.257$ Mg m^{-3}
Monoclinic, $P2_1/c$	Mo $K\alpha$ radiation, $\lambda = 0.71073$ Å
Hall symbol: –P 2ybc	Cell parameters from 13682 reflections
$a = 11.220$ (2) Å	$\theta = 2.9$–$27.5°$
$b = 45.582$ (15) Å	$\mu = 0.16$ mm^{-1}
$c = 11.974$ (3) Å	$T = 120$ K
$\beta = 100.860$ (16)°	Block, colourless
$V = 6014$ (3) Å^3	0.12 × 0.10 × 0.08 mm
$Z = 12$	

Data collection

Bruker–Nonius APEX II CCD camera on κ–goniostat diffractometer	13684 independent reflections
Radiation source: Bruker–Nonius FR591 rotating anode	9995 reflections with $I > 2\sigma(I)$
10cm confocal mirrors monochromator	$R_{int} = 0.061$
Detector resolution: 4096x4096pixels / 62x62mm pixels mm^{-1}	$\theta_{max} = 27.6°$, $\theta_{min} = 3.1°$
ϕ & ω scans	$h = -14 \rightarrow 14$
Absorption correction: multi–scan *SADABS* v2007/2, Sheldrick, G.M., (2007)	$k = -59 \rightarrow 59$
$T_{min} = 0.981$, $T_{max} = 0.988$	$l = -15 \rightarrow 15$
59441 measured reflections	

Refinement

Refinement on F^2	Primary atom site location: structure–invariant direct methods
Least–squares matrix: full	Secondary atom site location: difference Fourier map
$R[F^2 > 2\sigma(F^2)] = 0.093$	Hydrogen site location: geom except NH coords freely refined
$wR(F^2) = 0.199$	H atoms treated by a mixture of independent and constrained refinement
$S = 1.06$	$w = 1/[\sigma^2(F_o^2) + (0.0246P)^2 + 24.5662P]$ where $P = (F_o^2 + 2F_c^2)/3$
13684 reflections	$(\Delta/\sigma)_{max} < 0.001$
724 parameters	$\Delta\rangle_{max} = 0.44$ e Å^{-3}
0 restraints	$\Delta\rangle_{min} = -0.43$ e Å^{-3}

4.7

Crystal data

$C_{21}H_{22}NP$	$F(000) = 680$
$M_r = 319.36$	$D_x = 1.204$ Mg m^{-3}
Monoclinic, $P2_1/n$	Mo $K\alpha$ radiation, $\lambda = 0.71073$ Å
$a = 9.8158$ (12) Å	Cell parameters from 3200 reflections
$b = 9.5286$ (12) Å	$\theta = 2.2$–$25.2°$
$c = 18.871$ (2) Å	$\mu = 0.16$ mm^{-1}
$\beta = 93.716$ (2)°	$T = 150$ K
$V = 1761.3$ (4) Å^3	Block, colourless
$Z = 4$	0.37 × 0.34 × 0.07 mm

Data collection

Bruker APEX 2 CCD diffractometer	3605 independent reflections
Radiation source: fine–focus sealed tube	2789 reflections with $I > 2\sigma(I)$
graphite	$R_{int} = 0.051$
ω rotation with narrow frames scans	$\theta_{max} = 26.4°$, $\theta_{min} = 2.2°$
Absorption correction: multi–scan *SADABS* v2012/1, Sheldrick, G.M., (2012)	$h = -12 \rightarrow 12$
$T_{min} = 0.945$, $T_{max} = 0.989$	$k = -11 \rightarrow 11$
20304 measured reflections	$l = -23 \rightarrow 23$

Refinement

Refinement on F^2	Primary atom site location: structure–invariant direct methods
Least–squares matrix: full	Secondary atom site location: all non–H atoms found by direct methods
$R[F^2 > 2\sigma(F^2)] = 0.043$	Hydrogen site location: mixed
$wR(F^2) = 0.109$	H atoms treated by a mixture of independent and constrained refinement
$S = 1.07$	$w = 1/[\sigma^2(F_o^2) + (0.0449P)^2 + 0.5313P]$ where $P = (F_o^2 + 2F_c^2)/3$
3605 reflections	$(\Delta/\sigma)_{max} < 0.001$
217 parameters	$\Delta\rangle_{max} = 0.33$ e Å^{-3}
0 restraints	$\Delta\rangle_{min} = -0.30$ e Å^{-3}

4.9

Crystal data

$C_{34}H_{33}NP_2$	$Z = 2$
$M_r = 517.55$	$F(000) = 548$
Triclinic, $P\bar{1}$	$D_x = 1.235$ Mg m^{-3}
$a = 10.0528$ (8) Å	Mo $K\alpha$ radiation, $\lambda = 0.71073$ Å
$b = 10.3979$ (8) Å	$\theta = 2.2$–$28.7°$
$c = 14.2163$ (11) Å	$\mu = 0.18$ mm^{-1}
$\alpha = 73.275$ (1)°	$T = 150$ K
$\beta = 81.776$ (1)°	Block, colourless
$\gamma = 79.305$ (1)°	0.45 × 0.35 × 0.20 mm
$V = 1392.06$ (19) Å^3	

Data collection

Bruker APEX 2 CCD diffractometer	7218 independent reflections
Radiation source: fine–focus sealed tube	5975 reflections with $I > 2\sigma(I)$
graphite	$R_{int} = 0.025$
ω rotation with narrow frames scans	$\theta_{max} = 28.8°$, $\theta_{min} = 2.1°$
Absorption correction: multi–scan *SADABS* v2012/1, Sheldrick, G.M., (2012)	$h = -13 \rightarrow 13$
$T_{min} = 0.923$, $T_{max} = 0.965$	$k = -14 \rightarrow 14$
19755 measured reflections	$l = -19 \rightarrow 19$

Refinement

Refinement on F^2	Primary atom site location: structure–invariant direct methods
Least–squares matrix: full	Secondary atom site location: all non–H atoms found by direct methods
$R[F^2 > 2\sigma(F^2)] = 0.040$	Hydrogen site location: mixed
$wR(F^2) = 0.111$	H atoms treated by a mixture of independent and constrained refinement
$S = 1.04$	$w = 1/[\sigma^2(F_o^2) + (0.0562P)^2 + 0.4122P]$ where $P = (F_o^2 + 2F_c^2)/3$
7218 reflections	$(\Delta/\sigma)_{max} = 0.001$
338 parameters	$\Delta\rangle_{max} = 0.90$ e Å^{-3}
0 restraints	$\Delta\rangle_{min} = -0.23$ e Å^{-3}

4.10a

Crystal data

$C_{32}H_{46}Cl_5NO_6P_2Pt{\cdot}CHCl_3$	$F(000) = 1944$
$M_r = 974.98$	$D_x = 1.693$ Mg m^{-3}
Monoclinic, $P2_1/c$	Mo $K\alpha$ radiation, $\lambda = 0.71073$ Å
$a = 12.2484$ (9) Å	Cell parameters from 6933 reflections
$b = 22.3032$ (17) Å	$\theta = 2.3–22.8°$
$c = 14.065$ (1) Å	$\mu = 4.14$ mm^{-1}
$\beta = 95.2802$ (14)°	$T = 150$ K
$V = 3826.0$ (5) Å^3	Block, colourless
$Z = 4$	0.27 × 0.13 × 0.10 mm

Data collection

Bruker APEX 2 CCD diffractometer	7824 independent reflections
Radiation source: fine–focus sealed tube	5786 reflections with $I > 2\sigma(I)$
Graphite monochromator	$R_{int} = 0.076$
ω rotation with narrow frames scans	$\theta_{max} = 26.4°$, $\theta_{min} = 1.7°$
Absorption correction: multi–scan *SADABS* v2014/1 Sheldrick, G.M., (2014)	$h = –15\rightarrow15$
$T_{min} = 0.401$, $T_{max} = 0.682$	$k = –27\rightarrow27$
34244 measured reflections	$l = –17\rightarrow17$

Refinement

Refinement on F^2	Primary atom site location: structure–invariant direct methods
Least–squares matrix: full	Secondary atom site location: difference Fourier map
$R[F^2 > 2\sigma(F^2)] = 0.037$	Hydrogen site location: inferred from neighbouring sites
$wR(F^2) = 0.084$	H–atom parameters constrained
$S = 0.99$	$w = 1/[\sigma^2(F_o^2) + (0.0348P)^2]$ where $P = (F_o^2 + 2F_c^2)/3$
7824 reflections	$(\Delta/\sigma)_{max} = 0.001$
380 parameters	$\Delta\rangle_{max} = 1.11$ e Å^{-3}
0 restraints	$\Delta\rangle_{min} = –1.00$ e Å^{-3}

4.12a

Crystal data

$C_{32}H_{51}Cl_2NO_6P_2Pt{\cdot}CHCl_3$	$F(000) = 1992$
$M_r = 993.03$	$D_x = 1.663$ Mg m^{-3}
Monoclinic, $P2_1/c$	Mo $K\alpha$ radiation, $\lambda = 0.71073$ Å
$a = 11.4946$ (9) Å	Cell parameters from 3537 reflections
$b = 14.6212$ (10) Å	$\theta = 2.8–27.6°$
$c = 26.000$ (2) Å	$\mu = 4.00$ mm^{-1}
$\beta = 114.781$ (10)°	$T = 100$ K
$V = 3967.3$ (6) Å^3	Lath, colourless
$Z = 4$	0.18 × 0.09 × 0.03 mm

Data collection

SuperNova, Dual, Cu at zero, Atlas diffractometer	9163 independent reflections
Radiation source: SuperNova (Mo) X–ray Source	5365 reflections with $I > 2\sigma(I)$
Detector resolution: 5.2474 pixels mm^{-1}	$R_{int} = 0.058$
ω scans	$\theta_{max} = 29.7°$, $\theta_{min} = 2.2°$
Absorption correction: gaussian *CrysAlis PRO*, Agilent Technologies, Version 1.171.36.31a (release 02–08–2013 CrysAlis171.NET) (compiled Aug 2 2013,12:40:55) Empirical absorption correction using spherical harmonics, implemented in SCALE3 ABSPACK scaling algorithm.	$h = –15\rightarrow12$
$T_{min} = 0.533$, $T_{max} = 0.890$	$k = –15\rightarrow20$
17908 measured reflections	$l = –35\rightarrow32$

Refinement

Refinement on F^2	Primary atom site location: iterative
Least–squares matrix: full	Secondary atom site location: difference Fourier map
$R[F^2 > 2\sigma(F^2)] = 0.055$	Hydrogen site location: inferred from neighbouring sites
$wR(F^2) = 0.128$	H–atom parameters constrained
$S = 1.02$	$w = 1/[\sigma^2(F_o^2) + (0.0388P)^2]$ where $P = (F_o^2 + 2F_c^2)/3$
9163 reflections	$(\Delta/\sigma)_{max} = 0.001$
406 parameters	$\Delta\rangle_{max} = 1.32$ e Å^{-3}
36 restraints	$\Delta\rangle_{min} = –1.27$ e Å^{-3}

4.16

Crystal data

$C_{32}H_{36}Cl_2NPRu$	$F(000) = 2624$
$M_r = 637.56$	$D_x = 1.430$ Mg m^{-3}
Monoclinic, $P2_1/c$	Mo $K\alpha$ radiation, $\lambda = 0.71073$ Å
$a = 13.5885$ (11) Å	Cell parameters from 10727 reflections
$b = 23.8087$ (19) Å	$\theta = 2.2–25.9°$
$c = 18.8940$ (15) Å	$\mu = 0.79$ mm^{-1}
$\beta = 104.3232$ (13)°	$T = 150$ K
$V = 5922.7$ (8) Å^3	Block, red
$Z = 8$	0.24 × 0.13 × 0.08 mm

Data collection

Bruker SMART APEX 2 CCD diffractometer	9429 reflections with $I > 2\sigma(I)$
Radiation source: fine–focus sealed tube	$R_{int} = 0.086$
ω rotation with narrow frames scans	$\theta_{max} = 28.4°$, $\theta_{min} = 1.4°$
Absorption correction: multi–scan *SADABS* v2008/1, Sheldrick, G.M., (2008)	$h = –18\rightarrow18$
$T_{min} = 0.834$, $T_{max} = 0.940$	$k = –31\rightarrow31$
60154 measured reflections	$l = –25\rightarrow25$
14781 independent reflections	

Refinement

Refinement on F^2	Primary atom site location: structure–invariant direct methods
Least–squares matrix: full	Secondary atom site location: all non–H atoms found by direct methods
$R[F^2 > 2\sigma(F^2)] = 0.050$	Hydrogen site location: mixed
$wR(F^2) = 0.129$	H atoms treated by a mixture of independent and constrained refinement
$S = 0.99$	$w = 1/[\sigma^2(F_o^2) + (0.0613P)^2]$ where $P = (F_o^2 + 2F_c^2)/3$
14781 reflections	$(\Delta/\sigma)_{max} = 0.002$
677 parameters	$\Delta\rangle_{max} = 1.16$ e Å^{-3}
24 restraints	$\Delta\rangle_{min} = –1.05$ e Å^{-3}

4.19

Crystal data

$C_{56}H_{54}Cl_2NPRu$	$F(000) = 1960$
$M_r = 943.94$	$D_x = 1.332$ Mg m^{-3}
Monoclinic, $P2_1/c$	Mo $K\alpha$ radiation, $\lambda = 0.71073$ Å
$a = 15.8597$ (6) Å	Cell parameters from 12506 reflections
$b = 16.3786$ (6) Å	$\theta = 2.2–26.4°$
$c = 18.3111$ (7) Å	$\mu = 0.52$ mm^{-1}
$\beta = 98.3686$ (6)°	$T = 150$ K
$V = 4705.8$ (3) Å^3	Block, red
$Z = 4$	0.46 × 0.41 × 0.16 mm

Data collection

Bruker APEX 2 CCD diffractometer	7895 reflections with $I > 2\sigma(I)$
Radiation source: fine–focus sealed tube	$R_{int} = 0.042$
ω rotation with narrow frames scans	$\theta_{max} = 26.4°$, $\theta_{min} = 1.7°$
Absorption correction: multi–scan *SADABS* v2008/1, Sheldrick, G.M., (2008)	$h = –19\rightarrow19$
$T_{min} = 0.796$, $T_{max} = 0.922$	$k = –20\rightarrow20$
41450 measured reflections	$l = –22\rightarrow22$
9643 independent reflections	

Refinement

Refinement on F^2	Primary atom site location: structure–invariant direct methods
Least–squares matrix: full	Secondary atom site location: all non–H found by direct methods
$R[F^2 > 2\sigma(F^2)] = 0.032$	Hydrogen site location: mixed
$wR(F^2) = 0.081$	H atoms treated by a mixture of independent and constrained refinement
$S = 1.04$	$w = 1/[\sigma^2(F_o^2) + (0.0338P)^2 + 3.0334P]$ where $P = (F_o^2 + 2F_c^2)/3$
9643 reflections	$(\Delta/\sigma)_{max} = 0.002$
557 parameters	$\Delta\rangle_{max} = 0.55$ e Å^{-3}
74 restraints	$\Delta\rangle_{min} = –0.45$ e Å^{-3}